Proceedings of the

IWCEM-2014

International Conference and Technology Meet on Defence, Marine and Aero Applications



Date

24^{th} to 26^{th} May 2014

Address

Hotel Four Points by Sheraton,
Viman Nagar, Nagar Road,
Pune

Organized by

Manipal INSPIRED BY LIFE

MANIPAL UNIVERSITY JAIPUR

INSTITUTE OF MARINE ENGINEERS INDIA

Editorial Team

Vidhya Shinde
Dept. of E & TC,
VPCOE, Baramati,
University of Pune, India.

Prof. Rajveer Shastri
Dept. of E & TC,
VPCOE, Baramati,
University of Pune, India.

Cdr. (Dr.) Arnab Das
MILIT, Girinagar,
Sinhgad Road,
Pune, India.

Proceedings of the **IWCEM-2014**
International Conference and Technology Meet on Defence, Marine and Aero Applications

Published by
:.....

Electronic version

Copyright © 2014 by the authors.

Foreword

India's destiny has always been intricately linked to the sea, and events in history testify the same. Right from ancient to medieval and modern history, every era of intense maritime activity has been associated with economic prosperity and political stability. Maritime trade has been the mainstay till the 1200 AD and Indian share in world GDP was higher than other contemporary nations and empires. The 13th century saw establishment of dynasties of Central Asian origins leading to a continental outlook taking root ensuring reduced maritime activity. The Indian share in world trade dwindled, and India's naval power was at its all time low, when the Europeans arrived in the late 15^{th} century. The inability to contest the European access of the Indian Ocean in the 18th century, led to the nearly two centuries of foreign domination. The strong message is that India with its over 7,500 km long coastline cannot ignore its maritime dimension while formulating its national strategy.

We have traditionally been considered as sea blind. However, in the 21^{st} century our grand strategy has been extremely sensitive to the maritime dimension and consequently, significant resource allocation and policy initiatives have taken place. The Ministry of Shipping (MoS) announced its first ever comprehensive Maritime Agenda 2010–2020 in Jan 2011. There on, the planning commission on its part constituted a working group for implementing the provisions of this Maritime Agenda 2010–2020, in the 12th plan (2012-2017). The Ministry of Defence (MoD) on its part constituted joint Confederation of Indian Industries (CII) and Boston Consulting Group (BCG) report titled "Creating a Vibrant Domestic Defence Manufacturing Sector" dated March 2012 which is a serious effort to revamp the domestic defence sector. The report analyzes the growth potential of the warship production in India in line with the 12^{th} plan and the Maritime Agenda (2010-2020). Inclusion of a new chapter on ship building in the Defence Procurement Procedure (DPP) to address special requirements of shipbuilding, has facilitated participation of the private players in the warship building industry in India.

The renewed emphasis on the maritime dimension has to be supported by appropriate technology availability. The tropical littoral waters in the IOR, presents very unique challenges and demands significant research efforts to be able to sustain the technology applications. In a globalized world today, researchers from multi-disciplinary aspects across continents need to collaborate and evolve realistic solutions to harness the undersea resources towards economic prosperity and provide safe access to the vast oceans in the IOR and beyond.

International Workshops, Conferences and Expo for Military and Marine Applications (IWCEM), provides the right platform for researchers, academicians, industrialists and the users of the maritime technologies that is the navy and the coast guard across the globe to communicate, network and collaborate. IWCEM 14, comes up with yet another edition that has gone beyond the earlier editions and included multiple new areas to come close to being a comprehensive platform for researcher interaction between all stakeholders. We are pleased to submit that the enthusiasm among the participants has been overwhelming this time and we received significantly more entries this year. We encourage all the participants to take advantage of the heterogeneous group of delegates representing users, academia and the industry and evolve new research leads for a better tomorrow.

This compendium showcases the papers shortlisted for presentation during IWCEM 2014 . The best six out of these as selected after multiple reviews would be published in the Journal of Institute of Marine Engineers.

The IWCEM 2014 organising committee
May 2014.

Reviewers

Reviewers IWCEM 2014			
Sr. No.	**Name**	**Designation and Address**	**Contact Details**
1.	Dr. Vevekanand Kain	Head, Corrosion Science Section Materials Science Div. Bhabha Atomic Research Center, Mumbai 400 085, India	Tel.: +91-22-25595067 Fax: +91-22-25505151 Email: vivek_kain@yahoo.com
2.	Dr. V. S. Raja	Professor, Dept. of Metallurgical Engineering and Materials Science, IIT Bombay, Mumbai 400075, India	Tel (Office): +91-22-25767892 Tel. (Resi.): 25768892, 25760406 Fax: 25723480 Email: Rajavs.Rajavs@gmail.com
3.	Prof. Arun Mahajan	Sr. Associate Prof. (Marine Engg.) Tolani Maritime Institute, Pune	Mob. No. : +919860274144 Email: arunm44@gmail.com
4.	Cmde A. N. Sonasale	Head of Faculty (Navy), MILIT, Girinagar, Sinhgad Road, Pune-411025	Mob. No: 7350589386 Office: 020-24389630, 24304211 Resi- 020-24304212 Email: anand.sonsale@gmail.com
5.	Cdr. (Dr.) Arnab Das	MILIT, Girinagar, Sinhgad Road, Pune 411025	Mob. No.:+919665033463 Email: arnabdas1972@hotmail.com

Contents

Foreword **iii**

Reviewers **iv**

Invited papers **1**

Navantia LHDs: Main characteristics and customization options of the one of most capable, safe, reliable and sophisticated amphibious deployment systems in the world
Abel Méndez 1

Class Approvals - The Role of Classification in Naval Vessel Certification
James A. Stamm 11

Reviewed papers **20**

Tecnhical Session 1A: Shipbuilding & Class Approvals **20**

Propulsion System Integration - A Critical Gap in Indigenous Warship Building
Capt (IN) Sameer Agarwal, Lt Cdr V Kumaran 20

Developments in Shipborne Controls and Electronic Systems
Commander (Veteran) Alok Bhagwat 25

Numerical Investigation on Response of Air-backed and Water-backed Plates Subjected to Underwater Explosion
Debashis Wadadar, Masud Ali, Asokendu Samanta 35

Challenges in Aluminium Planing Craft Design and Production - Structural Aspects
Tathagat Kumar Parthsarthy, Anand Suresh Chimanpure,Cdr (Retd.) Atul Killedar . 40

Tecnhical Session 1B: Corrosion Assessment & Control **49**

Influence of Biofouling on the Metallic Corrosion in Singapore Seawater
D.J. Blackwood, C.S. Lim, S. L. M. Teo 49

Smart Nano-Composite Coatings for Aerospace Applications - A Holistic Approach Smart Anti-Corrosion Coatings
Amitha rani B.E., Prakashaiah. B.G. 54

Chemically Modified Metal/ Hetero-Metal Alkoxides as Molecular Precursors for Nano-Sized Ceramic Materials
Veena Dhayal, Aparna Pareek 58

Corrosion Predictive Modeling for Aging Ships
Cdr Nitin Agarwala 64

Stress Corrosion Cracking of SS 304 L Inchloride Environment at Near Boiling Temperatures - Mitigation & Acceleration
Harshad Tarate, Geogy Abrahami, Vivekanand Kain 71

Tecnhical Session 2A: Modeling & Simulation **78**

Development of Tools for Evaluating the Operational Effectiveness of Competing Hull Forms in the Design of Ship for Seakeeping
Cdr. (Dr.) R. Vijayakumar, Lt. Vivek Tewari, Lt. Cdr. B. Praveen 78

Wavelet Transform an Emerging Time Frequency Analysis Tool for Rolling Element Bearing Fault Diagnosis
Commandant(JG) (Dr.) Angello Innocent Devasigamani, Dr. Animesh Chatterjee . . 85

Comparative Evaluation of Adaptive Algorithms for Filtering of Underwater Ambient Noise
Vidhya Shinde, Rajveer Shastri, Arnab Das, Shankar Deosarkar 91

CFD Modeling For Optimizing Ballast Tank Structural Design in A Ship
Cdr Vinay G Ankalgi 95
Study of Combustion in Gas Turbine Engines
Lt Cdr MSN Murthy 106
Numerical Resistance and Self Propulsion Simulations for Early-Stage Ship Design Evaluation
Lt. Cdr. IS Makkar, Cdr. (Dr.) R. Vijayakumar 113

Tecnhical Session 2B: Environment & Energy **120**
Marine Pollution Control by Ballast Water Management System
Ashvin Wanzul, Sameer Mamluskar, Rohit Mathur 120
Spectrogram Denoising and Extraction of Dolphin Whistles from Noisy Underwater Environment
Bhagyashri Patil, Rajveer Shastri, Arnab Das 127
Super Eco Ship using Green Technology for Energy Conservation
Sanjay Dabadgaonkar, Asim Kumar Sen 130
Application of Solar (Photo Voltaic) Cells for Power Generation onboard Naval Ships
Captain(IN) Naresh Chhabra 137
Acoustic Characterisation of Marine Mammals using Spectrogram Image Correlation
Lt Cdr Aayush Verma, Cdr (Dr) Arnab Das 141
Underwater Sediment Classification using Characteristics of Echoes
Priya V. Bothe, J.A. Sadalage, Cdr Dr. Arnab Das 145

Tecnhical Session 3: STS-1 **149**
Under Water Electromagnetic Remote Sensing
Karan Datta 149
Quick Detection of Incipient Corrosion in AA2024-T3
Prakashaiah B. G., Deepa M. K., Amitha Rani B. E. 152
Analysis of Effects of the Anti-Fouling Paints on the Environment and their Economic Impact on Sea Transport
Cdt. Malay Phadke, Cdt. Kshitish Kumar Dubey 158
Waste Generation & Handling on Board the Vessel
Cadet Anubhav Kumar, Cadet Rohit Kumar 164
Geothermal Power Plant on the Concept of Organic Rankine Cycle
Cadet Akshay Shetty, Cadet Mayur Agarwal, Cadet Preetish Sengupta 170
Marine Air Pollution Control-Sulphur Emissions and Their Control
Cadet Rahul Dewan 173

Tecnhical Session 4: STS-2 **180**
The Nitrogen Revolution
Cdt. Neeraj Mehta, Cdt. Kevin Parmar 180
Need of Physical Fitness and Lifestyle Management for a Seafarer
Animesh Padhi, Arvind Kaushal 187
Object Detection for Maritime Surveillance
Avani Agarwal, Disha Mehra 190
Era of Advanced Materials
Sumit Jain 195
Naval Weapon Systems: An Introduction and Study of Overcoming Limitations with Ellipsometry and Improved Geometric Dilution of Precision Model
Anubhav Shankar 201

Piezoelectricity uses and Possible Incorporation to Harness Clean Energy
Kabir Roy 205
Frugal Flying Machine Building a Frugal Aircraft using Balsa
Ankur Kumar, Kastubh Kalla 207

Tecnhical Session 5: Students Contributory **210**
Dynamic Feature Extraction of ECG Signal
Juie Peshave, Rajveer Shastri, Arnab Das, Shankar Deosarkar 210
Cetaceans Detection and Classification Algorithms for use in Automated Passive Acoustic Monitoring
Suchita Nanaware, Rajveer Shastri,Arnab Das 214
EEG Signal Analysis Using Empirical Mode Decomposition
Nilima Mohite, Rajveer Shastri, Arnab Das, Shankar Deosarkar 219
Application of ICA for Fetal ECG Separation
Sonal Nikam, Rajveer Shastri, Arnab Das, Shankar Deosarkar 224
Detection of Leukemia in Microscopic Images Using LabVIEW
Chaitali Raje, Jyoti Rangole 228
Detection of Optic Disc in Fundus Images
Snehal Akhade,Vikas Deshmukh, Shankar Deosarkar 231

Tecnhical Session 6A: Design & Optimization **235**
Human Factors Perspective is Necessity of Modern Ship-Building
Lt. Cdr. Sumit Singh 235
Classification Techniques For Sediment Analysis
Ankika H. Rasal, J.A. Sadalage, Arnab Das 239
Optimization of Exhaust Systems in Warships
Ashvin Wanzul, Sameer Mamluskar, Rohit Mathur 243
Design Deviations During Retrofits: Boon or Bane A Case Study
Cdr. Vikram Gulwadi 249

Tecnhical Session 6B: Surveillance & Underwater Technology **255**
Coastal Area Surveillance Technology for Indian Ocean Region
Chakshu Malviya, Arnab Das 255
Implementation of Embedded Platform for Underwater Glider Prototype
Lt. Cdr. MD Nair, Mr. Abhilash MT, Cdr.(Dr.)Vijayakumar, Cdr. (Dr.) Arnab Das 263
Underwater Sensor Networks for Coastal Surveillance- The 'Indian Seaweb'
Lt Cdr Soubhagya Roul, Arnab Das 268
FPGA Realisation of QPSK Modulated OFDM Transceiver
K. Sandeep, Abhilash M. T. 273

Tecnhical Session 7A: Materials & Failure Analysis **278**
Constraint Weldment of Austenitic Stainless Steel Strain Development at Weld Fusion Zone and its Control
Lt Cdr Ramandeep Singh Sawhney, Vivekanand Kain, SP Srivastava 278
Failure Analysis of Axial Flow Impulse Turbine Rotor Disk
E. Bhaskar Rao Sc'C', R.Srihari Sc'F', C. Kedarnath Sc'F',AVS Chari Sc'G 289
Development of Improved Welding Technique for Naval Structural Material (Dmr249a)
Cdr Rishi Pamnani, Dr M Vasudevan, P Vasantharaja, Dr T Jayakumar 292

Effect of Hydrogen Content and Hydrides on Oxidation Behavior of Zirconium Base Alloys used for Fuel Cladding of Nuclear Reactors
Lt Cdr Sk Tiwari, M. Kiran Kumar, Vivekanand Kain, Sanjay Singh 296
A Theoretical Survey of the Effective Electron Mass in Nano-Wires invoking DFT Methodolgy
Dr. Ajay Kumar 305
A Brief Survey of Nano Materials invoking DFT based Descriptors
Prabhat Ranjan1, Ajay Kumar2, Tanmoy Chakraborty 310

Tecnhical Session 7B: Propulsion & Controls **313**
Air Independent Propulsion (Aip) for Submarines - A Strategic Necessity
Cdr Av Agashe 313
Electric Propulsion: A Strategic Choice for the Indian Navy
Commander PS Vombatkere 318
Rudder Roll Stabilisation: An Perspective
Lt Cdr Swarup Das, Cmde AN Sonsale 327
Design of a ships autopilot using state space feedback control methodology
U. Dheeraj, Swarup Das, SK Panigrahi 332
Evolution of Control in Marine Engineering
Lt Cdr PK Mishra 336

Tecnhical Session 8: Health Monitoring **340**
Comparative IR Thermography Changing Paradigms in Condition monitoring
Lt Cdr TS Sathya Narayanan, Lt Cdr Sumit Singh 340
Noise Transmission Analysis Onboard Marine Platforms- A Review
Cdr KK Mahapatra, Arnab Das 344
Condition Monitoring of Ships Hull using ICCP System- A Case Study
Dr N. Vasudeva Rao, K. Jaya Prakasa Rao 348
Zigbee Based Ship Health Monitoring and Warning System
Lt. Cdr. M. Vinodh, Dr. K. Krishna Naik 351

Navantia LHDs

Main characteristics and customization options of the one of most capable, safe, reliable and sophisticated amphibious deployment systems in the world

Abel Méndez
Design Manager. Australia LHDs
NAVANTIA S.A.
Madrid, Spain
amendezd@navantia.es

Abstract— *Navantia is a Spanish shipbuilding company with more than 300 years of history. Navantia is an international reference in the design and construction of complex submarine and surface ships, including aircraft carriers, frigates, destroyers, LPDs and Offshore Patrol Vessels.*

In the last decade, Navantia has delivered three state-of-the art LHD ships (Landing Helicopter Dock); one for the Spanish Navy and two for the Australian Defense Force. The LHD ships designed and built by Navantia represent one of the most capable, safe, reliable and sophisticated amphibious deployment systems in the world.

The LHDs are multipurpose ships capable of operating world-wide, inclusive of hot ambient and seawater temperatures as well as cold sub-artic conditions. They are provided with superior facilities for troop transportation, and can support amphibious watercraft operations from a floodable dock built inside of the ship. The LHDs can also be used as a roll-on/roll-off ships since they are provided of side ramp doors, vehicle lifts and heavy cargo and lightweight garages to accommodate combatant tanks and a variety of vehicles. Helicopters are operated from the lightweight cargo garage and maintained at a dedicated hangar. Aircraft access to the flight deck is done from two aircraft lifts. The LHDs can also be used for launching pads for UAVs and can operate short/vertical take-off fighters. The LHD ships are also provided with ammunition magazines, armories, refrigerated spaces, store areas, and various workshops. Furthermore, her very well outfitted medical facilities, large mess areas and ample spaces permit to carry out and support humanitarian missions.

The LHD design meets a very robust certification basis, including SOLAS, MARPOL and other IMO standards. The Australian LHDs HMAS Canberra and HMAS Adelaide are in fact the first new built military built ships ever classified by Lloyds Register under the Naval Rules. These ships utilize the Platform of the Spanish Navy Juan Carlos I, which was thoroughly tailored to satisfy the Royal Australian Navy mission system requirements and Australian standards. The Juan Carlos I, benefits from the experience gained by Navantia in the design, fabrication and operational feedback of the LPDs Galicia and Castilla delivered to the Spanish Navy in year the 2000, and the aircraft carrier "Principe de Asturias".

Navantia's design is flexible and versatile, and can be adapted to meet the specific needs of navies and flag states whilst maintaining the spirit, stylish and class which make Navantia LHDs recognizable worldwide.

This paper identifies some ship particulars, characteristics and provides some examples of customization options of the LHD ship design.

Keywords—Navantia, LHD; LPD, Ship, Amphibious, helicoper; aircraft, troops, dock, survability, hospital, truck, tank, garage, hangar, Classified, Lloyds

I. INTRODUCTION

In 25 June 2007 the Australian Government selected the proposal offered by Tenix, who are now BAE Systems Australia, and their partner Navantia for the design and construction of two LHD (Landing Helicopter Dock) ships. The Reference Ship in which such designs were based is the Navantia's 28,000 tonne 'Juan Carlos I', which was at that time under construction by Navantia for the Spanish Navy. The Spanish LHD design was appraised by Lloyds Register based upon the Rules for Ships in relevant areas with a merchant notation.

The Australian ships, HMAS Canberra and HMAS Adelaide, implement more than 2,000 modifications with respect to the Reference Ship to meet the Royal Australian Navy's (RAN) requirements. They are also the first new-built ships classified under the Lloyds Register (LR) Naval Ship Rule.

The LHD ships for the Spanish Navy is in service and performing well. The first Australian LHD is in the final commissioning stage and is planned to be in service by mid-2014, whilst the third ship remains under construction and will be delivered in 2015.

More recently, in January 2014, the Government of Turkey has announced that the partnership formed by Navantia and SEDEF, the Turkish shipyard, had been selected in first place for the design and construction of one LHD. The Navantia basic configuration has been tailored to meet the mission system requirements of the Turkish Navy. Fulfilment with the requirements of the class society Türk Loydu has also been made.

The last customization of the Navantia design was made for the Indian Navy in response to a Request For Proposal (RFP) to be presented in partnership with Larsen & Toubro by July 2014. Such work implied the design of a Platform Dock (LPD) ship meeting the navy requirements and high indigenous content. The Navantia design solution is based on the LR Naval Code, with the Indian Register of Shipping (IRS) as dual classification society.

This paper describes the main features of the basic LHD Navantia configuration utilized both for the Spanish and Australian designs already in service. Such Platform has also been used as starting point for adaptation to the requirements of the Turkish and Indian Navy projects.

II. BASIC CONFIGURATIONS

A. Generation of alterntives

Navantia, as a global contractor, can cover and coordinate the integration of the entire design and construction of the LHDs, including Platform and Combat System.

Conceptual engineering of the Spanish LHD was developed in cooperation with the Spanish Navy. Many of the ship systems are inspired in other Navantia designs such as the LPD vessels of the "Galicia Class", and the aircraft carrier "Principe de Asturias".

The Spanish LHD "Juan Carlos I" features a Combat System from Navantia Systems (formerly known as FABA)/INDRA, and communications from Rhode & Schwarz.. Lockheed Martin's CMS, which uses an Aegis Display System and Command & Decision System. Because this CMS has its origin in the Aegis Open Architecture software suite, it supports future change and growth, including the ability to later incorporate a Cooperative Engagement Capability. This system provides the best interoperability with the U.S. Navy.

Navantia coordinated the design of the above systems, and developed a fully integrated solution.

With respect to the Australian design, Navantia and the Commonwealth of Australia (CoA) evaluated the Operational Functional and Performance Requirements from the Navy at a very early stage, and developed alternatives based on Reference Ship. Due to local content requirements, Navantia was then asked to select a suitable yard in Australia, which resulted to be the Tenix yard (today BAE Systems) at Williamstown, Melbourne. Upon selection of the Navantia and BAE systems proposal, Navantia became back-to-back subcontractor to BAE systems, which then signed the head contract with the CoA for the supply of two LHD ships.

During the pre-contract period of the Australian project, two Combat System alternatives were developed; one based on the Lockheed Martin AEGIS solution, and one incorporating a Saab Combat Management System (CMS) with Communications from L3.

The preferred choice was the Saab 9LV CMS. This system evolved out of a Swedish Navy system developed in the late 70s and early 80s. It was one of the first to adopt the ADA programming language and computer-based software development environment. The system was upgraded, expanded and evolved for commonality with the Australian ANZAC frigates, and therefore transitioned to militarized COTS hardware and commercial operating system in 2004 prior to being installed on HMAS PERTH. The current Saab 9LV CMS was developed in close cooperation with the Royan Australian Navy.

Basic detail of the Combat System was under the scope of BAE Systems, whilst Navantia executed the detail design and final Platform integration.

With respect the ship information and control systems, both projects; the Spanish and the Australia, integrate a modern Platform Management System (IPMS) developed by a sister Navantia.

Many other changes have been assessed, but finally not implemented, such as for instance the removal of the ski jump, or implemented only with as necessary to enable future installation (i.e. fitted for but not with, reserve of space and weight, reserve of space only, etc). These last categories of changes are proposed mainly in respect to combat system, communications and weapons.

In summary, more than. 2,000 changes were implemented in the Australian LHD with respect to the Reference Ship, the Spanish "Juan Carlos I".All ship blocks and many equipment items were modified.

Other changes are also possible, and can be implemented as necessary for specific projects, including shortening or lengthening the hull, changes to the propulsion system for incorporation of conventional propellers, changes in the generation system, type and/or number of aircraft lifts, changes in the configuration of the dock (i.e. removal of the central fender, services to the dock, etc)

B. Project management

The design of both the Spanish and Australian ships was reviewed and approved following System Engineering standards tailored to the project. Several Design Review meetings were held to consolidate design baselines: the System Requirements Review (SRR), Preliminary Design Review (PDR), Detail Design Review (DDR) and TRR (Test Readiness Review).

Each of the above Design Reviews were organized separately for the Platform and Combat System designs, with a final joint Whole of Ship review.

Day to day design activities were followed closely by the end customer, the CoA, which was co-located with Navantia and BAE System engineers for the sake of mutual understanding of the requirements and real time awareness of design progress.

In addition to the above, several Working Groups (WG) were created to ensure good communication lines and facilitate the decision making process. GW members met regularly during project development, with some of them holding weekly meetings for the first four years of the project. The WG

included the CoA representatives, BAE Systems and Lloyds Register.

The following WG were created: Platform Engineering, Combat System, Safety, Human Factors engineering, interface management, EMI/EMC, Aviation and Antenna, Design of Command and Control spaces Upper deck design and related performance.

Furthermore, in planning this project, Lloyd's Register and Navantia considered that its scope and complexity required a full time Project Manager resident within the Navantia Ferrol project design office to coordinate the review and appraisal activities, and to act as the primary liaison point for Navantia, BAE Systems, and the CoA's project team.

Fulfilment of the project requirements was verified through the sell-off process, which was the end piece of a thorough Verification, Validation and Assurance process implemented by Navantia and BAE Systems, where each Contract requirement was flown down to suppliers through procurement specifications, and its implementation checked at various stages through verification points in design drawings, fabrication tests, harbor and sea trials.

C. *Certification basis*

The certification process necessary to meet the platform requirements followed different routes for the Spanish and the Australian LHDs, constituting two different standards.

The Spanish LHD "Juan Carlos I" was designed to meet a a Lloyds Register notation set with a commercial focus, this is, following the Rules for Ships, and with the consideration of a Roll On-Roll Off Special purpose ship.:

The ship was also designed to meet some selected Naval standards including NATO, NAVSEA, STANAG, MIL-STD and Spanish Navy Specific. With respect to statutory requirements, the design meets chapters of selected IMO Regulations such as SOLAS, MARPOL.

For the Australian LHD, Lloyd's Register provided Classification for the platform under the Naval Ship Rules. The Naval Ship Rules cater for the particular requirements of naval ships and their operators. Furthermore, allow tailoring of requirements relevant to the Navy or Naval Authority subject that they can be demonstrated that they are based on recognized standards which provide the same or improved safety levels. For the Australian LHDs, a number of specific Australian Navy requirements such as the DEF(AUST)5000 series were also taken into account. Consideration of the LR Naval Rules, tailored by Navy requirements, required project-specific certification for an important number of ships Systems and Equipment items, therefore requiring effort from suppliers which had to adapt and submit their COT solutions for design appraisal, and have the fabrication and installation of their supplies surveyed and approved by Lloyds.

The scope of the classification of the Australian LHDs includes: structure, machinery, electrical and control systems, machinery redundancy, replenishment at sea, fire safety, escape and evacuation and environmental protection.

D. *Project Execution*

The build strategy for the LHD ships can be adapted to local content requirements imposed by each specific Client.

The Spanish LHD was built totally in Spain at the Fene/Ferrol Yard, whilst the Australian LHD had two main construction sites, Navantia (Fene/Ferrol, Spain) and BAE Systems Australia (Williamstown, Australia).

Principally Navantia constructed the platform up to the flight deck, at which point the ship was wet transported by heavy lift ship to Williamstown for consolidation of the superstructure which was built in Australia by BAE Systems. Validation and trials were completed in Australia, with delivery of the ships to the Navy in Sydney.

Transport of the 231 meter LHDs to Australia was made with Dockwise's Blue Marlin heavy lift ship. Recognizing that the ship's structure would be subjected to different loading patterns during the lift operation and transport, Lloyd's Register was asked to assess the loads imposed on the LHD structure.

Navantia was responsible of the detail design, workshop drawings and work orders for the fabrications in Australia. In order to ensure a proper understanding or the production facilities in Australia, and also to make sure that Navantia drawings are interpreted correctly, a resident team including engineers, foreman and shop personnel were moved to Australia. Some companies who participated as subcontractors to Navantia in the fabrication of the LHD in Spain, created sister companies in Australia and offered up their services until the vessel completion.

III. MAIN DESIGN FEATURES

This section provides some details of the basic configuration of the LHDs.

A. *Key features*

The LHD ship possesses the following key operational features:

a. Capacity to conduct all forms of operations. The integrated amphibious capability has utility at all levels of military operations – from presence or deterrence, to disaster relief or humanitarian assistance, to policing operations or special recovery operations, or in the most extreme circumstances – warfighting

b. Integrated solutions. The LHD provides the complex amphibious capabilities that can only be successfully delivered through sound design and seamless integration of the physical elements of the LHD, and the functionality of the combat system

c. Command facilities. Fir for purpose designed functional command facilities and a robust Communication Information System (CIS) framework combined to support all forms of military support and warfighting operations. Together these facilities provide physical and electronic co-location of the commanders and tactical battle staffs in order to provide the

greatest opportunity for unity of effort and timeliness of response

d. Operational tempo. The LHD ships possess a very capable flight deck, dock and supporting facilities, which are integral to the generation of amphibious operational tempo – the speed at which a credible force with sufficient combat power can be established before an adversary can effectively respond to the landings

e. Underway reconfiguration. The current maxim of "first on is last off" is undesirable to the LHD ship design. Operational imperatives highlight the need of being able to reconfigure loads during transit to the amphibious objective area, in the early stages of the amphibious assault

f. Sea basing and logistics. Implies the provision of the tactical and operational capacity to enable playing a strategic role without reliance on ports, airfields or host nation support. Indeed, the sea basing capability of the ship will ensure that the naval forces footprint on the ground is limited to essential personnel thereby improving total force security.

g. Habitability. Whether providing a presence or supporting an operational embarked landing force, or participating in a regional engagement deployment, the embarked forces must remain highly trained and in good physical and mental condition despite a prolonged period at sea. The LHD ship can service these readiness demands through superior living conditions provided by a raft of facilities including 18 recreational rooms, two reading rooms, two gymnasiums, purpose designed cabins and extensive laundry facilities

h. Survivability. The design characteristics of the LHD afford exceptional survivability and flexibility during military operations. The LHD has a high level of survivability. In addition to a capable damage control system, it has a Citadel for defending against Nuclear, Biological and Chemical Warfare. The Citadel can be segregated into six sub-citadels. Personnel inside a sub-citadel are not at risk of contamination for four days, even while wearing no protective clothing or equipment. This enables them to carry out normal duties in key areas of the ship, including habitability, command and control, and hospital spaces. Survivability in combat is improved by being able to execute missions quickly and efficiently, reducing the exposure of the ship and its embarked forces to danger. Survivability is further enhanced by equipping the ship with excellent point defense systems

B. LHD Capabilities

The LHDs are able to carry more than 1400 persons, with 25% of the accommodation suitable for gender segregation.

The LHD ships are equipped for air operations featuring 6 helicopter spots (suitable also for vertical take-off and landing of fix wing aircraft) and a flight deck with 'ski jump' This enable operations to be carried out with the vessel's own rotary wing aircraft or a selection of other types as required. Two large aircraft elevators, forward and aft, each with a 27 tonne capacity, transport aircraft from the flight deck to the full length light weight vehicle/hanger hangar deck. Full support facilities including aircraft servicing and safety systems are supplied in accordance with the requirements of the Navy.

Two garages are provided, one light weight vehicle/hanger hangar and one heavy weight vehicle garage. These two garages (cargo spaces) are connected by a 20 tonne cargo elevator and vehicle ramp. Two side and a stern ramp provide shore side access for cargo, the stern ramp can also be used for amphibious operations.

The aft part of the heavy weight garage also forms part of the amphibious dock facility. With the dock flooded and the stern ramp open, four Landing Craft Motorized units (LCM) can load/unload in the protected confines of the dock and transfer the cargo ashore or to another vessel. Other craft such as RHIBs (Rigid Hull Inflatable Boats), and LCACs (Landing Craft Air Cushion) could also operate using this facility.

Replenishment at Sea (RAS) capability is provided by two stations for fluids and one station for heavy solids.

In addition to the platform's crew, and facilities personnel, the LHDs will have the arrangements to support troops personnel including accommodation, recreation spaces, mess rooms and a hospital.

Advanced weapons and communication systems are integrated into the ship's other systems.

To provide the LHDs with a sufficient and flexible power supply, a COmbined Diesel-electric And Gas turbine (CODAG) configuration is provided in the Navantia design. This comprises of one LM2500 gas turbine (22,000 kW) and two MAN B&W 32/40 diesels (7,680 kW each) driving the generation plant. The power management system manages the ship to provide power to the numerous platform consumers.

Propulsion is provided by two Siemens-Schottel PODS (POdded Drives), each rated at 11 MW, and in combination with the two bow thrusters, a high degree of maneuverability can be achieved.

An advanced Integrated Platform Management System (IPMS) of Navantia design and manufacture is being provided to monitor and control numerous critical, essential and auxiliary systems. This system spans the whole platform and integrates most of the platform's significant systems including: navigation, propulsion, communications, safety and weapons systems.

C. Aircraft Operations

The embarked aircraft can project assault force elements from over the horizon and as far inland as their operating radius in order to concentrate, strike or threaten an adversary's flanks and rear areas. Indeed, the number and type of helicopters and capabilities of the embarked air assault forces will define the size of the littoral battle space. The LHD ship provides an ability to conduct "Ship To Objective Maneuvers" (STOM) anywhere within this littoral battle space. The STOM capability provided by the air assault combat power is a credible threat that would cause an adversary to divert or disperse forces to protect vital infrastructure and key terrain over 100 nautical miles inland. While sea state conditions may limit the time or duration of an air assault, the LHD capability

to launch aircraft in Sea State 5 (SS5) conditions ensures that such interruptions are not common.

In order to generate such a credible air assault threat the LHD provides 990 m^2 of hangar space to accommodate eight troop lift helicopters with the blades folded. Smoke and fire curtain separates the adjoining 1880 m^2 Lightweight Cargo Garage. Like the hangar, it includes a dedicated aircraft elevator providing commanders with the opportunity to tailor the size and capabilities of their air assault forces in response to operational requirements.

A key tenet of surprise is the generation of tempo; the speed at which a credible force with sufficient combat power can be established before an adversary can effectively respond to the landings. Surprise and tempo also serve to limit the exposure of amphibious forces during the difficult transition period of ship to shore movement. The LHD ship flight deck and supporting facilities are integral to the generation of this tempo. The six spots on the 4750 m^2 flight deck (each serviced by refueling and de-fuelling points) are supported by up to five operational (blades spread) aircraft parking spots on the starboard side. Combined with the forward and aft aircraft elevators, which can also park one additional helicopter each with blades spread, a total of 13 helicopters may be positioned on the flight deck with the blades spread.

This capacity will enable to launch or recover two waves of aircraft from one LHD ship within 30 minutes. Furthermore, when the Helicopter In flight Refueling (HIFR) capability is added to the support package, it ensures that the tempo of assault waves can be sustained by a constant rotary wing (RW) effort, since the LHDs design enables refueling, loading and re-launching aircraft. Indeed, the limiting factor in the amphibious air assault tempo is likely to be the number of pilots and deck crew personnel, particularly during night operations.

The tempo of aircraft unloading and loading is controlled and monitored by a combination of physical and electronic means.

D. Dock Operations

The dimensions of the LHD dock ensure that the naval forces can poise at sea, raid or land on a potentially hostile coastline at the time and place of political choice entirely independent of shore infrastructure. As part of the integrated maritime capability the LHD has utility at all levels of military operations, from presence, to humanitarian assistance, to policing operations or Special Recovery Operations, or in the most extreme circumstances – warfighting.

As with the air assault forces and other naval forces, the surface assault forces that can be embarked in the LHD. Whilst the Embarked Landing Forces (ELF) is onboard, they can remain poised for 49 days; and once ashore the LHD can sustain the landing force for up to 20 days.

Each LHD is provided with a 1165 m^2 dock. The LHD dock provides a most effective means to generate operational tempo as the four embarked LCMs have capacity to insert a mechanized combat team in conditions up to and including SS4. The LHD is provided with an inclined dock floor, central steel fender, responsive stern ramp, gantry crane and adjoining 1880 m^2 Heavyweight Cargo Garage to provide effective and efficient reception, unloading and loading facilities and areas for landing craft. These facilities assist the surface assault to project maximum combat power across the shore in the 24 hours before an adversary can effectively respond to the landings.

The net capability of the LHD to unload and project the ELF during the surface and air assaults maximizes the shock effect on an adversary.

The Dock stern ramp can be lowered 30 degrees to facilitate ramp-to-dock floor marriages with landing craft or can operate in cantilever mode for ramp-to-ramp marriages (weight limit of 18 tonnes). The stern ramp can be raised within 30 seconds to aid safer Dock operations.

The tempo of landing craft unloading and loading is controlled and monitored by a combination of physical and electronic means. CIS support systems, including the Personnel and Material Control System (PMCS), assist onboard commanders to efficiently queue and respond assault waves through respective Troop Meeting Areas, the Deck 4 Troop Assembly Area and beyond to waiting landing craft. Closed Circuit Television (CCT) subsystems and individual communications between controllers (like the Dock Control Officer) and assault guides, provide the means to maximize the efficiency and effectiveness of the Dock embarkation processes. Progress is closely monitored by the LHD Operations Rooms and reported verbally or electronically to the Primary Control Officer.

The LHD dock can support a wide variety of craft ranging from small craft up to the size of USN Landing Craft Air Cushion (LCAC)

E. Vehicle Operations

The imperatives of landing vehicles ashore in a tactically configured formation ready for combat are paramount. While considerable effort is directed towards avoiding compromise, there is no guarantee that adversarial forces have been identified, isolated or destroyed. Therefore the first priority, once the first combat teams are ashore, is to introduce sufficient combat power to detect and destroy or neutralize potential threats to his forces. However, the need to strike and establish combat power ashore and developing appropriate beach infrastructure and support echelons before the follow-on combat teams need to be balanced. Often this balance is difficult to assess correctly in the planning stages where intelligence is always insufficient and tidal windows and beach gradients inadequately defined.

The above imperatives highlight a requirement to be able to reconfigure loads during transit of the LHD, and in the early stages of the amphibious assault. The current maxim of “first on is last off” is undesirable to the LHD. Indeed, the LHD’s 1158 lane meters do not include the Dock, the Troop Assembly Areas on Deck 1 (Lightweight Cargo garage) and Deck 4 (Heavyweight Cargo Garage), the Deck 1 maneuvers area and the two Deck 4 access ramp spaces. Combined with the gantry cranes on both decks, the Lightweight Cargo Elevator, forward aircraft elevator (leading directly from the lightweight cargo

garage to the flight deck), and space requirements around each vehicle, there is capacity to reorganize some elements of the load in transit and during disembarkation.

The 1410 m^2 Heavyweight Cargo Garage adjoins the Dock and its size ensures efficiency and effectiveness of vehicle positioning and maneuvers during the landing craft loading process. Similarly, the Dock Control Station positioned on Deck 3 has uninterrupted visibility of the Dock and approaches to the steel beach. CCTV subsystems and individual communications between controllers (like the Dock Control Officer) and assault guides provide the means to maximize the efficiency and effectiveness of the Dock embarkation processes. Progress is closely monitored by the LHD Operations Rooms and reported by CIS means to the officers onboard.

F. Cargo Operations and Sea Basing

Traditionally in amphibious operations, once the initial assault waves are ashore the majority of helicopter and landing craft effort is dedicated to the landing of Combat Service Support (CSS). Unfortunately offloading all CSS capabilities may remove significant amphibious force agility, particularly in the initial phase of an assault, or during an amphibious raid. Therefore, the ability of the LHD to support the ELF ashore for up to 20 days provides a "Sea basing" capability, and ability to integrate into a larger coalition sea base construct.

During short duration operations or raids command levels, the Primary Casualty Reception Facility (PCRF) and a significant slice of the first and second line assets may remain embarked. Such sea basing of non-essential maneuver elements offers a number of advantages including an ability to replace some vehicles with more combat vehicles. The superior cargo and accommodation capacity of the LHD offers significantly greater operational flexibility from this perspective. In so ensuring that the naval force footprint on the ground is limited to essential personnel only, total force security will be enhanced.

The Defense Integrated Distribution System and LHD IPMS will facilitate the tracking of stores and equipment from the Main Support Area or units forward through the logistic and amphibious support architecture until it is delivered. Staff charged with logistic support will have intimate visibility and management responsibility for what should be the seamless continuum of cargo, stores and equipment in transit or aboard.

G. Personnel Operations

Whether providing a presence or supporting an operational landing force, or participating in a regional engagement deployment, the embarked troops must remain highly trained and in good physical and mental condition despite a prolonged period at sea. The LHD can service these readiness demands through the following facilities:

a. Accommodation. Individual lockers, some of them with space reserve for installation of sit-up bunks (i.e a special bunk system with a L form which permits sitting comfortably on the bunk) and some en suite facilities combine with generous storage spaces to ensure that more than 1100 persons can be comfortably accommodated on board the LHD for in excess of one month. There is extra capacity of the LHD to also accommodate 243 persons crew, including 36 extra bunks available for the various ranks. Auxiliary services and lifesaving appliances are fitted for the overall capacity

b. Rest, Recreation and Fitness. Eighteen recreational rooms are provided across all accommodation levels of the LHD. These facilities ensure that troops have a wide range of entertainment mediums at their fingertips including video, TV, music, and facilities for reading material. Reading Rooms are also provided to the senior enlisted ranks and officers. These recreational spaces are ideal for briefings down to platoon level and serve a variety of social and military functions leading to improved morale and cohesion. Two gymnasiums combine with the functional flight deck spaces to ensure that troops can maintain high levels of physical fitness throughout their deployment

c. Hospital and Morgue. The LHD has comprehensive Level Three medical facilities, including two operating theatres, intensive care and dependent care wards, laboratory, X-Ray, pharmacy and dental surgery. Routes from the two embarkation triage points facilitate the movement of patients on roller-beds via a dedicated PCRF elevator to prep and surgery. Morgue facilities provide another level of flexibility. Innovative door and passage design features ensure that casualties can be wheeled on litter beds from initial triage locations on the Flight Deck or Dock, via the casualty elevator and stabilization facility to the most advanced operating theaters.

d. Galley. A centralized galley on Deck 2 ensures that catering facilities are efficient in every respect

e. Personnel Services. The functional layout of Deck 2 provides capacity for a raft of personnel services in the one accessible area. Facilities include Canteen, Administration, telephones, bars etc.

f. Access Routes. The LHD facilitates the unobstructed movement of EF personnel in marching order as they pass to and from points of embarkation and disembarkation

H. Embarked Forces C4I operations

Command, Control, Communications, Computer & Intelligence (C4I) amphibious operations rely on the integration of all components to achieve decisive theatre entry. Fighting in the difficult interface between sea, land and air requires an intimate understanding of mutual obligations and the special capabilities and problems of component elements. The LHD communications assets that will support the situational awareness and C4I networking include:

a. HF

b. VHF

c. UHF

d. SATCOM – INMARSAT, MILSATCOM and ASTIS-M

e. Link 11, Link 16 and VMF

f. Air Traffic Control (ATC) Communications for HF, VHF and UHF

g. Internal Ships Communications, both tactical and administrative.

These LHD communications assets provide an extensive and comprehensive capability for communications support to:

a. Strategic communications for Command and Intelligence Systems (CIS)

b. Command, control and coordination of embarked and deployed force elements using HF, VHF, UHF, VMF and MILSATCOM capabilities

c. Tactical Data link exchange with Link 11 and Link 16 for ship to ship and ship to air communications, including information exchange and coordination with allied forces

d. Coordination and control of helicopter and other air assets through HF, UHF, Link 11, Link 16 and ATC capabilities

e. Internal LHD communications in order to facilitate the coordination of all on-ship activities through the use of ships intercom, Tactical Intercom, ships broadcast and alarm, and telephone systems, flight deck communications, Sound Powered Telephone and wireless communications systems.

The above CIS architecture and situational awareness tools will support the following types of amphibious operations in hostile, uncertain and permissive environments:

a. Amphibious assault. This is the principal type of amphibious operation in that it establishes an Embarked Landing Force (ELF) ashore with some permanence on a hostile or potentially hostile shore. The intention will be to land the ELF in an undefended area. An example may include peace enforcement operations launched into an unstable regional country

b. Amphibious raid. A raid differs from an assault in that it is a swift and temporary incursion with limited objective/s. Examples may include Special Forces Special Recovery Operations launched offshore

c. Amphibious demonstration. Often demonstrations are conducted to deceive an adversary with a show of force into taking action unfavorable to his circumstances.

d. Amphibious withdrawal. Withdrawal operations entail the withdrawal of land based or landing forces by sea from hostile or uncertain environments. These operations may also include Non Combatant Evacuation Operations of evacuees and refugees from world trouble spots

e. Military support operations. These operations are not limited to periods of conflict and may be conducted throughout the operational continuum.

Purpose designed functional command facilities and a robust CIS framework of the LHD combine to support these military support and warfighting operations. Located aft and adjoining the Ship's Operations Room are the Supporting Arms Coordination Centre (SACC) and the Joint Operations Room (JOR). Together these facilities provide physical and electronic co-location of the commanders and tactical battle staffs in order to provide the greatest opportunity for unity of effort and timeliness of response.

The SACC is responsible for the coordination of offensive fire support during the landing operation and indeed performs a much wider coordination role due to its need to be intimately aware of activities across the maritime, land and air environments. To effectively manage this responsibility the SACC will also require timely voice and electronic connectivity with the ATC element.

The Level 04 Secondary Joint Operations Room (SJOR) is available to support another level of command. The SJOR may also be made available to a supporting headquarters or perhaps a major maneuver unit during raid operations where only a tactical sub-unit headquarters may be deployed ashore.

Two large planning or multi-functional rooms are available on Level 03 to service the requirements of the various component elements of the amphibious operations. Briefings may be conducted in Joint Briefing Room (Level 02), the JOR or one of the planning rooms as appropriate.

I. Ship Operations

The 231m long LHD has been designed to undertake operations across the entire amphibious spectrum of operations ranging from military support through to war fighting operations. In the most demanding context, the LHD ships will provide a critical enabling facility for a joint force with maritime, land and air elements operating in a complex warfare environment, linked to an operationally displaced national headquarters and possibly operating as part of a combined force. The LHD ship provides a balance mix of the functionality including, but not limited to:

a. Dedicated helicopter lift for vertical envelopment operations and support helicopter operations

b. Surface assault and follow-on surface lift of personnel, stores and equipment, including Logistics Over the Shore (LOTS) if required

c. Operational and tactical levels of command and control

d. Level Three medical support

e. Accommodation, rest and recreational facilities for EF, and ELF post insertion

f. Logistic support operations.

The strategic relevance of the joint force and the limited assets within the LHD ships will also demand that layered area defense and direct support forces will provide LHD protection.

To achieve assigned tasks the LHD will have access to CIS functionality, which is distributed across, and provided by, a range of elements, notably:

a. Combat System (mainly the Combat Management System functions such as Air Traffic Control and coordinated own ship protection)

b. Embarked Direct Support Element in the Electronic Warfare Office

c. Internal and External Communications Systems and Networks including Link 16 and Intelligence terminals, together with suitable control mechanisms

d. Embarked C2 and C4I Amphibious systems and applications (mainly located in the JOR, SACC and other embarked forces command spaces)

e. The Integrated Platform Management System (IPMS)

f. The Personnel and Material Control System (PMCS)

g. The Aircraft Control System (ACS)

h. The Broadcast and Alarm System (BAS)

i. The Entertainment and Training System (ETS).

Furthermore, the LHD has a high level of survivability and is protected from air and surface threats by point defense weapons. In addition to the capable damage control system, it has Nuclear Biological and Chemical (NBC) defense with a citadel that can be segregated into six sub-citadels within which personnel are not at risk of contamination for four days without wearing protective clothing or equipment, including habitability, command and control and hospital spaces.

Overall the design characteristics afford the LHD with exceptional survivability and flexibility for military operations, providing excellent support and protection for both ship's company and embarked forces.

J. Weapon Systems Operations

Sea and air superiority are essential pre-requisites to an amphibious operation. Achieving such a pre-condition however does not guarantee security to the LHD as effective and relatively cheap weapon systems, which are freely available worldwide, are likely to be widely available in the battle space. Such air, surface and sub-surface weapon systems may be delivered or fired by conventional, unconventional or asymmetric means and have the potential to inflict significant damage and casualties with unacceptable political consequences.

The LHD is not a surface combatant and is reliant on other supporting assets to provide its primary defense against conventional air, surface and sub-surface threats. Its weapons system is defensive in nature and can be generally split into the following component elements:

a. Radar

b. Radar ESM

c. Torpedo Defense

d. Mine Obstacle Avoidance Sonar (MOAS)

e. Electro Optic Surveillance (EOS)

f. Weapons

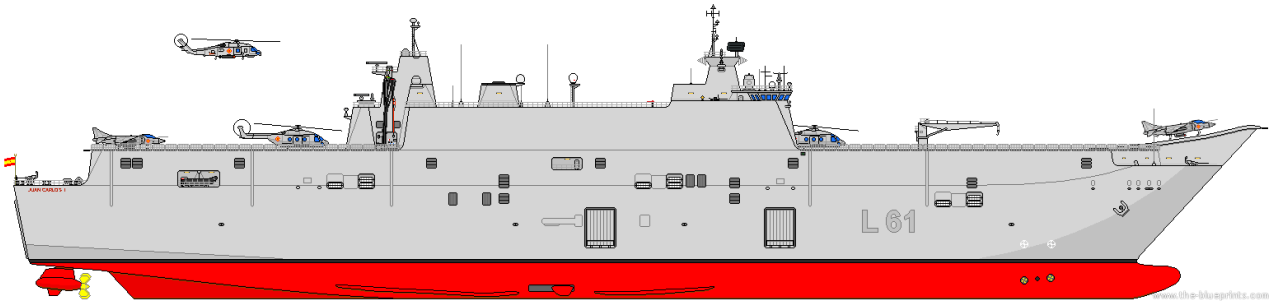
Radars and other sensors permit the LHD to detect and classify air and surface targets at ranges that exceed its organic engagement capabilities. To defeat or avoid a threat it may request engagement by other Navy or coalition assets maneuver to avoid contact, or position herself to ensure the highest probability of a successful engagement.

Weapons aboard the LHD will include 25mm Guns, 12.7mm Guns and Torpedo Defense. They are capable of engaging and defeating unconventional and asymmetric air and surface threats. Passive optical sensors will direct weapons and enhance the LHD's ability to provide a measure of self-defense, whilst eliminating radar emissions.

Some combat system options provide a self-defense hard-kill capability against conventional threats and a torpedo detection capability.

ACKNOWLEDGMENT

Navantia acknowledges the support and direction of the Spanish Navy, Royal Australian Navy, BAE Systems Australia and Lloyds Register, during the design and construction phases of the LHD Ships..



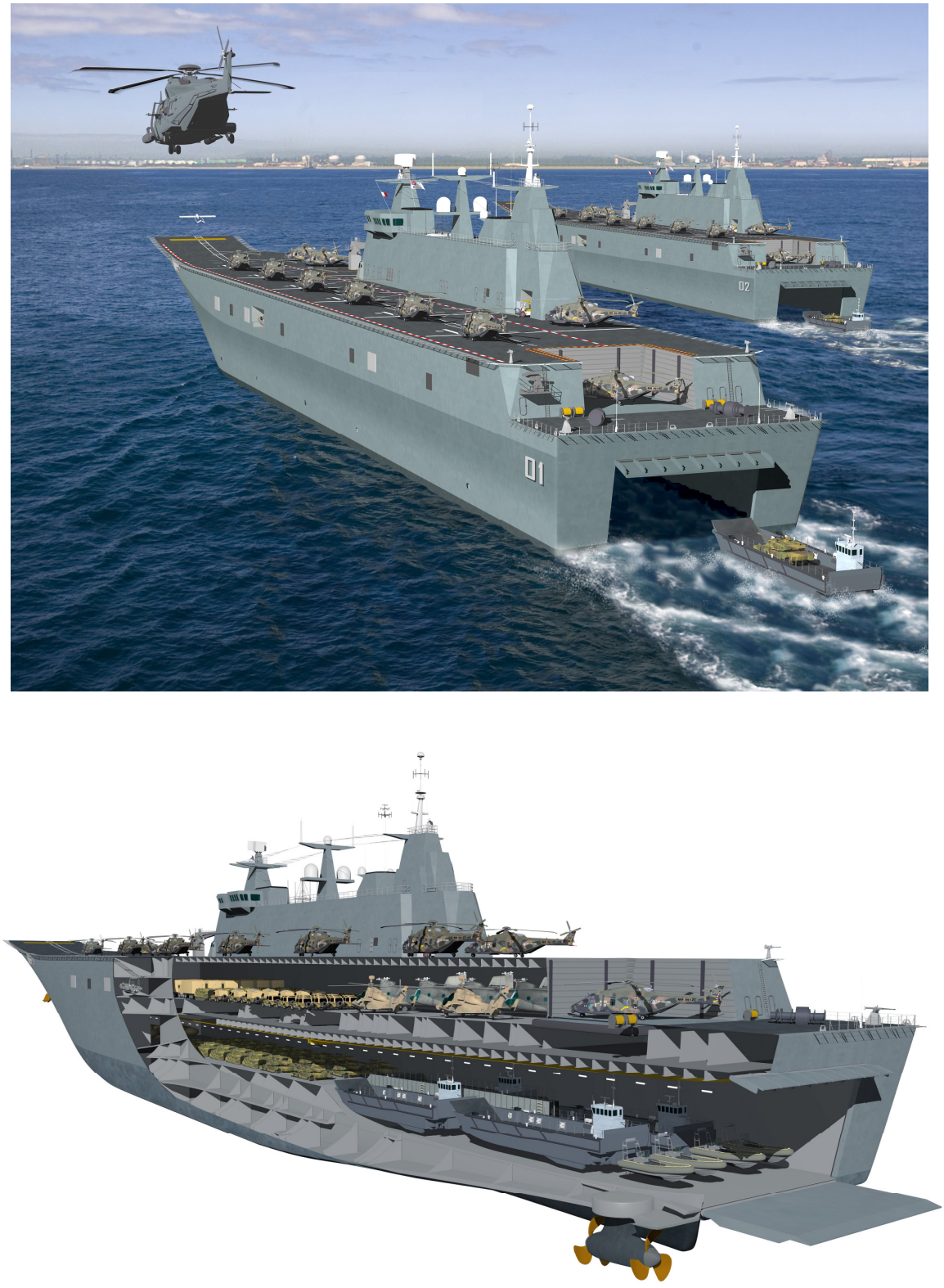
Picture 1.- Profile of the Spanish LHD “Juan Carlos I”



Picture 2.- Spanish LHD “Juan Carlos I”. Picture sailing (top) and taken from a watercraft (bottom)



Picture 3.- LHD Canberra transport between Spain and Australia (top), and sailing in Sidney (bottom)



Picture 4.- Artistic pictures of the Australian LHDs HMAS Canberra and HMAS Adelaide (top), and cutaway (bottom)

Class Approvals

The Role of Classification in Naval Vessel Certification

James A. Stamm
Government Operations Office
American Bureau of Shipping
Alexandria, Virginia, USA
jstamm@eagle.org

Abstract— **Shipbuilders have been making safe, seaworthy vessels for centuries. It was when operation and maintenance of ships surfaced as weak links in the safety chain and were attributed to a lack of crew competency that Classification Societies were established as an industry-grown mechanism to address these safety concerns. As crew competencies improved, and as governments began to assume the role of evaluating crew competency, further improvements to safe shipping required closer scrutiny of the vessels themselves. This led to Class Societies turning their attention to the development of minimum safety standards and independent assessment of vessels against those standards, a central role that has continued to present day and has evolved over time to maintain pace with technological advances and the changing needs of the maritime.**

When the focus of Class Societies turned to ship structures and ship systems, there was expanded outreach to maritime professionals and academia for developing and improving minimum safety standards, known as Rules. This imbedded the use of technical committees comprised of a broad spectrum of experts as central to the Rule development process and grew a deep seeded rooting of marine technology and best practices in the ship design, construction and maintenance standards contained in the Rules. Although originally conceived to address the safety of merchant shipping, the resulting core aspects of ship safety were, and are, not unique to merchant ships. Classification was conceived by industry but has grown to become the nucleus around which Governments and the international maritime community build programs for verifying compliance of vessels and marine structures with minimum safety standards.

Historically, government agencies that own or operate vessels for safety, security or defense purposes (primarily vessels of navies and coast guards) independently developed their own standards for vessel design, construction, operation and maintenance. Certain standards are unique as they apply to specific systems, features, or capabilities unique to the intended purpose of their vessels; however, a significant portion of the standards are based on fundamental principles for engineering design and construction of structures and basic systems common to all vessels. These agencies also developed the internal infrastructure and processes needed for conducting their own verification of compliance with their established standards. While the certification of certain systems or capabilities needs to remain the domain of these agencies, all agencies are continually seeking ways to control costs and find acceptable alternatives to maintaining standards and infrastructure. ABS Classification and certification services to US Government agencies spans more than eight decades, and the past four decades seen steadily growing interest by Navy and Coast Guard Administrations worldwide. Today, many are actively seeking Class as a foundational element in their approach to overall certification of their vessels. The promulgation of ANEP-77 (NATO Naval Ship Code), which relies heavily on Classification Society requirements as a primary means for evidencing compliance, is an example of the degree to which the naval community has come to recognize and utilize the core benefits of Class.

This paper discusses Class Approvals in general for naval vessels and with regard to technological advances and meeting operational needs. In addition to discussing the Rules, the role of research and development, and how the Rules are applied with regard to new technology, the paper also describes the Class process with respect to naval vessel acquisition projects and acceptance of new technologies.

Keywords—class societies; classification; certification; system approvals; equipment approvals; research and development.

I. INTRODUCTION

A. The Origin of Class

The beginnings of Class Societies dates back to the 18th century. Since their inception, their main function has been the safety of shipping. Originally the safety assessment of ships was based on the competency of crews with respect to ship operation and maintenance and later turned to the adequacy of the ship itself and its installed equipment. Ships were "classified" based on relative scales; A, E, I, O, U for ship structures, and G, M, B for machinery and equipment. Classifying ships in this manner benefited owners, insurers and funding institutions as it gave them a degree of assurance with respect to decisions they made on their assets and investments. Once the attention of Class Societies turned to the ships themselves and their installed equipment, Class Societies began the development and publication of minimum standards for materials, arrangements, methods of construction, etc., known as Rules. As the Rules matured and became recognized as minimums for safety, the initial relative rankings gave way to the singular Class notations we have today for the vessel and its equipment and machinery, and the term "classified" gave way to simply referring to vessels as

classed. This move toward the Rules representing a set of minimum requirements for safety, combined with the fact that Rules were developed with industry input and consensus, firmly established two of the core values that Class brings to the maritime industry. It made Class a valid mechanism for industry self-regulation by an independent third party and it solidified the central role of Class with regard to maritime safety in providing an objective, unbiased, level playing field assessment of vessel compliance to an agreed set of minimum standards for design and construction.

B. The The Evolution of Class

Class was created by industry for industry and has evolved over the years to maintain pace with the changing needs of industry, but has also come to be a trusted, recognized asset to many maritime stakeholders. These changes over time are reflected in the scope and detail of the Rules, but also in the range of classification related services provided and the ways in which maritime stakeholders view, value and rely upon Class as an integral component of vessel safety programs and safety regimes. Figure 1 shows the primary stakeholders with respect to commercial vessel safety regimes. All have analogous counterparts with respect to naval vessel safety regimes, most of them by way of the functional authorities and responsibilities of internal offices and departments that exist within a given Navy or Coast Guard organization.



Fig. 1. Commercial Vessel Safety Regime Stakeholders

The first Rules published primarily addressed physical aspects of vessels with respect to basic engineering design and construction, and they still do today and for the same purpose –safety, but the issues that affect maritime safety have come to include much more than the physical aspects of vessels. In addition to new requirements to address advances in engineering and technology, new requirements emerged to address environmental protection, quality management systems, human factors, and now are moving into aspects of efficiency and performance of systems (primarily for achieving new goals regarding environmental protection). As each of these received maritime focus and attention, national and international regulatory bodies and standards organizations revised codes and standards to encompass and address them. Likewise, the products and services of Class Societies expanded and matured to provide continuing support of maritime safety initiatives and programs.

Class Societies began as nationally based organizations primarily serving national clients. Although still nationally based, most today have an international footprint and client base. There are over 50 organizations worldwide that offer some type of classification service; 12 formal societies comprise the members of the International Association of Classification Societies (IACS). These 12 member societies of IACS Class over 90% of the world's commercial vessels and offshore structures and, through IACS participation at the International Maritime Organization (IMO), contribute to the development and implementation of international safety codes, conventions and treaties that signatory Flag States then enforce. Individually, numerous Flag States have delegated certain enforcement functions and activities to Class Societies to perform on their behalf. As an example, ABS was authorized its first delegation in the early 1900s and currently has 177 individual Flag State delegations covering various statutory approvals and certifications. These evidence the trust the world's safety organizations have placed in Class Societies and their confidence in the Class process.

C. The ABS Classification Process

The Classification of vessels has always been the core function of Class Societies, but the role of Class has evolved. The primary activities of ABS include: classification, statutory certifications, Rule development, third party certifications (to standards other than the Rules), and research and development. In addition, and in support of these, ABS also has broad participation on professional and technical societies and standards organizations worldwide. Though the role of Class has evolved and led to activities beyond mere Classification of vessels, the basic Classification process has remained the same.

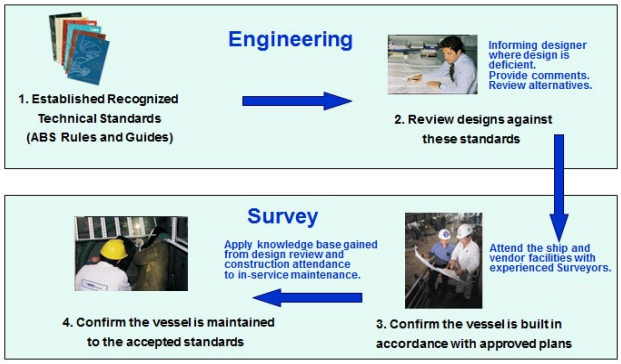


Fig. 2. The ABS Classification Process

The basic process is simple and straightforward as shown in Figure 2. It begins with the selection (or development if necessary) of Rules applicable for a given vessel type and service, then verification that the vessel design meets the Rules, followed by verification that all end products (vessel, materials, equipment, systems) meet the Rules; and for vessels that remain in Class beyond delivery, periodic surveys to verify the vessel is being maintained in compliance with the Rules.

All Class Societies assign Class notations that identify the requirements that a vessel has been shown to meet, and typically are a combination of basic notations (minimums for Class) and optional notations (requested additional notations with regard to special features, systems, or capabilities). For example, the basic Class notations assigned by ABS are A1 (for structures), Circle E (for anchor chain and equipment), and AMS (for machinery). The A1 and AMS notations are prefaced with a Maltese Cross symbol for vessels attended by ABS during construction; for vessels not attended during construction (such as existing vessels that enter Class for the first time or vessels that transfer Class to ABS), the Maltese Cross symbol is omitted. With regard to optional notations, ABS offers many (over 200), but the most commonly requested ones for naval vessels are: NIBS (for integrated navigation bridge), ACC or ACCU (for degrees of vessel automation that allow for reduced manning), R2-N (for propulsion system redundancy), DLA (Dynamic Loading Approach for assessing hull structures for dynamic loads), SFA (Spectral Fatigue Analysis for assessing hull fatigue life), and OE (Operational Envelope for safe operation of high speed craft in various sea states).

There is no singular “Class Approval”, per se, with regard to ABS Classification. ABS “approvals” are implicit throughout the Classification process by way of drawings for structures, machinery, electrical and piping systems that are reviewed and stamped ‘Approved’ or ‘Reviewed’ and by way of individual survey reports issued upon satisfactory completion of survey and test of materials or equipment. The Classification process does, however, include the issuance of a singular Class Certificate which signifies that ABS found the vessel and its machinery and equipment to be in compliance with the Rules and acceptable for enrollment in Class. At delivery of the vessel from the shipyard to the owner (or, in the case of naval vessels, typically after successful sea trials), ABS issues an Interim Class Certificate, and subsequently the full term Class Certificate is issued subject to satisfactory review of vessel engineering review and survey records by the ABS Classification Committee.

II. RULE DEVELOPMENT AND MAINTENANCE

A. ABS Rules and Guides

The Rules contain the minimum requirements for obtaining the basic Class notations and symbols; requirements for obtaining optional notations are also contained in the Rules or, in some cases, in separately published Guides. Changes to Rules and Guides occur due to improvements in materials, processes, quality, technology, and to industry standards that are incorporated by reference. As the types of vessels and installed systems changed over time, from wooden vessels propelled by sail to welded steel vessels fitted with nuclear propulsion, Rules have been developed and updated to maintain their applicability and relevancy to engineering and technology norms and trends. Rules are initially established based on known or perceived risks at the time they are written and evolve over time as risks change due to advances in engineering or technology. For example, safety factors can reduce or allowable stress values for materials can increase as improved material or process technologies reduce uncertainties and improve quality control.

One of the main values Naval Administrations see in the Class process is the Rules themselves, and primarily with regard to the process followed in their development and maintenance. Three specific advantages seen are: (1) the Rules are developed and updated via input and consensus of a broad cross cut of industry experts and academia, (2) the Rules are revisited annually for update and thus see technology refresh that can keep pace with industry trends, and (3) a large input to updates comes from experience and lessons learned from application of the Rules on projects as well as feedback from operations, which provides timely, continuous improvement to the requirements and the processes governing their application.

Depending upon the type and service or primary mission of naval vessels, Naval Administrations have utilized different Rule sets. For naval auxiliary and support vessels and most Coast Guard vessels, there is little if any armament and minimal application of military standards, thus the redominant hull forms and systems are such that either *ABS Steel Vessel Rules* or *ABS High Speed Craft Rules* have been found uitable and adequate. To address the needs of high speed craft whose missions are more military, ABS developed the *ABS High Speed Naval Craft Guide* in cooperation with the US Navy and industry and has been classing vessels to that Guide for over a decade. In 2004, recognizing a similar need for larger vessels, ABS worked with US Navy and US Coast Guard technical authorities and developed the *ABS Naval Vessel Rules*. That Rule set contains requirements peculiar to large combatant vessels, but is available for application to US Navy and US Coast Guard vessels only. To address the broader need for such a Rule set, ABS has since developed the *ABS International Naval Ship Guide* which is presently being finalized and will be available for application to Navy and Coast Guard vessels worldwide, and to other types of government owned vessels in non-commercial service.

B. ABS Rules Committees

As an international technical organization, it is essential that ABS be current with maritime-related developments worldwide. ABS accomplishes this through a general committee structure organized by country, region or special interest. Comprising individuals eminent in marine, offshore and related industries, these committees serve as forums for ABS management and members worldwide. They also provide an opportunity for ABS members and other prominent executives around the world to participate in the discussion and development of broad strategic policies related to marine safety.

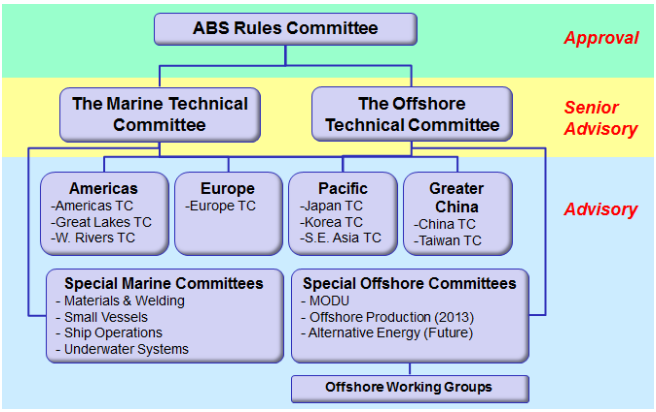


Fig. 3. ABS Rule Development Committees

ABS Rules are derived from the principles of naval architecture, marine engineering and other kindred disciplines. ABS develops and updates its Rules through the use of divisional, special, technical and Rules committees. These committees permit ABS to maintain close contact with the numerous technological and scientific disciplines associated with the design, construction and maintenance of ships and other maritime structures around the world. Each committee is comprised of individuals eminent in their field of endeavor. They are underwriters, ship owners, shipbuilders, materials manufacturers, machinery manufacturers, naval architects, marine engineers, government representatives and others who all serve without compensation. As a result of this arrangement, the Rules developed by this broad-based group from the marine, offshore and related industries are authoritative, impartial and current. A proposed change to the Rules originates with a committee or ABS staff. Once a proposal is made, a formal draft is prepared by ABS staff and then submitted for review to the appropriate special or divisional technical committee. When it is accepted by this committee, the proposal is presented to the Marine or Offshore Technical Committee for review and recommendation. The proposal then goes to the ABS Rules Committee consisting of officers and employees who have the final approval authority for all new or modified Rules.

C. Technology Insertion

New technology insertion into the Rules can result from: new safety focuses of international regulatory bodies (such as IMO) or national regulatory bodies (such as Flag States, Port States, or other national authorities having jurisdiction over geographic regions with regard to transportation safety or environmental protection), new or revised criteria being considered by national or international standards organizations, new technology that surfaces on new construction or major modification projects, research and development conducted by ABS, and ABS participation on joint industry projects and standards development organizations.

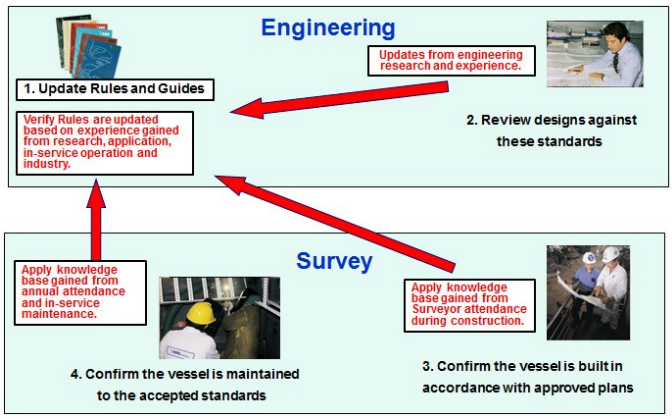


Fig. 4. Inputs to Rules Updates

Historically, new initiatives or safety focus areas of national or international regulatory bodies are slow to develop which affords ample time for identifying the need for supporting research or technology. Examples would be double hulls for tank ships, arrangements and equipment for oil pollution abatement, ballast water management systems and equipment, and engine modifications for increased efficiency and performance to meet new air pollution standards. Each of these called for research and development to prove out new technologies, and the Rule development process enabled resultant new requirements to be vetted by industry experts to identify those deemed appropriate to be incorporated directly into the Rules.

New systems or new approaches to meet the Rules sometimes arise on projects, especially projects involving technically sophisticated designs for high value assets. The

Rules account for this is two ways. For truly novel systems or equipment not covered by the Rules, the Rules refer to the *ABS Guide for Novel Concepts* which lays out formal analysis methods for addressing them. For new and different but less novel systems or equipment, throughout the Rules there are statements regarding acceptance of alternative or equivalent standards, arrangements or details. In both cases, ABS works with the designer, builder or manufacturer to identify appropriate criteria against which the design and the final products should be assessed with respect to ABS Classification. As a separate effort, the resulting criteria typically will be revisited by ABS to make it generic (i.e., remove project-specific requirements) and therefore suitable for potential incorporation into existing ABS Rules and Guides.

When new technology surfaces on projects or new safety goals or focus areas emerge, ABS initiates internal research and development projects when necessary prior to proposing new requirements or updates to the Rules. The list of ABS projects is prioritized and scheduled to synchronize results with associated Rules update schedules and for coordination with outside organizations which may have complementary efforts planned or underway. In 2013 ABS had nearly 190 individual projects; for 2014 there are 217 projects planned covering a wide range of research categories including: offshore structures, hydrodynamics, marine structures, LNG/FLNG/Gas, harsh environment studies, propulsion machinery, software, subsea pipe lines and equipment, human factors, materials and coatings, energy and efficiency, controls and automation, environment, station keeping, stability, renewable energy, oil and gas production, and regulatory initiatives.

Similar but separate research and development efforts are conducted through joint industry projects in which ABS participates and in some cases leads. Project types are similar to and often complementary to projects that are planned or underway within ABS, and also include research areas unrelated to Rule development that are of special interest to industry or to regulatory bodies or otherwise generally contribute to maritime safety.

In addition to and in support of all the above, ABS participates on over 135 professional societies, technical societies, and industry standards organizations and associations worldwide. This allows ABS to maintain awareness and involvement in maritime related fields, but also to directly monitor and actively contribute to the development and maintenance of standards that have been incorporated by reference into the Rules.

III. CLASSIFICATION AND CERTIFICATION SERVICES

A. Commercial and Naval vessel experience - similarities

Commercial vessels range from simple river barges to sophisticated, complex, high technology, high risk assets for the oil and gas industry and other specialty services. For all these, but especially the high end assets, over the years there has been steady growth in international recognition of the value of classification and in the number of Flag State delegations. The use of Class in commercial vessel safety programs is formalized internationally via Conventions and Codes; nationally its use in Flag State safety programs is typically formalized via organizational agreements in place between Flag Administrations and Class Societies. The consistency and simplicity of the Class process, coupled with the ease of insertion of new technology and timely update of Rules and Guides, has long afforded the commercial vessel industry an efficient mechanism for certification of structures and systems to life cycle focused sets of requirements applied in a systems approach to safety. These same benefits are afforded the naval vessel community.

While the requirements and type of systems are different for naval vessels, the core Classification and certification services provided for commercial vessels and the processes by which they are executed offer a reliable, time-tested, efficient, cost-effective approach for the certification of hull, mechanical and electrical (HM&E) systems on naval vessels. With regard to vessel classification, core ABS services include:

Review in Principle: design review of preliminary or contract designs; reviews are done to the level of maturity of the design; this review is not required for Class, but carried out upon request of the client; the scope of the review and approval is agreed between ABS and the client; clients who request this typically do so for early technical risk mitigation.

Detailed Design Review: review of system drawings and supporting data/calculations as required by the Rules to obtain basic and optional notations, but also includes review of other required submittals such as welding procedures, fabrication processes, operating manuals, and similar documents.

Material certifications: surveys at the place of manufacture for materials (plates, shapes, piping, castings), anchor chain, welding electrodes, etc.

Equipment certifications: engineering review and survey of major items of machinery and equipment such as engines, turbines, generators, gears, shafts, propellers, pumps, motors, switchboards, boilers, pressure vessels, anchors, steering gear, rudders, etc.; many items may qualify for ABS Type Approval

which offers manufacturers an optional, more cost effective alternative.

Statutory certifications: certifications to codes and conventions for which compliance is required by a given Flag State authority; these are not required for Class, but are provided by ABS if specifically requested by the owner or shipyard; in most cases Flag Administrations have programs in place with respect to delegation of these certifications to ABS to perform on their behalf.

Survey during construction/test/sea trials: survey of the vessel during construction; ABS Surveyors coordinate with the builder on construction hold points and on Surveyor attendance to conduct inspections or witness scheduled test and trial events; otherwise Surveyors conduct random patrols of work underway; upon satisfactory completion of all required surveys/tests/trials an Interim Classification Certificate is issued and followed later by a Full Term Classification Certificate upon satisfactory review of vessel records by the ABS Classification Committee.

Surveys after construction (required for retaining a vessel in Class): through-life surveys of the vessel by ABS to verify continued compliance with the Rules; surveys include: annual surveys (once a year), intermediate survey (once every five years), special survey (once every five years), and drydock survey or underwater examination in lieu of drydock (twice in every five years). In addition to required periodic surveys after construction, surveys and supporting engineering reviews as may be necessary are also required for casualty assessment, damage repairs, and vessel modifications or alterations.

Miscellaneous certifications requested by the owner or builder: third party certification of items not required by the Rules; the owner or builder provides the applicable standard or set of requirements.

Statement of Fact reviews and/or surveys requested by the owner or builder: review and/or survey for verifying compliance with additional requirements (most often requirements in the ship or product specifications that are above and beyond what is required by the Rules) that ABS is asked to also verify concurrent with ABS review or survey of items as required by the Rules.

Austere budgets are forcing most Naval Administrations to make existing fleet resources last longer. For existing naval vessels that are not enrolled in Class, of high interest and value to Naval Administrations has been the application of ABS survey processes long used on commercial tank ships and bulk carriers with regard to condition assessments of in-service vessels. The condition assessments of naval vessels included visual inspections of tanks and structure and comprehensive thickness measurements, followed by development of structural models and advanced engineering analysis of the models in both original and corroded conditions. The resulting strength and fatigue life assessments yielded estimated range of remaining service life and provided essential technical input to fix-or-replace decisions and to the maintenance prioritization and planning decisions of naval fleet maintenance organizations.

B. Commercial and Naval vessel experience - differences

ABS has been providing Classification and certification services to the US Navy since 1918 and has classed over 4,000 US Navy vessels. This has included numerous vessel types and mostly vessels for which commercial Rule sets applied, but all involving some degree of application of military specifications and standards and the attendant need for tailoring of criteria for intended use. Other than applicability of international conventions and codes, the Classification of naval auxiliary vessels mimics that for commercial vessels. The sophistication and complexity of naval combatants make them analogous in many ways to high end commercial assets; however, the use and application of products and services offered by ABS varies. While Naval Administrations have long used ABS services for augmentation and support of naval programs, the sustained use of Classification in naval combatant programs has taken time to root; but slowly and steadily has been on the rise. The slow pace was mainly due to Naval Administrations being relatively new to the full use of Class and their need to take measured steps in gaining experience on how best to integrate Class and other related services into their existing programs, processes and procedures for acquisition, verification, certification and through life maintenance of combatant fleets. The past decade has seen a marked increase in the application of Classification in acquisition projects for navy and coast guard patrol boats and for high end combatant. More and more, Naval Administrations are including Classification and other Class services in their certification policies and their fleet acquisition and maintenance strategies. Most naval vessels were primarily built for defense, but mission areas have changed and expanded greatly over time to include pollution response, border patrol, drug interdiction, search and rescue, disaster relief, humanitarian relief, piracy, and general security and support to regions of potential unrest. As mission areas grew, so too did the type and number of unique systems to meet the need for new capabilities. Naval vessels today are still largely designed and built to detailed designs and/or ship specifications prepared by the Naval Administration to achieve these capabilities, as well as all other “-ilities” that must be considered for modern warships (mobility, survivability, operability, reliability, maintainability, affordability, producibility, commonality, interoperability, etc.). Collectively, these contribute to a significant difference between commercial and naval vessels (especially combatants); the scope, detail and number of requirements,

specifications and standards for systems and features unique to naval vessels. Along with the increased number of special systems and associated requirements and standards comes the number of separate authorities and agencies having jurisdiction over certification of the vessel with respect to systems and capabilities. In addition, the Naval Administration itself functions as both the owner and the technical authority and is much more intimately involved throughout a vessel acquisition process than the commercial counterparts for these roles. Most of the certification authorities address mission systems and features that are not addressed by the Rules; however, the role and relationship of these other certifications with respect to Class does present a much larger Venn diagram than seen on commercial vessels. Early communication and coordination is important as the dividing line between HM&E systems and mission systems is not always obvious, but also because some systems or equipment may serve multiple purposes and thus be of shared interest to multiple authorities which has the potential to lead to conflicting requirements.

ABS Rules contain provisions for accepting alternatives and this provides for many of the special considerations needed due to the uniqueness of naval vessels with respect to their missions and operational needs. Naval vessel projects draw upon this provision in the Rules to a greater degree than commercial vessel projects, but the Rules (especially those written specifically for application to military vessels) also recognize the role of the Naval Administration as the technical authority. The Rules, and how ABS applies them, allow for tailoring of criteria and for special decisions where needed to meet operational needs, while still fulfilling the safety mission of class. Examples would be the acceptance of overrides for certain shutdowns, modifications to Voyage Data Recorders, and alternative machinery arrangements and configurations to meet Naval Administration reliability and survivability requirements.

The above are examples that address differences in vessel systems and requirements, but one of the obvious and perhaps more impactful differences on naval projects has to do with the acquisition process itself; i.e., the duration of the acquisition phases. Naval projects have far more extensive periods for preliminary design, contract design, detailed design, construction and test. In and of itself this is not a problem, but it does open the door to a cascading cause-and-effect list of other differences. The increased time allows for greater amount (or at least likelihood) of change to many things such as requirements, specifications, schedules, funding cycles, and in some cases even fundamental features of the design. The increased time and the potential for attendant changes lead to increased emphasis and importance for more robust documentation, metrics, process definition, decision-tracking and similar project management and technical management needs. Continuity and consistency over time and having a simple and clear audit trail are essential in order to efficiently deal with systemic issues on long duration projects such as technical uncertainties which linger pending results of certain analyses or validation tests, technical issues that resurface as the design matures, changes to project personnel or to organizational elements, etc.

With regard to ABS Classification, of all the differences mentioned above, of greatest significance is the potential for change to the requirements or the design and the potential impact on compliance with the Rules. Changes that may lead to non-compliance with the Rules can cause unnecessary process churn and rework. To address this concern, many have included ABS in the early steps of their change control process.

IV. THE ABS CLASSIFICATION PROCESS WITH RESPECT TO NAVAL VESSEL ACQUISITION PROJECTS

The Class process on naval vessel acquisition projects follows the same process as on commercial projects, but Class involvement is typically deeper and starts much sooner in the project. Figure 5 shows a generic naval vessel acquisition timeline and where and when Class activities typically occur.

In most cases on commercial projects, ABS activity only starts with the Request For Class (RFC), which is the official Class contract between ABS and the client (typically the builder) and marks the beginning of required ABS activities for obtaining Classification.

The activities preceding the RFC (activities shown with dashed lines) are not activities ABS must perform as part of the Classification process for either commercial or naval projects; they are done in response to a client's request. On commercial projects the activities prior to the RFC (other than the Review in Principle) occur over a very brief time period (weeks) and typically done by the owner or builder with very little assistance needed from ABS. This is mainly due to the familiarity that most commercial clients have with the Rules and the Classification process.

From the RFC on down (activities shown with solid lines), all activities occur on both commercial and naval projects as these are the formal steps of the Class process. Experience on naval projects has been that naval clients often request ABS assistance in the pre-RFC activities, including an ABS Review in Principle, for the benefits these bring with regard to advanced planning of acquisition events and for reasons of early contract, schedule, and technical risk mitigation.

Not shown in the figure as an ABS activity is project management as it is a fundamental activity on all projects and

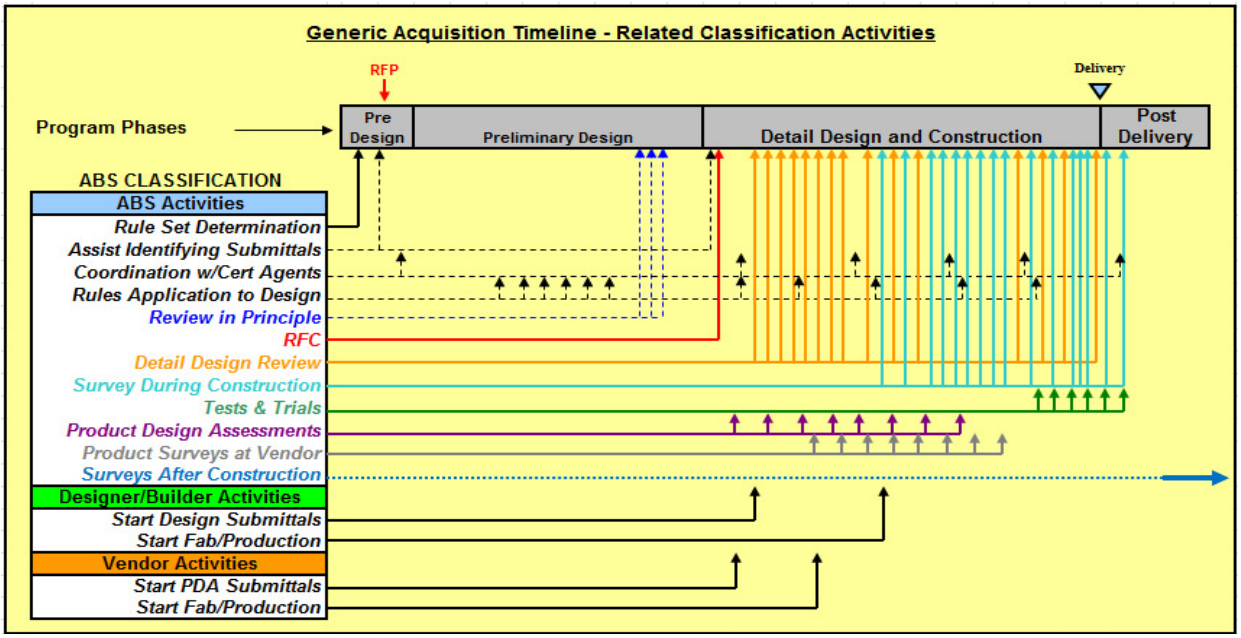


Fig 5. ABS Classification Activities on Naval Acquisition Projects

not unique to Classification, but is essential on naval projects and typically requires a much greater level of effort than required for most commercial projects. The following provides a brief description of those ABS activities that are depicted in the figure.

Rule Set Determination – early discussions between ABS and Naval Administration to identify appropriate Rule set and notations, sets stage for proper wording in RFPs and contracts.

Identification of Submittals – ABS works with Naval Administration and/or designer or builder to identify the submittals (drawings and supporting technical data) to be provided for ABS review.

Coordination with Certification Authorities/Agents – ABS works with Naval Administration to identify role, relationship and interaction regarding ABS and other Certification Authorities, including scheduling of activities that both need to attend (inspections, tests, etc.); for complex naval vessel projects ABS has always advocated developing a project specific Certification Plan and/or Matrix to map out certifications, standards, and certifying agents (ANEP-77 calls for similar in what it refers to as a "Standards Plan").

Rules Application to Design – occurs throughout project but started early to identify applicable portions of the selected Rule set and early look at system boundaries and interfaces (both functional and physical) with regard to HM&E versus mission systems, especially where systems may be dual use. Related to this, having ABS review the vessel detailed specifications is not required but is often requested for early detection of potential conflicts with the Rules. Alternatives are always considered but must be technically justified.

Review in Principle – not required for Class but often requested on larger, more complex projects as an early risk mitigation step during preliminary or contract design stage; major advantage is it is completely scalable (up to submitter what drawings and data to be reviewed); also often done separately from any given project, such as request from a designer or shipbuilder for ABS review of a concept or preliminary design.

RFC – Request For Class agreement - the formal Class contract (usually between ABS and the builder) containing basic terms and conditions for ABS Class, vessel particulars (length, breadth, draft, displacement, major items of equipment, and similar details needed for proper application of the Rules), the Rule set to apply along with Class notations and optional notations that are requested, and identification of statutory certifications ABS is requested to provide, as well as Fig 5. ABS Classification Activities on Naval Acquisition Projects miscellaneous third party certifications and Statement of Fact reviews and surveys.

Detailed Design Review – formal ABS engineering review and analysis of vessel, system and equipment detail drawings and associated supporting calculations and data; specific submittals are identified throughout the Rules and Guides for obtaining the basic and optional notations requested; submittals are appropriately stamped and returned to the submitter under cover of an ABS review response letter along with technical and survey comments as necessary.

Survey During Construction – ABS Surveyors attend the vessel during construction; initial discussions with shipyard representatives review the normal routines for scheduling callouts and tests, for routine meetings to address status, and for methods of communicating non-compliances that are found; separate from callouts, Surveyors conduct patrols to survey welding, fabrication, assembly and installation work in progress as required by the Rules and to the extent deemed necessary by the Surveyor; activities typically culminate with Surveyor attendance on sea trials.

Tests & Trials – the builder is responsible for scheduling and conducting tests and trials and including the attending ABS Surveyor for those that must be witnessed by ABS per the Rules; in general, no system is considered "approved" by ABS until all technical and survey comments have been addressed (closed) and all required testing has been satisfactorily performed and witnessed by an ABS Surveyor.

Product Design Assessments – engineering review of vendor equipment drawings and associated calculations and data for all items of equipment that are required by the Rules to be certified by ABS (certain items may be certified by the manufacturer, where this is the case it is specified as such in the Rules); this activity also includes items of equipment for which manufacturers may have requested ABS Type Approval.

Product Surveys at Vendor – survey of items of equipment that are required by the Rules to be certified by ABS (certain items may be certified by the manufacturer, where this is the case it is specified as such in the Rules); this activity also includes items of equipment for which manufacturers may have requested ABS Type Approval. Surveys After Construction – for vessels in service that are to remain in Class there are periodic surveys required in order for the Class Certificate to remain in effect; Class Certificates are valid for five years; periodic surveys include: annual surveys, intermediate survey, special survey, and drydocking or underwater inspection in lieu of drydocking; in addition, surveys are required in cases of casualty damage, or modifications/alterations to the vessel.

V. CONCLUSION

Classification has long been recognized for its contributions to commercial vessel safety, nationally and internationally. Classification has come to be at the core of all safety regimes and programs as a time-tested, efficient, and cost effective process upon which to build overall strategies for incorporating safety and best marine practices into the design, construction, operation, and maintenance of vessels and marine structures. The Rules are constantly evolving and improving to maintain pace with advances in engineering and technology. In addition, inherent to their application is the flexibility to address new technology and operational considerations unique to vessel types and services. ABS services offered in addition to Classification extend these same benefits to meet the unique needs of existing naval vessels for support to in-service fleets with respect to vessel maintenance, repair, casualty response, and service life extension decisions. A key enabler for the validity and continued relevancy of ABS products and services is ABS initiation of and/or participation in research and development projects. Such efforts keep the Rules current regarding industry capabilities and future trends and support the evolution of ABS services to meet the ever changing needs of both commercial and naval maritime interests.

PROPULSION SYSTEM INTEGRATION - A CRITICAL GAP IN INDIGENOUS WARSHIP BUILDING

Capt (IN) Sameer Agarwal[1], **Lt Cdr V Kumaran**[2]
[1,2]PSI Centre, NSTL (V) PSI Centre, NSTL (V) Visakhapatnam 27
[1]encpsicnstl-navy@nic.in

***Abstract*—The Indian Navy has transformed itself from a Buyers Navy of yesteryears to a modern Blue water Navy fully capable to design, build and maintain own warships. However, certain deficient areas do exist in the shipbuilding process where the indigenous technical capability and capacity has not yet matured to an extent to support the endeavors locally. Propulsion System Integration is the bedrock of shipbuilding process and involves a broad spectrum of activities right from design board to delivery. These critical activities comprise of selection and integration of propulsion elements such as prime mover, gearbox, transmission system and propeller along with the associated system necessary to provide designed propulsion. The importance of PSI can be gauged from the fact that the overall propulsive efficiency of the ship in terms of optimum performance at all regimes of engine operation critically depends upon accuracy and depth of PSI studies undertaken at the design stage. This paper aims to bring out critical capability gaps in this area and suggests various ways to bridge them. It is concluded from the paper that concerted efforts towards PSI self-reliance within the country can prove to be a game-changer for warship construction in the country.**

***Index Terms*—Propulsion System Integration.**

I. Introduction

India's foray into shipbuilding dates back to ancient times. More recently, during the colonial rule also, there was a great demand for ships made in India, specially the Bombay Dock, as they were made of fine wood and were sturdy to withstand any onslaught of war or weather. But that was in the era of wood. In the latter half of the 19th century, the European prowess in shipbuilding showed tremendous pace, post Industrial revolution and Indian indigenous shipbuilding expertise was lost in some manner. Till independence, the country was in a state of transition and there was hardly any shipbuilding activity, of importance, taking place in the country. During this era, most home grown industry had been either shut down or had been merged with much larger British firms. The Royal Indian Navy too, was operating warships constructed in Britain, which became the main source of warships for India even post independence.

The Indian Navy was born with just a few ships handed over by the then colonial masters at the time of granting Independence. However, gradual expansions through the 50s and 60s saw a steady induction of warships and submarines bought from other countries. In about half a century post independence, the Indian Navy has had a laudable transition from being a minor littoral force to the fifth largest Naval power in the world today. Today, it has transformed itself into a "Builders Navy", thanks to a steadfast indigenisation program started in the late 70s, and is now considered a modern and professional Blue Water Force to reckon with.

Despite a slow start, the Indian Shipbuilding industry has indeed come of age and has produced world class ships for the Indian Navy. A big percentage of our frontline warships today are of Indian origin and this trend is here to stay. As per the Indian Navy's Maritime Capability Perspective Plan (2005-27), it is envisaged that about 45-50 major warships of various kinds will be inducted in the next 15 years. When added with about 150 ships for Coast Guard contracted so far and likely to be increased substantially in the next financial year, the total figure comes to around 300-350 ships required in the next 12-15 years. As a result, despite a gloomy scenario in the world of shipbuilding today, there lies a healthy opportunity for warship building within India.

However, although great strides have been made by the indigenous warship building industry, discernable inadequacies still persist in certain critical technological frontiers. These deficiencies are resulting in continued dependence on foreign sources for required technology as well as expertise. Although, the Indian Navy, in collaboration with the research laboratories, is undertaking R and D activities in some of these critical areas, these efforts need to be better supported by the industry and synergized with other stakeholders.

II. Indigenous Warship Construction

Warships are significantly more complex than even the largest, most modern commercial ships due to the complicated design and construction process. The critical requirements of Speed, Weapons and Sensors, Signature Management, Survivability and Multi role operations are some critical features that put a warship on a different level when compared to any commercial ship. These critical requirements lead to significant changes in the design and construction process which are iterative in nature and may take more than a decade from drawing board to delivery.

Design of a warship is a complex task which starts with an assessment of requirement in accordance with the envisaged role and threat perception. The roles envisaged for a warship can cover an entire gamut of operations, right from peaceful

search and rescue, support action in littoral waters and full combat missions in blue waters. Further, a warship has to cater for robustness of design and obsolescence of critical equipment to ensure optimal performance in the intended role through the designed life which may extend to more than 40 years. The construction process also is unique in terms of basic parameters and configuration. While the external features of a warship are determined by its hull profile, weapons package and deck machinery, the internal features are determined by its operational space, machinery and propulsion systems. In short, to carry out its function, a warship has to be well designed and equipped with all capabilities.

It is to the credit of the Indian Navy that as part of the indegenisation, more than 80 warships comprising of 17 different classes have been designed in-house. The path of indigenization in terms of design and construction of warships, that the Indian Navy has traversed, has yielded excellent results in terms of development of required expertise, creation of specific skill sets, and mastering of modern shipbuilding technology. However, though an in-house capability exists for most of shipbuilding processes, capability related to production and integration of critical equipment such as Weapons, Sensors and Propulsion System is yet be fully realized more so because of lack of indigenous expertise and Industry support. While the Weapons and Sensors belong to a fully defence related industry and therefore has limited appeal in the outside world, the propulsion equipment and its integration with other systems is of equal use to defence as to the other sectors such as Shipping, Aviation and Power Generation etc..

III. Propulsion System Integration Capability Gap

Propulsion System Design and integration is a process that combines prime movers, transmission elements and propulsors in an optimum manner to achieve required propulsive performance of the ship in all regimes of operation. The Propulsion System is the backbone of a warship and its design, selection and integration forms an integral part of the ship design and construction process. Unlike other system and equipment, which may undergo a change with better equipment during ships life, the propulsion system is designed for the life of the ship and is seldom changed and even so, minimally. It is necessary to incorporate the configurations of the propulsion system at the initial stages of ship design itself. The importance of Propulsion System Integration (PSI) can be gauged from the fact that the overall propulsive efficiency of the ship in terms of optimum performance at all regimes of engine operation critically depends upon accuracy and depth of PSI studies undertaken at the design stage. Being a significant facet of the ship building process, the PSI expertise in terms of critical knowhow, technology tools such as specialized software, reference data and experience available within the country is extremely limited. Due to the paucity of necessary PSI infrastructure and dearth of technical expertise available within the country, initiating appropriate steps to bridge this critical capability gap remains a closely targeted area for the IN.

The process of selection of individual components of a propulsion system and their integration for achieving overall efficiency can be done in a variety of ways to obtain a number of possible solutions for a given requirement. None of the solutions can be termed as most perfect as there can be more than one solution to each scenario. Factors such as Size and Weight, Cost, Availability, Reliability, Maintainability (ARM), Speed and Power requirement and complexity etc have a large bearing on the solution chosen for a particular warship. All the solutions, carefullt calculated based on critical parameters, are evaluated over the above factors before a decision to select a single solution gets taken.

Propulsion System Integration has a wide scope of activities right from design board to delivery of the warship. It is a process which has interfaces with all other system installed onboard and is therefore critical for achieving the intended role of the ship. The complete scope of Propulsion system integration includes the following:-

1. Resistance Calculations and Powering Estimation
2. Design and Selection of Propulsion equipment
3. Design of propulsion train including:-
   - Propeller design
   - Engine propeller matching
   - Shaft design and analysis
   - Gear Box design
4. System design based on:-
   - Torsional and bending moments
   - System Dynamics
   - Signature Management
5. Selection of propulsion plant control system
6. Intake / Exhaust design
7. Endurance and fuel consumption calculations
8. Stability Analysis as a result of Propulsion Equipment installation
9. Integration of Propulsion and Auxiliary systems
10. Interfacing of systems and components
11. Performance curves and design of IPMS

The above is an indicative list of activities only. Nevertheless, it can be seen that the PSI covers a wide canvas of critical activities in the design of a ship, right from Concept design to Functional Design and then on to Detailed Design encompassing complete design and construction phases of the ship till induction. It is not difficult to gauge that all these activities require extensive scientific calculations and data analysis backed up by specialized software. Accurate in-depth studies are required for selection and integration of the prime mover, Gearbox and shafting arrangement for evolving an effective propulsion system to match the ships hull and tonnage.

The Propulsion System Integration can be applied equally to all ships, however, due to large number of commercial ships built to the same design, its importance is never felt in the merchant marine world. On the other hand, a warship, not only more complex due to varied requirements, is also constructed in lesser numbers before the design gets changed, necessitated due to role change. For example, the IN typically, has been ordering construction of three warships of a given class before

the critical parameters are changed signalling a new improved class. Therefore PSI assumes enormous significance in case of warships.

The Propulsion System Integration can be applied equally to all ships, however, due to large number of commercial ships built to the same design, its importance is never felt in the merchant marine world. On the other hand, a warship, not only more complex due to varied requirements, is also constructed in lesser numbers before the design gets changed, necessitated due to role change. For example, the IN typically, has been ordering construction of three warships of a given class before the critical parameters are changed signalling a new improved class. Therefore PSI assumes enormous significance in case of warships.

Due to a lack of necessary expertise and infrastructure in the country, the propulsion system design and integration studies are presently being sub contracted to foreign ship designers and vendors at exorbitant costs. What is of more concern is the fact that by contracting the system integration study to external agencies, what is achieved is only an end product in the form of a report which is applicable only for that specific project and no transfer of technology takes place. Moreover, as there is no single optimum solution for a PSI Design, the foreign consultant or the integrator generally offers a design ensuring procurement of PSI equipment in a way so as to gain commercially by limiting the choices for the Navy. Due to a lack of in house expertise and experience, the offered solution is generally concurred with and is seldom questioned. With a large number of indigenous ship building programs envisaged in the future, there is a dire need to acquire adequate expertise and in house competence in this field to bridge this critical capability gap.

This capability gap exists due to varying reasons, starting from limitation of adequate infrastructure, to lack of emphasis on this subject. The technology, tools, skill set, expertise and experience required to undertake PSI tasks is presently not available in-house or indigenously. Few limitations are brought out in the succeeding paragraphs:-

1 **Lack of Expertise**

The Propulsion System Integration is a highly complicated and specialised technology having extremely focused end use. Due to this reason, the development of technology has been highly concentrated in few countries or companies only. Consequently, a very limited number of specialists agencies exist who can undertake the PSI design and none of them are of Indian origin. It may be of interest to note that while more than 80% of worlds shipbuilding happens in East Asian countries like S Korea and China, almost entire expertise and tools for PSI are of European Origin. One of the reasons of lack of availability of expertise is the fact that undertaking a PSI design requires skills in multiple engineering fields such as Mechanical, Marine, Structural, Naval Architecture, Fluid Dynamics,Hydrodynamics etc. It also requires skills for in depth analysis of propulsion equipment and components using advanced tools such as scientific software. Due to relatively low requirement of PSI in fields other than shipping or aviation, the expertise required is extremely rare worldwide and more so in India. Although, it is being undertaken with help of foreign consultants so far by focusing on the immediate requirement but in the long run, there is a need to establish dedicated Centres of Excellence to provide a range of services from developing design technology, establishing benchmark Standards, promulgating guidelines and undertaking Independent Validation and Verification (IVV) of selected design.

2 **Lack of Benchmarks and Guidelines**

Together with the expertise, there is also a lack of available standards and guidelines to undertake the propulsion system design indigenously. Though, there are standards or guidelines available from Admiralty, NATO standards and Classification Societies, they all have subtle differences owing to the specific conditions such as ambient temperature, seawater temperature, salinity, humidity etc. prevalent in their regions. Moreover, as has been said earlier, a PSI design brings out multiple solutions which are workable and have to be evaluated with respect to other factors. Presently, there are no home grown benchmarks or guidelines and the study has to depend on the guidelines borrowed from other agencies.

3 **Lack of Available Tools and Technology**

As discussed earlier, during the course of a PSI design development, a multitude of different tools and technologies are required. Some of them are:-

- Technology / Tools for Specialised Design for shafting, propellers and Gearbox etc.
- Technology / Tools for Intake / Exhaust Design
- Technology / Tools for Signature Management. including technology for Raft Mounted Equipment.
- Technology for alternative forms of propulsion such as Water Jets and Pump Jets.
- Lack of sufficient data for integrating different hull forms with alternative propulsion for specialised operations.
- Lack of technology for manufacturing such as Propellers, CPP etc.

4 **Lack of Indigenous Equipment**

A major hurdle in achieving self-sufficiency in PSI is an almost complete lack of Indigenous equipment for propulsion. Significant development has been made in the production of Boilers and steam turbine and small diesel engines. Diesel engines available within the country which can be installed on board IN ships for main propulsion are limited to the range of 1-7 MW only and majority of them do not comply IMO emission norms. This is mainly because our OEMs are yet to bring in the necessary technology and infrastructure. Specialised equipment such as high powered Main Engines (Diesels and Gas Turbines) to Gear boxes, Transmission equipment such as shafting, Thrust Block

and Fixed and Controllable Pitch Propellers etc are almost invariably sourced from foreign companies. Even minor equipment like high capacity S and V mounts and TMDs utilised in critical equipment for limiting the Radiated Noise Levels are sourced from abroad. Sourcing these equipment from abroad not only has a long term cascading effect in terms of spares and support but also entails sourcing of other auxiliary equipment for reasons of better integration and single point responsibility.Leading OEMs have a virtual monopoly in this regards. Selecting their equipment invariably leads to practically limiting the procurement of related auxiliary equipment also from the vendors designated by them. Often, even the control system or the IPMS is also required to be procured from the vendor designated by equipment OEMs. Further, most of the time, equipment subscribing to the latest stipulations such as Tier 2 norms of IMO Annexure VI for reduction of NOx emissions are not available within the country. It is well understood that all the equipment to be installed on board cannot be indigenised and neither there is any requirement to do so provided the tools and technology for integrating such bought out equipment is available within the country and atleast the minor equipment can be sourced from indigenous resources. On the question of maintenance and spares support also, the system at large should be supportable indigenously. It is often observed that minor equipment like PCBs which form a critical component of any control system, cannot be repaired within India and have to be shipped abroad for maintenance causing avoidable delays and costing substantially more than costs of such repairs in India.

5 **Lack of Higher Learning and Skill Set Build Up**

The PSI is mainly a ship design requirement, particularly required by Navy, and therefore has limited utility in the civil world. Further, it encompasses multiple engineering streams and skills which prevents its introduction below Post Graduation level. Therefore, for obvious reasons, there is a visible lack of higher learning in PSI available in India. In the European world, there is a substantial focus on advanced ship design by various organisations including leading companies like Rolls Royce, Wartsila, and shipbuilding industry. These organisations come together to run specially designed courses in various aspects of PSI and advanced ship design. The graduates from these courses are absorbed by the companies themselves or other design organisations including Classification Societies. An in-depth understanding of these subjects is considered essential for our designers and marine engineers also who are involved in design and construction of ships within the country. It is, therefore, unfortunate that these fundamentals are not covered in any engineering stream offered anywhere within the country. There is, thus, a dire need to carve out a suitable syllabus for PSI and offer the same along with practical skills at Graduate and Post-Graduate levels. Similarly, there is a requirement to upgrade the skill set of general marine engineers and Architect by undertaking Resistance Calculations, Powering estimation, Propeller Design, Marine Shafting Design using specialised software. At present no short or long courses of this nature are offered anywhere in the country. Our institutes of higher learning can collaborate or tie up with universities / institutes abroad which offer these courses and make these courses available in India. Gradually, as the expertise grows, the dependence on foreign universities will become redundant.

6 **Propulsion System Integration Centre at NSTL A Navy & DRDO Initiative**

A. To bridge the capability gap brought out above, Indian Navy and DRDO have collectively embarked upon an initiative to establish the PSI Centre at Naval Science and Technological Laboratory at Visakhapatnam. This centre has been established with a broad charter of duties with the aim of becoming the Centre of Excellence for all PSI related activities of IN and to carry out research into new propulsion technologies, integration studies, creation and maintenance of data bank of reference documents etc. In addition to being a CoE on PSI, the charter of duties of the Centre include the following:-

- Selection and Design of Propulsion system
- Model testing of hull forms, generation of propeller curves for establishing power requirements and design of high efficient propellers
- Design and interfacing of propulsion system components.
- Dynamic simulation and Platform management of complete propulsion system.
- Design and Evaluate layout, installation and trials of propulsion / power generation systems.
- Formulation of Guideline Documents, Benchmarks and Specifications.
- Generation and maintenance of reference data bank in specialized areas of technology.
- Research in new propulsion technologies and re-engining studies of existing naval platforms.

B. The PSI Centre has been located inside NSTL at Visakhapatnam as a large no. of critical activities pertaining to the PSI are also being undertaken at the laboratory, albeit, under different projects. NSTL, over the years, have developed capabilities in specialised area for warship design such as assessment of Hydrodynamic performance, shock and vibration testing of equipment, equipment mounting systems and stealth technology. These aspects have been traditionally dealt as part of different projects by different Technology Centres. The same would now be harnessed for undertaking PSI related research also. Few test facilities that exists in NSTL which are considered essential for carrying to PSI studies are:-

i. High Speed Towing Tank (HSTT)

It is a Hydrodynamic Test Facility recognised by International Towing Tank Conference. It is equipped with a model makings workshop to make scale down models of

ships and submarines to carry out model tests for determining characteristics and evaluation of power plant requirements. The tests performed at HSTT are:-

- Resistance and self-propulsion tests to assess speed power characteristics.
- Flow visualisation to identify flow separation, if any.
- Open water tests to obtain propeller characteristics.
- Wake survey to determine flow velocities.
- Sea-keeping tests for head sea only.
- Dynamic tests for high speed vessel such as planing, multi-hulls, hydrofoil, SES etc.

ii. Cavitation Tunnel

It is a state-of-art facility for study of cavitation inception of body profile and propellers. It is also used for the study of Acoustic measurements due to cavitation of propellers. The other tests performed in cavitation tunnel are:-

- Propeller tests in open water to measure performance characteristics in cavitating and non-cavitating conditions.
- Tests with hull propeller model to measure self-propulsion characteristics, propeller working in the wake of the model in cavitating and non-cavitating conditions. Hull propeller interaction.
- Measurement of forces and moments on surface ships and submerged bodies including their control surfaces.
- Determination of towing resistance of surface ships and submerged bodies.
- Cavitation tests - Inception and decay
- Flow visualisation and Wake survey
- Measurement of hull pressure fluctuations induced by propeller and cavitation.
- Measurement of acoustic radiation caused by cavitating and non-cavitating propeller and hull.

iii. Signature Management

Measurement, study, analysis and mitigation of signatures of ships and submarines are essential for a stealthy fleet. Towards this, several facilities exists at NSTL and a few which are part of PSI studies include Shock, Noise and vibration and IR suppression studies. NSTL also holds the distinction for being the shock qualifying agency for equipment to be fitted on board Naval ships. For undertaking shock, Noise and Vibration measurement, facilities such as a floating shock platform, shock testing tank, Shock testing machine, Vibration shaker and Acoustic test Centre are available. The lab also undertakes Radiated Noise Levels (RNL) measurement for Naval ships at an inhouse underwater ranging facility. NSTL has also created test facilities for measuring ships' RCS and IR signatures. In addition to these, dedicated research is also in progress for ELFE, De-perming, Raft Mounted equipment, CLDs and UCLDs etc.

IV. Conclusion

Having identified Propulsion System Integration and its wide array of critical activities as a bedrock for warship design, it is essential to identify core areas where the skill set and expertise can be created indigenously. It is extremely important to create a healthy ecosystem of various stakeholders for creating opportunity for development of technologies related to production and integration of reliable equipment within the country. This will not only lead to advancement in technology and necessary infrastructure for manufacturing, but will also spearhead the creation of specialised agencies, promulgation of Indian Standards and development of skill sets essential to pursue this key component of shipbuilding thus preventing undue dependence on foreign sources. This ecosystem has to attain sustainability at each level and gradually move beyond focus on Indian shipbuilding industry. This indeed will be a true testimony of harnessing local talent for global solutions.

References

[1] Ciidefence.com/15-years-Indigenous plan of Indian Navy.
[2] SPs Naval Forces Feb-Mar 2012, Vol-7
[3] www.nrbdrdo.res.in/nstl.html



Captain (IN) Sameer Agarwal Captain (IN) Sameer Agarwal did his Marine Engineering from Naval College of Engineering and was commissioned in the Indian Navy in 1989. He has a post-graduate degree in Computer Science from IIT Kharagpur and has done his PG Diploma in Management Studies from JBIMS, Mumbai. The Officer has held various appointments onboard ships and ashore. Prior taking up his present assignment of setting up the Propulsion System Integration Centre at NSTL, the officer has been the Engineer Officer of a frontline Destroyer, Deputy General Manager of Naval Dockyard and Fleet Engineer Officer.



Lt Cdr V Kumaran Lt Cdr V Kumaran was commissioned in Indian Navy in 2005. He did his post-graduation in Internal Combustion Engines and Gas Turbines from IIT Madras. The officer prior joining the PSI Centre has held appointments as Senior Engineer Officer onboard INS Khukri and Engineer Officer onboard INS Battimalv.

Developments in Shipborne Controls and Electronic Systems

Commander (Veteran) Alok Bhagwat, NM
Joint General Manager
Larsen & Toubro - EAIC Marine Business
Rabale, Navi Mumbai India
Email: Alok.Bhagwat@LNTEBG.com

***Abstract*--The Newbuild Programmes of Indian Navy and Indian Coast Guard have seen rapid advancements in the level of technology onboard. There is an unprecedented increase in the level of automation throwing open complex integration and interface risks. In the past 20 years or so, the IN Ships have seen proliferation of automation in equipment, machinery and systems in almost all areas onboard viz. navigation, hull, engineering and electrical. However, there is a need to develop expertise within the country to be able master all the facets of new technologies viz. operation, maintenance, repair and Life Cycle Support. The paper covers these advancements, contemporary technologies in the modern control systems and suggests ways to master these.**

The modern warship has IPMS and IBS that control & monitor almost all ship systems, be it navigation, hull, engineering and electrical machinery. The monitored systems include propulsion machinery, auxiliary machinery, damage control, stability, power management, surveillance, intercom, navigation, communication dynamic positioning, amongst others. The modern control & automation technology has been introduced in the Indian Navy in a gradual way. Kolkata Class ships, presently under commissioning stage were the first to have indigenous Auto Power Management Systems (APMS). LST (L) witnessed the introduction of IPMS with propulsion machinery & auxiliary machinery control. Naval OPVs built by GSL have an elaborate power, machinery, systems and equipment control. INS Makar was the first vessel where the entire electrical, automation, electronic and hydrography package was executed under 'Turnkey Electrical & Automation' concept. INS maker has very sophisticated and state-of-the-art equipment & systems. Further, Shivalik Class ships have modern APMS and IPMS systems. The degaussing system onboard has undergone rapid change with modern controls including IGBT making the rotating machinery technology for DC current obsolete. The Coast Guard vessels viz. FPVs, IPVs, OPVs, Interceptor Boats and Training Vessel have similar complex and sophisticate technology onboard. The future warships are bound to see further complex systems, at par with the World Navies.

Whereas, Indian Navy is gradually increasing the technology levels in these areas in subsequent vessels, the refit programmes have not seen such advancements, thereby depriving the crew of crucial proficiency in operation & maintenance of such systems onboard. The repair agencies are now gearing up for these systems with RFIs being issued recently for such setup. The adaptation of contemporary technologies for retrofits and modernization has commenced and the future refit programmes are aiming to bridge the technological gap between an old and a new warship.

The future ships with electric propulsion are slated for further advancements with medium voltage switchgear and associated equipment. These ships will have different and elaborate power management as an integrated part of IPMS, dynamic positioning systems integrated with IBS and MV switchboards & motors with active front end drives. Indian Navy has embarked upon a programme to master these technologies with a proposed MV system setup at INS Valsura. But a cohesive and synergistic approach with Industry as an active partner is highly desirable to master these technologies and preparing the crew to effectively manage the same.

This paper brings out these advancements mapping change in the technology in IN and ICG vessels. The paper brings out the role played by Larsen & Toubro in ushering-in the technology. The paper addresses the way ahead for Indian Navy and Indian Industry to be able to manage the technology and keep pace with the advancements in future warships.

I. INTRODUCTION

The Indian Navy has migrated from a 'Buyers' Navy to a 'Builders' Navy long time ago. With the successful launch of the first Indigenous Aircraft Career last year, Indian has 'gate crashed' into the league of 'select few' countries capable of building naval platforms -including underwater platforms- of strategic dimensions. Indian Navy has embarked upon an ambitious fleet expansion plan with fifty odd warships in various stages of planning and construction. Simultaneously, Indian Coast Guard has been steadily inducting vessels after vessels in its quest of effectively defending the long coast line and EEZ. With most of the IN and ICG vessels being built within the country, the Indian Shipbuilding fraternity has a credible order backlog attracting global technology giants to flock to Indian coast and claim a pie of this growing market. With this scenario prevailing within the country for over a decade now, Indian Navy and Indian Coast Guard have been offered the best of the technologies earlier available to the western world only. IN and ICG, quick on the uptake in this area, selected equipment with the state-of-the-art technology for their newbuild programmes ushering in

warships with modern control and electronic systems. This paper aims to cover the modern shipborne control and electronic systems. The paper will touch upon the level of indigenization and expertise available within the country in various facets of new technologies viz. operation, maintenance and repair. The paper will briefly dwell upon the methodology adopted by Larsen & Toubro through global acquisitions and tie-ups with an aim to provide Life Cycle Support from within the country while reaping the benefits of global developments in these areas by a win-win model to all stakeholders, including global partners.

The control systems onboard can be broadly classified into navigation & bridge management, propulsion machinery management, auxiliary machinery management, power management, damage control & stability management, surveillance, habitability and domestic systems. These are elaborated upon in succeeding paragraphs.

II. CONTROL SYSTEMS IN IN/ ICG SHIPS

Navigation and Bridge Management

Contrary to the discrete bridge where there were hardwired and dedicated displays for navigation sensors, radars, Chart and other devices, the modern bridge uses multi-functionality concept. This concept permits greater flexibility and is much more fault tolerant than the traditional discrete bridge. In this concept, all the navigation sensors are serially connected to redundant intelligence devices called 'Data Concentrator'. The output of these devices is made available on a redundant network. The network is connected to Human Machine Interface (HMI) through computer based workstations and the operator commands are routed in similar manner. In addition, the sensor inputs are connected hardwired to select displays for fool proof redundancy in the event of failure of the integrated system. The operator can choose to select any workstation as a radar display or Chart display or Conning display. A rigid hierarchical protocol transfer logic ensures authorized access and prevents possible clash due multiple access bid. The flexibility and redundancy permits the navigating officer or captain to monitor the navigation inputs from any location in the ship through a laptop specially configured with the necessary software. The commands can also be transmitted from the same location. A Training Simulator is embedded for self training or tutorial sessions.

The modern Integrated Bridge System (IBS) uses a PLC (Programmable Logic Control) data concentrator where all the sensors are connected through serial links over standard protocols. The protocols are defined by IMO and IEEE standards. Therefore, the IBS can be configured and interfaced with all the sensors irrespective of the make of the equipment. Both the concentrators work in redundant manner and in the event of failure of one, the second takes over seamlessly. The dual concentrators provide first layer of redundancy. The processed data from the data concentrators is routed on ether network. The Ethernet network has fibre optic backbone running throughout the ship. Dual networks are used for second layer of redundancy. The HMI is provided by multi function workstations. The workstations are connected to both the networks and are redundant to that effect. Any authorized operator can switch any workstation into desired operation mode viz. radar, chart or conning. The workstations use latest computers with fast speeds so that the response time is within limits. Therefore, to summarize, an IBS uses PLC for data processing, Ethernet network for data transmission in the ship and standard computers for HMI functions. All the hardware components are required to be compliant to marine Class Societies and IEEE standards.

The softwares used are required to be developed in line with IEC or Mil standards to ensure robustness. The power supply arrangement is provided through UPS for 230V AC as well as 24V DC. The UPS is designed to provide 30 mts backup supply in the event of total power failure.

The entire IBS hardware including the interfaces and data transmission is monitored continuously with a robust BITE (Built In Test Facility). The BITS runs a health check on the system constituents on power ON and establishes communication with the devices disconnecting faulty components. The health check continues in the background and the operator is notified of any malfunction or defects online. The system rearranges itself with healthy components to ensure full functionality and availability. The replacement of faulty hardware from On Board Spares brings back the system to full operational status without compromising on system availability.

The IBS includes a simulator that can be brought in the circuit as and when required to carry out crew training. The simulator runs separately without obstructing the real data management.

Propulsion Machinery Management

The modern marine engines and monitored and controlled by a PLC based Local Operating Panel (LOP). The LOP makes it feasible to monitor the engine performance online and take corrective action viz. slowdown or shutdown automatically. Thus, the engine is prevented of any damages without human intervention. The limits are set at the factory and fine tuned during trials onboard. The other elements of the propulsion machinery viz. gear box and shafting are also monitored through engine or local intelligent LOP.

The propulsion machinery onboard IN Ships is managed by an Integrated Platform Management System (IPMS). The IPMS has a data acquisition layer configured with geographically distributed Remote Terminal Units (RTU). The RTU is a VME Processor Based device in line with IN specifications. The RTU interfaces with the engine, gear box, shafting and propulsion auxiliaries through analog, digital and serial interfaces. These interfaces use standard or proprietary protocols although Indian Navy specifies standard and open protocols so as to achieve seamless interface between all devices. The RTU provides processing of the data from the machinery and makes the data available throughout the ship using fibre optic based dual redundant Ethernet network. The operator interface is achieved using multi function workstations located in MCR, DCHQ, MSB, Bridge, Section Bases and other such locations. The system has full flexibility of controlling machinery from MCR or Bridge by a rigid 'Station In Control (SIC) protocol.

The software is developed suing Mil Std 498, upgraded recently to ISO Std 12207 ensuring robustness of the software. The entire system is monitored with a BITE system.

The ICG ships use similar arrangement for propulsion machinery control but with a subtle difference. The data acquisition units are PLC based and not VME based. The other constituents of the system are same. The system is called IMCS in CG vessels.

Power Management and other Machinery Management.

The IPMS extends to monitoring and control of generators and switchboard with a operator friendly APMS (Automated Power Management System). The APMS uses generator protection and synchronizing modules and can function along with IPMS on the same RTUs or can be configured using dedicated PLC based DAUs. Both the variants are available in IN ships, whereas ICG ships have a separate APMS.

The IPMS, whether VME based or PLC based, extends to monitoring and control of all the machinery and systems of the ship. These are listed below: -

- Auxiliary Machinery viz. fire pump, Cooling pump, compressors, fresh water pump etc
- AC and Ref plants
- Fire main system
- AVCAT system
- Tank gauging
- Fire & Flood detection
- Damage Control and Stability management
- CCTV
- STP
- Ventilation
- HVAC
- Any other machinery or system or equipment

Therefore, it can be seen that the modern vessels of IN and ICG use state-of-the-art control systems for entire ship machinery, equipment and systems. The control systems are intelligent, PLC or VME based, use advance networking techniques using active managed Ethernet switches and have wide bandwidth to ensure fast response time. The characteristics of these control systems are summarized below:-

- Redundancy
- Availability
- Reliability
- Maintainability
- Graceful degradation and avoidance of catastrophic failure
- Using latest processors and computers
- Fast communication with low latency to achieve a typical response time of less than 500 m sec
- User friendly and customized graphics
- Easy parameter calibration and configuration
- Online Health Monitoring with BITE
- MTBF of 8000 hrs or better
- MTTR of 30 mts or better
- Dynamic Analysis of critical machinery
- Training Simulator customized to User requirement
- Modularity
- Growth margin for future expansion
- Software developed in accordance with IEC and Military norms
- Strict Configuration Control
- Type Approved hardware compliant to JSS 55555 or Marine Class Rules and EMI/ EMC Norms
- Hardware and software compliant to Human Engineering Norms

Power Electronics and micro controller based equipment

While the major machinery monitoring & control systems onboard IN and ICG use platform management and integrated systems explained above, a large number of power electronics and electronic systems are finding increasing use. These are described briefly in succeeding paragraphs.

SCR and IGBT Based Systems

Every ship has large number of equipment requiring low voltage DC supply. The 24V DC supply onboard is required for engine control, generator control, navigation and communication. These equipment are fed through Transformer Rectifier Units (TRU) and Battery Charger Units (BCU). The IGBT based systems are slowly replacing SCR based systems as the devices are more reliable and compact. EMI/ EMC compliance and ruggedisation along with compact design and heart dissipation are the challenges to any designer. But IN ships have modern degaussing systems that use IGBT based current controllers. Similarly DC soft starters onboard submarines use IGBT based controllers. The future ships will see more of IGBT based systems.

Micro Controller Based Systems

The advancements in micro-controller technology and robust ICs permit their use for applications such as Engineer Calling System (ECS), Navigation Light Control System, Emergency EOT, POT and many such applications onboard.

III. L&T'S APPROACH

The Electrical & Automation Independent Company of L&T (L&T EAIC) set up a dedicated focused Marine Group in year 2004 and commenced marine approvals of basic switchgear. By year 2005, the group bagged the first major order for PGD of P15A ships at MDL, including APMS. The group bagged another major order for degaussing system for ASW Corvettes at GRSE. Then there was no looking back. Expanding the portfolio gradually, the group bagged the first IPMS order for NOPV at GSL in year 2007. The projects were successfully executed and equipment delivered to the shipyards in time. However, the ship activities were taking time and the equipment commissioning on board were delayed. In the interim, L&T ushered-in a novel concept of Turnkey Electrical & Automation Solution, wherein the complete responsibility from Design,

Engineering, cable routing, working level drawings, termination chart etc for the electrical & automation system onboard was entrusted to single party to mitigate the risks involved in integration and interfaces of the ever growing complex package onboard naval platforms. INS Makar was the first such ship commissioned with this approach in year 2012. This concept was adopted with varying scope in small and large vessels viz. IN Fuel Barges at Modest, IN Tugs at Tebma, ICG Interceptor Boats at L&T etc. In the interim, L&T undertook retrofitment cum modernization projects of Indian Navy wherein the traditional systems were modernized with the new control systems. Some of the examples are Al MSB of INS Agray with auto synchronization provision, SS MSB of SNMs at Vizag, MSB of Kora Class ships with APMS, GT monitoring system of INS Vipul, to name a few.

As on date, the following ships of Indian Navy have L&T supplied modern control systems: -

- IN Ships Saryu, Sunayna, Sumedha with MSB, APMS, IPMS
- INS Makar with MSB, APMS, IPMS, IBS, TRU, BCU
- Five Fuel Barges with MSB, ESB, AMS, Tank gauging, AFDS, AFAS, ECS,
- Ten Tugs with MSB, ESB, AMS, Tank gauging, AFDS, AFAS, ECS,
- Ten CG IBs with PGD, GA System, AFDS, AFAS, TRU, BCU,

L&T's model in the CSV project at AAGL, Bhavnagar has ushered in a novel model of undertaking E&A package onboard a Naval or Coast Guard platform in a Turnkey approach for expeditious execution. L&T undertook the following activities for this project: -

- Finalization of DG set capacity and load distribution after approval of load analysis and single line drawing by IRS and ETMA.
- Design & Supply of IRS & Navy approved Main Switchboards, Group Starter Panels, Distribution boards, Transformers, TRUs, etc.
- Design of complete PGD System
  - Cable tray layouts and cable schedules
  - Lighting calculations and lighting layouts
  - Compartment layouts for Galley, Survey Chart Room, Bridge, MCR, Gyro cum ECP room, WT Office, Antennae Layout as per NEC (MB) requirements, etc.
  - As fitted drawings for all electrical sub-systems
- Design of internal wiring drawings for L&T/Yard supplied equipment
  - Main Engines, Main DG sets, Emergency DG Set, STP, AC Plant & other machineries
  - External Communication Equipment – VHF/UHF sets, VLF sets, HF sets, etc.
  - Hydrographic Equipment – AUV, ROV, Multibeam Echo Sounder, SONAR, etc.

- Design, Supply & Installation of Integrated Propulsion and Machinery Control System and Auto Power Management System. The architecture of the systems are appended at the end of the document. The system has following controls: -
  - Remote Terminal Units (RTUs) with VME technology,
  - Drop-in plate for engine control,
  - MCR Console, Bridge Console and APMS standalone consoles
  - Engine Order Telegraphs, UPS, AFDS
  - Soft control for Main Engines and other auxiliary machineries i.e. bilge pumps, ventilation fans, salvage pumps, FM 200
  - Equipment Health Monitoring System & Dynamic Analysis

- Design, Supply & Installation of Integrated Bridge System. The architecture of the system is appended at the end of the document. The system has following constituents: -
  - Bridge Management System including RADAR, Conning and ECDIS operation
  - Navigation & Communication Equipment i.e. RADAR, Gyro Compass, Magnetic Compass, AIS, Navtax, Weather Chart Facsimile, INMARSAT C, INMARSAT M etc.
  - Intercom System, Auto Telephone System, Talk Back System

Some photographs of these systems onboard INS Makar are reproduced below.



Gyro Compass



Main Switchboard and Group Starter Panel



Main Switchboard with APMS Console



Ship's Bridge with Navigation Equipment and IBS Console



Operations Room (Ops Room) or Survey Chart Room

The modern control systems supplied by L&T onboard a number of Naval and CG vessels are operational for more than three years now. L&T has been involved in STW and commissioning activities for these systems for more than six years. This can be termed as the first



INS Makar

phase of ushering in modern indigenous control systems onboard Indian vessels. The journey has not been smooth and a number of teething troubles were encountered. However, L&T's capability and wherewithal to support these system from within the country has found favours with the naval fraternity and L&T is now involved in setting up test, repair and training facility for these systems in naval dockyards repair yards and training establ;shments.

While, the maintenance set up gets stabilized with time, there is a need to enhance the crew familiarity for operation and maintenance of these systems onboard. While the new projects take their own time to materialize, a large number of ships are getting retrofitted. There is a need to augment these ships with modern control systems so as to make the crew as familiar with the new technology as the old systems. There is a need to bring in a focused approach by IN in this regard so that in each refit, the ship is modernized with new control systems in a Turnkey manner. L&T has taken baby steps towards this and some of the projects undertaken on existing shuips are listed below: -

- GT Monitoring System of INS Vipul
- IBS for INS Tir

L&T has also forwarded various proposals for modernization as given below: -

- IPMS for Delhi Class ships
- Degaussing for SNF, LST and other ships
- Helo Rectifiers for refit ships

As brought out earlier, a focused approach towards retrofit/ modernization is required for extending the benefits of indigenous control systems to the existing platforms and, therefore, enhancing the operation and maintenance skills of the crew.

IV. GLOBAL PARTNERSHIP

Thou Shalt Not Reinvent The Wheel' Following this principle and understanding IN requirement of a 'Proven Track Record' L&T scouted for global technology leaders to arrive at a workshare arrangement that will satisfy all stakeholders. The Technology Leader got business in India, Indian Navy got state-of-the-art

technology with Life Cycle Support from within the country and L&T adopted 'Knowledge Acquisition Model' to enhance its portfolio. The journey began with degaussing system project of ASW Corvette. L&T partnered with M/ s Thales Underwater System (TUS), France. The workshare was such that the critical areas of coil design and controller software were handled by TUS. L&T took the responsibility of the balance work including complete hardware design & manufacturing, detailed design & engineering, project management and site commissioning activities. The next tie-up was for IPMS of NOPV. L&T partnered with M./ s Servowatch Systems, UK. A mutually agreeable worksharle with significant indigenisation level in first vessel, increasing levels in subsequent vessels, and touching a 90% level in last vessel, was drawn up. Indian Navy approved the workshare arrangement. L&T finally achieved over 90% indigenisation levels by the end of the project. Comparable levels were achieved for INS Makar also. L&T has been providing fully indigenous support to Ins Ships Saryu, Sunayna, Sumedha and Makar. Subsequently, L&T acquired Servowatch and today Servowatchh is a 100% L&T Subsidiary company.

The 'Knowledge Acquisition' model has been rigorously pursued by L&T in enhancing the portfolio to almost all the equipment and systems of the Electrical & Automation chain in a ship. The model is further being adopted to enhance the portfolio to include Auto-Pilot, Dynamic Positioning and Electric Propulsion elements. Today, L&T has achieved partnership with following technology leaders: -

- M/ s Thales Underwater Systems, France for Onboard Degaussing Systems
- M/ s Servowatch, UK for IPMS and IBS
- M/ s Ultra, UK for Onboard degaussing including degaussing of underwater platforms
- M/ s STL, Germany for magnetic measurement and treatment
- M/ s TAMCO, Malaysia (a 100% L&T Company) for MV switchgear
- M/ s Iffen for onboard degaussing system
- M/ s Krylov, Russia for magnetic studies
- M/ s Seatech for electrical design studies
- M/ s Navis for auto-pilot systems

As brought out earlier, a focused approach towards retrofit/ modernization is required for extending the benefits of indigenous control systems to the existing platforms and, therefore, enhancing the operation and maintenance skills of the crew.

V. SUMMARY

As a true Blue Ocean Navy, Indian Navy has tremendous responsibility in defending the SLOCS and keeping the Indian Ocean Region free for trade and free from piracy. At the same time, Indian Coast Guard has also to play a vital role in defending the vast coast line and EEZ from terrorism and piracy. Therefore, it is imperative that IN and ICG induct vessels with the systems having state-of-the-art technology at par with those onboard International Navies. It ia also imperative that IN and ICG embark upon retrofitment and modernization plans to replicate the new technology in existing vessels. This will ensure crew competence in mastering all the facets of managing the new technology, viz. operation, maintenance and repairs. Last, but not the least, Indian MOD should prepare a 'Policy Framework' to ensure participation with Indian Industry in a 'Partnership Approach' so as to ensure Life Cycle Support' from within the country. It is for consideration that such a framework is not existing today in India and the Indigenous suppliers are at a distinct disadvantage from imports in 'Taxation' and 'Certification' areas. Being a purely technical paper, the author wishes to refrain from dwelling upon the commercial aspects of the Defence Procurement Policy in this fora. However, until such a level playing field is made available to Indian Industry, India's dream of attaining Self-Reliance in critical defence projects will remain a distant dream. /It is pertinent to mention here that many countries have framed policy guidelines that tilt the balance heavily in favour of local suppliers. We should learn from them and, at least, provide a level playing field to indigenous suppliers, if not favouring them.

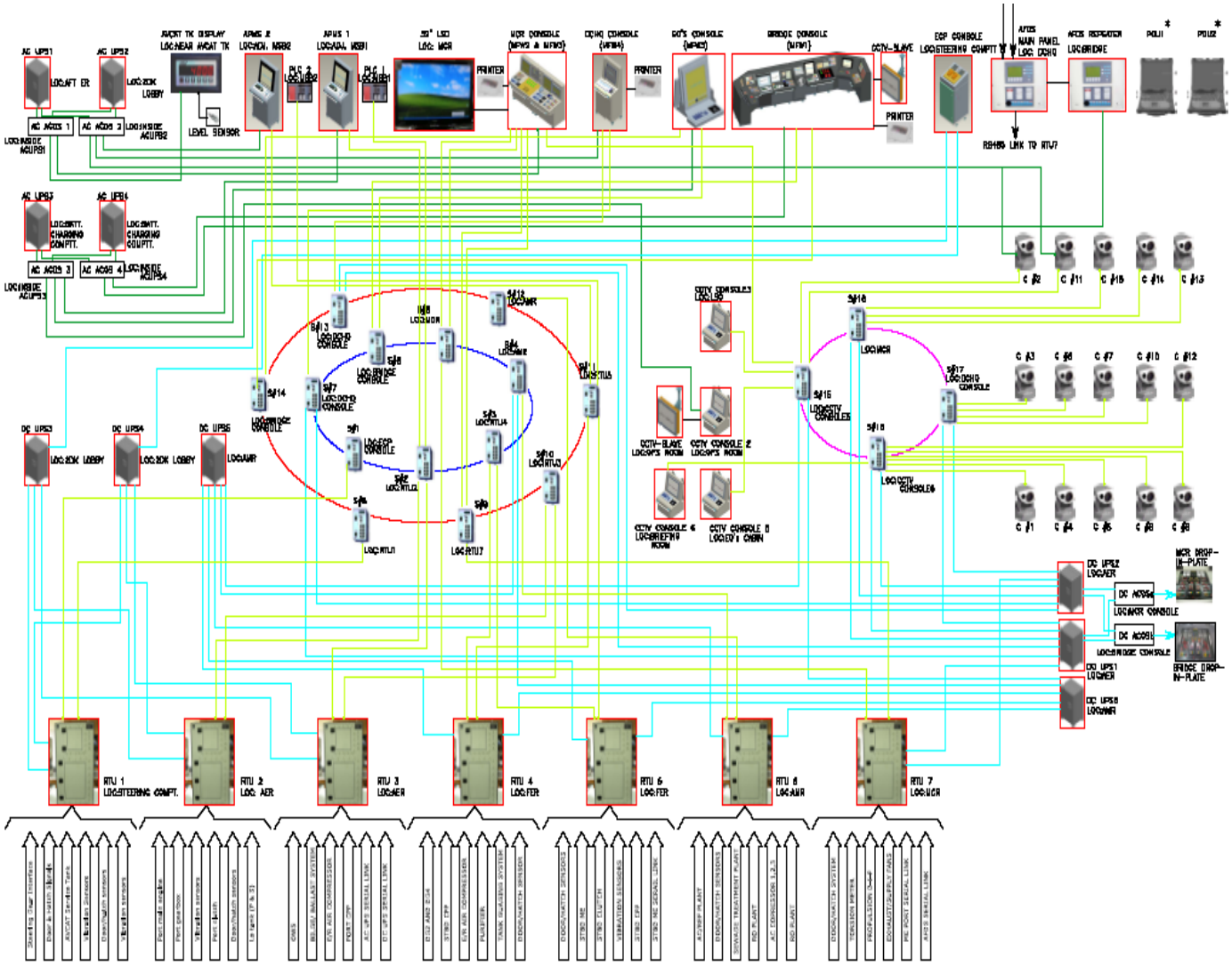
In the end I would like to reiterate the merits of the 'Turnkey Electrical & Automation' approach practiced by Larsen & Toubro in ushering cutting-edge technology on IN Ships with 'Global Partnership' and 'Knowledge Acquisition' model. The model has successfully been implemented on a number of operational ships. L&T is committed to take forward this model to retrofitment and modernization solutions as well and seek support from the IN and ICG towards achieving this goal.

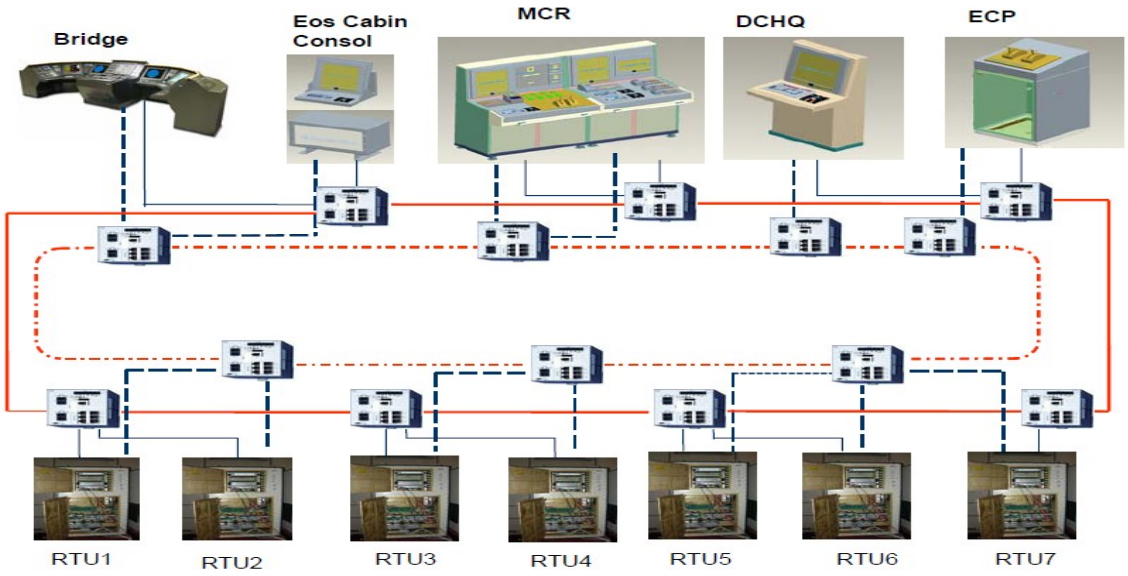
VI. ABBREVIATIONS

IPMS: Integrated Platform Management system
MFW: Multifunction Workstation
RTU: Remote Terminal Unit
UPS: Uninterruptable Power Supply
EOT: Engine Order Telegraph
ME: Main Engine
HMI: Human Machine Interface
FO: Fiber Optic
ACOS: Auto Change Over Switch
IEEE: Institute of Electrical and Electronics Engineers
BITE: Built In Test Equipment
BDCS: Battle Damage Control System
OBTS: On-Board Training System
APMS – Automated Power Management System
AI - Analog Input
CAT 6 – Category 6
DAU – Data Acquisition Unit
DI - Digital Input
DO – Digital Output
EDC – Energy Distribution Centre
MSB – Main Switchboard
PLC – Programmable Logic Controller
AIS -Automatic Identification System
ARPA – Automatic Radar Plotting Aids

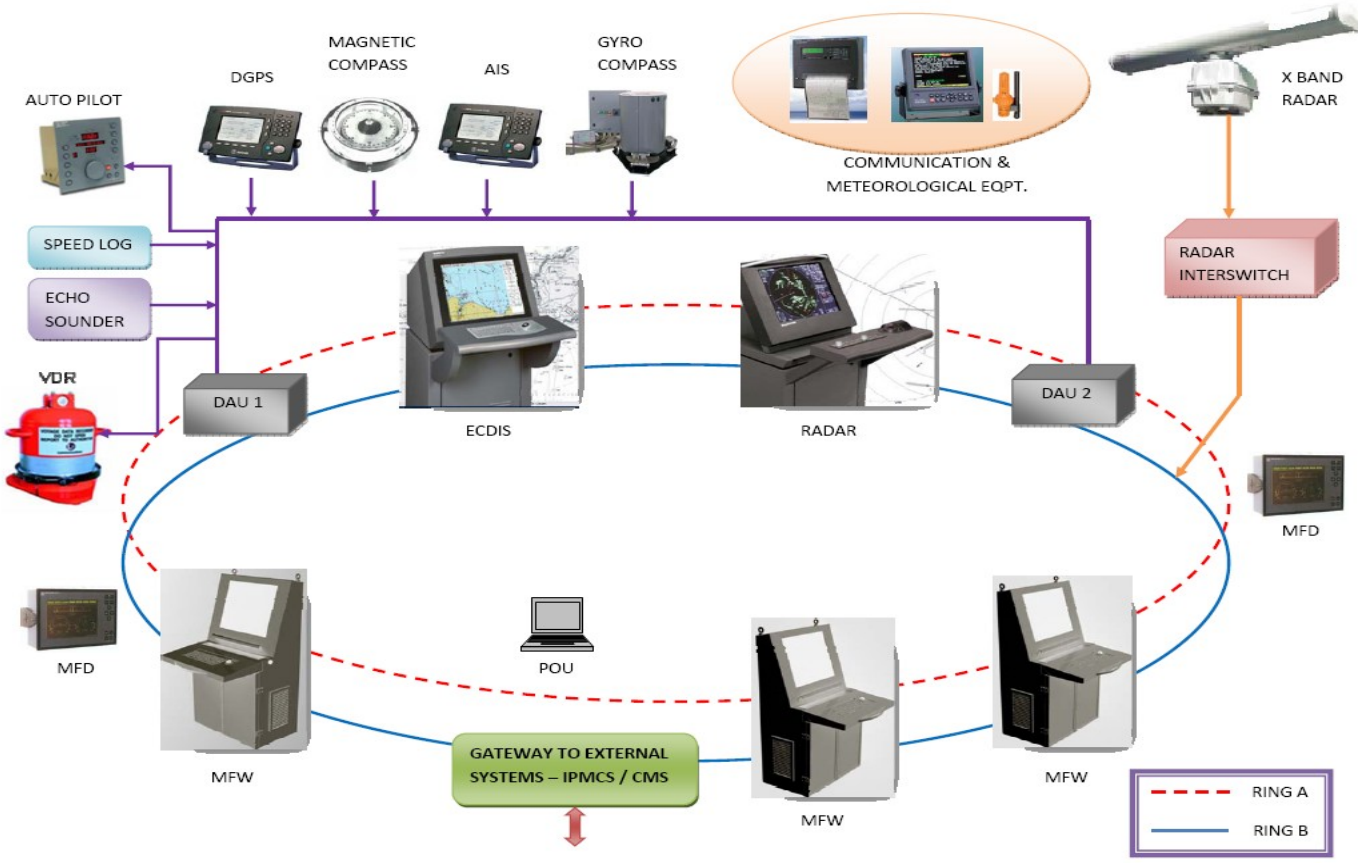
CCTV – Closed Circuit Television
CMS -Combat Management System
ECDIS – Electronic Chart Display and Information System
EMI -Electro-Magnetic Interference
ENC – Electronic Navigation Chart
GMDSS – Global Maritime Distress Safety System
GPS – Global Positioning System
IBS -Integrated Bridge System
IRS – Indian Register of Shipping
IHQ MoD(N)–Integrated Headquarter MoD(Navy)
ETMA – Electrical Trials & Modification Suthority
IMO – International Maritime Organization
IN – Indian Navy
ICG – Indian Coast Guard
MTBF – Mean Time Between Failures
MTTR – Mean Time to Replace
OEM – Original Equipment Manufacturer
RRB -Radio Receiver Beacon
SATCOM – Satellite Communication
SATs – Sea Acceptance Trials
SDN -Ship's Data Network
SOG – Speed Over Ground
SPT – Sound Powered Telephone
STW – Setting To Work

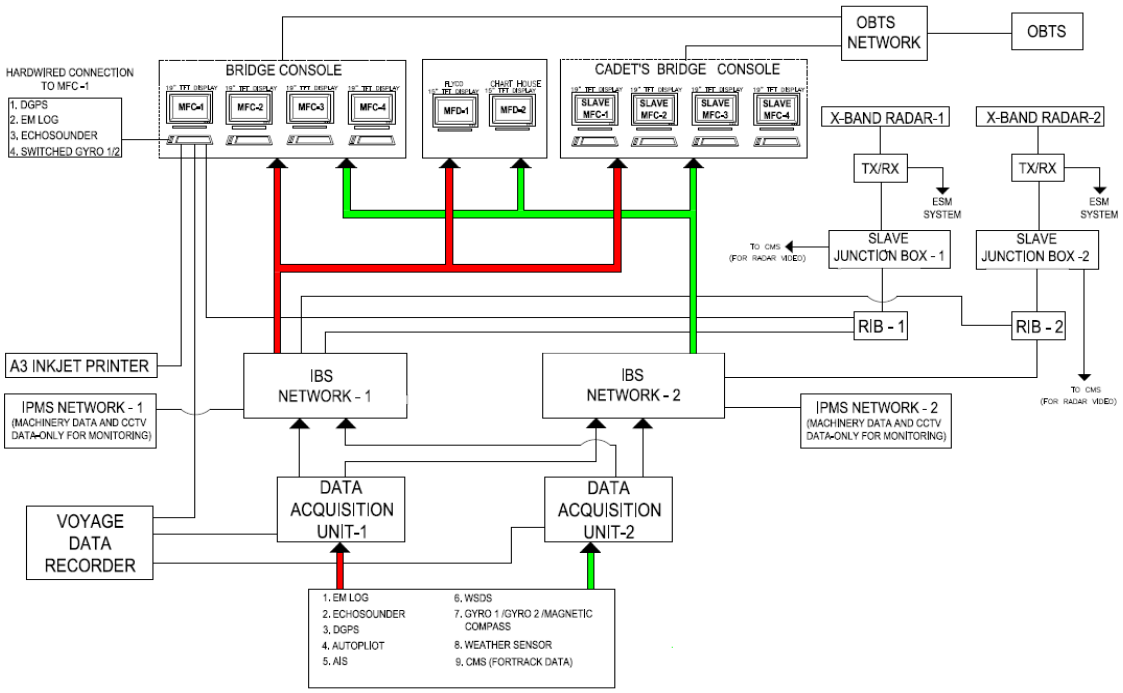
VII. DRAWINGS & ILLUSTRATIONS



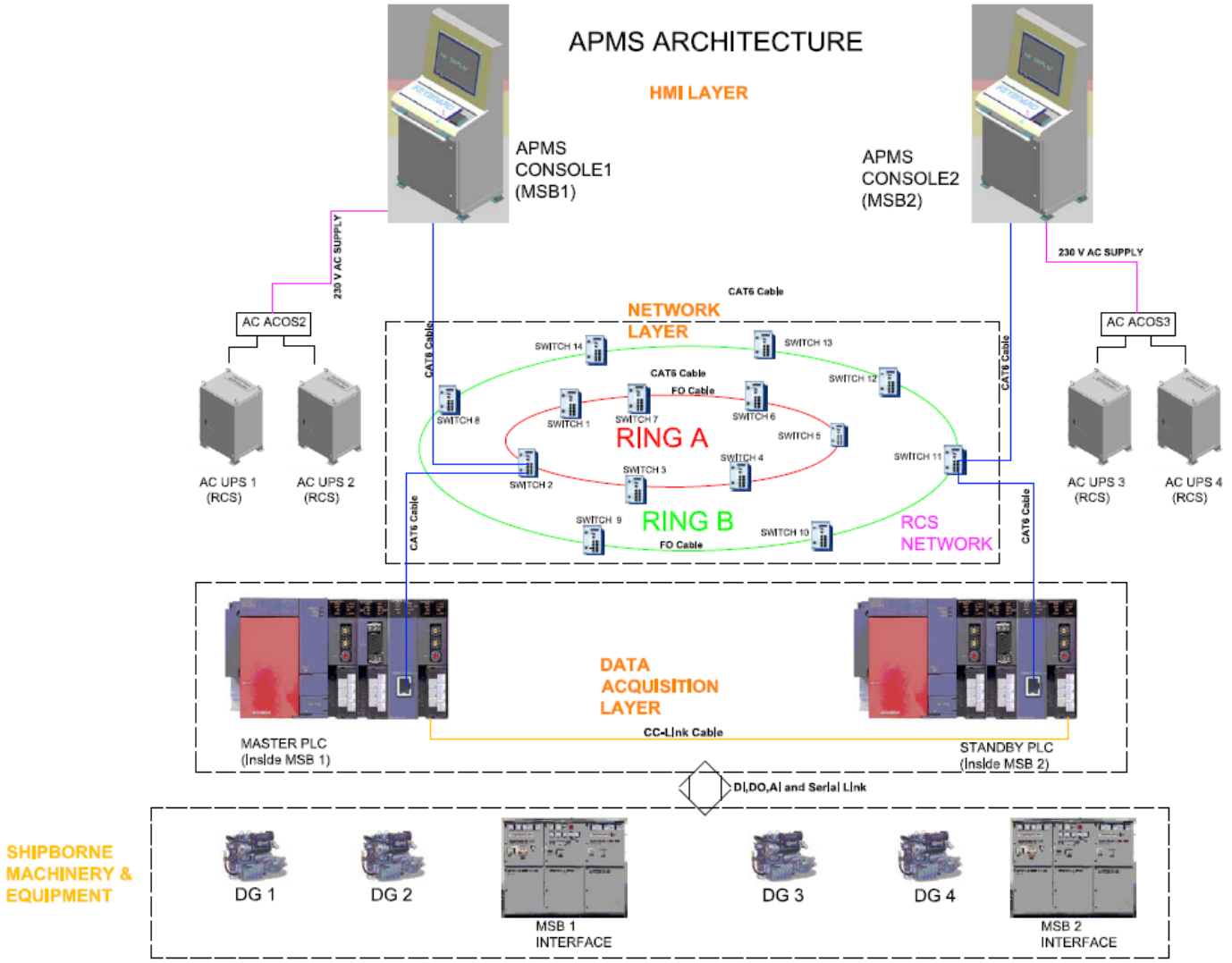


IPMS Architecture





IBS Architecture



APMS Architecture



Cdr Alok Bhagwat is a B.E. Electronics & Communication from IIT Roorkee and Master of Engineering (Mechanical/ Guided Missiles) from Pune University. During his career of 23 years in Navy, he held number of appointments in Warship building fields. On prematurely retiring from Indian Navy, he joined the newly formed Marine Business Group of Larsen & Toubro Electrical & Automation IC. He is presently working as Joint General Manager. He has published number of papers on 'Turnkey Electricals & Automation package for Warships' and "PLC Based Marine Controllers for GT and. Cdr Alok Bhagwat was conferred 'Naosena Medal for Devotion to Duty' in year 2000 for his contributions to Naval Shipbuilding.

Numerical Investigation on Response of Air-backed and Water-backed Plates Subjected to Underwater Explosion

Debashis Wadadar[1], Masud Ali[2], Asokendu Samanta[3]
[1,2,3]Research and Rule development division
Indian Register of Shipping
Powai, Mumbai, India
[1]debashis.wadadar@irclass.org ; [3]a.samanta@irclass.org

***Abstract*— The structural components of a warship can be subjected to the threat of underwater explosion caused by the sudden impact of a torpedo or mine placed well below the free water surface. The present study has been carried out to understand the effects of underwater explosion on an air-backed and a water-backed plate. Using commercial software package Patran as pre & post-processor and Dytran as solver, the modeling and numerical analyses of the air-backed as well as the water-backed plate have been carried out following a General Lagrangian-Eulerian (GLE) coupling technique which is being used to simulate the interaction between structure and surrounding fluid (air or water). Deflection of water-backed plate is compared and correlated with the deflection of air-backed plate. It has been observed that air-backed condition is more susceptible to damage compared to water-backed condition**.

***Index Terms*— Air-backed, Cavitation, Reloading, Water-backed**

I. INTRODUCTION

The explosions caused by torpedoes and underwater mines can pose serious threats to warships used in combat operations. Past researchers have focused mainly on the effect of explosion on air-backed plate. Taylor [1] proposed a one dimensional fluid-structure interaction model to analyze an air-backed plate subjected to exponentially decaying plane shock wave. Analytical solution for wetted surface pressure and plate response were derived. It was concluded that the peak momentum transmitted to the plate decreases with increasing fluid structure interaction (FSI) effect. Experimental and numerical investigations were carried out by Ramajeyathilagam et al. [2] on clamped rectangular plates subjected to underwater explosion. The test plate, considered to be air-backed, was submerged in a water tank. Numerical studies with and without strain rate effects were carried out on the plate to demonstrate the fact that if strain rate effects are not considered, the deflection is over-predicted by around 60%. The numerical results were compared with the experimental results for various shock factors (SF). Liu & Young [3] extended Taylor's floating air-backed plate model to submerged water-backed plate model within acoustic range. A systematic investigation on peak momentum transmission, peak response time, and cavitation inception time, leads to the conclusion that, if all the other parameters remain same, water-backed plate experiences lower net pressure loading, reduced structural response, and lower peak momentum transmission compared to an air-backed plate. Although cavitation is found inevitable for an air-backed plate, it is relevant only for a small range of FSI parameters in case of a water-backed plate. Rajendran & Lee [4] conducted a study on air-backed and water-backed plate based on Taylor's air-backed plate model and correlated the responses of water-backed plate with that of the air-backed plate. It was found that if other explosion parameters are kept the same, the analytical deflection and velocity of water-backed plate turns out to be 50% and 65% of the deflection and velocity respectively of an air-backed plate.

A comparative study of the response of a plate in air-backed and water-backed condition available in standard literature clearly reveals that damages induced in a water-backed plate is less compared to the damages of an air-backed plate subjected to underwater blast loading. This paper deals with the numerical simulation of air-backed and water-backed plates considering both FSI and strain rate effects.

II. THEORETICAL BACKGROUND

In general, a sudden release of huge amount of energy from an explosive material leads to the formation of highly pressurized, superheated gas. The expression for the peak pressure generated by shock wave produced by explosion as given by Cole [5] and Swisdak [6] is

$$P_m = k_1 \left(\frac{W^{\frac{1}{3}}}{R} \right)^{A_1} \quad (1)$$

Here, R is the distance to the point of interest from the centre of explosive and W is the charge weight. The pressure distribution behind the shock front is given by equation (2) as

$$P(t) = P_m exp^{-t/\theta} \tag{2}$$

Here $\boldsymbol{\theta}$ is the decay constant. When the shock wave passes through a fixed location, the water at that location flows with a velocity $\boldsymbol{v(t)}$ in the direction of shock wave resulting in transient pressure, the magnitude of which is given by Keil [7] as

$$P_w(t) = \rho_w c_w v(t) \tag{3}$$

Here, $\boldsymbol{\rho_w}$ is the density of water and $\boldsymbol{c_w}$ is the speed of sound in water. When the shock wave impinges upon a free standing plate the total pressure on the plate is due to the contribution of pressure at the front face as well as the back face of the plate. For air-backed plate back face pressure is zero whereas a water-backed plate will be subjected to back face pressure of magnitude $\boldsymbol{P_w}$.

According to Taylor's [1] model, the resultant pressure acting on the front face of the plate is the summation of incident, reflected and rarefactive pressure components resulting from the propagation of shock wave. Hence, the total pressure in an air-backed plate is

$$P_a(t) = 2P_m exp^{-t/\theta} - \rho_w c_w \dot{w} \tag{4}$$

Where, $\boldsymbol{w}$ is the deflection of the plate as well as the water that is in contact with the plate and $\boldsymbol{\theta}$ is the decay constant. The deflection of the plate leads to partial reflection of incident wave, thereby, resulting in a pressure reduction of magnitude. So, the equation of motion of the plate can be written as

$$m\frac{d^2w}{dt^2} = 2P_m exp^{-t/\theta} - \rho_w c_w \frac{dw}{dt} \tag{5}$$

The solution of the motion equation leads to plate displacement given by Rajendran & Lee [4] as

$$w(t) = \frac{2P_m\theta^2}{m(\phi_a - 1)\phi_a}[(\phi_a - 1) + exp^{-\phi_a t/\theta} - \phi_a exp^{-t/\theta}] \tag{6}$$

At time t tends to infinity the permanent deformation of the plate as given by Rajendran & Lee [4] is

$$w_{t=\infty} = \frac{2P_m\theta}{\rho_w c_w} \tag{7}$$

Taylor's floating air-backed plate model has been extended by Liu & Young [3] to water-backed plate. Water pressure at the back face of water-backed plate is adjoined with the Taylor's model. So, the total pressure can now be modified as

$$P_w(t) = 2P_m exp^{-t/\theta} - 2\rho_w c_w \dot{w} \tag{8}$$

The equation of motion of the plate given by Liu & Young [3] and Rajendran & Lee [4] is as follows

$$m\frac{d^2w}{dt^2} = 2P_m exp^{-t/\theta} - 2\rho_w c_w \frac{dw}{dt} \tag{9}$$

The solution to the differential equation as given by Liu & Young [3] and Rajendran & Lee [4] is as follows:

$$w(t) = \frac{2P_m\theta^2}{m(\phi_w - 1)\phi_w}[(\phi_w - 1) + exp^{-\phi_w t/\theta} - \phi_w exp^{-t/\theta}] \tag{10}$$

Here $\boldsymbol{\varphi}$ is the dimensionless inverse mass number. The permanent deformation of the plate when time t tends to infinity calculated from equation (10) is as follows:

$$w_{t=\infty} = \frac{P_m\theta}{\rho_w c_w} \tag{11}$$

Comparison of equation (7) with (11) reveals that permanent deformation is twice in case of an air-backed plate as compared to water backed plate.

III. NUMERICAL STUDIES ON AN AIR-BACKED AND A WATER-BACKED PLATE

The plate considered for numerical analysis has effective dimensions of 0.3 m × 0.25 m and thickness of 0.004 m. The modeling, meshing and set-up for the analysis have been made in Patran. Lagrangian shell elements have been used to discretize the plate into finite elements. To consider the high strain rate effect, Cowper-Symonds relation is used to compute the dynamic yield stress

$$\sigma_{dy} = \sigma_y\left(1 + \left|\frac{\dot{\varepsilon}}{D}\right|^{\frac{1}{p}}\right) \tag{12}$$

Other properties associated with the plate are as follows:

Young's modulus	= 210 GPa
Poisson's ratio	= 0.3
Density	= 7800 kg/m^3
Maximum plastic strain	= 0.23
Yield stress	= 400 MPa

Two Euler domains are used to model the fluid in front of and behind the plate. First Euler domain contains water in front of the plate within which the explosive is located and the second Euler domain behind the plate contains either air or water,

depending upon whether it is an air-backed plate or a water-backed plate. The gamma law equation of state (EOS) is used in this study to model air. The relevant properties are:

Air density = 1.225 kg/m^3
Ratio of specific heat (γ) = 1.4

Water is modeled using polynomial equation of state, given by Dytran user's guide. The Jones-Wilkins-Lee (JWL) equation of state is used to model the TNT explosive charge. In JWL equation, pressure is defined as

$$P = A\left(1 - \frac{\omega\eta}{R_1}\right)exp^{-\frac{R_1}{\eta}} + B\left(1 - \frac{\omega\eta}{-R_2}\right)exp^{-\frac{R_2}{\eta}} + \omega\eta\rho_0 e \quad (13)$$

In this current study fixed boundary condition is assigned along the plate boundary and non-reflecting boundary condition to the exterior surface of the fluid domain. Two Euler domains are separately coupled with the same coupling surface containing the plate.

The schematic diagram (Fig. 1) clearly shows the numerical model and the relative position of the plate with respect to the Euler domains.

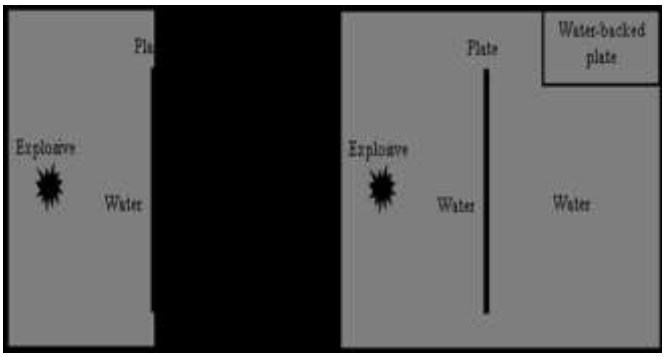


Figure 1 Schematic diagram of air-backed and water-backed plate condition

IV. RESULTS

The permanent displacements of plates are calculated for the specified problems in both air-backed and water-backed conditions. The displacements obtained from air-backed conditions are compared with the displacements obtained from water-backed conditions. Table 1 gives a comparative study between an air-backed and a water-backed plate.

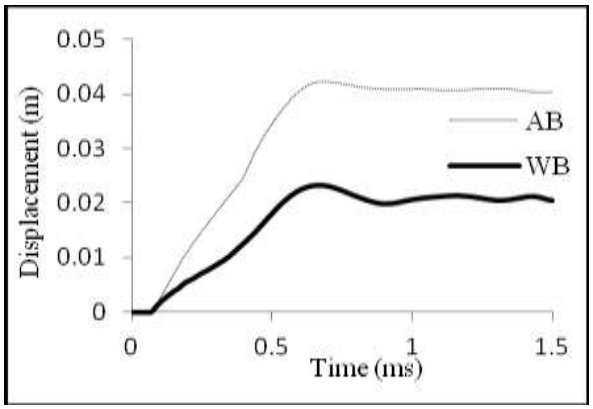


Figure 2 Displacement-time history at the central node of air-backed and water-backed plate for, 60 gm explosive with 0.15 m stand-off distance

The numerical results show that displacement of water-backed plate is almost 50% of air-backed plate which is in good agreement with the analytical study carried out by Rajendran & Lee [4]. The displacement time plots are shown in Fig. 2 to Fig. 4 for various stand-off distances.

V. CONCLUSIONS

Behavior of air-backed and water-backed plates subjected to underwater explosion have been studied numerically and damage severity is defined in terms of central displacement of the plate. The displacement of a water-backed plate is compared with the displacement of an air-backed plate. It is concluded that compared to an air-backed plate, displacement reduces drastically for a water-backed plate.

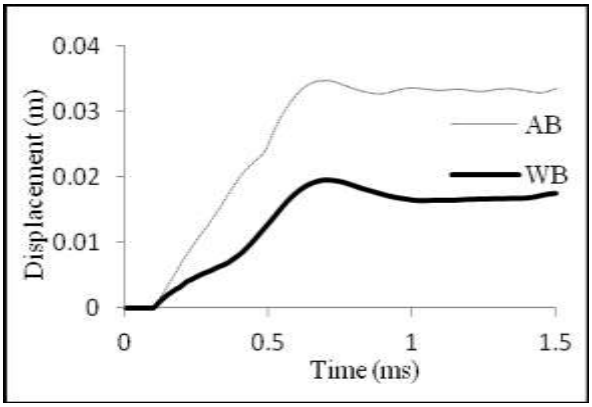


Figure 3 Displacement-time history at the central node of air-backed and water-backed plate for, 60 gm explosive with 0.2 m stand-off distance

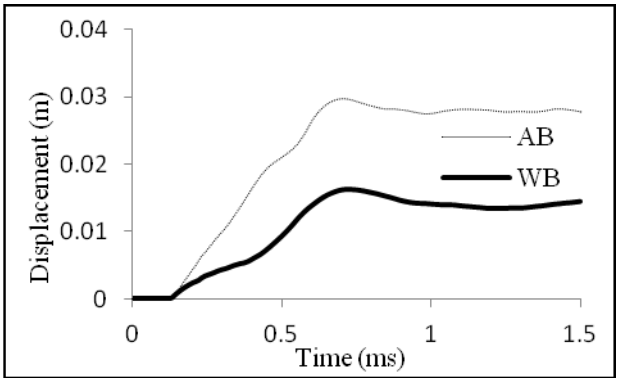


Figure 4 Displacement-time history at the central node of air-backed and water-backed plate for, 60 gm explosive with 0.25 m stand-off distance

Table 1 Permanent displacement at central point of air-backed and water-backed plates

No.	Charge weight (kg)	Stand-off distance (m)	Permanent displacement of air backed plate (m)	Permanent displacement of water backed plate (m)	Displacement ratio of water backed to air backed plate
1	0.06	0.15	0.0409	0.0208	50.85
2	0.06	0.20	0.0333	0.0168	50.45
3	0.06	0.25	0.0279	0.0141	50.54

REFERENCES

[1] G. I. Taylor, The Pressure and impulse of submarine explosion waves on plates, Scientific Papers of G. I. Taylor III, Cambridge University Press, Cambridge, UK, 1(1941) 1155- 1174.

[2] K. Ramajeyathilagam, C. P. Vendhan, V. Bhujanga Rao, Non-linear transient dynamic response of rectangular plates under shock loading, International Journal of Impact Engineering, 24(2000) 999-1015.

[3] Z. Liu, Y. L. Young, Transient response of submerged plates subject to underwater shock loading: An analytical perspective, Journal of Applied Mechanics, 75(2008) 0445041-0445045.

[4] R. Rajendran, J. M. Lee, A comparative damage study of air- and water-backed plates subjected to non-contact underwater explosion, International Journal of Modern Physics B, 22(2008) 1311-1318.

[5] R. H. Cole, Underwater Explosion. Princeton University Press, Princeton, New Jersey, 1948.

[6] M. Swisdak, Explosion Effects and Properties: Part II – Explosion Effects in Water, Naval Surface Warfare Center Report, NSWC/WOL TR (1978) 76-116.

[7] Keil, Introduction to underwater explosion research, UERD, Norfolk Naval Shipyard, Portsmouth, Virginia, 1956.



Mr. Debashis Wadadar is an Indian by Nationality. Having obtained his Bachelor degree (B.Tech) in Civil Engineering with First class Honours in the year 2011 from Jadavpur University, Kolkata, he took his Post-graduate degree (M.Tech) with First class from the Indian Institute of Technology, Bombay in Structural Engineering in 2013. Debashis Wadadar has been working in the Research Division of Indian Register of Shipping, Mumbai since 2013. His area of research is underwater explosion. He is currently an Assistant Surveyor in the Structures group in the Research and Rule Development Division of Indian Register of Shipping, Mumbai, India.



Mr. Masud Ali is an Indian by Nationality. Having obtained his Bachelor degree (B.Tech) in Civil Engineering with First class in the year 2008 from Jalpaiguri Government Engineering College, Jalpaiguri, he took his Post-graduate degree (M.Tech) with First class from the Indian Institute of Technology, Kharagpur with specialization in Structural Engineering in 2011. Masud Ali has been working in the Research Division of Indian Register of Shipping, Mumbai since 2011. His area of research is underwater explosion and its effects on floating and submerged structures. Masud Ali is presently working as Assistant Surveyor in the Structures group in the Research and Rule Development Division of Indian Register of Shipping, Mumbai, India.



Dr. Asokendu Samanta is an Indian by Nationality. Having obtained his Bachelor degree (B.E.) in Civil Engineering with First class in the year 1991 from Bengal Engineering College, University of Calcutta, he took his Post-graduate degree (M.E.) with First class First from the same university with

specialization in Structural Engineering in 1993. Subsequently, he obtained his Doctorate Degree (Ph.D) from the Department of Ocean Engineering, Indian Institute of Technology, Kharagpur in the year 1999. He worked as a Post-doctoral research fellow at the Robert Gordon University, UK during 2003-2004. He also completed Post Graduation in Business Management from XLRI, Jamshedpur in 2011. Dr. Samanta worked as a Visiting Faculty of Ocean Education and Research Centre, Mumbai, Reviewer of an International Journal. He is a Chartered Engineer (C.Eng) and a member of several distinguished societies. Dr. Samanta has experience in working in the field of finite element with structure for more than twenty years and has several publications in the reputed international journals to his credit. He is listed in Marquis Who's Who in the World, for his outstanding achievement in his field. Dr. Samanta has been working in the Research Division of Indian Register of Shipping, Mumbai for more than fifteen years and is presently holding the post of Vice President and Head of Structures Group in that concern.

Challenges in Aluminium Planing Craft Design and Production - Structural Aspects

[1]Mr. Tathagat Kumar Parthsarthy
Marine Engineering Centre
Larsen & Toubro
Chennai, India
Tathagat.parthsarthy@larsentoubro.com

[2]Mr. Anand Suresh Chimanpure
Marine Engineering Centre
Larsen & Toubro
Mumbai, India
Anand.chimanpure@larsentoubro.com

[3]Cdr (Retd.) Atul Killedar
Marine Engineering Centre
Larsen & Toubro
Chennai, India
Atul.killedar@larsentoubro.com

Abstract— **Aluminium Boat building throws huge challenges towards Shipbuilders worldwide. Moreover, problems intensify many folds when it comes to design and manufacture the planing craft with aluminium for the first time. Some precautions, if taken at the stage of initial design itself; would surely help in delivering final product with superior quality and performance. This paper is a case study of the planing craft indigenously designed and manufactured by L&T's Shipbuilding Division.**

Keywords—Aluminium, Plannig Craft, Structure Optimization, Weight, Welding, Distortion

I. INTRODUCTION

Ship Design in general and structure design in particular is an iterative process. Design of structure is influenced by many important factors like loading, ship speed, yard capabilities etc. To give the justice to each factor while designing brings in the need for optimization with holistic approach. There is a closer link between design and fabrication, and the design must often have to be changed to fit the advantages and limitations of construction capabilities.

The paper will be touching upon various challenges faced during design as well as production stage and will describe the steps taken towards addressing the challenges with typical examples. Paper will also discuss some lessons learnt during the project as Do's and Don'ts of designing and manufacturing the Aluminium planing craft.

II. DESIGN STAGE

A. Design optimisation:

The structure has to be optimized taking into account the ease of production (assessing advantages and limitations of construction capabilities) and strength requirements, given that the material in question is Aluminium. Many aspects such as Weight, availability of raw material, welding accessibility, and structure testing requirements though seem trivial initially, may become critical in later stage of fabrication. Following typical examples would portray the challenges involved in optimising the design at pre-manufacturing stage as well as post-manufacturing as lessons learnt.

1) Prevention of Fatigue Cracking:

Aluminium is more sensitive to fatigue as compared to steel. Studies have revealed that Aluminium has a crack propagation rate under fatigue loading that can be as much as 30 times greater than that of steel under the same applied stress intensity factor range. When a crack reaches appreciable size in an aluminium hull, it can grow quickly and lead to catastrophic hull failure. This calls for thorough study of the structural detail at the design stage. Earlier studies in this aspect show that fatigue sensitivity and notch sensitivity go hand in hand. In-service experiences have also revealed that lesser the welds, better the fatigue properties of the structure. In Interceptor boat, care has been taken to keep the weld butts away from the shape discontinuities by introducing integrated brackets. Where the chances of fatigue failure are high, the end connections are made with soft toe brackets.

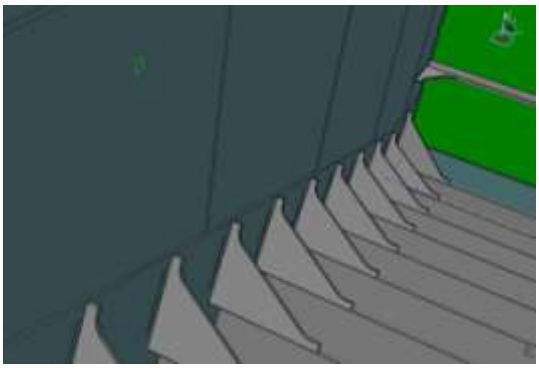


Fig. 1. Soft Toe Brackets for Bottom Shell stiffeners

2) Optimised Selection of raw material sizes to reduce the no. of seams/butts:

Selection of raw material sizes plays an important role in the detail designing. Raw material sizes have to be optimized for least weld seams/butts keeping in mind yard's material

handling and fabrication capabilities. Post first boat fabrication, a thorough study to reduce the number of weld seams/butts was carried out for entire ship plating. Significant reduction in the seams and butts for shell, deck and superstructure plating was achieved. A major weld seam reduction was achieved by combining Sheer strake (acting as fender base plate) with adjoining strake. Replacing two plates with a single plate was difficult in the forward region where 3D bending would have required. A prototype was prepared and tested for required bending. The results were positive. More than 50 m of butt welding could be reduced on the shell by joining these two plates. Similarly other design units could yield a reduction of more than 40 m additionally.

3) Structural Connections:

Structural connections should allow smooth flow of stress. Integrated brackets are highly effective in transferring the stresses in addition to their resistance to fatigue cracking. Locations such as the connection between deck frame and side shell frame, Bulkhead center girders terminating on bottom shell and deck center girders, etc. have been provided with integrated brackets. Additionally, this arrangement requires lesser welding unlike the conventional girder and bracket joints. This improves the strength of the joint and eases the fabrication efforts.

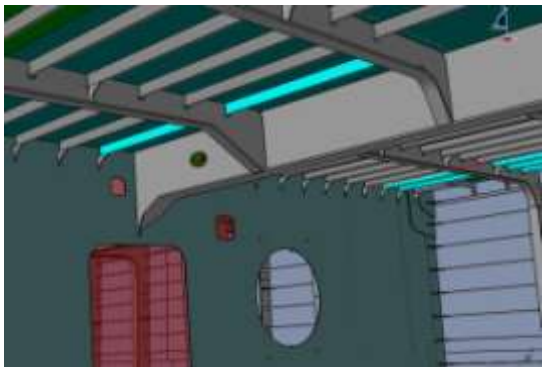


Fig. 2. End Brackets Integrated with Web Frames & Center Girder

4) Engine removal Soft patch support arrangements - A case study:

Being a maiden design, there were many avenues for improvement & optimization; one distinctive example being the Engine removal soft patch on main deck and superstructure deck. The interceptor boat is provided with two Engine removal soft patches per deck of the size of 3600mm X 1800mm. The cover is designed to take up the same loading as that of the deck. The seating for the cover, which also forms the part of primary deck framing, is designed to cater for holding the cover as well as compensate for the structural discontinuities formed due to the big cut-out. In addition, structural configuration has to be such that it provides clear area for engine movement through soft patch. The initial design though satisfying all the requirements had some drawbacks. Firstly, the arrangement was complex, and also had a large number of structural members which needed voluminous welding. After a careful re-look at the design, it was decided to do away with the bracketing support and introduce a simpler support arrangement which would also be better in strength. The new arrangement designed had almost 40% less parts and significant reduction in the weld length. Table showing the comparison between original design of Main deck soft patch support and the optimized design is provided below. Similar Results were obtained for Superstructure soft patch support also. Though the values seem small but for 50 boats, significant saving in terms of Man-Machine-Material would be achieved.

TABLE I. COMPARISON OF DESIGN PARAMETERS

Sr. No.	Parameter	Original Design	Post Optimisation	% Reduction
1	No. of structural members (Primary & Secondary)	130	82	37
2	Weight of the Arrangement (Kg)	231.4	163.7	29.3
3	Seam length (m)	126.4	110.1	12.9

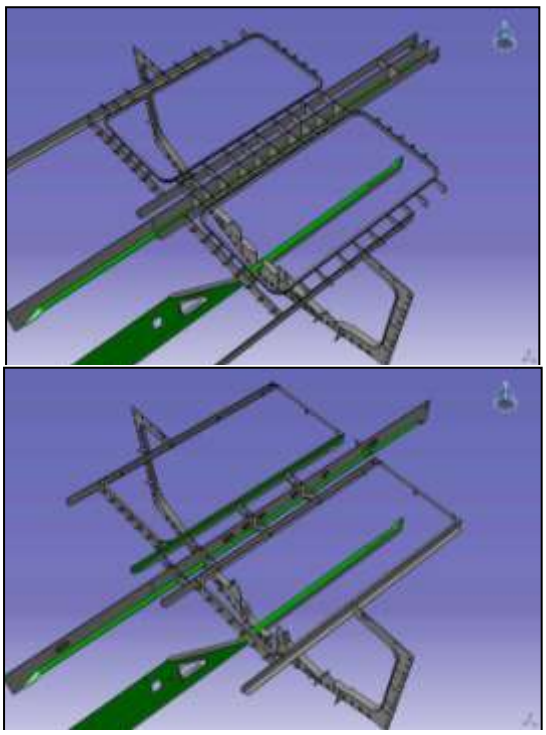


Fig. 3. Main Deck Soft patch Support Arrangement before (Above) & after (Below) Modification

5) Intercostal Arrangement:

Tanks which were designed as an integral part of either the side or bottom shell encountered a peculiar issue of leaks while undergoing tank pressure testing. The most common areas from where the leaking was observed were the weld joints between watertight collars and stiffeners/profiles.

The stiffeners were deigned to run continuously and tanks were made watertight with the use of collars. Later, the arrangement was altered to 'intercostal arrangement'. In this arrangement, stiffeners and other sections were terminated on the tank boundaries, completely eliminating the use of collars & associated welding. However, additional brackets were required on either side of tank boundaries to maintain the structural continuity. This arrangement not only saved time and effort of welding on complex profiles of bulb bars but also reduced the chances of repeated leaks observed during tank testing.

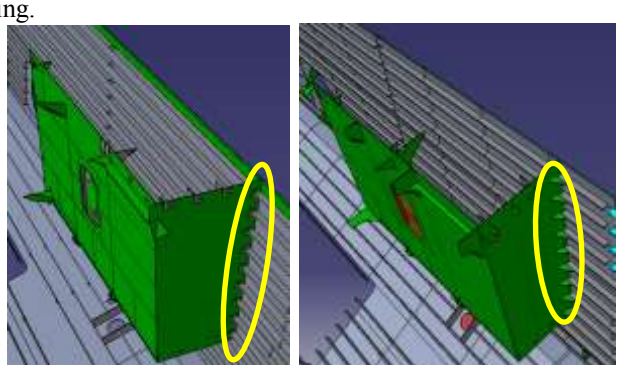


Fig. 4. Continuous Stiffener Arrangement (Left) & Intercostal Arrangement (Right)

6) Use of Flat bars in Forward Area:

Determining the structural configuration in forward area especially forward of collision bulkhead is vital. The area experiences heavy slamming loads hence needs to be adequately strengthened, on the other hand the bow area is quite narrow because higher dead-rise angle with the hull form having 3D bending. This brings in the challenge of forming the stiffener as well welding in-situ. To tackle this issue, longitudinal stiffeners in the forward were cut from plates (of material 5083 instead of using usual 6082 Bulb bars).The developed size of these plates, extracted from 3D modelling software could take care of bending along one of the axes. Thus required stiffener profile could be achieved by mere uni-axial bending.



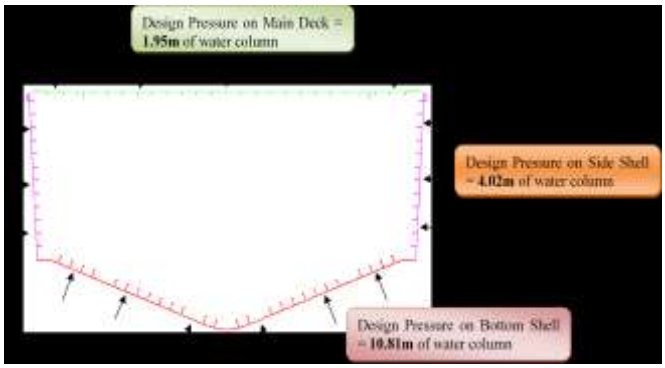
Fig. 5. Flat bars used as Longitudinal Secondary members

B. Weight sensitivity:

In a typical planing craft, both the weight and the centre of gravity play a vital role in determining the speed of the craft in addition to the hull form. Even with a marginal change in the theoretical displacement, speed criteria would become difficult to achieve. It is like walking a tightrope to manufacture a boat with the final displacement same as that of the design stage displacement values. During the design stage itself some target areas as discussed below, were identified and focused to optimize the structural weight. This was supplemented by meticulous weight monitoring at each stage of the fabrication.

1) Plate thickness optimisation:

Plates constitute nearly 70% of the total structure weight hence is the primary target area when it comes to structural weight optimization. However, areas like bottom shell & Bulkheads experience heavy loads and can be detrimental if they are over optimized.



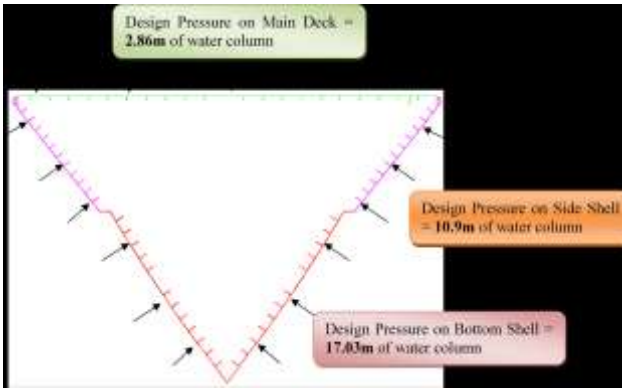


Fig. 6. Pressure Distribution At Forward And Aft Sections

To select the midway, in the Interceptor boats, areas were identified namely side shell, inner deck, part of main deck and superstructure to optimize the plate thickness depending on the global as well as local loads they will experience during service life. It was observed, even for these structural members, the design pressure values were higher in forward as compared to aft due to predominant slamming pressures in the forward. Following figures show the typical pressure distribution across the transverse sections in forward and aft of ship which is summarized in the succeeding table.

TABLE II. COMPARISON OF PRESSURE VALUES IN FORWARD AND AFT REGION

Sr. No.	Locations	Pressure at FWD Frames (m of water column)	Pressure at AFT Frames (m of water column)	Difference (m of water column)
1	Bottom Shell	17.03	10.81	6.22
2	Side Shell	10.9	4.02	6.88
3	Main Deck	2.86	1.95	0.91

For majority of these locations like main deck & side shell (in the aft half of the ship) as well as superstructure, 4 mm thick plate has been used which is quite rare in this type of ships.
A saving of approximately 15 % which amounts close to half a tonne could be achieved.

2) Scantling optimisation based on the detailed FE analysis:

Optimization of some of structural members (designed as per LR- SSC rules) was also done with the help of detailed Finite Element Analysis. The aim of the exercise was to redistribute the material as per stress requirements. The final scantling of structural members in water jet compartment is an example of such optimization. It is pertinent to mention that even classification societies approved the reduction in scantlings based on the detailed FE analysis. The scheme was further extended to other critical structures like Engine foundation, towing post etc. which has resulted in significant weight reduction.

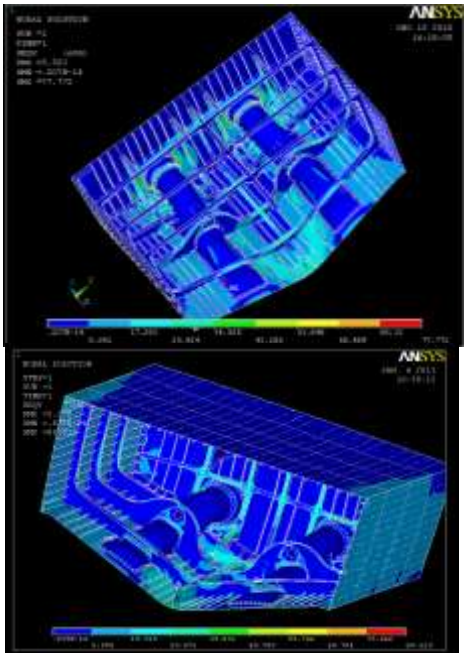


Fig. 7. Waterjet Compartment Stress Graph Before (Above) & After (Below) Optimisation

3) Weight optimisation in non critical areas:

Areas where structural strength was not of prime importance, arrangements which could yield light weight solutions were adopted. Partitions for galley, Compartment below wheelhouse deck were made of corrugated plates. The stiffened plate panel would have weighed 27 kg /m, as compared to 12.5 kg/m for corrugated plates, resulting in the weight saving of more than 50%. Some of the Primary structural members like Transverse frames and Center girders which were not coming in high impact load areas were provided with lightening holes. Holes were sized to achieve maximum weight reduction within the guidelines of classification society. At many places the cut-outs were used to pass through the cables & pipes which facilitated in decongesting the headroom area. Waterjet compartment though a critical area but was studied thoroughly for weight reduction. Waterjet ducts were changed from aluminium to GRP which gave substantial saving in the weight.

III. PRODUCTION STAGE:

A. Welding:

Welding is one of the most challenging activities in aluminium boat building. The sophistication of the process and high chances of distortion make welding a nightmare for many shipyards. To ensure an acceptable weld quality, there are two basic factors to consider; proper preparations to be done before welding commences and precautions to be taken during and after welding.

1) Aluminium: A different (Difficult?) material to weld:

Welding aluminium alloys is not more difficult or complicated than welding steel rather it is just different and requires specific training. Aluminium and its alloys are easy to weld, but their welding characteristics need to be understood and the proper procedures employed. Workers have to be trained to understand the differences between aluminium and steel fabrication, especially workers, who need to learn new procedures. Welding in an enclosed area is desirable for steel but it is a necessity for aluminium as they are prone to contamination.

Listed below are some of the interesting properties of Aluminium which make it a different metal to weld.

TABLE III. COMPARISON BETWEEN MATERIAL PROPERTIES OF ALUMINIUM AND STEEL

Property	Description	Implication
Melting Point of metal & their oxides	Aluminium oxides melts at 2060°C, 1400° C above AL whereas Iron oxide's melting point is close to or below the melting point of Metal	In Welding process it is essential to remove and disperse this oxide film before and during welding in order to achieve the required weld quality.
Specific heat	The specific heat of aluminium is twice that of steel.	Double heat input is required for welding Aluminium
Coefficient of thermal conductivity	The coefficient of thermal conductivity of aluminium is six times that of steel	The heat source for welding aluminium needs to be far more intense and concentrated than that for steel.
Coefficient of thermal expansion	The coefficient of thermal expansion of aluminium is approximately twice that of steel	Unacceptable buckling and distortion during welding.
Modulus of elasticity	Aluminium has a modulus of elasticity three times that of steel.	AL will deflect three times as much as steel under load
Colour change with temperature rise	Aluminium does not change colour as its temperature rises unlike steel, making it difficult for the welders to judge when melting is about to occur.	Adequate training of the welder when converting from steel to aluminium welding.

Aluminium suffers a reduction in strength in the weld area unlike Steel. When stressed, a welded aluminium structure will incur local deformation in the welded area first. The reduction in mechanical properties that occurs across the weld zone when aluminium alloys are welded can be easily seen as per the details shown below:

TABLE IV. ALUMINIUM: MECHANICAL PROPERTIES

Metal	Yield strength (N/mm2)		% Reduction	Ultimate Tensile Strength (N/mm2)		% Reduction
	Un-welded	*Welded*		*Un-welded*	*Welded*	
Al 5083 H 116	215	125	41.86	305	275	9.83

Keeping all the above aspects in mind right from the beginning of construction, L&T Shipyards have invested heavily in the facilities to augment the aluminium welding expertise. The yards have been provided with fully covered dust free weld zones. These zones help in protecting weld from the wind, Moisture, even high humidity, which can have a serious effect on the quality of aluminium welds. Enclosures also prevent the welded assemblies from exposure to sun light, thus reducing the distortion/Warping caused by regular temperature variations.

Training of welders has been pacified with the use of welding simulators. These sophisticated simulators working on VR technology, had an edge over conventional training as these are interactive tools for self learning. Welders could do the experimentation themselves and understand the process thoroughly.

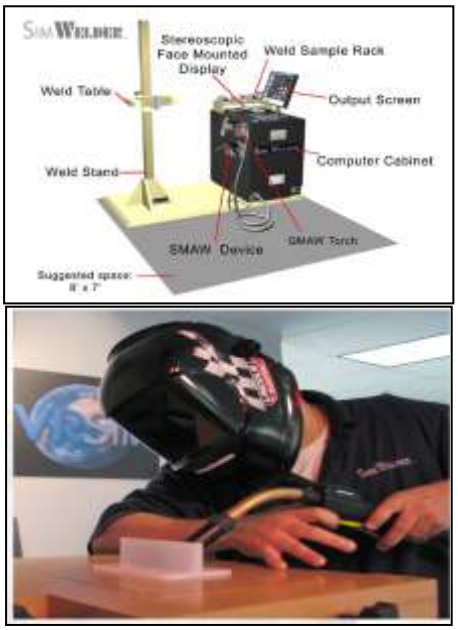


Fig. 8. Welding Simulator & practicing with the Simulator

Quality of aluminium welding primarily depends on the skill level of the welder. To minimise this manual intervention, robotic welding was introduced in L&T's Hazira yard. Robotic welding has got dual advantage of speed as well as defect free welding. Majority of weld joints on flat panels like Bulkhead plating, superstructure assemblies and even welding of flange to web of T-frames have been carried out by robot. Controlled and constant heat input ensured significant reduction in weld distortion.



Fig. 9. Robotic Welding in Progress & Enclosure with sliding roof for Robotic Welding

2) Weld type optimisation:

After successful sea trials of first of total 54 boats, need was felt to relook at the weld types being used, for rationalization. Aim was to reduce the yard efforts, distortion and time spent during welding. Areas were identified where double continuous fillet weld could be reduced to chain intermittent or staggered intermittent fillet welding. The changes were in accordance with the class requirement. Total of about 620 meters of reduction in weld length has been achieved per boat. Following table shows the design unit wise optimization done in weld types. It is evident from the table that almost all structural members have undergone through this exercise and sizable changes could also take place, the reason might be the extra conservative approach followed initially, as this was first of its kind project for L&T shipbuilding.

TABLE V. DESIGN UNIT WISE OPTIMISATION

Sr. No.	Design Unit	Targeted Members	Weld Type Change
1	Side Shell	Primary & Secondary	CIF to SIF
2	Main Deck	Primary & Secondary	DC to SIF & CIF to SIF
3	Inner Deck	Primary & Secondary	DC to SIF & CIF to SIF
4	Bulkhead & Transom	Primary & Secondary	DC to CIF & CIF to SIF
5	Superstructure	Primary & Secondary	DC to CIF & CIF to SIF

DC= Double Continuous Fillet, SIF=Staggered Intermittent Fillet, CIF= Chain Intermittent Fillet

B. Distortion:

Aluminium is more prone to distortion from welding than steel. In addition, the physical and mechanical properties make aluminium more vulnerable for distortions and deviate from tolerances even during handling of panels/subassemblies. A small deviation in hull form may lead to significant change in the Resistance and eventually the performance. Distortions can occur in welded structure for a variety of reasons, including initial distortion of plates and shapes, residual stress in plates and shapes, misalignment and mismatch of structural elements, thermal loading, straightening stresses, and welding shrinkage. Typical types of distortion include longitudinal shrinkage, transverse shrinkage, angular distortion, Buckling and bowing. Succeeding sections deal with the distortion and the measures taken to minimize it.

1) Distortion Due to welding:

Welding is the prime cause for distortion. It becomes very difficult to contain the distortion values within tolerance limits for plates with lower thicknesses such as 4 mm. During the welding of main deck plating of Interceptor boat, deviation observed in flatness was quite alarming.



Fig. 10. Welding Distortion

Various methods were tried on the mock-up plates for reducing the distortion. The sequence of welding is very important to reduce weld distortion. In addition, heat input, nature of joints, amount of root gap etc. have to be also taken into consideration to address the problem. There are some guidelines laid by past studies on the topic which can be summarized as under;

- Butts and seams in plating should progress outward from the center, with butts in strakes of plating welded before the longitudinal seams.
- It is beneficial to weld only small portions at a time, welding short intermittent beads, and returning to the weld seam, after structure farther away has been welded.
- For smaller craft and in not-critical structure, such as deckhouses, intermittent fillet welds may be used to reduce distortion.
- The plate should not be free to rotate about the axis of the weld during welding.
- The design of the joint should be symmetrical, as should the welding procedures.
- Pre-setting the parts such that the contracting weld metal pulls them into proper alignment when the weld cools is a common way of using the shrinkage of the weld metal to advantage.
- Minimum welding heat should be used, and excessive filler material should be avoided. Fillet welds should also be made with minimum heat input, and the fillets should be no greater than required for strength.
- To minimize weld size, the fit-up should be made as accurate as possible to minimize root gaps and irregularities in the root gaps. Small, uniform root gaps will minimize the amount of weld metal required.

Majority of the above points were incorporated as applicable during the mock up testing. In addition, some novel options like Roller Jacking fixture and Beam Box Assemblies were tried.

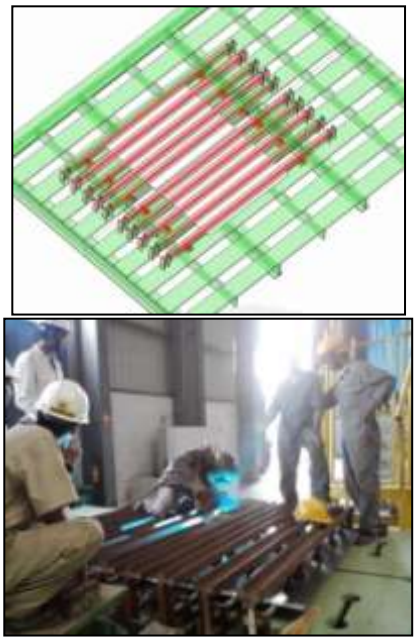


Fig. 11. Roller Jack Fixture Assembly

Roller jacking fixture comprised of two sets of roller arrays. The plates to be welded were sandwiched between the two arrays. This would constrain the movement of plate along the axis of weld but allowed the in-plane movement perpendicular to the weld.

Beam box assembly on the other hand is the simpler option with two heavy beam boxes being used for constraining the movement of plates being welded. The results were compared and it was concluded that the use of beam boxes combined with implementation of some of the above guidelines yielded least distortion values (within the tolerance limit).

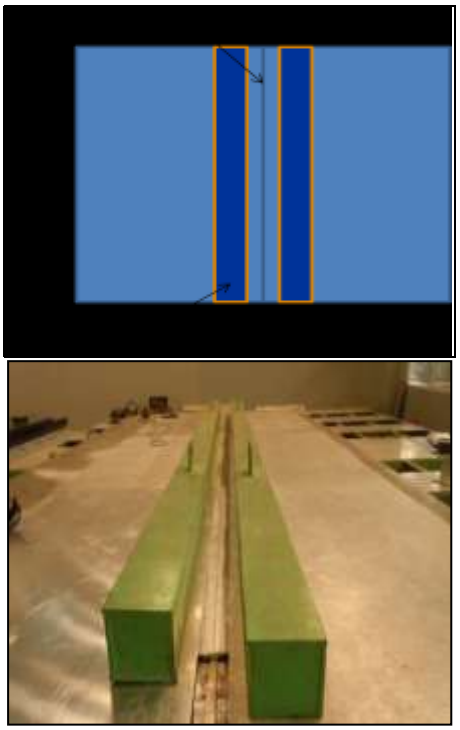


Fig. 12. Beam Box Arrangement

2) Distortion Due to Reasons other Than Welding :

Distortion in shipbuilding is cumulative, with the distortions occurring at one stage of construction carried over to the next. If distortion and misalignment is corrected at an early stage, there will be fewer distortions in the latter stages of construction. For this reason, it is important that initial panel fabrication be as free of distortion as possible. When distorted shapes are welded to uneven plate to form a stiffened panel, forces are required to bring the two together. The shapes are much stiffer than the plate, but residual stresses will remain after fabrication, and these stresses will contribute to the overall distortion of the panel. When a structural assembly is fabricated, the above distortions, the distortions produced by

welding, and errors and tolerances in cutting will mean that adjacent structural assemblies will not fit together precisely. Adjustments to align assemblies include forcing them together, which produces residual stresses that can lead to distortions of the combined structure, and overall distortion of the hull. Welded aluminium structure generally has less residual stress than comparable steel structure. However, the reduced buckling strength of aluminium means that it will tend to have greater distortion for the same level of residual stress, especially in plating.

Broadly there are two philosophies for producing the structure. Some shipyards produce stiffened panels, and have special aluminium panel lines for this purpose. In such panel construction, plates are butt welded to form large panels prior to the welding of frames and stiffeners. Stiffeners are welded first in mechanized stations, and then the frames are fitted over the stiffeners and welded. Curved hull sections are formed by laying the plates in jigs that are curved to the shape of the hull; butt welding them, and then fitting the stiffeners and frames. L&T Shipyards have favored "stick" construction methodology, an alternative to panel construction which is very advantageous for small planing crafts. Bulkheads and frames are first laid up and tack welded together. Stiffeners are then fitted to the frames, and the entire assembly is welded. The plating is then laid over the stiffening, and welded to the frames and stiffeners. Access to the details of stiffener-frame intersections is better prior to welding the plate, and makes these details easier to weld, especially for the small stiffeners typical of smaller craft. Alignment of intercostal members is easily accomplished when they are welded prior to welding the plate. The hull is constructed in the inverted position, so the welding of plating to stiffeners will be in the overhead position. Studies have shown that the method yields significant reduction (30-40%) in distortion.



Fig. 13. Stick Construction Methodology

A well-aligned structure when subjected to uneven temperatures, such as heating from the sun, will distort appreciably. The higher thermal coefficient of expansion of aluminium makes it more susceptible to this type of distortion, and therefore fabrication of aluminium is generally done under cover. The facilities provided in the yard to take care of this concern are covered under section about welding.

During the fabrication stage of the interceptor boats, due care has been taken during handling of the structural assemblies and also entire hull during turning. Flat panels were handled with pneumatic vacuum cups.



Fig. 14. lifting of Bulkhead with frame of Vacuum cups

For safe and distortion free turning of the main hull body, a rotating fixture assembly was designed. Not only the fixture ensured the uniform loading on structural members, it also ensured avoidance of sudden jerks during the entire turning process.



Fig. 15. Innovative Boat Turning Fixture

3) Distortion Monitoring:

Distortion control is a closed loop activity which starts with preventive measures and ends with monitoring as a feedback. During the Interceptor boat manufacturing, stage wise distortion monitoring was ensured. Hull measurements were taken meticulously at every stage, be it a keel sighting, panel fabrication level, pre-turning and post-turning of hull or after final welding. Sophisticated instruments such as Faro tracker were deployed for the task. This ensured precise inspection data and eventually helped in deciding corrective measures.



Fig. 16. 364 Points Inspection for Skid Using Optical Instrument Faro Tracker

IV. CONCLUSION

Aluminium has become the material of choice for many types of vessels, particularly high-speed vessels where Lightweight structure is important for meeting design goals. The methods of design and fabrication of aluminium contain many areas of conservatism. This approach escalates for beginners even further because of fear to go wrong. Paradigm shift in this thinking can be brought in by aggressive research, and determination to take bold steps for continuous improvement. This would surely result in greater performance of the product at reduced cost.

REFERENCES

[1] Ship Structure Committee 2007, SSC-452 “Aluminium Structure Design and Fabrication Guide”

[2] Robert A. Sielski, “Research Needs in Aluminium Structure”, 10th International Symposium on Practical Design of Ships and Other Floating Structures Houston, Texas, United States of America © 2007 American Bureau of Shipping

[3] Matthew Collette, University of Michigan, Robert Sielski, Consultant, “Aluminium Ship Structures”

Influence of Biofouling on the Metallic Corrosion in Singapore Seawater

D.J. Blackwood[1],
[1]Department of Materials Science& Engineering
National University of Singapore
Singapore 117576
e-mail: msedjb@nus.edu.sg

C.S. Lim[2] and S. L. M. Teo,[2]
[2]Tropical Marine Science Institute
National University of Singapore
Singapore 117574

Abstract— **Biologically induced corrosion various metals and alloys was investigated at three different test sites off coast of Singapore. By inspection of fouling species on the coupons after exposure revealed that the fouling species varied with both location and type of metal. Moreover, these fouling species showed different influences on the metallic corrosion, which was microscopically examined. The extent of fouling was found to decrease with increasing copper content in the alloys. For 316L stainless steel fouling was more diverse than on mild steel with barnacles which caused localized corrosion in a manner that appeared to be related to shape of the barnacle base, with most of corrosion sites were found under dead barnacles located at the edge of the colony and with sizes around 8-12mm. On some specimens serve localised corrosion was observed that appeared to be initiated by oysters. Although the extent of the attack on the surface looked low, within the metal long tracks (centimetres) of internal corrosion developed.**

Keywords— Biofouling, Localized corrosion, Metals & alloys

I. INTRODUCTION

Marine corrosion of metals in natural seawater is the result of interactions between the metal, living organisms and seawater chemistry [1]. When metal is immersed into seawater, corrosion and biofouling occur on approximately the same time scales [2]. Biofouling is the colonization of organisms, initiated by planktonic larvae attracted onto the surface and then increasing in thickness [3]. During the early stages of biofouling, the metal surface is in equilibrium with the biofilm, which consists mainly of bacteria and microbes. After a longer time exposure, the biofilm is overgrown by larger organisms like diatom and macro-organisms such as barnacles. Corrosion can start in the early biofilm or micro-fouling stage and be propagated in the macro-fouling stage.

Most of the previous research on biocorrosion focused on the effect of bacteria on metallic surfaces in the early micro-fouling stages [4]. With respect to macro-fouling, field exposure experiments can provide general corrosion data, such as corrosion rate and corrosion form [5]. Less attention has been placed on the macro-fouling stage, due to the difficulty of monitoring the effects of macro-foulers. The present model for corrosion during the macro-fouling stage focuses on the formation of oxygen concentration cells between the metals' surfaces and the macro-fouler attachment [6]. The relationship between macro-fouling and corrosion on metals is less discussed, especially, for metals with different corrosion resistances. Biofouling has been reported to cause some localized corrosion [6], but the processed leading to this is poorly understood.

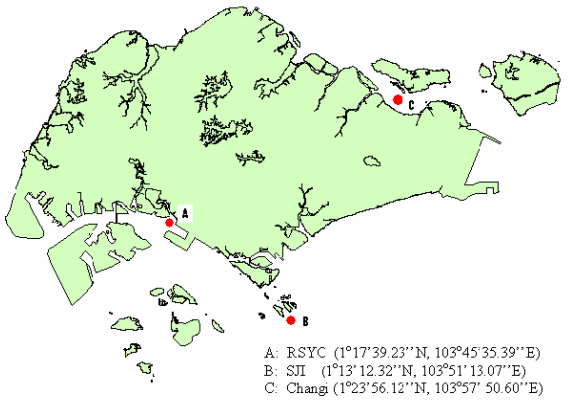
The marine environment around Singapore is typical of Southeast Asia coastal seas: temperatures vary only slightly throughout the year, 29 ±1°C, and the seas support a high biodiversity, which contributes to a high settlement rate of fouling organisms [7,8l]. In this present work exposure experiments and in-situ open-circuit potential (OCP) monitoring were used to study the corrosion and fouling patterns on dissimilar metals, in different coastal areas around Singapore, which has allowed a discussion on the influence of fouling on metallic corrosion.

II. EXPERIMENTAL

Six different metallic alloys; mild steel (MS), grade 316L stainless steel (SS316L), Monel (30Cu-70Ni) and a 70Cu-30Ni cupronickel alloy (Cu-Ni), having poor to very good corrosion resistances, along with highly corrosion resistant titanium and grade UNS S31254 stainless steel (SMO) were chosen to be exposed at three different test sites around Singapore offshore seawaters; namely the Republic of Singapore Yacht Club (RSYC), Changi, and St. John's Island (SJI) the locations of which are marked on the map in Fig. 1[a].

In exposure experiments clusters of pre-weighed samples measuring 100mm x 100mm x 2mm were arranged at equal distances by placing them on a stainless steel rod coated with silicone tubing (10mm diameter) to provide electrical isolation.

The experimental setup was designed to allow samples to be retrieved for examination after set periods of immersion to allow fouling weight, sample weight, fouling species composition and distribution of fouling on different panels to be assessed. Fouling species scoring was conducted with Photogrid 2.0 on 200 random points on both sides.



a

Fig. 1. Locations of three test sites around Singapore.

Weight loss testing panels of most of the alloys were retrieved after exposures of 3 (steels only), 6, 12, 24 and 30 months; expect for the highly corrosion resistant Ti and SMO stainless steel that were only retrieved after 24 and 30 months. Fouling species was scored after 40 psi water jet cleaning. Corrosion product was removed by specific acid treatments as shown in Table I[b] and corrosion rates were evaluated from weight loss. Corrosion morphology at the metal surface was investigated by visual inspections and SEM observations.

III. RESULTS

A. Biofouling Species Composition and Weight

The dominant fouling species was different at each test site, being: at SJI initially being from algae settlement but with time the variety of fouling species increased so that after 12 months oysters and barnacles dominated; at Changi barnacles, mussels and sponges were initially the main species with very few oysters, but over time green mussels became completely dominate; at RSYC the initial fouling pressure was from calcareous polychaetes but these were quickly overtaken by oyster and barnacle settlement. Fig. 2 shows that biofouling diversities at SJI and Changi location were higher than RSYC, possibly due to leaching of antifoulants from the hulls of yachts moored at the latter. The abbreviations for fouling species are: Barn: barnacles, Mag: green algae, Mol: mollusks, Stun: solitary tunicates, Pcal: polychaete tubeworms with calcareous tubes, Rst: rust, Psed: polychaete tubeworms with sedimentary tubes, Mab: brown algae, Br: arborescent bryozoans, Eb: encrusting bryozoans, Clut: colonial or compound tunicates. The diversity of fouling species materials decreased with increasing copper content, which is consistent with the release of toxic cupric ions [9].

TABLE I. [b]

Reagent for cleaning and removal of corrosion products from retrieved coupons		
Material	***Chemicals***	***Temperature and time***
Mild steel	20% NaOH, 200 g/L zinc dust	Boiling for 5 min
Stainless steels	10% HNO3	60 °C until clean (3-5mins)
Monel	15% HCl	25 °C until clean(10mins)
70Cu-30Ni	15% HCl	25 °C for 2-3 min
Titanium	No corrosion	-

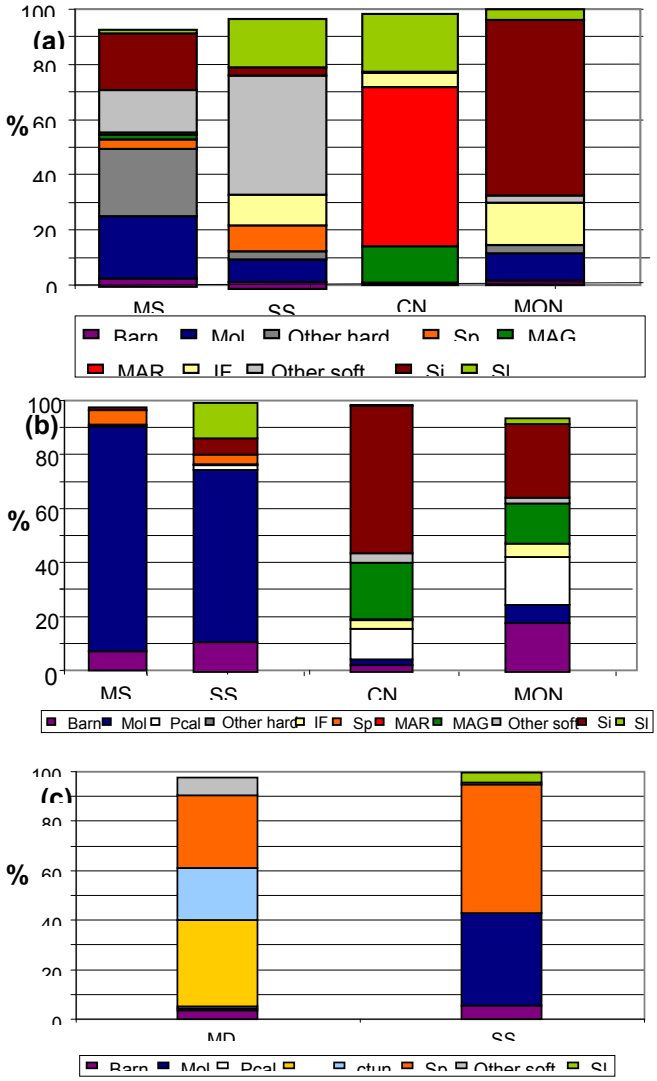


Fig. 2: Percentage covered by various fouling species after 12 months at (a) SJI; (b) RSYC; and (c) Change test sites.

B. Weight Loss

The weight loss experiments showed that the corrosion rates at SJI and Changi slowly declined by about 30% over the course of the 30 month duration. However, at RSYC there was a minimum in the corrosion rate at 12 months, which corresponds to the maximum in the fouling rate. It thus appears that the mass of the biofouling was protective. For the stainless steels the corrosion rate was higher during the first 3 to 6 months, but then declined by about 50% and adopted a fairly stable vale for the remainder of the 30 month duration. Comparing the corrosion rates of the 316L stainless steel at the three locations, during the first 3 months of immersion the weight loss was inversely proportional to the extent of biofouling, indicating that the fouling was protective. However, this correlation was lost in the 6 months data, suggesting that protection offer by the biofilm is only short-lived, possibly due to the growth of more macro-foulers in the long-term inducing localized corrosion. The copper based alloys corrosion rates did not vary considerably with time, whereas no measurable weight loss occurred from the Ti and SMO stainless steel. Table II shows the corrosion rates as determined from the weight-loss coupons. Based on the Monel, mild steel and 316L stainless steel, it seems that the on the corrosion rates are higher at SJI, than RSYC and least at Changi. The low corrosion rate of the 316L stainless steel at Changi might be associated with the lower incidence of oysters at this location, where the green mussels were the dominate mollusc found.

The corrosion rates at SJI and RSYC are higher than most literature values (Table II), although part of this may be due to the higher temperatures in the tropics this cannot explain why the Monel at SJI was corroding at almost twice the rate compared to the same material located in RSYC. At both locations the extent of biofouling on the Monel was low, due to the toxicity of Cu^{2+} ions, and not largely different in terms of weight. However, the nature of the biofoulers were different with composition at SJI being dominated by encrusting bryozoans, algae and tubeworms/vermetids, while at RSYC barnacles, tubeworms and oysters were dominant. Thus unlike 316L stainless steel it seem that soft foulers are more aggressive to Monel than hard foulers. In contrast the corrosion rate for cupronickel was remarkably similar at both SJI and RSYC with neither cupronickel nor Monel were tested at Changi, perhaps because the barnacles that caused shallow pitting were ubiquitous to all sites.

TABLE II

Summary of corrosion rates determined from weight loss monitoring (mm/yr)						
Test site	*MS*	*SS316*	*Cu-Ni*	*Monel*	*SMO*	*Ti*
SJI	0.25-0.35	0.005-0.01	0.01	0.04-0.06	0	0
RSYC	0.20-0.25	0.005-0.01	0.01	0.03-0.035	0	0
Changi	0.20-0.25	0.005-0.01	Not tested	Not tested	0	0
Literature [11]	0.12	<0.005	0.02	0.01	< 0.001	< 0.001

C. Mophology of Corrosion After Chemical Cleaning

Mild steel

The mild steel showed evidence of extensive general corrosion over all its surfaces, although pitting attack was also severe at localized regions. As a result of the corrosion rates were at the high end of those previously reported for steels in seawater, with complete penetration of the 2mm thick specimens occurring over a large fraction (ca. 20%) of the surface (especially at RSYC).

Stainless steel

On the 316L stainless steel pitting initiated within 3 months of immersion. Some of the corrosion pits were found under barnacle bases, especially under dead barnacles at the edges of colonies with diameters between 8 and 12 mm. Although it was noted that not all barnacles caused pitting corrosion two types of attack traces were found; one under the centre of barnacle base and the other under the edge of the base. The cause of the localized corrosion could be due to crevices forming under the barnacle bases resulting in differential oxygen cells on the metal surface [10]. Taxonomical examinations show that all of the barnacles, both those causing and not causing pitting corrosion, belonged to the same species *Balanus reticulatus*.

The most damaging localized corrosion appeared to have been oysters, being especially bad when attack occurred at the coupon edges. In some cases tracks of crevice corrosion extended several centimetres inside the stainless steel and it is possible that this attack was imparted due to initiation from the grain boundaries at the edges from sheet rolling of the alloy, with the corrosion cutting a path between the grain boundaries. Almost complete penetration of the 2 mm 316L stainless was observed on specimen retrieved from Changi after just 6 months, with the pit initiation site being found under an oyster (Fig. 3). On the surface this pit appeared a small pin-hole (Fig. 3c) but cross sectional analysis shows that acidification of the solution in the occluded cell caused extensive corrosion below the surface (Fig. 3d).

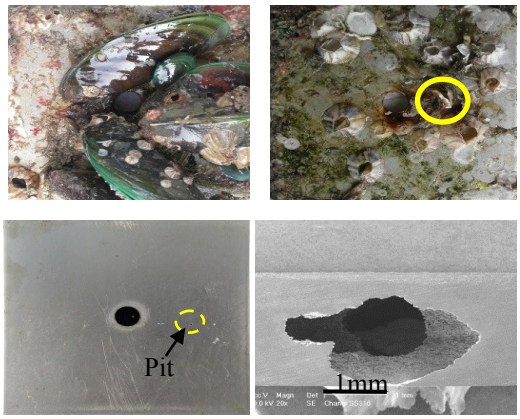


Fig. 3: Photographs of 316L stainless steel coupon removed from Changi test site after 6 months of immersion. (a) Prior to cleaning green mussels are the dominant species; (b) After water jet cleaning at 120 psi an oyster can be seen (circled); (c) chemical cleaning revealed a pit opening beneath this oyster; (d) cross-section of the pit revealing extensive subsurface corrosion.

However, later specimens retrieved from the same site did not show similar attack, these also did not have any oysters attached, but did displaying broad hemi-spherical crevice attack under barnacles up to 0.5 mm deep.

Complete pit penetration of the 316L stainless, similar to that of the 6 month Changi sample, was observed on all specimens retrieved after 12 months or more exposure from both RSYC and SJI. In each case the penetration was restricted to a single cluster of pin-holes no more than 10mm apart and the initiation sites seem to be associated with oysters, which are far more prevalent at these two sites than at Changi.

Once the biofoluing was removed it could be seen that crevice corrosion had also occurred around the central connection point, i.e. between the sample and the silicone tubing, even within three months. However, this was much less evident at Changi than the other two locations so it appears this crevice corrosion is accelerated by the macro-foulers predominately found at SJI and RYSC, i.e. oysters and not the green mussels found at Changi. A possible reason for the more extensive corrosion under oysters is they cement themselves down to give a much stronger attachment than mussels that attach by only a disk which is attached to the byssus thread. The secretions between the oysters are also very different from barnacles and mussels, likely less permeable.

Copper-nickel alloys

The 70Cu-30Ni alloy had the least amount of attached fouling, but many corrosion pits were still associated to barnacles. In this case, the pits were shallow and distributed across the whole area beneath the barnacle (Fig. 4d). Reddish areas appeared on the surface, a sign of denickelification, resulting in a higher surface copper content rendering the surface toxic and less favourable for larvae settlement. For the Monel alloy weight loss was mainly caused by a combination of both crevice and pitting corrosion, but only a few pits appeared to be caused by barnacles, even though many barnacles were present on the panels.

Most of the pits on the Monel appeared as pinholes, similar to those seen in sterile saline solutions, and distributed across the whole surface (Fig. 4 c). However, some of these pits were deeper than seen on the cupronickel alloy, being up to 1 mm after 12 months and SEM observations revealed that the corrosion in these pits was intergranular in nature (Fig. 5). The edges of the Monel specimens were also severely than on cupronickel, suggesting end grain attack (a form of integranular corrosion).

In addition to the number of corrosion sites the extent of the weight loss due to localized corrosion also depended on both the corrosion morphology and its depth. For example, the weight loss on Monel was more than on the 70Cu-30Ni alloy, even though the localized corrosion coverage on Monel was lower, since the pits were deeper in the Monel alloy.

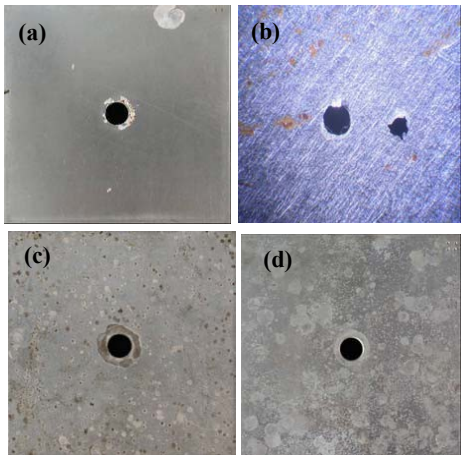


Fig. 4. Photographs showing pitting corrosion on different alloys retrieved after 6 months of immersion and chemically cleaned: (a) SS 316L panel from RSYC;(b) Pits on SS316L panel from Changi; (c) Pits on Monel panel from RSYC; (d) Pits on 70Cu-30Ni panel from RSYC.

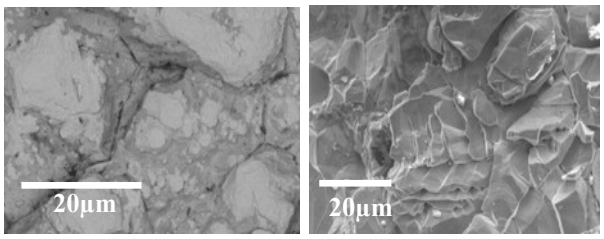


Fig. 5. SEM view of corrosion morphology of Monel and 70Cu-30Ni panels after 6 months exposure.

Titanium and UNS S31254 stainless steel

Both Ti and SMO showed characteristically strong corrosion resistance after 30 months immersion at the 3 test locations in RSYC, SJI and Changi. Despite being heavily fouled there were no noticeable corrosion signs on the metal surfaces or weight loss measured from these coupons.

IV. CONCLUSIONS

Biologically induced corrosion of various common metal alloys have been investigated at three different test sites off the northeast and south coasts of Singapore over a 30 month period. A wide range of bio-organisms were found at each site, with the dominant fouling species being different at each test site. There was less variety at RSYC, possibly due to leaching of antifoulants from the moored yachts. Although the extent of fouling generally increased with time it varied considerably with location, with the SJI site producing less fouling than the other two sites. However, no correlation was found between the extent of biofouling on the various alloys and their relative corrosion rates, although the presence of oysters did induce the worse corrosion in 316L stainless steel.

The biofilms formed on both mild steel and 316L stainless steel were initially protective. However, over time the mild steel's loose corrosion products fail from the surface, taking the biofilm with it, revealing fresh material to be attacked. As a result the long-term corrosion rate of mild steel are higher in Singapore seawater than most of the literature values (in part due to higher tropical temperatures) with 2 mm thick plates being completely penetrated by general corrosion inside of 30 months (especially at RSYC).

Likewise in the longer term the protection afforded to the stainless steel was lost, possibly due to the growth of oysters and barnacles that induced localized corrosion. For corrosion related to barnacles, especially under dead barnacles at the edges of colonies, two types of attack traces were found; one under the centre of barnacle base and the other under the edge of the base, though both gave rise to hemispherical pits consistent with crevice corrosion. However, it was also found that not all barnacles caused pitting corrosion, even though taxonomical examinations show that all of the barnacles present were *Balanus reticulatus*, it is still not known why only certain dead barnacles initiate corrosion. However, the fact that the deepest pits in the 316L stainless steels, with complete pin-hole penetration of the 2mm thick plates within 12 months, were associated with oysters and this was especially bad when attack occurred at the coupon edges; in some cases tracks of crevice corrosion extended several centimetres inside the stainless steel. For the 316L stainless steel it is claim that oysters cause more localised corrosion (deep pits) than barnacles (shallow crevices) than green mussels (limited attack).

At all the sites both the diversity of the foulers and the weight of the fouling decreased with increasing copper content in the test alloy, due to the release of toxic cupric ions, nevertheless organisms still attached to even the 70Cu:30Ni cupronickel alloy and barnacles induced shallow pitting corrosion of this material, but there was little variation in the corrosion rate of this allow with location, perhaps because barnacles were ubiquitous to all sites. In contrast Monel was found to suffer end grain corrosion such that its weight loss was about four times that expected from the literature and this seem to be worse in the presence of soft-foulers; as yet no mechanism for the involvement of the biofoulers in the end grain attack has been established.

Despite attracting heavy fouling titanium and the high grade SMO stainless steel both appear to be almost immune to corrosion in Singapore seawater.

V. ACKNOWLEGMENTS

The authors acknowledge support from the US Office for Naval Research Award No. N00014-04-1-0789, the Singapore Defence Research & Technology Office Grant POD0411835 and partial funding under SERC grant No. 1123004034.

The authors thank Mr Razali and Ms Hu Xiaoping for their assistance in the early stages of the project.

References

[1] S.M. Gerchakov and B. Sallman, "Effect of marine organisms," in Seawater Corrosion Handbook, Noyes Data Corporation, 1979.

[2] A. Mollica, "Biofilm and corrosion on active-passive alloys in seawater," Int. Biodeter. Biodegr., vol. 29, pp. 213-229, 1992.

[3] H.A.Videla, "Biofilms and corrosion interaction on stainless steel in seawater," Int. Biodeter. Biodegr., vol. 34, pp. 245-257, 1994.

[4] D.A Shifler, "Understanding material interactions in marine environments to promote extended structural life," Corro. Sci., vol, 47, pp.2335-2352, 2005.

[5] S. C. Dexter, "Biofouling and biocorrosion," B. Electrochem., vol 12, pp. 1-7, 1996.

[6] A.H.L. Chamberlain, S.E. Simmonds and B. J. Garner, "Marine 'copper-tolerant' sulphate reducing bacteria and their effects on 90/10 copper-nickel (CA706)," Int. Biodeterior., vol. 24, pp. 213-219, 1998.

[7] G. Swain, A.C. Anil, R.E. Baier, F.S. Chia, E. Conte, A. Cook, M. Hadfield, E. Haslbeck, E. Holm, C. Kavanagh, D. Kohrs, B. Kovach, C. Lee, L. Mazella, A.E. Meyer, P.Y. Qian, S.S. Sawant, M. Schultz, J. Sigurdsson, C. Smith, L. Soo, A. Terlizzi, A. Wagh, R. Zimmerman. And V. Zupo, "Biofouling and barnacle adhesion data for fouling-release coatings subjected to static immersion at seven marine sites," Biofouling, vol. 16, pp. 331-34, 2000.

[8] M. Eashwar, G. Subramanian, S. Palanichamy, G. Rajagopal, S. Madhu and P. Kamaraj, "Cathodic behaviour of stainless steel in coastal Indian seawater: calcareous deposits overwhelm biofilms," Biofouling, vol. 25, pp. 191-201, 2009.

[9] S. Maruthamuthu, G. Rajagopal, S.S. Narayanan, M. Eashwar, and K. Balakrishnan, B. Electrochem., vol. 12, pp. 86-90, 1996,

[10] I. B. Beech, J. A. Sunner and K. Hiraoka, "Microbe-surface interactions in biofouling and biocorrosion processes," Int. Microbiol. Vol. 8, pp. 157-168, 2005.

[11] D. A. Jones, "Principles and Prevention of Corrosion,"Prentice Hall, 1996.



Associate Professor Daniel J. Blackwood obtained his PhD degree in Electrochemistry under Prof. Laurie Peter (University of Southampton 1986). He was a postdoc at University of Utah whefre he worked on developing FTIR techniques for exploring the electrochemical interface. In 1989 he received an Alexander von Humboldt fellowship to work at the Universität der Bundeswehr München on conducting polymer vapour sensors. In 1990 if he joined the United Kingdom Atomic Energy Authority at Harwell Laboratories as a project manager in the aqueous corrosion section, where he work on a number of industrial projects for both Government agencies and commercial companies. Since 1996 he has been in the Department of Materials Science & Engineering, National University of Singapore where his current research interests are in the fields of corrosion, porous silicon and electrochromic windows. Between 2000 and 2009 he was the chairman of the Corrosion Association Singapore.

Smart Nano-Composite Coatings for Aerospace Applications - A Holistic Approach

Smart Anti-Corrosion Coatings

Amitha rani B.E.[1], **Prakashaiah. B.G.**[2]
[1,2]Surface Engineering Division,
CSIR- National Aerospace Laboratories,
Bengaluru-560017,India
[1]amitharani@nal.res.in, [2]bgprakashaiah@gmail.com

***Abstract*—With the ban on hexavalent chromium corrosion coatings, there has been a boom of a plethora of coatings, vying as alternate replacement coatings. However, no coating till date has been able to match the chromium coating in totality. Our research involves an holistic approach to corrosion mitigation understanding, identification and fabrication of sustainable coatings. Our focus has been to primarily understand the substrate-coating interface interaction, through first-principles calculations using Density functional theory, rapid methods to zero down on a few promising coatings and subsequently development of sustainable aerospace coatings, instead of trial and error method. Polymer and sol-gel coatings doped with inhibitor loaded nano-containers have shown promise as selfhealing coatings on the aluminum alloy AA2024-T3. Interestingly, these coatings could function as standalone films in corrosion sensing and could be adapted to develop a corrosion sensor device. It would be idealistic to have a film that could sense and heal corrosion, thus lowering the loss encumbered by aircraft grounding and reducing economic loss.**

***Keywords*—AA2024-T3, scratch cell, indicator test, quick diagnostic, corrosion, smart coatings, self healing, corrosion sensor, first-principles ,sol- gel coating.**

I. Introduction

Several coatings are being fabricated to serve as alternate to the unmatched hexavalent chromium coating for corrosion protection. However, a holistic approach including prognosis, diagnosis and prevention would be the ideal way to combat corrosion and reduce exorbitant costs and downtime, especially with respect to the aerospace industry. The components of this approach are as follows, Prognosis - a sensor/test/film to detect any changes in the environmental factors that could result in corrosion initiation in the incipient stages. Diagnosis- first-principles calculations to understand how the environmental factors cause corrosion, interaction of the inhibitors/coatings with the substrate under study and subsequently using the first-principles knowledge to re-tailor or redesign sustainable smart coatings would be the prevention and control approach.

Corrosion sensors are available in various forms such as films, devices etc [1]. Corrosion in aircrafts generally is undetected in the joints, under skin and goes unnoticed. Thus, a flexible corrosion film that could be easily placed in these inaccessible locations would be desirable.

We have been working on the fabrication of polymer- CNT based flexible corrosion films [2] [3]. The films were fabricated by The corrosion sensor film in the present study was fabricated by three methods (Fig. 1).(i) Layer by Layer method (LBL) with the polyelectrolyte - Polydimethyldiallyl ammonium chloride (PDADMA) and single wall carbon nano tubes $(PDADMA/SWCNT)_{10}$ and $(PDADMA/SWCNT)_{20}$ layers. Polyelectrolytes are known to have pH sensing properties which qualify their use in corrosion sensors [4]. Polyelectrolytes have the further advantage of being 'green' in nature and combination of different polyelectrolytes can be engineered depending on the pH of the environment their use is desired. (ii) Electro-deposition of polyaniline (PANI) - CNT film was carried out on a carbon paste electrode in a cyclic voltameter [5]. The optimum strength of the two electrolytes Sulphuric acid and Hydrochloric acid containing PANI - CNT were optimised along with scan rate and other CV conditions. PANI is an ideal conducting polymer for a corrosion sensor as it can detect changes in most corrosion factors such as pH, ions, gas, humidity and optical changes [6]. (iii) Casting The PANI-CNT film was drop cast on glass slides and Polyethylene terephthalate films.

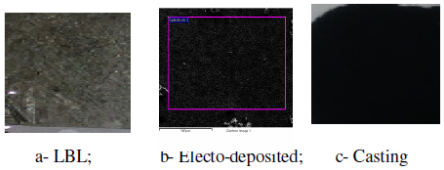


Fig. 1. FE-SEM of Polymer-CNT based corrosion sensing films

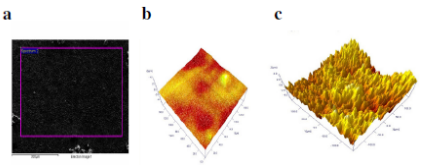


Fig. 2. AFM of electrodeposited Polymer-CNT corrosion sensing film

The film obtained by the LBL method was the best and was converted into a free standing film,while the the film obtained by electro-deposition was sensitive to pH changes but fragile. Also film obtained with HCl as the electrolyte was almost 4 times smoother than the one obtained with H2SO4 as the electrolyte (Fig. 2) The film obtained by the casting method was also a free standing film, but powdery in nature. Thus all further evaluations were performed using the LBL film.

A. Testing prototype Device:

The device was fabricated as shown in Fig. 3. The LBL film was cut into suitable size and a piece placed on a substrate. A small plastic well was set on the film with a diameter of 5mm to hold the pH solution. A four probe connection was obtained with copper tape and electrical contact was established with silver paste. A Keithley nanovoltameter was employed detect changes in resistance via a four point probe method. Solutions of pH ranging from 2 to 12 were pipetted into the chamber, while the nanovoltameter simultaneously measured resistance changes.

B. pH sensitivity

The LBL film showed a high sensitivity to different pH solutions and the bulk resistivity increased linearly progressively with increase in pH (Fig. 4).The pH sensing was viable for both acidic and alkaline solutions ranging from 1- 12. The pH sensitivity(Sp) was calculated using the formula [7]

$$Sp = \frac{\triangle R/A}{\triangle pH} \quad (1)$$

where, R is the change in resistance when the film is in contact with a pH solution, A- the surface area of the film. By plotting the resistance vs pH , a linear graph was obtained and the Sp was determined to be 3K Ohms.

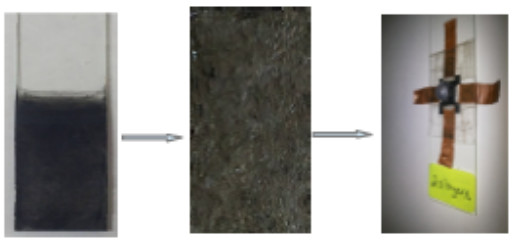


Fig. 3. Device fabrication

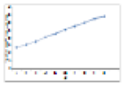


Fig. 4. pH sensitivity of LBL film at 25^0 C

The signal response time was a few seconds. Immersion of the film in water prior to a pH solution improved the signal, probably due to the swelling of the polyelectrolytes.

Environmental studies: Corrosion is influenced by different environmental conditions such as temperature and humidity , thus the sensor developed was tested for its stability and sensitivity to different temperature and humidity conditions. The results indicated that the film was most stable at -40^0C upto 48h. At 70^0 C/85 % humidity, the film with 20 bilayers was stable upto 24h, while, the film with 10 bilayers was stable only for 6h indicating that higher numbers of layers were desirable.

Quick diagnostic methods

1) Scratch cell set up
To detect corrosion reliable and simple diagnostic methods are also valuable in corrosion mianagement and mitigation. Scratch cell proposed by Palanivelu (2005) [10] involves a simple set up as shown in Fig. 5. The set up involves two coupons , generally a coated bottom coupon loaded with the inhibitor and the coated /bare top coupon without the inhibitor.

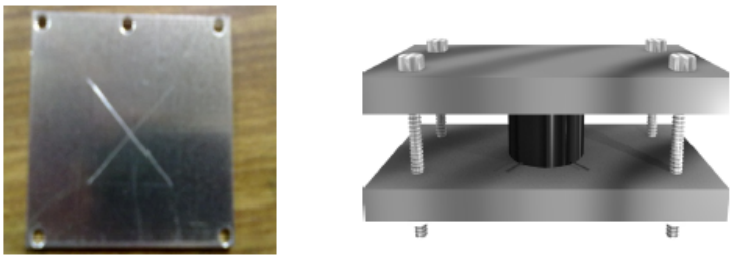


Fig. 5. Scratch cell set up

A neoprene 'O' ring filled with the electrolyte (3.5 % NaCl) was sandwiched between the two coupons and tightly held by screws on all four corners. Both the top and bottom coupon were scribed. This set up helps understand the movement of the inhibitor from the bottom coupon to the top coupon. The cell set up was dismantled at regular intervals (0,6,12,24,48...188h) to (i) monitor the leaching and movement of the inhibitor from the bottom coupon coating to the top coupon via the electrolyte (ii) self-healing of the scribed region and (iii) ensure the presence of electrolyte. The volume of the electrolyte was measured and made up to the original volume of 0.5ml.
The kinetics of the inhibitor movement and the scribe closure can be monitored by using a simple optical microscope. Detailed understanding of the mechanism of corrosion or self- healing can be obtained by Electrochemical Impedance studies/ potentiodynamic studies of the positive coupons.
The three commonly used inhibitors 8- hydroxy quinoline (8-HQ), benzotriazole and Cerium nitrate were

evaluated by the scratch cell test for their self healing ability on AA2024-T3 alloy. The inhibitors were loaded as nano- containers in a room temperature cured sol-gel ormosil coating [8] [9]. Methacryloxypropyl trimethoxy silane (MEMO), was used as the continuous phase i.e., matrix, Tetraethyl orthosilane (TEOS), as the nonhydrolysable organic binder, Triethoxy vinylsilane (VTEOS) as the discontinuous phase organic precursor i.e., filler and nitric acid as catalyst. Nano containers aid the controlled & /or "on demand" release of the inhibitor. Alodine- commercial hexavalent conversion coating was used as a positive control. The self- healing ability of the three inhibitors was evaluated relative to the Alodine coatings.

The results are depicted in Fig. 6 a-b. As expected selfhealing was best in the Alodine coatings. Self-healing was best in coatings loaded with 8-HQ followed by benzotriazole and Cerium.

Self- healing was initiated within 12h in the Alodine coatings in the top coupon. Chromium was detectable in the electrolyte but not in the top coupon, although scribe closure was observed in the top coupon. In the three inhibitors the inhibitor was detected by EDX analysis in the scribed region by 188h. EIS studies confirmed self- healing.

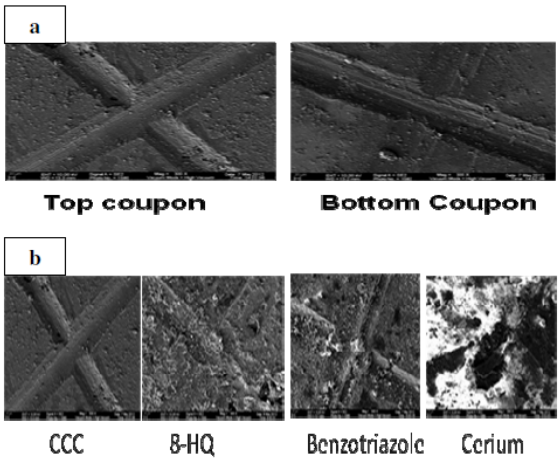


Fig. 6. a- Alodine coating ; b- Self- healing after scratch cell test in the bottom coupons

Indicator test using a suitable indicator dye is an excellent test to understand the mechanism of corrosion initiation and pitting (Fig. 7).It is easy to understand if the reaction is anodic/ cathodic and also self healing [11]. Frankel et al (2003) [12] in their patent describe the practical application of this method in real situation analysis.

The diagnostic test give us information of the extent of corrosion protection the coatings evaluated offer and also the extent of self healing. Minor modifications in the structure or use of analogs of the inhibitors could increase the efficiency of the coatings or inhibitors.

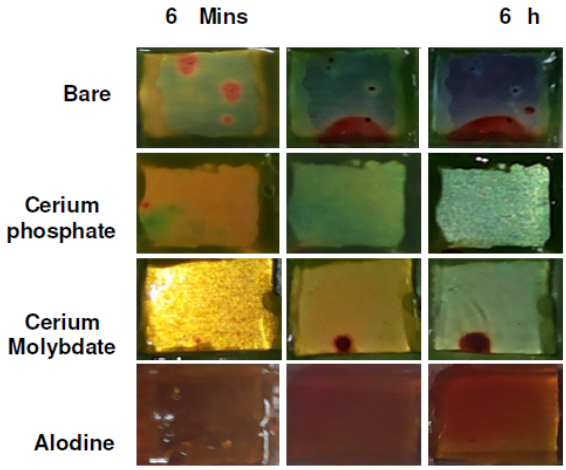


Fig. 7. Indicator test of smart sol- gel coatings

Laboratory trials for synthesis of these new compounds could be time consuming. Computational modeling could aid in the understanding of the coating/substrate and inhibitor interactions and evaluation of the new molecules [13] [14].

We have been using first- principles calculations Density Functional Theory calculations to understand the interaction of the different inter-metallics (Al_2Cu, Al_2CuMg) of AA2024-T3 and bulk Aluminum, Copper and Magnesium with the inhibitor benzotriazole (Fig. 8). This study would help in understanding the grain boundary effect as pitting is initiated by the dislodgement of the inter-metallic particles.

A 2X2 super cell has been created to study the interactions (Fig. 9). We adopted first-principles calculations based on density functional theory (DFT) as implemented in the Quantum ESPRESSO code with a plane-wave basis set and an ultrasoft pseudopotential. We adapted local density approximated functional of Perdew. We use an energy cutoff of 30 Ry for the plane-wave basis used for the wave functions and 180 Ry for that used to represent the charge density. Structures were determined through minimization of energy until Hellmann-Feynman forces on each atom were smaller than 0.03 $eV/^0$A in magnitude. The integrations were carried out over a $3 \times 3 \times 1$
mesh of k points in vc- relax mode. The smearing was fd with a degauss value of 0.01. The convergence threshold was fixed at 1.0E-05.The atomic co-ordinates were designated based on the wyckoff positions of different space groups. The structural geometry was visualized using XCRYSDEN software package. The calculations for the inter-metallics and inhibitor have converged(Fig. 6). The computed lattice constant and bulk modulus were comparable with the reported values.

Further, with computational modeling the most suitable

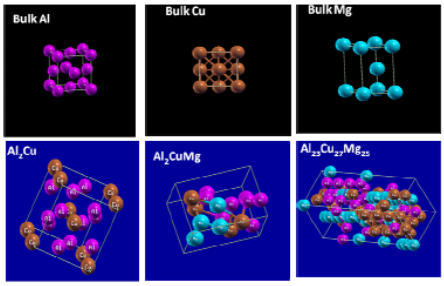


Fig. 8. Relaxed structures of the inter-metallics of AA2024-T3

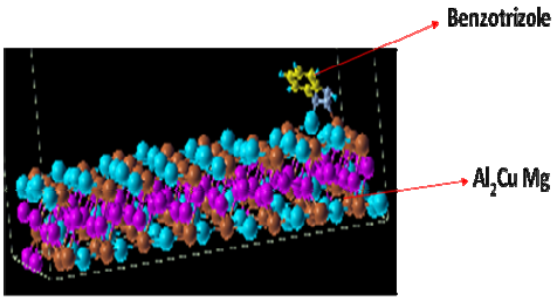


Fig. 9. Interaction of Al_2CuMg with Benzotriazole

plane of the alloy- inhibitor interaction can be evolved and the alloy fabricated suitably.

ACKNOWLEDGMENT

The authors are thankful to Director, NAL, Bengaluru and Head, Surface Engineering Division for their support and encouragement. The first author is also thankful to Prof. Umesh V Waghmare and Ms. Sharmila N Shirodkar, Materials Theory Group, JNCASR , Jakkur, Bengaluru, Coinvestigator for introducing me to DFT. I am also thankful to 4- PI, Bengaluru for permitting me to use the HPC system for the computational work.

REFERENCES

[1] Vinod S. Agarwala (2005) Sensors in corrosion, Tri-service corrosion conference.1-14.

[2] Jordi Prez-Puigdemont, Nuria Ferrer-Anglada, (2008). Transparent, flexible electrodes and sensors based on carbon nanotube thin films, contributions to science, 4 (2): 193201.

[3] Olga Korostynska, Khalil Arshak, Edric Gill and Arousian Arshak, Review on State-of-the-art in Polymer Based pH Sensors, Sensors 2007, 7, 3027-3042.

[4] Dongjin Lee and Tianhong Cui, "Layer-by-Layer Self-Assembly of Single-Walled Carbon Nanotubes with Amine-Functionalised Weak Polyelectrolytes for Electrochemically Tunable pH Sensitivity", Langmuir 2011,27,3348-3354.

[5] Jun Ge, Guanghui Cheng and Liwei Chen, "Transparent and flexible electrodes and super capacitors using polyaniline/single-walled carbon nanotubes composite thin films" Nanoscale, 2011,3,3084-3088.

[6] N. Ferrer-Anglada, M. Kaempgen2, and S. Roth, "Transparent and flexible carbon nanotube/ polypyrrole and carbon nanotube/polyaniline pH sensors", Phys. Stat. Sol.(2006) (B) 243, (13), 35193523.

[7] Kenneth J Loh et,al, "Multifunctional layer-by-layer carbon nanotube-polyelectrolyte thin films for strain and corrosion sensing" Smart Mates,Struct, 2007,16 429-438.

[8] T.L.Metroke and Apblett. A, Effect of solvent dilution on corrosion protective properties of Ormosil coating on 2024-T3 aluminum alloy, Prog.Org.Coat, 2004,51,1,36.

[9] D. G Shchukin, Zheludkevich.M, Yasakau, Lamaka.S,Ferreira. M.G.S, et al, Layer-by-layer Assembled nanocontainers for Self-Healing Corrosion Protection,Adv.Mater , 2006, 18 (13) ,1672.

[10] Palanivel V, Huang Y, van Ooij WJ. Prog Org Coat 2005, 53:153-168.

[11] W. Li and L. M. Calle, "pH and Electrochemical Responsive Materials for Corrosion Control Applications", CORROSION/08, paper no. 08214, (Houston, TX: NACE,2008.

[12] G.S.Frankel ,R.D.Buchheit and J.Zhang (2003) Corrosion sensing composition and use ,US 2003/0068824/A1.

[13] Wang, H., F. Presuel, and R. G. Kelly. Computational modeling of inhibitor release and transport from multifunctional organic coatings. Electrochimica Acta, 2004, 49, 239-255.

[14] Wang, W., Z. Li, Q. Sun, A. Du, Y. Li, J. Wang, S. Bi, and P. Li: Insights into the nature of the coupling interactions between uracil corrosion inhibitors and copper: A DFT and molecular dynamics study. Corrosion Science, 2012, 61, 101-110.



Amitha Rani B.E. received a PhD, Univ. of Mysore, Karnataka,India, 1991. During her career of of 22 years she has been working on development of quick diagnostic analytical methods. She is presently working as Principal Scientist. She has published 80 papers in refereed journals and conferences, written 3 book chapters, and has 10 US patents to her credit. Her areas of research interest are corrosion prognosis and mitigation for aerospace applications. Dr Amitha has won 10 awards for best paper, research fellowships etc.

Chemically modified metal/ hetero-metal alkoxides as molecular precursors for nano-sized ceramic materials

Veena Dhayal[1], Aparna Pareek[2]
[1]Department of Chemistry, [2]Department of mechanical engineering,
Manipal University Jaipur, Jaipur, India
[1]veena.dhayal@jaipur.manipal.edu
[2]aparna.pareek@jaipur.manipal.edu

Abstract— **Metal/hetero-metal oxides nanostructures play a very important role in many areas of chemistry, physics and materials science because of their many-fold practical applications. In technological applications, oxides are widely used in the fabrication of microelectronic circuits, sensors, piezoelectric devices, solar cells, coatings; Anti-scratch, anti-corrosive, acoustic, antifouling, heat insulation and as catalysts. The unique physical and chemical properties of oxide nanoparticles are due to their limited size.**

Bottom-up approach seems to be a promising method to provide materials at nano-scale but it requires suitable tailor-made precursors. Chemically modified metal/ hetero-metal alkoxides appear to be suitable potential precursors for the synthesis of pure nano-sized metal/ hetero-metal oxides. Such precursors have a high potential for innovative materials syntheses because they permit control of the precursor reactivity in sol–gel process and the preparation of inorganic–organic hybrid materials. Modification of alkoxides can be done by replacing some or all of the alkoxy groups with chelating ligands such as, oximes, Schiff's bases, glycols, carboxylic acids, etc. These chelating ligands modify the alkoxide precursor at a molecular level therefore modifying the whole hydrolysis condensation process and ultimately act as structure directing and size controlling agents.

Keywords— Metal/hetero-metal oxides nanostructures; Bottom-up approach; tailor-made precursors; Chemically modified metal/ hetero-metal alkoxides; sol–gel process

I. INTRODUCTION

Recently, considerable attention has been paid on the synthesis of metal/hetero-metal oxide nanostructures owing to their wide range of applications. They are often used in microelectronic circuits [1], as sensors [2], as piezoelectric devices [3] and in solar cells [4]. They are used as coatings which possess anti-scratch [5], anti-corrosive [6], acoustic [7], antifouling [8], and heat insulation properties [9]. The nanostructures are also being used as catalysts [10].

There are many approaches to synthesize metal oxide nanostructure among which sol-gel technique is being extensively employed to produce crystalline, pure materials with controlled microstructure and morphology. Sol-gel process provides a unique feasibility to control the entire synthetic route from precursors to the final targeted material at the molecular level, which is unachievable by other traditional methods like, sintering or precipitation methods.

Metal/hetero-metal alkoxides are often used as sol-gel molecular precursors for the synthesis of materials. However, on hydrolysis of these solutions, a massive uncontrolled phase separation, precipitation occurs. Hence, the search for more stable metal alkoxide precursors have led to the development of chemical modification of parent alkoxides, which can be achieved by substituting some of the or all the alkoxy groups with chelating ligands such as, oximes, Schiff's bases, glycols, carboxylic acids, etc [11]. It appears that the modification of the parent alkoxide with chelating ligands not only controls the hydrolysis and condensation reactions but also gives rise to new molecular precursors exhibiting interesting structural variations. Understanding of the structural and chemical aspects of the modified precursors is a prerequisite condition for tailoring the properties of the materials.

Therefore, the current research interest focuses on the synthesis and characterization of chemically modified metal/hetero-metal alkoxides, suitable to act as single source precursors (SSPs) for the syntheses of desired nano-sized ceramic materials.

II. SYNTHESIS AND CHARACTERIZATION OF CHEMICALLY MODIFIED METAL/HETERO-METAL ALKOXIDES

Synthesis of chemically modified metal/ hetero-metal alkoxides of some main group (Al [12], Si [13], Ge [14], Sn [15], Sb [16]) and some transition metals (Ti [17], V [18], Zr [19], Nb [20]) have been done by replacing some or all of the alkoxy groups with mixed atom multidentate chelating ligands according to the materials required. The objectivity is to prepare single source molecular precursors having greater solubility and volatility as compared to metal/ hetero-metal

alkoxides which can be easily purified (by distillation/crystallization) so that these can be used for making high purity nano-materials.

To draw meaningful connections between a precursor and the properties of materials generated from it, the structure of the starting compound must be fully understood. Therefore, the newly synthesized complexes have been characterized by elemental analyses, molecular weight and FAB mass studies and spectroscopic (FT-IR, NMR) techniques. Some of the compounds have been fully characterized by single crystals X-ray diffraction studies.

It is worthwhile to mention here that oximes including functionalized oximes served themselves as excellent chemical modifiers because they have a tendency to change their coordination mode from side-on to end-on to bridging as per the steric demand and chemical composition of the central metal (fig.1).

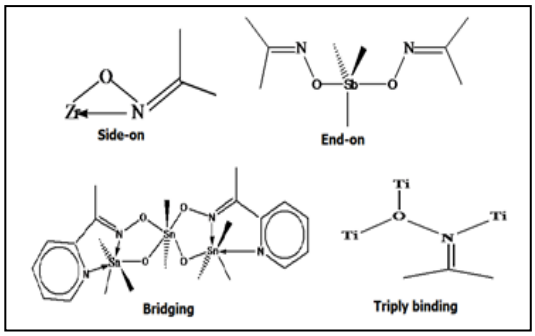


Fig. 1 Various coordination modes of oximes

Our recent studies indicate that coordination environment around central atom not only depends on nature of modifiers but also on the extent of modification. As reported in the case of titanium [17], di-substitution generates six coordinated environment (fig. 2 & 4) while tetra-substitution creates eight coordinated environment around Ti(IV) center (fig. 3). In di-substituted titanium(IV) alkoxide, schiff's base derivative are monomeric in nature while oxime derivatives are dimer.

Modifications of Ti(IV) alkoxides have also been done using other modifiers [21].

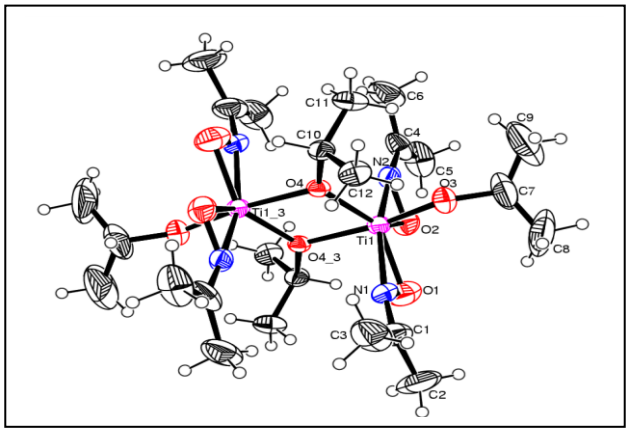


Fig. 2. Crystal structure of $[Ti\{OPr^i\}_2\{ONC(CH_3)\}]_2$

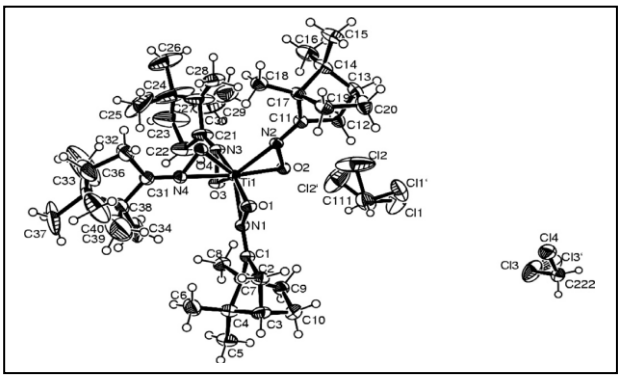


Fig. 3. Crystal structure of $[Ti\{ONC_{10}H_{16}\}_4.2CH_2Cl_2]$

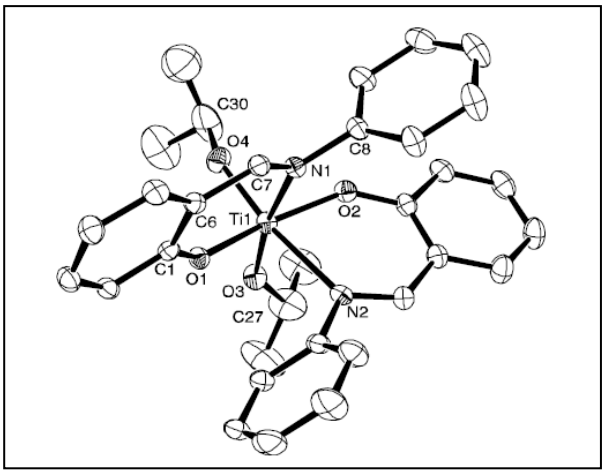


Fig. 4. Crystal structure of $[Ti\{O(C_6H_4)CH=NPh\}_2(OPr^i)_2]$

In addition to titanium alkoxides, other metal (Al, Si, Ge, Sb, Sn, V, Nb) alkoxides have also been modified using oximes and other modifiers [12-20].

The quest for single source precursors (SSPs) of hetero-metal oxides led to the synthesis of precursors having preformed M-O-Si bond. These precursors served themselves as SSPs for homogenous metallosilicates by pyrolysis. But sol-gel conversions of these SSP to materials demands modification as indicated in my earlier report [17].

Some of the hetero-metal alkoxides have been fully characterized by single crystal X-ray diffraction studies (fig. 5 & 6).

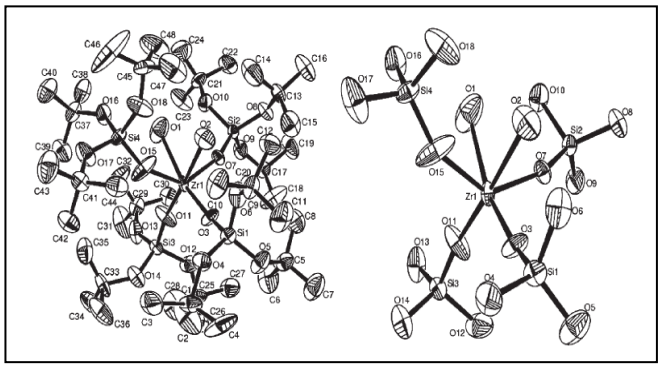


Fig. 5. Crystal structure of $[Zr\{OSi(O^tBu)_3\}_4(H_2O)_2]\cdot 2H_2O$ (i) with and (ii) without t-butyl groups.

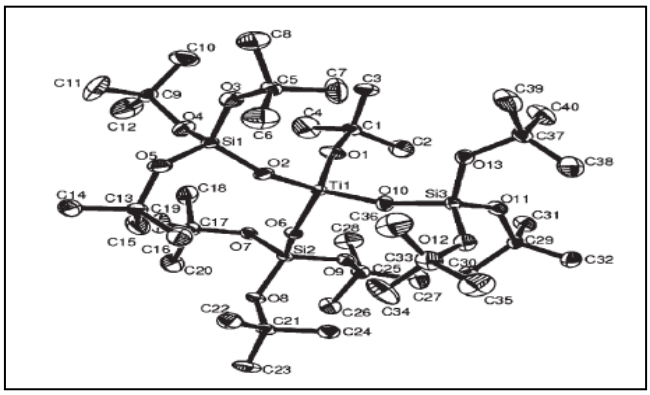
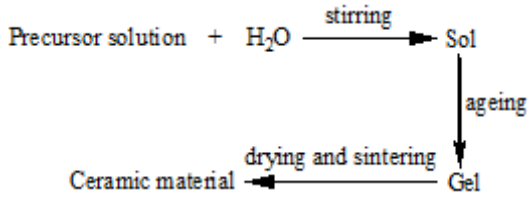


Fig. 6. Crystal structure of $[Ti(O^tBu)\{OSi(O^tBu)_3\}_3]$

III. SYNTHESIS OF NANOSIZED CERAMIC MATERIALS FROM CHEMICALLY MODIFIED METAL/HETERO-METAL ALKOXIDES AND THEIR CHARACTERIZATION

Previous studies indicate that sol/gel transition of alkoxides can be controlled when traditional sol-gel precursor, alkoxides are modified with chelating ligands. It is the sol/ gel transition that controls the particle size of the ceramic materials.



Scheme 1 Sol-gel process

An intermediate hydrolysis product, $\{Ti(O(C_6H_4)CH=NPh)_2\}O]_3$ (fig. 7) was obtained on controlled hydrolysis of precursor, $[Ti\{O(C_6H_4)CH=NPh\}_2(OPr^i)_2]$ [17] which supports that chelating ligands provides some stability and controls the basic sol-gel reactions, hydrolysis and condensation and ultimately affect the sol/gel transition.

It is worthwhile to mention here that the formation of titanoxane is reproducible, suggests that it is kinetically stable species during hydrolysis pathway of Precursor $[Ti\{O(C_6H_4)CH=NPh\}_2(OPr^i)_2]$ (scheme 2).

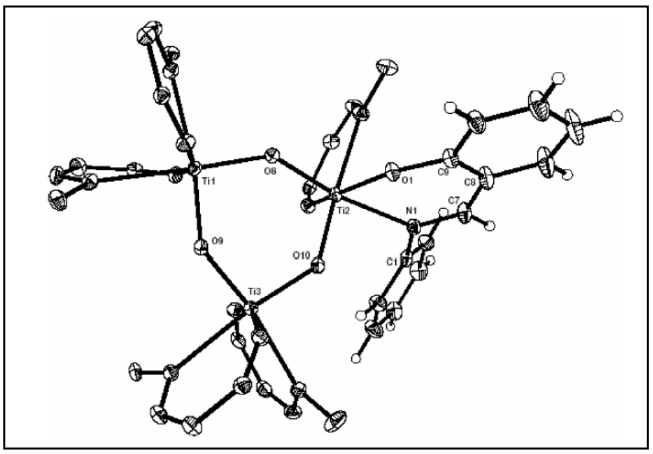
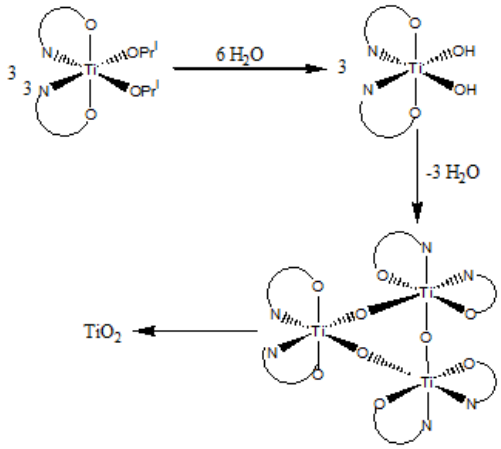


Fig. 7. Crystal structure of $[\{Ti(O(C_6H_4)CH=NPh)_2\}O]_3$

Pure TiO_2 is obtained on complete hydrolysis of $[Ti\{O(C_6H_4)CH=NPh\}_2(OPr^i)_2]$. The structure of trinuclear titanoxane reveals a non-planar six-membered ring system of alternating three titanium and three oxygen atoms while dinuclear titanoxane, $Ti(acac)_2O$ reveals a planar ring of Ti_2O_2 [17].



Scheme 2

Several other metal/ hetero-metal oxides ($MeSiO_{3/2}$, SiO_2, Al_2O_3, GeO_2, TiO_2, ZrO_2, V_2O_5, Nb_2O_5, $Al_2O_3.SiO_2$, $TiSiO_4$, $ZrSiO_4$) have also been prepared using chemically modified precursors [12-21].

It is interesting to mention here that as the extent of modification increases, particle size of the formed material decreases. Eg. In the case of titanium(IV) alkoxides: tetra-substituted Ti(IV) alkoxide yielded particles of 5.22 nm, tri-substitution provides particles of 10.39 nm and di-substitution yielded particles of 31.89 nm of TiO_2 by sol-gel process [17]. The particle sizes of TiO_2 were calculated using Debye Scherrer equation for the longest peak in the XRD spectra (Fig. 8).

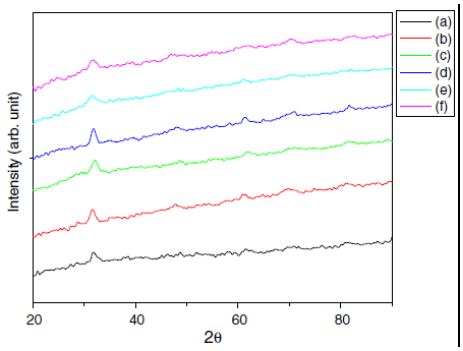


Fig. 8. XRD patterns of TiO_2 samples (a)&(d) obtained from di-substituted, (b)&(e) obtained from tri-substituted and (c)&(f) obtained from tetra-substituted titanium(IV) alkoxides.

Thermal studies of some of the compounds have been done by TG analyses. TG curves showed a precipitous weight loss consistent to the stoichiometric formation of metal/hetero-metal oxides (fig. 9).

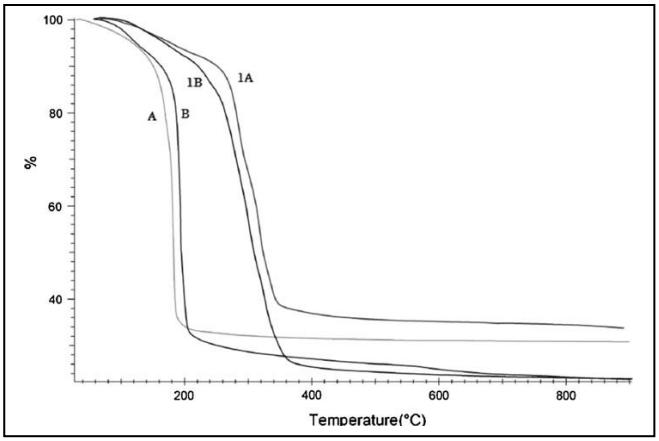


Fig. 9. TG curves (weight% vs. temperature) of $[Ti(OPr^i)_3\{OSi(O^tBu)_3\}]$ (A), $[Ti(OPr^i)_2\{OSi(O^tBu)_3\}_2]$ (B), $[Ti(OPr^i)\{O(CH_2)_2O\}\{OSi(O^tBu)_3\}]$ (1A) and $[Ti\{O(CH_2)_2O\}\{OSi(O^tBu)_3\}_2]$ (1B)

It suggests that modified alkoxides may be used as SSPs for materials by pyrolysis. Pyrolysis of titanosiloxane precursor, $[Ti(OPr^i)_3\{OSi(O^tBu)_3\}]$ afforded titania-silica material, $TiSiO_4$ approved the above statement (Scheme 3) (Fig. 10).

Schematic representation of the pyrolysis process can be shown as indicated below:

$$[Ti(OPr^i)_3\{OSi(O^tBu)_3\}] \xrightarrow[\text{Reflux}]{\text{Xylene}} TiSiO_4 + 3\,CH_2{=}CMe_2 + 3\,Pr^iOH$$

Scheme 3

As indicated above hetero-metal alkoxides having preformed M-O-M' bond served themselves as single source precursors for hetero-metal oxides by pyrolysis. But in sol-gel method the presence of M-O-M' bond does not guarantee to provide homogenous Hetero-metal oxides. Compatible hydrolytic reactivity of M-OR and M'-OR is essential.

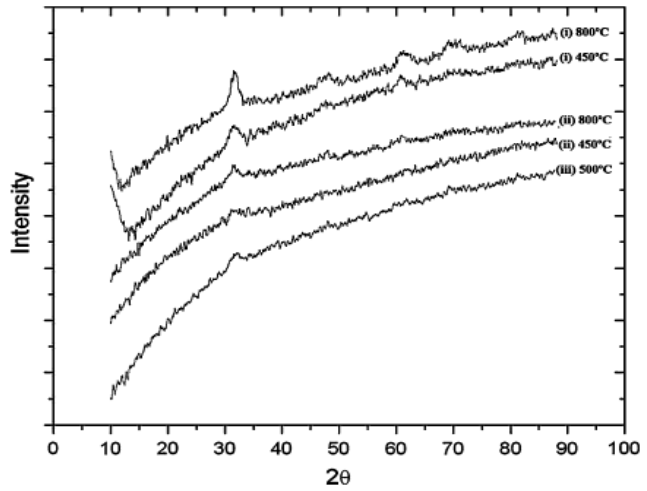


Fig. 10 Powder XRD patterns of xerogels i obtained from $[Ti(OPr^i)_3\{OSi(O^tBu)_3\}]$ by Sol–Gel process sintered at 450 and 800 °C; ii obtained from $[Ti(OPr^i)\{O(CH_2)_2O\}\{OSi(O^tBu)_3\}]$ by Sol–Gel process sintered at 450 and 800 °C and iii obtained from $[Ti(OPr^i)_3\{OSi(O^tBu)_3\}]$ by solvo-thermal process and sintered at 500 °C

Hetero-metal alkoxides having non-compatible hydrolytic reactivity of M-OR and M'-OR can generate homogeneity in materials on modification with chelating ligands as reported in my earlier report [17] (fig. 10). Characterization of ceramic materials has been done by various techniques such as, powder XRD (Fig. 8, 10 & 11), SEM (Fig. 12), EDX (Fig. 13), IR and Raman analysis.

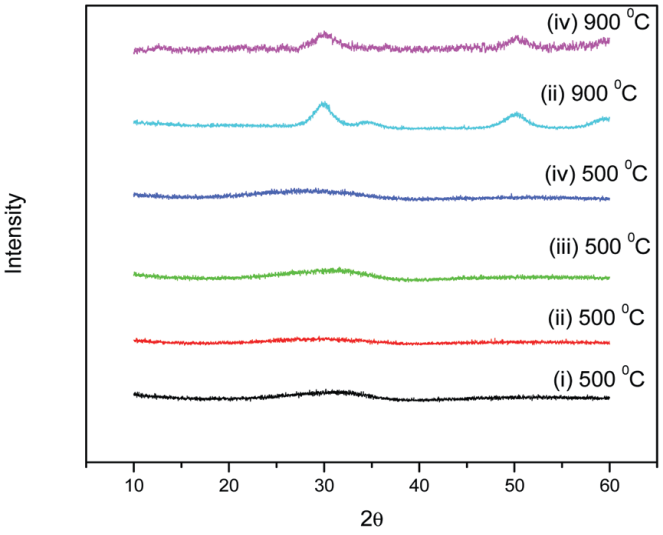


Fig. 11 Powder XRD patterns of the zirconia–silica materials sintered at 500 °C and 900 °C and obtained from (i) $[Zr(OPr^i)_3\{OSi(O^tBu)_3\}]$ (ii) $[Zr(OPr^i)_2\{OSi(O^tBu)_3\}_2]$ (iii) $[Zr(OPr^i)\{O(CH_2)_2CH(CH_3)O\}\{OSi(O^tBu)_3\}]$ and (iv) $[Zr\{O(CH_2)_2CH(CH_3)O\}\{OSi(O^tBu)_3\}_2]$

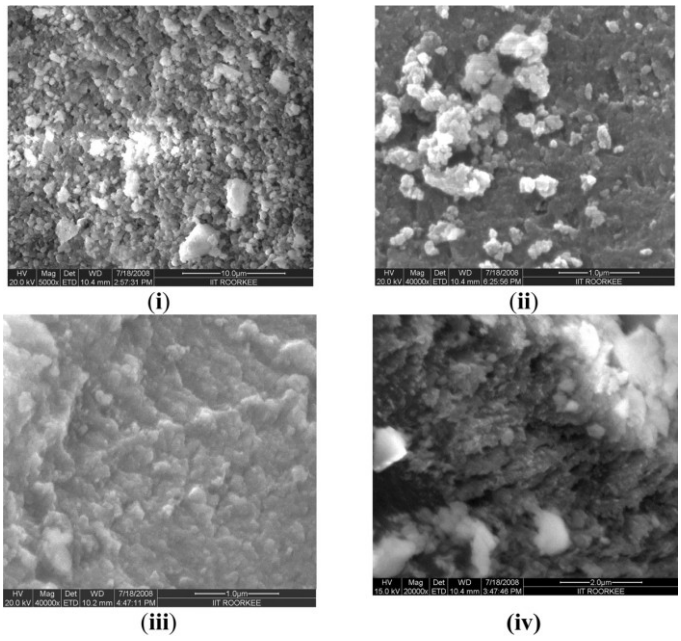


Fig. 12 SEM images of the zirconia–silica materials sintered at 500 °C and obtained from (i) $[Zr(OPr^i)_3\{OSi(O^tBu)_3\}]$ (ii) $[Zr(OPr^i)_2\{OSi(O^tBu)_3\}_2]$ (iii) $[Zr(OPr^i)\{O(CH_2)_2CH(CH_3)O\}\{OSi(O^tBu)_3\}]$ and (iv) $[Zr\{O(CH_2)_2CH(CH_3)O\}\{OSi(O^tBu)_3\}_2]$

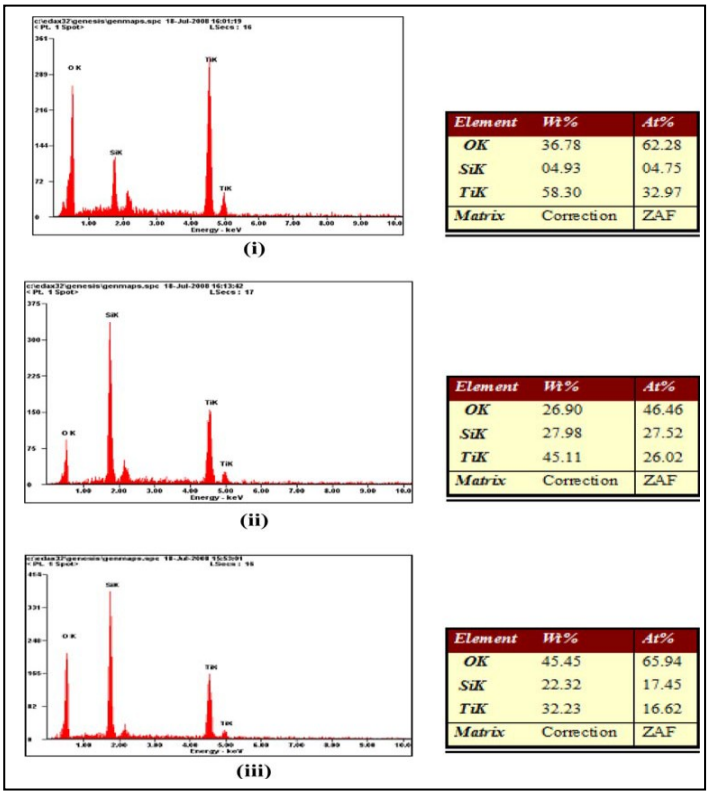


Fig. 13 EDX analyses of xerogels i obtained from [Ti(OPr^i)$_3${OSi(O^{t}Bu)$_3$}] & ii obtained from [Ti(OPr^i){O(CH$_2$)$_2$O}{OSi(O^{t}Bu)$_3$}] by the Sol–Gel and iii obtained from [Ti(OPr^i)$_3${OSi(O^{t}Bu)$_3$}] by solvo-thermal processes

CONCLUSION

For a rational material design, understanding the chemistry and the structural aspects of precursors are quite important. The substitution of alkoxy groups in metal/ hetero-metal alkoxides with chelating ligands offer a great scope for the development of new functional precursors for sol-gel/ solvothermal preparation of materials at nano-scale.

ACKNOWLEDGMENT

We are thankful to ONRG, UK for financial support. We are also thankful to Dr. D. C. Agarwal, Director SET, Manipal University Jaipur for his kind help in the preparation of the manuscript.

REFERENCES

[1] R. Ramesh and V. G. Keramidas, "Metal-oxide nanostructures," Annu. Rev. Mater. Sci. 25, 647, 1995.

[2] T. Fischer, A. P. Singh, T. Singh, F. Hernández Ramírez, D. Prades, S. Mathur, "Multi-component Metal-oxide Nano-architectures for Chemical Sensors," Publisher Springer, Metal Oxide Nanomaterials for Chemical Sensors, Ed. S. Mathur, A. Kolmakov and M. A. Carpenter, 2012.

[3] Y.-R. Wu and J. Singh, "Metal piezoelectric semiconductor field effect transistors for piezoelectric strain sensors," Appl. Phys. Lett. 85, 1223, 2004.

[4] L. Zhu, G. Shao and J. K. Luo, "Numerical study of metal oxide hetero-junction solar cells with defects and interface states," Semicond. Sci. Technol. 28, 55004, 2013.

[5] H.J. Gläsel, F. Bauer, H. Ernst, M. Findeisen,E. Hartmann, H. Langguth, R. Mehnert, R. Schubert, "Preparation of scratch and abrasion resistant polymeric nanocomposites by monomer grafting onto nanoparticles, 2 Characterization of radiation-cured polymeric nanocomposites," Macromol.Chem. Phys. 201, 2765, 2000.

[6] (a) S. E. Potts, L. Schmalz, M. Fenker, B. Díaz, J. Światowska, V. Maurice, A. Seyeux, P. Marcus, G. Radnóczi, L. Tóth and W. M. M. Kessels, "Ultra-Thin Aluminium Oxide Films Deposited by Plasma-Enhanced Atomic Layer Deposition for Corrosion Protection," J. Electrochem. Soc. 158, C132-C1382011 (b) J. M. Fan, Q. Li, W. Kang, S. Y. Zhang, B. Chen, "Composite cerium oxide/titanium oxide thin films for corrosion protection of AZ91D magnesium alloy via sol–gel process Materials and Corrosion," 60, 438, 2009 (c) G. X. Shen, Y. C. Chen, L. Lin, C. J. Lin and D. Scantlebury, "Study on a hydrophobic nano-TiO$_2$ coating and its properties for corrosion protection of metals," Electrochim. Acta. 50, 5083, 2005.

[7] S.-H. Nam, S.-J. Cho and J.-H. Boo, "Physical properties of metal-doped zinc oxide films for surface acoustic wave application," Nano. Res. Lett. 7, 25, 2012.

[8] (a) A. J. Trogolo, C. F. Rossitto, K. E. Welch, II, World patent, WO 03/055941, July 10 2013.(b) Wagener, Hygienic Coatings & Surfaces, PRA Coatings Technology centre, Paris, 16-17 March 2005, paper 14. (c) P. P. Karmali, Y. Chao, J. H. Park, M. J. Sailor, E. Ruoslahti, S. C. Esener, D. Simberg, "Different effect of hydrogelation on antifouling and circulation properties of dextran-iron oxide nanoparticles," Mol Pharm. 9, 539, 2012.

[9] (a) T. Kashiwagi, J. W. Gilman, in: fire retardance of polymeric materials (Ed. C. A. Wilkie, A. F. Grand), Chapter 10, Marcel Dekker, Inc., New York, 2000, pp 353-389. (b) B. Kandola, S. Nazare, R. Horrocks and various papers in: Fire and polymers, Polym. Mater. Sci. Eng. Preprints, American Chemical Society, August 22-26, 2004.

[10] X. Chen, S. Shen, L. Guo, S. M. Samuel, "Semiconductor based photocatalytic hydrogen generation," Chem. Rev. 6503, 2010.

[11] (a) R. Bohra "Structural aspects of some modified metal-alkoxides and related molecular precursors to ceramic materials by the sol–gel processing," J Indian Chem Soc. 82, 197, 2005 (b) U Schubert, "Organically Modified transition metal alkoxides: Chemical problems and structural issue on the way to material synthesis," Acc. Chem. Res. 40, 730, 2007.

[12] N. Sharma, A.R. Sanwaria, M. Nagar and R. Bohra, "Synthesis and structural characterization of some binuclear acetylacetone and schiff's base complexes containing aluminium(iii) atoms in different coordination states," Main Group Met. Chem. 36, 109, 2013.

[13] V. Dhayal, N. Sharma, V. Sharma, R. Bohra, J. E. Drake and C. L. B. MacDonald, "Synthesis and characterization of some dimethylsilicon(IV) Complexes with internally functionalized oximes: Crystal and molecular structure of [Me$_2$Si{ON=C(H)C$_4$H$_3$O-2}$_2$]. Formation of mesoporous materials by the hydrolytic study of [Me$_2$Si{ON=C(CH$_3$)C$_4$H$_3$O-2}$_2$] in presence of Al(OPr^i)$_3$," Polyhedron, 26, 3168, 2007.

[14] Y. Shah, A. Wadawale, B. S. Naidu, V. Sudarsan, R. K. Vatsa, V. K. Jain, V. Dhayal, M. Nagar and R. Bohra, "Germanium tetra(tertiary butoxide): Synthesis, structure and its utility as a precursor for the preparation of europium doped GeO$_2$ nanoparticle," Inorg. Chim. Acta., 363, 3680, 2010.

[15] V. Sharma, S. Agrawal, R. Bohra, R. Ratnani, J.E. Drake, M.B. Hursthouse and M.E. Light, "Synthesis and Characterization of some monoorganotin(IV) chloride adducts with internally functionallized oximes: Crystal and molecular structures of nBuSnCl$_3$.HON=C(Me)Py-2 and a trinuclear hydroxobridged stannoxane [nBuSnCl$_2$(ON=C(Me)Py-2)OH]$_2$Sn nBuCl.0.5 HON=C(Me)Py-2," Inorg. Chim. Acta, 359, 1404, 2006.

[16] N. Yadav, M. Nagar and R. Bohra, "New sol-gel precursors for binary oxides of antimony, Sb$_2$O$_3$(senarmonite) and α-Sb$_2$O$_4$: synthesis and characterization of some ketoximate modified antimony(III) alkoxides," J Sol-Gel Sci Technol, 54, 119, 2010.

[17] (a) M. Pathak, R.Bohra, R. C. Mehrotra, Ingo-Peter Lorenz and Holger Piotrowski, "Synthetic studies and structural aspects of some novel metallacyclic compounds of titanium(IV) incorporating nitrogen, oxygen and sulphur: 1. Reactions of *cis*-dialkoxy-bis(acetylacetonato)titanium(IV) with alkoxyalkanols and crystal

structure of a new modification di-m- oxo-bis[diacetylacetonato titanium(IV)]$_2$, Trans. Met. Chem., 28, 187, 2003 (b) N. Sharma, V. Sharma, R. Bohra, V. S. Raju, I. P. Lorenz, C. Krinninger and P. Mayer, Glycol modified cis-diisopropoxy-bis(N-phenylsalicylideneiminato) titanium(IV). Syntheses, characterization, X-ray structures of $Ti\{O(C_6H_4)CHNPh\}_2(OPr^i)_2$, $[\{Ti(O(C_6H_4)CHNPh)_2\}O]_3$ and their low temperature transformation to pure grains of nanosized titania. Inorg. Chim. Acta, 360, 3002, 2007 (c) V. Dhayal, M. K. Atal, B. L. Choudhary, M. Nagar and R. Bohra "Glycol modified titanosiloxane as molecular precursor for homogeneous titania-silica materials: Synthesis and characterization," J. Sol-gel Sci. Technol., 52, 97, 2009. (d) A. Chaudhary, V. Dhayal, M. Nagar, R. Bohra, M.M. Shaikh and P. Mathur, "Chemically modified oximato complexes of titanium(IV) isopropoxide as new precursors for the sol–gel preparation of nano-sized titania: crystal and molecular structures of $[Ti\{ONC_{10}H_{16}\}_4.2CH_2Cl_2]$," Polyhedron, 30, 821, 2011.

[18] M.K. Atal, V. Dhayal, M. Nagar, R. Bohra, K.S. Rathore and N.S. Saxena, "Synthesis and characterization of glycol-modified vanadium(V) oxoisopropoxide and their oximato derivatives: sol–gel transformations of $[VO(OPr^i)_3]$, $[VO\{OCH_2CH_2OCH_2CH_2O\}\{OPr^i\}]$ and $[VO\{OCH_2CH_2OCH_2CH_2O\}\{ON = C(CH_3)(C_4H_3S\text{-}2)\}]$ to vanadia," J Sol–Gel Sci Technol., 53, 67, 2010.

[19] (a) V. Dhayal, A. Chaudhary, M. Nagar, R. Bohra, S. M. Mobin and P. Mathur, "Synthesis and characterization of some single source molecular precursors for the preparation of homogenous zirconia-silica materials by hydrolytic sol-gel process in organic media. Crystal structures of $[Zr\{OSi(O^tBu)_3\}_4(H_2O)_2].2H_2O$ and $[Ti(O^tBu)\{OSi(O^tBu)_3\}_3]$," Dalton Trans, 41, 9439, 2012 (b) A.Chaudhary, R. Gopal, M. Nagar, R. Bohra, "Syntheses and characterization of a new class of zirconia precursors of oxime-modified zirconium(IV) isopropoxide," J Sol-Gel Sci Technol, in press.

[20] M. K. Atal, J. Jain, V. Dhayal, M. Nagar, R. Bohra, K. S. Rathore and N. S. Saxena "Synthesis and characterization of glycol and oxime modified precursors of niobium(V) for soft transformation to niobia," J. Sol-gel Sci. Technol. 67, 88, 2013.

[21] M. Pathak, B. Samuel, K. Tummalapalli, P.V. Giri, S. Koppala, R.Bohra, and K.J.Kim, "Alkoxyalkanol modified $Ti(OCHMe_2)_4$: synthesis and characterization of novel $[(OPr^i)_{4-n}Ti(OC_2H_4OR)n]$" Adv. Mat. Res.,584,415, 2012.



Veena Dayal received PhD from Department of Chemistry, University of Rajasthan, Jaipur, Rajasthan, India 2009. She is working as Assistant Professor, in Department of chemistry, Manipal University Jaipur, and Co-Investigator, NICOP Project funded by ONRG, UK & Singapore (US$ 345800). She has published 9 papers in refereed journals and 7 conferences. She has won awards for research fellowships etc. Her areas of research interest are coordination chemistry, organometallic chemistry, nanomaterials and coatings.

Corrosion Predictive Modeling for Aging Ships

Cdr Nitin Agarwala[1]
[1]Officer-in-charge,
Hull Inspection and Trials Unit,
Vishakhapatnam - 530 014, India
[1]nitindu@yahoo.com

***Abstract*—Ship inspections are inspector oriented and depend purely on his experience leading to subjectivity. It is hence essential that a rationalized approach on what to inspect, when to inspect, where to inspect and how much to inspect is put in place. To remove this subjectivity, one needs to develop a corrosion model to predict the corrosion rate. This model development is not straightforward since corrosion is a function of many variables and uncertainties, such as type of corrosion protection system employed, type of cargo, temperature, humidity etc. The corrosion model thus developed is different for different types of ship and cargo or structural member, location and category.**

Since the existing corrosion models are never 100% complete and need to be continuously updated with addition of more corrosion data as may be available, the field of corrosion predictive modeling is dynamic. The present paper discusses the available models, limitations and future of these models.

***Keywords*—Corrosion model; Marine environement; Aging ships; Corrosion mechanism; Corrosion.**

I. INTRODUCTION

During the service life of a ship, the hull structure is subjected to different damage scenarios, one of which is corrosion deterioration. Various forms of corrosion such as localized corrosion, pitting corrosion, crevice corrosion, stress corrosion cracking, corrosion fatigue etc. frequently occur without any visible signs of damage and often result in sudden and catastrophic failures. To minimize this unfavourable deterioration during service, focus of the owner remains on inspection and maintenance, timely and adequate repairs, crew training, imposing limits to cargo loading / unloading procedures to name a few. Presently inspections and maintenance operations for ships are based on calendar time with extent of inspection being governed by age of the vessel. Accordingly, any corrosion damage detected is repaired. However in actual practice, it is impractical, if not impossible, to execute perfect inspections and hence inspections become inspector oriented and depend largely on his experience. To remove subjectivity, it is essential to develop effective damage prediction technologies for successful avoidance of unscheduled downtime and for successful life extension strategies.

One such prediction technology used is that of developing a corrosion wastage predicting model. However developing a corrosion model solely based on theory is normally not straightforward because corrosion is a function of many variables and uncertainties involved. Many factors contribute to the corrosion deterioration. These include type of cargoes (acidity of the cargo), frequency of ballasting, frequency and method of tank cleaning, trapped water or oil, oxygen concentration, sulphur concentration, salinity of ballast water, temperature, humidity, pollution, trade route, structural flexibility, corrosion protection effectiveness, marine fouling, corrosion films, speed of flow, stray-current, cargo residues and mechanical abrasion, maintenance and repair, material of construction, microbial attack, sludge / scale accumulation, etc. These factors act individually or in combination, and their influences are difficult to quantify. As a result, corrosion wastage of structural members is dependent on the location of the member. This implies that the corrosion model developed by statistical means will usually be different for different types of ship and cargo or structural member, location and categories.

Over the years a number of studies related to corrosion evaluation in ship structures have been performed and various guidelines and rules have been developed by the classification societies. Since the existing corrosion models are never 100% complete and need to be continuously updated with addition of more corrosion data as may be available, the field of corrosion predictive modeling is dynamic. The present paper discusses the available models, limitations and future developments of these models.

II. APPROACHES USED

To assess corrosion damage, one must be able to predict the timeframe in which corrosion margin will be depleted. To do this predictive modeling is undertaken. One thus needs to develop a mathematical relationship between a target, response (or dependent) variable and various predictor (or independent) variables to measure future values of those predictors and inserting them into the mathematical relationship to predict future values of the target variable. Traditionally, corrosion rate predictions have been based on either empiricism (statistical) methods or determinism (analytical) methods.

A. Empiricism (Statistical) Method

Believes in the philosophy that everything we know must have been experienced. These methods are expensive and require large databases. They fail to capture the mechanism of failure and rarely represent failure since data available is usually for intact ships. These methods include correlating laboratory data to field measurements and field surveys. Two main types of statistical methods used for ships are:

- Polarization Potential Rate Prediction Methods: In these methods the corrosion potential of a corroded area (e) and associated current (i) is measured and compared to the developed i/e curves for a given corrosion process. One such i/e curve called the Tafel curve is often used where the constants for medium range are assumed constant, however they are not. Sometimes when the plot of e vs the logarithm of i yields a straight line, extrapolation is required hence the Tafel Extrapolation Method is used. Both these methods use graphical calculations which are cumbersome and often inaccurate.
- Statistical Rate Prediction Methods: These methods are concerned only with the end result of corrosion loss and provide an alternative method for predicting corrosion rates. Corrosion rate so measured is equal to the averaged metal loss / time between measurements for a given location.

B. Determinism (Analytical) Method

Believes in predicting future from the past via natural laws. The method deals with prediction of corrosion rates by solving the Laplace equation (the governing equation for potential distributions in electrochemical cells). However these efforts are limited to simple geometries and constant material properties. By combining numerical methods, these methods are capable of accommodating varying inhomogeneous, nonlinear properties for electrolyte and constituent metals. These methods need careful representation of the complex phenomenon of corrosion, kinetic parameters of the corroding system and the corrosion evolutionary path (CEP). Some analytical methods used are:

- Finite Element Method is used for galvanic corrosion problems and can handle general and arbitrary geometries and effect of nonlinear polarization behavior.
- Finite Difference Method is used to solve the Poisson equation for the electrochemical potential distribution in an electrolyte containing an array of fixed-potential electrodes and electrodes with activation, passivation, and diffusion-controlled polarization kinetics.
- Boundary Integral Method is similar to the finite element and finite difference methods in that it solves the Laplace equation to obtain the potential distribution in electrochemical cells. However, this numerical method is more efficient than the others because it does not require modeling the electrolyte bodies to obtain the potential distribution on the surface of the structure thus saving computer time.

Up to now, the prediction of corrosion damage has been largely based on the application of empirical models thus providing many time-variant corrosion models for different member location / category groups for bulk carriers, tankers and FPSOs. Only in the past decade, or so, have deterministic models been developed. Since a deterministic prediction is based, on our imagination, and is based upon inputs from imperfect senses, a working deterministic model can yield only an approximate description of a real system. Accordingly, pure determinism is an ideal concept that is probably never achieved in reality. Similarly identifying key issues that can lead to corrosion cannot be achieved through statistical investigations of corroded aging ships alone. Using corrosion mechanisms and corrosion wastage databases together, models have been developed to achieve a better understanding as well as improved prediction of corrosion damage in marine structures.

III. MODELS USED

Large numbers of parameters that can affect corrosion make developing corrosion wastage model for ships a difficult task. Notwithstanding, efforts of various researchers have resulted into many workable models. Three fundamental approaches have normally been applied.

- The conventional approach considering that corrosion grows linearly. This may lead to overestimation of the corrosion deterioration or underestimation of the corrosion effects in early life.
- Based on results of experiments in specific conditions, which suggest laws of corrosion deterioration as a function of specific parameters. This approach involves generalising results of laboratory tests to full-scale conditions while neglecting effect of environmental conditions.
- Develop a model that provides a trend that is derived from the dominating mechanism and then fit it to the field data.

These models provide a start point for analyzing corrosion of ships and are based on either analytical or statistical methods. Some of the major models developed are discussed herein.

A. Based on Data Collected from ships

The earliest corrosion models were developed entirely from empirical data sourced from thickness measurement surveys for bulk carriers and tankers. This work was undertaken due to numerous marine accidents particularly of bulk carriers. These models presented corrosion loss in terms of a constant corrosion rate, implying a constant rate of plate thickness reduction over time and an estimate of nominal or calculated variation. This allowed these models to be used in structural reliability analysis although these models exhibited a high degree of variability and thus tended to produce poor estimates of the lifetime risk of failure.

The most common databases of corrosion wastage in the public domain include the Tanker Structure Co-operative Forum (TSCF) [1] which published results of corrosion data from 52 oil tankers, Yamamoto and Ikegami [2] who introduced a database of 50 bulk carriers, Paik et al. who developed a probabilistic corrosion rate estimation model based on the measurements of 44 bulk carriers [3] and more than 100 oil tankers [4], Harada et al. [5] who collected a database from 197 oil tankers and ABS which developed a database based on 140 oil tankers.

To express the corrosion wastage at t years old the following equation is used.

$$\text{C(t)}=\alpha(t - t_0)^{\beta}$$

where $C(t)$ is the corrosion wastage at age t, t_0 the year when thickness of plates starts to deviate from as-built condition, α and β are constants that can be determined according to the measurement data.

Age when the corrosion starts, t_0, which can vary in a wide range, is itself a random variable. It can follow a log normal distribution, a normal distribution or a Weibull distribution. Since coating breakdown starts to take place in certain places when a ship is 2 to 10 years old,t_0 is considered to vary from 2 to 10 years. As the number of data points vary from year to year, as there may be more data points in some years than in others, it is meaningless to attempt to create a curve fitting all data points. While deriving the formulae for mean values and standard deviations by best fitting the data set, following are considered:

- Mean value of corrosion wastage increases with ships age.
- Standard deviation of corrosion wastage increases with ships age.
- Trends are better revealed or presented by ship with more data points.
- Coating life t_0 is assumed to be a constant value.
- Estimated equations cover the most severe investigated data due to the conservative consideration.

Weibull distribution is a good candidate for representing the corrosion wastage over a ships life. It is assumed that corrosion wastage at t years old follows a Weibull distribution or probability density function:

$$pdf(C;k,\lambda) = (\frac{k}{\lambda})(\frac{C}{\lambda})^{k-1}\exp\left(-(\frac{C}{\lambda})^{k}\right)$$

where k and λ are the shape and scale parameters, respectively, which are functions of ships age.

These studies represent a thorough presentation of corrosion loss data; however, due to large variations it has limited importance for prediction and assessment of remaining life. Since these models are based on historical data and on data collected from ships operating under quite varied operational conditions, they have limited capability for use in predictive studies for any one particular vessel.

B. Based on Actual Corrosion Process

A more refined empirical approach is based on the actual physical phenomena of the corrosion process. This means that models must take into account various factors such as oxygen concentration, marine growth and bacteriological effects, pit formation and growth and diffusion of reactants through the rust layer etc known to be important in the corrosion of steel in natural seawaters. Assuming a constant corrosion rate and a linear relationship between the material lost and time and by dividing the process in three stages namely effective coating life, transition time and corrosion progress, various researchers have refined the model as seen in Figure 2.

Curve 1 in Figure 1 given by Southwell et al., [6] shows that the wastage thickness increases non-linearly in a period of 2-5 years of exposure, but afterwards it becomes relatively constant. This means that after a period of initial non-linear corrosion, the oxidized material that is produced remains on the surface of the plate and does not allow the continued contact of the plate surface with the corrosive environment thus stopping corrosion. They proposed a linear and a bilinear model for design purposes. Both models are conservative in the early stages, overestimating the corrosion wastage.

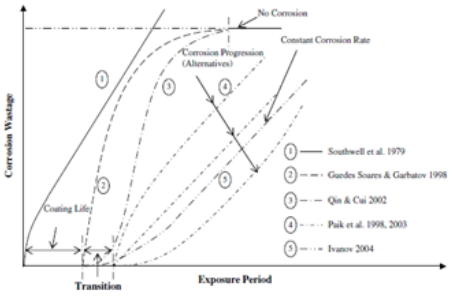


Fig. 1. Schematic Corrosion Wastage Models in previous literature

Yamamoto [7] proposed a corrosion model based on a pitting corrosion mechanism and plate thickness measurement data. He also presented results of the analysis of corrosion wastage in different locations of many ships, exhibiting the non-linear dependence of time with tendency of leveling off.

Guedes Soares and Garbatov [8] proposed a model for non-linear time dependent function of general corrosion wastage to obtain curve 2 in Figure 1. Their time dependent model separates corrosion degradation into three phases.

- First phase has no corrosion because the protection of the metal surface works properly. Statistics show that in ships the first phase varies in the range of 1.5 to 5.5 years.
- The second phase is initiated when corrosion protection is damaged and corresponds to the start of corrosion, which decreases the thickness of the plate. This process was observed to last a period around 4-5 years.
- The third phase corresponds to a stoppage in the corrosion process and the corrosion rate becomes zero. Corroded material stays on the plate surface, protecting it from coming in contact with the corrosive environment. Cleaning the surface or any involuntary action that removes the surface material initiates a new start of the non-linear corrosion growth process.

This model given below is flexible enough to represent realistic situations, due to the free parameters included in it, which can be adjusted to the data of specific situation. Hence where $d(t)$ is corrosion wastage at time t, d_∞ is the long-

$$d(t) = \begin{cases} d_\infty\left\{1 - exp\left[-\left(\frac{t-\tau_c}{\tau_t}\right)\right]\right\} & t > \tau_c \\ 0 & t \le \tau_c \end{cases}$$

term thickness of the corrosion wastage, defined as maximum corrosion depth in observed time interval, τ_c is time without

corrosion which corresponds to start of failure of corrosion protection coating and τ_t is transition time duration.

Sun and Bai [9] suggested a time variant corrosion rate model, adapting the Guedes Soares and Garbatovs [8] model, to describe the corrosion rate instead of the corrosion wastage. In the model, the corrosion rate increases as an experimental function of time and finally tends to be a constant value in the third phase.

Qin & Cui [10] proposed a model in which the coating protection system (CPS) such as coating was assumed to deteriorate gradually and the corrosion may start as pitting corrosion before the CPS loses its complete effectiveness. The corrosion rate was defined by equating the volume of pitting corrosion to uniform corrosion. This was regarded as the transition period and the corrosion rate increases. After the CPS loses its complete effectiveness, general corrosion starts and the corrosion rate decreases due to the increasing thickness of the corrosion product as seen in curve 3 of Figure 1. Hence, the whole corrosion process was divided into three stages:

- No corrosion when the CPS is fully effective
- Corrosion accelerating when pitting corrosion generates and progresses
- Corrosion decelerating

In this model, the Weibull probability density function was recommended to describe the corrosion rate. This model has enough flexibility to describe different models of corrosion rate using the same format and is given as: where $d(t)$ is

$$d(t) = \begin{cases} 0 & 0 \le t \le T_{st} \\ d_\infty \left\{ 1 - exp\left[-\left(\frac{t - T_{st}}{\eta} \right)^{\beta} \right] \right\} & T_{st} \le t \le T_L \end{cases}$$

the corrosion thickness, d_∞ is the long-term thickness of the corrosion wastage, T_{st} is the coating life and β and η are Weibull parameters.

Paik & Thayamballi [3], [4] also suggested that the corrosion behavior could be categorized into three phases:

- Durability of coating
- Transition to visibility obvious corrosion
- Progress of such corrosion.

Coating life was assumed to follow the log normal distribution. The transition time was considered to be an exponentially distributed random variable as seen in curve 4 of Figure 1. The main contribution of this model is somewhat sophisticated modeling procedure for predicting corrosion wastage in primary member locations or category groups of components in single and double hull tankers and FSPs / FPSOs as a function of age.

$$t_r = C_1 \ (T - T_C - T_t)^{c_2}$$

where t_r is depth of corrosion (thickness loss due to corrosion), T_c is coating life, T_t is transition time between coating durability and corrosion initiation, T is structure age, C_1 is coefficient indicative of annualized corrosion rate and C_2 is coefficients taking account of the characteristics of corrosion progress.

Melchers [11], [12] proposed a marine immersion corrosion model. This model consists of five phases that describe the phenomenon of corrosion progression as seen in Figure 2. Phase 0 consists of very short-term kinetic and bacterial influences that may be ignored in practical applications. Phase 1 represents the situation when the rate of corrosion is controlled by the diffusion of oxygen from the seawater. It may be modeled, closely, as a straight line, implying a constant corrosion rate (r_0). Phase 2 is non-linear and controlled by the rate of oxygen diffusion through the (increasing thickness of the) rust layers, assumed, theoretically, to be have uniform diffusion properties. Evidently, there is a smooth transition from Phase 1 to Phase 2. Phase 2 will proceed until point AP is reached, at which time anaerobic conditions begin to occur under the rust layers next to the corroding steel. In practice there is likely to be a smooth transition around AP as not all points on a corroding surface are precisely at the same stage. Phase 3 is the theoretical start of predominantly anaerobic controlled corrosion, associated with the metabolic activity of sulphate reducing bacteria. At first this activity is high owing to the high availability of nutrients but as this settles down the corrosion rate slows to the rate described by Phase 4. This may be modeled, closely, as linear with time. The model has been proposed in a probabilistic setting with the mean value function for corrosion loss given by f(t,T) as a function of time (t) and temperature (T). Each phase may be described mathematically as follows:

$$f(t,T) = \begin{cases} r_0 = 0.0539(2)^{0.1T} \frac{mm}{year} & Phase\ I \\ [3(Et+F)]^{1/3}\ mm & Phase\ II \\ r_a = 0.066 \exp(0.061T) \frac{mm}{year} & Phase\ III \\ r_s = 0.045 \exp(0.017\,T) \frac{mm}{year} & Phase\ IV \end{cases}$$

The coefficients E and F are functions of temperature and the point AP is described by parameters c_s, c_a and time t_a, given by

$$t_a = 6.61 \exp(-0.088T)$$
$$c_a = 0.32 \exp[(-0.038T)]$$
$$c_s = 0.075 + 5678T^{-4}$$

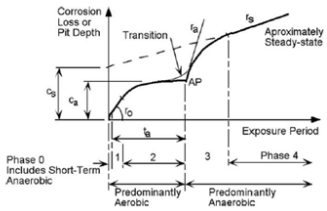


Fig. 2. Corrosion loss exposure time model.

Ivanov et al [13] proposed a model with similar features to the one of Guedes Soares and Garbatov [8]. The first phase is while the protective coating is intact and there is

no corrosion wastage of the structure. The second phase is a gradual acceleration of corrosion as the coating breaks down and has a linear dependency with time. The final phase is when the coating has completely failed, and the corrosion rate reaches its maximum. For the third phase, corrosion rates of the steel structure have been treated as constant over the rest of the ships lifetime. This argument, though not quite true, is believed to be reasonable for practical use.

In all these models referred above, corrosion models require calibration to empirical corrosion loss data to determine values of parameters in the model.

C. Based on Environment

Since the above mentioned models make no effort to establish realistic corrosion rates as a function of different environmental conditions, different areas of the ship hull as well as different types of ships, new corrosion models accounting for the environmental conditions were considered essential. Hence

Marine Atmospheric Corrosion:: The other form of corrosion relevant to ship structures and to ballast tanks is marine atmospheric corrosion. The model proposed by Gardiner and Melchers [11] accounts for the chemical and physical processes of ship corrosion in an enclosed atmospheric environment and, as is usual for atmospheric corrosion, depends on temperature, time of wetness and salt deposition, but also on the voyage time. They considered the topside ballast tanks, double bottom ballast tanks and cargo spaces in bulk carriers. Factors include tank status, effectiveness of protective coatings and presence or otherwise of sacrificial anodes. The model is given by

Mass loss / voyage=WF .VT .$(k_1 + k_2[Salt] + k_3 T)$ with the units of mass loss being millimeters and WF expressed as percentage wetting fraction. VT is the voyage time in years, [Salt] is the salt concentration in parts per million (ppm), T is temperature (degree C) and k_1, k_2 and k_3 are constants.

Marine Environmental Factors: : Guedes Soares et al [14] studied the effect of major marine environmental factors on corrosion wastage of immersed external hull surfaces. They developed a model for long-term corrosion wastage of submerged shell plating. This model is based on immersion corrosion mechanisms, and calibrated with measured corrosion wastage database for tankers. This long-term corrosion model express the corrosion wastage as a nonlinear function of time; it accounts for different trading routes, the associated environmental conditions, and the percentage of time spent in each of these environments. This model has the advantage over most others that, instead of providing only the average corrosion wastage, it also provides information about how the corrosion wastage changes with respect to the environmental factors associated with the navigation routes which can also be reflected in the entire life of ship. Hence

$d_L(t) = \sum_{i=1}^{n} p_i d_{c,i}(t)$

where $d_L(t)$ is the long term prediction of corrosion wastage for the entire life of ship, p_i is the weighting factor representing the relative duration of the i^{th} stationary period along the lifetime of ship $d_{c,i}$(t) is the short term corrosion wastage of the i^{th} period given by

$d_{c,i}(t) = \pi_{j=1}^{5} f_{i,j} d_{n,i}(t)$

where $d_{c,i}(t)$ is the corrected corrosion wastage, $f_{i,j}$ are the environmental correction factors such as salt content, Temperature, dissolved oxygen, pH and water velocity.

D. Based on Electric Potential

Measurement of Electric potential provides a global tool to get clues about the state of an underwater iron structure with an appropriate cathodic protection. This method works with internal or external problems with any cathodic protection (impressed current or sacrificial). Diagnosis of ships hull corrosion from electric measurements in the electrolyte and not on the bounds can hence be studied. Using Greens equations, a few data and an appropriate series of electric potential measurements, one can get clues and even precise locations of damaged areas on the hull. These results are obtained with efficiency and a great time saving, compared to existing methods.

E. Based on Probability

Noor et al [15] gave a probabilistic time-dependent growth model of marine corrosion as an alternative approach to analyzing corrosion data randomly collected from a large number of like ballast tanks. Rather than making an assumption on the time to the start of the corrosion process and then develop a linear model of corrosion rate, two corrosion depth models which are a function of time have been proposed. The new model can be used to predict the likely variation of corrosion depth at any point of time without having to estimate the corrosion growth rate for each single defect. Even though the value of correlation coefficient were not more than 0.16 indicating poor correlation between averaged depth and vessel age, the incorporation of probability model into the analysis methodology can improve the reliability of the prediction results as well as minimizing the errors. The proposed model simplifies the modeling process so the available data can be fully utilized for prediction purposes.

The Weibull distribution based on linear fitting of the probability plot and verified by the Chi-square goodness-of-fit test is utilized to construct a distribution for all the data by removing the effects of time. This distribution function for all of the data can be expressed as follows:

where x_d is corrosion depth, x_{norm} is normalized depth given

$$F(x_{norm}) = 1 - exp\left[-\left(\frac{x_d}{0.0056 t_v + 0.4475}\right)^{1.05}\right]$$

by $x_{norm} = x_d / d_{(ave(t_v))}$, d_{ave} is linear regression model of defect depth average, t_v is age of vessel in years.

Sanja Bauk and Spiro Ivosevic [16] using the Monte Carlo simulation method developed a predictive model of corrosion wastage over three most sensitive hull structure member areas

of ten aged bulk carriers, being more than 25 years in exploitation. They extended their work [17] to give an optimal procedure of pre-processing the collected data for a better fit into the Weibull distribution function.

IV. LIMITATIONS

Some major work done over the years and the models proposed by various researchers for the prediction of corrosion have been discussed in this paper. Each model has its own limitation over which it is applicable and can be used. It is important to bear in mind that prediction made using predictive models may be incorrect because of the assumptions involved and that they are not to be believed too strongly. Before using predictive modeling or the output obtained, it is important to realize and take account of the limitations involved, including:

- Each model is based on a single deterioration mechanism, however more than one mechanism may be present.
- Quality of output will depend, on applicability of chosen mechanism and quality of input data.
- User of the model, or just the output, may not fully appreciate practical variability of input parameters and magnitude of variation on the output.
- Output from deterministic models is a single value that can be expressed to any level of precision desired. This can give a false impression of the validity of the number.
- Predictions of long-term behaviour are necessarily based on relatively short-term observations
- The simplest model is the one which assumes constant corrosion rate, estimated entirely from observations made as part of normal surveys. Due to the products of corrosion, the corrosion rate decreases with time. However observations from oil tankers showed that in most cases the corrosion rate appears to increase with time and then keep constant. The reason for this appears to be related to dynamic loading that spill off corrosion products in ocean environments. This reasoning makes the output of the available models suspect.
- Simply collecting data without detailed analysis will only result in statistical models with very large degrees of uncertainty and with consequent low predictive capability. Such models are unlikely to be of much practical use for decision-making. Moreover, as they are based on historical data, they may be inapplicable to more modern applications with different operational and maintenance practices. For example, much of the ship data for bulk carriers applies to vessels which did not have coatings for their ballast tanks, a practice which is no longer condoned. Hence, the historical, statistical information, while interesting, is not likely to be applicable to new situations nor is it capable of generalization.
- Extrapolation of models outside range of data to which they were calibrated, is not possible with empirical (statistical) models. As a consequence, statistical models have to be calibrated to a set of structural components (plates, stiffeners) identical from a structural point of view (same type of elements, same type of materials) and submitted to similar conditions: same loading, same environmental conditions, and same operational conditions.

V. CONCLUSION

Development of shipbuilding standards has evolved on the basis of previous experience and knowledge of material behavior rather than on fundamental principles. These standards have worked well with failures limited to elements not built to standards. Nevertheless, significant unscheduled maintenance or repair before completion of design life has resulted in the belief that some requirements in these standards are inadequate. These available codes are probably acceptable for structures with an intended working life. Nevertheless, a more rigorous approach is considered appropriate under circumstances such as:

- Intended working life significantly greater than designed for
- Environmental conditions significantly more severe than those covered by codes
- Where conditions for construction and / or maintenance are particularly difficult
- Where there is a detailed knowledge of the micro-environment

To address these issues, predictive models that mathematically define the assumed mechanism of deterioration are used. Sometimes attempts to model processes at a fundamental level using quantitative relation between degradation rate (obtained from failure data) and operational conditions may also be used. Having decided on the mathematical description it is necessary to determine suitable values for the input parameters obtained from observations of structures or laboratory tests. These models may be deterministic or probabilistic. Deterministic models are usually as simple as spreadsheets while probabilistic models require considerably more detailed input. These models may be utilized to predict the residual thickness, determine the effect of coating longevity on the hull girder properties and evaluate the maintenance needs of the vessel even at the design stage. The use of an appropriate corrosion model is hence crucial for inspection and maintenance planning.

Efforts towards establishing realistic corrosion rates as a function of different environmental conditions, different areas of ship as well as different types of ships is a relatively newer area of development and needs to be progressed further to account for various environmental factors such as salinity, temperature, dissolved oxygen, pH and flow velocity including the effect of ships service life in different routes etc. For the development of generalized models, the following are considered essential

- Detailed understanding of factors and their influence
- Reference back to fundamental corrosion mechanics

In attempting to understand the influences of various factors, it is necessary to move away from observations on actual structures (and the concomitant large uncertainties in the data)

to a study of the behaviour of corrosion specimens. Development of such mathematical corrosion models and introduction of sophisticated hull condition monitoring programmes has lead to utilization of reliability techniques to predict the future behaviour of ship structures. Methods such as predictor-corrector methods are hence one of the futures of corrosion modeling.

REFERENCES

[1] TSCF (Tanker Structure Co-operative Forum), 1992, "Condition evaluation and maintenance of tanker structures", Witherby & Co. Ltd, London. 1992.

[2] Yamamoto N., Ikegami K., "A study on the degradation of coating and corrosion of ships hull based on the probabilistic approach", *Journal of Offshore Mechanics and Arctic Engineering*, 120, 1998, pp. 121-128.

[3] J.K. Paik, S.K. Kim, S. Lee, Y.E. Park, "A probabilistic corrosion rate estimation model for longitudinal strength members of bulk carriers", *Journal of Ship and Ocean Technology*, 2 (1), 1998, pp.5870.

[4] Jeom Kee Paik, Ge Wang, Anil Kumar Thayamballi, Jae Myung Lee, Young Il Park, "Time-Dependent Risk Assessment of Aging Ships Accounting for General / Pit Corrosion, Fatigue Cracking and Local Denting Damage", ABS Tech Paper 2003.

[5] Harada S, Yamamoto N, Magaino A, Sone H, "Corrosion analysis and determination of corrosion margin", Part 1and 2, IACS discussion paper, 2001.

[6] Southwell CR, Bultman JD, Hummer Jr CW, "Estimating of service life of steel in seawater", Seawater corrosion handbook, New Jersey, USA: Noyes Data Corporation; 1979, 374-87.

[7] Yamamoto N. "Reliability based criteria for measures to corrosion", *Proceedings of the 17th International Conference on Offshore Mechanics and Arctic Engineering (OMAE98), Safety and Reliability Symposium*, New York, USA: ASME, 1998.

[8] Guedes Soares C, Garbatov Y, "Reliability of maintained, corrosion protected plate subjected to non-linear corrosion and compressive loads", Marine Structures, 12, 1999, pp. 42545.

[9] Sun, H. and Bai, Y., "Time-Variant Reliability of FPSO Hulls", *Trans. SNAME*, 109, 2001, pp. 341-366.

[10] S.P. Qin, W.C. Cui, "A discussion of the ultimate strength of ageing ships, with particular reference to the corrosion model", *Proceedings of the Institution of Mechanical Engineers: Part M, Journal of Engineering for the Maritime Environment*, 216, 2002, pp. 155-160.

[11] C.P. Gardiner, R.E. Melchers, "Enclosed atmospheric corrosion in ship spaces", *British Corrosion Journal* 36 (4), 2001, pp. 272276.

[12] R.E. Melchers, Probabilistic models for corrosion in structural reliability assessment Part 2: models based on mechanics, *Journal of Offshore Mechanics and Arctic Engineering*, 125 (4), 2003, pp. 272280

[13] L.D. Ivanov, G.E. Wang, A.K. Seah, "Evaluating corrosion wastage and structural safety of aging ships," Pacific international maritime conference (Sydney, Australia, Feb 25, 2004)

[14] C. Guedes Soares, Y. Garbatov, A. Zayed, G. Wang, "Non-linear corrosion model for immersed steel plates accounting for environmental factors", *Transactions of the Society of Naval Architects and Marine Engineers*, 113, 2005, pp. 306322

[15] Norhazilan Md Noor, George H. Smith, Nordin Yahaya, "The Weibull time-dependent growth model of marine corrosion in seawater ballast tank", *Malaysian Journal of Civil Engineering* 19(2), 2007, pp. 142-155

[16] Sanja Bauk and piro Ivoevi, "Analyzing the Corrosion Wastage over Some of the Bulk Carriers' Member Locations", *Journal of Mechanics Engineering and Automation*, 1, 2011, pp. 377-384

[17] Sanja Bauk and piro Ivoevi, "Combining Weibull Distribution Function and Monte Carlo simulations in Predicting Corrosion Losses Over Inner bottom and Hoper Plating of Ageing bulk-Carriers", *Journal of Maritime Research*, Vol. IX. No. 3, 2012, pp. 75 80



Nitin Agarwala Cdr Nitin Agarwala, is a PhD from Cochin Univ. of Science and Technology, India, 2014. He was commissioned in the Indian Navy in 1993. The officer is a Naval Architect with both field and teaching experience. He has served on-board a naval ship, the Fabrication Department of Naval Dockyards Mumbai and Vishakhapatnam and Headquarters of Western Naval Command. He is presently the officer-in-charge of the Hull Inspections and Trials Unit at Vishakhapatnam. During his career of 20 years in the Navy he has published 10 papers in refereed journals and conferences. His areas of research interest are Wave structure interaction problems, Acoustic structure interaction problems, Hydroelasticity related ship structure problems and Corrosion problems associated with ships. He has been commended by the Chief of Naval Staff in 2005 and Flag Officer Commanding-in-chief in 2010.

Stress Corrosion Cracking of SS 304 L Inchloride Environment at Near Boiling Temperatures - Mitigation & Acceleration

Harshad Tarate
Geogy Abraham, Vivekanand Kain
Homi Bhabha National Institute, Anushaktinagar,
Mumbai 400094, India,
htarate@gmail.com

***Abstract*—Stress corrosion cracking (SCC) refers to cracking caused by the simultaneous presence of tensile stress and a specific corrosive medium. During stress corrosion cracking, the alloy is virtually un-attacked over most of its surface, while fine cracks progress through it. The cracking phenomenon has serious consequences since it can occur at stresses within the range of typical design stress. Stainless steels readily crack in chloride bearing environment. A crack may take time to initiate but once initiated, it grows at an increasing speed. Stainless steels undergo SCC in hot chloride, sulphide and seawater environments. Residual tensile stresses, even those arising from welding are sufficient to cause SCC. The paper details the work done to establish the various factors that can mitigate or accelerate SCC in SS 304 L grade steels especially focussing on the effect of oxygen and potential at temperatures near boiling. The study has been carried out by using Slow Strain Rate Testing (SSRT) technique under different chloride environments, and oxygen concentrations. The paper finally suggests the methods by which the life of SS 304 L components could be increased by regulating the parameters.**

Keywords: Slow Strain Rate Test, Sensitization, DL-EPR test, electrochemical polarization test.

I. INTRODUCTION

Austenitic stainless steels have excellent resistance to uniform corrosion in various environments ranging from mildly acidic to alkaline [1-6]. The main reason for its good corrosion resistance is the formation of a strong, protective passive film over surfaces. This passive film is primarily chromium oxide and an air formed film is around a few nm thick. This film is a self healing film i.e. stainless steels tend to repassivate instantaneously when the passive film is damaged. However, austenitic stainless steels are particularly susceptible to localized forms of corrosion viz. pitting, crevice and stress corrosion cracking (SCC) [1-6].

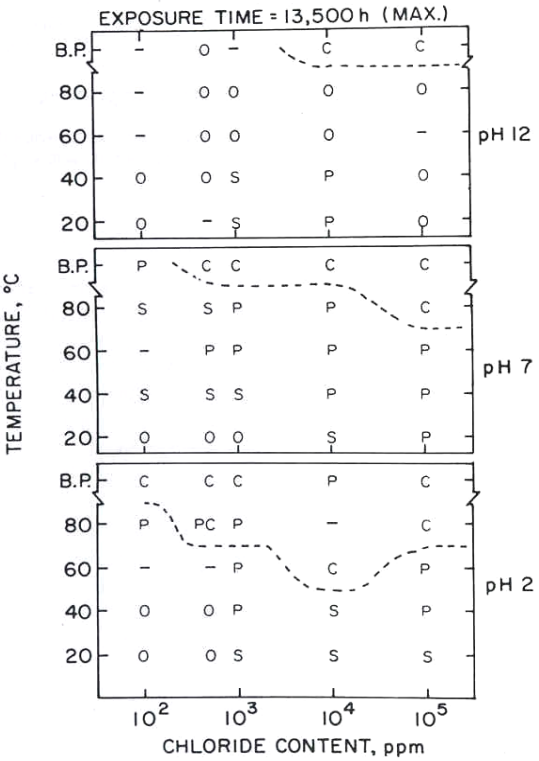
Austenitic stainless steels are particularly prone to SCC in chloride and sulfide environments. As with all cases of SCC, it requires a synergistic action of a susceptible material, particular environment and tensile stresses [1-6]. While the austenitic stainless steel – chloride environment combination is a known combination that results in SCC, the tensile stresses are invariably present in components either as applied stresses (from the process) or due to residual stresses (from various fabrication processes e.g. bending, welding etc.) [1-6].

The austenitic stainless steels and chloride environment mostly results in transgranular stress corrosion cracking (TGSCC). SCC in chloride environment shows a typical branching nature and the cracks are very fine. The rate of cracking goes on increasing as the un-cracked ligament reduces.

Typically SS is not known to undergo SCC at low temperatures (i.e. below 60 °C) in chloride solutions. An exhaustive study [7] on the effect of chloride ion concentration and temperature of exposure on pitting and SCC behaviour was done and the summary of the results is shown in Fig. 1. This study included annealed, heat treated, welded and bent stainless steel samples for 13,500 h in solutions with varying chloride ion concentration, pH and temperature. This study showed that at pH of 7, the SCC of austenitic stainless steels did not take place till the chloride concentration increased beyond 10^5 parts per million (ppm). At pH ~ 2, it took only 10^4 ppm chloride ions to cause SCC. Even pitting corrosion took place at chloride concentrations above 500 ppm at 60°C in water with pH ~ 7. Using fracture mechanics approach (measuring SCC growth rate at different temperatures in 22% sodium chloride solution), it has been shown [8] that stress corrosion cracks do grow at even 50 °C in case of type 304 (solution annealed condition) and even at lower (ambient) temperatures for type 304 (sensitized condition), although the rate of growth was very low (of the order of 10^{-11} m/s).

Boiling solutions of chloride have been used for long to test the susceptibility to SCC. Magnesium chloride is known to be a particularly aggressive solution that produces SCC for stainless steels. The boiling point of magnesium chloride changes with the concentration of the salt. A standard procedure (G36 ASTM, 2007) is to test in 45 per cent solution of magnesium chloride that boils at 155 °C. The magnesium

and calcium chlorides hydrolyze to produce acidic solutions and therefore are aggressive than sodium chloride in producing SCC of stainless steels. The pH of the solution at the tip of a crack in type 304 stainless steel undergoing SCC in boiling magnesium chloride test is shown [9] to be between 1.2 and 2.0. Long term boiling leads to reduction in acidity of the solution and it is known [10] to reduce the aggressiveness (makes it more alkaline) of the solution to cause SCC. It is also reported [11] that with lowering of pH (by acid addition) in magnesium chloride solution, cracking propensity increases while there is no change in cracking propensity when pH is lowered for calcium chloride solution. The boiling magnesium chloride solutions are known to be the most aggressive chloride solution to cause SCC and austenitic stainless steels are known to undergo SCC in this solution even when only residual stresses are present (i.e. without application of external stress) in a few hours. Calcium chloride solution that boils at high temperature (155 °C) and also forms acidic solution upon dissolution also is known to cause severe SCC [12]. Sodium chloride solution (22%) acidified to a pH of 1.5 is used in other standard test procedure (G123 ASTM, 2007) to evaluate the susceptibility to SCC.



C – SCC, P – pitting, S – stains, O – no effect

Fig. 1 Occurrence of SCC and pitting for austenitic stainless steels on exposure for 13,500 h in solutions of 10^2 – 10^5 ppm chloride ions at pH values 2, 7 and 12 at various temperatures upto boiling [7].

The crack growth rates in boiling 22% chloride solution have been measured and for type 304/304L stainless steels in sensitized condition and were of the order of 10^{-8} m/s [8]. These were three orders of magnitude higher than that measured at ambient temperatures. Lowering the chloride concentration leads to very high resistance to SCC. At boiling temperature of 100 °C, type 304 stainless steel showed extensive cracking (in a few days) in 1500 ppm chloride solution compared to over 6 months that it took to obtain the same extent of cracking in a 10 ppm chloride solution [13]. At 250 °C in an autoclave test, type 347 stainless steel was shown to crack readily in a few hours in 3% chloride solution but it took over 1000 hours to crack it when the chloride concentration was reduced to 0.01% [14]. This reinforces the view that the laboratory tests done to obtain SCC in a short testing time (by accelerating the test either by increasing the aggressiveness of the solution, temperature or stress) are difficult to correlate to the long term behavior in field applications. However, a relative ranking of the resistance to SCC of different alloys is readily obtained in laboratory tests.

An exhaustive investigation [15] established the corrosion behavior of low carbon 18Cr-10Ni stainless steel (type 304L) in various (boiling) chloride solutions and listed time to failures in each case. It clearly shows accelerated cracking in chloride solutions in which additions of ferric chloride or sodium dichromate are done but no cracking (heavy uniform corrosion) in mercuric or chromic chloride solutions. Therefore, the cation present in the solution also has a role in determining if passivity prevails over most of the metallic surface and the chloride ion is allowed to cause a local breakage of the passive film to initiate SCC.

Now it is commonly accepted that iron contamination on components made of stainless steels (and in solution annealed condition) results in transgranular SCC even when stored in coastal environments at ambient temperature [16-17]. The corrosion of the embedded iron leads to (a) development of stresses due to a wedging action and (b) concentration of chloride ions. The SCC of components (partially) fabricated from austenitic stainless steel and stored in coastal environment for long term has been reported [18] even when there was no iron contamination on the surfaces. The SCC of stainless steels used as roofing in covered swimming pools in Europe in 1990s is another example of SCC occurring at ambient temperature [19]. Presence of various salts of chlorides (Al, Zn, Ca chlorides) in the corrosion products were related [20-22] to formation of a high chloride content and low pH on SS surfaces of the roof and the support structure above the pools. Chloramines (from body sweat) helped to carry the chlorides to the roof and pools that had fountains and surf makers further helped in carry over of chlorides to the roof and the support structures and also caused high relative humidity. In industries, presence of highly oxidizing ions (Fe^{+3}, Cr^{+6}etc) has been identified in cases where SS had undergone SCC at room or near ambient temperatures. Laboratory studies have also reportedly [17] demonstrated that presence of ferric ions in chloride solutions lead to faster SCC of austenitic stainless steel at room temperature. Type 304L stainless steel is reported [17] to have undergone SCC in an aqueous solution of 500 ppm chloride and hydrogen sulfide at room temperature in overnight exposures. Austenitic stainless steels are also reported [17] to have cracked by SCC in hydrochloric acid vapours at - 4 °C. Austenitic stainless steels

are also reported [23] to have shown SCC at ambient temperature in marine environments. It is estimated that 95% of the industrial and service occurrences of chloride SCC are due to sodium chloride [17]. However,all of these cracking are predominantly transgranular in nature.

The crack growth rate in 22% chloride solution (from ambient to boiling temperatures) has been measured [8] for type 304/304L stainless steels in annealed and sensitized conditions. At ambient temperatures, the crack growth rates were found to be of the order of 10^{-11} m/s which are of consequence for design life of components (10^{-11} m/s leads to crack growth of 0.3 mm in one year). This test does not assess the SCC initiation process but suggests that once initiated, the stress corrosion cracks would certainly grow at these slow rates in components fabricated from stainless steels.

Studies have also shown that the crack growth rate is a direct function of temperature. Pitting is considered by many as a precursor event for initiation of SCC however it was proved by established by Mancia and Tamba [24] that SCC can occur independently under certain environmental conditions.

Therefore in this study, an attempt is being made to assess if chloride ions at concentrations below 10 – 10000 ppm are able to cause SCC at 90 °C and 60 °C. The technique employed in this study to assess susceptibility to SCC is slow strain rate testing (SSRT). SSRT provides a quick enough assessment of the susceptibility to SCC and if done at slow strain rates, observation of SCC in this test implies susceptibility to SCC.

II. EXPERIMENTAL

A. Material and Heat Treatments

The SS304 LN1 used in this present study was in the form of a sheet having a thickness of 6.4 mm. The wet chemical analysis was carried out for the SS sheet. The chemical composition (wt. %) of the alloy used is given in Table 1. The heat treatments employed in this study with corresponding designations are further tabulated in Table 2.

B. Microstructural Characterization

All the specimens were mechanically ground on successively finer grits of emery papers up to 1000 grit finish followed by fine polishing using 1 µm diamond paste. The samples were cleaned in distilled water and then dried in acetone prior to microstructural examination. The samples were examined under an optical microscope after etching. The etchant used to reveal microstructure is listed in Table 3.

C. Hardness Measurement

The micro hardness was measured by Vickers micro-indenter at $100g_f$ load. The dwell time used was 10 seconds. The hardness measurements were an average of 10 readings along the surface.

Table 1.The chemical composition (wt. %) of SS304 LN1.

C	**N**	**P**	**S**	**Cr**
0.018+/- 0.002	<0.1	0.011+/- 0.001	0.003+/- 0.001	18.54+/- 0.18
Mn	**Fe**	**Ni**	**Si**	**Mo**
1.61+/- 0.01	68.94+/- 0.20	9.87+/- 0.10	0.82+/- 0.01	0.018+/- 0.001

Table 2. Heat treatments applied for alloy SS 304 LN samples.

Sample Designation	**Heat treatment condition**
AR	As Received
2	AR + 675 ^oC (60 min) + WQ

WQ: Water Quenching

Table 3.Etching as per Practice A, A262, ASTM used for SS-304LN1.

Solution	**Etching Procedure**
10% Oxalic acid	Electrolytic, 10 V at 1 A/cm^2, time 90 sec

D. Electrochemical Tests

The electrochemical tests carried out for SS304LN included potentiodynamic polarization, potentiostatic measurements and double loop electrochemical potentiokinetic reactivation (DL-EPR) measurements. The measurements were carried out using a potentiostat. The tests were carried out in a conventional three-electrode cell using a Pt foil as the auxiliary (counter) electrode and a saturated calomel electrode (SCE) as the reference electrode **(Ref. 7).** All the electrochemical measurements were done at room temperature and the test solution was bubbled (de-aerated) with Argon gas. The working electrode which was SS304 specimen was mounted in an cold setting epoxy resin to obtain an exposed sample area of 10 mm x 10 mm. The test specimen was provided an electrical contact by spot welding an SS wire and plastic sleeve covering the wire for insulation from solution. The mounted specimen was ground on successively finer grits of emery papers and polished with a diamond paste to obtain a surface finish of 1 µm, rinsed in acetone and dried before each experiment. It was ensured that there is no crevice being formed between the sample and the mount by applying lacquer. At the start of each electrochemical experiment, the specimen was cathodically polarized at - 1000 mV_{SCE} for 60 sec to remove any air-formed oxide film. The tests were initiated after a nearly steady-state open circuit potential (OCP) had developed.

D.1 The double loop - electrochemical potentiokinetic reactivation tests

DL-EPR tests were carried out in 0.5 M H_2SO_4 and 0.01 M KSCN to measure the degree of sensitization (DOS) for as received (AR) and sensitized "sample 2" of SS 304LN1. The solution was used in a deaerated condition at room temperature. Subsequent to each DL-EPR test the specimens were examined by optical microscopy. The DOS values were calculated as the ratio of the maximum current density during reactivation (i_r) and the maximum current density during activation scan (i_a) multiplied by 100.

D.2. Potentiodynamic polarization tests

Potentiodynamic polarization tests onSS samples were carried out in different concentrations of NaCl solutions. These tests were carried out to electrochemically establish the open circuit potential, active dissolution region, passivation potential and potential regions of passivation and start of transpassivity. After obtaining the stable open circuit potential, potential was scanned from 50mV_{SCE} cathodic to OCP to transpassive potential at a scan rate of 20 mV/min. The tests were repeated for specimen (at a given heat treatment condition) to establish reproducibility and in different mediums to distinguish polarization behaviour. The microstructures were examined and recorded after each polarization test to establish the nature of attack. The purpose is to establish the potential at which SSRT tests need to be done in order to demonstrate SCC protection/proneness.

E. Slow Strain Rate Testing

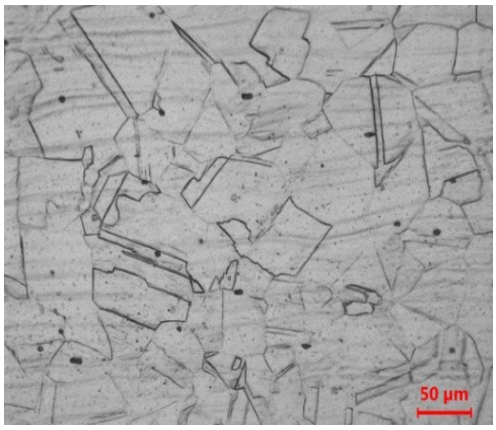
Before starting any SSRT experiment, the material was first tested in air for its mechanical properties and change of surface appearance by straining the tensile specimen in air at room temperature at a strain rate of 10^{-6} s^{-1} to ~ 80% strain/failure. After the test the gauge section surface area became extremely rough such that it was difficult to characterize. Gauge length marking was done on the specimen and actual plastic strain was measured for all tests. The SSRTs were performed on diamond polished flat tensile specimens strained and exposed in different conditions of chloride concentrations at two sets of temperatures, 60°C and 90°C. There was an environment chamber in which a given test solution could be maintained at a given temperature. The accuracy of temperature during the test duration was ± 1 °C. The samples were insulated by Teflon along with the load pins. This was done to prevent the effect of galvanic corrosion as well as to insulate the tensile sample from the pull rods.

In one of the test, a certain potential was applied while doing the SSRT. In this case, both potential and current from the specimen were monitored throughout the test duration. For this purpose, luggin probes were inserted in the experimental set up and a reference electrode (saturated calomel electrode (SCE) and a counter electrode (Pt electrode) were used. Since the test was done at 90 °C, the reference electrode was kept outside the SSRT chamber, in a beaker kept at room temperature and connected to the specimen chamber through two luggin probes.

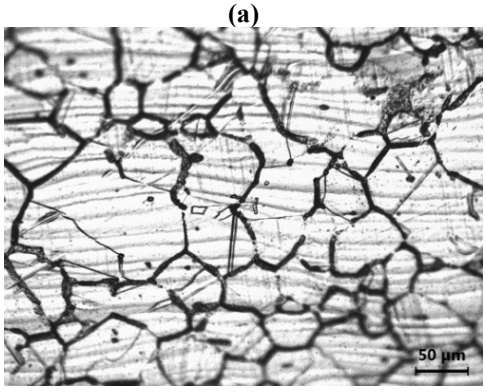
III. RESULTS AND DISCUSSION

A. Microstructural Evolution with Heat Treatment

The microstructural characterization was done for the as received material and also after heat treatment of 675°C one hour and water quenched which has been shown in figure 2(a) and figure 2(b) respectively. Figure 2(a) shows a step structure as the grain boundary was clearly revealed by oxalic acid test during electro etching and is not susceptible to intergranular attack as per ASTM A 262-02a-practice A. Figure 2(b) shows ditch microstructure at the grain boundaries which indicates chromium carbide precipitation and depletion of chromium along the grain boundaries The average grain size is ~ 50 µm.



(a)



(b)

Figure 2.Optical microscopic photographs of SS 304 samples, (a) as received, (b) after 675 °C, 1 h heat treatment.

B. Hardness

Micro-hardness measurements were done on the test sample to characterise the material in terms of hardness. The micro-

hardness measured in as received condition was close to the typical value known for solution annealed SS i.e. 190HV.

C. Electrochemical Measurements

C.1. Double loop electrochemical Potentiokinetic reactivation tests (DL-EPR)

The DL-EPR test results have been analyzed for as received specimen and for heat-treated specimen (675°C for one hour). The DL-EPR curves for as received specimen (Sample AR) is shown in figure 3 (a) indicates higher activation current density and lower reactivation current density as compared to DL-EPR curve shown in figure 3 (b) for the heat-treated sample (Sample 2). For both the specimen, passivation current density is of the order of microamperes/cm^2.The DOS calculated from the plots for as received and sensitized samples are 0.202 and 17.58 respectively.

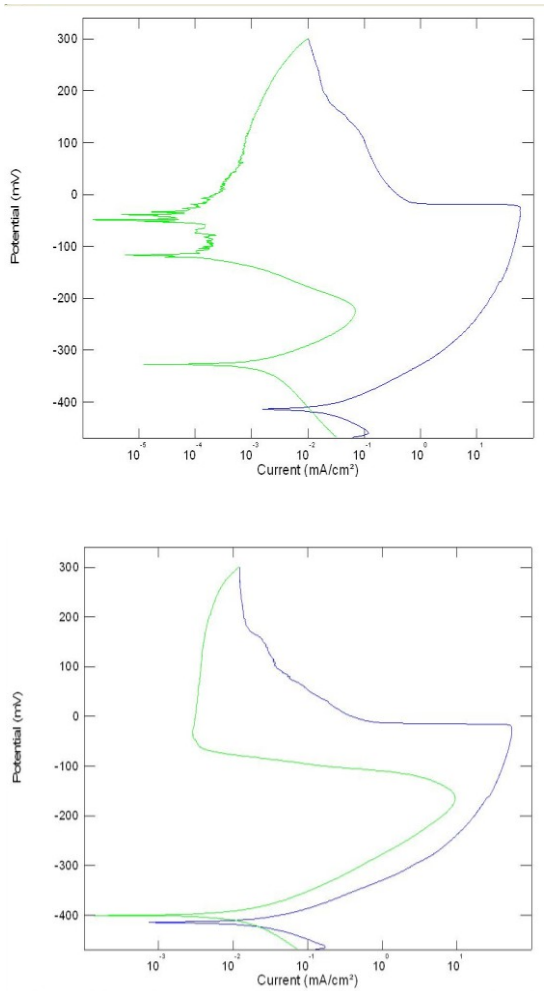


Figure 3: potential vs current density DL-EPR curves; (a) as received material with DOS = 0.202 and (b) heat treated sample (675ºC one hour treatment) with DOS = 17.58.

C.2 Potentiodynamic polarization tests

The potentiodynamic polarization curves in different concentrations of NaCl solution (at 60°C and 90 °C temperature) for the as-received specimen are shown in Figure 3. The current fluctuations in Figure4 were due to the initiation and repassivation of pits (i.e. metastable pitting). Passivation potentials were ranging from -270 mV_{SCE} to 170 mV_{SCE} for the 100 ppm chloride solution whose pH was adjusted to pH3.

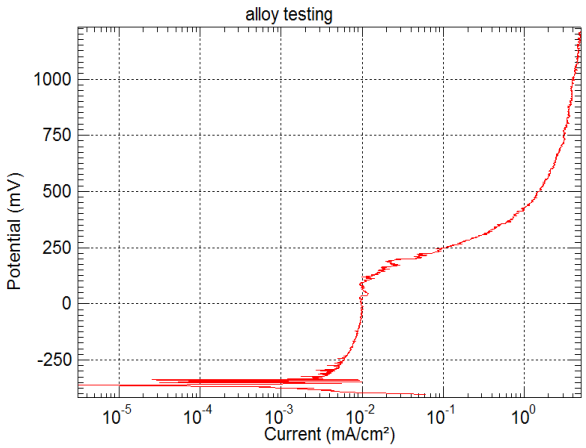


Figure 4(a) Potentiodynamic polarization 100 ppm chloride solution at 90 °C with pH adjusted to 3.

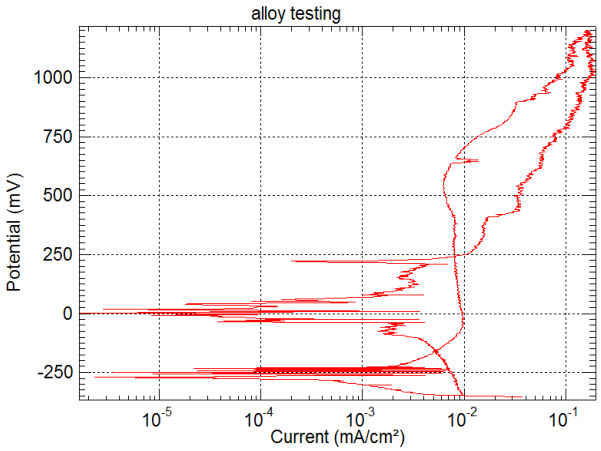


Figure4(b) Cyclic polarization of SS 304 LN1 in 10 ppm chloride solution at 90 °C with pH adjusted to 3.

D. Slow Strain Rate Testing

SSR tests were carried out at different concentrations of chloride ions and exposure temperatures were 90 °C and 60 °C as shown in Figure 5(a). The tensile specimen was provided with electrical connection by spot welding an SS wire on its shoulder. The specimen were insulated from other metallic components in the test system. Potential was monitored for all experiments by means of a potentiostat.

The SSRT testing was done only for the as-received condition of the stainless steel. This was done essentially because chloride SCC has been observed to be non-sensitive to microstructure and is TGSCC for a properly solution annealed stainless steel as well as for a lightly sensitized stainless steel.

As a base line behavior, the test was done in air at room temperature. The stress-strain curve is reported in Fig. 5a. The total elongation obtained was 88%. This stress-strain curve also shows the yield strength and ultimate tensile strength and the stress-strain curve serves as a comparison curve for the behavior we obtain in a given test solution at the same strain rate. The strain at which failure took place for the specimen in 100 ppm and 10 000 ppm solutions at 90 °C was 54 and 45 % respectively (Fig. 5a). This clearly indicates that SCC has taken place as otherwise the specimen would have shown a strain till failure of ~ 88%. This observation was supported by fracture surface examination of the failed sample after the SSRT.

The SSRT at 60 °C in 100 ppm and 10 000 ppm chloride solutions showed strains till failure of 76 and 73 % respectively (Fig. 5). This shows a tendency for SCC though much less than that observed at 90 °C.

Since the test employed to establish the susceptibility was SSRT, the test duration was relatively short (maximum time to failure in air was 10 days), the results showing a high SCC susceptibility at 90 °C and a much lower susceptibility at 60 °C are applicable to short exposures to 100 – 10 000 ppm chloride environment. A long exposure (at lower levels of tensile stresses e.g. residual stresses) may result in a relatively similar difference in susceptibility though the time to failure would be very different (it is dependent on the tensile stress present on the component). SSRT relies on increasing levels of load being applied to the specimen, in order to cause rupture of the passive film (as also strain being produced in the material). Therefore, acceleration in the SCC tendency in SSRT is done by increasing load levels and breakage of passive film by the applied load. Therefore, if the environment is able to cause SCC, we shall see lowered strain to failure.

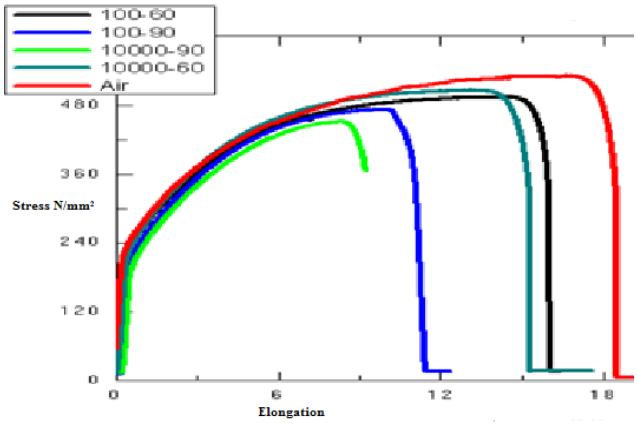


Figure 5(a) - Comparative Stess - elongation plots for SS 304LN1 in air and in 100 and 10,000 ppm water at 60 °C and 90 °C.

The other philosophy of controlling SCC that we wanted to examine in this project was to support repassivation of the specimen by applied potential. For this purpose we had established the polarization curve in the test environment (Fig. 4). Therefore, in the first test, a potential of – 150 mV_{SCE} was applied while doing the SSR test at a strain rate of 10^{-6} s^{-1}. SSRT in 100 ppm chloride solution was done at 60 °C and 90 °C and the stress-strain curves are shown in Fig. 5b. The strain to failure was 76% and 54% at 60 and 90 °C respectively. This data is in line with the results reported earlier in Fig. 5a that there is an enhanced SCC susceptibility at 90 °C compared to that at 60 °C.

The main demonstration of being able to suppress SCC by avoiding passive region (i.e remaining in cathodic potential region) OR by supporting repassivation (i.e. remaining in the strongly passive potential region – Fig. 4) was done in this study. A potential of -150 mV_{SCE} was applied throughout the SSRT. It was found that the current was negative (i.e. cathodic). This implied that the specimen was under cathodic potential regime. The stress –s strain curve for this case is also shown superimposed on the stress-strain curves for the tests where no potential was applied and is shown in Fig. 5b. The strain to failure in case of applied potential of -150 mV_{SCE}in 100 ppm chloride solution at 90 °C was 70% while it was 54% strain when no potential was applied. This behavior (Fig. 5b) shows that the SCC was suppressed as compared to the case when no potential was applied.

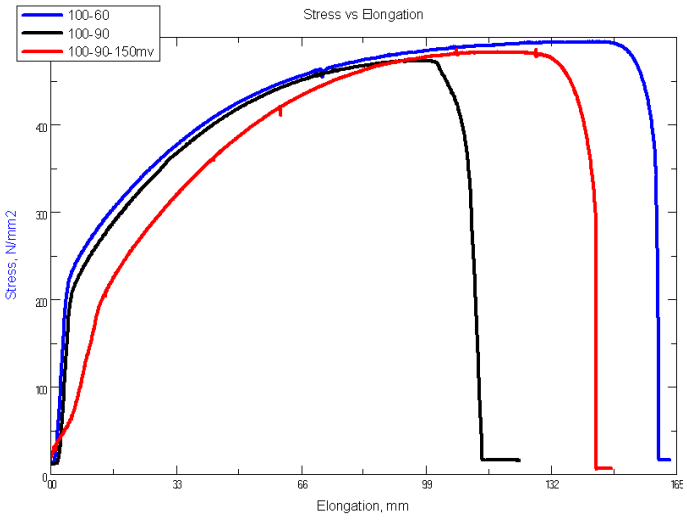


Figure 5(b) SCC in 100 ppm at 90 °C suppressed by application of potential V1=-150mV_{SCE}.

Another philosphy to be tried in this project is to apply a potential in anodic region (correspodning to passivation potential) and do the test at the same parameters (i.e. 90 °C in 100 ppm chloride solution). This test is under progress and result would be presented at the time of presnetation.

The tests done at a potential other than OCP indicate how the austenitic stainles steel would behave when the test

solution/process fluid has saturation with oxygen or with other oxidizing ions. In those cases, the operating potential is expected to increase into the passivation regime and unless it is too oxidizing, it should provide passive film stability and would make brekage of the passive film more difficult. Even if the passive film breaks, the repassivation would be quick enough and in such cases, SCC would become difficult.

IV. CONCLUSIONS

The present study focused on showing the effect of chloride concentration and effect of temperature (both on the lower end) on the susceptibility of an austenitic stainless steel to SCC. Also demonstrated was the effect of application of potential during the SSR test conducted at low levels of chloride at 90 °C. The following conclusions are drawn from the present study:

1. SSRT was clearly able to establish the susceptibility to SCC at temperatures of 60 °C / 90 °C in low concentrations of chloride ions.
2. The SSRT results showed that the strain to failure was in a lower range for tests done at 90 °C and on the higher range for tests done at 60 °C. This was true for chloride concentrations ranging from 100 to 10 000 ppm.
2. Upon application of potential of -150mV$_{SCE}$ on the tensile specimen in the chloride test solution of 100 ppm at 90 °C, the SCC was delayed/suppressed. The same was indicated by a shift of the stress-strain curve towards the right. It is to be noted that the applied potential resulted in cathodic current throughout the test.
4. It is anticipated that an application of higher potential – in the passivation regime, would result in positive current consumption hence anodic protection,

ACKNOWLEDGEMENTS

The authors are thankful to Dr. Gaonkar SO(F), Mr. Sunil Kumar SO(D), Mr. Prafful Sinha SO(C), Mr. Sai Karthik Noduru SO(C) and Mr. V N. Choudhary for their valuable assistance during the period of this research work.

REFERENCES

[1] A. J. Sedriks, “Corrosion of Stainless Steels”, John Wiley & Sons, 2nd edition, New York, 1996.
[2] M. G. Fontana, “Corrosion Engineering”, Tata McGraw Hill, New Delhi, 2005.
[3] D. A. Jones, “Principles and prevention of corrosion”, 2nd Edition, Prentice Hall, 1992.
[4] ASM Handbook, Vol 13, ASM International, Ohio, 1998.
[5] Vivekanand Kain, Corrosion Resistant Materials, chapter in the book entitled Functional Materials: Preparation, Processing and Applications, Eds. S. Banerjee and A. K. Tyagi, Elsevier, 2011.
[6] Vivekanand Kain, Stainless steels: Composition-processing-structure-environment relation to SCC, chapter in the book Stress corrosion cracking: mechanisms, materials and application to industrial problems, Eds V. S. Raja and Tetsuo Shoji, Woodhead Publishing Ltd, 2011.
[7] J. L. Truman, “The influence of chloride content, pH and temperature on the occurrence of stress corrosion cracking with austenitic stainless steels”, Corrosion Science, vol. 17, pp. 737-746, 1977.
[8] M. O. Speidel, “Stress corrosion cracking of stainless steels in NaCl solutions”, Metall. Trans. A., vol. 12, pp. 779-789, 1981.
[9] H. R. Baker, M. C. Bloom, R. N. Bolster and C. R. Singleterry, “Film and pH effects in the stress corrosion cracking of type 304 stainless steel”, Corrosion, vol. 26, pp. 420-426, 1970.
[10] I. A. Maier, C Manfredi and J. R. Galvele, , “The stress corrosion cracking of an austenitic stainless steel in HCl+NaCl solutions at room temperature”, Corrosion Science, vol. 25, pp. 15-34, 1985.
[11] K. C. Thomas, H. M. Ferrari and R. J. Allio, “Stress corrosion of type 304 stainless steel in chloride environments”, Corrosion, vol. 20, pp. 89t-92t, 1964.
[12] J. E. Truman, “The effects of composition and structure on the resistance to stress corrosion cracking of stainless steels”, in British Nuclear Energy Society symposium on Effects of environment on materials properties in nuclear systems, paper no. 10, Institute of civil engineers, 1971.
[13] D. Warren, “Chloride bearing cooling water and the stress corrosion cracking of austenitic stainless steel”, in Proc. 15th annual Purdue industrial waste conference, Purdue University: May 1960, p1.
[14] J. E. Truman, “Methods available for avoiding SCC of austenitic stainless steels in potentially dangerous environments”, in Stainless Steels, ISI publication 117, Iron and steel institute, p101, 1969.
[15] C. Edeleanu, “Transgranular stress corrosion in Cr-Ni stainless steels”, J. Iron Steel Inst., vol. 173, pp. 140-146, 1953
[16] J. B. Gnanamorrthy, “Stress corrosion cracking of un-sensitized stainless steels in ambient temperature coastal atmosphere”, Materials Performance, vol. 29(12), pp. 63-65, 1990.
[17] C. P. Dillon (1990), “Imponderables in chloride stress corrosion cracking of stainless steels”, Materials performance, vol. 29(12), pp. 66-67, 1990.
[18] V. Kain, R. C. Prasad and P. K. De, “Testing sensitization and predicting susceptibility to intergranular corrosion and intergranular stress corrosion cracking”, Corrosion, vol. 58, pp. 15-38, 2002.
[19] J. W. Oldfield and B. Todd, “Ambient temperature stress corrosion cracking of austenitic stainless steels in swimming pools”, Materials Performance, vol. 29 (12), pp. 57-58, 1990.
[20] S. Torchio, “Stress corrosion cracking of type 304 stainless steel at room temperature: influence of chloride concentration and acidity”, Corros. Sci., vol. 20, pp. 555-561, 1980.
[21] J. W. Oldfield and B. Todd, “Room temperature stress corrosion cracking of stainless steels in indoor swimming pool atmospheres”, British corrosion journal, vol. 26 (3), pp. 173-182, 1991.
[22] Prosek T, Iversen A and Taxen C (2008), “Low temperature stress corrosion cracking of stainless steels in the atmosphere in presence of chloride deposits”, Paper no. 8484, CORROSION 2008, NACE International, USA.
[23] R. M. Kain, ‘Marine atmospheric stress corrosion cracking of austenitic stainless steels’, Mater. Perf., vol. 29(12), pp. 60-62, 1990.
[24] F. Mancia and A.Tamba, “Electrochemical Prediction and Control of Localized Corrosion and SCC of Stainless Steels” Corrosion 1988,NACE International, USA, Ohio.



Lt Cdr Harshad Tarate is an alumnus of the 18th Naval Engineering Courseand was commissioned on 01 Jan 2006. He joined the submarine arm in 2008 and has served as senior engineer officer on board INS Sindhushastra. The officer has also carried out instructor duties at submarine school INS Satavahana. Presently he is undertaking his Masters of Technology degree project under the guidance of Dr. Vivekanand Kain at Homi Bhabha National Institute (HBNI)

Development of Tools for Evaluating the Operational Effectiveness of Competing Hull Forms in the Design of Ship for Seakeeping

[1]Cdr (Dr) R Vijayakumar, [2]Lt Vivek Tewari, [3]Lt Cdr B Praveen
[1,3]Deputy Officer in Charge, [2]Trainee Officer,
[1,2,3]Naval Construction Wing,
IIT Delhi, New Delhi, 110016.
[1]vijay2028@gmail.com, [2]vtlko26@gmail.com, [3]praveen2000in@yahoo.com

Abstract— **The performance of a ship in a seaway is a major determinant of its overall functional purpose for which it is designed. This functional purpose encompasses, successfully achieving all the targets set by the role and mission requirements for a vessel. For a warship, this will include successful operation of the entire military payload that she is required to carry and for a merchant vessel, it will include safe carriage of cargo in high seas. Thus, the success of a ship design, to a large extent, depends on the ship's performance in a sea way as dictated by the customer's requirements. Till date, owing to the complexities involved in evaluating the seaway performance combining various roles and missions which a vessel is required to accomplish, it has not been common practice to assess the seakeeping capabilities of various hull configurations competing for a given design requirement. Therefore, it is imperative to evolve and incorporate a comprehensive criterion, which can be used to evaluate the seakeeping performance of a ship, the design for which is primarily based on calm water performance without considering the sea and weather conditions prevailing over the route on which they are required to operate.**

This paper brings out a way for evaluating competing hull forms for their performance against individual mission based criteria and emerges with quantification of the functional purpose of a ship in terms of operational effectiveness. The operational effectiveness of a vessel is defined as the ability of the ship to go to sea and accomplish its mission in whatever weather conditions. Further, the paper also demonstrates development of an in-house software tool that will be able to evaluate the operational effectiveness of competing hull configurations and aid in the choice of a better hull form for the given functional requirement.

Keywords—seakeeping, seakeeping analysis, seakeeping criteria, operational effectiveness

I. INTRODUCTION (*Heading 1*)

Seakeeping is generally regarded as the study of the behaviour of ships in rough weather; ships with good seakeeping qualities are able to go to sea and successfully execute their missions despite adverse weather conditions. Thus the seakeeping performance of a ship is a major determinant of its overall operational effectiveness. At present the experimental/software packages available for seakeeping analysis limit to the calculation of motion responses of the vessel for particular sea condition. However the overall performance for wide variety of sea state and the season conditions are not possible to evaluate experimentally. But it is pertinent for the operator/owner to know the ship overall operational effectiveness of the designed hull form.

Monetary constraints together with the desire to maximise operational effectiveness demand that naval ships, with their ever increasingly sophisticated systems, are designed with known operational capabilities. These capabilities, which should be known in specific environments, must play an important role in the ship design process. The operational capability of a warship in all its major roles will be reduced due to excessive motions and related phenomena in bad weather. A long term analysis of the operational effectiveness of the vessel operating in a specific sea area is thus essential. The tools available today for seakeeping analysis, both experimental and software packages restrict to determination of motion response in a specific sea area. Also it becomes difficult to ascertain the better option from the given design variants of hull form

In view of the same a literature review was carried out based on which a generalised model was developed for seakeeping analysis of warship and comparison of operational effectiveness of two design variants in terms of seakeeping behaviour. A preliminary software tool was developed for calculation of operational effectiveness of ship.The developed software requires Response amplitude Operators as input.

Thus a generic hull form of warship was modelled and its operational effectiveness calculated using the software.

Thus this paper presents the analysis for long term operational effectiveness of the vessel operating in a specific sea area and hence determine the more operational effective option from the given design variables in terms of seakeeping behaviour. The paper also explains the developed software for calculating the overall operational effectiveness of the designed hull form of naval vessel.

II. Generalized Model for Seakeeping Analysis

Seakeeping performance of a vessel is a function of the environment condition under which it is operating, mission it requires to perform and the measure of performance. Based on the same a generic model for this real time problem was developed. The model is given in schematic form in Fig 1.

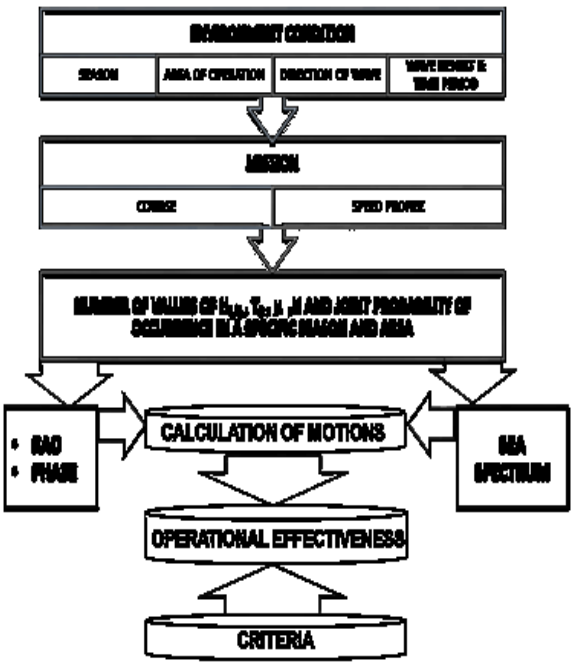


Fig 1: Generalised model developed for seakeeping analysis

From the above model, operational effectiveness (which is in percentage) of a design variant can be calculated for given areas of operation and mission profile. Thus for similar operating conditions two design variants can be compared for their operational effectiveness and a better option can be chosen. Each component of the model is detailed in the following sections.

A. Environment

A very comprehensive atlas based on over 55 million visual observations from ships on passage between 1854 and 1984 was published as Global Wave Statistics by Hogben, Dacunha and Quiver (1986). This superseded the earlier work by Hogben and Lumb (1967). The new atlas covers virtually the entire globe and gives the probabilities of occurrence of significant wave heights and zero-crossing periods for all the sea areas shown in Fig 2. Of the given areas in wave atlas the areas 39, 50, 60, 69, 70, 61, 51 are important for operation near Indian subcontinent as shown in Fig 2.

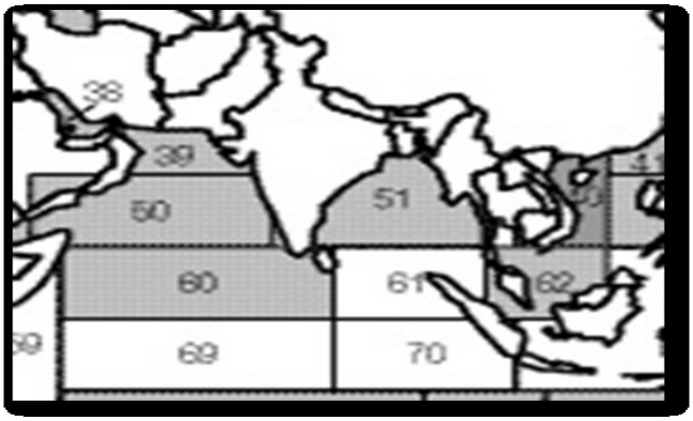


Fig 2: Areas for operation near Indian Subcontinent [1]

The wave atlas gives joint probability of occurrence of a significant wave height and zero crossing periods in an area for a given season.it also gives the probability of occurrence of the wave direction as a percentage of the total observation. An extract from the data is given in Fig 3.Due to the unavailability of wave atlas same abstract data was used for the software development with templates to fill in the correct data on availability.

Area 9; December to February; North West; Percentage of observations = 11.28%

Significant wave height [m]	< 4	4 - 5	5 - 6	6 - 7	7 - 8	8 - 9	9 - 10	10 - 11	11 - 12	12 - 13	> 13	Total
Total	0	1	10	73	210	286	236	120	50	14	0	1000
> 14												0
13 - 14								1	1			2
12 - 13							1	1	1			3
11 - 12							1	2	1	1		5
10 - 11						1	2	2	2	1		8
9 - 10						2	4	4	2	1		13
8 - 9					1	3	6	7	4	1		22
7 - 8					2	6	11	10	5	2		36
6 - 7					4	12	19	14	8	2		59
5 - 6				1	8	24	31	22	8	2		96
4 - 5				2	17	43	44	25	8	2		141
3 - 4				6	37	66	53	14	6	1		183
2 - 3			1	16	63	76	46	14	3	1		220
1 - 2			4	33	66	49	17	4	1			174
0 - 1		1	5	15	12	4	1					38
Total												1000

Fig 3: Wave height and period statistics (after Hogben and Lumb 1967) [2]

We can get an approximation of frequency distribution of the operation profile of the vessel in terms of frequency distribution of season and area number from previous similar ships. Frequency distributions presently used as input for evaluation are shown in Table 1 and Table 2.

Table 1: Frequency distribution of season

Season	Frequency
Spring	0.5
Summer	0.5
Autumn	0
Winter	0

Table 2: Frequency distribution of area

Area Number	Frequency
39	0
50	0
51	1
60	0
61	0
69	0
70	0

B. Mission of Ship

Each mission is associated with a mission speed profile.it is affected by particular navies operating doctrine, specific ship type and system being used. Fig 4 gives a representative Mission Speed Profile (MSP) for transit and patrol. From a previous ship with similar operational profile we can get a fair idea of the annual frequency distribution of the course and speed followed by ship. A sample distribution used as input is given in Table 3 and 4. Thus the joint probability of a vessel travelling in a specific sea area in a specific season with a given speed in a given heading with respect to wave direction encountering a wave of specific wave height and time period can be calculated.

C. Response Amplitude Operators (RAO

Response amplitude operators(RAO) can be calculated for motion of vessel in regular waves using various methods (e.g. strip theory) and is a general output of the present available seakeeping analysis softwares. In this paper RAO's are taken as input. A generic cruiser hull form was modeled using the software Maxsurf Version 11.12.

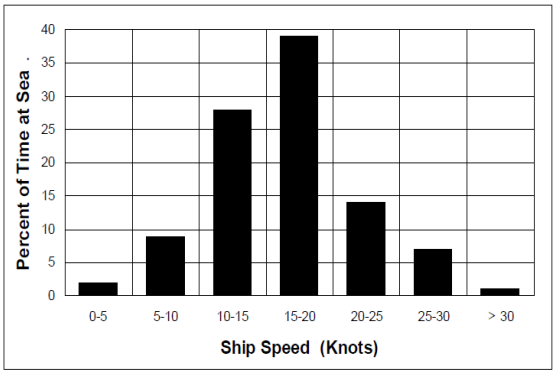


Fig 4: Example of Mission speed profile [3]

Table 3: Frequency distribution of speed

Course	Frequency
N	0.125
NE	0.125
E	0.125
SE	0.125
S	0.125
SW	0.125
W	0.125
NW	0.125

Table 4: Frequency distribution of course

Speed (Knots)	Frequency
10	0.15
20	0.75
30	0.1
40	0

Fig 5 shows the generrated model with main particulars. The model was imported in software Seakeeper Version 11.12 to get the response amplitude operators and phase angles for input. Assumed data for calculation and plots of RAO for 20 knots speed, 135 degrees headind have been given in Table 6 and Fig 6 respectively

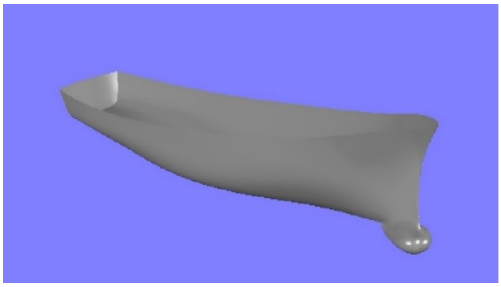


Fig 5: Generated Cruiser Hull form in Maxsurf v11.12 with main particulars

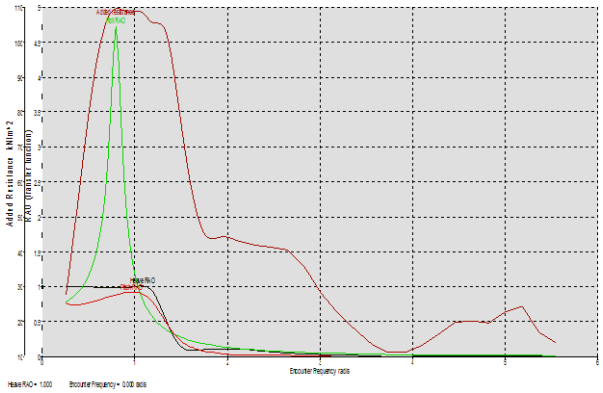


Fig 6: RAO plots for 20 Knots speed and 135 degrees heading generated from Seakeeper v11.12

Table 5: Ship Data For Calculating RAO

Length Overall	123.42 m	Pitch Gyration (% LOA)	25
Beam	16.5 m	Roll Gyration (% BOA)	30
Draft	7.94 m	VCG	7.94
Displacement	4539 tons	Roll Damping Factor	0.075

D. Wave Spectrum [4].

The wave spectrum to be applied in the short term seakeeping calculations is based on the characteristics of the sea area where the ship is going to operate. In this paper Bretschneider spectrum has been used. For a given significant wave height and zero crossing time period the Bretschneider spectrum, or two parameter Pierson-Moskowitz spectrum, is defined as

$$S(w) = \frac{H_S^2}{4\Pi}\left(\frac{2\Pi}{T_z}\right)^4 w^{-5} \exp\left(-\frac{1}{\Pi}\left(\frac{2\Pi}{T_z}\right)^4 w^{-4}\right) \quad \text{.....(1)}$$

E. Calculation of Motions and Parameters [2].

Once the response amplitude operators are known and from the wave spectrum for the area in which vessel is operating motion spectrum of the centre of gravity of vessel easily. The heave motion energy spectrum ordinates are given by:

$$S_{x3}(w_e) = S_\zeta(w_e)\left(\frac{x_{30}}{\zeta_0}\right)^2 \quad \text{....(2)}$$

And similar expression applies for other motion. After calculation of the motions at the center of gravity absolute motions and relative motions at a point with known coordinates from center of gravity can be calculated.

F. Seakeeping Criteria[3,5].

In most cases, naval ships have a variety of missions and support activities, many of which are performed at the same time. It is useful to arrange the seakeeping criteria for these different missions and activities in "mission criteria sets". It is important so that any individual criterion or task is dominant in limiting the ship's performance may be identified and in order that both the criteria limit values and locations of location-dependent seakeeping criteria can be retained for assessment throughout the design process

Mission criteria sets are given in Table 6 and defined for Transit and patrol (TAP), Antisubmarine warfare (ASW), Antiair warfare (AAW), Naval air operations(NAO), Weapon reload (WRL), Replenishment at sea (RAS).These criteria sets can be applied individually or can be combined to provide a measure of overall seakeeping performance. Mission criteria sets can be combined in two basic manners:

- A functional grouping of criteria sets to assess overall performance when the ship is expected to perform more than one mission or activity at the same time; and,
- A combination and reduction of criteria sets to reduce the number of individual criteria that must be evaluated by eliminating the less demanding criteria.

Table 6: Mission Criteria sets [3]

		Location-Dependent Criteria						
		Roll (deg)	Pitch (deg)	No.	MII / min	Vacc (g)	L.acc (g)	Vvel (m/s)
TAP	deck wetness / hr			30				
	slamming / hr			20				
	personnel, bridge	4.0	1.5		1.0	0.2	0.1	
	MSI, bridge (percent)			20				
	MII helm				1.0			
	MII hangar				1.0			
	MII flight deck				1.0			
	propeller emergence / hr			90				
ASW	TAP criteria , plus...							
	sonar emergence / hr			24				
	active sonar	7.5	2.5					
	towed array launch				0.5			
	torpedo launch	3.8	3.8					
AAW	TAP criteria , plus...							
	foredeck gun fire	3.8	3.8					0.5
	VLS launch	8.8	1.5			0.30	0.35	
	CIWS fire	3.8	3.8					0.5
NAO	TAP criteria , plus...							
	helicopter landing	3.0	1.0					3.7[i]
	helicopter traverse	5.0	1.0					
WRL	TAP criteria , plus...							
	VLS reload (3/hour)	3.8	1.0			0.15	0.15	
	chaff reload				0.5			
	torpedo manual reload	1.5	1.5					
	CIWS reload				0.5			
	support equipment	1.8	1.8					
RAS	TAP criteria , plus...							
	magazine				0.5			
	stores room (fwd)				0.5			
	stores room (aft)				0.5			
	deck submergence / hr			0.5				

G. Operational effectiveness [1].

Full operability calculations are rather more complicated because they involve predicting operability in all likely-to-be-encountered wind and waves conditions and speed/heading combinations; such methods are described in detail in [Lloyd, 1989]. In this case there will be, possibly, a trade-off between meeting a specific seakeeping capability and cost, based upon the probability of not being able to perform in some scenarios which occur less frequently and are regarded as less important.

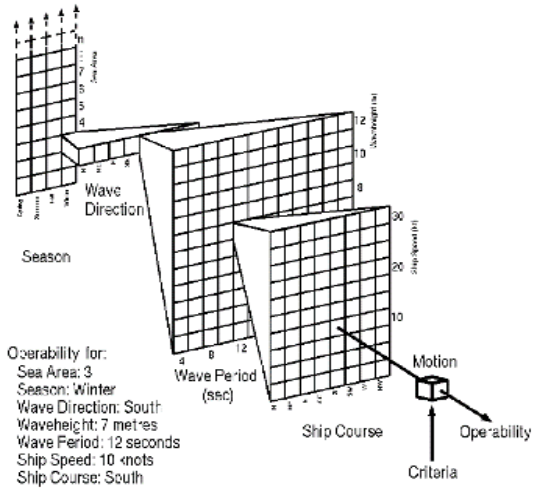


Fig 7: Calculation of operational effectiveness. [1]

Once the operating scenario has been specified using the scatter diagrams as shown earlier, and the conditional frequency distribution of wave direction has been determined from suitable wave atlases, it is possible to determine all relevant ship motions from the short term responses for every combination of ship course and heading, as illustrated in the Fig 7 taken from [Lloyd, 1989].The proportion of time the ship spends in a given season, sea area, wave direction, zero-crossing period, and significant wave height at a given speed and course is given by

$$P = F_{SEASON}\, F_{AREA}\, F_X\, F_{TH}\, F_{COURSE}\, F_U \text{ ----------(3)}$$

The ship can successfully execute its mission if all the responses are less than the critical levels for the mission being considered. The proportion of time for which this is the case (the operational effectiveness) is obtained from the weighted sum of all the possible values of P. Mathematically this may be written as:

$$\text{Operational Effectiveness} = \sum_{season} \sum_{area} \sum_{x} \sum_{th} \sum_{course} \sum_{u} (P\, \lceil_1\, \lceil_2\, \lceil_3\, \lceil_4 \ldots .. \lceil_n) \text{ -------- (4)}$$

Where,

$\lceil_n$ is counting function

$\lceil_n = 1$ for $r_n < r_{crit}$

$\lceil_n = 0$ for $r_n > r_{crit}$

III. DEVELOPMENT OF THE SOFTWARE TOOL

The real time problem modelled as explained was converted into a software for calculating the operational effectiveness of the vessel. Visual basic was used at the front end as a user interface and Microsoft Excel was used as back end for storing data and as well as for all the calculation. The unique combination of two provided the advantage of friendly user interface and reduction in programming in visual basic.

A common template was used for interaction between visual basic and Microsoft excel. Visual basic provided the input data forms in which the user enters data. The data then is transferred to Microsoft excel for storage or computation. The result is then communicated back to visual basic, which displays it as the output form.

Following features have been included in the software:

(a) Stores and displays the available seakeeping criteria. It also provides an option for editing the criteria to the user as with time the criteria gets refined.

(b) Takes as input the response amplitude operators for the vessel at different speed and heading angle, and Calculates of rms roll and pitch, relative motions, absolute motions and probability of slam etc. and Motion Sickness Index (MSI), Motion Induced Interference (MII)

(c) Calculates overall and individual operational effectiveness of criteria.

The software in total has six forms. The various forms used are described as follows:

(a)The first form is a splash screen which is displays while the program loads and picks up stored values from excel sheet. It is shown in Fig 8.



Fig 8: Splash Screen during Loading of Software

(b)After the splash screen the main user option form is displayed as shown in Fig 9.

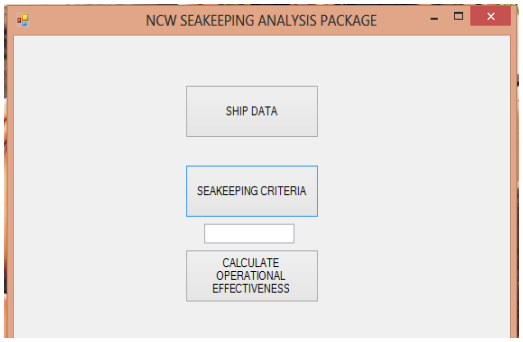


Fig 9: Main User Option Form

(c). Using the ship data form by cicking the SHIP DATA button, the main particulars and data regarding the operating profile of the ship are taken. Fig 10 describes the form.

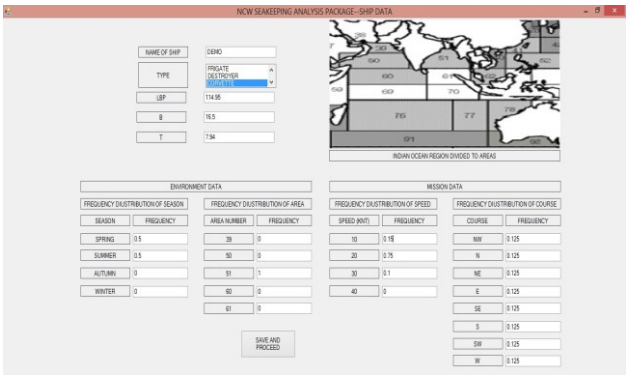


Fig10 Ship Data Entry Form

(d) Appears on pressing the "CRITERIA" button in Main User Option Form. Criteria form displays the criteria stored in the software. The criteria can be edited using the "EDIT" button in form. Criteria Form along with the selected criteria for evaluation are shown in Fig 11.

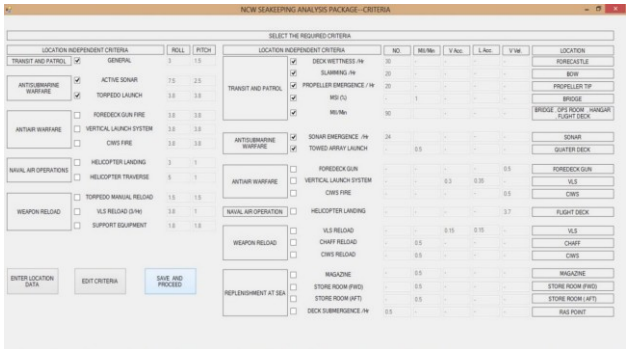


Fig 11: Seakeeping Criteria Form

(e) The data of various locations in ship required for calculation are entered using Location Data Form. The form appears on pressing "ENTER LOCATION DATA" button in Criteria Form. The form along with assumed location data are shown in Figure 12

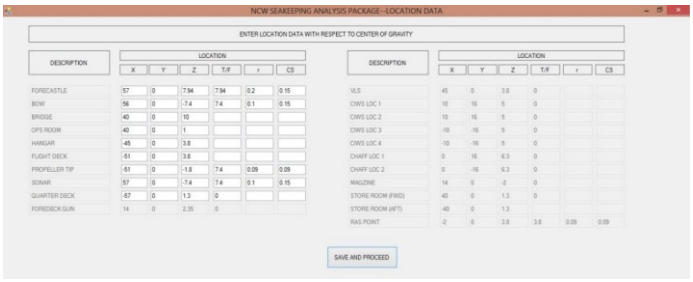


Fig 12: Location Data Form

(f) Final output is displayed as form "OPERATIONAL EFFECTIVENESS" shown in Fig 13

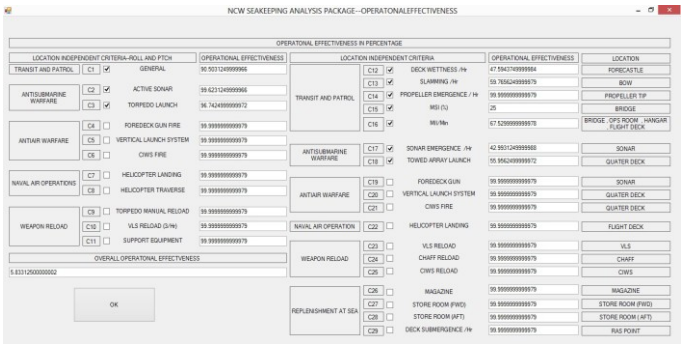


Fig 13: Final Output Form

IV. Results and Discussion

A generic cruiser hull form was modeled using the software Maxsurf v11.12.. The model was imported in software Seakeeper v11.12 to get the response amplitude operators and phase angles for input. The hull form was analysed for operational effectiveness for Anti-Submarine Warfare mission using assumed location data (for weapons etc.). Result obtained is shown in Fig. 13.Overall effectiveness is found to be 5.83 percent. It can be seen that though effectiveness of individual criterias is higher, still overall effectiveness is low. The main reason behind this is that the overall effectiveness is a representation of when all criterias are being satisfied simultaneously. The results obtained are expected to have high amount of error due to following reasons:

- Non availability of complete wave atlas the same wave data of one sea area in one season and in one direction was fed for all entries.
- Assumptions of locations data was assumed
- Swell up coefficient is not correctly known for the hull form thus assumed.

V. CONCLUSION AND FUTURE SCOPE OF WORK

A generalised model for seakeeping analysis of design variants was developed. The modelled real time problem was converted into a software having visual basic as front end and having Microsoft excel as Back end for storing data and calculation.

Due to lack of data operational effectiveness was calculated using an assumed model and limited wave data. The result obtained may have error. Despite of the error in result the problem has been modelled as a software and just requires feeding of correct wave and model data when available. Different design variants can be analysed using this tool for selecting the appropriate variant as per mission requirements.

The software developed is still at a preliminary stage and requires following work to be incorporated:

- Data for Joint probability of HS and Tz for specific area to be entered in excel of the programme once the complete wave atlas is available.
- Once the wave data is fed in the programme the software requires validation with real time data of warship including operational profile, RAO's and location data for weapons.
- Seakeeping criteria for core aviation integration with warship (for aircraft carriers) has not been included and may be worked upon.
- There are no available seakeeping criterias for mission like minesweeping, amphibious operation and launching of boats. A direction towards development of these criteria may be envisaged.

References

[1] A R J M Lloyd (1989)."Seakeeping : Ship behaviour in rough weather", Ellis Horwood Limited, 1989

[2] P. Couser, "Seakeeping analysis for preliminary design. formation design systems".

[3] "STANAG 4154 : Common Procedures for Seakeeping in the ship Design Process" Military Agency for Standardisation, 2004

[4] "Seakeeping Assessment, Part E , Chapter1", Bureau Veritas Rules For Naval Ships, 2011

[6] T C Smith, "A survey and comparision of criteria for Naval missions", David Taylor Research Center, 1990



Cdr (Dr) R Vijayakumar is a Ph.D. from Indian Institute of Technology Delhi in 2009. During his career of 20 years he has served in both the Naval Dockyards and Design Directorate. He is presently appointed as Adjunct Faculty at the Naval Construction Wing, Department of Applied Mechanics at Indian Institute of Technology, Delhi where he teaches the subjects of warship design, structural design of warship and Ship Dynamics. He has published 18 papers in refereed journals and conference. His fields of interest include Warship Design, Ship Hydrodynamics, Ship Dynamics and Computational Fluid Dynamics (CFD).



Lt Vivek Tewari is a PGDIIT form from Indian Institute of Technology Delhi in 2013. He is presently working as Assistant Manager in SBC (V). His areas of research interest are Ship Hydrodynamics, Ship Dynamics.



Lt Cdr B Praveen is a graduate of Naval Architecture from the Cochin University of Science and Technology. He has done a PG Diploma in Naval Construction from Indian Institute of Technology, Delhi and M Tech in Ocean Engineering and Naval Architecture from Indian Institute of Technology, Kharagpur. He is presently appointed as Adjunct Faculty at the Naval Construction Wing, Department of Applied Mechanics at Indian Institute of Technology, Delhi, where he teaches the subjects of Resistance, Propulsion and Ship Dynamics. He is a member of the Institution of Naval Architects, India. His fields of interest include Warshi Design, Propulsion and Ship Dynamics

WAVELET TRANSFORM AN EMERGING TIME FREQUENCY ANALYSIS TOOL FOR ROLLING ELEMENT BEARING FAULT DIAGNOSIS

Commandant(JG) (Dr.) Angello Innocent Devasigamani[1], **Dr. Animesh Chatterjee**[2]
[1]750 SQN(CG), Daman Indian Coast Guard
[2]Department of Mechanical Engineering,
Visvesvaraya National Institute of Technology, Nagpur
[1]angellomani@gmail.com, [2]achatterjee@mec.vnit.ac.in

***Abstract*—Rolling element bearings are one of the most essential parts in rotating machinery. During operation, bearings are often subjected to high loading and severe conditions. Under this severe operating condition, defects are often developed on the bearing components. Rolling element bearing failure can cause production loss or even catastrophic damage such as large production-line equipment failure or even human casualties. One way to increase operational reliability and machine availability is to diagnose bearing faults at the incipient stage. Of the numerous bearing fault diagnosis techniques available to date, Fast Fourier Transform(FFT) is one of the most popular. However, the drawback of FFT is that it does not give time information and is not suitable for non- stationary signal. As rolling element bearing defects are often non stationary in nature, thus Fast Fourier Transform cannot be effectively used for bearing fault diagnosis. To overcome the above drawback a joint Time-Frequency analysis technique is required for fault diagnosis. In this paper an attempt has been made to study the distinct advantages offered by new Time-Frequency analysis technique known as Wavelet Transform towards easy identification of types of bearing defects in comparison with the existing widely used bearing fault diagnosis technique known as Fast Fourier Transform(FFT). The paper also deals with the main limitations of FFT in terms of handling non – stationary signal and how the easily the same difficulty can be overcome by using Wavelet Transform.**

I. Introduction

Rolling element bearings are one of the important components of rotating machineries. Bearings generally fail under fatigue conditions. Manufacturing defects, improper installation or lack of lubrication also significantly shortens bearing Fatigue life. The bearing defects are either a localized or distributed defect such as wear, flaking, crack or other miscellaneous defects in bearing components. In the past it has been observed that, bearing failure often leads to breakdowns in machines, which at times lead to serious damages to machine, interruption in production and sometimes even human casualties. One way to increase the operational reliability and availability of these machineries is by detecting bearing faults at the very incipient stage, thereby assisting in reducing maintenance costs and avoiding catastrophic failures. In order to prevent these kinds of failures from happening, various bearing fault diagnosis techniques have evolved over a period of time.

Some of these techniques include bearing temperature monitoring, lubricant analysis and bearing vibration monitoring. However, the limitation with bearing housing temperature monitoring or simple vibration measurement is that, they don't exclusively pinpoint the presence of bearing fault in the machine. Recently, researchers have shown that bearing fault generates a series of impulses whenever the rolling element passes over the defect. These impacts can be observed at bearing defect characteristic frequencies in vibration spectrum. The defect characteristic frequency depends upon bearing geometry and rotational speed and hence measured vibration signal from the bearing housing can be used for detecting presence as well as type of various bearing faults in the machines.

Analytical Representation of Bearing Defect Characteristic Frequencies

Rolling element bearings generate vibration with characteristic defect frequencies, which are related to bearing geometry, number of rolling elements and shaft speed[1]. The expressions for these characteristic frequencies are presented below in terms of following notations

$\omega_{i,g,e}$- Angular speed of inner race, cage and outer race

$f_{i,g,e,r}$- Rotational frequency of inner race, cage, outer race and rolling element.

d - Diameter of rolling element

D_P - Pitch diameter

θ - Contact angle

N - Number of rolling elements

The cage angular speed is given by

$$\omega_g = \frac{1}{2}\left[\omega_i\left(1-\frac{dcos\theta}{D_p}\right)+\omega_e\left(1+\frac{dcos\theta}{D_p}\right)\right] \quad (1)$$

The Ball Pass frequency Outer Race(BPFO) can be evaluated by multiplying the number of rolling elements with the relative angular speed between cage and outer race. Thus, BPFO can be given as

$$BPFO = N(\omega_g - \omega_e) \quad (2)$$

Substituting equation 1 into 2, using the relation ω = 2πf and by considering that outer race is stationary BPFO can be further simplified and expressed as

$$BPFO = \frac{N}{2}(f_i)\left(1 - \frac{dcos\theta}{D_p}\right) \quad (3)$$

Ball Pass Frequency Inner Race (BPFI) can be evaluated by multiplying the number of rolling elements by the relative angular speed between cage and inner race. It is given by the equation

$$BPFI = N(\omega_i - \omega_g) \quad (4)$$

Putting equation 1 into 4 and by considering that outer race is stationary BPFI can be further simplified and expressed as,

$$BPFI = \frac{N}{2}(f_i)\left[1 + \left(\frac{dcos\theta}{D_p}\right)\right] \quad (5)$$

Ball Spin Frequency (BSF) is the rolling element rotation frequency of ball or roller by it's own centre. Considering that only a pure rotation exists, there is no sliding and outer race is stationary, equation pertaining to defect frequency BSF is obtained as

$$BSF = \frac{D_p}{2d}(f_i)\left[1 - \left(\frac{dcos\theta}{D_p}\right)^2\right] \quad (6)$$

Feature Extraction for Bearing Fault Diagnosis

The procedure for fault diagnosis starts with data acquisition, followed by feature extraction, fault detection and identification. Feature extraction is critical for the success of the diagnostic procedure. Rolling element bearing often fails due to cracked defects in the inner, outer races and the rolling elements. Bearing defects induces impacts at the characteristic defect frequency. The characteristic defect frequency are determined by shaft speed and bearing geometry. The peak values at these frequency components are the features one seeks in interpreting bearing faults. Numerous vibration feature extraction techniques have been developed to date. Mathematical transformations are applied to signals to obtain further information from signal that is not readily available in the raw signal. There are a number of transformations that can be applied, among which the Fourier Transform is probably the most popular. The Fourier transform shows the frequency spectrum of a signal, thereby indicating what all frequencies exist in the signal. The drawback of FFT is that it does not give time information and is not suitable for non- stationary signals [2]. Also in the case of the transfer of non- stationary feature to frequency domain using Fourier Transform, most of the information about the transient components of the signal is lost. Consider a stationary signal with 5, 25 and 50 Hz frequency. Time domain representation of the signal is as shown in Figure 1. FFT spectrum of the signal is as shown in Figure 2.

Now let us consider a non stationary signal having a frequency of 5Hz, 25 Hz and 50 Hz at different time intervals as shown in the Figure 3. FFT spectrum of the signal is as shown in Figure 4.

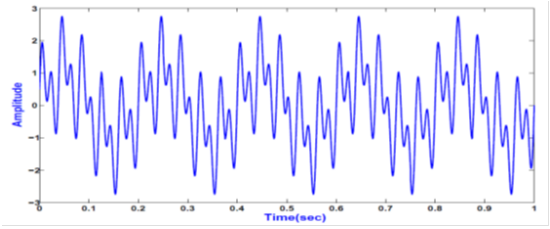


Fig. 1. Time Domain Representation of Stationary Signal with 5, 25 and 50 Hz Frequency Components.

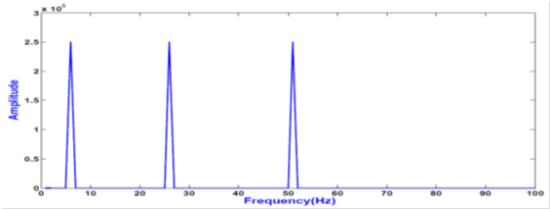


Fig. 2. FFT Spectrum of Stationary Signal with 5, 25 and 50 Hz Frequency Components.

On comparing both the Frequency spectrum i.e (Figure 2 & Figure 4), spectral components /peaks are evident at same frequency i.e., at 5, 25, and 50Hz irrespective of the fact that one is stationary signal while the other is non stationary signal. FFT thus gives only the spectral content of the signal, however it gives no information regarding where in time those spectral components appear. Hence, FFT is does not give correct interpretation of non-stationary characteristic of any signal.

Bearing fault vibration signals are generally non stationary/transient in nature. Hence Time-Frequancy analysis technique known as Wavelet Transform is ideal for these types of applications. Unlike traditional frequency domain analysis methods, wavelet analysis has the key advantage of being able to localize information in time. Fig. 5 and Fig. 6 show Continuous wavelet Transform of both stationary and non-stationary signal with 05, 25, and 50 Hz frequency components. In Wavelet spectrum stationary and non-stationary characteristic of a signal can be clearly exhibited. The multiresolution property of Wavelet Transform allows for both good time resolution at high frequencies and good frequency resolution at low frequencies. Thus Wavelet Transform are best suited for detecting bearing faults.

Wavelet Transform an Emerging Time-Frequency Analysis Tool

Time–frequency analysis performs mapping of one-dimensional signal to a two- dimensional function of time and frequency, thereby providing true time–frequency representations for the signal. Wavelet analysis is a recently developed time frequency analysis tool. Wavelets are mathematical functions that cut up data into different frequency components, and then study each component with a resolution matched to its scale. Wavelets can be either symmetric or asymmetric, sharp or smooth, regular or irregular. For different types of

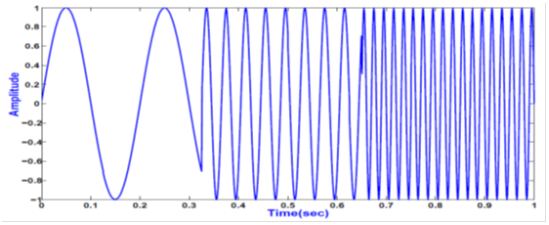


Fig. 3. Time Domain Representation of Non-Stationary Signal with 5, 25 and 50 Hz Frequency Components.

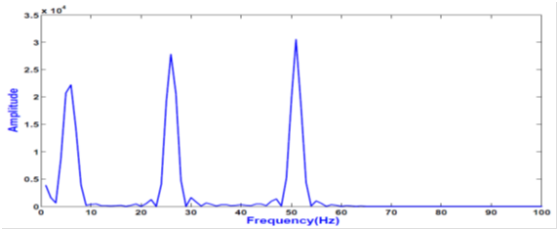


Fig. 4. FFT Spectrum of Non-Stationary Signal with 5, 25 and 50 Hz Frequency Components.

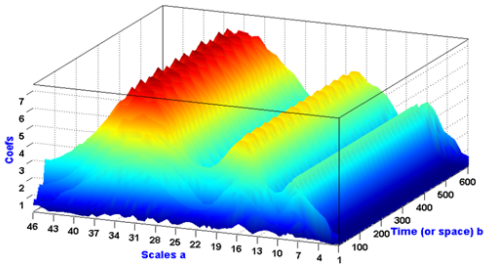


Fig. 5. Continuous Wavelet Transform of Stationary Signal with 5, 25 and 50 Hz Frequency Components.

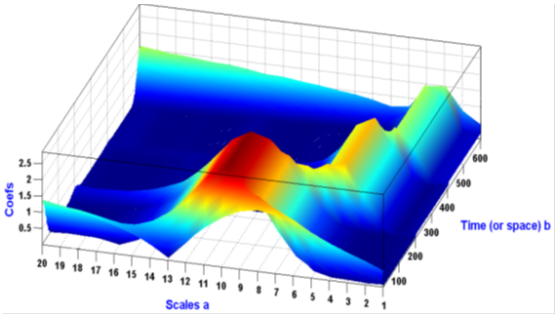


Fig. 6. Continuous Wavelet Transform of Stationary Signal with 5, 25 and 50 Hz Frequency Components.

signals, we can select different types of wavelets that best match the features of the signal we want to analyze. Wavelet Transform has the ability to identify frequency (or scale) components, simultaneously with their locations in time. The vibration signals from faulty bearings are more like impulses, instead of smooth and continuous curves. Wavelet Transform has advantages over traditional Fourier methods in analyzing physical situations where the signal contains discontinuities and sharp spikes. It is a suitable tool for transient, non-stationary or time-varying phenomena. As Wavelet Transform can efficiently represent non stationary characteristic of a signal, they can be effectively used for detecting bearing faults.

De-noising and extraction of the weak signature are crucial to fault prognostics in which case features are often very weak and masked by noise. Wavelet denoising/thresholding attempts to remove the noise present in the signal while preserving the signal characteristics, regardless of its frequency content. It has been shown that that wavelet filter is more suitable and reliable to detect a weak signature of mechanical impulse-like defect signals. Wavelet transform can be broadly classified into Continuous Wavelet Transform, Discrete Wavelet Transform and Complex Wavelet Transform.

Continuous Wavelet Transform

The continuous wavelet transform (CWT) provides a method for analyzing characteristic of signals that are dependent on time and scale. The CWT is defined with respect to a particular function, called mother wavelet, which satisfies some particular properties. Continuous Wavelet Transform (CWT) is defined as the sum over all time of the signal multiplied by scaled, shifted versions of the wavelet function ψ [3].

$$C(scale, position) = \int_{-\infty}^{\infty} f(t)\,\psi(scale, position, t)\,dt \tag{7}$$

In Continuous Wavelet Transform the scale and position are varied smoothly. It's flexible time-frequency provides a very finely detailed description of a signal in terms of both time and frequencies. The results of the CWT are many *wavelet coefficients* C, which are a function of scale and position. These coefficients indicate how close the signal is to a particular basis function. For a prototype function $\psi(t) \in L^2(R)$ called the mother wavelet, the family of functions can be obtained by shifting and scaling this $\psi(t)$ [4]–[6] as

$$\psi_{a,b}(t) = \frac{1}{\sqrt{a}}\psi\left(\frac{t-b}{a}\right), where\ a, b \in R(a > 0) \tag{8}$$

Parameter **a** is a scaling factor and **b** is shifting factor. Normalization ensures that $||\psi_{a,b}(t)||= ||\psi(t)||$. $\psi_{a,b}(t)$ is the wavelet coefficient at time t and scale a.

Discrete Wavelet Transform

As parameters (a,b) take continuous values, the resulting CoWT is a very redundant representation. Calculating all possible wavelet coefficients, on continuous time and scale axes, generates a fair amount of data. Towards a practical implementation, discretization of the dilation and translation parameter is done using Discrete Wavelet Transform (DWT). It involves the choice of only a subset of possible scales and position at which calculations are made. It has been proved that scales and positions based on powers of two, so called dyadic scales and positions, are accurate and efficient. The mother wavelet is rescaled or dilated by powers of two and translated by integers [7]. The numbers *a(L,K)* are known as the approximation coefficients at scale *L*, while *d(j,k)* are known as the detail coefficients at scale *j*. The approximation

and detail coefficients can be expressed as

$$a(L,k) = \frac{1}{\sqrt{2^L}} \int_{-\infty}^{\infty} f(t)\, \varnothing(2^{-L}t - k)dt \qquad (9)$$

$$d(j,k) = \frac{1}{\sqrt{2^j}} \int_{-\infty}^{\infty} f(t)\, \Psi(2^{-j}t - k)dt \qquad (10)$$

Complex Wavelet Transform

Complex Wavelets Transforms (CWT) use complex-valued filtering (analytic filter) that decomposes the real/complex signals into real and imaginary parts in transform domain. The real and imaginary coefficients are used to compute amplitude and phase information, just the type of information needed to accurately describe the energy localisation of oscillating functions (wavelet basis). Complex wavelets provide more detail information in transient signal detection than real-valued wavelets. The complex-valued transform coefficients allow for processing capabilities that are impossible with real-valued coefficients. Real valued Discrete wavelet transforms are very much useful for several signal processing application. However, these transforms suffer from disadvantages named shift sensitivity and phase information. Complex wavelet transform provides important phase information of the signal and it is shift- invariant [8]. Due to these added advantages it can be very much useful for signal processing applications. Of all the mother wavelets used during experimentation work, Complex Gaussian Wavelet of order 8 gave the best results for bearing faults.

Bearing Vibration Signal in Time Domain

Time domain signal of healthy bearing, bearing with inner race fault, outer race fault and ball fault are shown in Figure 7 to Figure 10 respectively.

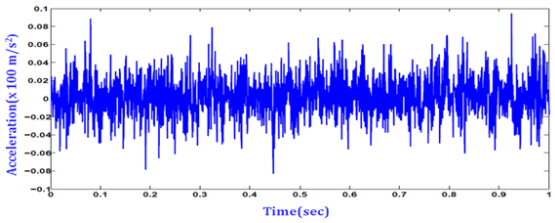


Fig. 7. Time Domain Acceleration Signal of Healthy Bearing Running at 1200 RPM (20 Hz) and Sampled at the Rate of 2048 Samples/Sec.

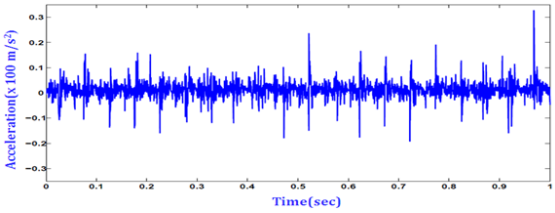


Fig. 8. Time Domain Acceleration Signal of Bearing with Inner Race Fault Running at 1200 RPM (20 Hz) and Sampled at the Rate of 2048 Samples/Sec.

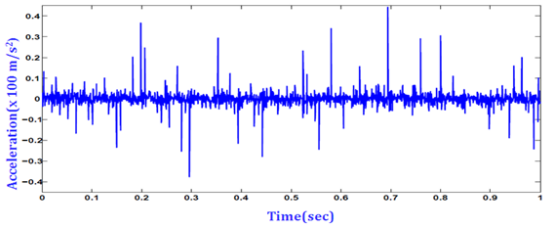


Fig. 9. Time Domain Acceleration Signal of Bearing with Outer Race Fault Running at 1200 RPM(20 Hz) and Sampled at the Rate of 2048 Samples/Sec.

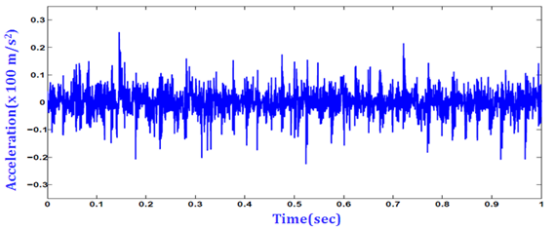


Fig. 10. Time Domain Acceleration Signal of Bearing with Ball Fault Running at 1200 RPM (20 Hz) and Sampled at the Rate of 2048 Samples/Sec.

FFT Spectra of Bearing Vibration Signal

FFT spectra of vibration signal of healthy bearing, bearing with inner race fault, outer race fault and ball fault are shown in Figure 11 to Figure 14.

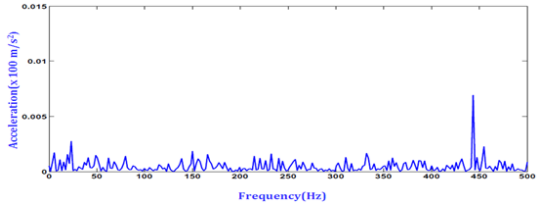


Fig. 11. FFT of Healthy Bearing Running at 1200 RPM (20 Hz).

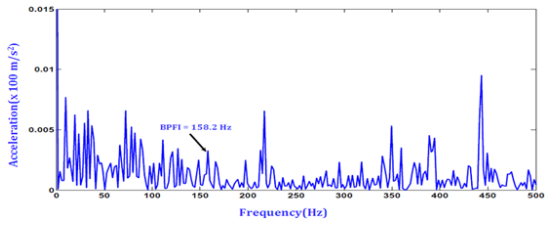


Fig. 12. FFT of Bearing with Inner Race Fault Running at 1200 RPM (20 Hz).

Theoretically, in FFT spectra, the characteristic defect frequency corresponding to the bearing defect should be distinctly visible. However, in practical scenario the impulses generated by defects are often masked by noise. The bearing defect characteristic frequencies BPFI, BPFO and BSF for the bearing are 157.285 Hz, 122.715 Hz, and 79.759 Hz respectively [9]. In Figures 12, 13 and 14 we are getting peaks at 158.2 Hz, 123 Hz and 80.2 Hz respectively, however

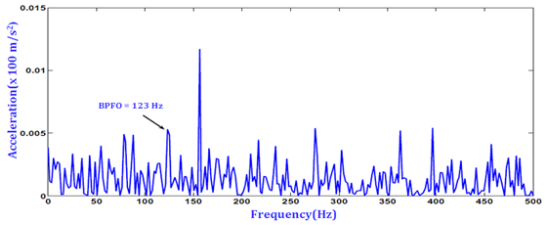


Fig. 13. FFT of Bearing with Outer Race Fault Running at 1200 RPM (20 Hz).

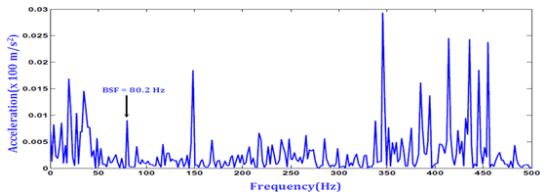


Fig. 14. FFT of Bearing with Ball Fault running at 1200 RPM (20 Hz).

they are not distinctly visible view a number of peaks are evident along with the bearing defect characteristic frequency. As it is evident from spectra that the bearing vibration signal contains large amount of noise components, which in turn is affecting clear representation of bearing defect characteristic frequencies. The above problem can be resolved by using Wavelet Transform post filtering and denoising of acquired vibration data. Wavelet spectrum of the vibration data of Healthy bearing, bearing with inner race fault , outer race fault and ball fault are as shown in figures 15, 16, 17 and 18 respectively.

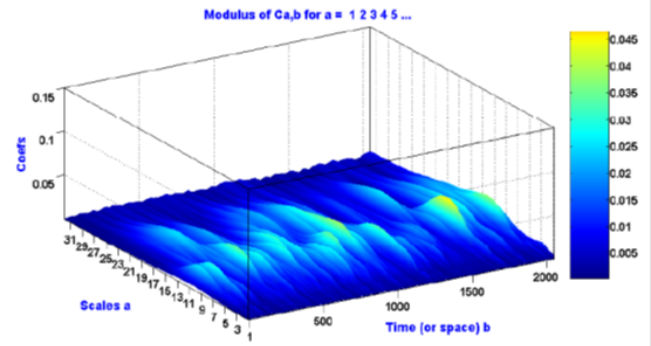


Fig. 15. Wavelet Spectrum of Filtered and Denoised Vibration Data of Healthy Bearing Running at 1200 RPM (20 Hz) and Sampling Rate of 2048 Samples/Sec using Complex Gaussian Wavelet of Order 8.

On using Complex Gaussian Wavelet of order 8(cgau8) as mother wavelet, the scales corresponding to these defect frequencies are 09, 12 and 18 respectively. On taking Continuous wavelet transform of pre-processed bearing vibration data, hilly region/peaks corresponding to respective defect characteristic frequency scale were clearly and distinctly visible. For example in case of bearing with inner race defect, the peaks were concentrated somewhere closer to

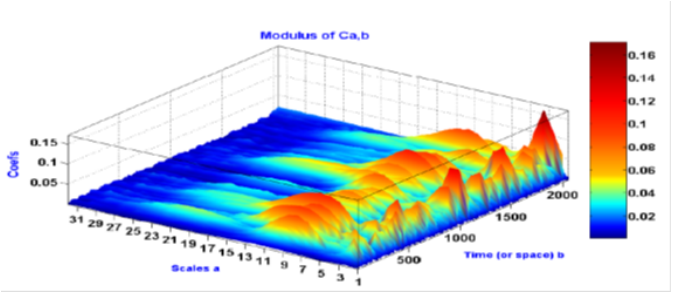


Fig. 16. Wavelet Spectrum of Filtered and Denoised Vibration Data of Bearing with Inner Race Fault Running at 1200 RPM (20 Hz) and Sampling Rate of 2048 Samples/Sec using Complex Gaussian Wavelet of Order 8.

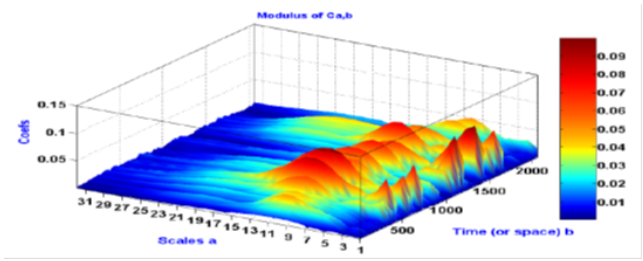


Fig. 17. Wavelet Spectrum of Filtered and Denoised Vibration Data of Bearing with Outer Race Fault Running at 1200 RPM (20 Hz) and Sampling Rate of 2048 Samples/Sec using Complex Gaussian Wavelet of Order 8.

the scale of 09 (Figure 16) which in turn represents Ball pass frequency inner race (BPFI). Similarly, for bearing with outer race defect the peaks were concentrated closer to the scale of 12(Figure 17) which in turn represents Ball pass frequency outer race(BPFO) and for bearing with ball defect the hilly region is concentrated closer to the scale to 18(Figure 18) which in turn represents Ball spin frequency(BSF). Thus bearing defect frequency can be easily identified in Wavelet spectrum. In case of healthy bearing, peaks were also observed (Figure 15) however, the amplitude of these peaks were less compared to defective bearing spectrum. The magnitudes of these peaks in general, were observed to be less than 0.04. These peaks in general were indicating waviness of the bearings raceways.

CONCLUSION

It can be concluded that feature extraction of vibration signal generated by rolling element bearings of rotating machinery plays a vital role towards early fault detection. Various bearing fault detection techniques have evolved over a period of time. Out of these evolved techniques, FFT is one of the widely accepted/ used techniques. However, FFT has certain inherent limitations i.e it does not give time representation of signal and also is not effective in detecting non stationary characteristics of vibration signal. As vibration generated by defects in bearings is generally non stationary in nature, hence FFT can't be effectively used for bearing fault diagnosis. In this study it has been brought out that the above limitations can

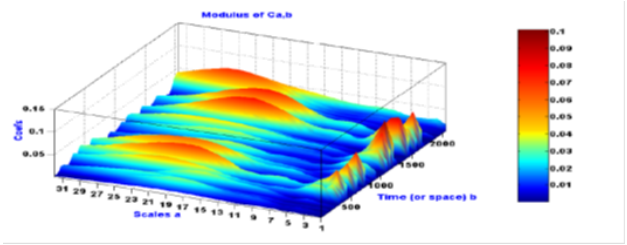


Fig. 18. Wavelet Spectrum of Filtered and Denoised Vibration Data of Bearing with Ball Fault Running at 1200 RPM (20 Hz) and Sampling Rate of 2048 Samples/Sec using Complex Gaussian Wavelet of Order 8.

be easily overcome by using one of the fast emerging Time-Frequency analysis technique known as Wavelet Transform. It has also been shown that in Wavelet spectrum bearing faults can be easily identified because of it's distinct advantages.

REFERENCES

[1] A. A. Roque, T. A. N. Silva, J. M. F. Calado and J. C. Q. Dias, "An approach to Fault Diagnosis of Rolling Bearings", WSEAS Transactions on Systems and Control, Vol 4(4), 2009, pp 188-197.
[2] R. Polikar, The Wavelet Tutoria, AMES, IOWA, 1996, pp 1-67.
[3] M. Misiti, Y. Misiti, G. Oppenheim and J.M. Poggi 2007, The Wavelet Toolbox^{TM} 4, User's Guide, The Mathworks^{TM}.
[4] K. P. Soman and K. I. Ramachandran, Insight into Wavelets from Theory to Practice, 20052nd edn. New Delhi: Prentice Hall of India.
[5] C. Junsheng, Y. Dejie and Y. Yu, "Application of an impulse response wavelet to fault diagnosis of rolling bearings", Mechanical Systems and Signal Processing 2007, Vol 21, pp 920-929.
[6] J. M. Haan, "A Survey on Methods for Time-Frequency Analysis MEE-98-01", Master Thesis, Ronneby, Sweden, University of Karlskrona, 1998, pp 1-106.
[7] N. Rao, "Speech Compression using Wavelets", Thesis, School of Information Technology and Electrical Engineering, St Lucia, Queensland, University Of Queensland, 2001, pp 1-62.
[8] A. Khare and U. S. Tiwary, "Multilevel Analysis in Complex Wavelet Transform Domain for Signal Processing Applications", Proceedings of the 9thWSEAS International Conference on Applied Mathematics, Istanbul, Turkey, 27-29 May, 2006, pp 115-120.
[9] WWW: http:// www.skf.com
[10] I. Angello and A. Chatterjee, "Development of Rolling Element Bearing Test Bench Facility and Application of Wavelet Transform for Fault Diagnosis", Journal of Aerospace Sciences and Technologies, Vol.63, No.2, May 2011.
[11] I. Angello, "Fault Diagnosis of Rolling Element Bearing using Wavelet Analysis", PhD Thesis, Visvesvaraya National Institute of Technology, Jun 2012.



Commandant (JG) Angello Innocent Devasigamani joined Indian Coast Guard on 11 Jan 03. Post joining the service he got specialized in Marine Engineering and Aeronautical Engineering. The officer has done B.E in Mechanical Engineering and M. Tech in Industrial Engineering from Nagpur University. The officer was awarded PhD on the topic "Fault Diagnosis of Rolling Element Bearing using Wavelet Analysis" from Visvesvaraya National Institute of Technology, Nagpur. The officer has held various important appointments viz. Technical Officer of Indian Coast Guard Ships Lakshmibai and Savitribai Phule. He has also carried out the duties of Air Engineer Officer at 750 Squadron (CG), Daman. The officer is presently carrying out the duties of Engineer Officer of Indian Coast Guard Ship Varad based at Port Blair. The officer has published 02 research papers in National level Journals. He has also presented 04 research papers in International/ National level conferences.

Comparative Evaluation of Adaptive Algorithms for Filtering of Underwater Ambient Noise

Vidhya Shinde[1], **Rajveer Shastri**[2], **Arnab Das**[3], **Shankar Deosarkar**[4]
[1,2,4]VPCOE, Baramati, University of Pune, India
[3]MILIT, Pune, India
[1]vidyashinde99@gmail.com , [2]rajveer_shastri@yahoo.com , [3]arnabdas1972@hotmail.com,
[4]sbdeosarkar@yahoo.com

***Abstract*—The ambient noise in the ocean environment affects the underwater acoustic signal transmission. Working with shallow water environment is extremely challenging since the environment can change in both time and space drastically. This effect can be reduced by adaptive cancellation of ambient noise from the signal of interest i.e. desired signal. The main objective of designing an adaptive filter is to reach certain accuracy with the least amount of complexity. This paper includes the adaptive filtering of ambient noise from the specific ambient noise source. The two adaptive algorithms LMS (Least Mean Squares) and NLMS (Normalized Least Mean Squares) have been implemented and evaluated by comparing the performance parameters such as SNR (Signal-to-Noise Ratio) and MSE (Mean Square Error). From a comparative study, it is found that the NLMS is better adaptive algorithm for filtering and separation of the ambient noise sources and thus, can improve performance of SONAR (SOund Navigation And Ranging) systems. The ambient noise data used in this experimentation has been recorded at 30 m depth from the sea surface.**

***Index Terms*—Underwater Ambient Noise, Adaptive Filtering, LMS Algorithm, NLMS Algorithm.**

I. Introduction

The acoustic waves are used as the best medium of underwater signal transmission, as the Electromagnetic (EM) waves gets spread because of its high frequency. The identification and recognition of acoustic signals have become as the primary issue of underwater techniques. Since acoustic environment of the ocean is highly variable, the underwater transmission is highly affected by ambient noise [1]. Ocean ambient noise is the unwanted background noise in the absence of individual sources. In an ocean environment, the sources of ambient noise consist of man-made as well as natural activities. These ambient noise sources include fishing, commercial shipping, naval operations, wind-driven waves, ice breaking, earthquakes, bio-acoustic sound generation, rainfall and thermal agitation of the seawater [2].

The ambient noise is highly nonstationary signal which varies with the varying environment in shallow water. The acoustic signal gets highly affected by the unwanted ambient noise [3]. It is important to reconstruct the signal of interest in the presence of ambient noise. A more efficient technique is to use an adaptive filter. Hence the adaptive algorithm for filtering the specific ambient noise from desired signal is required to be investigated which plays the significant role in tracking the changes of signal and noise.

Working with SONAR requires knowledge of both, the signal as well as the ambient noise within which the signal must be detected. Therefore, the analysis of ambient noise is required to improve the performance of SONAR [4]. It is necessary to know the spectral representation of ambient noise sources and predict the same. A more efficient method is to use an adaptive filter. Hence the adaptive algorithm for filtering the specific ambient noise from desired signal is required to be investigated. It is necessary to reconstruct the desired signal affected by the ambient noise in shallow water.

A. Das [5], in 2011, carried out spectral analysis of the real ambient noise recordings in very shallow water condition close to the commercial port with heavy shipping activity. The purpose was to study and characterize the distant shipping noise component and variations due to tides. Spectral characterization of ambient noise data has been explored in the same environment [6]. S. K. Veni et al. [7] has presented the spectral estimation of the wind driven ambient noise using different non-parametric methods. Also, they have developed an adaptive algorithm as LMS, modified LMS, RLS, etc., for filtering ambient noise for various wind speeds. Various adaptive algorithms are processed and compared to achieving maximum SNR [8], [9].

The Section II explains the concept of adaptive filtering. In Section III, the steps for different adaptive algorithms are discussed. The simulation results achieved are presented in Section IV. Section V gives the concluding remarks.

II. Adaptive Filtering

Filtering is the signal processing operation whose aim is, to obtain the information included in the signal. In digital signal processing, the adaptive signal processing has developed extremely due to the increasing availability of technology for the implementation of the emerging algorithms. These algorithms have been applied to an extensive number of problems including noise and echo canceling, channel equalization, signal prediction, adaptive arrays and many others.

The filter with fixed coefficient is useful to achieve the desired signal from the additive noise, only when the signal and noise are stationary. In the condition when both the signal and noise are nonstationary the fixed coefficient filter is unable to track the changes of signal and noise. In such a condition, the adaptive filter is to be designed instead of the filter with fixed coefficient.

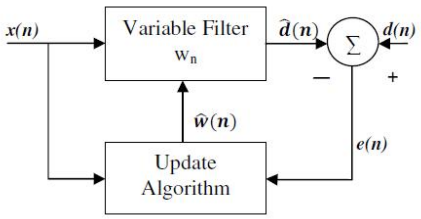


Fig. 1. Structure of Adaptive Filter

The adaptive filters have the capability of adaptively tracking the signal under nonstationary conditions. The filter is used to reject unwanted signals and to achieve desired spectral characteristics of the signal. A possible solution is to first estimate the statistical parameters of the appropriate signals and then compute the filter parameters [10]. Adaptive filter has self-regulation and tracking capacities. The general structure of an adaptive filter is shown in Fig. 1.

Mathematical model:

The mathematical model of adaptive filter is given as below,

- Output signal: The output signal of the filter is given by,

$$y(n) = \sum_{p=0}^{N} w_p(n).x(n-p) \tag{1}$$

where, $w_p(n)$ = Weight vector of filter
$x(n-p)$ = Samples of input signal

- Input Noisy Signal: The input signal $x(n)$ to the adaptive filter at the receiver side is the sum of a desired signal $d(n)$ and interfering noise $e(n)$ in the channel.

$$x(n) = d(n) + e(n) \tag{2}$$

- Error Signal: The error signal $e(n)$ is the difference between the desired signal $d(n)$ and the estimated signal $\hat{d}(n)$.

$$e(n) = d(n) - \hat{d}(n) \tag{3}$$

- Filter Coefficients: The variable filter has a Finite Impulse Response (FIR) structure. For FIR structures the impulse response is equal to the filter coefficients. The coefficients for a filter of order p is defined as,

$$w(n) = [w_n(0), w_n(1), ..., w_n(p)]^T \tag{4}$$

- Impulse Response: The variable filter estimates the desired signal by convolving the input signal with the impulse response given by,

$$\hat{d}(n) = w(n) * x(n) \tag{5}$$

- Update Filter Coefficients: Moreover, the variable filter updates the filter coefficients at every time instant.

$$w_{n+1} = w_n + \delta w_n \tag{6}$$

where δw_n , is a correction factor for the filter coefficient. The adaptive algorithm generates this correction factor based on the input and error signals.

III. Adaptive Algorithm

There are several least squares adaptive filtering algorithms. This section describes steps of LMS and NLMS algorithms.

A. LMS Algorithm

The LMS algorithm is a linear adaptive filtering algorithm based on an approximation of the steepest descent algorithm. The LMS algorithm is built on the transversal filter concept. This component is efficient for performing the filtering process using a mechanism for achieving the adaptive control process on the tap weights of the transversal filter. The LMS algorithm is designed to find a set of filter coefficients w that reduce the expected value of the quadratic error signal, i.e., to obtain the least mean squared error.

The LMS algorithm is designed using following steps,

1) Adaptive filter output

$$y(n) = \hat{w}^T(n).x(n) \tag{7}$$

2) Estimation error or error signal is,

$$e(n) = d(n) - y(n) \tag{8}$$

3) Tap-weight adaptation is given by

$$\hat{w}(n+1) = \hat{w}(n) + \mu x(n)e(n) \tag{9}$$

where, $e(n)$ is the error signal, $x(n)$ is the input signal vector, μ is the step-size parameter. Choose $\mu > 0$ but it should not be too large. $\hat{w}(n)$ is the tap-weight vector, $d(n)$ is the desired response.

Advantage of LMS algorithm is its computational simplicity. Unfortunately as the step size parameter reduced the rate of convergence of LMS algorithm correspondingly get decreased.

B. NLMS Algorithm

The LMS algorithm is very sensitive to the scaling of its input $x(n)$, which makes it difficult to select a learning rate μ that guarantees stability of the algorithm. The NLMS filter is a modification of the LMS algorithm that resolves this problem by normalizing with the power of the input.

The NLMS algorithm is designed using following steps,

1) Tap-weight adaptation is given by

$$\hat{w}(n+1) = \hat{w}(n) + \mu(n)x(n)e(n) \tag{10}$$

where,
$\mu(n) = \dfrac{\mu}{\alpha x^T(n)x(n)}$
α = small positive constant
μ = small step size

IV. Results

The adaptive filter is implemented by using least square algorithm to separate specific ambient noise source. The algorithm is also evaluated for the test signals as ship, whale, dolphin and the corresponding sinusoidal successfully. The various combinations of desired signals have been carried out to evaluate adaptive filters. The parameters of an adaptive filter, such as step size and filter order affects on performance of

adaptive filters. Performance of algorithms has been compared on the basis of SNR and MSE. It is reported that the NLMS algorithm provieds the better SNR as compared to that of the LMS algorithm.

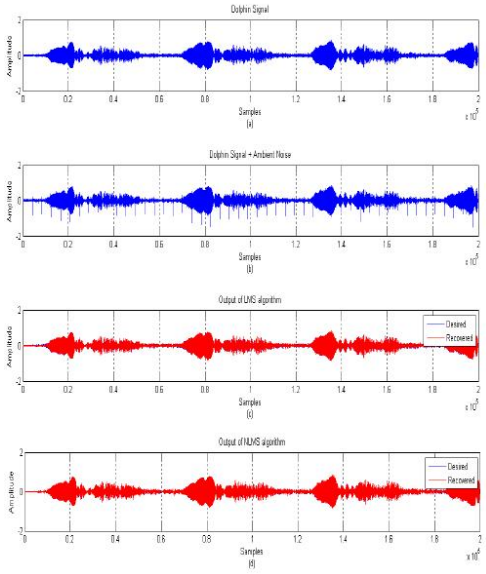


Fig. 2. Ambient Noise Cancellation

The Fig. 2 shows the separation of ambient noise sources using adaptive algorithms. The ambient noise generated by dolphin with signature frequency about 775 Hz is the signal of interest as shown in Fig. 2(a), which has to be reconstructed using an adaptive algorithm in the presence of noise. The noisy signal as shown in Fig. 2(b), is a combination of dolphin signal, and the ambient noise and this noisy signal is then given as input to the adaptive filter. The aim is to separate the dolphin signal from the ambient noise. The output of the filter using LMS and NLMS adaptive algorithm is shown in Fig. 2(c) and Fig. 2(d) respectively. From the results of both adaptive algorithms, it is reported that the reference signal is recovered successfully.

The spectral, as well as the temporal characteristics of recovered signal, are verified using the spectrogram method as shown in Fig. 3. The Fig. 3(a) and 3(b) shows the spectrogram of the dolphin signature and the ambient noise respectively. The spectrogram of combined signal is as shown in Fig. 3(c). The spectral and temporal characteristics of the recovered signal are shown in Fig. 3(d). From the Fig. 3(a) and 3(d) it is observed that the spectral and temporal characteristics of the reference signal are matches with that of the recovered signal. The output SNR achieved using NLMS algorithm is 26.1216 dB.

V. Conclusion and Future Work

The adaptive algorithms are found useful for separation of different ambient noise sources such as Dolphin, ship, Humpback Whale sounds, etc. The LMS and NLMS adaptive algorithms are able to filter the ambient noise at acceptable level. The results of both algorithms have been evaluated by

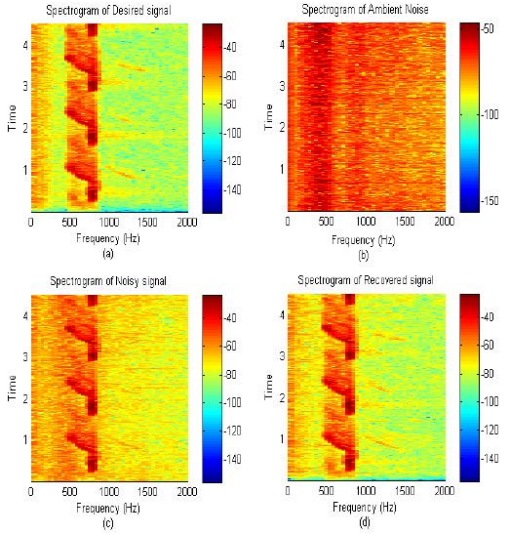


Fig. 3. Performance of Adaptive Filtering Algorithm

TABLE I
COMPARATIVE ANALYSIS OF ADAPTIVE ALGORITHM

Sr. No	Input to Filter	Adaptive Algorithm	SNR (dB)	MSE
1.	Dolphin + Ambient Noise	LMS	(dB)	3.260610-4
		NLMS	26.1216	1.023710-4
2.	Ship+ Ambient Noise	LMS	20.1667	1.2801 10-4
		NLMS	24.4526	1.256010-4
3.	500Hz + Dolphin Noise	LMS	34.4870	1.780710-4
		NLMS	35.0774	1.552410-4

performance parameters as SNR and MSE are listed in Table I. It has been found that the NLMS algorithm provides the improved SNR as compared to that of the LMS algorithm. These findings can be used to develop intelligent signal processing algorithms to improve SONAR performance. Other different adaptive algorithms like Block LMS, RLS (Recursive Least Squares), QR-RLS (Square Root-RLS), Kalman filter, etc., can be evaluated to find best suitable adaptive algorithm for filtering of ambient noise.

References

[1] Peter H. Dahl, James H. Miller, Douglas H. Cato, Rex K. Andrew, "Underwater Ambient Noise", *Acoustics Today*, January 2007.
[2] John A. Hildebrand, "Anthropogenic and natural sources of ambient noise in the ocean", *Acoustics in marine ecology*, vol. 395: 520, 2009.
[3] Gordon M. Wenz, "Acoustic Ambient Noise in the Ocean: Spectra and Sources", *The Journal of the Acoustical Society of America*, vol 34. No. 12 December 1962.
[4] Website-http://www.dosits.org/science/soundsinthesea
[5] A. Das, "Shallow ambient noise variability due to distant shipping noise and tide", *Applied Acoustics*, vol. 72, no. 9, pp. 66064, Sep. 2011.
[6] R. K. Shastri, Y. V. Joshi, A. Das, "Spectral Analysis of Littoral Water Ambient Noise in the Tropical Region", *Acoustics in Underwater Geosciences Symposium (RIO Acoustics), IEEE/OES*, Rio de Janeiro, pp. 1-4, (24-26 July 2013).
[7] S. K. Veni, S. S. Murugun, S. Radha,"Adaptive Algorithms for Detection of Underwater Acoustic Signals against Ambient Noise in Shallow Sea", *IEEE- Int. conf. Emerging Trends in Electrical and Computer Technology (ICETECT)*, 2011 Chennai, Tamil Nadu, pp. 758 761, (23-24 Mar. 2011).
[8] S. S. Murugan, V. Natarajan, R. R. Kumar, "Estimation Of Noise Model and Denoising of Wind Driven Ambient Noise in Shallow Water Using The LMS Algorithm", *Acoustics Australia*, Vol. 40, No. 2, August 2012 111.

[9] R. R. Kumar, S. S. Murugun, V. Natarajan, S. Radha, "Analysis of Power Spectral Density and Development of an Adaptive Algorithm for Filtering Wind Driven Ambient Noise in Shallow Water", *IEEE*, 2011.
[10] Simon Haykin, Thomas Kailath, *Adaptive Filter Theory*, Pearson Education, 4th ed. 2005.



Vidhya Shinde received the B.E. Electronics and Telecommunication in 2009 from Dr. Babasaheb Ambedkar Marathawada University, Aurangabad and she is pursuing M.E. Degree in Electronics with specialization in Digital System from Vidya Pratishthan's college of Engineering, Baramati, India. She has Published paper in National Conference held at GOA College of Engineering, Farmagudi, Ponda-Goa. Her area of research is Underwater Signal Processing.



Rajveer Shastri received the B.E. Electronics and Telecommunication in 2000 from Dr. Babasaheb Ambedkar Marathawada University, Aurangabad, the M.E. Degree in Electronics with specialization in Computer Technology from Shri Guru Govind Singh Engineering and Technology, Nanded, He is now pursuing Ph.D. degree, in Electronics from Swami Ramanand Tirth Marathawada Univeristy Nanded. He worked as lecturer from 2002 to 2008 and from 2008 to till date he is working as assistant professor in Vidya Pratishthan's college of Engineering, Baramati, India. He is life member of IEEE, ISTE and IETE. He has published 10 international journal, conference papers and 5 national conference papers.



Arnab Das received B. Tech degree in Electrical Engineering from Naval College of Engineering, Lonavala, India in 1995. He obtained M. Tech degree in Radar and Communication with specialization in Underwater Signal Processing in 2002and PhD degree in 2009 from Indian Institute of Technology, Delhi, India. He was commissioned into the Indian Navy in 1994. He worked as Project Officer at CARE, IIT Delhi for R & D in Underwater Signal processing and hardware design in 2003-2007. Currently he is instructor at MILIT Pune, India. His research interests are Underwater Passive Surveillance, Underwater Communication and Pattern recognition.



Shankar Deosarkar received his BE Degree in Electronics in 1988 from Amravati University and his both M. Tech and Doctorate Degrees in the area of Microwave Communication in 1990 and 2004 respectively from S.G.G.S. Institute of Engineering and Technology, Nanded. He has to his credit about 35 research publications at the National and International level. At present he is guiding three Research Scholars in the area of EMI / EMC and Microstrip Antenna Design. He was invited to deliver scholarly lectures at McGill University, Montreal, Canada, Electromagnetic Research Center Ottawa, Government of Canada and Princeton University, New Jersey, USA and UGC / AICTE Refresher Courses.

CFD Modeling For Optimizing Ballast Tank Structural Design in A Ship

Cdr Vinay G Ankalgi
Officer – in – Charge, Diesel Testing & Tuning Team (Vzg)
Indian Navy
Visakhapatnam, India, Pin - 530014
vinay.ankalgi@rediffmail.com

Abstract— This paper describes computational fluid dynamics study for optimizing ballast tank structural design in a Ship by applying the technique of flow-through method of ballast water exchange and thus analyzing the flow dynamics in a typical ballast tank. It also examines the effects of shape of tank on the effectiveness of exchange in replacing coastal water in the tank and thus assists in optimizing the tank design. Mid-ocean Ballast Water Exchange (BWE) has been the primary management practice with widespread acceptance aimed at reducing or preventing the spread of non-indigenous aquatic species via ballast water.

There are two types of BWE approaches: sequential (or empty-refill), and flow-through (or flushing). The former requires that ballast tanks be emptied completely and then refilled at sea, while the latter requires pumping of mid-ocean water, usually entering at the tank bottom, into a full or partially full ballast tank and allowing the water to overflow the tank for a given tank volume multiple. Flow-through exchange has a target of three tank volume overflows based on a theoretical calculation that assumes perfect and instantaneous mixing between the original ballast water and the incoming mid-ocean water.

International Maritime Organization (IMO) has set acceptable standard of ballasting, which is generally based on empirical formulae. The phenomenon of ballast water exchange involves flow and mixing of two liquids, which will be an interesting application of computational fluid dynamics (CFD). This study will give an understanding of the flow process of a complicated engineering problem.

A CFD model offers the possibility of forecasting ballast water exchange "effectiveness," for individual ballast tank architectures. The model is portable and is tailored to different tank types and geometries, different ballasting and de-ballasting flow rates, and different starting conditions. A computer model could also be used to improve the sampling design of on-board ballast exchange experiments and to test the effects of modifications to internal tank architecture.

Reynolds Averaged Navier Stokes (RANS) Equation was solved using Fluent 6.2 software. ICEM CFD Ver 10.0 was used for generating the grid. The mixing process is basically turbulent, so adequate care was taken to handle Reynold's stress terms in RANS equation through suitable turbulence model. In all of the simulations, multiphase turbulence models are being evaluated. The turbulence models used is the standard k-ε model.

The results of this study may help explain the variable results of ballast water exchange experiments documented to date, lead to ballast tank structural modifications to improve overall ballast water exchange effectiveness, minimize the dead spots, reduce sediment deposition and accumulation, and provide the insight and knowledge to select and enhance treatment technologies, thus reducing the threat of coastal invasive species being discharged in coastal ecosystems.

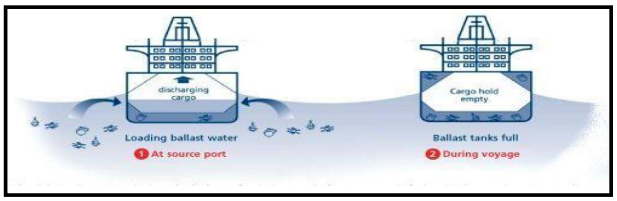
Keywords—Optimization; Ballast Tank; Ballast Water Exchange; Standard k-e Turbulence Model; Reynold's Averaged Navier Stokes Equation

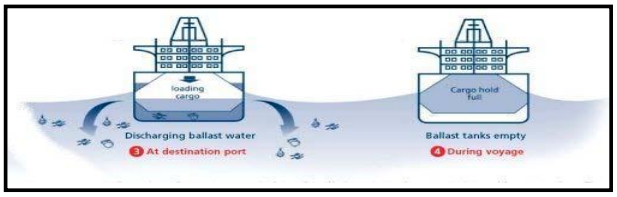
I. INTRODUCTION

A. International Maritime Organization (IMO) has set acceptable standard of ballasting, which is generally based on empirical formulae. The phenomenon of ballast water exchange involves flow and mixing of two liquids, which will be an interesting application of computational fluid dynamics (CFD). The study will present an understanding of the flow process of a complicated engineering problem and thus facilitate in ballast tank designing procedure. It is therefore essential to fully understand the ballast water exchange process, the flow dynamics inside a ballast tank during exchange, and how tank architectures affect the outcome.

B. Before entering into ports abroad, a ship requires to discharge and refill its ballast water in outer sea. This process is called ballast water exchange (BWE) and is a widespread practice for reducing the spread of non-indigenous aquatic species via ballast water. Ballast Water Exchange is carried out to replace coastal ballast water and entrained organisms with mid-ocean surface seawater. Ballast water exchange is practiced in routine manner since for a long time. However, there is ample scope for efficient design of the ballast tanks to reduce the required time for exchange. A CFD model offers the possibility of forecasting ballast water exchange "effectiveness," for individual ballast tank architectures. The model is portable and is tailored to different tank types and geometries, different ballasting and de-ballasting flow rates, and different starting conditions. A computer model could also be used to improve the sampling design of on-board ballast exchange experiments and to test the effects of modifications to internal tank architecture. This paper describes computational fluid dynamics study for optimizing the ballast tank structural design using the concept of flow dynamics in a

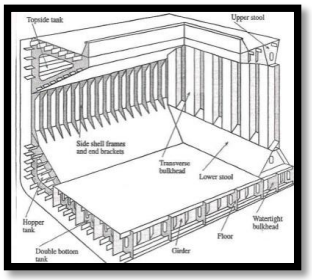
typical ballast tank during flow-through method of ballast water exchange.





C. **Structure of Ballast Tank**. Ballast Tank is a large void space, or specially designed cargo hold, used to store ballast water on board a ship. Individual ballast tanks can range in size from a cubic meter or less on small vessels, such as fishing boats, to thousands of cubic meters each on large vessels, such as commercial cargo vessels. Each vessel will usually have multiple ballast tanks and there are many different configurations of ballast tanks across and within ship types. Most ballast tanks are subdivided by internal interconnected compartments that make it structurally complex and subject to sediment accumulation. There are many different types of ballast tanks , composed of interconnected bays separated by girders, floors, frames and plating, with associated lightening holes, limber holes and slots for drainage, and longitudinal frames or stiffeners as shown in figures appended below.





II. MULTI PHASE FLOW IN FLUENT

A. Continuum multiphase models can be categorized into either mixture models or multi-fluid models. True multiphase modeling involves the consideration of each phase as a distinct fluid, which leads to multi-fluid models. Here, the primary conservation equations of mass, momentum and energy are written individually for each phase, and the phases interact via inter-phase transfer terms. Primary applications for multi-fluid models involve cases where the general flow pattern of the two phases is not known, and the flow is not amenable to simplifying assumptions. These models are somewhat complicated because of the introduction of numerous momentum equations in the formulation (i.e. one set of momentum equations per phase) presents mathematical difficulties and because proper specification of the inter-phase transfer terms is not always easy. Computationally, these models are expensive and difficult to solve. For a three dimensional, transient problem with a turbulence model, as many as 12-14 transport equations must be solved at each time step for a two-phase flow.

B. Another class of models, described as mixture models, is formulated by considering the multiphase mixture as a single fictitious fluid. These models are usually the result of first considering the equations given by a multi-fluid model and then making simplifying assumptions, about the flow in question. The basic concept is to consider the two-phase mixture as a whole, rather than as two separate phases. These models make use of a set of mixture variables for the velocity, density, and viscosity as some combination of the unmixed phase values of these quantities. Here the crucial problem is the determination of the physical properties of the fictitious fluid, and the definitions of the mixture variables.

C. The multiphase models that are used for this study were mixture models, where only one set of momentum equations was solved for the given two-phase (two-fluid) flow. More specifically, two different models were studied for purpose of Ballast Water Exchange by flow through method, one involving immiscible fluids, and the other model for the simulations involving miscible fluids. Basically, the present study adopts the definitions for the mixture quantities and the form of the individual phase mass and momentum equations. Both of these models are, to some extent, simplified variations of the drift flux model as given by Ishii [5]. From these definitions and equations a model is developed for turbulent flows where two liquids mix and the relative velocity between the liquids is non-zero as is typical for buoyant, immiscible flows. This model is described as being a single fluid, scalar transport (SFST) model referred to as SFST2. For cases where the relative velocity between the phases is negligible, SFST2 can be further simplified to give a model that is typically used for miscible fluids which is our area of interest for this work. This model is referred to as SFST1.

D. Inherent Assumptions

Three of the main assumptions that are used in formulating the SFST models are that the individual phases are incompressible, that the flow is isothermal, and that the density difference between the phases is small compared to the density of either phase. These assumptions allow certain terms to be neglected in the form of the model equations for turbulent flows. Another important modeling assumption

involves using a gradient diffusion model for the average turbulent stresses in the momentum equations.

III. COMPUTATIONAL DETAILS

A. The CFD simulations are performed using the commercial viscous flow solver, Fluent 6.2, developed by Fluent, Inc. The 2D, Pressure-based unsteady RANS solver was used. Mixture model was enabled to handle flow of two liquids. Standard k-ε was used to model the turbulence. The detailed description of the solver code is available in Fluent Users Guide. The code uses a cell-centered finite volume approach to solving the governing equations of mass and momentum. **FLUENT** code uses a control-volume based technique to convert the governing equations to algebraic equations that can be solved numerically. This control volume technique consists of integrating the governing equations about each control volume yielding discrete equations that conserve each quantity on a control-volume basis. In addition, a transport equation is solved for the volume fraction of one of the fluids, with the algebraic constraint that the volume fraction of both fluids must sum to unity.

B. The QUICK (Quadratic upstream Interpolation for Convective Kinetics) scheme was used to discretise the velocity components; this scheme should give at least second order accuracy on the grids in the present simulations. The volume fraction equation was discretised using first order upwind while the turbulent quantities were also discretized using QUICK scheme. In order to solve the physical and temporal distribution of two fluids, the mixture multi-phase model in Fluent was used. This seems appropriate for this type of problem, where the two fluids are miscible, and have nearly equal densities. The time derivative terms are discretized using the first order implicit scheme. The SIMPLE (Semi Implicit Pressure Linked Equations) procedure is used for calculation of pressure field from the continuity equation. In this algorithm, originally put forward by Patankar and Spalding, the convective fluxes are evaluated from an estimated velocity field. Furthermore, estimation for the pressure distribution is used to solve the momentum equations. The continuity equation then yields a pressure correction equation, which yields a pressure correction field. This pressure correction term is used in turn to update the estimated velocity and pressure field. This process is iterated until the velocity and pressure fields are converged.

IV STANDARD k- ε TURBULENCE MODEL

A. The general approach has been to use the single-phase form of a turbulence model and assume the model is sufficient to account for the desired features of the turbulence in a multiphase flow. This is equivalent to assume that the turbulence of each phase is approximately the same at each point in the flow field. Additional transport terms are then usually added to the turbulence model to account for any significant effects that the two-phase mixture might have on the turbulence, such as buoyant production or dissipation of turbulent kinetic energy.

B. Two-equation models have been the most popular turbulence models for a wide range of engineering analysis and research. These models provide independent transport equations for both the turbulence length scale, or some equivalent parameter, and the turbulent kinetic energy. This part will focus primarily on the use of the *k*- ε model, where *k* is the turbulent kinetic energy and ε is the rate of dissipation of *k*, and its application to multiphase flows. The modeled *k*-equation is given by

$$\frac{\partial \rho k}{\partial t} + \frac{\partial \rho u_j k}{\partial x_j} = \tau_{ij} \frac{\partial u_i}{\partial x_j} - \rho\varepsilon + \frac{\partial}{\partial x_j}[\left(\mu + \frac{\mu_T}{\sigma_k}\right)\frac{\partial k}{\partial x_j}]$$

The modeled ε -equation is given by

$$\frac{\partial \rho \varepsilon}{\partial t} + \frac{\partial \rho u_j \varepsilon}{\partial x_j} = C_{\varepsilon 1}\frac{\varepsilon}{k}\tau_{ij}\frac{\partial u_i}{\partial x_j} - C_{\varepsilon 2}\rho\frac{\varepsilon^2}{k} + \frac{\partial}{\partial x_j}[\left(\mu + \frac{\mu_T}{\sigma_\varepsilon}\right)\frac{\partial \varepsilon}{\partial x_j}]$$

where the right hand side terms represent production of dissipation, dissipation of dissipation and diffusion of dissipation. The turbulence model based on the equation for the rate of dissipation of *k* is based on the exact equation for ε. Standard values for five closure coefficients of k-ε turbulence model as listed below were used:-

C_μ	$C_{\varepsilon 1}$	$C_{\varepsilon 2}$	σ_ε	σ_k
0.09	1.44	1.92	1.22	1.00

C. Grid Generation

Three different shapes of same volume were considered for the tank. Fig 1 shows three different geometrical configurations. Three different girds were generated in commercial software ICEM CFD Ver 10.0. In view of the fact that there is no significant variation in the flow along in depth of the tank, the flow inside the ballast tank was considered as two-dimensional phenomenon. Complete structured grid was generated for all the cases. To represent the flow field a total around 10,200 quadrilaterals cells were employed. Views of the grid for three tank shapes are shown in Fig 2.

V SIMULATION OF THE PROBLEM

A. Problem Parameters

	Model	Real
Inflow	135.72 l/min	510 cu m/hr
Inlet Velocity at pipe end	1.8 m/sec	0.18 m/sec
Bore of pipe	0.04 m	1 m
Tank Representative length	1 m	10 m
Reynolds number	1.7×10^5	

B. Calculation of Time for Three Tank Volume Exchanges.

Prevailing practice is to allow flow into the ballast tank for duration sufficient to fill three times the volume of the tank. The volume of the present ballast tank (V) is 1 m^3. Inlet Flow Rate possible by the pump (Q) is 135.72 liter/min. The volume of the tank, bore of pipe and flow rate is so chosen to simulate the actual Reynold's Number $1.7X10^5$. However, actual dimensions of the tank and flow rate are not reported here.

Volume of tank = V = 1 m^3
Inlet Flow Rate = Q = 0.002262 m^3/secm^3/sec (135.72 litres/min)

$$\text{Time in sec for One tank volume exchange} = \zeta = \frac{\text{Volume of Tank}}{Inlet\ Flow\ Rate} = \frac{V}{Q}$$

$$\zeta = \frac{1}{0.002262} = 442\ sec$$

Total elapsed time for three complete tank volume exchanges = 3 ζ =1326 sec

C. Three different shapes of the tanks, square, rectangular and L shaped profile have been considered to check the relative efficiency. The initial condition was that of quiescent fresh water in the tank. At the start of the simulation, sea- water was introduced through the opening at the bottom of the tank at a flow rate of 135.72 litres/min. The time step was set at 0.25 seconds and 100 iterations were performed at each time step. The simulations were carried out until the total elapsed time reached 1326.0 seconds.

D. After the flow pattern was established, velocity vectors in square, rectangular and L shaped tank are shown in Fig. 3, 4 and 5 respectively. This big separation in flow inside the square tank is detrimental for mixing. The size of separation bubble is reduced in rectangular tank. Multiple separation bubbles of smaller sizes are observed in the L shaped tank, which provides the condition for best mixing. This is reflected in terms of exchange time as given in Table 1.

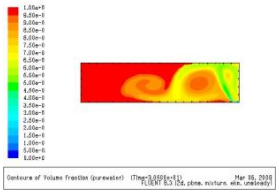
E. The progress of ballast water exchange has been monitored with time for three different tanks. Fig. 6 shows the contour of volume fraction of sea water at different time in the tank for its three different shapes. The figure shows the mixing pattern. Table 1 below gives the measure of mixing obtained at different time in the tanks of different shapes.

Table 1 % of Sea Water in the Tank at different Time

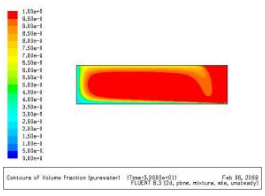
Tank Shape / Time	Square	Rectangle	L Shaped
0	0	0	0
1ζζ	75.1	78.1	82.9
2ζ ζζ	91.5	91.9	95.6
3ζζ ζ	96.2	97.0	98.5

F. Influence of Stringers in Tank Designs

The lack of stiffeners allows the incoming fluid to spread more quickly through the tank, while the presence of the stiffeners causes the incoming fluid to be trapped at various locations near the inlet. In addition, there are several small-scale mixing events that occur as the salt water is impeded by the structure and then spills over the stiffeners. When the stiffeners are neglected, there is significantly less obstruction to the dispersion of the incoming fluid, and the tank acts more like an open box. A larger amount of the incoming fluid reaches the tank exit much sooner than if the stiffeners were present.



Tank without stringers



Tank with stringers

VI RESULTS AND CONCLUSION

A. Computational Fluid Dynamic Method can be used successfully to investigate the flow phenomena present in Ballast Tanks and thus assess the exchange efficiency during flow through Ballast Water Exchange.

B. If seawater of three times of the ballast tank capacity is overflowed by using the flow through method, about 95% of exchange of the fluid in a tank is possible. All the tank models used in our study satisfy the International Maritime Organization (IMO) regulation for replacing Ballast Water in Tank. The time scale has been converted to multiples of a single tank volume exchange (t* = tank volume/inlet flow rate), and the exchange efficiencies for all three tank configurations are as tabulated below.

t*	Exchange Efficiency			
	Square Tank	Rectangular Tank	L-Type tank	Theory
1ζζ	0.75	0.78	0.83	0.63
2ζ ζζ	0.91	0.92	0.95	0.75
3ζζ ζ	0.96	0.97	0.98	0.95

C. **Comparative Study and Analysis of Tank Geometries**. Simulation results for all three tank configurations confirms that the predicted exchange efficiency using L shaped tank design would be most efficient as it gives upto 98.5% exchange within 3ζζ time. It is also observed that for L shaped tank, time of 2ζζ itself is sufficient for attaining 95% exchange. Based on the exchange effectiveness, it is concluded that an L-Type tank would be the best Ballast Tank design configuration followed by the Rectangular Tank Model and then the square tank design.

D. **Ballast Tank Structural Modifications**. Simulation results with structural modifications like inclusion of stringers in the Ballast Tank design improves the exchange efficiency. A comparison of the predicted exchange efficiency for the two tank geometries shows n in Table appended below. It is also observed that for L shaped tank, time of 2ζζ itself is sufficient for attaining 95% exchange.:-

t*	Exchange Efficiency	
	Tank with no Stringers	Tank with stringers
1ζζ	0.78	0.870
2ζ ζζ	0.92	0.956
3ζζ ζ	0.97	0.985

E. The study exhibits the capabilities of CFD to solve industry problems involving complex flow of multiple liquids.

F. CFD can also be effectively applied for other complex marine applications.

References

[1] Koichi Kamada, Minami and Ishida, "Study of Ballast Water Exchange by Pumping –Through Method".

[2] Wesley Wilson, Peter Chang, David Reid, "Computational and experimental Analysis of Ballast Water Exchange", American Society of Naval Engineers.

[3] MTECH Dissertation by Lt Cdr Vinay G Ankalgi, "Computational Fluid Modeling of Ballast Water Exchange by Flow through Method", DIAT, Pune, May 07

[4] International Maritime Organization (IMO), "International Convention for the Control and Management of Ships' Ballast Water and Sediments," International Maritime Organization: London, 2004.

[5] Ishii, M. 1977, "One-Dimensional Drift-Flux Model and Constitutive Equations for Relative Motion between Phases in Various Two-Phase Flow Regimes," Argonne National Laboratory Report, ANL-77-47.

[6] FLUENT® 6.2 Documentation

[7] Matthew R. Umbel, "Prediction of Turbulent Mixing at the Interface of Density Stratified, Shear Flows using CFD".

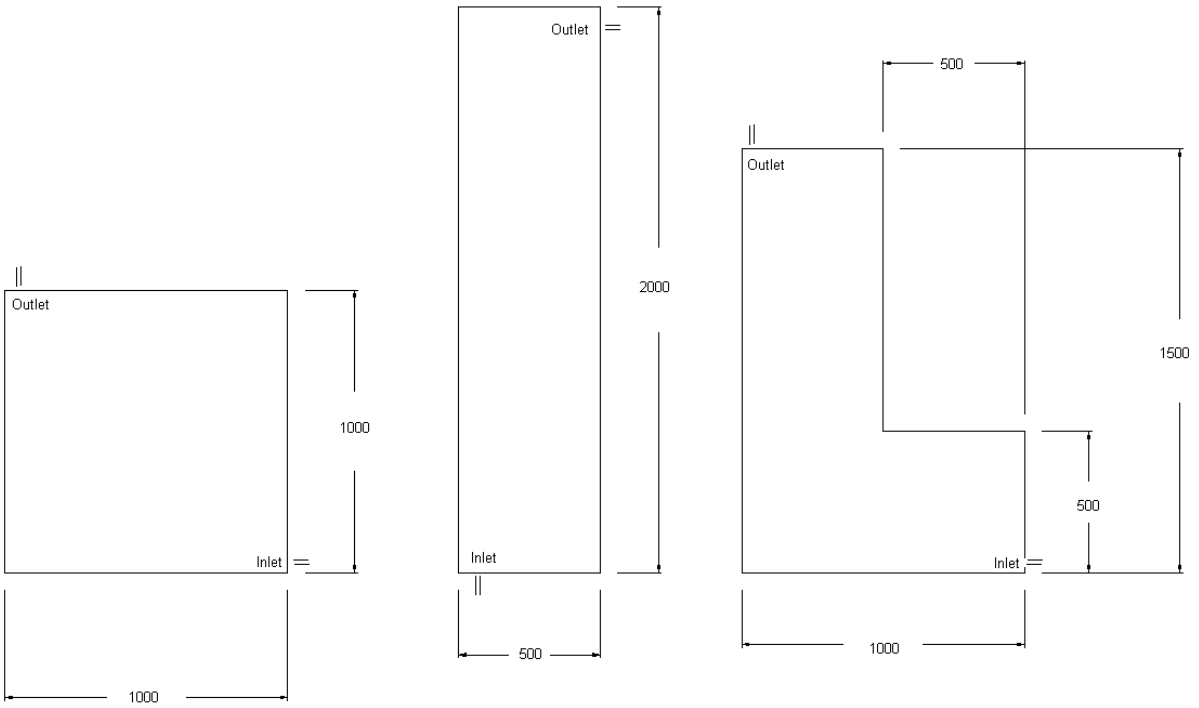


Fig 1 - Three different shapes of Ballast Water Tank

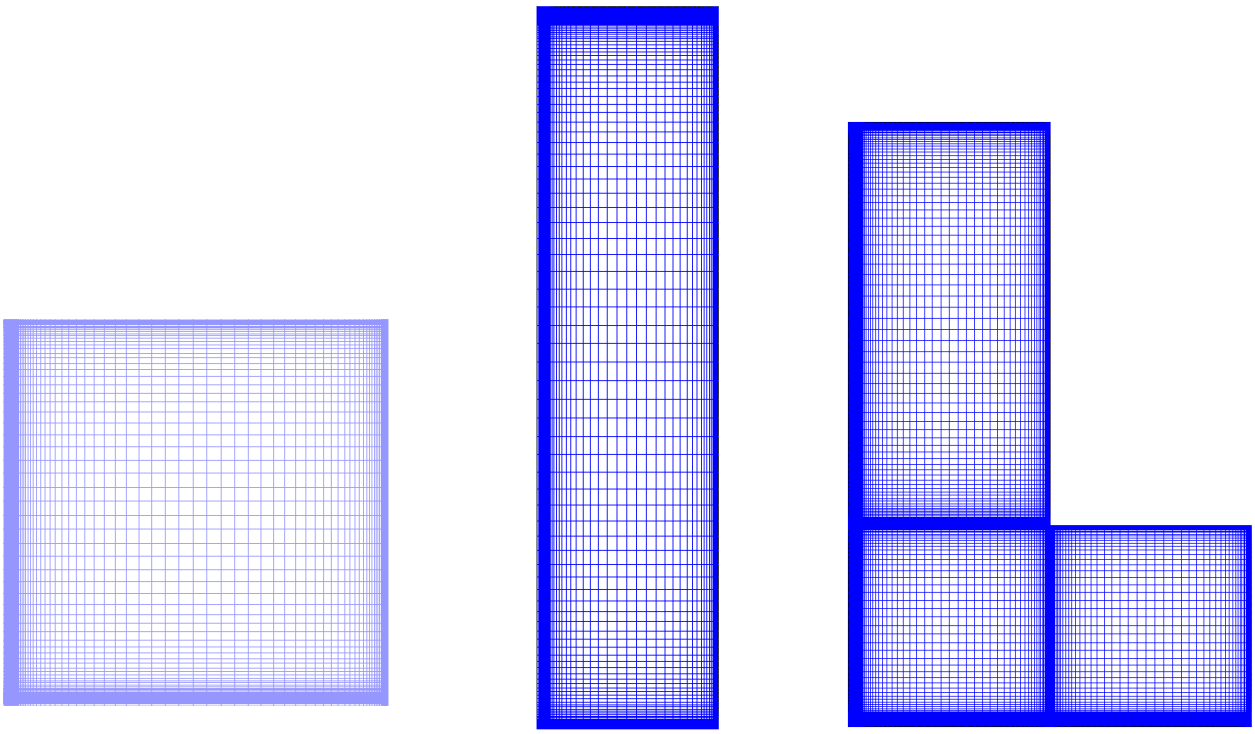


Fig 2- Grid for three configurations

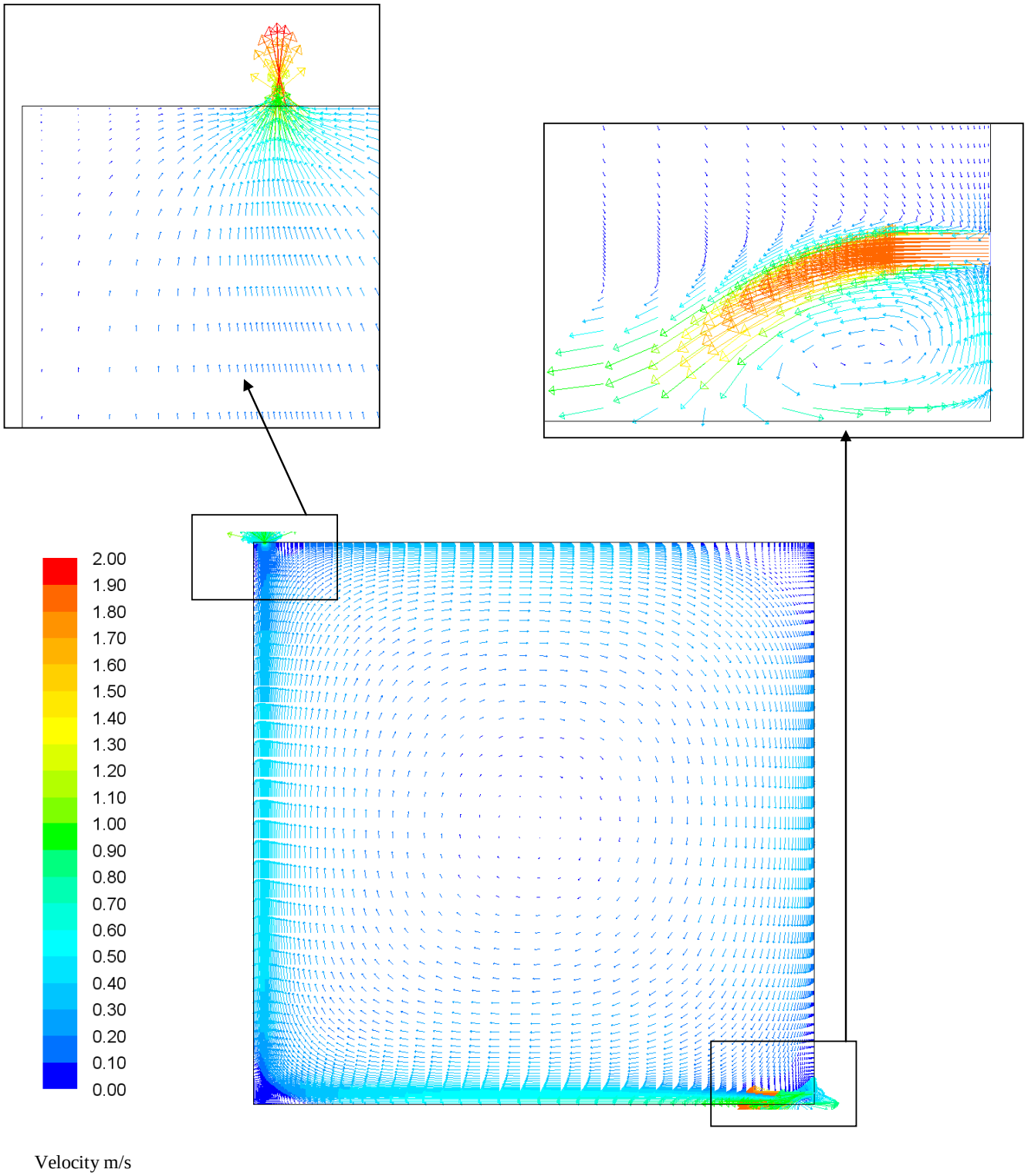


Fig 3 - Velocity vectors inside Square Tank

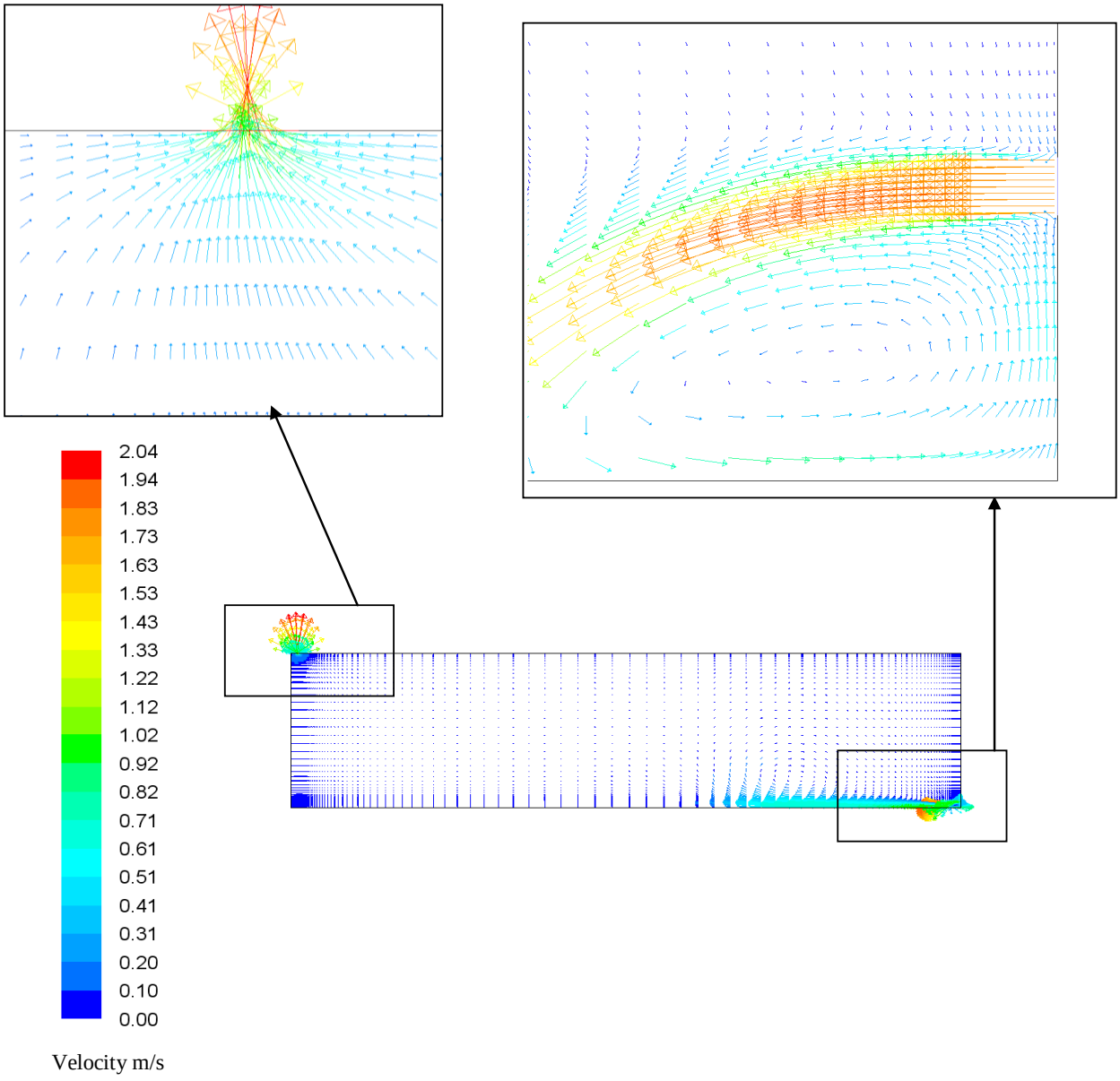


Fig 4 -Velocity vectors inside Rectangular Tank

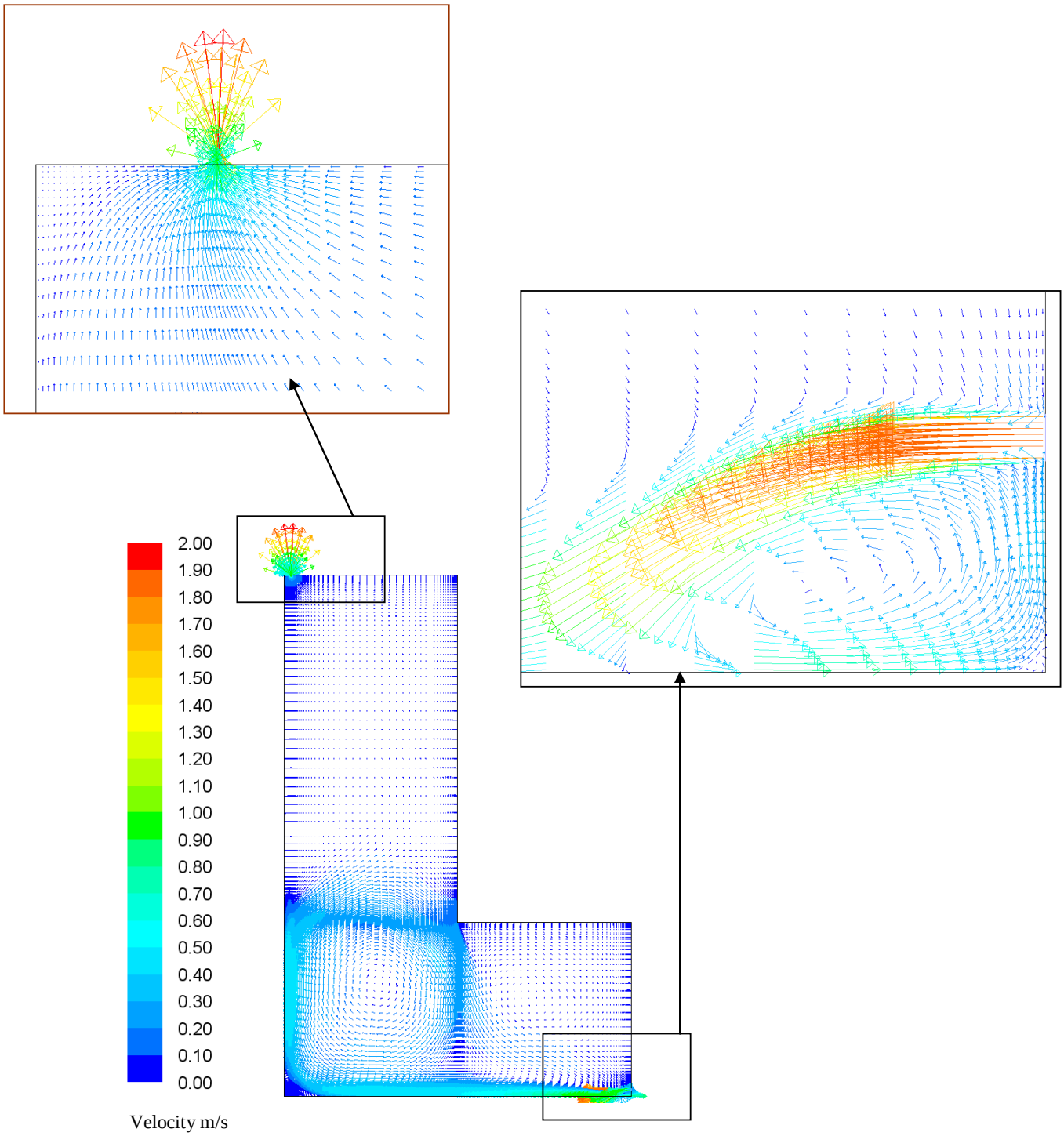


Fig 5 - Velocity vectors inside L shaped Tank

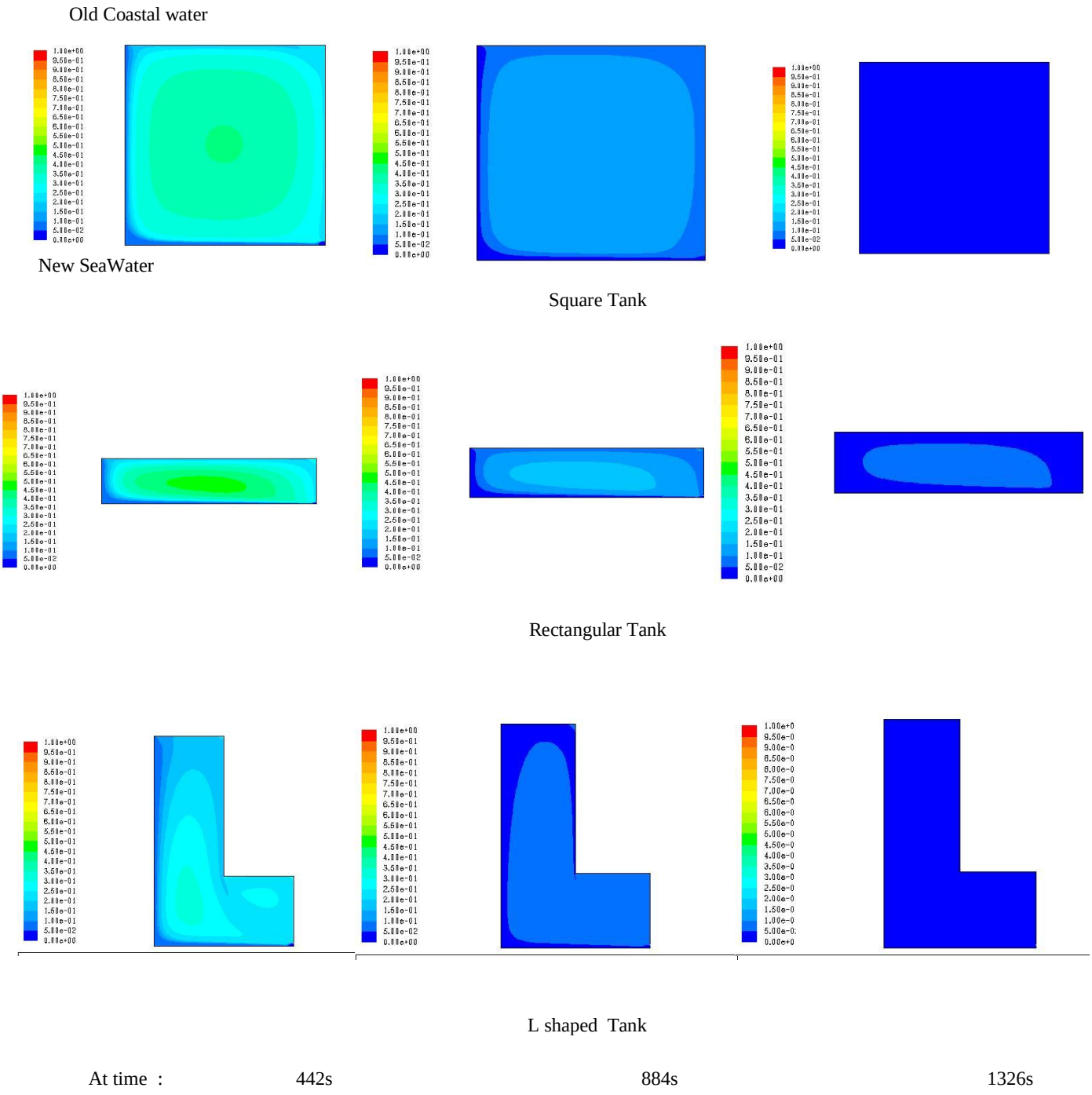


Fig 6 - Mixing of seawater with time progressive in three different tanks



Cdr Vinay G Ankalgi, is a MTECH in Mathematical Modeling & Simulation, from DIAT Pune, 2009. During his career of 15 years in the Indian Navy, he has held various prestigious appointments including Replenishment Engineer Officer and Senior Engineer Officer of INS Jyoti, Asst and Deputy Manager of Engineering Department at Naval Dockyard, Visakhapatnam. He is presently serving as Officer-in-Charge of Diesel Testing & Tuning Team, Visakhapatnam. He has published 02 papers in refereed journals and conferences. His areas of research interest are Enhanced Performance Monitoring and Analysis of Combustion related pressure signatures in Diesel Engines.

STUDY OF COMBUSTION IN GAS TURBINE ENGINES

Lt Cdr MSN Murthy[1]
[1]Centre of Marine Engineering Technology
INS Shivaji, Lonavala, India.
[1]msnmariner@gmail.com

***Abstract*—High specific power output or high power to weight ratio is perhaps the most important feature of a Gas Turbine Engine (GT) which makes it the most sought after source for propulsion and power generation on marine platforms. The ability of a GT to deliver such high power is obtained by the possibility of supplying large quantities of air to support combustion of large amounts of fuel. One of the major challenges involved in achieving this significant feature is flame stabilization within high velocity air streams, others being advanced fluid dynamics along with complex design of compressor and turbine blades, advanced metallurgy and manufacturing processes. Understanding the reactive and non-reactive flow fields inside a GT Combustor and its influence on combustion characteristics, can aid in higher reliability and optimization of combustion and thereby the GT. Experimental analysis of GT combustion is both cost and time intensive whereas numerical analysis though widely attempted is dependent on accurate experimental data for validation. A validated numerical model of GT combustion is a promising option for optimization of combustor design, analysis of performance and for improving the efficiency of GT. The present study pertains to analysis of detailed characteristics of combustion in a GT through an experimental setup to imitate combustion as it happens in a real life GT. Numerical simulations are undertaken using ANSYS, FLUENT with same inputs used for experimental analysis for comparison. Valuable insights into the combustion characteristics like combustion stability efficiency, emissions and exit temperature profile are obtained for the combustion process in a Gas Turbine Engine.**

***Keywords*—Combustor, Combustion efficiency, FLUENT, Gas Turbine, Simulation, Stability, Swirler.**

I. INTRODUCTION

In a typical gas turbine combustor, flame is stabilized using a swirler, which provides re-circulation zone within a high velocity stream of air. The swirl flow field inside the combustor also aids in mixing of air and fuel and thus has a direct influence on combustor performance. The flow in this region is generally associated with high shear stresses and strong turbulence intensity resulting from vortex break-down. Understanding the flow field inside a combustor and its influence on combustion characteristics, can give valuable inputs for combustor optimization. Experimental analysis of nonreactive and reactive flow fields is both cost and time intensive whereas numerical analysis though widely attempted, is dependent on accurate experimental data for validation. A validated numerical model of gas turbine combustion is a very promising option for optimization of combustor design. Therefore to obtain experimental data for benchmarking of the numerical model, an experimental facility is developed using a real life gas turbine combustor.

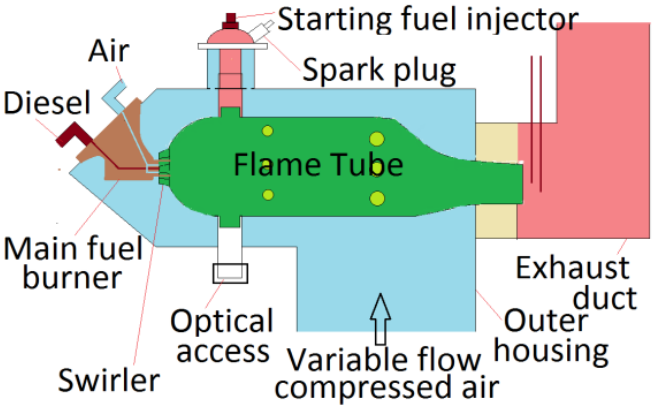


Fig. 1. Schematic of the experimental setup

II. METHODOLOGY

1.Experimental Facility. The approach adopted in building up the experimental facility is to match the conditions of combustion of the actual gas turbine engine (GT). The combustor/flame tube is housed inside a cylindrical outer housing as shown in Fig. 1. The cylindrical outer housing is fabricated using suitable dimensions to cater for equivalent flow rate of air to one combustor as against nine can annular combustors in the actual GT. The flame tube is connected to pilot ignition unit through the periphery of outer housing. The pilot ignition unit consisted of a starting fuel injector and a spark plug. Sparking voltage is provided by an igniter unit powered by 24 V DC supply. An optical access is provided on the other side of the periphery of the outer housing, to visualize the flame. Main fuel burner, is connected at the center of the combustor through the hub of the swirler.

2.The outer housing is fabricated in such a way that the asymmetric exit section of the combustor remained out of the outer housing. An exhaust hood fabricated in two halves is fastened onto the outer housing, over the exit section of the combustor. The outer edge of the exit section of the combustor

is leak proofed using asbestos paste. The exhaust duct is flanged onto the exhaust hood. A variable speed air blower is connected to the outer housing through a 6 m long circular duct to provide for developing length for the air flow. A pre-calibrated venturimeter is incorporated between the air duct and the outer housing for measurement of air flow rate into the outer housing. The starting fuel injector and main fuel burner are connected to a pressurized fuel tankthrough flow regulator valves by means of 10 mm SS piping. Nitrogen is used to pressurize the fuel tank upto a pressure of 2 bar. A pre-calibrated rotameter and two flow regulating valves are provided in the circuit for measurement and metering of fuel flow rate respectively. The other instrumentation used in the setup include K-type thermocouples for measuring temperature profile at the exit of combustor, and a QUINTOX flue gas analyzer for measurement of combustion products.

3.Combustion Experiments. Combustion experiments are conducted as follows. First the air blower and sparking igniter are switched on. Starting/pilot fuel is opened to initiate combustion. The flame obtained is seen through the optical access. Now main fuel along with the atomizing air at 6 bar is opened gradually. As the main fuel gets ignited, the pilot fuel is gradually closed ensuring the flame is stabilized. After obtaining a stable flame, equivalence ratio is varied by varying either the air flow rate or fuel flow rate. Input and output parameters are recorded at various equivalence ratios for parametric analysis. The input values measured are mass flow rate of air, mass flow rate of fuel and ambient temperature. The output variables measured are centerline temperature inside the recirculation zone, exit temperature at nodes of a 50 mm 70 mm grid, mean flue gas temperature, and mole fractions of exhaust products like CO, CO2, SO2, NOx and un-burnt hydrocarbons.

4.Extinction Tests. Combustion stability is determined by carrying out a series of extinction tests at constant, air temperature and pressure, as follows. After achieving stable combustion at a particular equivalence ratio as discussed above, the fuel flow rate is lowered gradually until extinction of the flame occurs. This fuel flow rate at which extinction occurs is recorded as lower extinction limit at that equivalence ratio. Similarly experiments are repeated with different equivalence ratios to get a trend of lower extinction limit. Upper extinction limits can be determined in the same manner by increasing the fuel flow rate gradually till extinction occurs at a constant air flow rate. However this study is limited to analysis of only lower extinction limits as determining higher extinction limits involved prohibitively large heat release rates.

5.Experimental Uncertainty. The experimental uncertainties associated with measurement of various parameters as well as the derived quantities using these parameters are listed in Table 1. Errors associated with the derived parameters have been computed by using the approach of differential method of propagating errors based on Taylor theorem [1]. Effect of radiation on temperature measurements is found negligible due to high value of Reynolds number at the exit of combustor.

Numerical Approach

6.The physical model refers to the combustion of a continuously injected liquid-fuel spray in a can type combustor. ANSYS FLUENT 14.0 was used to investigate the 3D swirling, reacting and non-reacting flow inside the combustor. The exact geometry of the flame tube along with its complicated design of swirler is incorporated in CATIA V5 and later exported to ANSYS for meshing and numerical analysis. As shown in Fig. 2, the fluid domain of the combustor is meshed using tetrahedral mesh with the smallest element size of 5 mm for which grid independence was achieved. Number of node points and number of elements are 78582 and 435841 respectively.

TABLE I. UNCERTAINTIES ASSOCIATED WITH EXPERIMENTS

Variable	Instrument	Uncertainty in perscent
a	Venturimeter	0.84
f	Rotameter	0.91
Temperature	K-type thermocouples	4.83
Products	Quintox flue gas analyzer	5
Equivalence ratio	Computed Parameter	0.4
Combustion efficiency	Computed Parameter	17.4



Fig. 2. Actual and Meshed geometry of the combustor

7.In a can-combustor, the swirl induced flow patterns affect not only mixing of products and reactants, but also the mixing of fuel and air.Swirlerproduces Central Toroidal Recirculation Zones (CTRZs) that providedominant flame stabilization mechanism. The k- model has been universally used for turbulence closure. However Xia et al., [**?**] claims that though the k- model performs well for simple flow cases, it is less satisfactory for swirling flows and poorly predicts the size and strength of recirculation zones, whereas the Differential Reynolds Stress Model (DRSM) captures all the major features of the swirling flows. Shamami and Birouk [3] assessed the performances of RANS turbulence models for simulating turbulent swirling can-combustor flows with different inlet swirl intensities i.e. S=0.4 andS=0.81. It was suggested that all turbulence models can predict the CTRZ in the strongly swirling flow (S=0.81), although with different sizes of recirculation zone. But, in the weakly swirling flow (S=0.4), only the Reynolds Stress Model (RSM) and the SSG could predict the existence of the CTRZ in the flow field. In the present study, all numerical simulations have been performed using standard k- turbulence model because it is easy to implement and computationally cheap. k- model is suitable for initial screening of alternate designs of combustors and parametric studies. The actual swirler of the combustor and the fluid domain created is shown in Fig. 3. The swirler has 14 vanes at a vane angle of 33. The swirl number obtained

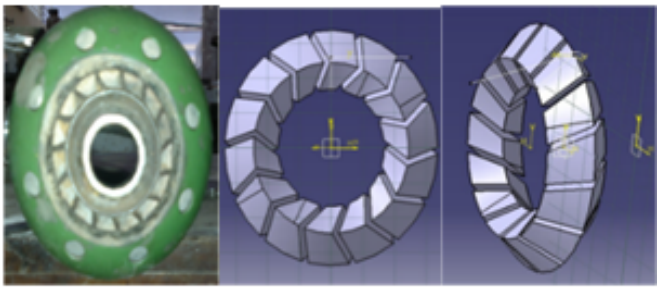


Fig. 3. Actual Swirler and its CAD model

TABLE II. MASS FLOW SPILT

Part	Area (m2)	perscentage of flow
Swirler	0.001658	43.98
Primary holes	0.000628	16.67
Dilution holes	0.001232	32.69
Cooling holes	0.000251r	6.67
Total	0.003769	100.00

using the relation in Eq. (1) is

$$S = \frac{2}{3}\{\frac{1-(D_{hub}/D_{sw})^3}{1-(D_{hub}/D_{sw})^2}\}tan\theta \quad (1)$$

Where, S is the swirl number, Dhub is the diameter of swirler hub, Dsw is the outer diameter of swirler, and is the swirler vane angle.

8.The following assumptions have been made during the numerical study:-

(a) Body and buoyancy forces are neglected.

(b) The droplet collisions and interactions are neglected and spray is assumed to be dilute in nature.

(c) Convective and radiative heat loss is neglected.

9.The conservation equations of mass, momentum and energy in the turbulent flow field are solved in conjunction with the standard k turbulence model with initial turbulence intensity as 10 perscent [4]. The mass flow split of air into the combustor through swirler, primary and dilution wall jets, based on the cross sectional area of the inlets is shown in Table 1. The mass flow rate of air through a large number of film cooling holes on the combustor surface is accounted for by increasing the size of primary and dilution jet holes in the combustor geometry.

10. In addition to solving transport equations for the continuous phase, a discrete second phase is calculated using a Lagrangian frame of reference that includes the discrete phase inertia, hydrodynamic drag, and the force of gravity, for both steady and unsteady flows. This second phase consists of droplets dispersed in the continuous phase. The discrete phase patterns are predicted using a coupled approach where continuous phase is impacted by discrete phase. The dispersion of particles due to turbulence in the fluid phase is predicted using the stochastic tracking model.

11. Air-assisted atomizer is incorporated in FLUENT by defining initial position, relative velocity between the liquid sheet and air, mass flow rate of fuel, and temperature of individual particles of diesel. Fuel spray is injected from an atomizer located at the hub of the swirler. The fuel is considered to be diesel (C10H22). The combined effect of pressurized air and fuel is defined in terms of relative velocity. Numerical analysis is carried out at two values of relative velocities; 100 m/s and 75 m/s, to study the effect of relative velocity and spray penetration on mean outlet temperature and NOx emission.

12. Non-premixed equilibrium combustion model is used for modeling combustion. Assumed-shaped Probability Density Function (PDF) is used to solve the closure problem. The post-processing computation of NOx is employed and implemented in FLUENT since it is a good compromise between CPU time and prediction accuracy. In the post-processing approach, NOx emissions are computed on the basis of previously determined temperature fields and chemical species concentrations by solving a transport equation for each nitrogen species of interest [5], [6] or only for NO species. CO is more difficult to predict accurately, because CO formation is also kinetically limited and it is not a trace species.

Results and Comparison

13.Experimental Results. Following variables are analyzed from the experimental results:-

a. Combustion Temperature. Variation of recirculation zone centerline temperature, and the exit temperature, with increase in equivalence ratio is shown in Fig. 4. The local equivalence ratio inside the recirculation zone is determined by considering the mass flow of air only through the swirler i.e., inside the primary zone. Total mass flow of air into the combustor, i.e., through swirler, primary and dilution jet holes is considered for global equivalence ratio. Exit temperature increases with increase in equivalence ratio as expected, because of higher heat release rate due to longer residence time available for the fuel. Longer residence time for the fuel is obtained due to lower velocity of air, since decreasing mass flow rate of air is related to increasing equivalence ratio. The graph is expected to decline at global equivalence ratio beyond unity. Similarly the center line temperature in the recirculation zone is found to increase with increasing equivalence ratio till about stoichiometric value and then found to drop with further increase in equivalence ratio. The drop in recirculation zone temperature can be explained as follows. The recirculation zone temperature reflects the reversal of hot products from the downstream, which is dependent on the strength of the swirl flow. At larger equivalence ratios, the velocity of air being lesser, will result in weaker swirl and thereby center line pressure deficit obtained by the flow across swirler is lower. Therefore inspite of higher downstream temperature, the back flow being less after a particular swirl intensity, the recirculation zone temperature is found to reduce with increasing equivalence ratio beyond a limit.

b.Combustion Efficiency. Combustion efficiency is deter-

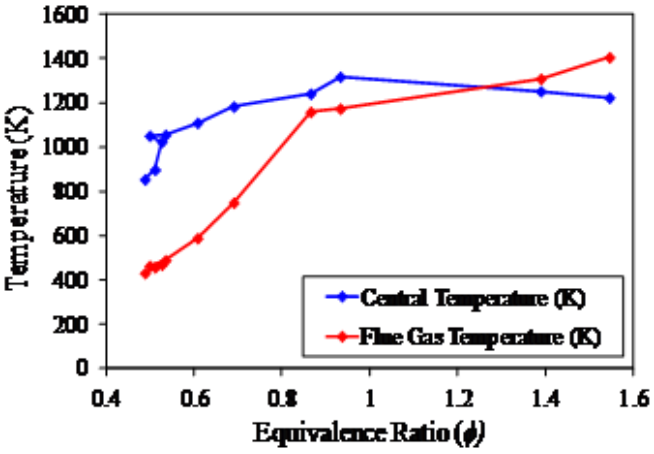


Fig. 4. Variation of recirculation zone temperature and exit temperature with local equivalence ratio

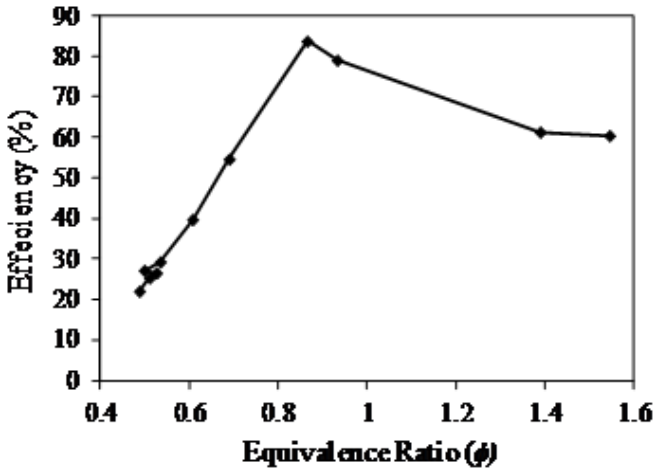


Fig. 5. Variation of combustion efficiency with local equivalence ratio

mined from the ratio of mean heat release rate at the exit of combustor to the total calorific value of the burning fuel rate expressed in terms of percentile. Combustion efficiency is a function of the residence time available for combustion of fuel which is governed by the air velocity and the mixing of fuel and air which is governed by the turbulence induced by the swirl flow. The conflicting effects of air velocity i.e., fuel residence time and turbulence due to swirl, decide the overall combustion efficiency. As shown below, the variation of combustion efficiency with increasing equivalence ratio is plotted in Fig. 5.

Combustion efficiency is found to increase steeply with increase in equivalence ratio till an equivalence ratio of about 0.85, there after the efficiency drops gradually with further increase in the equivalence ratio. The upward trend of efficiency can be explained as a result of increasing residence time due to reduction of air flow velocity and the decreasing trend can be explained as due to insufficient mixing of fuel and air, and also lower entrainment rate of hot products from downstream into the recirculation zone.

c.Combustion Products.CO, CO2, NOx, SOx and CxHy measured using QUINTOX flue gas analyzer are plotted against equivalence ratio along with exit temperature in Fig. 6. Higher values of unburnt hydrocarbons are recorded at lower equivalence ratios compared to the lower values at higher equivalence ratios.

At higher equivalence ratios, air velocities being lower, the fuel has higher residence time to burn. Therefore lower values of unburnt hydrocarbons are recorded at higher equivalence ratios owing to near complete combustion. The initial increasing trend of unburnt hydrocarbons is due to the insufficient residence time of fuel in the recirculation zone as well as lower entrainment of hot products from downstream leading to incomplete combustion. Production of SOx, is found to decrease with increase in equivalence ratio. NOx is found to increase with increase in equivalence ratio, since thermal NOx is dependent on temperature, and higher temperatures are achieved at higher equivalence ratios as discussed earlier. The trend of CO2 shows upward gradient till about stoichiometry which is the zone of higher overall temperatures and then remains steady for rest of the higher equivalence ratios, where the overall temperatures are low. CO concentrations show an increasing trend till about equivalence ratio and then rapidly fall along with the temperature. CO is formed at higher combustion temperatures as a result of dissociation of CO2 which is clearly depicted from the opposing trends of CO and CO2 upto the stoichiometric value of equivalence ratio. This trend is in vogue with the basic combustion literature [7].

d.Combustion Stability. Fig. 7 shows the lower extinction limits of combustion obtained from series of extinction tests conducted at atmospheric pressure. As the mass flow rate of air increases, it is found that fuel to air (f/a) ratio that can support stable combustion decreases.

Higher mass flow rate of air, which implies higher velocity of air (in this case of combustion at ambientpressure) results in lower residence time of fuel although aids in better mixing due to higher turbulence caused by the swirler, the net effect being reducing limits of fuel to air ratio that can yield stable combustion. However it is expected that a reverse trend may follow, if combustion is studied at higher pressures, the reason being at higher pressures the air flow velocities are expected to be lower even at higher mass flow rates of air, resulting in more residence time than in the present case.

14.Numerical Results. Fig. 8 shows the temperature distribution inside the combustor across mid-plane at =0.93. Lower temperature region and slight lift-off was observed near to the fuel-injector exit. Beyond the primary zone and near the stoichiometric mixture fraction, maximum temperature was observed. Maximum temperature inside the combustor is 1920 K.

15. The mean outlet temperature and NOx obtained numerically at different and with relative velocity as 100 m/s and 75 m/s, shown in Fig. 9 and Fig. 10 respectively, were compared

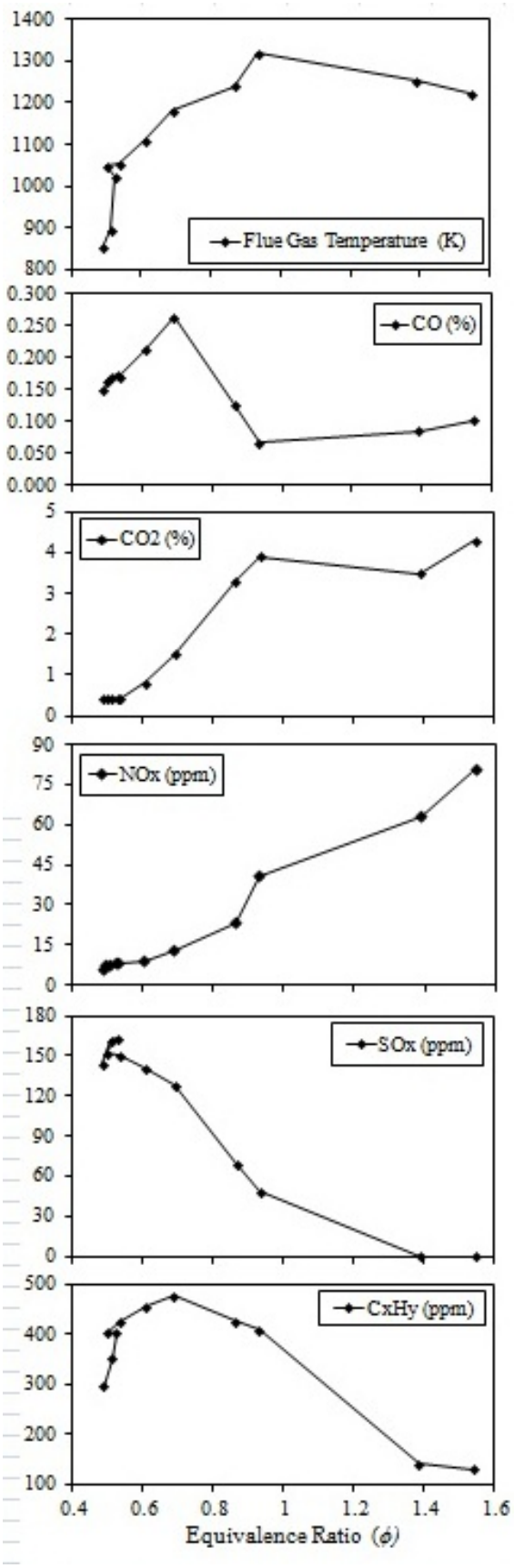


Fig. 6. Variation of Combustion products and flue gas temperature with local equivalence ratio

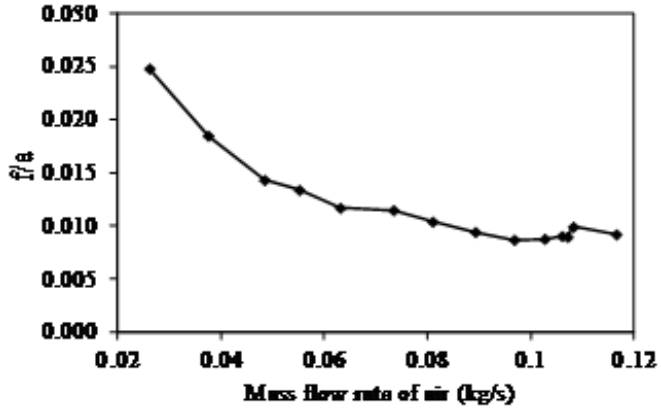


Fig. 7. Lower extinction limits

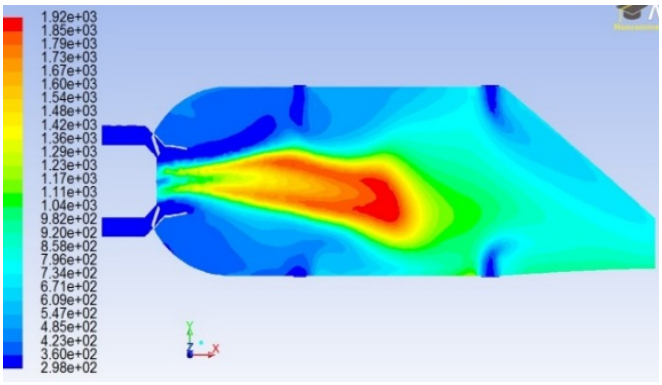


Fig. 8. Contours of temperature inside the combustor across mid-plane =0.93

against the experimental data. For higher , the mean outlet temperature agrees well with experimental data. The over-prediction of temperature at lower is because the standard k turbulence model fails to predict the recirculation zone inside the combustor and as a result under-predicts the mixing field. Also, since the extinction tests were carried out to obtain stability loop, fuel flow rate was varied for all . Hence, the relative velocity of the spray in each case is different. In numerical simulation, a constant and assumed value of 100 m/s and 75 m/s is taken. For simulation results with relative velocity=75 m/s, the mean outlet temperature is in very good agreement with experimental data as compared to that with 100 m/s. It implies that the temperature traverse varies with fuel spray characteristics, such as relative velocity and spray penetration even for a fixed equivalence ratio, because these control the pattern of burning and hence the distribution of temperature in the primary-zone and at the outlet. However it is observed that at lower , the mean outlet temperature obtained numerically with relative velocity as 100 m/s and 75 m/s is hardly distinguishable.

16. The approach adopted to evaluate NOx emissions is able to predict the trend as obtained experimentally but over-

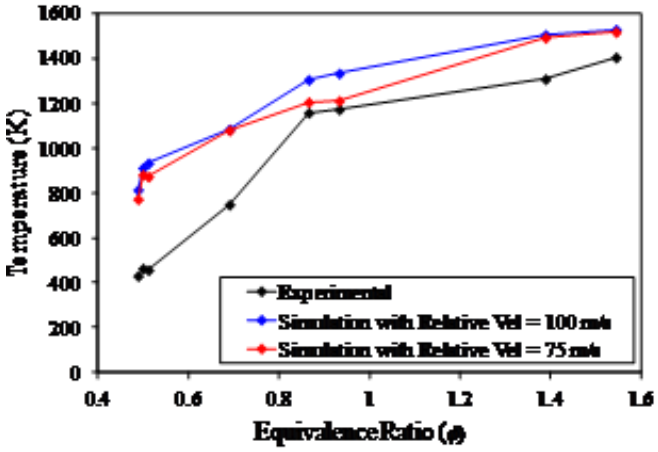


Fig. 9. Comparison of mean outlet temperature with experimental data

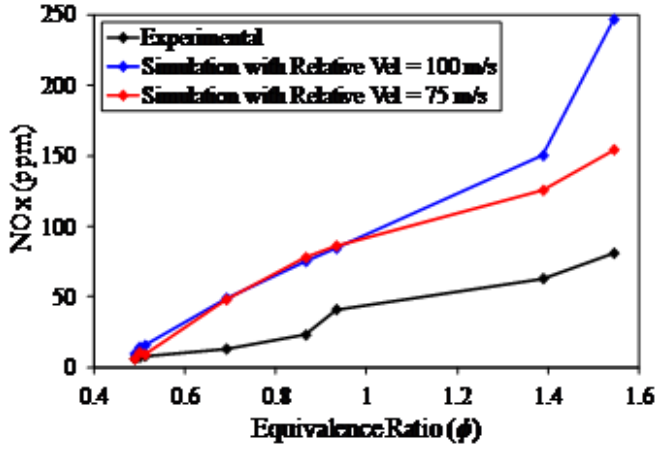


Fig. 10. Comparison of NOx results

predicts the value of NOx emission at higher . In the numerical simulation, the effect of radiation on the heat transfer is not modeled. The contribution of the radiative heat is lower because of the high bulk flow velocity and short residence times but it can have a significant impact on the chemical reactions and thus on the NOx formation [8].

17. Fig. 11 shows the contours of mean outlet temperature at =0.93 and 0.86. The pattern factor obtained at these is 0.33 and 0.43 respectively. The desired value of pattern factor is 0.25 [7]. The center line of the exit plane of combustor is offset from the axis of the combustor making the flow of hot products from the combustor asymmetric about centre line. This causes non uniform dilution of hot products in the combustor exit plane along the radial direction. The pattern factor reflects the effectiveness of dilution and the results indicate that leaner the equivalence ratio, higher is the pattern factor. Burning of residual fuel due to availability of air at leaner equivalence

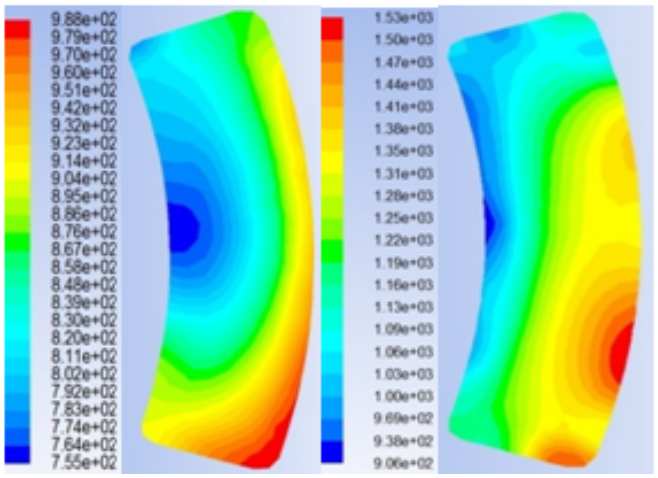


Fig. 11. Contours of mean outlet temperature at equivalence ratios () =0.93 and 0.86

ratios through dilution holes may have resulted in higher exit temperature as well as higher pattern factor. The dependency of all the results on overall combustion pressure is expected to be significant and is still to be verified.

18.Conclusions and Future Scope. Swirl stabilized liquid fuel combustion inside a real gas turbine combustor has been achieved using experimental setup and numerical simulation. Experiments are conducted by varying input parameters to obtain lower extinction limits which give a measure of stability and emissions. Maximum combustion efficiency is achieved at =0.83. Numerical analysis is conducted with standard k turbulence model. Values of mean outlet temperature and NOx obtained at different and with constant relative velocity of 100 m/s and 75 m/s, are in good agreement with experimental data.

20. Further scope in experimental work includes measurement of fuel spray velocity using Particle Droplet Image Analyzer (PDIA), and measurement of flow field data inside the combustor to determine accurate mass flow split and for comparison with numerical results. To study the dependency of pressure on stability, further tests are to be conducted at higher pressures. In case of numerical simulation, the radiative effects on the heat transfer will be modeled using the P1 thermal radiation model. The overall results obtained numerically are promising for further validation of experimental results.

REFERENCES

[1] P. Brijesh, A. Chowdhury and S. Sreedhara. Effect of Ultra-Cooled EGR and Retarded Injection Timing on Low Temperature Combustion in CI Engines. SAE International 2013. 01-0321.

[2] Xia J.L., Yadigaroglu G., Liu Y.S., Schmidli J., Smith B.L. Numerical and experimental study of swirling flow in a model combustor. International Journal of Heat and Fluid Flow [J], 1998. 41, PP1485-1497.

[3] K Shamami and M Birouk. Assessment of the Performances of RANS Models for Simulating Swirling Flows in a Can-Combustor, The Open Aerospace Engineering Journal, 1, 2008, 8-27,

[4] Peters, N. 2000. Turbulent combustion. Cambridge University Press.

[5] Gicquel O, Miquel P, Quilichini V, Hilka M, Thvenin D, Darabiha N. Numerical and experimental study of NO emission in laminar partially premixed flames. Proceedings of the Combustion Institute 2000; 28: 2419e25.

[6] Frassoldati, A., Cuoci, A., Faravelli, T., Ranzi, E., Colantuoni, S., Di Martino, P., Cinque, G., Kern, M., Marinov, S., Zarzalis, N., Da Costa, I., Guin, C., Fluid dynamics and detailed kinetic modeling of pollutant emissions from lean combustion systems Proceedings of the ASME Turbo Expo 2, 2010, (PARTS A AND B), pp. 451-459 .

[7] AH Lefebvre, Gas Turbine Combustion, Hemisphere Publishing Corporation, United States of America, 1983.

[8] A. Schultz, Convective and radiative heat transfer in Combustors, Institute fur Thermische Stromungsmachinen, Universitat Karlsruhe, 2005.

Numerical Resistance and Self Propulsion Simulations for Early-Stage Ship Design Evaluation

Lt Cdr IS Makkar [1], **Cdr (Dr) R Vijayakumar**[2]
[1,2] Naval Construction Wing,
Dept of Applied Mechanics
IIT Delhi, New Delhi-110016.
[1]ismakkar@iitd.ac.in, [2]vijay2028@gmail.com

***Abstract*—The use of Computational Fluid Dynamics as a tool for design evaluation of ships is of great importance to the present day designer. Due to improvements in code capabilities and computer performance, CFD use in practically all areas of naval architecture has increased dramatically over the past decade. The fields include resistance, propulsion, manoeuvring, seakeeping, propulsor design, ocean engineering, noise/acoustic analysis at model and full scale, forming the primary usability for this tool. The numerical techniques required by CFD for the physical modelling of viscous ship hydrodynamics have matured sufficiently that predictions of the steady state resistance of a ship hull at model scale can be estimated with a reasonable confidence. The users decisions are majorly guided by applicability, accuracy, reliability, time and cost.**

The design of an efficient hull form from the perspective of resistance and propulsion features has always been a designers dream. However, with conflicting requirements of the other elements in the design spiral, multiple iterations prior to finalisation of the design are essential. Qualitative analysis of multiple hull forms with major or minor modifications needs to be undertaken in an inexpensive and fast manner. Expensive and time consuming model testing procedures for detailed parametric study is restricted by the budget allocations for model testing in the project and the total value of the project for the operator.

The prime objective of this work was the study of flow characteristics, resistance and self propulsion simulation using RANS solver - SHIPFLOW. In the present work, investigations were carried out for known benchmark CFD model (Eg. KVLCC2, HTC). The results of the simulations are presented, which gave an insight into the modeling accuracy and confidence over the design tool for analysing live projects. Thus, the process provided a convenient initial design tool for resistance and propulsion evaluation of hull forms qualitatively.

***Keywords*—Numerical Estimation; Ship Resistance; Self Propulsion; CFD; Ship design.**

NOMENCLATURE Re Reynolds Number Fn Froude Number CV Coefficient of Viscous resistance CW Coefficient of wave-making resistance CT Coefficient of Total resistance

I. Introduction

Resistance of a ship is defined as the total tow force experienced on a ship for forward motion. The total resistance of the ship alongwith the related propulsive efficiencies in the propulsion train give the total propulsion requirement/ engine sizing for the ship. The engine output and numbers are further guided by the factor of safety, redundancy, volume requirements and stealth characteristics in the design.

An accurate prediction of resistance at the initial stages is a prerequisite to minimize design changes in later stages. Resistance and powering calculations in the design spiral are generally undertaken using the undermentioned procedures along with the related challenges:

- Admirality coefficients Rough estimates.
- Empirical/ Semi-empirical relations Depending on type of ship considered for formulation of equation.
- Statistical Methods /Regression methods Data availability.
- Parent ship data analysis Availability of detailed data for similar hull form.
- Experimental techniques/Model Testing Most trusted method, expensive and time consuming with inherent errors due to assumptions and experimental errors.
- CFD/Numerical Estimation New approach, Initial facility cost for computation/trained manpower, inherent errors and require detailed validation.

Among all the procedures mentioned above, only experimental techniques and CFD can predict changes in ships resistance and powering due to minor design modifications or inclusion of energy saving devices to optimize the hull form. Hull-form optimization is an important area of interest for present day designer trying to minimize fuel consumption and maximize endurance. A reduction of resistance even by 1-2 perscent, incorporating minor modification can result in a major saving during the life-cycle of the ship. Worldwide CFD studies have reached to a level of accuracy to predict the resistance and other propulsion estimates to decent levels of accuracy. Numerical simulation results of Ship propulsion can be further used to undertake a propeller performance estimation in open water and behind hull (Model/ Ship self propulsion points). The wake generated due to the presence of hull in uniform flow further affects the propulsive efficiency. Hence, numerical wake improvement studies is another field of interest for Ship designers. The wake inputs can be further used for vibrational studies [1], [2], [4]. Excessive vibration (with a major hydrodynamic component) can damage or adversely impact the in-service performance of the ships mechanical and electrical equipment. Prolonged exposure to vibration can also contribute to crew and passenger

discomfort, increasing the opportunities for human error. In addition to the above-mentioned aspects, acoustic signature reduction by study of vibration is critical for Warships, Submarines, research vessels and cruise vessels. Detailed vibrational studies with unsteady CFD formulation will provide estimates of the same with spatial as well as temporal variation and promises a bright future of numerical estimations in hydrodynamics, specifically for warships/submarines. CFD tools are also being used for estimation of:

- Shallow water operation
- Wake wash
- Seakeeping parameters prediction
- Maneuvering predictions
- Ship- Boat interaction
- Superstructure aerodynamics

The range of CFD tools available for these classes of problems discussed above is broad and varied. Furthermore, their development has followed different paths, with both specialised maritime CFD packages and more general engineering CFD tools being applied to these problems.

A. Review of Marine CFD Usage - International Scenario The International Towing Tank Conference (ITTC) has been specifying procedures for experimental methods, which are still being followed in most of the Towing tanks across the globe. ITTC 57 and ITTC 78 guidelines form the primary procedure with further corrections and improvements suggested during subsequent conferences of ITTC. With growing interest of the marine industry in CFD, a separate CFD specialist committee of ITTC has been constituted in all recent ITTC conferences. The agenda of the committee is to discuss the advancements in the field of Marine CFD, sharing experiences from various international workshops and formulation of standardized procedures for Numerical predictions. The accuracy of the suggested procedures is debatable; as few authors have suggested alternative higher accuracy guidelines. The latest ITTC conference (2011) convened in Brazil gives the international CFD usage statistics as shown in Fig. 1, Fig. 2 and Fig. 3. The global trends indicate an increased use of CFD in Model test basins and academia, followed by shipbuilding yards. The user profile shows a significant Intermediate user presence, employing generally commercial codes. In-house codes usage is also prevalent, but restricted to specific research area and rarely generic. The commercial code popularity statistics clearly indicates an increased use of ANSYS Fluent,CFX and Star CCM due to its generality in application. Other open source codes like Open Foam are also popular.

B. Review of Marine CFD Usage Indian Scenario In India the use of CFD in the marine industry, primarily for ship design is at nascent stages. Presently, commercial CFD codes for ship design (SHIPFLOW, STAR CCM, OPEN FOAM, ANSYS CFX/Fluent etc) are being employed for design evaluation by academia (IITs, IMU Vizag etc), research organisations (DRDO NSTL, CMFRI) and Class societies (IRS- Research Wing). All the three towing tank facilities in India at IIT Kharagpur, IIT Madras and NSTL use CFD tools

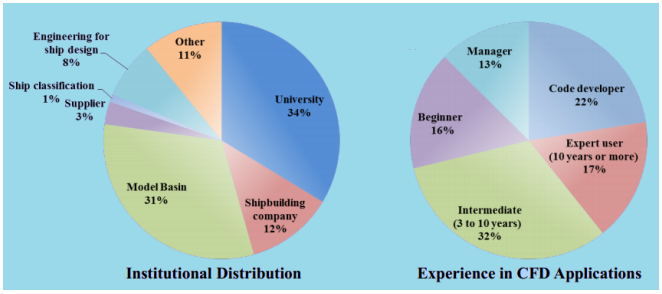


Fig. 1. International Distribution of Institutes for CFD usage in Hydrodynamics of Ships [25].

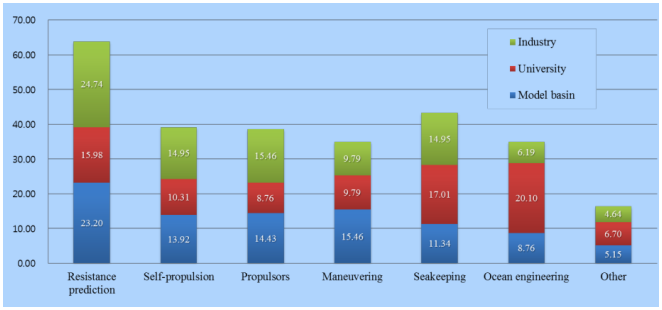


Fig. 2. Areas of Application CFD in Marine Hydrodynamics of Ships [25].

for design evaluation and validation. The generic CFD codes (Ansys Fluent, ANSYS CFX, STAR CCM) are more popular, due to their widespread applicability in auxiliary industries for system design in sync with the global trends. However, the shipyards and major design houses are yet to invest on the infrastructure for CFD evaluation techniques or development of in-house techniques. The primary argument against the same is the high initial cost for the commercial package, requirement of sustained trained manpower for operation/result evaluation, lack of robust in-house data for validation and minimal hull form design changes in orders. It has to be understood that such tools are more relevant for organizations involved in concept/ preliminary design and not for production design. Hence, with limited design variations for the yards, it is more prudent to invest on such capabilities to strengthen existing organisations by providing adequate consultancy problems, research funding for validation data creation and sharing of information by comparison of similar CFD models. Formation of international/ national conglomerates for design skill sharing under the aegis of organisations like NRB, NIRDESH etc is another alternative solution.

C. International CFD Workshops The advances in use of CFD in Marine hydrodynamics is studied in detail during various international CFD workshops and conferences. Guidelines from these workshops are being religiously followed in most of the Towing tanks. International conferences like the SIMMAN, Gothenburg workshop etc are also being organised for researchers in this field to meet and analyse their respective

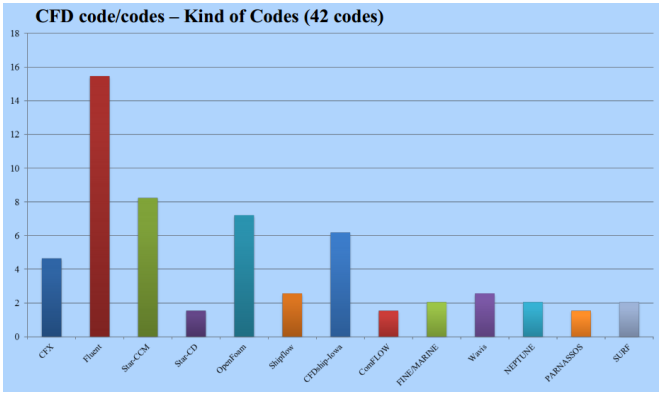


Fig. 3. CFD Commercial Codes Poplularity in Marine Hydrodynamics of Ships [25].

data. This study delves into part of the hydrodynamic resistance, wave elevation analysis, wake study and self propulsion estimation. Standard CFD hull form models used in the above-mentioned workshops have been used to ensure availability of experimental results for data validation. The study has proved that the numerical analysis can be effectively used for qualitative analysis of hull forms. The study was conducted at the Computational hydrodynamics lab, IIT Kharagpur, using the high end computing facility available for running commercial RANS code- SHIPFLOW(R).

II. SCOPE OF WORK

A. Objective The prime objective of this work is study of Numerical Resistance prediction and Self Propulsion simulation using Reynolds-Averaged Navier-Stokes (RANS) solver, SHIPFLOW(R); undertaken by integration of CAD, CFD, analytical and existing empirical methods. This will lead to the development of a convenient preliminary design stage evaluation tool/procedure for hull form optimisation.

—textbfB. CFD Software Description: SHIPFLOW(R) Introduction SHIPFLOW(R) is a special purpose computer code for predicting the flow around ship and around its components, developed at Chalmers University of Technology and FLOWTECH International, AB. To solve the flow around the hull two different approaches, i.e. global and zonal approaches are available in SHIPFLOW(R). A global approach means that the Navier-Stokes equations are solved in the whole flow domain. A zonal approach means that the flow domain is divided into different zones based on the flow characteristics inside, as shown in the Fig. 1. In Zone 1, which is characterised as inviscid and irrotational, a potential flow method is used. This method computes wave resistance and induced resistance, and provides input to a boundary layer method in Zone 2, where transition and boundary layer parameters on the forward half of the ship are predicted. In Zone 3 where the boundary layer gets very thick, a RANS code is used [6].

C. Modules of SHIPFLOW(R) In general, SHIPFLOW(R) includes six modules: XMESH, XPAN, XBOUND, XGRID,

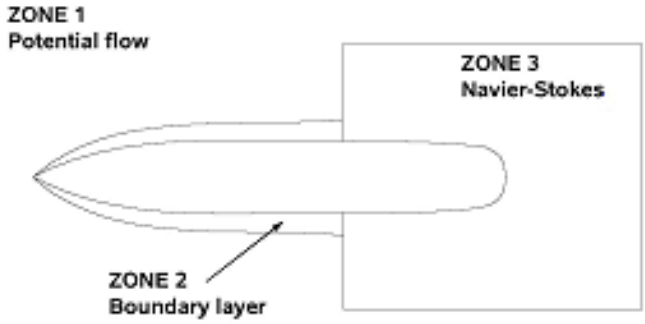


Fig. 4. Different zonal approach in SHIPFLOW

XVISC and XCHAP, as shown in the Table 1. The first two modules are used for the potential flow computations: XPAN is the solver for the free-surface potential flow based on a surface singularity panel method and XMESH provides the panelisation of the body and free-surface before the computation. XBOUND is a program for thin turbulent boundary layer computations and it is also able to compute the laminar boundary layer and the transition to the turbulent boundary layer for simpler cases with a well-defined stagnation point or line.

The other three modules are designed for viscous flow (RANS) computations: XGRID establishes the grids around a ship body (except appendages) used in the viscous computations in XVISC and XCHAP. XVISC is a finite difference code solving the RANS equations, in which the boundary conditions are generated from given boundary layer information or results provided by XPAN and XBOUND.

XCHAP is a finite volume code that solves the RANS equations, either in a zonal approach (like XVISC) or in a global approach where the same method is used in the entire computational domain. In particular, this module can compute more complicated geometries, as it is capable of handling overlapping grids of, e.g. rudder, shafts, brackets and vortex generators. The grids may be generated internally or imported from external grid generators. The flow can be computed with a double model or with a prescribed free surface from XPAN. In XCHAP, the two turbulence models introduced above are available: Menter k- SST model and EASM.

TABLE I. DIFFERENT MODULES OF SHIPFLOW

Pre- Processors		
X MESH X GRID		
Flow Programs		
Potential Flow	Boundary layer	Navier Stokes
XPAN	XBOUND	XCHAP XVISC
Post-Processor		
SPOST		

D. Propeller Analysis Model Lifting Line Method (LL): In the standard version of SHIPFLOW(R), a lifting line method

based propeller analysis code is coupled with the RANS solver XCHAP. In this model, a finite- bladed propeller is first replaced by an infinite bladed propeller. Then a series of vortex system, such as bound vortices, hub vortices and free (trailing) vortices, are distributed to represent the propeller. The slipstream contraction is not considered in this model because the pitch and the radius of each free vortex line are assumed to be constant. Only the steady part of the induced velocity is taken account of, although this is mainly proved for lightly loaded propellers. The method used in the calculations of the induced velocity of propeller can be found in standard procedures in self propulsion analysis. A determination of the non-dimensional blade circulation is made by incorporating a method based on Goldsteins kappa theory. The viscous drag of the blade is calculated in an approximate way.

E. Numerical Self Propulsion Estimation Methodology

The interactive coupling between RANS solver and XCHAP and the LL model via body forces is done with the following procedure at regular intervals, normally every 10 iterations in the RANS solver:

- Interpolate the current approximation of the velocity field to an embedded cylindrical grid concentric with the propeller.
- Obtain the effective wake on the blade of the propeller by subtracting the propeller induced velocities obtained in the previous iteration from the velocity field.
- Run the propeller model in the effective wake and calculate the blade circulation and the forces and the torques.
- Distribute the computed forces over the volume cells in the cylindrical grid.
- Interpolate the forces from the cylindrical grid and introduce them in the right hand side of the N-S equations. The fluid that passes through the cells has thus acquired a body force and is accelerated so that the time averaged action of the propeller is simulated. The sum of the forces will give the fluid passing through the propeller disc a longitudinal and angular momentum consistent with the thrust and torque on the propeller.
- At convergence two models are matched in the sense that the absolute wake computed by the RANS method, at points sampled in a circular disc in the middle of the cylindrical grid, will be equal to the total wake computed by the propeller model at the same point.

III. CASE STUDIES, OBSERVATIONS AND RESULTS

The hull form selected for the studies were standard CFD models of KVLCC2 tanker. Other CFD models HTC, KCS Container ships were also analysed by the author. In this paper the results of the KVLCC 2 are being discussed. These models are widely used for comparative CFD studies result comparison. The data for the hypothetic vessels are available from various CFD studies/model tests conducted by multiple agencies and CFD workshops. The vessel details, self propulsion simulation results and vibration analysis of some of the hull configurations are enumerated in the subsequent sections.

TABLE II. MAIN PARTICULARS KVLCC 2

Dimension	Ship	Model
LBP	320 m	4.97m
T	20.8m	0.323m
hline CB	0.8098	0.8098
hline Design Speed	15.57 knots	1 m/s

A. Numerical Study Methodology

SHIPFLOW(R) CFD code was used for the initial resistance simulation of the vessel model. The results obtained were; vessel resistance, wave cuts and nominal wake. In the second step Propeller Open Water (POW) simulation using the original propeller geometry was carried out and the propeller characteristics were obtained. Resistance results and POW simulation results were used as input file for the Self Propulsion Test (SPT) simulation for detailed Ship propulsion characteristics. The numerical simulations were carried out at model scales for comparison with available experimental/workshop simulation results. After gaining enough confidence in resistance estimation and wake validation, multiple drift conditions for further validation of wake with experimental results was undertaken. Grid independence studies were carried out by varying the grid density.

B. Ship Model Description KVLCC2

The MOERI KRISSO VLCC was conceived to provide data for both explication of flow physics and CFD validation for a modern 3,00,000 tonnes tanker ship with bulbous bow. Two stern variants were designed:

- KVLCC1 has barge type stern frame-lines with a fine stern end bulb i.e. relatively V-shaped frame-lines.
- KVLCC2 (Table 2) the second variant, has more U-shaped stern frame-lines.

KVLCC 2 with adequate experimental results from various workshop publications has been used as the hull form for the CFD study. No full-scale ship exists with this hull form. The corresponding Reynolds number is Re = 4.97 x 106, at model scale. The Froude number is Fn = 0.143. The main particulars of the ship are tabulated below:

C. Geometric Model- KVLCC 2 The geometric model of the vessel was generated from the available CAD model (MAXSURF) in IGES format Fig. 6, as part of the pre-processing procedure for the CFD study. The hull was further divided into four hull offset groups as shown in the figure, depending on the location and complexity in curvature for SHIFLOW evaluation.

D. Grid Arrangement KVLCC 2 The initial runs were undertaken with Coarse mesh and final runs of numerical simulation were run with Fine grid Fig. 7 in to check for grid sensitivity.

E. Resistance Simulation Validation - KVLCC 2 Resistance validation of the bare hull for KVLCC 2 hull was carried out with the existing results from CFD workshops and other CFD package results (Marine CFD -OPENFOAM). The validation was carried out at a Froude number of Fn = 0.143 corresponding to the design speed and others speeds (For resistance curve validation). It was observed that the results of the SHIFLOW CFD runs were comparable with other studies

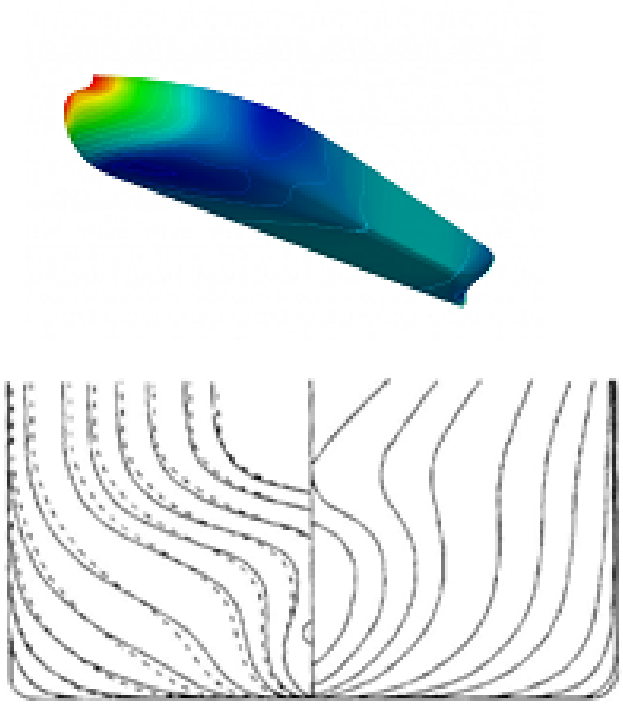
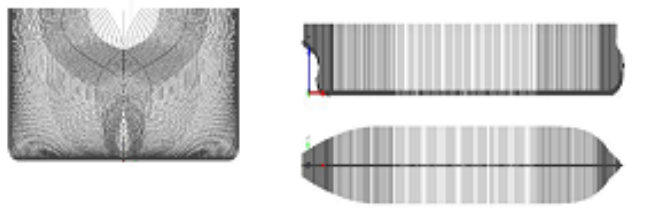


Fig. 5. Hull Geometry KVLCC 2



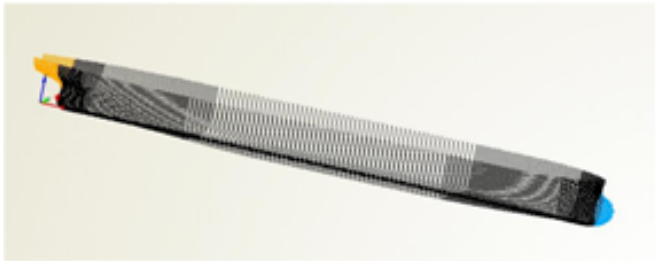


Fig. 6. Hull Geometry KVLCC 2

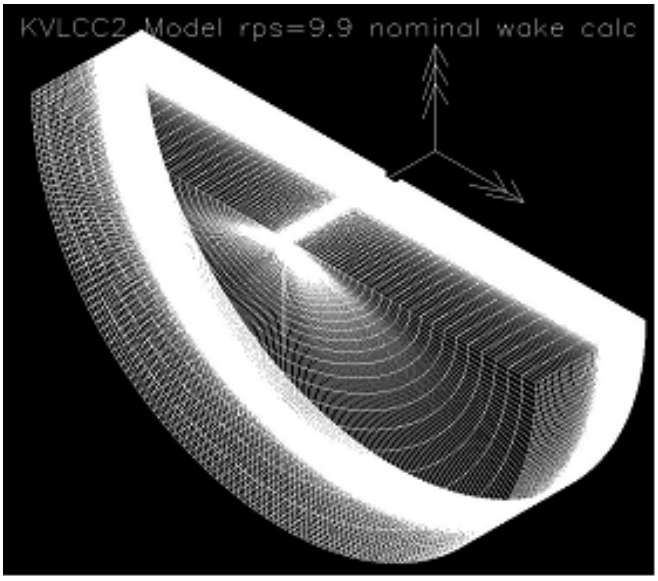


Fig. 7. Grid Arrangement KVLCC 2

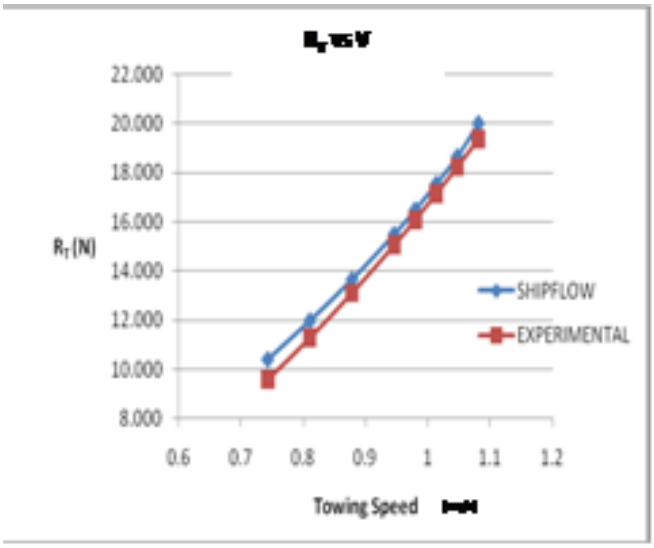


Fig. 8. Resistance Validation KVLCC 2

and the hull form/software could be used for further studies. The validation results is plotted in Fig. 8.

textbfF. Wake Validation KVLCC 2 The hull form was further validated with the wake results for KVLCC2 from SHIPFLOW, being compared with NMRI, Japan (2006) tank test results. The wake distribution trend was very closely replicated in the CFD study. The results were further validated in drift conditions with six and twelve degrees drift angles and showed comparable qualitative results as shown in Fig. 9.

G. POW and SPT Results - KVLCC 2 Propeller Open

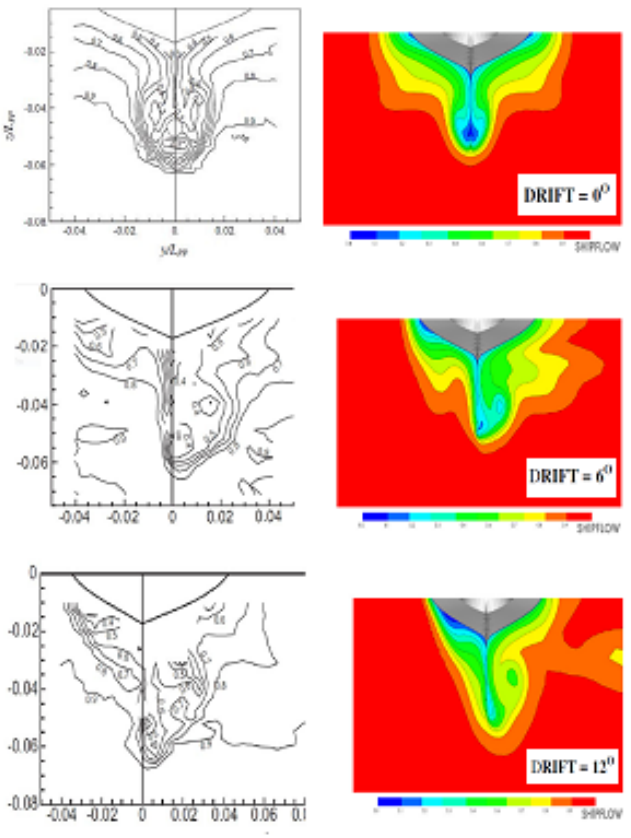


Fig. 9. Wake Validation: Drift Conditions KVLCC 2

water (POW) and Self Propulsion Test (SPT) simulation was carried out for the 4-bladed KVLCC 2 propeller model at the design speed and the results were validated with the experimental results from NMRI. Fig. 10 and Fig. 11 gives the plot showing the result validation with the available data and SPT result (Effective wake). KVLCC 2 Propeller data is given below (Model scale):

- Type - Fixed Pitch
- Scale ratio = 1:58
- Propeller Diameter = 0.17 m
- No. of blades = 4
- Direction of rotation - Right hand

IV. SUMMARY AND CONCLUSION

In the present work, investigation were carried out for detailed numerical self propulsion simulation for known CFD model - KVLCC 2. The RANS based CFD software SHIPFLOW(R) developed at Chalmers University of Technology and FLOWTECH has been used.

Validation of KVLCC 2 hull form model results using SHIPFLOW(R) was carried out for resistance and wake with available model test data and CFD workshop results. The results were found to be comparable. Open Water Test and

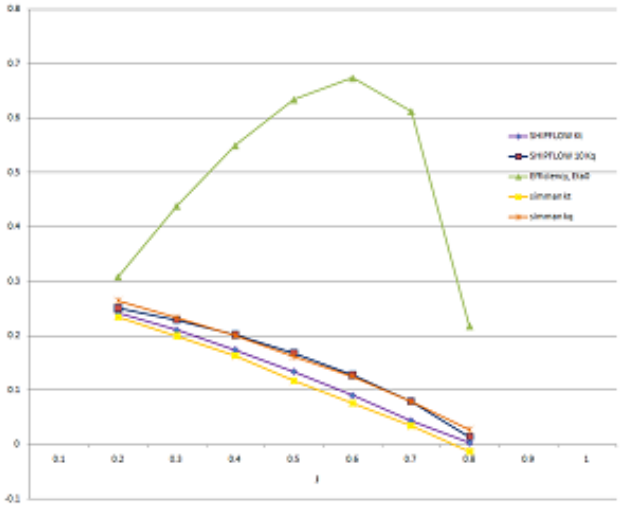


Fig. 10. POW Results KVLCC 2

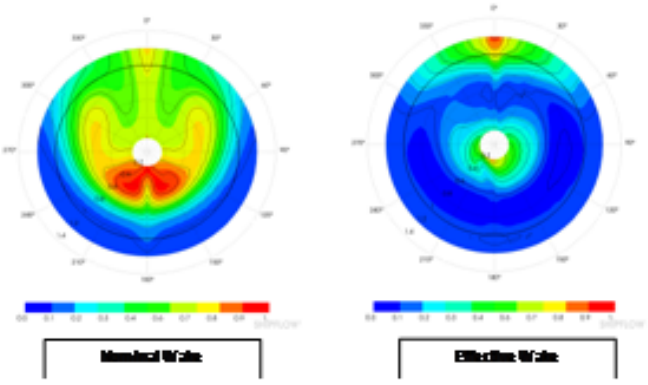


Fig. 11. SPT Results KVLCC 2

Self Propulsion Test were undertaken using SHIPFLOW(R) and effective wake for the model was evaluated. The results were validated with available experimental data. The results showed very good validation of the LL theory based code.

The results of wake were found to be sensitive to the Froude number and grid arrangement selected for the study. The wake distribution is also sensitive to the propeller location. High Froude number vessels pose a challenge for the numerical tool and might need to be analysed at model scale/ varying grid. The procedure can also be followed for more slender hull forms like warships. Results for validation exist for DTMB CFD model of a typical warship hull form. However, in-house development of experimental validation results is very critical for a successful CFD analysis tool usage. The procedure can be further extended to submarines and submersibles.

This process can thereby be used for resistance estimation, qualitative multiple hull form analysis, optimum hull selection for a given operational requirement, resistance reduction by hull form optimisation, stern configuration optimisation for better propulsive features etc. The results could be further utilized for vibrational characteristics assessment and acoustic signature analysis. The objective of the study was creation of a preliminary design tool, for multiple hull/propeller configuration performance evaluation. The tool is primarily intended for qualitative optimisation studies and not for quantitative powering estimation replacing experimental studies.

ACKNOWLEDGMENT

The authors would like to acknowledge the guidance of Prof OP Sha, Dept of Ocean Engineering and Naval Architecture, IIT Khargpur; Prof. RP Gokarn, Consultant at Ocean Engineering and Research Consultancy (OERC).

REFERENCES

[1] GHOSE, J.P and GOKARN, R.P. (2004), Basic Ship Propulsion, Allied Publishers Pvt Ltd.

[2] MAKKAR, I.S., SHA,O.P.(2013), Numerical Self Propulsion Simulation and Propeller Induced Vibration Study, Proceedings of

[3] LARSSON, L. and RAVEN H. C., Ship Resistance and Flow, The Society of Naval Architects and Marine Engineers, 2010, USA.

[4] VORUS, W.S. (2010), The Principles of Naval Architecture Series: Vibration, SNAME

[5] SSC-350. (1990), Ship Vibration Design Guide.

[6] AMERICAN BUREAU OF SHIPPING. (2006), Guidance Notes on Ship Vibration.

[7] SHIPFLOW 4.7 Users Manual (2012), FLOWTECH International, Gothenburg, Sweden.

[8] VAN, S.H, KIM, W.J, KIM, H.H and LEE, C.J (1998), Experimental Investigation of the Flow Characteristics around Practical Hull forms, Proceedings of 3rd Osaka Colloquium on Advanced CFD Applications to Ship Flow and Hull Form Design, Osaka, Japan.

[9] PAULLING, J.R. (2010), The Principles of Naval Architecture Series: Ship Resistance and Flow, SNAME.

[10] BRESLIN, J.P and ANDERSON, P. (1994), Hydrodynamics of Ship Propellers, Cambridge University Press.

[11] BERTRAM, V. (1999), Practical Ship Hydrodynamics, Butterworth-Heinemann, Elsevier.

[12] GERMANISCHER LLOYD. (2001), GL Technology-Ship Vibration.

[13] ITTC-Recommended Procedures and Guidelines (2011), Practical Guidelines for Ships CFD Applications, 26th ITTC Specialist Committee on CFD in Marine Hydrodynamics.

[14] ITTC-Recommended Procedures and Guidelines (2008), Uncertainty Analysis in CFD Verification and Validation Methodology and Procedures, 25th ITTC Resistance Committee.

[15] LEE, S.K.et al. (2006). Propeller Induced Hull Vibration Analytical Methods, 2nd International Ship Noise and Vibration Conference, London, UK.

[16] HAN, K.J. (2008), Numerical Optimisation of Hull/Propeller/Rudder Configurations, PhD Thesis, Chalmers University of Technology, Goteborg, Sweden.

[17] HYLARIDES, S. (1978), Some Hydrodynamic Considerations of Propeller-Induced Ship Vibrations, Ship Vibration Symposium 78, Washington, D.C.

[18] VERSTEEG, H.K and MALALASEKARA, W. (1995), An Introduction to Computational Fluid Dynamics- The Finite Volume Method, Pearson Education Ltd.

[19] [Stefan KRUGER, Manuel MANZKE, Thomas RUNG, Hendrik VORHOLTER, Introduction of RANS-CFD into the Initial Design Process.

[20] VAN, S. H. Et al. (1998b), Experimental investigation of the flow characteristics around practical hull forms, Proceedings of 3rd Osaka Colloquium on Advanced CFD Applications to Ship Flow and Hull Form Design, Osaka, Japan.

[21] VALKHOF.H and HOEKSTRA.M (1998), Model tests and CFD in Hull form Optimization, SNAME Transactions, Vol. 106, 1998, pp. 391-412.

[22] CARLTON, J. S., Marine Propellers and Propulsion, 2nd edition, Elsevier, 2007.

[23] TAHARA.Y, WILSON.R.V, CARRICA.P.M (2006), RANS simulation of a container ship using a single-phase level-set method with overset grids and the prognosis or extension to a self-propulsion simulator.

[24] LEWIS, E.V. (1988), Resistance Propulsion and Vibration, Principles of Naval Architecture Volume II.

[25] www. ittc.sname.org



Lt Cdr Ishaq S Makkar Lt Cdr Ishaq S Makkar is a graduate of Naval Architecture from the Cochin University of Science and Technology. He has done a PG Diploma in Naval Construction from Indian Institute of Technology, Delhi and M Tech in Ocean Engineering and Naval Architecture from Indian Institute of Technology, Kharagpur. He is presently appointed as Adjunct Faculty at the Naval Construction Wing, Department of Applied Mechanics at Indian Institute of Technology, Delhi, where he teaches the subjects of Warship Resistance & Propulsion and Submarine Design. He has published papers in in various international/national conferences in the area of Warship design/CFD. He is a member of the Institution of Naval Architects, India. His fields of interest include; Ship Resistance & Propulsion, Ship Hydrodynamics, CFD in Naval Architecture Ship Aerodynamics, Submarine Design, Submarine Construction and Overseeing.



Cdr (Dr) R Vijayakumar is a Ph.D. from Indian Institute of Technology Delhi in 2009. During his career of 20 years he has served in both the Naval Dockyards and Design Directorate. He is presently appointed as Adjunct Faculty at the Naval Construction Wing, Department of Applied Mechanics at Indian Institute of Technology, Delhi where he teaches the subjects of warship design, structural design of warship and Ship Dynamics. He has published 18 papers in refereed journals and conference. His fields of interest include Warship Design, Ship Hydrodynamics, Ship Dynamics and Computational Fluid Dynamics (CFD).

MARINE POLLUTION CONTROL BY BALLAST WATER MANAGEMENT SYSTEM

Ashvin Wanzul [1], **Sameer Mamluskar** [2], **Rohit Mathur**[3]
[1,2,3]Marine Engineering Center,
Larsen & Toubro limited,Mumbai, India
[1]ashvin.wanzul@larsentoubro.com, [2]sameer.mamluskar@larsentoubro.com, [3]rohit.mathur@larsentoubro.com

***Abstract*—Marine industry is continually facing challenges of marine pollution. We should care about the continuing environmental degradation of our oceans and coastal areas because it is detrimental to human health, economic development, climate and our planet's store of biodiversity. It is interfering with the sustainability of environment and its resources. It is also contributing to detrimental global warming and thus now time has come to prevent marine pollution and need to assess the size of this problem and solution for this.**

One of the major causes for marine pollution is exchange of ballast water. As the ballast water is discharged together with the plankton, etc. at another port, it possibly impacts the ecosystem in the sea area, causing a global-scale environmental damage. Ballast water contains local plankton, bacteria, viruses, mud and sand of the unloading port where the ballast water is taken.

In the late 1980s, Canada and Australia brought their concerns to the attention of IMO's Marine Environment Protection Committee (MEPC).

In 2004, IMO introduced "International Convention for the Control and Management of Ships' Ballast Water and Sediments", which is intended to address the ever growing issue of the introduction of non-native species in waters all over the world. When this convention is ratified, all ships above 100 GT needs to have a water ballast treatment system installed by 2012 (with all ships fitted by 2017) which shall meet the Standard on the water quality.

***Index Terms*—Ballast water treatment , Solid-liquid separation, Disinfection.**

I. INTRODUCTION

Around the world more than 10 billion tons (m3/h) of ballast water are carried in ships each year. Ballast water contains a variety of organisms including bacteria and viruses and the adult and larval stages of many marine and coastal plants and animals. While the vast majority of such organisms will not survive to the point when the ballast is discharged, some may survive and thrive in their new environment. These 'non-native species', if they become established, can have a serious ecological, economic and public health impact on the receiving environment creating problems for the marine environment and human health, threatening the aquatic flora and economies that depend on healthy aquatic ecosystems.

The transportation of ballast water cannot be stopped, but the transfer of harmful aquatic organisms and pathogens can be minimized by deep sea exchange or suitable treatment.

The International Maritime Organization (IMO) has developed international legislation, the International Convention for the Control and Management of Ships' Ballast Water and Sediments, to regulate discharges of ballast water and reduce the risk of introducing non-native species from ships' ballast water by the year 2016.

II. CAUSES FOR MARINE POLLUTION-

Marine pollution is mainly introduced by man, directly or indirectly, of substances or energy into the marine environment. It is harmful to living resources and marine life, hazardous to human health, hindrance to marine activities, including fishing and other legitimate uses of the sea, and impairment of quality for use of sea water and reduction of amenities.

The Marine pollution occurs due to following sources:

A. Black Water-

Backwater is any waste from a toilet or urinal. It contains disease causing organisms that can result in human illness by direct contact or by consumption of affected fish and shellfish. It also contributes to the build-up of unwanted nutrients in ecosystems.The black water is treated by Sewage treatment plant & discharged in to the sea. But sometimes it is directly discharged in to the sea.

B. Oil Spillage-

Ships can pollute waterways and oceans in many ways. Oil spills can have devastating effects. While being toxic to marine life, polycyclic aromatic hydrocarbons, found in crude oil, are very difficult to clean up, and last for years in the sediment and marine environment. Much of the oil in the world's seas comes from other smaller sources, such as tankers discharging ballast water from oil tanks used on return ships, leaking pipelines or engine oil disposed of down sewers.

Cargo residues Discharge-

Discharge of cargo residues from bulk carriers can pollute ports, waterways and oceans. In many instances vessels intentionally discharge illegal wastes despite foreign and domestic regulation prohibiting such actions. It has been estimated that container ships lose over 10,000 containers at sea each year (usually during storms).

C. Solid waste-

Solid waste includes Food waste; Food contaminated waste, Dry general waste, Plastic, Cardboard, Metal tins & cans, Glass, Hazardous waste & Dust. Many times this waste is directly thrown in to the sea.

D. Bilge Water-

It is the water that collects in the bilges & does not drain off the side of the deck drains down through the ship into the bilge. This water may be from rough seas, rain, leaks in the hull or stuffing box, or other interior spillage. The bilge water may contain water, oil, detergents, solvents, chemicals, pitch, particles, and other materials. The bilge water is stored in tanks & treated by oily water separator. But sometimes ships discharge it overboard directly adding it to water pollution.

E. Ballast water-

Ballast water taken up at sea and released in port is a major source of unwanted exotic marine life. Invasive species can take over once occupied areas facilitate the spread of new diseases, introduce new genetic material, alter underwater seascapes and jeopardize the ability of native species to obtain food.

F. Hull coating leachate-

It consists of constituents that leach, dissolve, or erode from the paint on the vessel's hull into the surrounding water. The anticipated standard will require Armed Forces vessels to use antifouling paints that meet a maximum allowable copper release rate.

G. Gray water-

Gray water is waste water from sinks, showers, washing machines, dish washers and so on. It is thrown overboard without treatment.

H. Deck Runoff-

Deck runoff occurs from all vessels as a result of deck cleaning. Constituents of deck runoff may include oil, grease, cleaner or detergent residue, paint chips, and general debris. Discharge rates for deck runoff vary from vessel to vessel and depend on weather, deck machinery, deck operations, and frequency of deck wash downs. Due to the nature of vessel operations, design, and safety, it is not always feasible to hold or treat all deck runoff which adds to sea water pollution

III. HARMFUL EFFECTS OF POLLUTANTS ON MARINE ORGANISMS

The organisms living in the oceans tend to concentrate the pollutants into their body by various mechanisms, like adsorption, absorption, ingestion etc. The concentration of pollutant increases with higher trophic levels, i.e. from primary producers to the tertiary consumer. The threshold limit of organisms to the pollutant concentration increases with

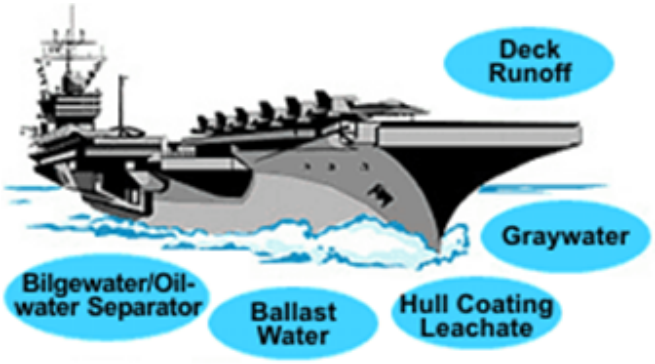


Fig. 1. Sources Of Marine Pollution

increasing trophic levels. Various mode of pollution transport in organisms are:

(a) Bio-concentration
(b) Bioaccumulation
(c) Bio-magnification
(d) Bio degradation

A. Bio concentration

The bio concentration is the process by which a contaminant such as oil is directly taken up (i.e., by absorption only) from water and is accumulated to levels greater than those found in the surrounding water.

B. Bio accumulation

Marine organisms can accumulate chemical species in amounts far exceeding their surrounding (sea water or sediment) concentrations. The bioaccumulation is the process by which a contaminant is taken up by organisms directly through the physical exposure pathway or through consumption of food containing the contaminated substance. Organisms may take up the chemical directly from seawater or from their food. Thus, depending upon the composition of the food, concentration factors can vary from one environment to another for specific organisms with a given chemical.

C. Bio magnification

Bio magnification is the increase in tissue concentrations of a bio accumulated chemical substance such as oil as it passes up though the trophic levels.

D. Biodegradation

Biodegradation is the process of degradation of a contaminant such as oil because of its use as a food a source for certain microorganisms. This process is limited to a great extent by temperature, nutrients and oxygen availability.

TABLE I
THE USCG COMPLIANCE SCHEDULE

Vessel Types	Ballast water capacity	Date constructed	Compliance date
New vessels	All	On or after 1 December, 2013	On delivery
Existing vessels	Less than 1,500m3	Before 1 December, 2013	First scheduled drydocking after 1 January, 2016
	1,500 – 5,000m3	Before 1 December, 2013	First scheduled drydocking after 1 January, 2014
	Greater than 5,000 m3	Before 1 December, 2013	First scheduled drydocking after 1 January, 2016

IV. NECESSITY OF BALLAST WATER TREATMENT

Ballast water plays an important role in maintaining the stability & maneuverability of the ship. Ballast water contains thousands of species of aquatic animals and plants. These invasive organisms are creating problems for the marine environment and human health, threatening the economies that depend on healthy aquatic ecosystems.

The transportation of ballast water cannot be stopped but the transfer of invasive aquatic organisms and pathogens can be minimized by deep-sea exchange or suitable treatment.

In order to reduce damage from aquatic invasive species the International Maritime Organization (IMO) developed the "International Convention for the Control and Management of Ship's Ballast Water and Sediments".

The BWM convention began with the IMO's Marine Environment Protection Committee (MEPC) in 1991.

A. Regulation for ballast water management system

1) The BWM Convention- The BWM Convention will apply to all ships including submersibles, floating craft, floating platforms, FSUs and FPSOs. It will not apply to:
   - ships not designed to carry ballast water
   - warships, naval auxiliary ships or other ships owned or operated by a state
   - ships only on non-commercial service, or
   - Ships with permanent ballast water in sealed tanks.

   Once the BWM Convention has entered into force, all ships will be required to manage their ballast water on every voyage by either exchanging or treating it using an approved ballast water treatment system & the Ships have to comply the schedule given by IMO till 2016.
2) The United States Coast Guard (USCG) regulations- All ships calling at US or Canadian ports and planning to discharge ballast water must carry out ballast water exchange or treatment in addition to sediment management. However, ballast water exchange will only be allowed until the implementation dates for treatment systems shown

TABLE II
THE IMO D-2 STANDARD FOR DISCHARGED BALLAST WATER

Organism category	Regulation
Plankton, >50 μm in minimum dimensions	<10 cells/m3
Plankton, 10-50 μm	<10 cells/ml
Toxicogenic Vibrio cholera (O1 and O139)	<1 colony forming unit (cfu)/100ml or less than 1cfu/g (wet weight)
Escherichia coli	<250 cfu/100ml
Intestinal Enterococci	<100cfu/100ml

3) European Union regulations
   - The European Commission has published a proposal for a regulation on the prevention and management of the introduction and spread of invasive alien species. The proposal's aim is to address the problem of invasive alien species to protect native biodiversity and ecosystem services; and to minimise and mitigate the impacts on human health and economy.
   - It is for three types of interventions: prevention; early warning and rapid response; and management.
   - The proposal states that a large proportion of invasive alien species are introduced unintentionally into the Union; therefore it is crucial to manage these pathways.

B. Standards for ballast water management system

Regulation D-2 of the BWM Convention sets the standard that ballast water treatment systems must meet and it is indicated in the table below. Ballast water treatment systems must have a type approval certificate in compliance with the IMO Guidelines for the Approval of Ballast Water Management Systems (Resolution MEPC. 174(58)), which updated Resolution MEPC.125(53).

V. BALLAST WATER TREATMENT PROCESSES

The technology used to treat ballast water has generally been derived from other industrial or municipal applications, such as wastewater treatment systems, in which forms of solid-liquid separation and disinfection processes were applied. However, their use is constrained by key factors such as space, cost and efficacy.

There are two generic types of process technology used in ballast water treatment:

A. Solid-liquid separation, and

B. Disinfection.

Solid-liquid separation- The separation process concerns the removal of solid suspended material from the ballast water by sedimentation or straining by means of a filter. This produces a waste stream that comprises backwash water from the filtering or a hydro cyclone operation. The waste stream is discharged during ballasting.

Waste streams require appropriate management and during ballasting they can be safely discharged at the point where they

TABLE III
PERCENTAGEWISE WEIGHTAGE OF PARAMETERS WHILE SELECTING BALLAST WATER TREATMENT SYSTEM

Item	Importance	Description
Power requirement	20%	System required power
Footprint	10%	Comparative grade
Pressure loss	20%	Pressure loss caused by installing treatment system
Required inlet pressure	10%	Minimum required pressure at system inlet
Investment cost	40%	Comparative grade
Ballast pump capacity	Critical	Flow rate of ballast pump
EX restrictions	Critical, if required	If the system can installed in hazardous areas, where required
Delivery time	Secondary	In months
Sampling system	Secondary	Delivered by vendor
Retention time	Secondary	Minimum time the ballast water has to retain in tanks for safe discharge without neutralizer

were taken up. On DE ballasting, the solid-liquid separation operation is generally bypassed.

Disinfection- It may be achieved in a number of ways. Chemical treatment uses oxidizing biocides that interfere with the microorganism's organic structure or non-oxidising biocides that interact with reproductive or metabolic functions. Disinfection removes and/or inactivates micro-organisms using one or more of the following methods:-

- Chemical inactivation of the micro-organisms through either by oxidizing biocides or by Non-oxidizing biocides .
- Physico-chemical treatment systems use UV light, heat or cavitation.
- DE oxygenation is another method, in which the organism is asphyxiated.

All of these disinfection methods have been applied to ballast water treatment, with different products employing different unit processes.

Most commercial systems comprise two or more stages of treatment with a solid-liquid separation stage being followed by disinfection shown in Fig. 2.

The range of system processes employed for ballast water treatment is shown in filtration and UV systems shown in Fig. 3 and 4 respectively. A typical treatment process is shown

Commercial systems differ mainly in the choice of disinfection technology and the overall system configuration.

VI. SELECTING A TREATMENT SYSTEM

- Various types of Ballast Water Treatment Processes, methods benefits are given in detail in Annexure-1

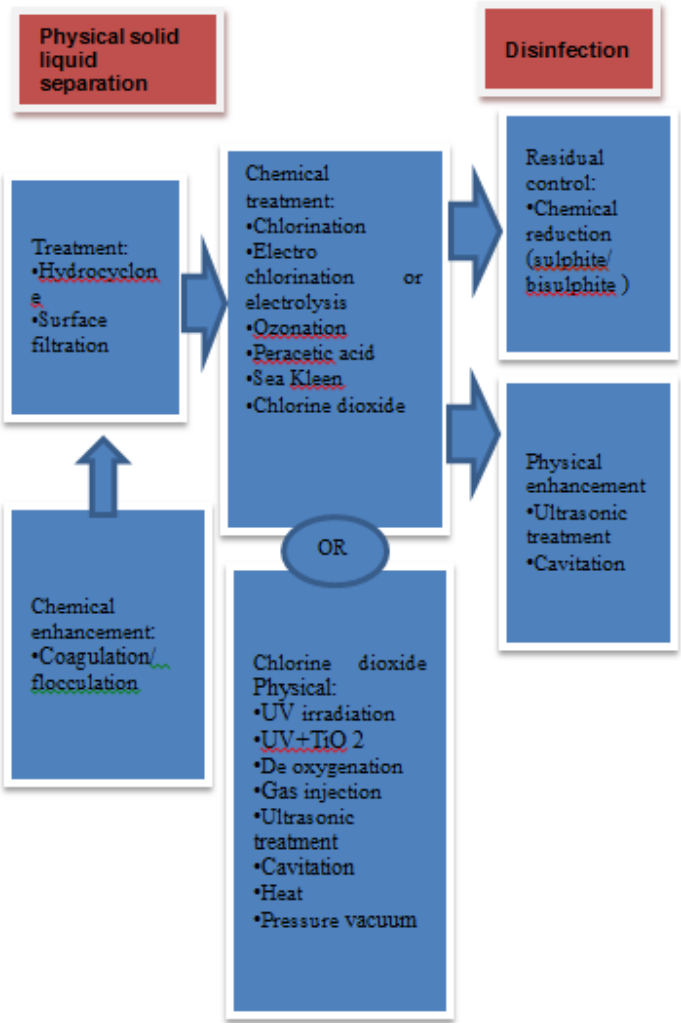


Fig. 2. Generic ballast water treatment technology process options

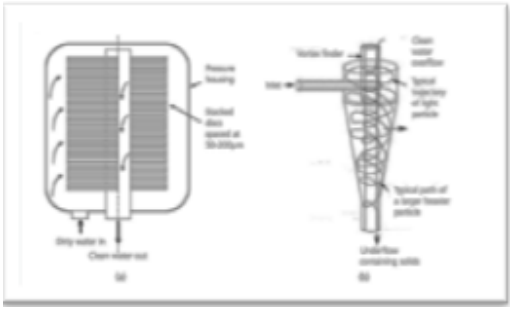


Fig. 3. Filtration (a) and hydro cyclone (b) processes

VII. GUIDE LINES FOR SELECTING A TREATMENT SYSTEM

Ballast water management system plays an important role in controlling the marine pollution. Based on the below parameters the most efficient & reliable system along with optimized cost & weight can be selected.

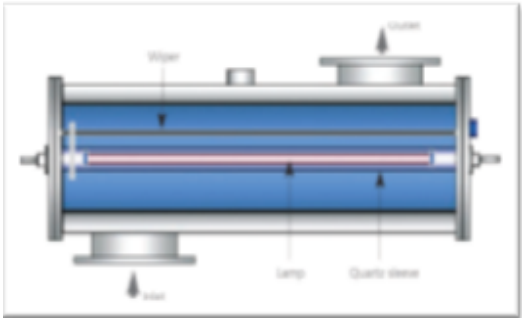


Fig. 4. UV tube and system

A. System supplier

- Is the supplier an established organization that can demonstrate marine water treatment experience?
- Is it likely that long-term maintenance contracts will be honored?
- Will spare parts still be available if the manufacturer ceases trading?

B. System status

- Does the system make use of an active substance?
- If so, has the substance been approved?
- Is the system type-approved?
- Can the manufacturer supply from stock or only to special order?

C. Active substances

- Is the active substance an additive?
- If so, is it readily available?
- Does it present any health risk to crew?
- Is there a risk that the active substance will affect ballast tank coatings? (For this to be established it may be necessary to discuss the matter with the coating manufacturer or require tests to be carried out.)

D. Cost considerations

- What will be the capital outlay per vessel?
- How much will the system cost to install?
- How long will it take to install?
- Is a fleet discount available?
- What are the system's running costs?
- What is the electrical power consumption of the system (minimum/maximum)?
- Replacement/additional filters/pumps?
- Maintenance and spare parts costs?
- Level of cost savings from less sediment and reduced damage to tank coatings?

E. Layout considerations

- How much space is available for installation?
- What are the installed system's dimensions?
- Piping and cabling requirements?
- Is it a modular system?
- Can the system be installed either vertically or horizontally?
- Space needed to store active substances?

F. System suitability

- Is the system designed and tested for prevailing realistic harbour conditions?
- Can the treatment process speed match the vessel's ballasting requirements?
- For scalable systems, how many will be required to match vessel requirements?
- If an active substance is used, will it be affected by salinity or temperature at ports in the vessel's normal area of operation?
- For vessels whose trading pattern involves short voyages, will the treatment process be completed in time for the next port call?
- If a retrofit, are existing pumps sufficient?

G. Operation and maintenance

- What level of training is needed by the crew?
- Is the system fully automatic or is crew intervention required during operation?
- Where substances must be added, is the dosing system fail-safe?
- How frequently do lamps or filters need to be changed?
- If a UV system, does the lamps' warm-up time affect the ship's ballast regime?
- What percentage of lamps must be operational for the system to be effective?
- Can off-the-shelf parts be used?

VIII. TECHNO-COMMERCIAL COMPARISON OF VARIOUS SUPPLIERS IS MENTIONED BELOW.

The comparison of various suppliers is given in below table

- Treatment Technology
- Power
- Pressure Loss
- Inlet Pressure Investment Cost

TABLE IV
THE COMPARISON OF VARIOUS SUPPLIERS

Suppliers	Treatment Technol-ogy	Power (MW)	Foot -print (m2)	Pressure Loss (bar)	Inlet Pres-sure (bar)	Invest ment Cost (Crore)
Optimarin	Filtration and UV	0.6	0.1	0.6	0.3	1.2
Alfa Laval	Filtration and UV	0.6	0.1	1	0.5	0.8
Ocean Saver	Filtration and electro dialysis	1.2	0.6	1.2	0.6	2.4
EcoCholer	Filt and eneration/ injection of ClO2	0.2	0.4	0.6	0.2	2
Techcross	EL and AO	0.2	0.2	0.2	0.2	0.8
Hyundai	Filtration and UV	0.2	0.6	0.2	0.2	0.4
RWO	Filtration, AO	1.2	0.3	1	1	2.4
NK	O3	0.6	0.3	1	0.2	0.8
JFE	Filt and chemical treatment	0.2	0.3	1	0.3	1.6

IX. STEPS IN SELECTING A TREATMENT SYSTEM

Steps in selecting a treatment system are show in Fig. 5.

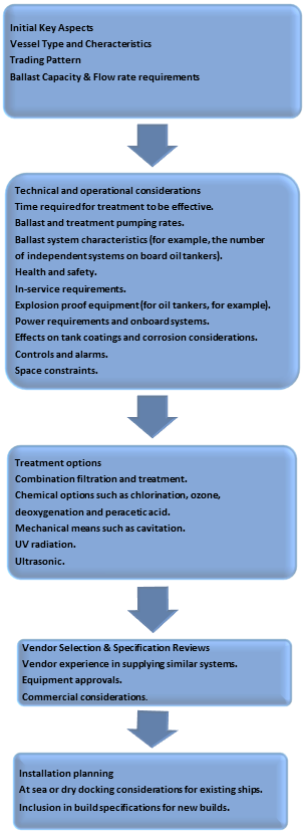


Fig. 5. STEPS IN SELECTING A TREATMENT SYSTEM

X. CONCLUSION

Ballast water management system plays a very important role in controlling the marine pollution.
According to IMO rules & regulations it is important to treat the ballast water so as to avoid the invasion of species.
The large numbers of technologies are available for treating the ballast water. The guidelines & steps for selection of these technologies are mentioned in systematic manner in this paper so that it will help to choose appropriate treatment while treating ballast water

REFERENCES

[1] Armstrong, G. (1997). Ballast system design for flow-through exchange of ballast water, Trans I Mar E. Vol.109, Part 3, 257-269.
[2] Bolch, C. J., Hallegraeff. G. M. (1993). Chemical and physical treatment options to kill toxic dinoflagellate cysts in ships' ballast water. J. Marine Env. Engg. (**??**): 23-29.
[3] Buck, E. H. (2004). Ballast Water Management to Combat Invasive Species, Congressional Research Service, Report to Congress, 8 Apr 2004, Pp.3.
[4] Carlton, J. T. (1995). Ballast water: the ecological roulette of marine biological invasions. ICES Annual Sci Conference, Aaborg, Denmark, Pp. 1–7.
[5] Carlton J. T. (2010). The Impact of Maritime Commerce on Marine Biodiversity. Brown Journal of World Affairs, Vol. XVI, Issue II. Section 138.
[6] Carlton, J. T., D. M. Reid, H. van Leeuwen. (1995). The role of shipping in the introduction of non-indigenous aquatic organisms to the coastal waters of the United States (other than the Great Lakes) and an analysis of control options. National Sea Grant College Program/CT Sea Grant Project R/ES6, Pp.213.



Ashvin Wanzul received his B.E. degree in Mechanical Engineering from Pune University and he is working as a ASSISTANT MANAGER DESIGN (L&T SHIPBUILDING) in Marine Engineering Center, Larsen & Toubro limited at Mumbai, India. He has presented paper in IWCEM 2012 conference. His area of research is PIPING SYSTEM, MACHINERY.



Sameer Mamluskar received his B.E. degree in Mechanical Engineering from Mumbai University and he is working as a ASSISTANT MANAGER DESIGN (L&T SHIPBUILDING) in Marine Engineering Center, Larsen & Toubro limited at Mumbai, India. He has presented paper in IWCEM 2012 conference. His area of research is PIPING SYSTEM, MACHINERY.



Rohit Mathur received his B.Tech degree in Mechanical Engineering from U.P.Tech University and he is working as a ASSISTANT MANAGER DESIGN (L&T SHIPBUILDING) in Marine Engineering Center, Larsen & Toubro limited at Mumbai, India. He has presented paper in IWCEM 2012 conference. His area of research is PIPING SYSTEM, MACHINERY.

TABLE V
ANNEXURE 1-BALLAST WATER TREATMENT PROCESSES

Process	Method	Benefit	Considerations	Comments
Solid-liquid separation				
Filtration	Generally using discs or fixed screens with automatic backwashing	Effective for larger particles and organisms	Maintaining flow with minimum pressure drop requires backwashing. Low membrane permeability means surface filtration of smaller micro-organisms is not practical.	Mesh sizes are proportional to size of organism filtered (e.g., larger organisms such as plankton require mesh between 10 and 50 m)
Hydrocyclone	High velocity centrifugal rotation of water to separate particles	Alternative to filtration and can be more effective	Effective only for larger particles	Effectiveness depends on density of particle & surrounding water, particle size, speed of rotation & time
Coagulation	Optional pre-treatment before separation to aggregate particles to increase their size	Increasing size of particles increases efficiency of filtration or hydrocyclone separation	May require additional tank space to store water which has been treated due to long residence time for process to be effective	Ballasted flocculation uses ancillary powder (e.g., magnetite or sand) to help generate flocs which settle more quickly
Chemical disinfection (oxidising biocides)				
Chlorination	Classed as an oxidising biocide that, when diluted in water, destroys cell walls of micro-organisms	Well established and used in municipal and industrial water disinfection applications	Virtually ineffective against cysts unless concentration of at least 2 mg/l used. May lead to by-products (e.g., chlorinated hydrocarbons/ trihalomethanes	Efficiency of these processes varies according to conditions of the water suchas pH, temperature and type of organism
Electro-chlorination	Creates oxidising solution by employing direct current into water which creates electrolytic reaction	As chlorination	As chlorination. Brine, needed to produce the chlorine, can be stored on board the vessel as feedstock for the system	Upstream pre-treatment of the water is desirable to reduce the 'demand' on the chlorination process
Ozonation	Ozone gas (1–2 mg/l) is bubbled into the water which decomposes and reacts with other chemicals to kill micro-organisms	Especially effective at killing micro-organisms	Not as effective at killing larger organisms. Produces bromate as a by-product. Ozonate generators are required in order to treat large volumes of ballast water. These may be expensive and require sufficient installation space	Systems in which chemicals are added normally need to be neutralised before discharge to avoid environmental damage in the ballast water area of discharge. Most ozone and chlorine systems are neutralised but some are not.
Chlorine dioxide	As chlorination	Effective on all micro-organisms as well as bacteria and other pathogens. It is also effective in high turbidity waters as it does not combine with organics.	Reagents used can be chemically hazardous	Chlorine dioxide has a half-life in the region of 6–12 hours, according to suppliers, but at the concentrations at which it is typically employed it can be safely discharged after a maximum of 24 hours.
Peracetic acid and hydrogen peroxide	As chlorination	Infinitely soluble in water. Produces few harmful by-products & relatively stable.	Reagent is typically dosed at high levels, requires suitable storage facilities and can be relatively expensive	
Chemical disinfection (non-oxidising biocides)				
Menadione/Vitamin K	Menadione is toxic to invertebrates	Natural product often used in catfish farming but produced synthetically for commercial use. Safe to handle.	Treated water will typically require neutralising before discharge	
Physical disinfection				
Ultraviolet (UV) irradiation	Amalgam lamps surrounded by quartz sleeves produce UV light which denatures the micro-organism's DNA and prevents it from reproducing	Well established, used extensively in municipal and industrial water treatment applications. Effective against wide range of micro-organisms	Relies on good UV transmission through the water. Hence, needs clear water and unfouled quartz sleeves to be effective	Can be enhanced by combining with other reagents such as ozone, hydrogen peroxide or titanium dioxide

Spectrogram denoising and extraction of dolphin whistles from noisy underwater environment

Bhagyashri Patil[1], **Rajveer Shastri**[2], **Arnab Das**[3]
[1,2]VPCOE, Baramati, University of Pune, India
[3]MILIT, Pune, India
[1]bhagyashreepatil24@yahoo.com, [2]rajveer_shastri@yahoo.com, [3]arnabdas1972@hotmail.com

***Abstract*—Marine mammal sounds are often analyzed using time-frequency representations which show the non-stationarities of these signals. One commonly used TFR is the spectrogram. The characteristic spectrogram of marine mammal sounds, play a significant role in classification of whistle from noisy recordings, because it helps for monitoring and identification of marine mammals. A major problem in the automated extraction of TF contours from spectrograms is underwater noise. This paper presents an algorithm which is developed for denoising and extraction of dolphin whistles from noisy underwater recordings. A procedure for measuring the accuracy of extracted spectrogram contours is also proposed in this paper.**

***Keywords*—- Underwater noise, TFR, Spectrogram Denoising.**

I. Introduction

Dolphins are known to communicate primarily through the use of frequency modulated pure tones, with whistles being the main area of interest. However, trying to extract these signals effectively and efficiently from underwater recordings has always been difficult because recordings of the many marine mammal vocalizations include combination of signals from echolocation clicks, vocalizations that seem to have an emotional content and other fairly nondescript sounds, snapping shrimp in warm shallow coastal waters (impulsive noise), general background noise and other specific sources of noise.

Marine mammal vocalizations are recorded and studied for a variety of purposes, including research on behavioral and contextual associations, animal detection and localization, and census surveys. Some of these natural signals of interest are non stationary waves well suited for analysis using time-frequency representations (TFRs). In this paper, we focus on the analysis of dolphin vocalizations using spectrograms, which are TFRs based on the short-time Fourier transform (STFT) [1] [2].

Dolphins vocalization can be divided into 3 categories:-
1) Broadband short-duration clicks, called sonar clicks
2) Broadband pulsed sounds, called burst pulses
3) Narrowband frequency-modulated whistles

Dolphins whistle using frequency modulated pure tones in order to communicate with dolphins of the same species. This appears to serve to identify an individual dolphin to its group members since each dolphin develops a signature whistle that is uniquely its own. Dolphins produce broadband clicks sometimes in click trains, during echolocation. [3].

Dolphin whistles are commonly characterized by their time-frequency contours in spectrograms that highlight non stationarities and provide effective visual means of differentiating whistles from other acoustic signals. Features extracted from spectrogram contours of dolphin whistles have been used in many classification studies.

Fig.2 shows database of dolphin sounds. The long term studies of identified individual dolphins allow us to relate the acoustic communication of bottlenose dolphins to the problems posed by their patterns of social behavior. Dolphins can use acoustic features of whistles to recognize different individuals [4] [5] [6].

The paper is organized as follows. Section II describes the methodology i.e. algorithm used for whistles signal extraction. Section III describes results and analysis. Section IV draws the conclusion from results.

II. Methodology

Fig.1 shows the Proposed algorithm for whistle segmantation. Which consist of spectrogram denoising, harmonic suppression, spectrogram segmentation and whistle tracing.

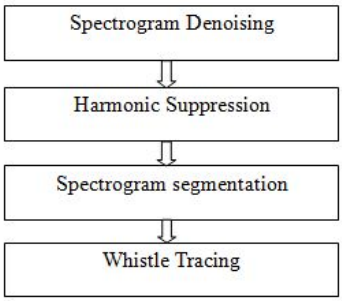


Fig. 1. Proposed algorithm for whistle segmentation

A spectrogram is obtained by converting time domain signal to the frequency domain signal. This transformation is done by using STFT. Generally, the STFT of a discrete-time function x[n] with respect to the window function w[n] calculated at the location w[m] in the frequency domain is defined as

$$X[w, m] = \sum_{n=-\infty}^{\infty} x[n]w[n-m]\exp(-jwn)$$

The columns of the matrix X[m] contain the time localized frequency content of the discrete signal x[n]. The values of matrix X are generally complex, and it is necessary to log-compress the absolute value of this transform for visual inspection due to the large dynamic range. This log compressed gray-level two-dimensional (2D) image is called the spectrogram of x[n], and is denoted by X [m].

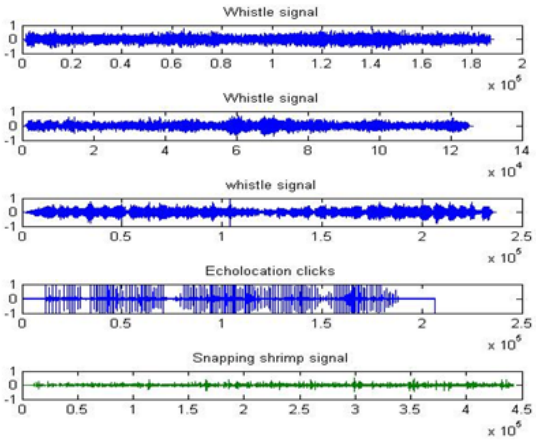


Fig. 2. Database of dolphin sound signals

A. Spectrogram denoising

While detecting dolphin whistle signals all other acoustic sources are considered as noise sources; hence all other spectrograms that are obtained during analysis are also considered as noise. The main objective of denoising a spectrogram is to extract the required dolphin whistle contours by ignoring all other noise sources. This paper presents different image processing techniques applied on spectrogram to complete this goal. Firstly the preprocessing is done. In the preprocessing step the low-frequency noises such as shipping noise are removed by high-pass filtering with a cut-off frequency set slightly below the lowest frequency at which dolphin whistles are expected (1.5 kHz). However, this method can also be used for denoising other types of signals, such as the low frequency noises of different fish species in underwater environment, the area of interest is modified accordingly. In the latter case, the low pass filter can also be applied according to need [7].

B. Harmonic suppression

Dolphin Whistles contain harmonics similar in shape with the original whistle contour but slightly shift in original frequency. The frequency of a harmonic of the whistle is an integer multiple of the original frequency of whistle contour, the goal is to completely remove the shift i.e. harmonic from the original whistle contour. This step should be used according to situation because when recorded whistles are taken for the analysis it is not necessary that all whistle recordings have strong harmonics. One drawback is that when more no of whistle contours overlap at a time the frequency variation of whistle intersects the harmonic of another whistle contour [7] [8].

C. Spectrogram segmentation

After the spectrogram denoising and harmonic suppression there is need to remove unwanted spectral patterns, Image segmentation techniques help to extract whistle contours. This paper presents the main goal that is to choose a simple and appropriate method to extract dolphin whistle contours from noisy underwater environment. To fulfill the objective a 3 stage segmentation algorithm is proposed. Different steps applied in the algorithm are starting with thresholding. Thresholding requires only one parameter to be specified. By selecting required threshold, this step is implemented. The care should be taken while selecting the threshold because intensity values of ambient noise can change from one signal to another because the spectrograms of recordings are taken from different sections of the same recording. The next step is morphological image processing on the spectrograms. This processing is applied on the output of thresholding. In the morphological image processing techniques closing followed by opening is done. While analyzing the results there may be misclassifying of start and ends of whistle contours. This care should be taken while analyzing contours [9] [10].

D. Whistle tracing

The final goal of proposed algorithm is to extract the dolphin whistle contour of the fundamental frequency variation of a whistle contour. For the visual inspection of whistle contours, the trace of extracted contour should be drawn on the spectrogram. Fig.6 shows the results of whistle tracing in which the traces of whistle contours are clearly shown. As compared to spectrogram denoising and spectrogram segmentation, the whistle tracing is simplest step as it does not contain algorithm. It only traces the resultant dolphin whistle contours [11] [12] [13].

After tracing of whistles user is able to understand that what the exactly whistle contour is. Due to filtering the high frequency noises are filtered and due to segmentation the exact trace of whistles is obtained.

III. Results and Discussions

Fig.3,4 and 5 shows the results of whistle contour extraction algorithm resectively. First the spectrogram denoising of whistle signal is done using high pass filttering and after that harmonics are suppressed.Spectrogram segmentation and tracing is done using image processing techniques.

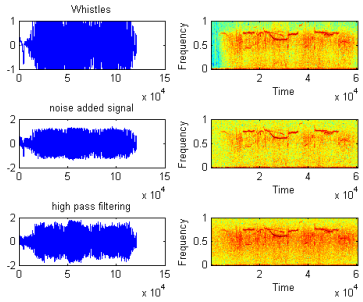


Fig. 3. Spetrogram denoising

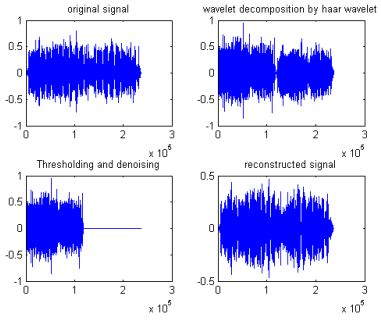


Fig. 4. Harmonic suppression

IV. Conclusion

The image processing based algorithm to extract dolphin whistles from underwater noisy environment is discussed in this paper. The algorithm consists of different steps applied on spectrograms. The algorithm is implemented using MATLAB environment.

References

[1] Taylor, P.J. Seekings,"Wavelet denoising with independent component analysis for the segmentation of dolphin whistles in a noisy underwater environment", IEEE jornal 2006.

[2] G. Latha and S. Ramji, "Identification and Analysis of Dolphin Signatures from Ocean Ambient Noise Measurements",. IEEE Journal of Oceanic Engineering, vol. 31, no. 2, 2006.

[3] DRC-Dolphin acoustics. 2004 at http://dolphins.org/Learn/1mm-acou.htm.

[4] Website-http://www.dosits.org/science/soundsinthesea

[5] Asitha Mallawaarachchi, S.H Ong, Mandar Chitre and Elizabeth Taylor, "A method for tracing dolphin whistles",Dolphins,2006.

[6] Asitha mallawaarachchi, "Spectrogram denoising for the automated Extraction of dolphin whistle contours".

[7] H. Carter Esch, Laela S. Sayigh, Randall S.Wel, Quantifying parameters of bottlenose dolphin signature whistles, Marine Mammal Science, 25(4): (October 2009) by the Society for Marine Mammalogy.

[8] J. R. Buck and P. L. Tyack,"A quantitative measure of similarity for tursiops truncates signature whistles", *IEEE- Int. conf. Emerging Trends in Electrical and Computer Technology (ICETECT)*,The Journal of the Acoustical Society of America, vol. 94, no. 5, pp. 2497.

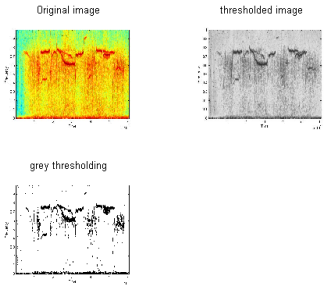


Fig. 5. Segmentation and tracing

[9] A thesis Spectrogram denoising for the automated extraction of dolphin whistle contours by Asitha Mallawaarachchi

[10] C. Sturtivant and S. Datta, "Techniques to isolate dolphin whistles and other tonal sounds from background noise", Acoust. Lett. 18, 189193,1995.

[11] C. Sturtivant and S. Datta, "The isolation from background noise and characterisation of bottlenose dolphin (tursiops truncates) whistles", J. Acoust. Soc . India 23, 199205, 1995.

[12] C. Tomasi and R. Manduchi, "Bilateral filtering for gray and color images",in Proceedings of the IEEE International Conference on Computer Vision, Bombay, India, Jan. 47, 1998.

[13] F. Yan, H. Zhang, and C. R. Kube, "A multistage adaptive thresholding method",Pattern Recogn. Lett. 26, 11831191 (2005).



Bhagyashri Patil received the B.E. Electronics and Telecommunication in 2012 from Solapur University, Solapur and she is pursuing M.E. Degree in Electronics with specialization in Digital System from Vidya Pratishthan's college of Engineering, Baramati, India. She has Published paper in International Conference held at Adhiparasakthi college of engineering,melmaruvathur,Tamilnadu. Her area of research is Underwater Signal Processing.



Rajveer Shastri received the B.E. Electronics and Telecommunication in 2000 from Dr. Babasaheb Ambedkar Marathawada University, Aurangabad, the M.E. Degree in Electronics with specialization in Computer Technology from Shri Guru Govind Singh Engineering and Technology, Nanded, He is now pursuing Ph.D. degree, in Electronics from Swami Ramanand Tirth Marathawada Univeristy Nanded. He worked as lecturer from 2002 to 2008 and from 2008 to till date he is working as assistant professor in Vidya Pratishthan's college of Engineering, Baramati, India. He is life member of IEEE, ISTE and IETE. He has published 10 international journal, conference papers and 5 national conference papers.



Arnab Das received B. Tech degree in Electrical Engineering from Naval College of Engineering, Lonavala, India in 1995. He obtained M. Tech degree in Radar and Communication with specialization in Underwater Signal Processing in 2002and PhD degree in 2009 from Indian Institute of Technology, Delhi, India. He was commissioned into the Indian Navy in 1994. He worked as Project Officer at CARE, IIT Delhi for R & D in Underwater Signal processing and hardware design in 2003-2007. Currently he is instructor at MILIT Pune, India. His research interests are Underwater Passive Surveillance, Underwater Communication and Pattern recognition.

Super Eco Ship using Green Technology for Energy Conservation

Sanjay Dabadgaonkar[1], **Asim Kumar Sen**[2]
[1] Sr. Associate Prof. (Electrical & Electronics
[2]Principal, St. Francis Institute of Technology,Mount Poinsur, Borivali (W),Mumbai 400103
[1]comsanjayd@tmi.tolani.edu
[2]asim_sen@linuxmail.org

***Abstract*—The importance of shipping industry is very much traced for international transportation. It is generally acknowledged that more than 90 percent of international trade is carried by sea. Throughout the last century the shipping industry has seen a general trend of increases in total trade volume. Advances in technology have also made shipping an increasingly efficient and swift method of transport. The shipping industry is facing ever greater challenges, especially regarding energy. Other than economical issues there are some environmental issues which are resulted due to burning of more fuel. In recent years, sustainability in a climate and an environmental perspective has become an issue of highest priority. It is estimated that 4 % of the global CO2, SOx and NOx emissions come from international shipping. The world wide increase in the price of oil has especially affected the shipping industry. Because the burning of diesel fuel ultimately generates the energy required onboard ship. Each kilo-watt of energy saved onboard has a direct effect on the consumption of diesel and the total operating cost. Therefore ship operators will put higher pressure on ship owners to obtain fuel efficient ships. These in turn will put pressure on ship yards to supply fuel efficient ships. As a result, we expect to see an improvement in the fuel consumption on ships. Shipping installations having higher fuel efficiency in all operational stages will be increasingly favored and will presumably have great potential for future growth. Parts of these requirements can easily be met by controlling the speed of electric motors used for centrifugal pumps onboard ship using variable frequency drives. This VFD uses Space vector pulse width modulation to generate three phase AC with fewer harmonics for controlling speed of three phase Induction Motor and Variable Flow output from CF Pump for ballast operation.**

***Index Terms*—Green Technology, Variable Frequency Drive,SVPWM Control, Energy Conservation.**

I. Introduction

Advances in technology have made shipping an increasingly efficient and swift method of transport. The amount of goods actually loaded aboard ships has reached up to 10 billion tons. Like all industrial sectors, shipping industry has also witnessed the worst global recession in over seven decades and the sharpest decline in the volume of global merchandise trade. The improvement of energy efficiency has become most important in shipping industry to achieve excellence in cost competitiveness. Energy cost is one of the major component not only necessities the installation of energy efficient technology but also inculcate energy efficient practices and methods to be used for eco-friendly sailing. Here we have developed a latest technique using advanced technology for sustainable energy conservation onboard ship. Now a days energy is a critical input for production & consumption activities in an economy. In spite of the increase in prices of electricity, consumption has also gone up. Substantial saving of electrical energy can be achieved by using methods such Variable speed drive. parOther than economical issues there are some environmental issues which are resulted due to burning of more fuel. In recent years, sustainability in a climate and an environmental perspective has become an issue of highest priority. As almost 90 % of the world trade is carried by ship. It is estimated that 4 % of the global CO2, Sox and Nox emissions come from international shipping. The world wide increase in the price of oil has especially affected the shipping industry. Because the burning of diesel fuel ultimately generates the energy required onboard ship. Each kilo-watt of energy saved onboard has a direct effect on the consumption of diesel and the total operating cost. Therefore ship operators will put higher pressure on ship owners to obtain fuel efficient ships. These in turn will put pressure on ship yards to supply fuel efficient ships. As a result, we expect to see an improvement in the fuel consumption on ships.

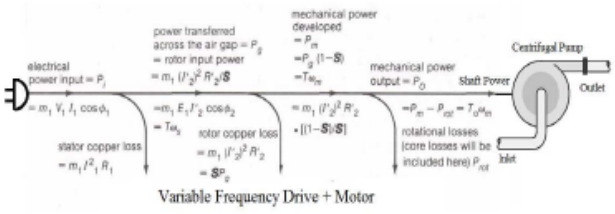


Fig. 1. Transfer of Power from VFD to Pump

On board ships, there are a great number of pumps serving multiple purposes. The vast majority of pumps used today are the centrifugal type. These pumps are used for water cooling systems, cargo and ballast operation onboard ship. Cooling water pumps are especially dimensioned to have their rated capacity at a water temperature of $30Cto40C$. When operating in cooler seas, this means that unnecessary high volumes of cooling water are pumped through the systems, resulting in high cost of energy and wear of the mechanical equipment. Vessels used for transporting fruit require very

stable temperature. In passing through climatic zones with changing temperature conditions, a Marine frequency converter controlled cooling system will ensure constant storage room temperature. On board passenger and cruise vessels, considerable energy is used for ventilation and air conditioning. Day cycles and changing environmental temperatures mean the motor power requirement for systems of this kind will undergo large variations. With temperature control, only the required motor power will be used to maintain the desired temperature.

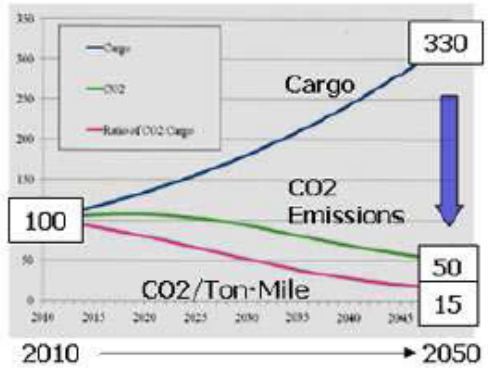


Fig. 2. Carbon emission expected till 2050

For supply vessels, the ballast pumps, cargo pumps for fuel, brine and mud, etc. are installed with speed regulation using Marine frequency converters. The use of Marine frequency converters in regulating engine room temperature has also proved to provide great savings in energy. The shipping industry is facing ever greater challenges, especially regarding energy saving and the environment. Lurking in the background are political shadows like CO2 duties and dire predictions concerning the cost of fuel in ten years time. Authorities and owners are consequently focusing more and more on shipping concepts involving less environmental risk and energy saving. Shipping installations having higher fuel efficiency in all operational stages will be increasingly favored and will presumably have great potential for future growth. Additionally, the requirements of reliability, redundancy, maneuverability and concerning long maintenance intervals and short service response time are gradually becoming stricter.

Competence is a key factor in smooth sailing. Parts of these requirements can easily be met by controlling the speed of electric motors. The Centrifugal pumps used on board ship for ballast operation, cargo operation, Sea water cooling operation, savage operation etc are major consumers of electrical power. In the past 10 years, variable speed control for fans, pumps, chillers and HVAC systems has become an affordable way to save energy, thanks to advances in microelectronics and control technology.

Variable frequency drives (VFDs) are gradually being recognized by maritime industries as one of the most effective tools for energy savings. Significant energy benefit can be realized from VFDs driven sea water cooling systems because the ambient sea water temperature varies greatly as ships travel through different sea areas. This research study of

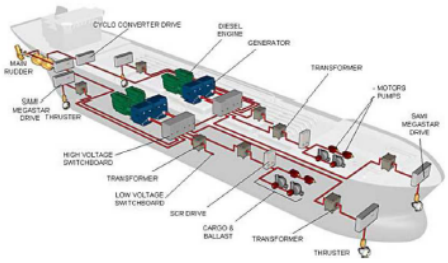


Fig. 3. Ship layout with motors and pump for ballast operation

environmental issues and energy management is aimed at reducing energy consumption and pollution onboard ship and at sea.

II. Ballast Operation

Ballast is any material used to weight and/or balance an object. Ships have carried solid ballast, in the form of rocks, sand or metal, for thousands of years. Since modern times, ships have used water as ballast. Shipping moves over 80 % of the worlds commodities and transfers approximately 3 to 5 billion tones of ballast water internationally each year. Ballast water is absolutely essential to the safe and efficient operation of modern shipping, providing balance and stability to unladen ships. It is much easier to load on and off a ship, and is therefore more efficient and economical than solid ballast. When a ship is empty of cargo, it fills with ballast water. When it Loads cargo, the ballast water is discharged.

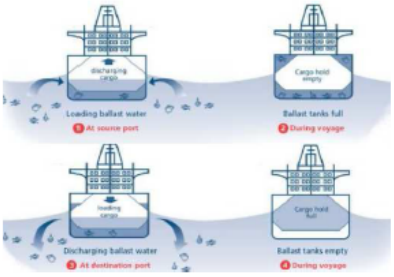


Fig. 4. Cross section of ship showing ballast water cycle

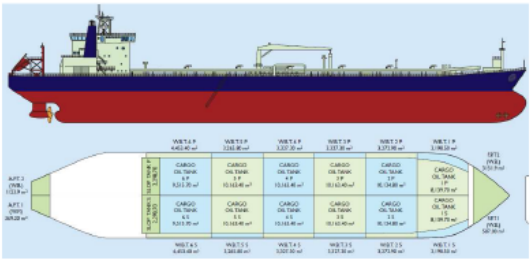


Fig. 5. Arrangement of ballast tank onboard ship

The centrifugal pumps are used onboard ship for loading and unloading ballast water. These pumps are traditionally

VESSEL TYPE	DWT	BALLAST CONDITION NORMAL (tonnes)	% of DWT	HEAVY (tonnes)	% of DWT
Bulk carrier	250,000	75,000	30	113,000	45
Bulk carrier	150,000	45,000	30	67,000	45
Bulk carrier	70,000	25,000	36	40,000	57
Bulk carrier	35,000	10,000	30	17,000	49
Tanker	100,000	40,000	40	45,000	45
Tanker	40,000	12,000	30	15,000	38
Container	40,000	12,000	30	15,000	38
Container	15,000	5,000	30	n/a	
General cargo	17,000	6,000	35	n/a	
General cargo	8,000	3,000	38	n/a	
Passenger/RORO	3,000	1,000	33	n/a	

Fig. 6. TABLE I. Ballast water capacities for different types of ships

Ballast needs	Vessel types	Typical pumping rates (m3/h)
Ballast replaces cargo Ballast required in large quantities, primarily for return voyage.	Dry bulk carriers Ore carriers Tankers Liquefied gas carriers Oil bulk ore carriers	5,000–10,000 10,000 5,000–20,000 5,000–10,000 10,000–15,000
Ballast for vessel control Ballast required in almost all loading conditions to control stability, trim, and heel.	Container ships Ferries General cargo vessels Passenger vessels Roll-on, roll-off vessels Fishing vessels Fish factory vessels Military vessels	1,000–2,000 200–500 1,000–2,000 200–500 1,000–2,000 50 500 50–100

Fig. 7. TABLE II. Typical pumping requirement for ballast water management

controlled by throttling valve control, hydraulic and pneumatic control systems, bypass control systems etc. These systems have few limitations and disadvantages. Therefore to improve the overall efficiency of ballast operation, we need to use advanced technology that will reduce fuel consumption, emission of CO2, NOx, Sox, save energy. This can be done by using Variable frequency drive and three phase induction motor for controlling centrifugal pump onboard ship. As suggested power electronic technology reduces the emission of CO2, NOx, Sox and fuel consumption, we call this as ecofriendly system and green technology used for ballast water management.

III. Variable Frequency Drive

Induction motors, the workhorses of shipping industry [1], rotate at a fixed speed that is determined by the frequency of the supply voltage. Alternating current applied to the stator windings produces a magnetic field that rotates at synchronous speed. This speed may be calculated by dividing line frequency by the number of magnetic pole pairs in the motor winding. A four-pole motor, for example, has two pole pairs, and therefore the magnetic field will rotate 60 Hz / 2 = 30 revolutions per second, or 1800 rpm. The rotor of an induction motor will attempt to follow this rotating magnetic field, and, under load, the rotor speed "slips" slightly behind the rotating field. This small slip speed generates an induced current, and the resulting magnetic field in the rotor produces torque. Since an induction motor rotates near synchronous speed, the most effective and energy-efficient way to change the motor speed is to change the frequency of the applied voltage. VFDs convert the fixed-frequency supply voltage to a continuously variable frequency, thereby allowing adjustable motor speed. A VFD converts 60 Hz power, for example, to a new frequency in two stages: the rectifier stage and the inverter stage. The conversion process incorporates four functions **Rectifier stage:** A full-wave, solid-state rectifier converts three-phase 60 Hz power from a standard 208, 460, 575 or higher utility supply to either fixed or adjustable DC voltage. **Breaking chopper:** The DC output of rectifier is controlled by chopper i.e. DC to DC converter. This output DC acts as input to three phase Inverter. **Inverter stage:** IGBT/IGCT power transistors or thyristors switches the rectified DC on and off, and produce AC current and voltage waveform at the desired new frequency. The amount of distortion depends on the design of the inverter and filter. The output of inverter is variable voltage variable frequency with minimum harmonics. **Control system:** It models a direct torque control (DTC) induction motor drive with space vector pulse width modulation. The particularity of this modified version is that the DTC is no longer based on hysteresis regulation that implies switching at variable frequency but on a fixed frequency PMW inverter. An electronic circuit receives feedback information from the driven motor and adjusts the output voltage or frequency to the selected values. Usually the output voltage is regulated to produce a constant ratio of voltage to frequency (V per Hz).

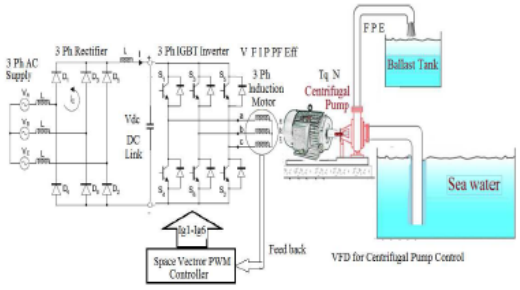


Fig. 8. Ballast water management using VFD

Controllers may incorporate many complex control functions. Inverters use Space Vector Pulse Width Modulation (SVPWM) because the output current waveform closely approximates a sine wave. IGBT switches DC voltage at high speed, producing a series of short-duration pulses of constant amplitude. Output voltage is varied by changing the width and polarity of the switched pulses. Output frequency is adjusted by changing the switching cycle time. The resulting current in an inductive motor simulates a sine wave of the desired output frequency. The high-speed switching of a SVPWM inverter results in less waveform distortion and, therefore, lowers harmonic losses. Low voltage variable speed drives offer powerful and accurate performance for any application in powers of 0.55 up to 5600 kW [7].

Induction motors: Three Phases high efficiency induction motors offers a comprehensive range up to 18000 kW are reliable. These machines are commonly used onboard ship as prime movers for centrifugal pumps. IM consume about 35 % of the total energy consumption. The simplicity of these machines allows them to be perfectly engineered according to requirements for application areas that include special and hazardous environments.

Centrifugal Pump: The load for the IM is variable torque

type centrifugal pump. In the simulated model 500 HP Pump with maximum of 3000 m3 per hr flow rate is controlled using SVPWM controlled Variable Speed Drive. Thus we can adjust flow rate of ballast water system using VFD and reduce the consumption of energy and fuel.

IV. Affinity laws

The affinity laws for specific pumps are, the volume (Flow) is proportional to speed. The Pressure (head) is proportional to square of the speed and the power absorbed is proportional to cube of the speed [2].

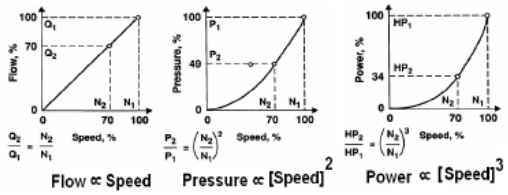


Fig. 9. Affinity laws for pump

The affinity curve shows that at 100 % rated speed and a fully loaded pump the horsepower consumption is maximum. If a 30% reduction in speed is allowable by the system process requirements then the pump may be driven at 70% of the maximum motor RPM with a nominal power consumption of 34.0% of the full load, full speed consumption. i.e. Power consumed = (0.7)3 = 0.343 = 34.3%. For 60 Hz / 2 Pole IM, If we reduce 1 Hz frequency then Speed will reduce by 60 RPM i.e. 10% reduction in speed can reduce power consumption up to .9x.9x.9=72.9 % i.e. Saving = 27.1% power. Thus VFD is useful in energy saving because it reduces the motor speed as demand decreases and saves fuel and energy. The pump and driving motor must then develop enough torque to actually move the fluid[3].

V. Modeling of Induction Motor

A variable frequency drive (VFD) is used to change the supply frequency. As a result, motor speed changes. For various frequencies; speed, output torque, power factor, efficiency are studied. Graphs are generated to describe the behavior. An induction motor can be considered like a transformer with an air-gap. The equivalent circuit can be used to form a mathematical model. In this simulation, the motor of following specifications is studied. A three phase Y connected 220-V (line to line voltage) 7.5 kW, 60 Hz, 6 pole induction motor has the following values in /phase referred to the stator. $r1 = 0.294, r2 = 0.144, x1 = 0.503, x2 = 0.209, Xm = 13.25$. The total friction, windage and core losses may be assumed as 6.5$ of the power input at any given load. At 2$ slip (loading condition), the motor offers its best performance [6].

It is assumed that the motor is tested for No Load and Blocked rotor tests at 60 Hz, because the motor is designed for this frequency and rated line voltage 220V. We are interested in predicting its behavior at various supply frequencies from a variable frequency drive. The range of frequencies will be 30 Hz to 90 Hz. For simplicity, we assume that the wave shape

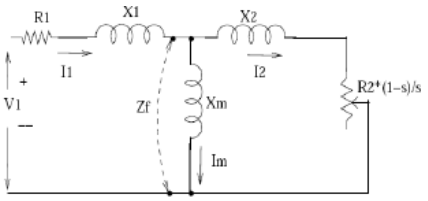


Fig. 10. Modified equivalent IM Model

is a pure sinusoid. The user can select the loading condition (no load to overload) by mentioning the slip in the range 0 to 0.1. The best performance is obtained at $slip = 0.02$. From the No load and Blocked rotor tests, the user finds X1, X2, R2 and Xm. R1 can be measured using an ohmmeter. The reactance values are for 60 Hz. From the reactance we can find the inductances L1, L2, M. This helps to calculate the values of reactance at different frequencies. Following equations and concepts play vital role in the script. The Total power transferred across the air gap from the stator is,

$$p_{gap} = 3 * I_1^1 * \frac{R1}{S} p_{rotor} = 3 * I_2^2 * R2 = S * p_{gap} \quad (1)$$

$$= 3 * I_2^2 * R2 = S * p_{gap} \quad (2)$$

Therefore the mechanical power output is given by $p_{mech} = p_{gap} - p_{rotor}$

$$= 3 * I_2^2 * R2 = S * p_{gap} \quad (3)$$
$$= 3 * I_2^2 * \frac{R_2}{S} - 3 * I_2^2 * R2$$
$$= 3 * I_2^2 * R_2 * \frac{l-S}{S} = (l - S) * p_{gap}$$

and the mechanical torque is given by

$$T_{mech} = \frac{P_{mech}}{\omega_m} = \frac{P_{gap}}{\omega_s 2}$$

$$= 3 * I_2 * \frac{R_2}{S * \omega_s} \quad (4)$$

i.e the shaft power and shaft torque is given by

$$P_{shaft} = P_{mech} - P_{rotor} \quad (5)$$

$$T_{shaft} = \frac{P_{shaft}}{\omega_m} = P_{mech} - P_{rotor} \quad (6)$$

i.e. the stator input power (Pin) is given by

$$P_{in} = 3 * []V_1 * I_1] \quad (7)$$

and Efficiency () is given by

$$\eta = \frac{P_{shaft}}{P_{in}} \quad (8)$$

All the above parameters are fixed except the slip. We can change the slip value within the range 0 to 0.1 (No load to overload) and see the behavior of the motor.

VI. Simulation using MATALB

It models a direct torque control (DTC) induction motor drive with a braking chopper for a 200HP AC motor. The induction motor is fed by a SVPWM voltage source inverter using IGBT. The speed control loop uses a proportional-integral controller to produce the flux and torque references for the DTC block. The DTC block computes the motor torque and flux estimates and compares them to their respective reference. The comparators outputs are then used by an optimal switching table which generates the inverter switching pulses. Motor current, speed, and torque signals are available at the output. After the simulation, we can observe the motor stator current, the rotor speed, the electromagnetic torque and the DC bus voltage on the scope. The speed set point and the torque set point are also shown.

At time t = 0 s, the speed set point is 500 rpm. Observe that the speed follows precisely the acceleration ramp. At t = 0.5 s, the full load torque is applied to the motor shaft while the motor speed is still ramping to its final value. This force the electromagnetic torque to increase to the user-defined maximum value 1200 N. m and then to stabilize at 820 N. m once the speed ramping is completed and the motor has reached 500 rpm. At t = 1 s, the speed set point is changed to 0 rpm. The speed decreases down to 0 rpm by following precisely the deceleration ramp even though the mechanical load is inverted abruptly, passing from 792 N. m to - 792 N. m, at t = 1.5 s. Shortly after, the motor speed stabilizes at 0 rpm. Finally, note how well the DC bus voltage is regulated during the whole simulation period. The power system has been discretised with a 2 us time step. The speed controller uses a 140 us sample and the DTC controller uses a 20 us sample time in order to simulate a microcontroller control device. In order to control centrifugal pump using VFD controlled three phase IM, pump system is also modeled and simulated for 3000m3/Hr flow rate [4].

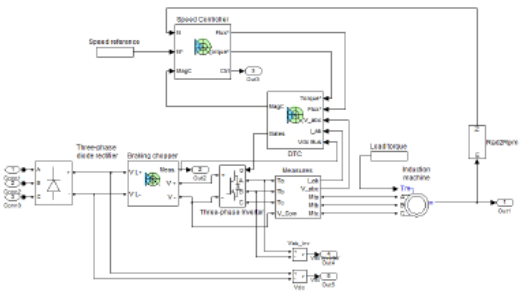


Fig. 11. DTC based VFD control for three phase IM.

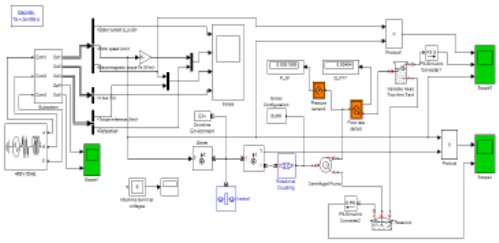


Fig. 12. VFD controlled centrifugal pump

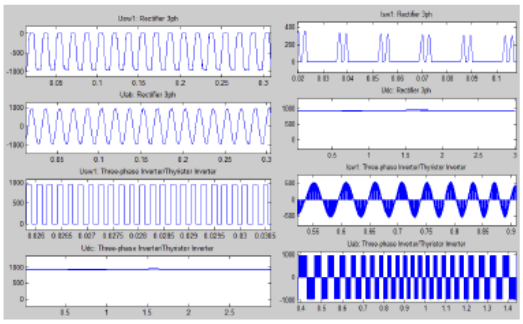


Fig. 13. Rectifier I/O and Inverter I/O waveforms

VII. Experimentation

The VFD controlled centrifugal pump with 400 HP power, 50 Hz, 380 V AC nominal voltage, 2 poles and 2900 RPM nominal speed squirrel cage three phase induction motor of 500 HP is used for validation of results. VFD efficiency is 98 %, IM efficiency is 90 % and Pump efficiency is 80%. Maximum head can be 30 meter. Pressure sensor is a 0-10 Bar ranged pressure switch in constant speed control strategy and an analog piezoelectric pressure transmitter with 24 V DC feed voltage and 4-20 mA output current in variable speed control strategy.

Flow	%	Throttled	VFD Static head in feet			
GPM	Flow	Valve	0 Ft	60 Ft	140 ft	210 Ft
170	50	19.7	3.2	6.35	10.44	14.08
204	60	20.95	5.46	8.7	12.7	16.02
238	70	22.21	8.68	11.75	15.42	18.3
272	80	23.47	13.06	15.58	18.61	20.9
306	90	24.73	18.83	20.31	22.31	23.77
340	100	25.99	26.19	26.02	26.52	26.89

Sr. No.	0 Ft	60 Ft	140 Ft	210 Ft
1	83.75635	67.7665	47.00508	28.52792
2	73.93795	58.47255	39.37947	23.53222
3	60.91851	47.0959	30.57181	17.60468
4	44.3545	33.61738	20.70729	10.95015
5	23.85766	17.87303	9.785685	3.881925
6	-0.76953	-0.11543	-2.03925	-3.46287

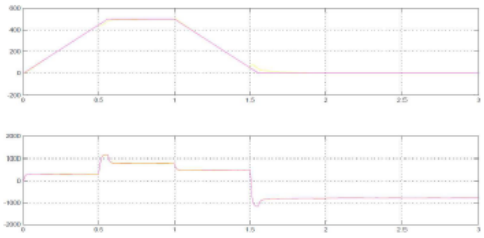


Fig. 14. Speed and torque response

Sr. No.	Cose saved /ytar @ 0.06 $ for 8 Hrs/250 days			
Head in Feet	0 Ft	60 Ft	140 Ft	210 Ft
1	1485	1201.5	833.4	505.8
2	1394.1	1102.5	742.5	443.7
3	1217.7	941.4	611.1	351.9
4	936.9	710.1	437.4	231.3
5	531	397.8	217.8	86.4
6	-18	-2.7	-47.7	-81

SPEED	VRLUME OO FLOW	I/P HP
100%	100%	100%
90%	90%	73%
80%	80%	51%
70%	70%	34%
60%	60%	22%
50%	50%	13%
40%	40%	6%
30%	30%	3%

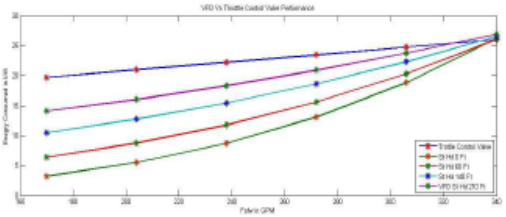


Fig. 15. Energy consumed using VFD and Throttling Valve.

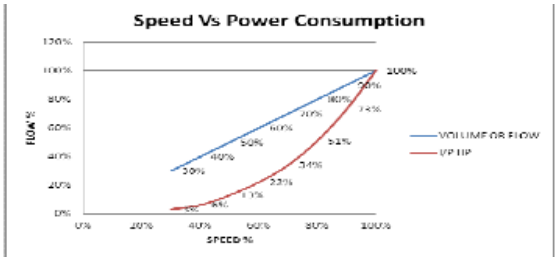


Fig. 16. Power consumption at various speed

VIII. Conclusion

A variable speed drive regulates the speed of the motor, and in turn the speed of the pump, by controlling the energy that goes into the motor, rather than restricting the flow of a process running constantly at full speed. A variable speed drive can save over 50 % of the energy. This is possible as it controls the energy at source, only using as much as is necessary to run the motor with the required speed and torque. Therefore variable speed drives are gaining much more importance for controlling centrifugal pumps and to conserve energy onboard ship [5]. Use of VFD improves process variability, VFD is faster, more linear and is invulnerable to backlash, reduced energy consumption, the pump supplies only enough energy to overcome the system head, the energy wasted across the control valve is eliminated, reduced maintenance costs, since the pump will operate close to the BEP over the entire operating range, reliability and efficiency are complementary. VFD improves the efficiency of motor-driven equipment by matching speed to changing load requirements and continuous process control over a wide range of speeds. In addition to saving of energy, it reduces consumption of CO/CO2, Sox and NOx etc. Therefore this eco-friendly power electronics technology act as green technology to protects environment in around at sea

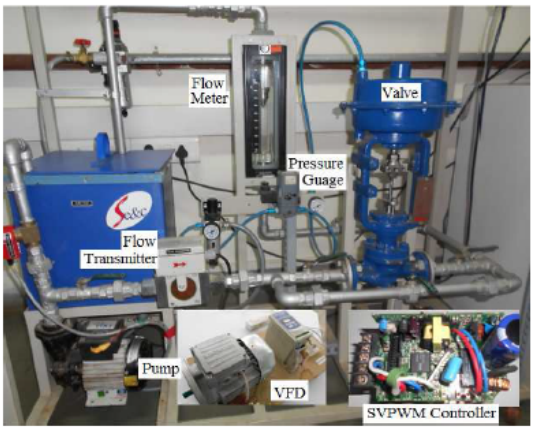


Fig. 17. Experimental setup for controlling pump using VFD

IX. Acknowledgment

I am very much thankful to Management of Tolani Maritime Institute, Induri, Pune and my colleagues for support extended to carry out this research activity.

References

[1] Transactions on Industry Applications, Vol. 1A-20, No. 1 January/February 1984, pp 23-31.
[2] Joseph R. Pottebaum, Optimal Characteristics of a Variable- Frequency, Centrifugal Pump Motor Drive, IEEE
[3] Ron Carlson, The Correct Method of Calculating Energy Savings to Justify Adjustable-Frequency Drives on Pumps, IEEE Transactions on Industry Applications, Vol. 36, No. 6 November/December 2000, pp 1725-1733.
[4] Exclusive Energy Savings: Centrifugal Pumps and Variable Speed Drives by Copyright 2002 Francis J. Martino
[5] Payback Analysis for variable frequency drives by Copyright 2003 Francis J. Martino
[6] P. C. Krause, Analysis of Electric Machinery, McGraw-Hill, 1986.
[7] Malcolm Barnes, Practical Variable Speed Drives and Power electronics.



Prof. Sanjay Dabadgaonkar Presently working as Senior Associate Professor, Department of Electrical and Electronics at Tolani Maritime Institute, Induri, Pune. Total Teaching experience of about 24 years. Worked as a Head of Dept. in Electronics and Telecommunication at College of Engineering under Dr. B A M U Auranbabad. Published 8 Papers in International / National Journals and Presented more than 50 papers in Inter-national / National Conferences. Attended several workshops, honored with a best teaching faculty award, Member of University LIC and Chairman / Head during NBA & AICTE Visit in COEO, Organised Two National Level conferences. Fellow member of IETE, ISTE, IE. Research in Simulation of Power Electronic systems is in progress.



Dr. ASIM KUMAR SEN Presently Working as a Principal and Professor, Saint Francis Institute of Technology, Borivali, Mumbai. Completed Ph.D. In 1995 from IIT Kharagpur. Fellow IE (India), LM of International Society for Reliability Engineers (India Chapter), LMISTE, Fellow of IETE, Honorary Council Member of Flash India Management Senate, Mumbai, Referee of the Journals published by A.M.S.E, France, Chartered Engineer, LM of Indian Nuclear Society, Experienced faculty in the field of Electronics, Instrumentation and control, Digital Signal Processing, Industrial Engineering and Management. Having administrative experience as a Principal for more than 12 years. More than 60 Publications in International / National Journals and Conference Proceedings. Guided several Projects and Ph. D. Thesis and in the panel of Supervisor for various Universities for guiding research related activities.

Application of Solar (Photo Voltaic) Cells for Power Generation onboard Naval Ships

Captain(IN) Naresh Chhabra[1]
Head of Faculty (Electronics and Communication Engineering)
Indian Naval Academy Ezhimala
narchhabra@hotmail.com

***Abstract*—Power generation capacity of a conventional warship is based on its weapon package and is done using conventional fuels. Power generated is mainly used for lighting, ventilation systems etc.**

A typical destroyer which has gas turbine generators eats up to 12 tons of fossil fuel to generate 800MW in a day. If we are able to reduce this consumption and start producing electricity using photovoltaic cell onboard ships we will save not only fuel but also save our exchequer pocket.

This paper aims to study a ship and where all, non conventional source of power can be used-its pros and cons, its effectiveness.

***Index Terms*—Electrocardiograph, Feature extraction, Discrete Wavelet Transform(DWT).**

I. Introduction

Power generation capacity of a ship, be it a merchant vessel or a warship, is governed by its own need and the role it plays. In merchant vessel the power generation capacity is based on the total load of domestic supplies and the cranes/davits etc whereas in the case of a warship it is based on its weapon package. Whatever may be the role, today the source of power generation is through gas turbines, steam turbines and diesel operated generators which implies that we use fossil fuels for the power generation. With the technological developments in the field of non conventional sources of power/energy, it is imperative for us that we start thinking about their usage onboard ships now because one day or the other we will have to tread the path which is less traversed. In the succeeding paragraphs the photovoltaic cell/module (solar cell) will be discussed in terms of its advantages, disadvantages and its applications onboard. Considering the financial aspects related to the solar technology, even if we make a miniscule progress, it will be worth the effort because it will make our nation less dependent on the fossil fuel.

NON-CONVENTIONAL SOURCES

The cost of conventional fossil fuel being used onboard ships is exorbitant. This can be gauged from the fact that a gas turbine generator eats up 12 tons of fossil fuel to generate 800MW in a day. This grave situation can be saved by the use of non conventional sources of energy like solar, wind etc. In the case of a ship, solar energy is a better candidate for obvious reasons.

Solar Generated Electricity- Photovoltaic

The solar generated electricity is called Photovoltaic(PV). These are the solar cells that convert sunlight to electricity which is direct current(DC). The solar cells are made of semi-conductor materials which emit electrons when light strikes on them. The electrical conductor on the P-N junction captures the electrons in the form of direct current (DC). This can be used directly to power a DC load, can be converted to AC to power an AC load and also can be stored in a battery. Solar modules produce electricity devoid of pollution, without odour, combustion, noise and vibration. Also, other power supply systems require professional competence for installation and operation, but solar cells have no moving parts and no special expertise is required. However, for their usage onboard ships we may have to come out with innovative installation and sun path tracking system.

A typical destroyer has a power requirement of 3.5- 4MW which may vary from ship to ship. This is the total load of the ship which is called the Action Load. However, the cruising load of the same ship is only about 800-1200KW. This load further comprises of both AC and DC. On a ship presently the DC load is supplied either by the batteries directly or using rectifiers. Thus using solar cells have an advantage that they can directly supply the DC load and they can replace the use of rectifiers onboard. In order to supply to AC loads we will need inverters. Considering the cost benefit ratio, it may be decided that only a part load will be supplied with the help of solar cells and the heavy load like SAM, SSM, Gun mount etc will be supplied by using the hybrid configuration of Photovoltaic-Gas Turbine Generator.

The advantages of using PV cells are:-

1 No moving parts
2 Negligible or nil maintenance
3 Modularity
4 High Mean Time Between Failure(MTBF)
5 Long effective life

In the last decade, technological innovations have led to increase in solar efficiency and reduction in the price levels. Theoretically, the efficiency of a solar PV cell is about 25-30% but only 17-18% is practically achieved. World over the work is in hand to find new PV cells which can withstand high concentration of light and heat and produce more output per unit area.

From the foxle (fore part of the ship) to the quarterdeck (aft part of the ship), there is space available where solar panels can be positioned.This is generally not true for a war ship however for merchant ships it is easily feasible. The panel can be mounted as a whole and suitable tracking arrangements

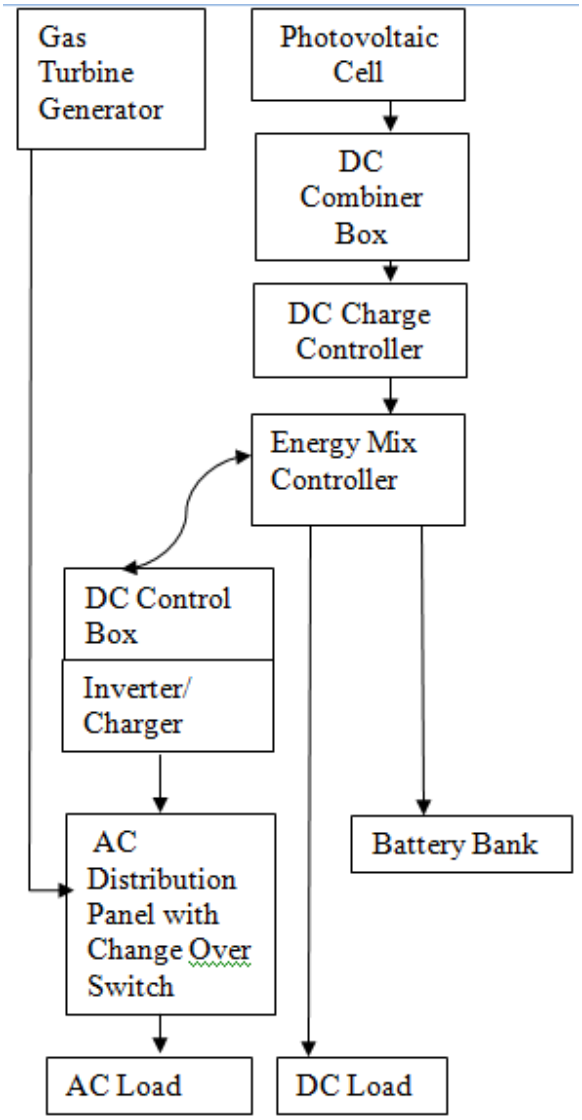


Fig. 1. Hybrid Solar-Fossil Fuel Power Source (PV-GT Generator)

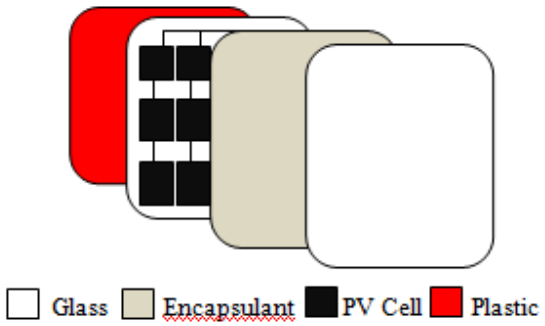


Fig. 2. Schematic of Modular Crystalline Silicon Cell

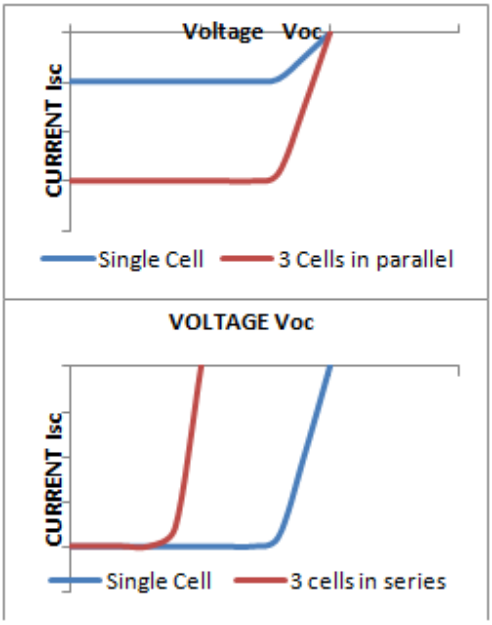


Fig. 3. I-V Characteristics

can be made. In addition one reflector on either side of the panel can be positioned at optimum angle to enhance the light collection. Here we may use 3 axis position control system considering the ship motion of roll, pitch and yaw.

A typical module construction for crystalline silicone is as shown in Fig 2. Onboard a ship PV cells are used in both series and parallel connection. Series where voltage needs to be increased and parallel where current capacity is to be high.

It is important to have well matched cells. In series connection, the matching should be w.r.t. current and in parallel connection, the matching should be w.r.t. voltage. The series/parallel configuration determines the current and voltage values obtained from the module under given illumination and load conditions. The test conditions are defined in the International Electro-technical Commission standard number 60904(IEC, 1987).

In a PV module, losses occur due to mismatch and efficiency depends on the configuration of the module and packing density. The module voltage reduces with increase in temperature although current increases slightly, overall efficiency reduces as temperature increases. In the case of ship, not only the modules required greater physical protection from the salty marine environment but also it was observed that it was mandatory to maintain the cell operating conditions. The cell is often at a temperature in the region of 50-80C when operating in good sunlight conditions and an ambient temperature of 25-35C. The ideal module also provides for a good heat transfer in order to keep the cell temperature as low as possible. The module used for this study is provided with a metal frame for ease of installation. The orientation of the module w.r.t the direction of the sun determines the intensity of the sunlight falling on the module surface. Latitudes where ship operates, weather condition and the load determines the optimum array orientation. Considering these factors, gyro stabilized orientation mechanism would be necessary to trade off the increase in sunlight from the optimum orientation as against any financial implication. Post trial installation of

PV cells, study of radar cross section would be imperative especially in the case of a naval vessel.

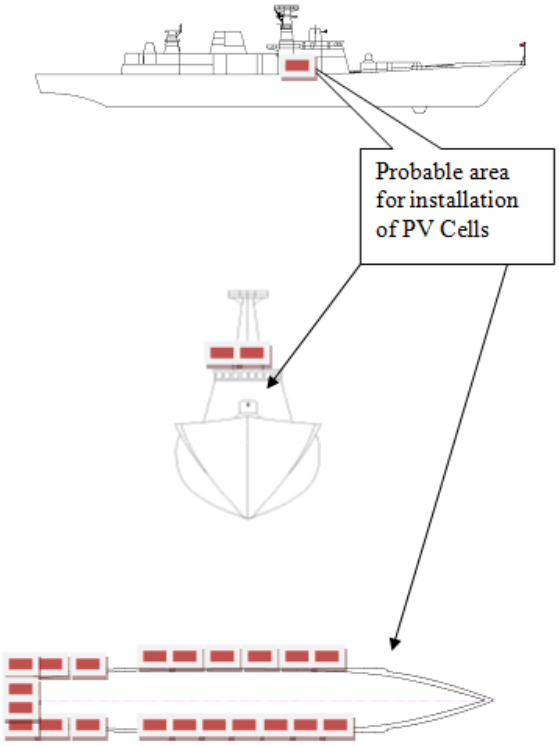


Fig. 4. Suggested Location

System Size and Its Operation

The system size needs to be optimum in order to ensure that it is not expensive and has performance levels. For arriving at an optimum system weather data and the lat long where the system is going to operate is a must. In our case we considered the Indian Ocean region however data wrt monthly average sunlight, ambient and max temperature was just with experience where more practical data is required.

The sample model was designed for a very small load because no actual experimental setup is available. As far as operation is concerned output of PV module depends on the sunlight conditions and is severely affected by the accumulation of dirt on the modules. In our Indian weather conditions it is a must to clean the modules so to maintain the efficiency of the modules. The efficiency of the system is defined as

$$\frac{poutput}{pinput} \quad (1)$$

Fig 5 below shows the efficiencies of Multi-junction cells, single-junction cells and crystalline Si cells. A line graph is also made for the cells with thin film technologies and the emerging PV cells. It can be seen that the efficiencies today are in the range of 40-45% as against 25-30% earlier stated. This indicate that time is not far when PV cells will be the main stay of power generation and integrated grid system. The efficiency of a solar cell may be broken down into reflectance efficiency, thermodynamic efficiency,charge carrier separation efficiency and conductive fficiency. The overall efficiency is the product of all of these individual efficiencies.

A solar cell usually has a voltage dependent efficiency curve, temperature coefficients, and shadow angles. Due to the difficulty in measuring these parameters directly, other parameters are measured instead: thermodynamic efficiency, quantum efficiency, integrated quantum efficiency, VOC ratio, and fill factor. Reflectance losses are a portion of the quantum efficiency under "external quantum efficiency". Recombination losses make up a portion of the quantum efficiency, VOC ratio, and fill factor. Resistive losses are predominantly categorized under fill factor, but also make up minor portions of the quantum efficiency, VOC ratio.

The fill factor is defined as the ratio of the actual maximum obtainable power to the product of the open circuit voltage and short circuit current. This is a key parameter in evaluating the performance of solar cells. Typical commercial solar cells have a fill factor ¿ 0.70. Cells with a high fill factor have a low equivalent series resistance and a high equivalent shunt resistance, so less of the current produced by the cell is dissipated in internal losses.

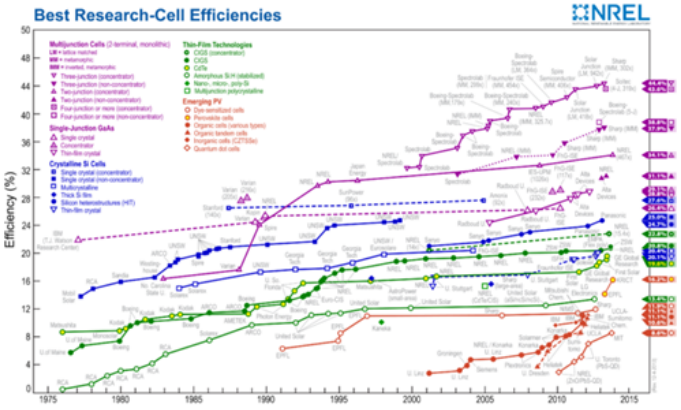


Fig. 5. Cell Efficiencies

II. CONCLUSION

PV cells have commercial value only when they are used in a system to provide a service. A PV module is an electricity generator and requires additional equipment. The sunlight reaching the Earth's surface is plentiful almost 10,000 times more than the equivalent of average power consumed in 2005 by humans. This abundance leads to the suggestion that it will not be long before solar energy will become the world's primary energy source. Additionally, solar electric generation has the highest power density among renewable energies.

Solar power is pollution-free during use. Production end-wastes and emissions are manageable using existing pollution controls. PV installations can operate for many years with little maintenance or intervention after their initial set-up, so after the initial capital cost of building any solar power plant, operating costs are extremely low compared to existing power technologies.

Compared to fossil and nuclear energy sources, very little research money has been invested in the development of solar cells, so there is considerable room for improvement. Nevertheless, experimental high efficiency solar cells already have efficiencies of over 40% in case of concentrating photovoltaic cells and efficiencies are rapidly rising while mass-production costs are rapidly falling.

The paper has discussed the economics of PV module and its probable application onboard ship. The study is in nascent stages and far futuristic. At times disadvantages outweigh the advantages for its use onboard but also lies the fact that fossils fuels have to make way for the non conventional sources of energy. The model of proposed hybrid system is feasible and it is a strong candidate for proving onboard a test platform.

REFERENCES

[1] Piao, Z.G.Park, J.M.Kim, J.H.Cho, G.B.Baek, H.L.,(2500) A study on the tracking photovoltaic system by program type, page(s):971-973 Vol.2
[2] Pritchard,"Sun tracking by peak power positioning for photovoltaic concentrator arrays, IEEE Control Systems Magazine, Volume3, Issue 3, August 1983, pp.2-8
[3] Hill R(1993),"Prospects for Photovoltaics Energy World, 208,8-11 original data updated by Hynes K and Hill R in 1999.
[4] IEC(1987), Photovoltaic Devices IEC 60904/EN60904:
[5] IEC(1996), Thin Film Terrestial Photovoltaic Modules-Design Qualification and Type Approval IEC 61646.



Captain Naresh Chhabra Commissioned in the Indian Navy on 01 Jul 1984, Captain Naresh Chhabra is an alumnus of Naval Academy Goa. He is an Electrical Engineer with Masters in Electronics and Telecommunications. He is a graduate of College of Naval Warfare Mumbai. The officer holds Master in Business Administration(MBA) degree from IGNOU(specializes in Marketing) and also PGDBA in HR from Indian Institute of Modern Management(IIMM) Pune. He is also a Member of Institution of Engineers India. Captain Naresh Chhabra has held various operational and staff appointments. He has served onboard Indian Naval Ships Sukanya, Ranvijay, Delhi and Trishul. He has held staff appointments as Trials Officer, Electrical Trials and Modification Authority (ETMA), Chief Instructor Electrical Equipment School(LES) INS Valsura, Joint Director, Directorate of Naval Design(Surface Ship Group), Staff Officer(SO) to Controller Warship Production and Acquisition(CWP&A), Technical Assistant(TA) to Chief of Material(COM). The Officer is presently serving as HoF(ECE) at INA. He is an avid reader and also plays Squash, Badminton.He has published 05 papers in refereed journals and conferences. His areas of research interest are solar cells and controls.

Acoustic Characterisation of Marine Mammals Using Spectrogram Image Correlation

Lt Cdr Aayush Verma[1], **Cdr (Dr) Arnab Das**[2]
[1]DIAT(DU), Girinagar, Pune
[2]MILIT, Girinagar, Pune
[1]vermaaayush@gmail.com, [2]arnabdas1972@hotmail.com

***Abstract*—The marine mammals are an important aspect of any marine ecosystem. Long-term, passive acoustic recorders are useful tools for monitoring some marine mammal populations, with potential applications ranging from providing information on behavioral ecology and abundance, to near-real-time localization and tracking of calling animals. A typical marine survey comprises of long-term recordings of ocean ambient noise, running into months/ years of recorded audio data and the task is to examine and identify the target species from such a long recording. However, manually detecting each species call in this large data set would potentially require hundreds of hours of human effort to scan spectrograms visually and to listen to recordings. In contrast, a computer using automated detection software could potentially process a year-long data set within hours to days, and human effort could be focused on reviewing automated detection results and searching for additional calls near times of automatic call detections. The paper examines spectrogram cross-correlation as a viable tool for real time automated call detection.**

***Keywords*—Spectrogram, Image Correlation, Marine Mammals, Identification, Common Dolphin, Matched Filtering**

I. Introduction

Marine Mammals are an integral part of any Ocean ecosystem. Owing to their long life spans, high trophic level (position an animal occupies in the food chain) feeding, extensive fat reserves acting as depots for anthropogenic toxins and low tolerance to rising ocean ambient noise, marine mammals serves as sentinel organism for coastal and ocean environments. Detection and localization of marine mammals in their natural habitat is an important and elaborate aspect of research and conservation. Visual detection and identification of marine species during shipboard surveys is often constrained by inclement weather, darkness, and animal behavior. Sound propagates long distances in the ocean [1] and many cetaceans are extremely vocal [2]. Most marine mammals have impressive vocalization capabilities that can be broadly categorized into three classes: (i) broadband short-duration clicks (ii) broadband pulsed sounds and (iii) narrow band frequency modulated whistles [3].

As a result, acoustic techniques can augment visual surveys by providing methods for detection and identification of cetaceans when they are likely to be missed by visual observers. The use of acoustic techniques to complement visual efforts has increased rates and distances of detection for several cetacean species, including: Humpback whales (Megaptera novaeangliae), Sperm whales (Physeter macrocephalus), Blue and Fin whales (Balaenoptera musculus and B. physalus), Bowhead whales (Balaena mysticetus) and other Delphinids. While the use of acoustic techniques to detect marine mammals is becoming an increasingly common element of shipboard surveys, acoustic species identification has, until recently, received less attention [4]. Numerous detection techniques have been employed to detect the presence of marine mammals in long audio recordings often limited by low SNR of the vocalizing mammal, high ambient noise, dense shipping traffic etc. This paper examines the third class of marine mammals vocalization i.e whistles, that are used in animal communication and implements the cross correlation on the transformed time-frequency space for species identification.

II. Approach Description

A. General Description

The method for detecting frequency-sweep calls uses convolution of a spectrogram image with a kernel designed for the desired type of call. This method is inspired by neural processes in the auditory cortex and cochlear nucleus that are responsive to frequency-modulated tones [key-7]. First, a spectrogram of the input sound signal is computed. Next, a kernel designed for the target call type is produced. This kernel, a two dimensional image, contains several segments, one for each of the frequency sweeps in the desired call type. The spectrogram image is then convolved with the kernel to-produce a sequence of output values; whenever the output value is above a certain threshold, a call is considered to have been detected. More specifically, the input signal is digitized, transferred to computer, and stored as a disk file. A spectrogram of it - a two-dimensional time vs. frequency image is computed. Spectrogram parameters (FFT size, hop size, zero padding. Window type, etc.) depend on the input signal sampling rate, frequency and duration of the target call type, and the rate of frequency sweep. They are set such that each frequency sweep of interest covers at least four, and preferably ten or more, output bins [7]. Next a kernel, specific to target call is designed and its spectrogram is correlated in 2-dimensions (time and frequency) with the input signal.

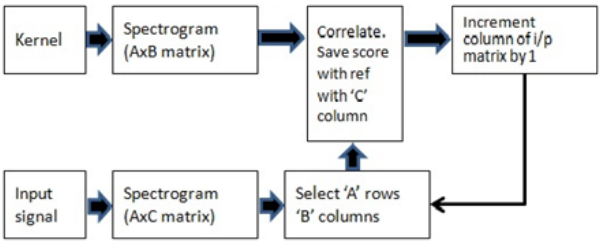


Fig. 1. Flowchart of General Description

B. Spectrogram Computation and choice of parameters

Spectrograms are being used to identify spoken words phonetically and to analysis the various calls of animals. They are used extensively in the development of the fields of music, sonar, radar, and speech processing, seismology, etc. Spectrograms are usually created in one of two ways: approximated as a filter-bank that results from a series of band pass filters (this was the only way before the advent of modern digital signal processing), or calculated from the time signal using the FFT. These two methods actually form two different Time-Frequency Distributions, but are equivalent under some conditions. The band pass filters method usually uses analog processing to divide the input signal into frequency bands; the magnitude of each filter's output controls a transducer that records the spectrogram as an image on paper. Creating a spectrogram using the FFT is a digital process. Digitally sampled data in the time domain is broken up into chunks, which usually overlap and Fourier transformed to calculate the magnitude of the frequency spectrum for each chunk. Each chunk then corresponds to a vertical line in the image; a measurement of magnitude versus frequency for a specific moment in time. These spectrum or time plots are then "laid side by side" to form the image or a three-dimensional surface. The spectrogram of a signal s(t) can be estimated by computing the squared magnitude of the STFT of the signal s(t), as follows:-

$$spectrogram(t,\omega) = |STFT(t,\omega)|^2 \tag{1}$$

where STFT is the Fourier Transform of the product of signal s(t) and a window function which is nonzero for only a short period of time. The Fourier transform (a one-dimensional function) of the resulting signal is taken as the window is slid along the time axis, resulting in a two-dimensional representation of the signal. Mathematically, this is written as:-

$$STFT\{x(t)\}(\tau,\omega) \equiv (\tau,\omega) = \int_{\infty}^{\infty} x(t)w(t-\tau)e^{-j\omega t}\,dt \tag{2}$$

where w(t) is the window function.

1) Choice of Analysis Window: The choice of the analysis window is important, since it directly affects the trade-off between frequency resolution and side-lobe attenuation. The simplest window function is the rectangular window of length M and whose DTFT is given by :-

$$W(\omega) = \frac{sin(\frac{M\omega}{2})}{sin(\frac{\omega}{2})} \tag{3}$$

The width of the main lobe of this function is $2f_s$/M, which corresponds to a width twice of a single frequency bin, B = 2 times Freq bins, giving a narrow main lobe. However, the height of the largest side lobe is -13dB relative to the main lobe peak which is poor for analysis as this leads to cross talk between DFT bins. In comparison, the Hamming window has a main lobe width B=4 times Freq bins, but the largest side lobe is at -43dB relative to the main lobe and hence a Hamming window is used for computation of Spectrograms. To resolve two closely spaced sinusoid at frequencies f_1 and f_2, a narrow main lobe is required so that the two modulated window transforms can be distinguished. If the minimum frequency separation we need to resolve is $\triangle$=f_2-f_1, then

$$B\frac{f_s}{M} \leqslant \triangle \tag{4}$$

And, thus for a Hamming window, we require that the length of the window function be at least:-

$$M \geq \frac{4f_s}{f_2 - f_1} \tag{5}$$

For this project a Hamming window of 512 points are used. The sampling frequency f_s is 44100Hz and thus the minimum frequency separation achieved is:-

$$\triangle f = \frac{4 * 44100}{512} = 344.5Hz \tag{6}$$

2) Choice of FFT Length: Once a window function and a length M is decided, we can compute the DFT of this frame. The size, N, of this DFT must be at least M, with any additional samples being produced via "zero-padding". Firstly, in order to take advantage of the computational efficiency of the FFT algorithm, N is taken to be a power of 2. Secondly, the visual display produced by the analysis will be represented by N samples of the DTFT. The larger the value of N, the closer the DFT will approximate the smooth function of represented by the DTFT. For the present application, more stress is laid on better frequency resolution and smooth frequency curves, hence Spectrograms of all the input samples are computed with 1024 point FFT.

3) Choice of Overlap: Overlap of the sliding window makes the STFT smoother along the time axis. However, overlap requires more computation time and memory. If the signal length is large and the spectral content evolves slowly, it is not necessary to overlap the sliding window. If the signal length is small, overlapping

is recommeded for the sliding window to obtain a smoother STFT. In the project, 50% overlap is used because an instance of call of most marine mammals last only for few millisecond.

C. Kernel design

The most important aspect of the correlation process is the kernel design. The presence or absence of the mammals is directly related to closeness of the actual vocalization to the designed kernel of the target species. An approach entailing design of synthetic kernel was developed by Mellinger and Clark [7], where the kernel is designed by separating each frequency sweep of the vocalizing mammals (also known as Segmentation) and later concatenated to produce the synthetic kernel resembling the spectrogram of the target species. In this work, the species specific kernel is chosen from the actual vocalizations of the species. Such a method of using the actual sound of vocalizing animal as the kernel has been used successfully by Christopher W. Clark et al. in their work [10] to analyze vocalizations of Swamp Sparrows. The vocalizations of animals captured in controlled environment offer some unique advantages such as, recordings are free from ambient environment induced noise and high SNR of vocalizing animals, that are particularly suitable for developing computationally inexpensive algorithms. This approach is also suitable when the training data or the samples of marine mammals vocalizations are limited and thus insufficient to apply statistical methods. Most of the marine mammals vocalizations are obtained from online repositories like http://aquaticacousticarchive.com/metadatalibrary.php, which is an index of most of the online marine mammals libraries, www.dosit.org and other online sources. Most marine mammals have impressive vocalization capabilities that can be broadly categorized into three classes: (i) broadband short-duration clicks (ii) broadband pulsed sounds and (iii) narrow band frequency modulated whistles. The recordings were then classified into the above mentioned classes and spectrograms of each recording was computed using Raven Lite freeware (Raven Lite is a free software program that lets users record, save, and visualize sounds as spectrograms and waveforms. Available at http://www.birds.cornell.edu/brp/raven/ravenoverview.html). Post examinations of numerous spectrograms (corresponding to each recording) of one species, one spectrogram is chosen as the kernel based on adequate frequency modulation lasting few mille seconds, good clarity of sound vocalization and minimum ambient noise. The time waveform corresponding to this chosen spectrogram was opened in a freeware sound editing tool like Audacity (Available at http://audacity.sourceforge.net/) and one instance of vocalization, lasting few mill seconds is extracted. This becomes the kernel to be used in all future correlation operation for that particular species. Spectrogram of these extracted sound files are computed in Matlab using the same parameters as discussed earlier.

D. Correlation operation with Kernel

It is pertinent to mention that the process is similar to Matched Filtering, which is an optimal solution for detecting a known signal in white Gaussian noise. The two requirements of this method is that the signal to be detected must have the same structure and the background noise is white [9]. However in the present case, the basic structure of the mammal calls varies reasonably from call to call and the ocean ambient noise cannot be assumed to be white and Gaussian. Therefore a kernel spectrogram correlation approach is presented, where correlation is performed in time-frequency space. The processed Spectrograms of input signal and kernel are compared. The cross correlation works because when the kernel is lined up with the target sound type for instance when kernel in Fig. 2(a) lines up with the Common Dolphin calls in Fig. 2(b), the regions of kernel lines up with the high Spectrogram values, resulting in a high correlation score. Thus the correlator outputs a high score whenever one of the target sound types occurs. The kernel spectrogram, having dimensions M-by-N is correlated with a part of the input spectrogram, having the same dimensions and successively incremented column-wise. The variable ‘N is dependent on the time duration of kernel signal and variable ‘M is controlled by the number of FFT points i.e.

$$M = \{\frac{FFT_{points}}{2}\} + 1 \tag{7}$$

Thus in effect the input signal spectrogram which is a 2-D matrix is divided into sub matrix of same dimensions as that of kernel and correlated with kernel. In next iteration the matrix column is incremented by 1 and again correlated with the kernel to produce a correlation score. This score is later plotted with time axis of the input signal to indicate the times at which mammals vocalization of interest occurs, as shown in Fig. 2(c).

III. RESULTS

The correlation score obtained post correlation of kernel with the input sound is plotted on y-axis with time duration of input signal placed on the x-axis as shown in Fig. 2(c). Thus correlation score which are higher than user defined threshold are indicative of presence of target species calls. There are various methods to set the threshold either manually or adaptively depending upon the required detection rate. These methods are not discussed here and the threshold value is set based on the loudness of the ambient noise. The above mentioned procedure was tested to indentify the calls of Common Dolphin (Delphinus tropicalis) and Dugong (Dugong dugon), which are a common species around Goa coast. Using the algorithm, it is found that a SNR of 6dB, threshold at 0.01 is sufficient to give 70% Probability of Detection in case of Dugong. For same detection probability, and threshold value, the SNR required must be around 20dB. This variability in detection probability is attributable to the unique signature whistles produced by the Common Dolphin.

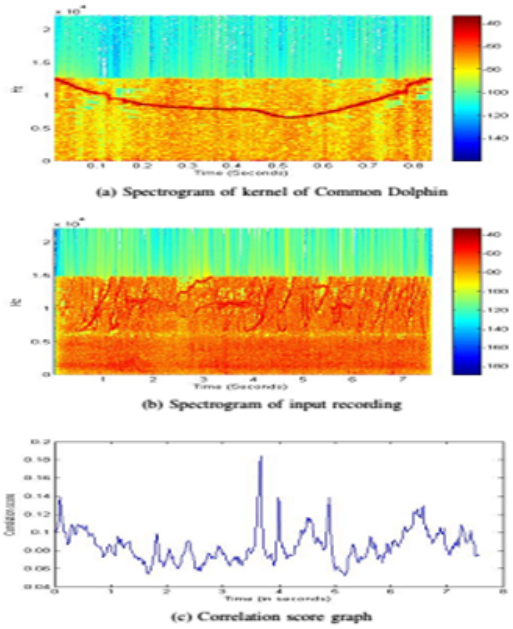


Fig. 2. Spectrograms of Common Dolphin

IV. CONCLUSION

Passive acoustic methods have been increasingly employed both as standalone surveys and in conjunction with visual surveys. Their utility has become clear over the past decade and many marine mammal surveys now include extensive acoustic component. One of the biggest hurdles prevalent is a general lack of understanding of the behavioral context of sound production for many species which is compounded by interspecies differences in acoustic behavior. For instance, Bottlenose Dolphins are highly vocal compared to baleen whales, however, because their vocalizations are higher in frequency than those of most baleen whales, they are detected at shorter distances. Therefore, assessment strategy may need to be tailored for individual species or suites of species.

REFERENCES

[1] Medwin, H., and C. S. Clay, "Fundamentals of acoustical oceanograph", Academic Press, San Diego, CA, 1998.

[2] Richardson , W. J., C. R. Green, C. I. Malme and D. H. Thomson, "Marine mammals and noise", Academic Press, San Diego, CA,1995.

[3] M. Greco, F. Gini, and L. Verrazzani, "Analysis and modeling of acoustic signals emitted by mediterranean bottlenose dolphins," in Proceedings of the *3rd IEEE International Symposium on Signal Processing and Information Technology*, Dip. di Ingegneria dell7Informazione, Pisa Univ., Italy, pp. 122 - 125 December 2003.

[4] Mellinger, D., and C. Clark, "Recognizing transient low-frequency whale sounds by spectrogram correlation", *Journal of the Acoustical Society of America* 107:3518 3529, 2000.

[5] Michalopoulou, Z-H "Underwater transient signal processing: marine mammal identification, localization, and source signal deconvolution" *Acoustics, Speech, and Signal Processing ICASSP*-97., IEEE International Conference on. Vol. 1. IEEE, 1997.

[6] W. J. Richardson, C. R. Greene, C. I. Malme, and D. H. Thomson, Marine Mammals and Noise. California: Academic Press, 1995.

[7] Mellinger, David K., and Ch W. Clark, "A method for filtering bio acoustic transients by spectrogram image convolution", OCEANS93, *Engineering in Harmony with Ocean*, Proceedings IEEE, 1993.

[8] Mallawaarachchi, Asitha, et al. "Spectrogram denoising and automated extraction of the fundamental frequency variation of dolphin whistles", *The Journal of the Acoustical Society of America* 124.2 (2008): 1159-1170.

[9] Mellinger, David K., and Christopher W. Clark "Methods for automatic detection of mysticete sounds", Marine & Freshwater Behaviour and Phy 29.1-4 (1997): 163-181.

[10] Clark, Christopher W., Peter Marler, and Kim Beeman, "Quantitative analysis of animal vocal phonology: an application to swamp sparrow song", Ethology 76.2 (1987): 101-115.



Lt Cdr Aayush Verma The officer pursued his bachelors degree in Electrical and Electronics Engineering from Naval College of Engineering, INS Shivaji, Lonavla. Post initial training, the officer assumed duties of Weapon Maintenance Officer and later Deputy Electrical Officer onboard a ASW platform. The officer was then appointed to Naval Dockyard, Mumbai, where was entrusted with the duties of System and Network Administrator of Yards Campus Area Network. Presently, the author is pursuing Post Graduation program from DIAT(DU), Girinagar, Pune on Signal Processing and Communication.



Cdr (Dr) Arnab Das Cdr. (Dr) Arnab Das is a graduate of Electrical and electronic Engineering from the Naval College of Engineering, Lonavala. He has done his M Tech in Radar and Communications with specialization in Underwater Electronics from Indian Institute of Technology, Delhi and Ph.D. from Indian Institute of Technology, Delhi. On completion of his graduate training, he has served on sea going platforms of the Indian Navy and performed the task of an Assistant Electrical Officer (Anti-Submarine Warfare). He was on deputation to IIT Delhi for seven years as a project officer and has been involved sponsored projects from the DRDO and the Indian Navy for technology development in the areas of underwater systems, signal processing algorithms and passive classification techniques. He has published a total of 7 technical papers in referred International Journals and several conference papers. His fields of interest include marine acoustics, anthropogenic noise and their impact on marine mammals, shallow water acoustics.

Underwater Sediment Classification Using Characteristics of Echoes

Priya V. Bothe[1], **J.A. Sadalage**[2], **Cdr Dr. Arnab Das**[3]
[1,2]VPCOE, Baramati, University of Pune, India
[3] MILIT, Pune, India
[1]priyabothev@gmail.com, [2]jyotika2k1@gmail.com, [3]arnabdas1972@hotmail.com

***Abstract*—In the seabed classification, analyzing the details of echoes from single-beam sounders is well established as a basis. Both echo shape and amplitude are analyzed to make maps of seabed sediment classes. Classification requires echo envelopes that are rich in seabed information and with few artifacts. The echoes should be influenced only by properties of the seabed, for accurate acoustic classification of the seabed. For seabeds with any significant roughness, the echo is not at the same frequency as the transmission. These frequency shifts may be valuable for characterisation. Depth, slope and system independent digital versions of the echo envelopes are also required for classification by segmentation. It has been observed that the direct application of echo-waveform data for seafloor classification indicates poor classification. The application of the echo signal preprocessing prior to the classification is unwarranted because it affects real-time classification activity. Therefore, possibilities to explore a better technique may then become essential. All classification methods use some kind of characteristic features (or attributes), which are extracted from the normalized backscatter echo envelopes. The normalization is essential to make these features independent of echo amplitude. These echo features are grouped into few categories: features that (a) represent the characteristics of acoustic backscatter energy, (b) describe the shape characteristics and the amplitude variability of echo envelopes, (c) represent the statistical characteristics of echoes, (d) describe the spectral characteristics of echo envelopes, and (e) other features such as fractal, Hausdorff dimension, and wavelet characteristics. This paper aims at review of sediment classification for river water using echo parameters. Based on the review a way ahead will be presented to facilitate research and development in riverbed mapping.**

***Index Terms*—Echo features, single beam echo-sounders, grain size, echo shape parameters.**

I. Introduction

Underwater sediment classification has been long considered as a useful tool for fast preliminary geological analysis. Every sediment is a mixture of grains of varying sizes. There have been different definitions of terms used for the different sizes of individual grains and similarly differing definitions for the terms used to describe the relative proportions of different grain sizes. A common classification used derives from that proposed by Folk (1954) in [5] that groups grains into mud, sand and gravel on the basis of their diameter with the boundary between mud and sand size grains at 63 micrometer (0.063 millimeter) and the boundary between sand and gravel size grains at 2mm. Acoustic methods for seabed identification and classification can be used in most of the fields including marine geology, hydrography, marine engineering, environmental sciences, military sonar, and fisheries. The advantage over conventional bottom grabs is a vast reduction in survey time and costs. Echo to echo variations are the difficulties included that may occur even for low sea states and homogeneous sea

beds, and the need for identification of echo parameters which are best suited to discriminate between various seafloors. For example, the presence of current ripples can affect certain echo features, but this is undesirable when the purpose is to discriminate between only sediment compositions. Behind the process of echo formation, the physical mechanisms are nontrivial and a theoretical treatment which includes specular reflection, surface backscattering and volume reverberation can be exceedingly complex, that depends on the level of completeness that is appeared.

Seafloor classification algorithms can be divided in two categories [10] model based methods and empirical methods. Model based methods attempt to characterize the seabed by translating echo signal properties directly into geological quantities through a physical model or into the physical properties of sediments. The knowledge about system characteristics such as sensitivity, emitted signals, and directivity patterns is often required for model-based methods. Empirical approaches depend on the observation that certain features of echo signals are correlated with the sediment type. The idea behind the use of a particular feature may very well be based on theorotical assumptions or expectations, but this theory is not used in the classification or signal processing. Two or more features are combined by means of a cluster analysis then after each identified cluster is associated with a particular type of sediment. The empirical methods have the disadvantage that it is not trivial to interpret the results otherwise these are easy to implement.

Fresh water is generally distinguished by having low concentrations of dissolved salts and other total dissolved salts than salt water. Sound is considered to travel faster in less denser mediums of the same state of matter. Salt water is having more density than fresh water, yet sound travels faster in salt water. Also, the speed of sound in fresh water is 1497 m/s, and 1500 m/s in salt water. This is because in terms of experimental uncertainty and the factors affecting the speed of sound (pressure, temperature, salinity, etc.), are essentially of the same value. And since the density of seawater is only 2.5

II. Methodology Employed

The set of the echo envelopes related to particular beams as a multibeam sonar output was obtained in [7] (the sonar had to operate in water column mode in order to register the beam echo waveforms, not only the bathymetry information). After detecting of bottom echo in the received signal, the set of echo parameters was calculated for the suitable part of each beam echo, with averaging of obtained values for whole set of echoes of the same transmission angle. The transmission angle was assumed to be equal to the incidence angle and the seafloor

was assumed to be approximately flat. Following group of echo parameters were calculated:

1) Basic parameters:
   a) The total echo energy calculated as a sum of squared acoustic pressure values of all echo samples.
   b) The maximum echo amplitude.
   c) The echo duration time or echo length.
2) Parameters related to statistics of the echo energy:
   a) The mean of echo energy.
   b) The standard deviation of echo energy.
   c) Echo energy skewness that is the normalized third statistical moment.
3) Parameters which describe the echo geometric shape:
   a) The centre of gravity along time axis of echo envelope.
   b) The normalized moment of inertia of echo envelope deter- mined with respect to axis containing its centre of gravity.
   c) Fractal dimension of echo envelope, determined as a mea- sure of its shape composedness which was calculated as a box dimension approximation of a Haussdorff dimension.

1) Echo Energy:
   Although the bottom sediment type remains the same, the shape of the backscatter envelope and the power of the returned signal can change significantly with depth. The normalized echo energy E is an important parameter for the classification of various sediments. It is expected to increase for increas- ing sediment grain sizes by discarding the effect of limited bandwidth. The total energy is [15],

$$E = \int_0^{t_0} i(t)\,dt$$

   where t0 : the truncated return pulse duration
   i(t) : water depth corrected intensity as a function of time. The total energy directly relates to the hardness and roughness
   of the seabed. The energy in the echo is expected to increase for increasing mean grain sizes, since both the sediment roughness mostly expressed as the spectral length and the impedance contrast increase.
2) Time-Spread:
   The time-spread T is considered to be a pure echo shape parameter and it is independent of the echo energy E. The time spread is expected to exhibit a minimum for intermediate grain sizes [2]. Because of the increased volume scattering, increased time-spreads are expected for small grain sizes. Also, for the coarser sediments because of the increased roughness the time spreads are expected to increase. As a second order moment, the time spread T is [15],

$$T = \sqrt{\frac{4}{E}\int_0^{t_0} i(t)(t-T_0)^2\,dt}$$

   where T0 in the equation for time spread is echo centre of mass and is given by equation below,

$$T_0 = \frac{1}{E}\int_0^{t_0} i(t)\,t\,dt$$

3) Skewness:
   The skewness is [15],

$$S = \frac{8}{T^3 E}\int_0^{t_0} i(t)(t-T_0)^3\,dt$$

   Since a measure of asymmetry, the skewness S is typically positive for all seafloor echoes. This shows that echo shape is right-skewed, means that mass of the shape is concentrated on the left hand side. Skewness is independent of echo duration because it is normalized by third power of T.
   Skewness of the distribution, an indicator of whether the grain-size histogram is symmetrical or is skewed to a higher percentage of coarser or finer material.

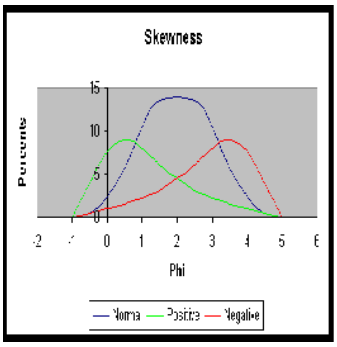


Fig. 1. Variation of Skewness.

4) The Flatness or Kurtosis:
   The fourth-order moment, the flatness or kurtosis is [15], This is the measure of the peakedness of the echo shape. An echo shape with higher kurtosis or less flatness leads to have distinct peak near the mean and also to have heavy tail(s). But an echo with low kurtosis has a flat top near the mean instead of a sharp peak, with short tail(s). Therefore, the term kurtosis

$$F = \frac{16}{T^4 E}\int_0^{t_0} i(t)(t-T_0)^4\,dt$$

is used as a measure for the kurtosis parameter. Kurtosis is independent of echo duration because it is normalized by fourth power of T.

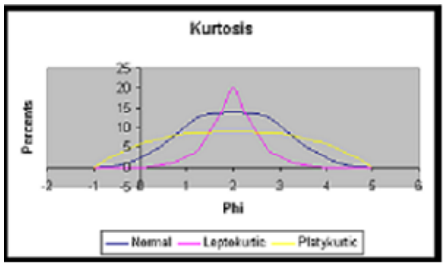


Fig. 2. Variation of Kurtosis.

The features provide different information but those are prob- ably statistically correlated. They contain independent infor- mation regarding the physical properties of the seabed and therefore they provide useful tools for classification.

Fig. 1 presents an illustration of the procedure in [12] based on the assumption of normally distributed backscatter strengths per sediment type to classify sediments. The thick solid black line in the figures corresponds to the histogram of the measured backscatter strengths. The fit is represented by the red line, with the individual PDFs represented by the thin black lines (4, 5, 6, and 7 for the different subplots, respectively).

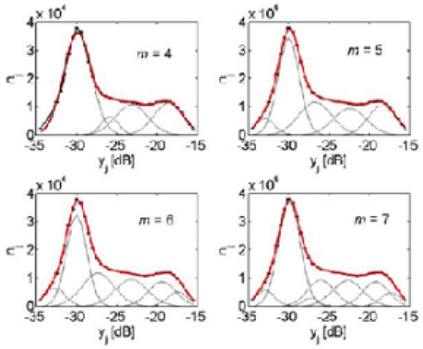


Fig. 3. Histograms of measured backscatter data (60 degree beam) fitted to the model for m = 4, 5, 6 and 7 respectively.

III. Conclusion

Echo parameters like energy, time spread, maximum amplitude, skewness, kurtosis plays vital role in sediment analysis.

Further advancements in sediment classification could be car- ried out through Shape Statistics.

Acknowledgment

This is to acknowledge and thank all the individuals who played defining role in shaping this IWCEM Conference paper. Without their Coordination, guidance and reviewing this task could not be completed alone. I avail this opportunity to express my deep sense of gratitude and whole hearted thanks to my guide Prof. J. S. Rangole madam for giving her valuable guidance, inspiration and encouragement to embark this paper. I also take great pleasure in thanking Dr. A. Das Sir for providing appropriate guidance. I would personally like to thank Prof. V.U. Deshmukh Sir, Head of Computer Dept. at Vidya Pratistaisthans College of Engineering (VPCOE), and our Honble principal Dr. S. B. Deosarkar sir who creates a healthy environment for all of us to learn in best possible way.

References

[1] Chanchal De and Bishwajit Chakraborty, Model-Based Acoustic Remote Sensing of Seafloor Characteristics, IEEE Transactions on Geoscience and Remote Sensing, vol. 49, no. 10, Oct. 2011.

[2] Haris K., Bishwajit Chakraborty, Chanchal De, Prabhudesai R.G., and William Fernandes, Model-based seafloor characterization employing multi-beam angular backscatter data a comparative study with dual-frequency single beam, J. Acoust. Soc. Am., vol.130(6); 2011.

[3] Ben R. Biffard, Jon M. Preston and N. Ross Chapman, Acoustic Classification with Single-Beam Echosounders: Processing Methods and Theory for Isolating Effects of the Seabed on Echoes, IEEE Oceans, Sept. 29 2007.

[4] Kerstin Siemes, Jean-Pierre Hermand and Mirjam Snellen, A multi-sensor approach for remotely modeling and mapping sediment properties, IEEE/OES RIO Acoustics, 2013.

[5] P.A. Van Walree, J. Tegowski, C. Laban, and D.G. Simons, Acoustic seabed discrimination with echo shape parameters: a comparison with the ground truth, Continental Shelf Research. 25:2273, 2005.

[6] Masahiko Furusawa, Echo Integration Near The Seabed, Journal of Marine Science and Technology, vol. 19, No. 3, pp. 259-266, Nov.2011.

[7] Z. Lubniewski, A. Chybicki, Using Multibeam Echoes in Seafloor Classification, IEEE Oceans, 2009.

[8] Bishwajit Chakraborty, and K. Haris, Seafloor Roughness Estimation Employing Bathymetric Systems: An Appraisal of the Classification and Characterization of High- Frequency Acoustic Data, AIP Conf. Proc. 1495, 283, 2012.

[9] Pierre Legendre, Kari Elsa Ellingsen, Erik Bjrnbom, and Philippe Casgrain, Acoustic seabed classification: improved statistical method, Can. J. Fish. Aquat. Sci. 59: 1085, 2002.

[10] D. D. Sternlicht and C. P. de Moustier, Remote sensing of sediment characteristics by optimized echo-envelope matching, J. Acoust. Soc. Amer., vol. 114, no. 5, pp. 2727, Nov. 2003.

[11] Mirjam Snellen, Kerstin Siemes, and Dick G. Simons, Model-based sediment classification using single-beam echosounder signals, J. Acoust. Soc. Am. 129 (5), May 2011.

[12] D.G. Simons, A. Amiri-Simkooei, K. Siemes, M. Snellen, Recent developments in multi-beam echo-sounder processingThe multi-beam potential for sediment classification and water column sound speed estimation, TU Delft, Acoustic Remote Sensing group, the Netherlands.

[13] Dimitrios Eleftherakis, AliReza Amiri-Simkooei, Mirjam Snellen and Dick G. Simons,Improving riverbed sediment classification using backscatter and depth residual features of multi-beam echo-sounder systems, J. Acoust. Soc. Am. 131 (5), May 2012.

[14] Bishwajit Chakraborty, K. Haris, G. Latha, Nicolas Maslov and Andrew Menezes, Multifractal Approach for Seafloor Characterization, IEEE Geosci. Remote Sens. Lett., vol.11(1), 2014.

[15] Ali R. Amiri-Simkooei, Mirjam Snellen, And Dick G. Simons, Principal Component Analysis Of Single-Beam Echo-Sounder Signal Features For Seafloor Classification, IEEE J. Ocean, Vol. 36, No. 2, April 2011.

[16] Chanchal De, Bishwajit Chakraborty, Estimation of Mean Grain Size of Seafloor Sediments using Neural Network, Mar. Geophys. Res., vol.33, 2012.

[17] I. Karoui, R. Fablet, J.-M. Boucher, and J.-M. Augustin, Seabed segmentation using optimized statistics of sonar textures, IEEE Trans. Geosci. Remote Sens., vol. 47, no. 6, pp. 1621, June 2009.

[18] P. A. van Walree, M. A. Ainslie, and D. G. Simons, Mean grain size mapping with single-beam echo sounders, J. Acoust. Soc. Amer., vol. 120, no. 5, pp. 2555, Nov. 2006.

[19] G. L. Chenadec, J.-M. Boucher, and X. Lurton, Angular dependence of K-distributed sonar data, IEEE Trans. Geosci. Remote Sens., vol. 45, no. 5, pp. 1224, May 2007.

[20] C. De and B. Chakraborty, Acoustic characterization of seafloor sediment employing a hybrid method of neural network architecture and fuzzy algorithm, IEEE Geosci. Remote Sens. Lett., vol. 6, no. 4, pp. 743, Oct. 2009.

[21] C. De and B. Chakraborty, Preference of echo features for classification of seafloor sediments using neural networks, Mar. Geophy. Res., vol. 31, no. 3, pp. 215, Sep. 2010.

[22] B. Chakraborty, V. Kodagali, and J. Baracho, Sea-floor classification using multibeam echo-sounding angular backscatter data: A real-time approach employing hybrid neural network architecture, IEEE J. Ocean. Eng., vol. 28, no. 1, pp. 121, Jan. 2003.
[23] C. de Moustier and D. Alexandrou, Angular dependence of 12 kHz seafloor acoustic backscatter, J. Acoust. Soc. Amer., vol. 90, no. 1, pp. 522, Jul. 1991.
[24] K. L. Williams, D. R. Jackson, E. I. Thorsos, D. Tang, and K. B. Briggs, Acoustic backscattering experiments in a well characterized sand sediments: Data/model comparisons using sediment fluid and Biot models, IEEE J. Ocean. Eng., vol. 27, no. 3, pp. 376, Jul. 2002.



Priya V. Bothe is pursuing M.E. Degree in Electronics with specialization in Digital System from Vidya Pratishthan's college of Engineering, Baramati, India. Her areas of interest are Sediment Classification Using Empirical Methods, Fresh water acoustic, Hydrographic Survey.



Jyoti Rangole M.Tech. in Digital System from C.O.E. Pune in 2009. She has worked as a reviewer for Pearson Publication for the book , Embedded System. She is working as an Assistant Professor in Electronics and Telecommunication Department. She has published 1. Data compression techniques, IEEE third international conference on Machine Learning Computing Conference, Singapur. 2. Implementation of image processing algorithms on FPGA published in international journal Technology World. 3. Automatic silkworm eggs counting mechanism for sericulture, journal of engineering technological research, ISSN 2229-9262 Quarterly Malaysia Journal. Her areas of research interest are Machine Vision, Implementation of Image processing algorithm using VLSI for sericulture automation, Multiresolution image analysis.



Arnab Das received B. Tech degree in Electrical Engineering from Naval College of Engineering, Lonavala, India in 1995. He obtained M. Tech degree in Radar and Communication with specialization in Underwater Signal Processing in 2002and PhD degree in 2009 from Indian Institute of Technology, Delhi, India. He was commissioned into the Indian Navy in 1994. He worked as Project Officer at CARE, IIT Delhi for R & D in Underwater Signal processing and hardware design in 2003-2007. Currently he is instructor at MILIT Pune, India. His research interests are Underwater Passive Surveillance, Underwater Communication and Pattern recognition.

UNDER WATER ELECTROMAGNETIC REMOTE SENSING

Karan Datta
Department of Electronic Engineering,
School of Engineering,
Manipal University,
Jaipur karandatta@muj.manipal.edu

***Abstract*—Utilization of non-destructive and non-invasive methods for the real-time underwater remote sensing is one of the challenging and desired tasks in the maritime security and safety as well as the harbour surveillance. Our aim is to develop and verify advanced electromagnetic sensors for a seabed objects detection and inspection. The seabed is a complex environment often covered with the sand, dense aquatic vegetation and rocks. Hence, it is difficult to investigate the seabed by only one conventional method. Usually a combination of the sonar and video system is used for the detection and classification of underwater targets. In this paper, we verify the operation and efficiency of two EM imaging sensors, a ground penetrating radar (GPR) and an electromagnetic continuous wave sensor (CWEMS).**

Keywords*—electromagnetic sensors, GPR, remote sensing, underwater detection.

I. Introduction

The underwater remote sensing technology plays a key role in investigations of the underwater environment and detection of unknown objects. Nowadays, several techniques exist in this field; the most important among them are acoustic, electromagnetic and optical devices. Electromagnetic (EM) sensors have long been recognized as a useful tool for the geophysical exploration and remote sensing. However, no system currently available in the market is capable to accurately survey and map the location of objects buried under the bottom sediments or vegetation. The technology selected includes an adapted version of the ground penetrating radar (GPR) and the continuous wave electromagnetic sensor (CWEMS) which are competing tools against the SONAR (sound navigation and ranging) and metal detector.

II. EM sensing methods

The EM propagation in water is very different from the propagation through air due to the high permittivity and electrical conductivity of water. In freshwater the conductivity is 0.1 - 10 mS/m, whereas in sea water this value is around 4 S/m. Another difference is a greater attenuation loss of the propagation pulses in water. It depends on the selected frequency and salinity of water. Hence, for the freshwater and sea water the attenuation loss at 100 MHz is 0.1 dBm-1 and 100 dBm-1, respectively, whereas at 1 GHz it increases to 1 dBm-1 and 1000 dBm-1, respectively. Furthermore, the propagation velocity and corresponding wavelength in water decrease by a factor of about 10 in comparison to the velocity and wavelength in air.

A. Ground penetrating radar

The ground penetrating radar or GPR is a non-destructive geophysical method based on the propagation of high frequency electromagnetic waves. The GPR method images structures in the ground that are related to changes in the dielectric properties. If a very short EM pulse is transmitted by an electric dipole into the medium, it propagates in the subsurface with a velocity depending on the electrical properties of the medium.

For a layered subsurface with contrasting electrical properties, a part of the EM energy is reflected back to the surface where it is detected by a receiver dipole and recorded. Synchronization between the transmitter and the receiver systems allows the determination of the time taken for the EM pulse to be reflected back.The antenna was placed in a rubber dinghy on the water surface. The experiment with a 50 MHz antenna is performed from the wooden pier at the lake shore. The 50 MHz antenna with a flexible snake-like design allows easy manoeuvring and provides optimum results in difficult environments as well as a deeper signal penetration into the medium.

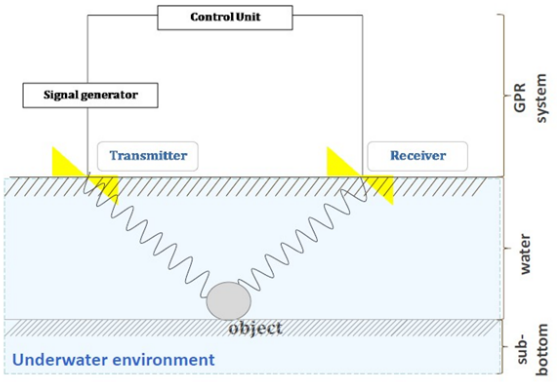


Fig. 1. The GPR system for underwater measurements

B. Continuous wave electromagnetic sensor

In the CWEMS method, the primary magnetic field produced by the transmitter coil is changed in such a way that a higher density of magnetic flux lines occurs due to the presence of metallic objects. The modified magnetic field is detected by a receiver coil. Additionally, eddy currents occur which originate from metallic objects and have an important effect on the induction of the receiver coil field. The CWEMS sensor has proven to be very effective in detecting both ferromagnetic and nonmagnetic metallic targets lying on the sea bottom or buried in the seabed. The scenario for CWEMS monitoring is comprised of the CWEMS sensor composed of eight probes mounted on a wooden pole (Fig. 2). Moreover, the constructed CWEMS sensor was moving on a quadratic holder made from wood to reduce destructive interferences from other objects. For the investigation purposes, samples with simple circular and rectangular cross sections is selected.

The samples are located on the wooden plate with the constant distance from the sensor which was in the range of a few centimetres. The investigated area is limited with dimensions of 45 cm by 90 cm. A special software is prepared to acquire signals from all eight probes simultaneously. The raw signals in a matrix form are imported in the Matlabprogramming environment. In order to obtain a more realistic circular or rectangular cross section of the detected objects, the 2-D interpolation between the data in matrix is applied. Furthermore, the obtained plots are smoothed using a MatLab built-in cubic interpolation function. The final results are visualized as an intensity plot.

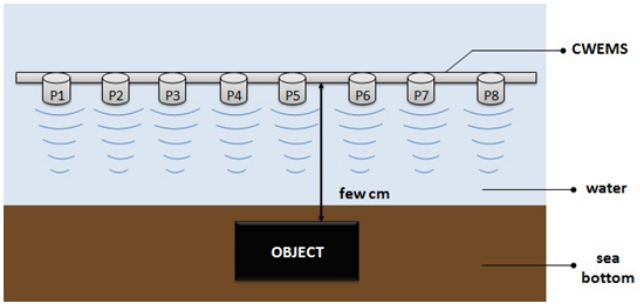


Fig. 2. The CWEMS sensor adapted for underwater operation.

III. Results and Discussion

The calculated GPR profile with a 50 MHz antenna shows that we reached a penetration depth of more than 3 m (Fig. 3, right). A distinct subsurface layer with a depth close to 1 m is also visible in addition to a rather homogenous layer observed up to at least 5 m in depth and possibly even lower. Namely, in the Fig. 3 the depth scale is given in the left-hand scale as the double time needed for the calculation of the electromagnetic waves to travel the distance from the transmitting antenna to the observed object or structure and back to the receiving antenna. In the right-hand scale, this double time is transformed to the real underwater depth, using the velocity of the transmission of electromagnetic waves through the water layer, which is about ten times lower than in the air.

For the subsurface layer, the velocity of the transmission of electromagnetic waves is much larger than in the water, usually three or four times. The size of the homogeneous subsurface layer is therefore much larger than depicted from the scale, and can be estimated to be at least 10 m. From the GPR profile with a 250 MHz antenna the results are similar (Fig. 3, left). While the penetration depth is not as deep as with the 50 MHz antenna, the resolution is better, so it is possible to see a more detailed structure of the first meter of the subsurface layer.

From Fig 3 it is clear that both selected frequencies are useful for the investigation of the subsurface below the lake bottom. The low frequency 50 MHz antenna provides the deep penetration of more than 10 m, and the higher frequency 250 MHz antenna provides a higher resolution of the observed region closer to the surface.

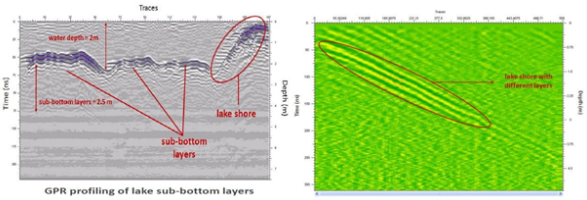


Fig. 3. 250 MHz (left) and 50 MHz (right) lake profiling with the GPR.

The CWEMS method is used to characterize whether the material within the sensor range is metallic or not. Apart from this, we found out that different metallic objects give the various responses. The probes in Fig. 2 are equidistantly positioned on a wooden pole. In this case, we investigated objects with different dimensions and shapes. The raw EM responses were recorded in a matrix form. With the basic imaging method based on cubic interpolation, 2-D images were obtained (Fig. 4). From these images one can notice that not only the shape and orientation of the objects could be detected, but also some information regarding the metal material characterization could be defined. In Fig. 4 there is a major difference in EM responses between aluminium and iron objects, due to the eddy currents which originate in metallic objects and they are particularly expressed in the case of conductor materials such as aluminium and not as much in the case of the ferromagnetic materials such as iron.

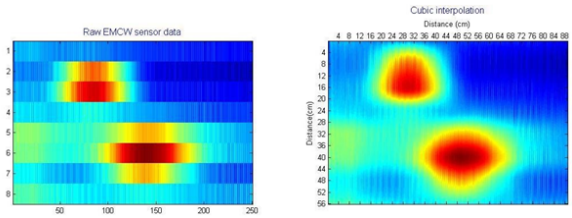


Fig. 4. CWEMS imaging.

IV. Conclusions

We measured the structure of the lake subsurface with a commercial GPR at frequencies of 50 MHz and 250 MHz, respectively. The used GPR system is capable to observe the subsurface below 10 m and through more than 3 m of water with the 50 MHz antenna. However, a more detailed structure can be obtained with a higher frequency 250 MHz antenna at the expense of a lower penetration depth. The GPR method has several potential applications in the general exploration and security of the underwater environment as well as in the oil and gas industry. In addition, we measured and imaged several metal objects of different sizes and shapes with the CWEMS sensor. The discrimination between various metallic object is possible, which makes the sensor appropriate for the underwater security imaging.

Acknowledgment

I would like to use this opportunity to express my gratitude towards my teacher, DR Kp Mishra and my senior Abhimanyu Kacker. Without their constant guidance and motivation this paper would be far from complete.

References

[1] D. J. Daniels, Ground Penetrating Radar, 2nd ed., UK: The Institute of Electrical Engineers, 2004, pp. 1-352.

[2] M. J. Harry, Ground Penetrating Radar: Theory and Applications, 1st ed., The Netherlands: Elsevier Science, 2009, pp. 1-176.

[3] D. Margetis, Pulse propagation in sea water: the modulated pulse, Progress In Electromagnetics Research, vol. 26, pp. 89-110, 2000.

[4] Annan, A. P. GPR Methods for Hydrogeological Studies, In: Hydrogeophysics, edited by. Y.Rubin and S.S. Hubbard, Springer, Netherlands, 2005, pp. 185-213.

[5] I. J. Won, D. A. Keiswetter, and T. H. Bell, Electromagnetic induction spectroscopy for clearing landmines, Geoscience and Remote Sensing, IEEE Transactions on, vol. 39, pp. 703- 709, 2001.

[6] T. Lasri, D. Glay, L. Achrat, A. Mamouni, and Y. Leroy, Microwave Methods and Systems for Nondestructive Control, Subsurface Sensing Technologies and Applications, vol. 1, pp. 141-160, 2000.



Karan Datta I have always been interested in the technological advancements in the sphere of electronics and communication. It all started with my first mobile phone and its subsequent developments and spread in our day to day life. I have now turned into an avid reader of engineering discoveries and try to keep myself abreast with the latest developments. I have produced my first research paper in the field of communication on Underwater Electromagnetic Remote Sensing. I am an alumnus of Sanskriti School, New Delhi and presently am pursuing my interests as a first year student of Electronics and Communication Engineering at Manipal University, Jaipur. My other interests are outdoor sports of Golf and Basketball.

Quick detection of incipient corrosion in AA2024-T3

Prakashaiah B. G. [1], **Deepa M. K.** [2], **Amitha Rani B. E.** [3]
[1,2,3]Surface Engineering Division
CSIR-National Aerospace Laboratories
Bangalore -560017,INDIA
[1]bgprakashaiah@gmail.com, [2]amitharani@nal.res.in

***Abstract*—Corrosion is a universal problem in any engineering industry, the major culprit being invisible corrosion. Aluminum alloy, AA2024-T3 faces major corrosion issues due to the presence of inter-metallic precipitates. Present methods of corrosion detection require time, elaborate infrastructure and a trained technician. Smart coatings or methods which could detect corrosion initiation, preferably visually are need of the hour.**

We report here a quick detection method by using indicator test, wherein, corrosion/self healing could be detected by the naked eye, or with minimum instrumentation even by less trained personnel, as early as a few seconds. Three types of coupons (i) bare, (ii) methacrylate based sol gel coating doped with cerium phosphate loaded nanocontainers and (iii) methacrylate based sol gel coating doped with cerium molybdate loaded nanocontainers were evaluated by this method. The kinetics of corrosion/self healing was evaluated at regular intervals in the presence of 1M NaCl. In the case of the indicator test, distinct changes in pH were observed at low-pH anodic sites and at high-pH cathodic sites. Pit initiation and growth could also be monitored by the indicator method. Pit was initiated within few seconds in the bare coupon, while in the coated coupon it was seen after 6 minutes. However, passivation was seen within few hours.

The mechanism of action was studied by performing accelerated corrosion studies of the coatings, to substantiate and understand the visual observations.

Keywords*—AA2023-T3, sol-gel, indicator test Methacrylate, Cerium phosphate, Cerium phosphate, nanocontainers, Electrochemical impedance studies.

I. INTRODUCTION

Corrosion is an expensive problem for a wide range of industries, affecting almost every facet of our lives and can lead to catastrophic metal failure if undetected.

It is essential to detect corrosion preferably in early stages, to avoid structural damage or loss of function of metals and their alloys. Pitting can be one of the most dangerous forms of corrosion, as it occurs very rapidly, and can penetrate a metal without significant weight loss.

Coatings are frequently used as corrosion protective barriers to protect the metallic substrates and often able to delay the corrosion process, but not completely prevent it. Different approaches have been used to develop a damage-responsive protective coating, such as semi-conducting coatings that serve as an electronic barrier at the metal coating interface, passive barrier sol-gel coatings that can be converted to smart active coatings with the inclusion of corrosion inhibitors in their controllable micro- or nano-structure. One way of preventing failures is to have a coating that can detect and heal localized corrosion.

Many different sensors and techniques are being developed to detect corrosion [1]. Among different technologies, corrosion sensing coatings are highly desired for corrosion control, especially if the signal can be detected through visual inspection by the naked eye, at a stage much earlier than the appearance of the observable corrosion products, at the incipient stages. Corrosion is an oxidative dissolution process whereby, metal atoms lose electrons and are transformed into an ionic species stoichiometrically represented in Equation (1)

$$M \longrightarrow M^{n+} + ne^{-}$$

Oxidation reactions are generally accompanied by reduction reactions that consume the electrons. The main cathodic reaction for any form of atmospheric corrosion is oxygen reduction and is chemically represented by Equation (2) Equations (3)

$$O_2 + 2H_2O + 4e^{-} \longrightarrow OH^{-}$$

and (4) represent the other cathodic reactions that often accompany corrosion, commonly referred to as hydrogen evolution or

$$2H^{+} + 2e^{-} \longrightarrow H_2$$

$$2H_2O + 2e^{-} \longrightarrow H_2 + OH^{-}$$

In localized corrosion such as pitting, crevice, and exfoliation corrosion, the cathodic reaction will tend to occur at more-accessible locations than the anodic reaction, i.e. nearer to the source of oxygen or water in the environment. The cathodic reactions cause an increase in the local pH at the

location where they occur. Therefore, a coating sensitive to pH changes will indirectly sensing corrosion occurring nearby generated by the alteration in pH due to the cathodic reaction.

Recently, pH-triggered release microcapsules have been used for early detection of corrosion and corrosion properties. Indicators have been used for many years to determine the location and mechanisms of corrosion. Some authors have used indicators to locate the presence of anodic and cathodic sites during the corrosion of iron. Gels with indicators were used to illustrate corrosion processes. Some authors have described the advantage of using indicators in early /hidden corrosion detection , while others used a wide range indicator to locate the presence of anodic and cathodic sites during the corrosion of different aluminum alloys [11].

In the present study, a wide range pH indicator was added to agar gel and used as media to locate the presence of anodic and cathodic sites during the corrosion of AA2024-T3. EIS was used to understand the corrosion protection efficiency of the coating and the corrosion mechanism to correlate the visual findings. Commercial hexavalent chromium conversion coating (Alodine) was used as the positive control.

II. EXPERIMENTAL PROCEDURE

A. Materials

Methyl orange, methyl red, phenolphthalein, bromothymol blue, Sodium chloride were purchased from Merck. The precursor silanes, Tetraethyl orthosilane (TE0S, 98), Methacryloxy propyltrimethoxy (MEMO, 98) And Vinyltriethoxy silane (VTEOS, 98) were purchased from Gelest, USA and used as received. Agar Agar was purchased from Hi-media. Nitric acid, Cerium (III) Phosphate (CP), Cerium molybidate(CM) and other solvents were purchased locally. AA2024-T3 aluminum alloy coupons were used as substrate and elemental composition of the alloy is shows in Table 1.

B. surface treatment

The surface of the test coupons was degreased with acetone, followed by chemical etching, which involved dipping in an alkaline aqueous solution for 4 minutes at 60C, followed by 2 minutes dip in nitric acid and finally in NaOH solution with rinsing in Mill-Q water after each step.

C. preparation of ormosil

The ormosil comprising of TEOS, MEMO and VTEOS was prepared as described in [12]. Hydrolysis and condensation was initiated by addition of 0.05N HNO3, and stirred for 1h at 25oC in a closed reactor. The water was supplied by the catalyst solution for complete hydrolysis and condensation through formation of Si-O-Si bonds. The resultant sol was diluted with equal volume of ethanol and used immediately.

D. Preparation of colloidal Ludox silica nanocontainers

Colloidal silica-PE nano-containers were prepared by the method of [13]. These nano-containers comprisedof the following layers (SiO2/PEI/PSS /PEI/PSS/PEI).The inhibitor doped nano-containers were prepared with inhibitor layer sandwiched between the PSS layer and comprised of the following layers (SiO2/PEI/PSS/ inhibitor/PSS/ inhibitor/PEI). The bound inhibitor concentration of the nano-containers was back calculated from the unbound inhibitor in the washes, analysed by spectroscopy. The undoped and doped nano-containers were stored at 8C until further use.

E. Preparation of Ormosil coatings with doped nanocontainers

A pre-determined quantity of undoped/inhibitor doped nanocontainers and ormosil were mixed, diluted with ethanol, and sonicated for one hour, to obtain the desired concentrations of inhibitor. A fixed volume of this mixture was then sprayed on fresh chemically etched AA-2024 coupons and clean glass slides.

F. Preparation of agar gel

The agar gel was prepared according to the modified method of [15]. Agar was added to 1M NaCl boiling salt solution to obtain a 1 wtthe universal indicator was added to the NaCl solution and the hot solution, poured to cast a film (2-3mm thick) and allowed to set. The cast gel was cut into suitable size pieces to cover the exposed area/window of the coupon, and placed directly on the bare and AA2024-T3 coated with different coatings - Ormosil Coating with CP and CM nanocontainers, hexavalent chromium conversion coating Alodine, anodized coupons. The experimental set up for the indicator test was as shown in Fig.1.The rest of the area was covered with a sealing tape or lacquer to prevent environmental induced corrosion and avoid edge effect.

	Substrate Composition (Wt %)								
	Al	Cu	Mg	Zn	Fe	Mn	Cr	Ni	Si
AA 2024-T3	93.52	4.24	1.26	0.08	0.15	0.65	0.01	ND	0.06

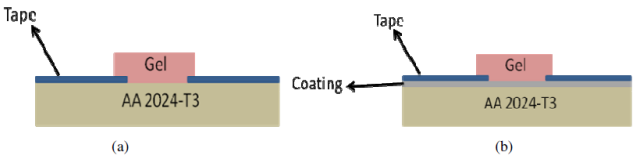


Fig. 1. Experimental set up for indicator test (a) Bare substrate (AA2024-T3) (b) Coated Al-alloy surface.

This experimental set up was placed on moist cotton bedding in an air tight, closed container to prevent drying of the gel slab. The progress of corrosion, changes in the anodic and cathodic sites due to corrosion initiation was recorded periodically and the visual changes captured with a camera.

G. Corrosion evaluation

The corrosion inhibition of the coatings was evaluated by Electrochemical Impedance studies and potentiostatic polarisation.

Chemically etched bare AA-2024, sol-gel coated, and conversion coating commercial hexavalent (Alodine) were potentiodynamically polarized to evaluate their corrosion protection efficiency using IVUM Instrument Electrochemical Workstation. Polarization test was carried out in de-aerated 1M NaCl solution using conventional three electrode cell equipped with the test coupon as working electrode (0.5 cm2) and platinum foil and SCE used as counter and reference electrodes respectively. The reference electrode was connected to a Luggin capillary and the tip of the Luggin capillary was placed very close to the surface of the working electrode to minimize IRu drop. The coupons were immersed in NaCl solution for an hour in order to stabilize the open circuit potential (EOCP). The change in open circuit potential (OCP) were monitored and represented as potential vs. time plot. EIS studies were carried out in the frequency range of 100 kHz 10 mHz with AC amplitude of 10mV. The impedance data was displayed as Nyquist plot - real (Z_{Γ}) vs imaginary impedance (($Z_{\rceil}$) and Bode plot —Z— vs frequency , where —Z— is the absolute impedance. The acquired plots were curve fitted and analyzed using Zman program. After EIS measurements, the system was allowed to attain open circuit potential, then the sample was polarized 200 mV on cathodic to anodic side from the OCP with scan rate of 1 mV/s.

Any recent upcoming systems are always validated for their environment friendliness and their expense in the long run. The problem of these mono nitrogen oxides cumulatively called as NOX has recently been one of the main causes contributing to air pollution .With the help of the proposed system design one can combat this issue along with gaining an increase in the ship speed with a reduction in fuel consumption.

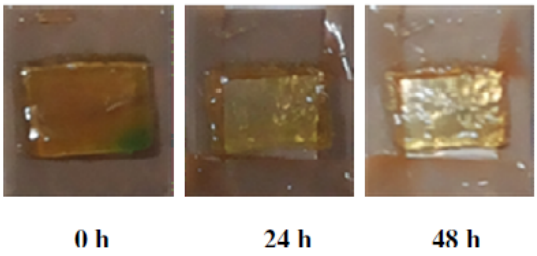


Fig. 2. Corrosion sensing using slab-indicator method on Alodine coated coupons.

Tafel plots obtained have been represented as potential vs. logi plot. The exposed area for EIS studies was similar to the exposed area in the indicator test to reduce the error/disparity due to the presence of intermetallics.

III. RESULT AND DISCUSSION

The results indicated that corrosion could be detected as early as few seconds. It is estimated that in normal environmental conditions, the corrosion that would occur in 1 hour would be visible in one minute by the indicator method. Of all the coatings tested, as expected Alodine/hexavalent chromium conversion coating was the best with no corrosion visible upto 48 hrs of testing period (Fig.2). No pitting or corrosion initiation was observed. Fig 3. shows the results of placing a 2-3mm agar gel on a bare AA2024-T3 surface. We observed that pitting initiated within few seconds. With time, the pit size and number increased, compared with coated coupons. In both sol-gel coated coupons with cerium phosphate and cerium molybdate. (Figs 4 and 5), corrosion was observed after 6 mins, the pit grew in size with time up to 48h. However, of the two inhibitors, cerium phosphate offered higher corrosion protection compared to cerium molybdate. This is evidenced in Fig. 4& 5, where, in coupons coated with sol -gel + cerium phosphate, although the pit was initiated within 6 minutes, it did not grow in size and remained constant almost upto 20h, while in coupons with cerium molybdate, the pit grew in size from 5h (Fig.5).

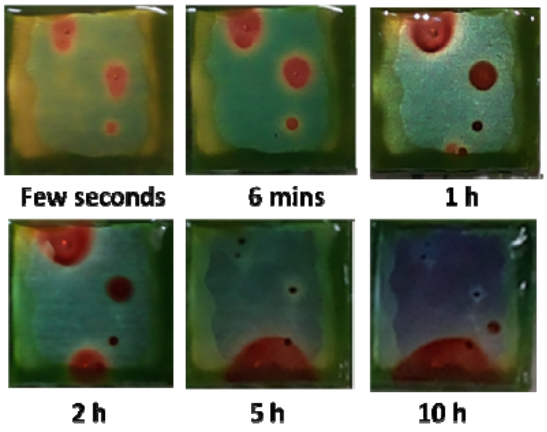


Fig. 3. Corrosion sensing using slab-indicator method on bare coupons.

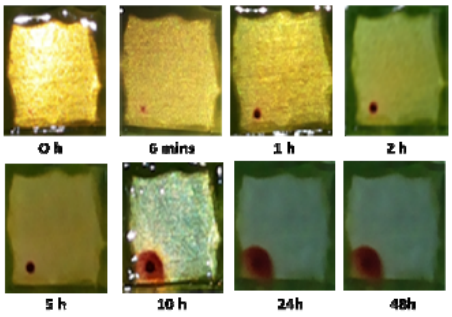


Fig. 4. Corrosion sensing using slab-indicator method on coatings with Cerium Phosphate.

To understand the movement of the inhibitor in aqueous medium, the coated coupons were immersed in both water

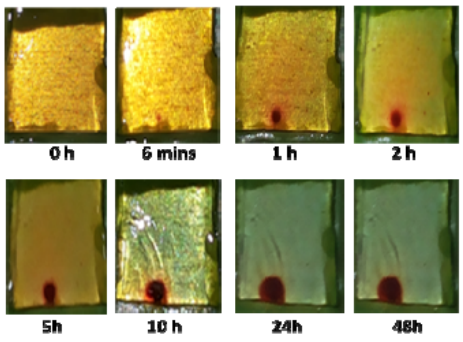


Fig. 5. Corrosion sensing using slab-indicator method on coatings with Cerium Molybdate.

and NaCl solution for 2h, prior to the indicator test. Interesting results were observed after 2h immersion (Figs 6-7). Although pit initiation was seen at 6 minutes in cerium phosphate coatings before immersion, interestingly, the pit reduced in size after immersion for 2h and finally with time, the pit disappeared by 1h (Fig.7). This could be indicative of the self healing property of the coating.

In cerium molybdate coatings, pitting was observed from 6 mins (Fig. 7). The pit size was smaller as compared to coatings without immersion, it gradually increased with time and remained constant, but did not disappear.

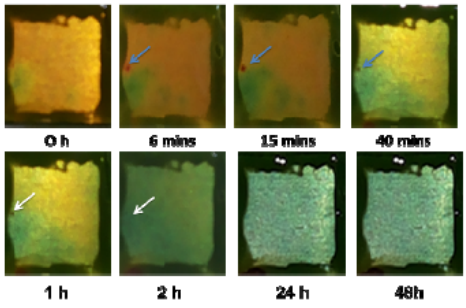


Fig. 6. Corrosion sensing using slab-indicator method on coatings with Cerium phosphate after 2 hour immersed in NaCl solution.

Interestingly, after removing the agar slab and washing the coupons to dislodge the corrosion products if any. No pits were observed in the sol-gel coated coupons (Fig.8).

EDX analysis of the coatings confirmed that the coating was intact in Cerium phosphate and Cerium molybdate (Fig. 9a-b) doped sol gel coatings as revealed by the low levels of Aluminium /substrate (8.2 and 2.4 wt3m.

Potentiodynamic studies also supported this finding

A. *Potentiodynamic studies*

The potentiodynamic polarization was used to evaluate the barriers properties of sol-gel coated aluminum AA-2024 Alloy

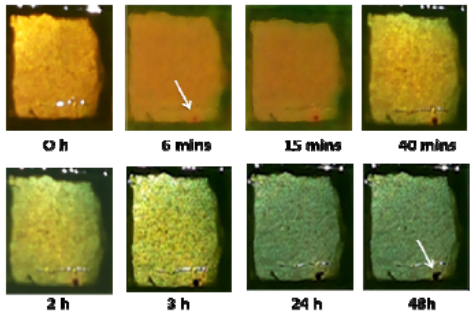


Fig. 7. Corrosion sensing using slab-indicator method on coatings with Cerium molyblade after 2 hour immersed in NaCl solution.

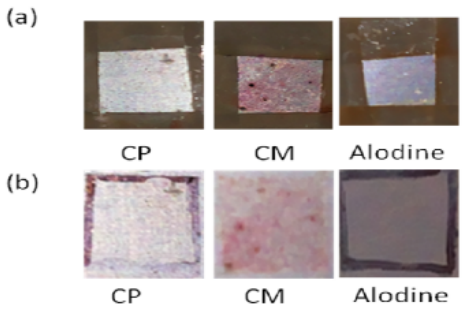


Fig. 8. Corrosion sensing using slab-indicator method after removing the slab (a)- before washing (b) after washing with milli-Q water

in 1M NaCl solution (Fig.10 and Table 2). As it can be seen, all the coated surfaces improved greatly the corrosion resistance of AA2024- T3. The current densities of the coating are 2-3 orders of magnitude lower than that of the bare, indicating lower corrosion rates of the coated AA2024-T3. With immersion, the corrosion efficiency of the coatings with Cerium molybdate increased enormously (Table 2). However, corrosion efficiency of coatings with cerium phosphate increased marginally, but still showed higher corrosion potential than Cerium molybdate. With immersion, the corrosion protection efficiency increased by at least one fold in coatings with inhibitors (Fig. 10, Table 1). The released cerium ion react with the OH ions generated by the cathodic reaction and giving rise to an insoluble oxide/ hydroxide film that precipitates on the alloy surface thereby, inhibiting the cathodic reaction (Equation 3). This insoluble layer is less conductive and reduces the rate of the oxygen reduction reaction. The percentage porosity and protection efficiency (PEpolarization data using the formulae [14].

Where, icorr and icorr are the corrosion current densities of the coating and bare substrate respectively. The corrosion current density was obtained from the intersection of anodic and cathodic curves in the Tafel.

The calculated porosities and protection efficiencies of the coatings are presented in Table 2 and indicated almost 4 times

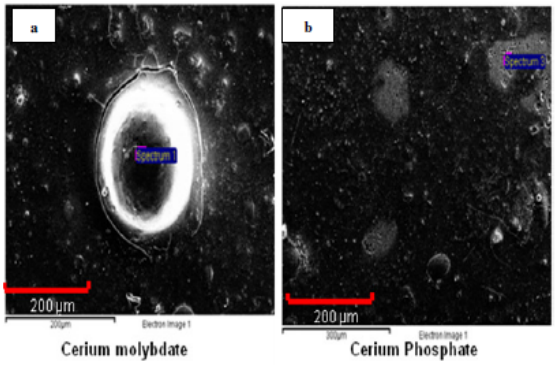


Fig. 9. FE-SEM of the coatings after 48h of indicator slab test.

$$\%\text{porosity} = (R_{ps}/R_p) \times 10^{(-\Delta ECorr/\beta a)} \times 100$$

Where,

R_P – polarization resistance of the coating, R_{ps} – polarization of the bare substrate, β_a – anodic Tafel slope of the bare substrate, ΔE_{Corr} – Difference in corrosion potential of the coated and the bare substrate

$$\text{Protective efficiency, PE (\%)} = \frac{i^{\circ}corr - I\,corr}{i^{\circ}corr} \times 100$$

lower porosity in the coatings with Cerium phosphate compared to Cerium molybdate , explaining its superior corrosion protection efficiency. These results are further corroborated by the decrease in porosity with immersion (Table.2). In both the coatings the porosity decreased with immersion. E corr value shifted towards negative potential indicating that the inhibitor acts as a cathodic protector.

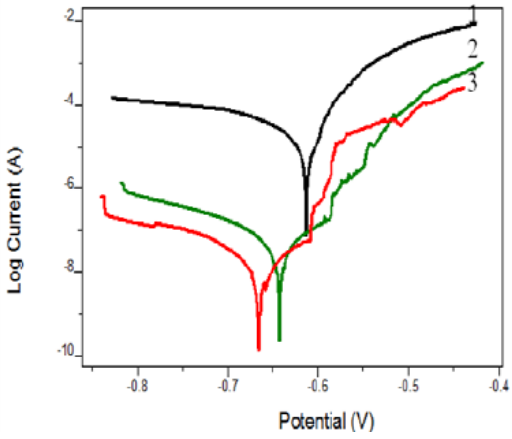
The released cerium ion react with the OH ions generated by the cathodic reaction and giving rise to an insoluble oxide/ hydroxide film that precipitates on the alloy surface there by inhibiting the cathodic reaction (Equation 3). This insoluble layer is less conductive and reduces the rate of the oxygen reduction reaction [15].

IV. CONCLUSION

The indicator test could reveal the corrosion trend within few seconds and also self healing ability of the coating. These findings were further corroborated with potentiodynamic studies and EIS studies which clearly indicated self healing ability of the sol gel coatings.

V. ACKNOWLEDGEMENT

The authors are grateful to Director, NAL for the support. The first author is grateful to NAL for the Junior Research Fellowship. The authors also thank Electroplating section, NAL for the Alodine coated coupons and Mr. Siju for the help in FESEM.



captionTafel curves of polarised sol- gel + Cerium Phophate coatings. (1) Bare (2) Before immersion (3) After 2h immersion in 1M NaCl.

Anodic:

$$Al \longrightarrow Al^{3+} + 3e^{-}$$

Cathodic:

$$O_2 + 2H_2O + 2e^{-} \longrightarrow H_2O_2 + 2OH^{-}$$

$$H_2O_2 + 2e^{-} \longrightarrow 2OH^{-}$$

$$Ce^{3+} + OH^{-} \longrightarrow Ce(OH)_3 \longrightarrow Ce_2O_3$$

REFERENCES

[1] W. L. Dunn, A. M. Yacout, Corrosion Detection in Aircraft by X-ray Backscatter Methods, Appl Radit Isotopes 53, 4-5, (2000): 625.

[2] M. Z. Silva, R Gouyon, and F. Lepoutre, "Hidden Corrosion Detection in Aircraft Aluminum Structures Using Laser, Ultrasonics and Wavelet Transform Signal Analysis, Ultrasonics, 41, 4 ,(2003): 301.

[3] J.H. Ali, W. B. Wang, P. P. Ho, R R Alfano, Detection of Corrosion Beneath a Paint Layer by Use of Spectral Polarization Optical Imaging, Opt Lett 25,17,(2000): 1303.

[4] V. Agarwala, S. Ahmad, "Corrosion Detection and Monitoring - A Review," Proceedings of Corrosion 2000, paper no.271 (Houston, TX: NACE International, (2000).

[5] W. Li and L. M. Calle, "A Smart Coating for the Early Detection and Inhibition of Corrosion," Proceeding of the Smart Coatings 2007 Conference, February (2007),191.

[6] U.R.Evans, Met.Ind. (London) (1926):29,281.

[7] U.R.Evans, The Corrosion and Oxidation of metals (London, U.K: Edward Arnold pub.Ltd.,(1960).

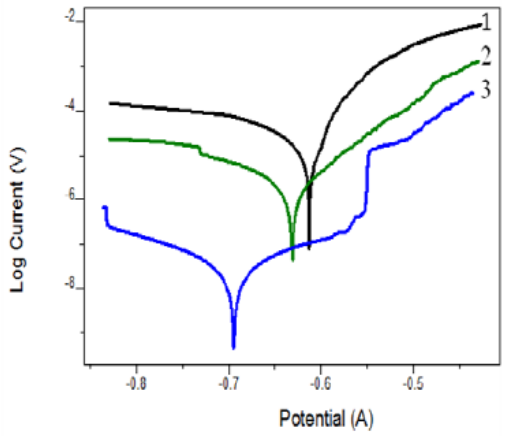


Fig. 10. Tafel curves of polarised sol gel + Cerium Molybdate coatings (1) Bare (2) before immersion (3) after 2h immersion in1M NaCl.

	Immersion time (h)	-Ecorr (V) vs SCE	Icorr (A/cm^2)	C. Rate mm/y	Porosity	Protective efficiency (%)
Bare		0.611	5.25E-5	0.1718	-	-
Cerium molybdate	0	0.632	1.622E-6	0.530E-2	0.168E-1	96.91
	2	0.6962	2.858E-8	9.351E-5	0.82E-2	99.94
Cerium phosphate	0	0.646	9.859E-8	0.32E-3	0.55E-2	99.81
	2	0.6645	1.059E-8	3.464E-5	0.53E-2	99.97

[8] F.L.Laque, T.P.May, H.H. Uhlig, Corrosion in Action (The International Nickel Co., Inc., (1970) in Corrosion and Protection of Light Metal Alloys: Proceedings of Electochemical Society Proceedings, edited by Rudolph G. Buchheit, 2003,23,105.

[9] J. Zhang and G. S. Frankel, Corrosion-Sensing Behavior of an Acrylic-Based Coating System, Corrosion 55 (1999): 957.

[10] Wenyan Li, Jerry W. Buhrow, and Scott Jolley (2010). Microencapsulation of corrosion indicators for smart coatings. NASA Project report

[11] H. S. Isaacs, G, Adzic, and C. S. Jeffcoate, Visualizing Corrosion, Corrosion 56, (2000):971-978.

[12] T.L.Metroke and Apblett. A, Effect of solvent dilution on corrosion protective properties of Ormosil coating on 2024-T3 aluminum alloy, Prog.Org.Coat, 51,1,(2004) 36.

[13] D. G Shchukin, Zheludkevich.M, Yasakau, Lamaka.S, Ferreira. M.G.S, et al,Layer-by-layer Assembled nanocontainers for Self- Healing Corrosion Protection, Adv.Mater ,18 (13) (2006) 1672.

[14] Ho-Gun Kim, Seung-Ho Ahn, Jung-Gu Kim, Se Jun Park, Kwang-Ryol Lee ,Electrochemical behavior of diamond-like carbon films for biomedical applications,Thin Solid Films 475 (2005) 291 297.

[15] Vignesh Palaniel, Y.Huang,Wim J, Van Ooij. Effect of addition of corrosion inhibitors to silane films on the performance of AA2024-T3 in a 0.5 M NaCl solution, progress in organic coatings53(2005),153- 168.

Analysis of effects of the anti-fouling paints on the environment and their economic impact on sea transport

Cdt. MALAY PHADKE
TOLANI MARITIME INSTITUTE,
INDURI, PUNE

Cdt. KSHITISH KUMAR DUBEY
TOLANI MARITIME INSTITUTE,
INDURI, PUNE

***Abstract*—ne of the major challenges that the marine community faces today is how to prevent corrosion and fouling of the most widely used metals and alloys in this field. The marine environment is very hostile to metals due to various factors like the saline sea water, which is a major cause of corrosion not just underwater but also on board, growth and sticking of marine organisms on the underwater parts of the ships cause the repair and maintenance cost of the ships to be very large. There is no second opinion about the fact that marine paints are an indispensible part of the shipping industry. The use of marine paints is the most effective way to prevent corrosion which helps the industry save millions. The counter effect of their use is the high level damage caused to the marine ecology. This lack of balance between the two options i.e. to make profits or to protect the environment forced the I.M.O (International Maritime Organisation) to enforce extremely strict laws regarding the marine pollution issue. Since then the marine pollution has been restricted to quiet a large extent, yet the problem of efficient eco-friendly paint systems (which also contribute majorly toward environment pollution) prevails even today. The need of the hour is eco-friendly paints and various paint techniques, which should not just optimize their use, but also take care of the marine pollution problems caused by them.ne of the major challenges that the marine community faces today is how to prevent corrosion and fouling of the most widely used metals and alloys in this field. The marine environment is very hostile to metals due to various factors like the saline sea water, which is a major cause of corrosion not just underwater but also on board, growth and sticking of marine organisms on the underwater parts of the ships cause the repair and maintenance cost of the ships to be very large. There is no second opinion about the fact that marine paints are an indispensible part of the shipping industry. The use of marine paints is the most effective way to prevent corrosion which helps the industry save millions. The counter effect of their use is the high level damage caused to the marine ecology. This lack of balance between the two options i.e. to make profits or to protect the environment forced the I.M.O (International Maritime Organisation) to enforce extremely strict laws regarding the marine pollution issue. Since then the marine pollution has been restricted to quiet a large extent, yet the problem of efficient eco-friendly paint systems (which also contribute majorly toward environment pollution) prevails even today. The need of the hour is eco-friendly paints and various paint techniques, which should not just optimize their use, but also take care of the marine pollution problems caused by them.O**

The aim of our paper is to create awareness regarding the impact of marine paint systems on the environment. We have discussed briefly upon the history of these paints and latest technological advancement that have taken place with respect to anti-fouling paints keeping in view the reduction of adverse ecological impact. We have also briefly delved upon the financial aspect of painting systems and how they have helped make sea transport more economical with least adverse effects on the marine environment.

I. INTRODUCTION

For the past decade the technological advancements made in the marine industry have been ones which have dramatically changed the working and efficiency of this field. But one such important part of this field MARINE PAINTS was untouched for a very long time. With time there came in need of variety of paints to be applied for specific actions on the ships. In the view of different kinds of the problem it posed, the underwater part of the ship became one of the most interesting places to be looked, worked and developed upon for better efficiency. Besides the need to assure efficient anticorrosive protection it was also necessary to keep the surface as smooth as possible in order to minimise the drag resistance when the ship is in movement and thus to reduce the fuel consumption. This demand was full-filled by the invention of anti-fouling paints which provided prevention against the sticking of wide variety of marine-organisms (both flora and fauna). In the recent decades the anti-fouling paints applied on the ships hull must not only prevent fouling but should also comply with the regulations and legislation laid down by the IMO. Thus the time for something special to be invented is already on the verge, and it need to be done as early as possible.

II. MARINE PAINTS

The anticorrosive protection of steel ships starts in the shipyard, which are now equipped with the automatic blasting and painting plants for both steel plates and steel profiles. The traditional painting systems used were very much into function till the 70s-80s decades, the changes that took place were slow and gradually occurring. In the recent decades the paint systems used in shipbuilding have undergone enormous development in correspondence with the emerging legislation, especially those related with protection of the environment and human health. These developments have concentrated above all reducing volatile organic compounds (VOC) contents and eliminating toxic and carcinogenic components from traditional paint products. Table 1 lists several examples of typical systems currently used in different critical areas in ship

painting. Underwater and boottop areas have been excluded from the following table.

TABLE 1 Examples of typical paint systems currently used in different critical area of ship painting [1].

Critical areas in ship painting	Main requirements	Typical paint systems
Sides and superstructures	Appearance, anticorrosive protection, wash ability, U.V. resistance	• Pure or modified epoxy primer. • Aliphatic polyurethane • Polysiloxane/epoxy hybrid
Decks	Appearance, anticorrosive protection, wash ability, U.V. resistance, non-slip	• Zinc silicate followed by two pack epoxy/polyurethane • Trowel-or-roller-applied elastomer • Topcoats should include aggregates like aluminium oxide, silica etc. To provide non slip properties.
Tanks – ballast	Resistance to alternating contact with sea water and with transported product.	• Modified epoxy • Special waterborne asphaltic emulsion. • Cement reinforced acrylic
Cargo • Crude or petroleum • Oils or hydrocarbon • Very aggressive products	Resistance to contact with specific cargo types.	• High-solid or solvent free plyamine-cured epoxy • High solid polyamine epoxy • Epoxy cyclosilicone

III. Protection of Underwater Ship Parts

It is mandatory the protective underwater coating systems should include anticorrosive primer and an antifouling topcoat. If the anticorrosive part of the coating negatively affects the adhesive properties of antifouling paints a suitable intermediate primer coat is applied. Modern paint systems typically include two pack epoxy primer. In view of the fact that fibre glass improves mechanical strength the water vapour impermeability, there has been a significant increase in the use of this material as reinforcement for the aforementioned primers, especially in the boottop area of the ships, which is subjected to considerable mechanical forces and to periods of exposure to the atmosphere. For economic reason, underwater hull of the ship should be kept smooth, so as to reduce the drag resistance and thus minimise the fuel consumption [1].

IV. Interaction Between Underwater Ship Hull and Sea Water

The rise in the price of fuel, increasing demand and limitations to the supply of oil are important incentives to maintain ship hulls in a smooth and fouling free condition. This is at a time when the most successful antifouling coating ever developed, the self-polishing copolymer organotin based coatings, are no longer available due to unacceptable environmental impacts on non-target marine organisms (Champ 2003, International Maritime Organization 2001, Swain 1999). The transfer to replacement technologies has created the need to identify the most efficient and cost effective system that will match an individual ship and its mode of operation. A considerable part of the power required to move ships is to overcome the frictional resistance between the ships hull and water. For low speed ships (bulk carriers and tankers) it may constitute some 70 - 90

V. Antifouling Paints

Fouling

Fouling is the undesirable growth of organisms on artificial structures immersed in seawater. The most visible form of such fouling are barnacles and seaweed which degrade the performance of ships considerably. Worldwide, the cost of keeping marine fouling at bay is estimated to at least 1.4 billion dollars a year, Clare (1995). For conventional ships, 50-80

Historical development of antifouling methods (from Bertram, 2000)

Ancient	Resistant wooden ship - coating of coal tar, oil, and wax - wooden and metallic (lead, copper) sheathing
1850 - 1900	Resistant wood and iron ship copper sheathing, galvanic action for iron "patent paints", almost Ineffective "Italian Moravian" hot plastic paint, fairly effective
1900 - 1950	Antifouling paint - various binders and copper oxide - hot plastic paint, followed by cold plastic paint
1950- present	Antifouling paint -Insoluble or soluble matrix used, containing copper oxide and mercuric oxide as toxics - organotin and copper oxide combinations - organotin polymer antifoulant (self-polishing co-polymer)
present - future	Paint and system - low and non toxic paint - electrolysis technology of seawater by electro-conductive coating system - use of copper alloy etc. - Low surface-energy paint

VI. What Led to Development in Anti-Fouling Paints?

Significant advances in the paint technology came about with the demand for higher performance, longer life coatings. These were eventually realized by the progressive introduction and development of synthetic raw material and intermediates helping not only to alleviate the restrictions imposed on the paint chemist by traditional technology but also to establish a much more scientifically based industry. Reproducible products with predictable performance resulted. In the years from 1970-2000 there were significant studies made to review the environmental impact of antifouling paint systems being used in the industry. The results were extremely shocking which forced the I.M.O to lay down strict rules.

During the 1960s the chemicals industry developed efficacious and cost-effective anti-fouling paints using metallic compounds, in particular the organotin compound tributylin (TBT). By the 1970s, most seagoing vessels had TBT painted on their hulls. However, it soon became clear there was a price to pay for the efficient anti-fouling paints containing TBT. Environmental studies provided evidence that organotin compounds persist in the water and in sediments, killing sea life other than that attached to the hulls of ships and possibly entering the food chain. Specifically, TBT was shown to cause shell deformations in oysters; sex changes (imposex) in

whelks; and immune response, neuro toxic and genetic affects in other marine species.

In the 1970s-1980s, high concentrations of TBT in shellfish on the coast of France caused the collapse of commercial shellfisheries in at least one area, and this prompted many States to act and enforce some restrictions on the use of TBT in anti-fouling paints. In 1988, the problem was brought to the attention of the Marine Environment Protection Committee (MEPC) of the International Maritime Organization (IMO), the United Nations Agency concerned with the safety of shipping and the prevention of marine pollution.

As a result, IMO in 1990 adopted a resolution recommending governments to adopt measures to eliminate anti-fouling paints containing TBT. In the 1990s, the MEPC continued to review the environmental issues surrounding anti-fouling systems, and in November 1999, IMO adopted an Assembly resolution that called on the MEPC to develop an instrument, legally binding throughout the world, to address the harmful effects of anti-fouling systems used on ships. The resolution called for a global prohibition on the application of organotin compounds which act as biocides in anti-fouling systems on ships by 1 January 2003, and a complete prohibition by 1 January 2008. In October 2001, IMO adopted a new International Convention on the Control of Harmful Anti-fouling Systems on Ships, which will prohibit the use of harmful organotin in anti-fouling paints used on ships and will establish a mechanism to prevent the potential future use of other harmful substances in anti-fouling systems [1].

VII. Law regarding anti-fouling paint systems

Annex I attached to the Convention states that by an effective date of 1 January 2003, all ships shall not apply or re-apply organotins compounds which act as biocides in anti-fouling systems, and by 1 January 2008 (effective date), ships either:

(a) shall not bear such compounds on their hulls or external parts or surfaces; or (b) shall bear a coating that forms a barrier to such compounds leaching from the underlying non-compliant anti-fouling systems. This applies to all ships (except fixed and floating platforms, floating storage units (FSUs), and floating production storage and off-loading units (FPSOs) that have been constructed prior to 1 January 2003 and that have not been in dry-dock on or after 1 January 2003. Ships of above 400 gross tonnage and above engaged in international voyages (excluding fixed or floating platforms, FSUs and FPSOs) will be required to undergo an initial survey before the ship is put into service or before the International Anti-fouling System Certificate is issued for the first time; and a survey when the anti-fouling systems are changed or replaced. Ships of 24 metres or more in length but less than 400 gross tonnage engaged in international voyages (excluding fixed or floating platforms, FSUs and FPSOs) will have to carry a Declaration on Anti-fouling Systems signed by the owner or authorized agent. The Declaration will have to be accompanied by appropriate documentation such as a paint receipt or contractor invoice. Anti-fouling systems to be prohibited or controlled will be listed in an annex (Annex 1) to the Convention, which will be updated as and when necessary.

Tributyltin (TBT) - harmful effects on the environment

Water and sediments	Tributyltin - organotin compound (TBT) is a broad spectrum algicide, fungicide, insecticide and miticide used in anti-fouling paints since the 1960s. TBT is toxic to humans. TBT can be broken down in water under the influence of light (photolysis) and micro-organisms (biodegradation) into less toxic di- and monobutyltin. Half-life varies from a few days to a few weeks, but decomposition is slower when TBT has accumulated in sediment - if oxygen is completely excluded, TBT half-life maybe several years. Therefore waters with heavily sedimented bottoms - such as harbours, ports, estuaries - are at risk of being contaminated with TBT for several years.
Shell malformations	TBT causes thickening of shells in sea oysters, caused by disturbance of calcium metabolism.
Imposex	Recorded in marine snails: females develop male sexual characteristics. Imposex has been recorded in 72 marine species. Concentration of just 2.4 nanograms of TBT per litre needed to produce sexual changes in dog-whelks, leading to sterility.
Marine mammals	Traces of TBT have been found in whales, dolphins and members of the seal family in the United States, south-east Asia, the Adriatic Sea and the Black Sea. The TBT is absorbed via the food chain.
Reduced resistance to infection	Research has shown TBT reduces resistance to infection in fish such as flounder and other flatfish which live on seabed and are exposed to relatively high levels of TBT, especially around areas with silty sediment like harbours and estuaries.

Ref: TBT in antifouling paints: National Institute for Coastal and Marine Management/RIKZ, Netherlands. MEPC

VIII. Why were TBTs release a problem?

The biggest breakthrough came in this field with the invention of self-polishing copolymer paints in the era of 1970s. But even the SPCs were biocide releasing paints. They were able to minimise the fuel consumption cost by upto 6

IX. Modern painting systems

Current technologies employ two basic strategies for non-biocidal coatings anti-fouling (deterrence of initial attachment) and fouling-release (weaken adhesion strength so the organisms can be easily removed). Both strategies, in principle, leave the fouling organisms unharmed and without releasing toxic chemicals into the organism or the marine environment.

X. Low surface energy, nonstick, fouling release technology

Non-stick fouling release coatings are based on a technology which initially prevents the adhesion of fouling organisms by providing a low-friction, ultra-smooth surface on which organisms have great difficulties adhering. Many sessile species rely on attaching mechanism involving some kind of glue, with the adhesion strength highly dependent on the ability of this glue to spread over the surface and bind physicochemical to it. For a given amount of glue, the higher the surface tension of the substrate the better the glue can wet the surface and the higher numbering of anchoring points translating into better adhesion of the organism. Some organisms, such as the blue mussel (callow et al., 2005), seem to compensate the latter by secreting larger amounts of glue when in contact to low surface energy surfaces. These fouling release coatings rather than killing the marine life makes it difficult for them to stick on the underwater surfaces.

XI. Self polishing copolymers

The main developments in TBT-free SPC antifoulings have been pioneered by Japanese paint companies, in response to the TBT application ban which was introduced in Japan in

the early 1990s. A series of new acrylic polymers have been synthesized which attempt to mimic the chemistry of TBT in seawater. There are three main types:

Copper Acrylate

Silyl Acrylate

Zinc Acrylate

The first of these to be introduced was the copper acrylate system, launched in 1990 under the brand name Ecoloflex SPC, by Nippon Paint Marine Coatings. The copper acrylate polymer reacts with seawater in exactly the same way as the TBT SPC co-polymer, producing a soluble micro-layer at the paint surface, resulting in the gradal polishing away of the coating. This mechanism ensures that there is no leached layer build up over time, and that the biocides in the system are released in a controlled way, to give long-term fouling protection, and with lifetime proportional to the thickness applied. The biocides in the Ecoloflex SPC products are copper oxide and zinc pyrithione. Copper itself is safe to man and the environment when used in antifouling paints for ships, and is registered for use as an antifouling biocide in products for commercial vessels with government authorities around the world. It is clearly accepted that its use in antifouling paints is much safer to the environment than TBT. Zinc pyrithione is degraded and becomes non-toxic quickly after release from the coating. It is not persistent and will result in minimal impact on the marine environment.

The other major use of zinc pyrithione is as an anti-dandruff agent in shampoos. As many thousands of tonnes of this substance is applied to human hair each morning and subsequently discharged into the environment via sewage treatment works without incident, its safety to humans and the environment is proven. Ecoloflex SPC products have been applied to the complete underwater hull of over 1,350 commercial vessels greater than 4,000 dwt. At present there are more than a dozen ships currently in-service with five year Ecoloflex SPC systems applied to the entire underwater hull. One of these has now completed 53 months in-service and a recent underwater inspection showed that performance was good. The Royal Australian Navy has also been carrying out long-term testing of Ecoloflex SPC on Patrol Boats, and after 64 months Ecoloflex SPC showed exactly equivalent performance to the standard TBT-SPC product used. This was far superior to the other tin-free products tested, which were all of the Controlled depletion type [4].

XII. How do SPCs work?

SPC technology antifouling work because the film contains a patented resin called an SPC-copolymer. This copolymer reacts with saltwater in a controlled way and as a result of the controlled reactions he biocide release is sustained throughout the lifetime of the paint without decline. The chemical reaction will take place at the same rate whether the vessel is underway or docked.

XIII. Tin-free controlled depletion paints (CDPS)

These paints which constitute the first generation of tin-free antifouling paints, are no more than a development of traditional soluble matrix paints, whose binder is reinforced by organically synthesized resins which are more resistant than resins and control the dissolution of the soluble binder. However, their working mechanisms are assumed to be similar to those of conventional resin-based paints. These paints are known as ablative paints, they contain a large proportion of physically drying, nontoxic, sea water-soluble binder, combined with polymeric ingredients capable of controlling the relative rate of the dissolution mechanisms by means of physical processes. General properties of these paints, mention may be of the longer than 3 years protection period that they can afford, their toxicant release economy, roughness control, and the fact that they do not need a tie coat during repainting in the dry docks, beside being less expensive than the TBT-based self-polishing paints. They are widely used on small boats and leisure vessels with relatively short service times.

XIV. Modern advancements in antifouling technology

Recently, anti-fouling methods inspired by living organisms have become the subjects of intense research by scientists looking for more environmentally friendly and effective ways of reducing biofouling. This type of design imitation is known as biomimicry. Biomimetic design describes the process of using living organisms as the inspiration for new functional materials. For instance, many large and slow moving marine animals like whales are able to effectively prevent biofouling on their skin. For marine anti-fouling purposes, biomimetic designs typically fall into two categories: physical and chemical.

Mussel adhesive proteins

One of the more common methods of anti-fouling come from growing polymer chains from a surface, often by poly(ethylene glycol) or PEG. However, challenges exist in creating a functionalized surface to which PEG chains may be grown from, especially in aqueous environments. Researchers have been able to study the methods by which the common blue mussel Mytilus edulis' is able to adhere to solid surfaces in marine environments using mussel adhesive proteins, or MAPs.

Barnacle cement

Similar to MAPs, barnacle cement is composed primarily of adhesive proteins. The composition of barnacle cement is known to be both non-toxic and stable over a long period of time and also shows a significant attachment strength as an adhesive. The sequence and composition of these proteins is highly dependent on the surface of attachment, allowing for the barnacle so securely attach to a number of surfaces. Barnacle cement proteins contain a significant amount of hydroxyl groups which can be used as starting points to grow antifouling polymer brushes from using ATRP using Atom Transfer Radical Polymerization (ATRP).

Shark skin

Shark skin, alongside that of many other large marine animals such as dolphins and whales, exhibits a high degree of nanoscale surface roughness that imparts a low wettability

which limits biofouling. The surface of shark skin consists of nanoscale overlapping plates that exhibit parallel ridges that effectively prevents sharks from becoming fouled even when moving at slow speeds. A commercial shark skin analogue coating has been developed at the University of Florida under the name of Sharklet AF.

XV. Economic impact of paints on sea transport

For comparing painting on the basis of costs involved. We can compare them on the basis of many factors and categories like paints ban, enclosed work areas, collection and disposal of wastes, sealed hard stand, approved handler, PPE requirements.

Expected Effects

Summary of Impacts

Category	Small boats	Large boats	Total
Paint bans	Some increase in costs: 5-10% in short run for those using banned paints; negligible in long run	Some increase in costs: 5-10% in short run for those using banned paints; negligible in long run	Less than $0.2 million per annum
Enclosed work areas	Can be managed through brush and roller painting. Fence screening likely to be acceptable	Potentially high costs if full encapsulation is required	Costs depend on whether complete enclosure is required. High costs for large boats
Collection and disposal of waste	Filtration systems equivalent to $120-170/marina berth	Mostly in place	$1-1.5 million for filtration systems
Sealed hard stand	80-85% of marinas already have sealed hard stands	Not applicable	$1.7-2.6 million up-front or $260-390,000 per annum.
Approved handler	Some impact – cost for DVD or on-line training (less than $100 per person)	Small impact	Total of less than $0.5 million
PPE requirement	Up-front costs of approximately $40	No impact – professional painters likely to have equipment already	$0.3 million
Total		<$5 million pa	

XVI. Paint Prices

To estimate the expected increase in costs we show retail prices. The cheapest variety currently on the market is the Diuron-based Awlcraft (also known as Coppercoat) imported by International Paints (Akzo Nobel). This is the only retail paint identified that would be affected by the ban. Alternatives to Awlcraft include the copper-based Warpaint available from small local producer Wet & Forget (a 9% increase in price) and thiram-based No.5 imported by Altex (a 19% increase in price). However, these price differences are based on a simple snapshot of prices in November 2012; prices change over time in absolute and relative terms. For example, a check on prices in 2011 from Smart Marine showed that Altex No.5 was at that time slightly (5%) cheaper than Awlcraft4 rather than the 19% more expensive that it is currently. Altex No. 5 is one of the most commonly used paints currently, so it is unlikely that it would retain a permanent price disadvantage. We have also observed that commercial operators offering painting services will allow purchasers the choice of either Altex or International Paint options, with no impact on price; the implication is that the prices are broadly the same.

Retail paint prices (including advertised discounts for card holders) November 2012.

Paint	Ingredient	Manufacturer/importer	Price ($/l)	% above
Awlcraft	Diuron	International Paints	39.75	
Warpaint MFI	Copper	Wet & Forget	43.50	9%
No 5	Thiram	Altex	47.25	19%
Ultra	Dichlofluanid	International Paints	62.25	57%
Micron Extra	Dichlofluanid	International Paints	67.25	69%
Trilux	Dichlofluanid	International Paints	72.25	82%
Pettit Vivid	Zinc pyrithione	Altex	100	150%
Micron 66	Zinc pyrithione	International Paints	121	203%

XVII. PPE Costs

International Paints (Akzo Nobel) recommends a number of Personal Protective Equipment (PPE) items should be used when applying antifouling paint. We have included an indicative price range from NZ Safety for each item (Table 5). The average cost is approximately $538 (based on 1 litre of barrier cream) for a professional painter. However, as professional painters are expected to own and use this equipment currently, the cost of compliance would be minimal.

Possible costs for Personal Protective Equipment

PPE	Azko Nobel Recommendation	NZ Safety Price Range
Face Mask	"Spray application will require the use of full face masks and respiratory protection"	$316 - $414
Gloves	"Chemical resistant gloves should be worn"	$5 - $81
Overalls	"A cotton overall (minimum 60% cotton) with full length sleeves and legs should be used"	$92 - $131
Barrier Cream	"Barrier cream should be used on exposed skin"	$13 - $24 (per litre)
Total		**$426 - $650**

Costs of DIY PPE

	Cost	Proportion	Number	Cost
Brush & roller	$30	75%	5,280	$158,400
Spray paint	$65	25%	1,760	$114,400
Total	Weighted average = $39	100%	7,040	$272,800

Acknowledgment

We would like to thank our principal Dr. B.K. Saxena, faculty members Mr. Bhaskar Walimbe and Mrs. Puja Awachat for their endless support and guidance that they gave us throughout our task of writing this technical paper. We would also like to show our gratitude towards all the faculty members who have assisted us through this paper.

References

[1] Marine Paints: particular case of antifouling paints by Elisabete Almeida.

[2] MEASURING THE PERFORMANCE OF TODAYS ANTIFOULING COATINGS Geoffrey W Swain, Brett Kovach, Arthur Touzot, Franck Casse, Christopher J Kavanagh.

[3] Focus on IMO Antifouling Systems (2002) released by IMO.

[4] M. Candries (2000), Paint systems for the marine industry, Notes to Complement the External Seminar on Antifoulings.

[5] Non-toxic Polymer Coatings for Fouling-Resistant Marine Surfaces - Windy Turchyn.

[6] Survey of Corrosion Cost in Japan- Japan Society of Corrosion Engineering.

[7] NATURAL PRODUCTS BASED ECOFRIENDLY ANTIFOULING PAINTS Bharati Phate Burande, Bhalchandra B. Gogte.

[8] Economic analysis to support the reassessment of antifouling paints - Tim Denne and Stephen Hoskins.

[9] HOW FOULING RELEASE COATINGS CAN SUPPORT YOUR FUEL EFFICIENCY - Sijmen ViSSer.

[10] Making Dollars and Sense of Nontoxic Antifouling Strategies for Boats Making Dollars and Sense of Nontoxic Antifouling Strategies for Boats - Leigh Taylor Johnson, Marine Advisor and Jamie Anne Miller.

[11] Wikipedia.

[12] Google search engine.

WASTE GENERATION & HANDLING ON BOARD THE VESSEL

Cadet Anubhav Kumar[1], **Cadet Rohit Kumar**[2]
[1,2]Marine Engineering & Research Institute, Indian Maritime University-Mumbai Campus, Mumbai, Maharashtra-400033
[1]anubhavgotam@gmail.com
[2]rohitsh223@gmail.com

***Abstract*—The scope of this paper is to address all types of waste generated on board, how the on board waste management process is managed, and to seek ways to handle this process in a more environmentally responsible way. The paper is divided into: Waste generated onboard and its environmental impact, waste management activities today and future more environmentally friendly ways. A description of the process and organisation and how it works today is done. What rules and regulations that we need to comply with, both onboard and in the ports is described. A main obstacle for introducing a more environment responsible process that can handle waste generation and treatment is the lack of continuity between the onboard waste management processes and the respective processes ashore. Waste, properly sorted and shredded or compacted onboard, is normally dumped into one container and sent to a landfill, or in best case incinerated. This paper describes an environmentally responsible way of combining the waste management processes onboard and ashore and thereby provides both Ship Owners and Port Authorities with a documented process for showing Corporate Social Responsibility and Environmentally Responsible waste management. The main philosophy is to use the 3R's. Reduce, Reuse or Recycle. A possible pilot project "Waste to Values" (W2V) is proposed.A table describing all types of waste, its impact on the environment and how it is treated is also presented in the paper.**

I. Introduction and background information

Background

In light of the climate crisis and enhanced focus on environmental protection, players at all levels are called upon to make a contribution to turn the development and/ or limit the impact of environmental pollution. The shipping industry has traditionally been regarded as a major contributor to environmental pollution. Through several initiatives the Norwegian Ship-owners Association has had the intention to initiate and coordinate efforts which can make the industry greener and through this improve the shipping industrys reputation in society. The working group NSA Environmental initiative consists of several other ship owning companies who want to make an effort to improve environmental performance in the shipping industry.

The 1973 MARPOL Convention sought to eliminate and reduce the amount of garbage being dumped into the sea from ships. Under Annex V of the Convention, garbage includes all kinds of food, domestic and operational waste, excluding fresh fish, generated during the normal operation of the vessel and liable to be disposed of continuously or periodically. Annex V totally prohibits of the disposal of plastics anywhere into the sea, and severely restricts discharges of other garbage from ships into coastal waters and "Special Areas". Despite the entry into force of Annex V in 1988, even recent surveys carried out in the United States each year have produced up to 10 tons of garbage per mile of coastline, a record that can probably be matched in many other parts of the world. Plastic forms the biggest single item found. (Ref. IMO Web page / Conventions / Marpol Annex V) Persuading people not to use the oceans as a rubbish tip is a matter of education - the old idea that the sea can cope with anything still prevails to some extent but it also involves much more vigorous enforcement of regulations such as Annex V. The Annex V also obliges Governments to ensure the provision of facilities at ports and terminals for the reception of garbage.

However, even if the MARPOLs Annex V has been in force for almost 20 years, and the ports have been required to receive the waste from ships, not much has happened on the port side to reflect the marine regulations. It is unacceptable and frustrating to see in most ports that well-sorted waste from the ships are thrown into one and the same skip and taken away with no evidence of any responsible treatment of the waste after this has been landed. The ship-generated waste is mostly incinerated or taken to a landfill, even if the domestic waste from the same port city is recycled. The waste service providers are predominately local waste handlers with little or no commitments to environmental responsible waste treatment. There is a total lack of standardization on port level and virtually every port has its own local way how to manage waste returned from ships with different waste notification forms to fill in and individual charging regimes for waste management services. Some ports are charging for landing waste, others are charging for not landing waste. Environmental conscious owners that enforcing a strict environmental control of their ships do like to see a port side service that can document environmental responsible treatment of the waste and see to that the good waste management job done aboard is respected when the waste is finally land.

Objective

To identify and evaluate existing as well as new technical and operational solutions for reducing wastes generated from

ships and managing the waste on the most environmentally responsible way.

Scope & description

The Section II explains the concept of adaptive filtering. In Section III, the steps for different adaptive algorithms are discussed. The simulation results achieved are presented in Section IV. Section V gives the concluding remarks.

1) Identify types of wastes generated onboard.
2) Describe the aspects and impacts from the wastes generated onboard.
3) Perform a fact finding study to see what procedures, equipment and initiatives that focus on reducing waste generated and the respective handling and treatment processes of these wastes, both onboard and ashore.
4) Identify areas for cooperation between members in order to become more environmental responsible in the Waste generation and Handling process.

To address the totality in the project the following approach has been taken;

Functional approach:

- How waste is handled and treated onboard ships today?
- How is waste handled and treated ashore today?
- Where can we look for areas for improvement in a systematic manner?

Holistic approach:

For embracing the fact that better waste handling is dependent on;

- Processes (on board/ashore)
- Technology utilization
- Organization (knowledge/training/efficiency)
- Supplier involvement in reducing packing material etc.

Sources of information

Main source of input has been participating members aggregated know how and experience in environmental technologies. In addition, Bellona has been involved as a sparring partner to complete a list over what actions can be taken to avoid contamination caused by wastes generated onboard.

Terminology and abbreviation

Food Wastes are any spoiled or unspoiled victual substances, such as fruits, vegetables, dairy products, poultry, meat products, food scraps, food particles, and all other materials contaminated with such wastes, generated onboard ships, principally in the galley or dining areas. Plastic means a solid material which contains as an essential ingredient one or more synthetic organic high polymers and which is formed (shaped) during either manufacture of the polymer or the fabrication into a finished product by heat and/or pressure. Plastics have material properties ranging from hard and brittle to soft and elastic.

Cargo associated waste means all materials which has become wastes as a result of use onboard a ship for cargo handling and stowage. Cargo associated waste includes but is not limited to Dunn age, shoring, pallets, lining and packing materials, plywood, paper, cardboard, wire and steel strapping. Maintenance waste means materials collected in the engine department or deck department while maintaining and operating the vessel, such as soot, machinery deposits, scraped paint, deck sweeping, wiping wastes and rags. Operational wastes means all cargo associated waste and maintenance waste, and cargo residues defined as garbage under cargo residues.Oily rags are rags which have been saturated with oil as controlled in Annex I to the convention. Contaminated rags are rags which have been saturated with a substance defined as harmful substances in the other Annexes to the convention.Cargo residues are the remnants of any cargo material onboard that cannot be placed in proper cargo holds or which remain in cargo holds and elsewhere after unloading procedures are completed.

II. Results

Waste Reduction activities today and after treatment/handling

The philosophy behind waste treatment can be described in the following order (the 3 Rs):



Starting with Reduce (waste not generated does not require treatment), reuse whatever can be reused and send remaining waste for recycling. What cannot be addressed by the three Rs should as far as possible be incinerated with energy recovery. Typical equipment onboard used in the Waste handling process is:

WILHELMSEN SHIP MANAGEMENT
GARBAGE MANAGEMENT PLAN

Equipment and Processing of Garbage:

1) Listed in the table below are the description, capacities and probable locations of the equipment utilised in processing various garbage.
2) The Department Heads are responsible for ensuring that the personnel operating and maintaining the equipment listed above are properly trained to do so. The Cheif Engineer should be consulted for detailed operating instructions and maintenance manuals.
3) Waste not incinerated are stored as per ch.9.2 until disposal to facilities ashore.
4) As a guide the functions and characteristics of various processing devices are as follows:
   - Compactors
     Comactors make garbage easier to store, to transfer to port reception facilities and to dispose of at sea when discharge limitations permit.

Type of Equipment	Location	Wastes Processed	Processed Waste
Galley comminuter or Grinder	Galleys	food waste	Into the sea and/or dried and incinerated.
Shredder Machine	Engine room	Bottles, glass, crockery	Bagged and stored until landed ashore
Bale Compactor	Engine room	Cardboard and paper	Bundled and stored until landed ashore or incinerated
Densifier	Engine room	Tins, cans, metal	Bundled and stored until landed ashore
Garbage Shredders	Engine room	Burnable waste	Incinerated
Incinerators	Engine room	Burnable waste	Ash bagged and stored until landed ashore

- Comminuters/grinders
  Ships operating primarily beyond 3 nautical miles from the nearest land are encouraged to install and use comminuters to grind food wastes to a particle size capable of passing through a screen with openings no larger than 25 milimeters. Such a process is recommended even beyond 12 nautical miles because the particle size hastens assimilation into the marine environment.
- Incinerators
  Marine incinerators are predominantly designed for intermittent operation, hand fired.

It is also fully legal to dump some of the waste overboard, following certain procedures :

WILHELMSEN SHIP MANAGEMENT
GARBAGE MANAGEMENT PLAN

SUMMARY OF GARBAGE DISPOSAL TO SEA FOR ALL SHIPS EXCEPT OIL PLATFORMS***		
Material	**Outside Special Areas**	**In Special Areas****
Plastics – Including but not limited to synthetic ropes, synthetic fishing nets, plastic garbage bags and incinerator ashes from plastic products which may contain toxic or heavy metal residues	***Disposal Prohibited***	***Disposal Prohibited***
Cargo residue, Floating Dunnage, Lining and packing materials	More than 25 miles from nearest land	***Disposal Prohibited***
Paper, rags, glass, metal, bottles, crockery and similar refuse	More than12 miles from the nearest land	***Disposal Prohibited***
All other garbage including paper rags, glass, etc. comminuted or ground*	More than 3 miles from the nearest land	***Disposal Prohibited***
Food waste not comminuted or ground	More than 12 miles from the nearest land	More than 12 miles from the nearest land
Food waste comminuted or ground*	More than 3 miles from the nearest land	More than 12 miles from the nearest land
Mixed refuse types	****	****

Designated Personnel Responsible for Carrying Out Plan

Chief Officer

Assisted by:

1. Chief Engineer
2. Department Heads
Environment Engineer (if available)*

Summary disposal requirements at sea in & outside special areas

Process and organization

Ensure crew competence:

All crew, especially members of the crew management team should be familiar with the ships garbage management plan and aware of their duties and responsibilities as described therein.

WILHELMSEN SHIP MANAGEMENT
GARBAGE MANAGEMENT PLAN

Designated Persons Responsible for Carrying Out Plan

The Master has the overall responsibility for the implementation of the company's Environmental Protection Policy

1) The Chief Officer is the Designated Person overall responsible for carrying out the plan and record keeping.:

2) The Chief Engineer is responsible for the overall management of all waste disposal devices and waste processing systems.:

3) The Department Heads are responsible for supervising the seperation of garbage at source and removel of garbage to the designated area for processing storage or disposal. For purpose of this plan the 2nd Engineer and Chief Cook/ cook(depending on ship's manning) is the person in the charge of their respective departments.:

4) The person in-charge may delegate the responsibility to others, who will work under his supervision and in compliance with the Garbage Management Plan.:

5) The Environmental Engineer (if available) assisted by waste operators is responsible for the day-by-day operation of waste disposal systems, waste management, disposal and record keeping.: Periodic training should be arranged and all crew be familiar with the waste management process as well as their individual roles.

Management Systems:

A Garbage management plan shall be the guiding document that describes the vessels Management system. See extract from a Garbage Management Plan below:

WILHELMSEN SHIP MANAGEMENT
GARBAGE MANAGEMENT PLAN

A. General Information

Gabage collection, storing, processing by the use of equipment on board (if available) and disposal should be cost-effective and always provide environmentally sound results. However onboard the vessel procedures in handling and storing garbage will vary depending on factors such as the type and size of the ship, the area of operation (e.g. distance from land), shipboard garbage processing equipment and storage space, crew size, duration of voltage, and resulations and reception facilities at ports of call. It is economically advantageous to keep garbage generation ar a minimum through a combination three complementary techniques as follows.

1) Source Reduction: The best means of reducing waste generation onboard the vessel is to prevent waste from being provisioning activities. To minimize the generation of waste, provisioning practices should be reviewed with ship's suppliers in order to determine the optimum packaging for the products.

Options include:

- Reusable packaging and use of containere. Disposable cups, utensils, dishes, towele and other convenience items should be limited and replaced by washable items when possible.
- Where practical options exist, provisions packaged in or made of materials other than disposable plastic should be selected to replenish ship's supplies unless a arusablle plastic alternatives is availble.
- Stowage systems and methods that resuse coverings, dunnage, shoring, lining and packing materials.
- Dunnage, lining and packaging materials generated in port during cargo discharge should preferably be disposed of at the port reception facilities and not retained onboard for dischrage at sea.

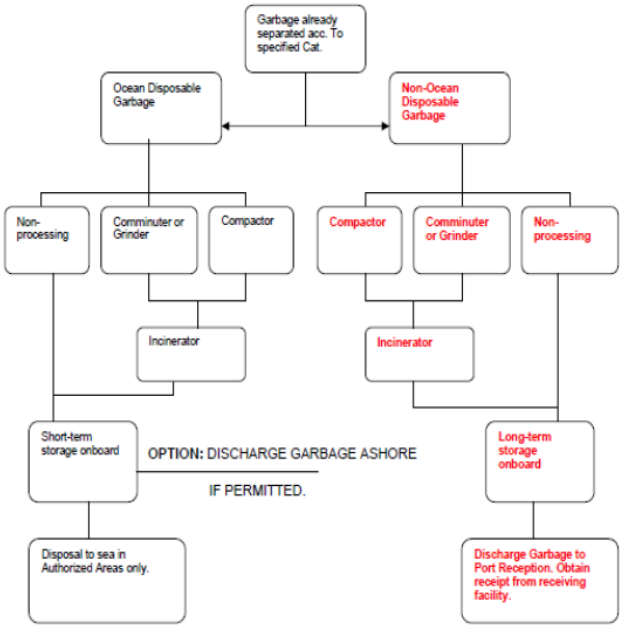
2) Recycling: If this is attempted due consideration must be given to the limited storage space available at the designated storage stations, company mandatory requirement for good house-keeping with regards to hygiene, safety i.e. fire risk and creation of any pollution threat.

3) Disposal: In view of the cost involved with the different ultimate disposal techniques, it may also be economically advantageous to keep garbage requiring special handling (e.g. hazardous wastes) separate from other garbage collection.

WILHELMSEN SHIP MANAGEMENT
GARBAGE MANAGEMENT PLAN
GARBAGE MANAGEMENT FLOWCHART

Regulatory compliance/Requirements:

- MARPOL residues/wastes is used to refer collectively to all waste streams that are generated on board ships during normal operations and are governed by the MARPOL Convention, including the following:
  1) MARPOL Annex I: Oil, oily waste, oily mixtures, oily bilge water, slops, sludge, oily tank washings, oily cargo residues, ballast water containing oily mixtures.
  2) MARPOL Annex II: Mixtures, tank washings, and cargo residues containing noxious liquid substances (NLS) as defined in MARPOL Annex II.



  3) MARPOL Annex III: Prevention of Pollution by Harmful Substances Carried by Sea in Packaged form.
  4) MARPOL Annex IV: Sewage.
  5) MARPOL Annex V: Garbage as defined in MARPOL Annex V including cargo residues not governed by Annex I or II (such as dry/bulk cargo residues) and cargo-associated waste (such as dunnage and packaging).
  6) MARPOL Annex VI: Ozone depleting substances and exhaust gas cleaning residues.
- Residues generally refer to all waste streams governed by Annexes I and II. These include, but are not limited to, oil, oily mixtures, oily bilge water, slops, sludge, tank washings, pre-washes, ballast water containing oily mixtures, oil or NLS cargo residues and other mixtures containing oil or NLS residues. In all cases, residues are expected to be in small quantities.
- Waste is used to mean useless, unneeded or superfluous matter which is to be discarded, and unless otherwise specified, interpretation of the term waste should be limited to the context of the MARPOL Convention (i.e., wastes generated on board ships in the course of normal operations).
- Every ship of 12 meter or more in length overall shall display placards which notify the crew and passengers of the disposal requirements.
- Every ship of 400 gross tons and above, and every ship which is certified to carry 15 persons or more, shall carry a Garbage Management Plan and a Garbage Record Book which the crew shall follow. The plan shall provide

written procedures for collecting, storing, processing and disposing of ship generated garbage, including the use of the equipment onboard. It shall also designate the person(s) in charge of carrying out the plan.

- The administration may waive the requirements for Garbage Record Book for:
  1. Waste management systems onboard any ships engaged on voyages of 1 hours or less in duration which is certified to carry 15 persons or more or: 2. Fixed or floating platforms while engaged in exploration and exploitation of the sea-bed.
- Port state or MARPOL inspectors may inspect your Garbage Record Book and may make a copy of any entry in that book, and may require the Master of that ship to certify that the copy is the true copy of this entry. Any copy so made, which has been certified by the master of a ship as a true copy of an entry in the Garbage record book, shall be admissible in any judicial proceedings as evidence of the facts stated in the entry. The inspection of a garbage record book and the taking of a certified copy by the competent authority shall be performed as expeditiously as possible without causing the ship to be unduly delayed.

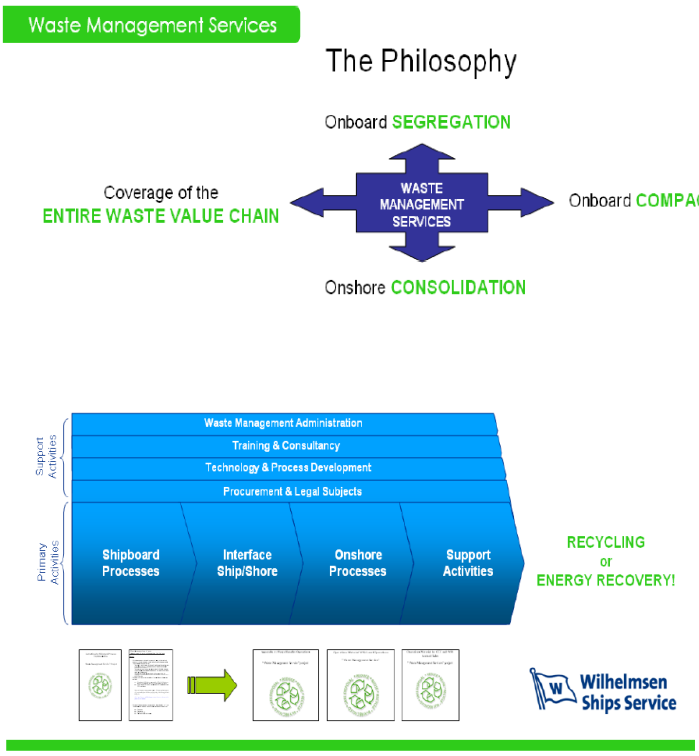
B. Waste Reduction activities in the future, what can be done?

To establish a procedure that links the onboard waste management process with the port waste management process will be essential in order to inspire the vessel and its crew to become even better in managing their waste. One such initiative is Wilhelmsen Ship Services (WSS) "Waste-to-Values" project (W2V). Waste-to-Values (W2V) "A predictable and environmentally responsible solution to ships generated wastes Wilhelmsen Ships Service (WSS) is in the process of developing a global solution for the environmentally responsible treatment of ships generated waste. The corner stones are onboard segregation & compaction, consolidation onshore with a strong preference for recycling before incineration with energy recovery. W2V addresses the harmonization of shipboard and onshore waste management practices through a unique Set of processes following the entire waste value chain, i.e. from the place where the waste is produced onboard ship all the way through to the final recycling station or incinerator with energy recovery. The W2V shipboard processes are in line with the requirements as laid down in Marpol Annex V, Reg. 9. Required products/equipment (such as waste bins, compactors, glass crushers, shredders and relevant consumables etc.) and awareness materials (process documentation and placards etc.) are included in the package and complemented by relevant crew training. In addition to this, WSS offers assistance in the establishment of Marpol Garbage Management Plans which reflect the W2V shipboard processes.

The W2V onshore processes will be developed and implemented in approx. 40 major liner ports world-wide in order to provide maximum flexibility for the ships and to come to a sufficient level of waste consolidation. WSS will ensure that all stakeholders in a particular port (such as shipping companies, port authorities, local waste management companies etc.) are integrated in the processes.

The shipboard and onshore processes are connected through a unique colour coding system for waste recycling as stated in the ISO/CD 21070 (Ship and marine technology Marine environmental protection Handling of ship generated garbage) which is currently being worked on by ISO.This means that the seaman in the galley or the engine control room onboard a ship uses the same colour code as the local waste manager in port, which harmonizes the waste management procedures.

WSS will charge an annual fixed fee per vessel for the W2V service in port and offer a complete range of marine waste management equipment complemented by a range of waste management products and awareness materials for shipboard use.



III. COST/BENEFIT OF ENVIRONMENTALLY RESPONSIBLE WASTE MANAGEMENT

A study that includes interviews and discussions with Environment responsible Ship Owners, International Port Authorities and International Waste Management Companies reveals that it may be a feasible business opportunity to have a holistic approach and link the onboard waste management processes to the shore waste management process in an environmental responsible manner. In order to make such a project fly it is important that a certain number of Pilot Ports and Pilot Customers participate to obtain proof of its operational and financial feasibility.

IV. Conclusion Value creation

- There is, indeed, a potential to improve the environmental performance by streamlining the waste management process onboard and ashore through a set of Pilot Ports and by including a number of Pilot Ship Owners.
- A responsible environmental profile for ship owners and ports can be achieved by having documented processes in place which are audited by an approved body.
- Most of the equipment needed is off-the-shelf type. Investment in a multi-chamber type compactor solution and other relevant waste management equipment is necessary.
- The shipboard and shore processes have been developed and are more-or-less ready to be launched provided that ports and ship owners sign up and Norwegian governmental funds (NRC or IFU) to support the industrialization phase is available. Indication on resources and funds needed for the pilot project.

References

[1] IMO Guidelines.

[2] Wilhelmsen Ship Management Garbage Management Plan.

[3] Wilhelmsen Ship Services W2V project.

GEOTHERMAL POWER PLANT ON THE CONCEPT OF ORGANIC RANKINE CYCLE

Cadet Akshay Shetty[1], **Cadet Mayur Agarwal**[2], **Cadet Preetish Sengupta**[3]
[1,2,3]Tolani Maritime Institute

***Abstract*—The objective of the project is to install two 200KW organic Rankine cycle Geothermal Power Plant for total generating capacity of approximately 400KW. Geothermal power is cost effective, reliable, sustainable, and environmentally friendly. Geothermal power has the potential to help mitigate global warming if widely deployed in place of fossil fuels. We intend to use refrigerant R134a in Rankine cycle to produce power using a hot-spring as a source. The hot-spring we have chosen is from Puga, Ladakh as its suits the required atmospheric conditions. The geothermal water in the hot-spring never reaches above 75-80 degree Celsius and the traditional steam turbine requires 120 degree Celsius. So instead a secondary fluid R134a which has low boiling point than water is used as the working fluid. The hot-spring heat will cause R134a to convert into vapors which will drive the turbine to produce power. As this is a closed loop system, virtually nothing is emitted to surrounding atmosphere. The thermodynamic calculation shows us that minimum pressure reached in condenser is 5 bar. Thus the plant is always is positive pressure condition which reduces the maintenance. As Ladakh is ecologically protected place, it will not adversely affect the surrounding, As the temperature of hot-spring is enough to boil the refrigerant, we virtually do not need any other source like oil and coal to be fired. Thus by using a free and renewable source of energy, we are producing power.**

***Keywords*—ORGANIC RANKINE CYCLE, PUGA HOT SPRING, REFRIGERANT R134a, EVAPORATOR, RADIAL FLOW TURBINE, AIR COOLED CONDENSOR.**

I. INTRODUCTION

The world energy consumption has risen to a level never reached before, releasing in the same process large quantities of CO2 into the atmosphere. Current concerns over climate change call for measures to reduce greenhouse gases emissions. New heat conversion technologies need to be developed and improved to take advantage of the necessary increase in the supply of renewable energy. The Organic Rankine Cycle is well suited for these applications, mainly because of its ability to recover low-grade heat and the possibility to be implemented in decentralized lower-capacity power plants. Conceptually, the Organic Rankine Cycle is similar to a Steam Rankine Cycle in that it is based on the vaporization of a high pressure liquid which is in turn expanded to a lower pressure thus releasing mechanical work. The cycle is closed by condensing the low pressure vapour and pumping it back to the high pressure. Therefore, the Organic Rankine Cycle involves the same components as a conventional steam power plant (a boiler, a work- producing expansion device, a condenser and a pump). However, the working fluid is an organic compound characterized by a lower boiling temperature than water and allowing power generation from low heat source temperatures. In this paper, we are proposing a project of a possible Geothermal Power plant in Ladakh, India using a geothermal source used for heating the working fluid refrigerant R134a .

II. HOW OUR GEOTHERMAL POWER PLANTWORKS

Geothermal water at Puga hot spring never reaches above 93 degree Celcius. Traditional steam turbine requires 120 degree Celcius to create steam. Instead a secondary fluid, R134a which has a lower boiling point than water pass through the heat exchanger with 93 degree water from our geothermal well. Heat from the geothermal water causes R134a to flash into vapour which then drives the turbine. As this is a closed loop system, virtually nothing is emitted to the atmosphere.

Here are the steps in the cycle:

- Hot water enters the evaporator at 93 degree celcius. After the hot water runs through the evaporator, it is return to the geothermal reservoir via pump.
- Evaporator is a giant heat exchanger where the hot water never comes contact with the refrigerant but transfer heat energy to it. The evaporator shell is filled with R134a, refrigerant found in many air conditioning system. The 93 degree water is hot enough to boil R134a. The R134a begins to boil and vaporise.
- On initial system start up, the vapour bypasses the turbine and returns directly to condenser via bypass valve. Once there is adequate boiling/evaporation of the refrigerant, the bypass valve closes and the vapour is routed to the turbine.
- The vapour is expanded through the turbine nozzle, causing the turbine blades to turn. The turbine is connected to generator which produces electrical power.
- Cooling water enters into the condenser at a rate of 52kg/s.
- The pump pushes the liquid refrigerant back to the evaporator. So the cycle can start again.

III. LOCATION

According to Indias ambitious energy programme, it appears that Renewable Energy Sources will be generating substantial

quantity of power in future. If the geothermal energy potential is exploited, then India will have surplus electrical power. This expansion should be planned to help the rural areas rather than the urban areas. In the very near future India may appear on the geothermal map of the world with the proposal of generating power and direct utilization of geothermal energy from the existing bore well. The Himalayan geothermal provinces, extending over a length of about 1500 km from NW to SE of India host more than 100 geothermal springs, the most prominent ones located within the NW Himalayas.



Fig. 1. STEAM RISING FROM A HOTSPRING IN PUGA

Considering the requirements for our power plant, we have found Puga Hot Spring most favourable. The surface temperatures of the thermal discharges atPuga are about 93 degree Celsius. In the Puga valley, more than ten thermal discharges can be seen with the above temperatures Discharge rate here varies from 30 to 40 L/s. Steam discharge is seen very prominently from one of the boreholes drilled by the Geological Survey of India and lies abandoned now which we plan to use for our project 1.

IV. WHY R134A?

- Heat transfer performance better than other refrigerant.
- Good safety performance(non flammable, non explosive, non toxic , non irritating).
- Eliminates needs for fire protection.
- Best for operating temperature around 60-90 degree
- Much better match for low temperature geothermal application and enables significant cost reduction as this is a low cost thermic oil and refrigerant than any other available in market.
- Equipment design risk is no greater than that of any other heat exchanger designed for power plant(conventional steam).
- Approved by EPA as environmentally safe.
- This do not contain chlorine atom so it has least effect on atmospheric ozone.
- Very low global warming potential.
- The ban on CFCS and HCFCs by the montreal protocol forced us to concentrate more on usage of environmental safe R134.

V. COMPONENT SPECIFICATION

A. TURBINE

A distinction is generally made between two main types of turbines: the axial turbine and the radial inflow turbine. Axial turbines show a distinct design when used in combination with high molecular weight working fluids. The main difference between organic fluids and steam is the enthalpy drop during the expansion, which is much higher for steam. As already mentioned, fewer stages are required in the case of an organic fluid. Even single-stage turbines can be employed for low or medium temperature ORC cycles. Radial inflow turbines are designed for high pressure ratios and low working fluid flow rates. Their geometry allows higher peripheral speeds than for axial turbines, and therefore a higher enthalpy drop per stage. They also have the advantage of maintaining an acceptable efficiency over a large range of part-load.

B. CONDENSOR

Considering the selected location conditions, we have decided to use water cooled condenser in summer conditions and air cooled condenser during winter. The Air-cooled heat exchanger is a device for rejecting heat from a fluid or gas directly to ambient air. When cooling both fluids and gases, there are two sources readily available, with a relatively low cost, to transfer heat to..air and water. The obvious advantage of an air cooler is that it does not require water, which means that equipment requiring cooling need not be near a supply of cooling water. In addition, the problems associated with treatment and disposal of water have become more costly with government regulations and environmental concerns. The air-cooled heat exchanger provides a means of transferring the heat from the fluid or gas into ambient air, without environmental concerns, or without great on-going cost.

C. EVAPORATOR

Heat exchangers represent a major share of the total module cost. Their optimization should therefore be carefully performed. Each heat exchanger in the cycle is sized according to the set parameters. Different types of heat exchangers can be used, the most common being shell & tube (mainly in larger-scale systems) and plate heat exchangers (mainly in small-scale systems, due to their compactness). A critical heat exchanger is usually the exchanger installed on the heat source. Depending on its nature, this heat exchanger must with stand high temperatures and can be subject to fouling and/or corrosion. Heat can be recovered by means of two different setups: (1) direct heat exchange between heat source and working fluid and (2)an intermediate heat transfer fluid loop that is integrated to transfer heat from the waste heat site to the evaporator usually using thermal oil.

D. PUMP

ORC feed pumps are key components and should be given particular care during the selection and sizing process. They should comply with the cycle requirement in terms of controllability, efficiency, tightness and NPSH.

VI. CALCULATIONS

Hot water available at 90-93 degree celcius.

Ambient temperature: Summer: 20 degrees winter : 15 degrees

During Summer : 26.32 bar
H(g)1 : 280.59 kJ/kg
S1 : 0.88912 kJ/kgK

:

During summer the temperature is brought down to 30degrees in condenser.

P2: 7.7 bar

s=s(f)+x*s(fg)

X= 0.951656

H2=h(f)+xh(fg)

H2= 258.3kJ/kg

Work done = h1-h2 = 22.30kJ/kg

Taking isentropic efficiency as 0.8,

Total work done = 0.8*22.30= 17.845kJ/kg

Let mass flow rate of refrigerant = 15kg/s

Therefore, work output = 15*17.845= 267.688kW

During winter, temperature is brought down to 6 degrees approx. (thus we use an air cooled condenser)

$$P2 : 7.7bar$$
$$s = s(f) + x * s(fg)$$
$$X = 0.951656$$

Work done = h1-h2 = 34.63

Let isentropic efficiency be 0.8

Therefore work output = 0.8*34.63=27.7058

Mass flow rate = 15kg/s

Work ouput=27.7058*15=415.58

Evaporator Calculations

Hot Fluid inlet temperature=93 degrees

Hot fluid outlet temperature=80 degrees

Cold fluid inlet temperature=20degrees

Cold fluid outlet temperature=80 degrees

M(cp)(deltaT) [water] =M(cp)(deltaT)[r134a]

Mass flow rate of water=21kg/s

LMTD=30.73

Ntu=1.95

c/s Area of tube=0.346m2

assuming inner dia=1.5cm

A=pie D1

L=7.5m

Taking 5 passes, length of each pass=1.5m

No.of tubes=119

Shell diameter=30cm

REFERENCES

[1] Geothermal energy resource of India: Past and the present, D. Chandrasekharam, Department of Earth Sciences, Indian Institute of Technology, Bombay, April 2005.

[2] Chena Power Geothermal Power Plant, February 4, 2007.

[3] Organic Rankine Cycle- Wikipedia www.wikipedia.com/organicrankinecycle.

[4] Website-http://www.dosits.org/science/soundsinthesea

[5] 4. Brasz, Lars J. and Bilbow, William M., "Ranking of Working Fluids for Organic Rankine Cycle Applications" (2004). International Refrigeration and Air Conditioning Conference.

Marine Air Pollution Control

Sulphur Emissions and Their Control

Cadet Rahul Dewan
Marine Engineering Cadet , III year
Tolani Maritime Institute
Talegaon –Chakkan Road, Pune. India
rahuldeewan1993@gmail.com

Abstract : **Air pollution in Maritime transportation is high on global agenda. Emissions from shipping in parts are transported to land, where they add to pollutant load. Emissions have affected human environment adversely leading to acid rains affecting vegetations and many other problems such as lung diseases. Therefore, current legislation is more restrictive about emissions and special attention is given to these components. More stringent measures have been adopted by International Maritime Organization (IMO) in relation to Sulphur Dioxides (SOx) and Nitrogen Dioxides (NOx) emissions from merchant ships, through the ANNEX VI of MARPOL. Under revised MARPOL ANNEX VI, the global sulphur cap is to be reduced to 0.50%, effective from 1-Januarary-2020. The paper analyses the quantum of SOx emissions from merchant ships and adverse effects it poses to inhabitants and facilities in the areas close to commercial shipping ports. The paper also looks at the present methods adopted by authorities for its control and cost analysis of these methods. This will be achieved through study of different approaches of sulphur emission control like use of low sulphur fuels including natural gas, neutralization of fuel sulphur by use of better cylinder lubrication mechanisms, after treatment of flue gases (FGD) and fuel cleaning.**

I. INTRODUCTION

The ocean covers approximately 71% of the earth's total surface area. 97% of the total water content of earth is present in the oceans. It harbors rich source of biodiversity,which population may exceeds in trillions. Oceans are the main regulatory agent of earth's climate. About 60% of the world's population live within 60 km of coastline and use the coastline as source of livelihood. It was thought that human beings, living only on one-third of the portion of globe, cannot pollute this vast amount of water, as the marine ecosystems are capable of serving as sink for all the pollution caused by mankind. However, inreality this is not true. We have come to realize that our waste, even in small quantities,have huge effects on ocean communities and species. Moreover, it is difficult to believethat something so massive and seemingly resilient can really be adversely affected by ouractivities. Environmental pollution of the coast, inshore water and deep oceans is one ofthe important topical issues in the context of human health and global warming.

Combustion of sulphur-containing fuels, such as coal and mineral oil, results in Sulphur Dioxide (SO_2) and Sulphur Trioxide (SO_3) formation. SOx emissions are known to cause detrimental impacts on human health and the environment. The major health concerns associated with exposure to high concentrations of SOx include breathing difficulties, respiratory illness, and aggravation of existing cardiovascular disease. In addition to the health impacts, SOx leads to acid deposition in the environment. This deposition causes acidification of lakes and streams and damage to tree foliage and agricultural crops. Furthermore, acid deposition accelerates the decay of buildings and monuments. While airborne, SOx and its particulate matter derivatives contribute visibility degradation.

II. FORMATION OF SULPHUR EMISSIONS

In diesel engines, fuel is injected at high pressures into air which has been compressed by the moving pistons. This compression raises the temperature of the air sufficiently to cause the fuel to ignite. Combustion proceeds around the periphery of the fuel spray at temperatures around 2000°C.

Oxides of nitrogen are formed during the combustion process due to combination of nitrogen and oxygen from the air at these high temperatures. The diesel combustion process inherently produces relatively high levels of NOx, and the fuel properties only have a minor influence on the amount produced.

Oxides of sulphur form during the combustion process, by combination of the sulphur in the fuel with oxygen. The prime constituent of SOx is SO2. The amount of SOx formed in an engine depends primarily on the concentration of sulphur in the fuel. SOx emissions from ship engines are relatively high because they burn fuel with high sulphur content.

III. IMPACTS ON ENVIRONMENT

- Emissions from shipping are in part transported over land where they add to the pollutant load.
- In sufficient concentrations SO2 can adversely affect lung function, leading to respiratory illness and breathing difficuilties.
- SOx emissions leads to Cardiovascular diseases.
- The SOx and NOx emissions contribute to acid rain, as well as affect air quality.

IV. REGULATIONS FOR CONTROL OF EXHAUST EMISSIONS

The International Maritime Organization (IMO) enacted a revised Convention in 2008 for control of exhaust emissions from ships. MARPOL is the International Convention for Prevention of Pollution by Ships. ANNEX VI of this convention deals with air pollution.

As per Regulation 14 of MARPOL 2008 revised ANNEX VI, general requirements for merchant ships for control of SOx emissions are:

1. *The sulphur content of any fuel oil used onboard ship shall **not** exceed the following limits outside Emission Control Areas (ECA) :-*

- 4.50% m/m prior to 1 January 2012;
- 3.50% m/m on and after 1 January 2012; and
- 0.50% m/m on and after 1 January 2020

2. *Requirements within ECA are:*

- 1.50% m/m prior to 1 July 2010;
- 1.00% m/m on and after 1 July 2010; and
- 0.10% m/m on and after 1 January 2015;

Table 1 :
Regulation for sulphur limit in fuel

Date	Sulfur Limit in Fuel (% m/m)	
	SOx ECA	Global
2000	1.5%	4.5%
2010.07	1.0%	
2012		3.5%
2015	0.1%	
2020[a]		0.5%
a – alternative date is 2025, to be decided by a review in 2018		

Alternative measures are also allowed (in the SOx ECAs and globally) to reduce sulfur emissions, such as through the use of scrubbers.

For example, in lieu of using the 1.5% sulphur content fuel in SOx ECAs, ships can fit an exhaust gas cleaning system or use any other technological method to **limit SOx emissions to ≤ 6 grams/kilowatt hours (as SO_2).**

V. METHODS AND TECHNOLOGIES FOR EMISSION CONTROL

A. Using Low Sulphur Fuels

The most straightforward method of reducing SOx emissions is to reduce fuel sulphur content.

Since sulphur emissions are proportional to the sulphur content of the fuel, an effective means of

reducing SOx emissions is to burn low-sulphur fuel such as natural gas, low-sulphur oil. Natural gas has the added advantage of emitting no particulate matter when burned.

There is a limit to how low the sulphur content of heavy fuel oil can be reduced. Heavy fuel oil is largely composed of the thick residue from the crude oil refining process, to which lighter components have been added to bring it to a useable consistency. It is black in colour. The majority of shipping runs on heavy fuel oil. MARPOL ANNEX VI will allow global fuel sulphur content of 3.5% until 2020, a further 6 years from now. States requiring lower fuel sulphur can make their own rules or declare Emission Control Areas (ECAs) under IMO MARPOL ANNEX VI. Higher quality marine diesel fuels are available, but at a greater cost. These lighter fuels are known as Marine Diesel Oil (MDO) or Marine Gas Oil (MGO). MGO and MDO are known generally as distillates. Some ships use MGO or MDO in their auxiliary engines for generating electricity. MDO and MGO are available at low sulphur content, down to around 0.1%. MDO and MGO are not generally available in Australia, and if ships were required to use fuel other than heavy fuel oil in or near port, they would either bring MDO or MGO with them which has very low sulphur content. Natural gas is another alternative fuel, but is not as easy to implement as low sulphur distillate.

B. Better Cylinder Lubrication- Alpha Lubricator

Good quality cylinder lubrication along with efficient control systems such as Pulse or Alpha lubrication systems can neutralize the sulphur in fuel and reduce Sox emissions from the engine. The cylinder oil feed rate has impact on the particulate emission. Tests show that when reducing the cylinder oil feed rate, the particulate emission is also reduced. Alpha Lubricator is a high pressure electronically controlled lubricator that injects the cylinder lube oil into the cylinder at the exact position and

time where the effect is optimal, which is not possible with conventional mechanical lubricators.
By applying a low oil dosage, about half of usual particulate emissions are lowered and also less cylinder oil is wasted in the engine where in case of 4-S engines, it could end up in system oil, resulting in increased TBN and viscosity.

C. *Speed Reductions*

Speed reduction is an operational measure which offers significant SOx reductions. A 10% speed reduction gives 20+% reductions in fuel consumption over the same distance. Engines can be derated to optimise operation at reduced speeds by measures such as increasing compression ratio or turbocharger boost pressure to recover cylinder pressures when less fuel is injected per cycle. Classification Society Germanischer Lloyd have recently suggested that container ship speeds of 12 to 14 knots would be optimum. The present norm is 20+ knots. This reduced optimum speed would save fuel costs and emissions as well as absorbing overcapacity in the fleet.

D. *Flue Gas Desulphurization - Scrubber Technology*

Under *Flue gas desulphurization (FGD)* technology, the exhaust gas from engine is passed through the scrubber tower where sea or fresh water is showered on it. Sea or fresh water blended with *Caustic Soda (NaoH*) is used as scrubbing medium which reduces Sox emissions by *95%.*
The scrubbing water is then sent to effluent emulsion breaking water treatment plant after which it can be discharged overboard. This may be carried out using either of two basic FGD systems: regenerable and throwaway. Both methods may include wet or dry processes. Currently, more than 90% of utility FGD systems use a wet throwaway system process.

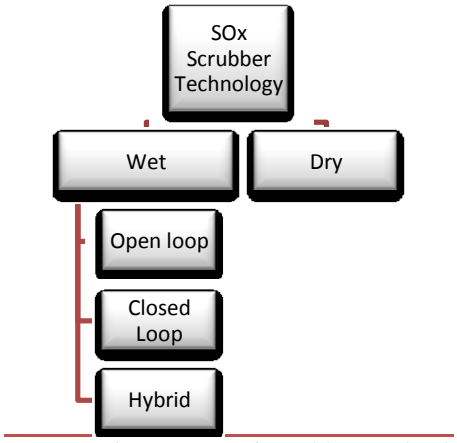


Fig 1. Types of Scrubber Technology

1) *Wet SOx Scrubbers :* Wet SOx scrubbing is simple, effective technology that has been used in industrial applications for many years. A wet SOx scrubber plant broadly comprises of the following components:

- A scrubber unit. A vessel or series of closely coupled components, that brings water into intimate contact with exhaust gas from combustion units. The unit is typically mounted high up in ship in or around the funnel.
- A treatment plant, for sludge separated from the wash water
- A Scrubber control and emission monitoring system
A wet SOx scrubber system may also include a heater to raise the exhaust gas temperature above dew point, and a demister to remove fine water droplets.

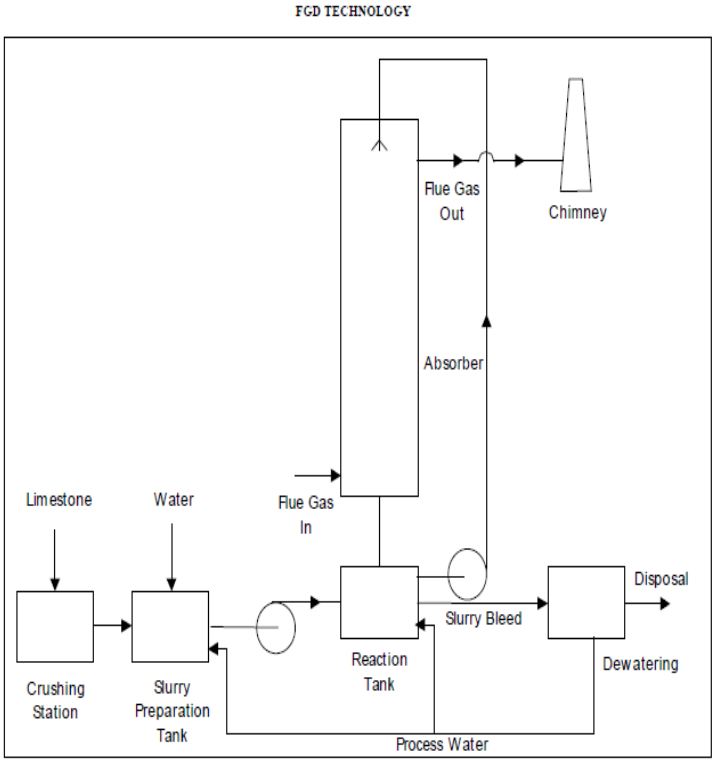


Fig 2. – Wet Scrubber Technology

Different types of Wet SOx Scrubber systems include :

i. **<u>Open loop system :</u>** In wet open loop scrubbing systems, seawater is pumped from sea through the scrubber, cleaned and then discharged back to sea. Wash water is not recirculated.

For SO_2:

$SO_2 + H_2O \rightarrow H_2SO_3 + HSO_3$ (Sulphurous Acid)

$HSO_3 + H \rightarrow 2SO_3 + 2H_2$ (Sulphite)
$2SO_3 + ½\ O2 \rightarrow 2SO_4$ (Sulphate)

For SO_3:

$SO_3 + H_2O \rightarrow HSO_4 + H_3O$
$H_2SO_4 + H_20 \rightarrow HSO4 + H_3O$
$HSO_4 + H2O \rightarrow 2SO_4 + H_2O$

The process requires no hazardous chemicals. The sea water is the only scrubbing agent. Also this system has fewer components than other wet systems. The SOx removal rate is close to 98%. In this process seawater temperature has also to be considered as SO_2 solubility reduces at higher seawater temperatures.

ii. **Closed loop system :** All main closed loop SOx scrubbers use fresh water treated with sodium hydroxide (NaOH) as the scrubbing media. This results in removal of SOx from exhaust gas stream as sodium sulphate. The chemical reactions are :

For SO_2:

$Na^+ + OH^- + SO_2 \rightarrow NaHSO_3$ (aq. Sodium bisulphite)
$2Na^+ + 2OH^- + SO_2 \rightarrow Na_2SO_3$ (aq. Sodium sulphite)
$2Na^+ + 2OH^- + SO_2 + ½\ O_2 \rightarrow Na_2SO_4 + H_2O$ (aq. Sodium sulphate)

For SO_3:

$SO_3 + H_2O \rightarrow H_2SO_4$ (sulphuric acid)
$2NaOH + H_2SO_4 \rightarrow Na_2SO_4 + 2H_2O$ (aq. Sodium sulphate)

Rather single flow as in an open loop scrubber, the wash water from closed loop scrubber passes into a process tank where it is cleaned before it is recirculated. The control of pH by dosing with sodium hydroxide enables the wash water circulation rate and therefore the power consumption to be half that of open loop systems. Closed loop systems can be operated when ship is operating in closed waters where alkanity would be too low for open loop operations. These systems typically control sodium hydroxide in 50% aqueous solution.

iii. **Hybrid system:** Hybrid system can be either operated in closed loop mode or in open loop mode.

This provides the flexibility to operate in closed loop mode where(including zero discharge mode) where the water alkanity is insufficient or where there is sensitivity to, or regulation of, wash water discharge, and in open loop mode without consuming sodium hydroxide at all other times.
The arrangement offers advantages in that sodium hydroxide is only used when necessary, reducing handling and storage and associated costs. Fresh water consumption is also reduced.

Hybrid Scrubbers are however more complex than open loop or closed loop scrubbers.

2) *Dry SOx Scrubbers :* Dry SOx scrubbers have been widely used in land based industries since 1970's. The main components of this technology are

- A Scrubber unit, Also known as absorber which brings exhaust gas from combustion units to Calcium Hydroxide granules. Unlike the majority of wet scrubbers the entry of exhaust gas is perpendicular to the vertical downward flow of scrubbing medium. No heat is removed from exhaust gas during scrubbing, infact the reaction is exothermic and it rather releases heat. So dry scrubbers can be placed before SCR and heat recovery units.
- A granule supply silo and screw conveyor. For discharge, positioned at top and bottom of absorber respectively. A pneumatic conveyor system enables granules to be transported from and returned back to onboard storage facilities.
- A Scrubber Control and emission monitoring System. Removal of used granules and any exhaust related particulate matter is automated process and either is continuous or intermittent to ensure the correct flow of fresh granules under gravity down through the absorber.

Dry scrubbers typically operate at exhaust temperatures between 240 - 450 C.

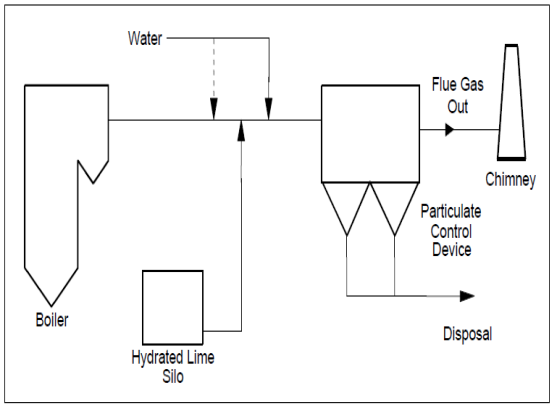


Fig 3. Dry scrubber technology

In dry SOx scrubber using calcium hydroxide, the reaction with sulphur dioxide forms calcium sulphate.
Ca(OH) 2 + SO2 → CaSO3 H2O

The sulphate is then oxidized and hydrated in exhaust stream to form calcium sulphate dihydrite, or gypsum
2CaSO3 + O2 → CaSO4

$Ca(SO)4 + H2O \rightarrow CaSO4 + 2H2O$ (calcium sulphate dihydrate gypsum)

Similarly, for $SO3$:
$SO3\ Ca\ (OH)\ 2 + H2O \rightarrow CaSO4.2H2O$ (calcium sulphate dihydrate gypsum)

VI. COST ANALYSIS

A. Using Alpha Lubricator.

Alpha ACC allows the cylinder oil dosage (g/bhph) to be controlled in such a way that it is proportional to the amount of sulphur (g/bhph) entering the cylinder with the fuel. This is achieved by making the cylinder oil dosage proportional to the sulphur percentage in the fuel and to the engine load (fuel amount).

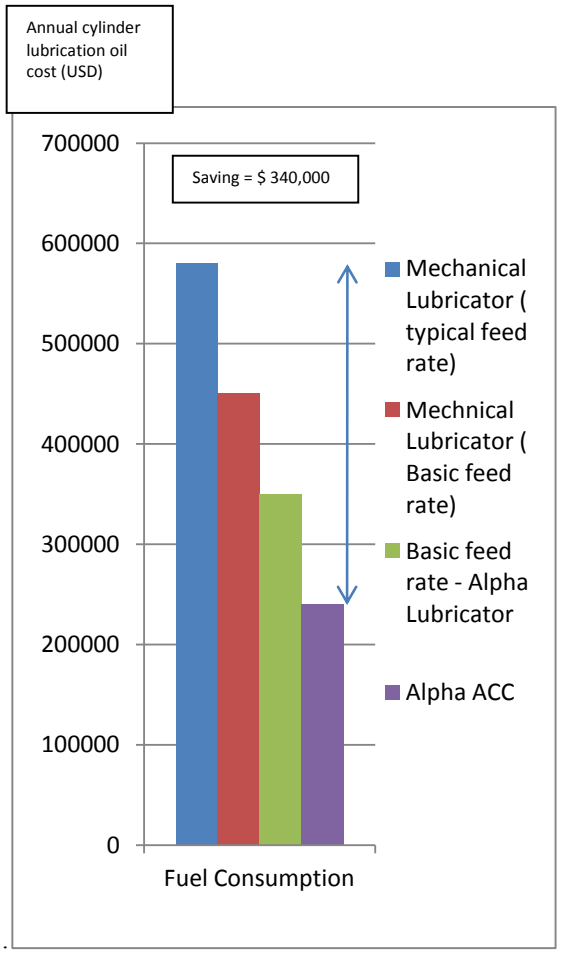


Fig 4. Fuel saving by use of Alpha Lubricator

Thus it is clear from the graph that the use of alpha lubricator results in saving of lubrication oil, thus reducing SOx emissions and saves $ 340,000 per year.

B. Using Low Sulphur Fuels

In practice, a switch to fuel with a maximum sulphur content of 0.1% will mean that vessels will have to use gas oil (MGO) as fuel, which is a lot more expensive than heavy fuel oils, owing to the way in which it is manufactured. Based on recent studies, the cost increases are represented below.

Table II
Additional estimate Cost for low sulphur fuel useage

Fuel sulphur content		Additional cost (Euros per tonne)	
From	To	Min.	Max.
1.0%	0.5%	115	30
0.5%	0.1%	200	
0.1%	10 ppm	20	

C. Dry versus wet scrubbers

The Dry chemical Gas Scrubber is approximately $100,000 - $120,000 less in cost than the Wet Scrubber. Therefore dry scrubbers are preferred over wet scrubbers.

Table III
Cost comparison between Wet and Dry Scrubbers

Capital costs	Dry scrubber system	Wet scrubber system
Equipment	$127,000	$90,000
Concrete Pad	$1,500	$1,200
Equipment Installation	$24,000	$36,000
Duct Work	$10,000	$15,000
Electrical & Instrumentation	$8,000	$14,000
Contractor OH&P (15%)	$25,575	$23,430
Contingency (20%)	$34,100	$31,240

Construction Cost	$230,175	$210,870
Engineering & Administration (20%)	$46,035	$42,174
Estimated Project Subtotal	$276,210	$253,044
Capital Depreciation Cost	$276,210 ($13,810/yr)	$253,040 ($12,652/yr)
Operation & Maintenance Costs	$12,000 ($600/yr)	$152,400 ($7,620/yr)
Total 20-Year Costs	**$288,200 ($14,410/yr)**	**$405,440 ($20,272/yr)**

Source : Purafil , Environmental System Dividion (ESD)

D. Comparison between Wet type scrubbers

The table below shows cost comparison between different types of wet scrubbers

Table IV. Wet type Scrubbers- Costs

	Open Loop	Closed Loop	Hybrid	Dry
Scrubber Ratings (by Engine Size)	(USD)	(USD)	(USD)	(USD)
36MW	3,100,000	3,850,000	3,600,000	6,050,000
16MW	2,900,000	3,600,000	3,120,000	3,200,000
12MW	2,000,000	2,500,000	2,220,000	1,900,000
10MW	1,800,000	2,150,000	1,920,000	1,600,000
3MW	1,300,000	1,850,000	1,560,000	1,250,000
1MW	1,000,000	1,750,000	1,260,000	930,000
Containership Transpacific	5,260,000	6,430,000	5,904,000	7,970,000
Containership Alaska to Puget Sound	5,060,000	6,180,000	5,424,000	5,120,000
Tankship US West Coast	3,960,000	4,730,000	4,224,000	3,520,000

Source :- The Glosten Associates , U.S Department of Transportation

Installation and commissioning is assumed to be 50% of the equipment cost for all technologies. Other costs are also based on percentages of equipment cost: 7% for engineering/design, and 2% for training and documentation.

VII. CONCLUSIONS

- Ship engine exhaust emissions are known to have adverse impacts in areas of high shipping
- The human health impacts of concern are short-term exposure to sulphur dioxide (SO2) concentrations above 1,000 micrograms per cubicmeter, measured as a 10-minute average. Priority therefore must be given to limiting exposures to peak concentrations.
- The use of alpha lubricator is very benificial in reducing consumption of cylinder lube oil and also reduces SOx emissions.
- The use of low sulphur fuels to reduce sulphur emissions is very costly , and thus not optimum. Therefore FGD is done to reduce sulphur content in exhaust.
- At present the most effective and economical method to reduce sulphur emissions is use of Exhaust Gas Scrubbers
- The Wet type exhaust scrubbers are better than Dry type scrubbers in terms of cost .
- In Wet type scrubbers Hybrid type is most economical.

ACKNOWLEDGEMENTS

I have worked very hard in writing this paper. However it would have not been possible without the blessings of Almighty and my Parents. I would like to extend my sincere thanks to many individuals who have helped me through this and their efforts should be appreciated.

I am extremely thankful to Tolani Maritime Institute for giving me the platform to prepare this project. I am highly indebted to my project guide, Dr. Rajendra Prasad, Captain S.G. Deshpande and Mr. Shailendra Kumar for encouraging me and giving me opportunity to work on this topic as well as for providing necessary information and their support for completing this paper.

My thanks and appreciations also go to my colleagues for helping me in writing this paper and people who have willingly helped me out with the best of their abilities and encouraged me.

REFERENCES

1. MARPOL – Consolidated Edition , 2011 – *Bhandharkar Publications*
2. Marine Engineers Review (INDIA), June 2013
3. Exhaust Emissions from Ship Engines, *by Laurie Goldsworthy*

4. Clean Coal Technology , *by The U.S department of Energy and Pure air*
5. Pollution Prevention and Abatement Handbook, *by WORLD BANK GROUP*
6. Controlling SO_2 Emissions , *by Ravi K. Shrivastava*
7. Economic comparisons , by *PURAFIL - ESD*
8. Tests for alpha lubricator , Press release , *by MAN B&W.*
9. Exhaust Gas Cleaning Systems , b*y GLOSTEN ASSOCIATES*
10. Marine Pollution , *by Raja Insanbir Singh*



Cadet Rahul Dewan Cadet Rahul Dewan is a Marine Engineering Cadet, Tolani Maritime Intitute, Pune, India, 2011. He is Presently Studying in Third year of Marine Engineering. His areas of research interest are Marine Air Pollution Control.

The Nitrogen Revolution

Cdt. Neeraj Mehta [1], **Cdt. Kevin Parmar** [2]
[1,2]Tolani Maritime Institute
Talegaon, Pune, India
[1]neeraj_mehta1993@yahoo.co.in
[2]kevindlhparmar@gmail.com

***Abstract*—With time the upcoming times the civilization demands for a cleaner environment including cheap and efficient systems. Presently the NO x emissions from ships have been of a great concern to all the international regulatory organizations and to cater to their demands a large number of reduction techniques have been proposed and implemented. But the key element in this emissions-NITROGEN has been neglected for its abundance and importance.**

In this paper we intend to propose a revolutionary idea for ships by use of NITROGEN on-board. For this we intend to install a nitrogen generator which would optimize the newly developed hull lubrication by the replacement of air with the inert nitrogen along with the use of same system for counteracting the NOx emissions and bringing a change in the overall combustion scenario. We intend also to use this nitrogen produced for cutting down the cost of painting operation performed on-board along with enhancing the life of the coating. With the development in the material and engineering sector the feasibility of installing such systems has increased significantly. To sum up we intend to showcase the benefits of the use of nitrogen over the present scenario and pave a path to a greener and efficient world on-board.

Keywords*—NOx, oxygen, nitrogen, hull lubrication, carbon dioxide.

I. INTRODUCTION

Installing any type of system onboard has always been a subject of great concern for all kinds of ships, trying hard to make the system as economical as possible along with coping up to satisfy the demands of the various international organizations regarding environmental protection. So, in this paper we intend to propose an idea of a system which will lead to increased efficiency of machinery onboard. In this system we propose to install a nitrogen generator as the primary component which would support the working of the other systems in line. With all the systems in live condition this can achieve greater vessel speed along with lesser specific fuel oil consumption leading to reduction in the carbon footprint, a significant reduction in mono nitrogen oxides i.e. nitric oxide (NO) and nitrogen dioxide(NO2) and an entire change in the combustion scenario [3].

II. NEED FOR NEW SYSTEM

Any recent upcoming systems are always validated for their environment friendliness and their expense in the long run. The problem of these mono nitrogen oxides cumulatively called as NOX has recently been one of the main causes contributing to air pollution .With the help of the proposed system design one can combat this issue along with gaining an increase in the ship speed with a reduction in fuel consumption.

III. INSPIRATION OF SYSTEM

Our first inspiration arose from the already present design of air hull lubrication present on some of ships owned by Mitsubishi Heavy Industries Ltd. (MHI), Nippon Yusen Kabushiki Kaisha Line (NYK line) [7]. In this our idea of combatting the problem of corrosion took us to think about inert gas application. This introduced us to the abundant nitrogen present in the atmosphere(78 percent). For this we propose a nitrogen generator and running such a system for hull lubrication only would not prove to be an idea worth investing. This leads to solving one of the most important hurdles in oxy-fuel combustion in the Marine Diesel Engines. On land, one of the most important problems is production of pure oxygen which is possible using nitrogen generators. Hence replacing air with nearly pure oxygen in engines and using the remaining nitrogen in air lubrication would help us in cutting out the NOx emissions from engines along with a much efficient combustion and a reduction in the fuel consumption leading to a reduction in the carbon-foot print and hence cost saving and a green system.

IV. COMBUSTION IN IC ENGINES

Presently, for combustion lean air-fuel mixture is preferred as it provides sufficient oxygen for combustion near to stoichiometric ratio leading to better fuel consumption efficiency and higher brake power. But higher power output led to higher peak pressures and temperatures in the combustion chamber leading to formation of nitrous oxide (thermal and prompt NOx) [3].The result of these higher temperatures above 1600 degree Celsius, molecular nitrogen (N2) reacts with molecular oxygen in air forming NOx through a series of reversible reactions. This leads to decrease in oxygen content for burning of fuel leading to incomplete combustion and reduction in brake power. To cater to this, turbochargers were installed to bridge the oxygen requirement and also for effective scavenging of unburned particles but problem of NOx still remains unsolved.

A. harmful effects of mono nitrogen oxides include [3]:

i. Formation of nitric acid with water, ammonia and other compounds leading to acid rain and various respiratory diseases

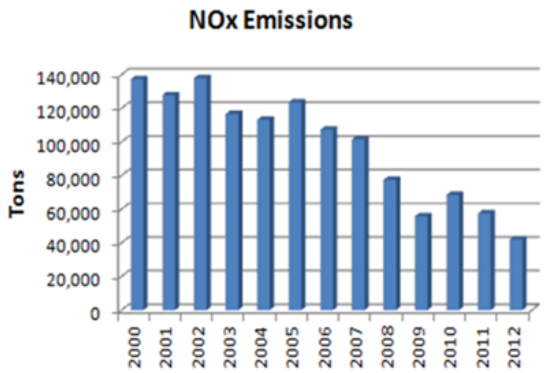


Fig. 1. NOx emissions throughout the years

ii. React with volatile organic compounds in presence of sunlight to form ozone causing lung disorders
ii. Also forms toxic chemicals with organic compounds like nitrosamines, nitroarenes and nitrate radical causing biological mutations
iv. Destruction of ozone layer in stratosphere.

B. MAPOL Annex VII Regulation 13:

In the maritime sector, for marine diesel engines with a power output more than 130 kilowatts the NOx limit in grams per kilowatt hour verses rated engine speed is shown in Fig. 2

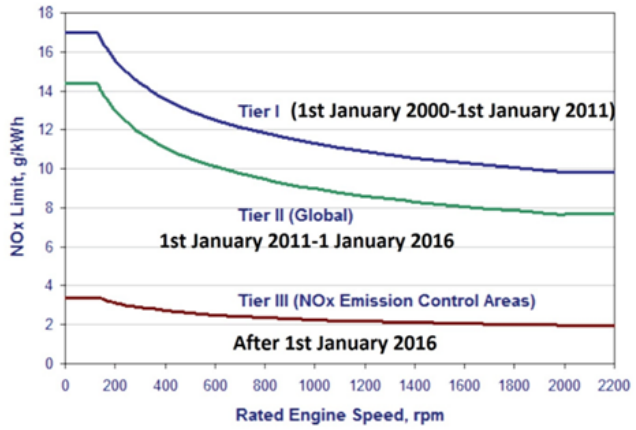


Fig. 2. Graph for NOx limit laid down by MARPOL

These limits have been brought into action after a detailed study of the effects of nitrous oxide. So in account of this various pre-treatment methods have been implemented in the maritime sector like water injection, humidified air motor (HAM) and post treatment methods like selective catalytic reduction (SCR) but each with its certain drawbacks.

V. PROPOSED SYSTEM

In this system, shown in Fig. 3, we intend to fit a nitrogen generator at the air suction of the engine. Thus, as air would enter the nitrogen generator, one outlet will be of pure oxygen and other outlet of nitrogen and other gases depending on the efficiency of the nitrogen generator. The pure oxygen would be sent to the main diesel engine for combustion while the nitrogen would be used for hull lubrication.

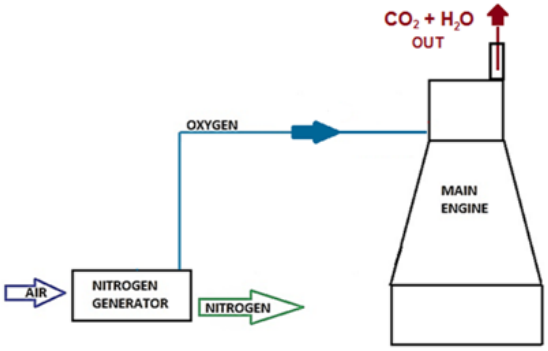


Fig. 3. Proposed system

VI. NEW COMBUTION ANALYSIS

When pure oxygen will be sent for combustion, it will lead to an ideal combustion process in which fuel will combust with oxygen in stoichiometric ratio forming carbon dioxide and water vapour. There will be a substantial reduction in heat losses due to absence of other gases. But it will lead to very higher temperatures and pressures with an increased power. It will lead to greater thermally induced vibration and pressure induced vibrations which would cause damage to an engine producing same power as a conventional engine using air for combustion. It also leads to generation of hot spots and flame spots. Also there is a problem of insufficient pressure development during the strokes due to lesser quantity of gas available for expansion. And if the oxygen content increases a little more than the stoichiometric ratio, it will lead to catastrophic destruction.

VII. SOLUTIONS TO THE PROBLEMS

A big solution to all these problems is recirculation of carbon dioxide which is produced during combustion.

i. Recirculation [1]: Carbon dioxide is an inert gas with high emissivity. After combustion, a part of the products thus formed is cooled and after water is condensed out carbon dioxide is recycled back and mixed with the incoming oxygen and is sent to scavenge space. Condensation leads increase in the density of Carbon dioxide. Thus due high emissivity of carbon dioxide it takes the heat of combustion maintaining the temperature and also reducing thermally induced vibrations.
ii. Ratio controller [1]: This also gives an additional degree

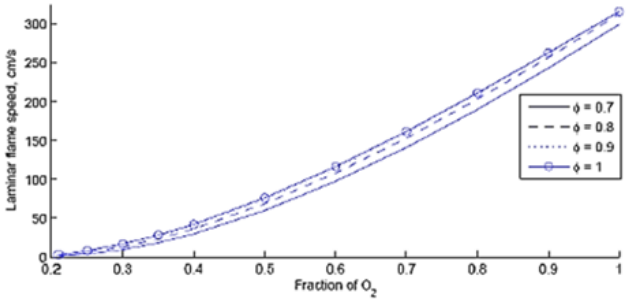


Fig. 4. Graph of fraction of O2 verses laminar flame speed

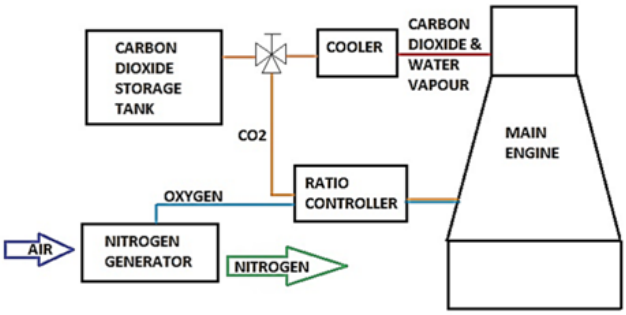


Fig. 5. System with carbon dioxide recirculation

of control i.e. the ratio of oxygen to carbon dioxide could be controlled as per the load on the engine maintaining sufficient oxygen for combustion and avoiding a disaster. For O2 content of 30, nearly 90 of CO2 is recirculated.
It is maintained by Oxidizer ratio given by [1]:

$$\lambda = \frac{\text{number of moles of } O_2}{\text{Number of moles of } O_2 + \text{number of moles of } CO_2}.$$

Demands of fluctuating load will be taken care of efficiently. From experiments conducted by Ditaranto and Hals (2006) [2], they show that up to a certain threshold in oxidizer composition, the vibrations induced due to pressure are similar to what is found when burning fuel with air. Above this threshold, however, the instabilities tend to grow even stronger so it is important for ratio to be maintained below this for safe running. Fig. 6 shows a system where oxidizer ratio exceeds threshold value.

iii. Placement of fuel injectors [1]: A usual performance measures for a combustion process is how fast the system is stabilized i.e. bandwidth. In practice nominal bandwidth is not critical as the dynamics are fast. Hence robustness, i.e. the ability to stabilize the system for a variety of disturbances

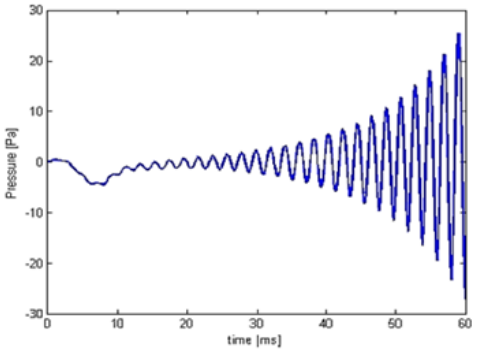


Fig. 6. Response of uncontrolled system to unbalance in oxidizer ratio

and operating conditions is the critical measure. Depending on the location of the injectors, there will be a time delay. The time delay will impose a serious limitation on the achievable bandwidth, because every control action will be delayed. A time delay is a phenomenon that might lead to oscillations if the design bandwidth of the controller is too high. Its effective positioning helps in reducing the induced vibrations to a greater extent.

iv. CO2 injectors [1]: When fuel is injected, it resulted in generation of hot spots on the flame surface, due to pockets of pure fuel entering the flame zone. In addition to hot spots, secondary diffusion flames due to poor mixing were reported in Hath out et al. (2002) [2]. If one uses carbon dioxide injectors for control, the opposite might occur. Pockets of CO2 might cause the flame temperature to be reduced. However, this is probably not as problematic as the hot spots. Also, use of carbon dioxide does not influence the total amount heat produced in the combustion, and will therefore not cause significant fluctuations in power production in engines.

There are two possibilities for injection: one can inject directly into the flame, or upstream of the flame. Injecting directly into the flame will not allow the injected gas to mix with the main flow before burning. This can cause hot spots on the flame surface, and secondary diffusion flames (Hath out et. al., 2000) [2]. Injection upstream of the flame gives better mixing, but will cause a time delay due to transport of the injected gas to the flame. Time delay depends on length of travel and velocity of gas. Thus, the injector placement will always be a tradeoff between good mixing and problems related to time delay. Even a small time delay can cause greater oscillations but if the time delay is taken into account during controller design, it is still possible to stabilize the system. Figs. 7 and 8 show the design of the combustion space.

The solution to these problems helps addressing several questions. The most important is where to place the injector. One wants the injector to be placed as far from the flame as possible, to ensure good mixing of the reactants before burning. However, the injector must be placed such that the system can be stabilized. As the time delay is a function of both injector location and operating conditions. The new system

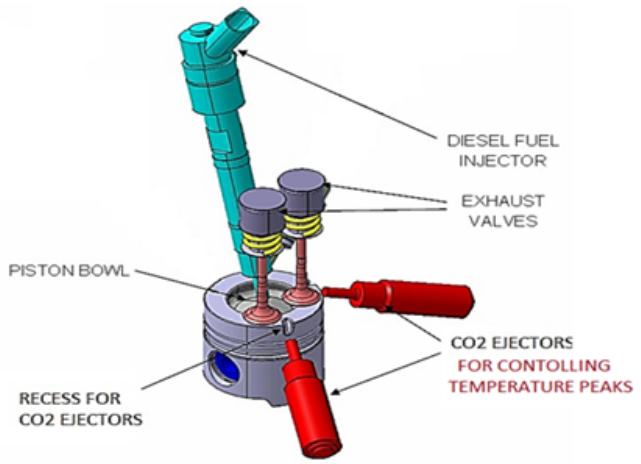


Fig. 7. Construction of cylinder head.

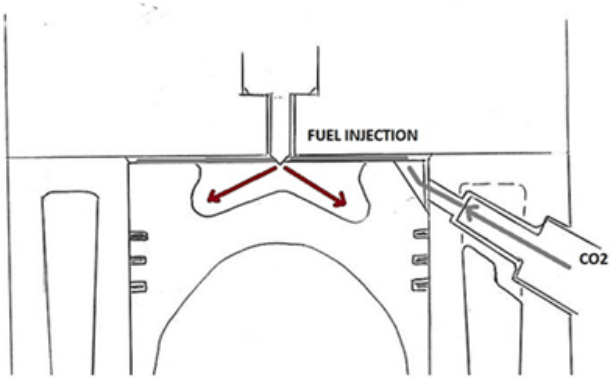


Fig. 8. Section view of combustion space

would not possess any threat of scavenge fires as the gas being stored in the space would not be pure oxygen but a mixture of oxygen and carbon dioxide.

VIII. FUEL ANALYSIS

A typical marine heavy fuel oil consists of 85 percent Carbon, 12 percent Hydrogen and 3 percent Sulphur by mass. In 1kg of fuel by considering their molecular weights, it comprises of 0.85kg carbon, 0.12kg Hydrogen and 0.03kg Sulphur, leading to formation of 2.27kg Carbon dioxide and 1.08kg water by consuming 3.26kg Oxygen. As air contains approx. 23 percent oxygen amount of air needed initially 14.17kg of air was needed now reduced to 3.26kg + 5 percent extra and remaining carbon dioxide for cooling.

IX. THE GAS SEPARATOR

The proposed gas separator is a membrane type construction which has been shown in Fig.9. It involves the use of BICUVOX (Bi2Cu0.1V0.9O5.35) which is a ceramic oxide [4]. Oxygen will be transported through the membrane through ionic conductivity. The air which is made to pass over the oxide membrane, due to the surface reaction at the cathode results in the formation of O2- ions. The ions forms then move through the oxygen vacancies towards the anode part where the dissipate electrons hence forming molecular oxygen. This separator is capable of generating a quantity of 5litres per minute of oxygen.

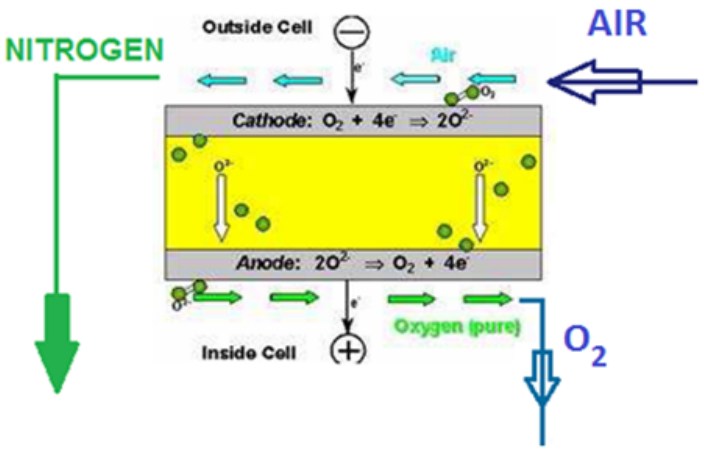


Fig. 9. The ceramic oxide membrane

X. WORKING OF THE SYSTEM

The working of the system has been represented in Fig. 10. The exhaust is sent to the turbine side of the turbocharger. Hence the air which is sucked in by the blower is sent to the membrane generator. It separates out the oxygen which is the sent to the ratio controller. Here the oxygen mixes with the carbon di oxide which is coming from the condenser. The mixture is formed in a stoichiometric ratio according to the load demand.

XI. AIR HULL LUBRICATION

In this system we use a pump which sucks in air and this is then pumped underneath the hull surface. This forms a blanket of air bubbles underneath the hull surface. This help in significant reduction in the viscous drag and hence the hull resistance reduces. This design claims to reduce the CO2 emissions and the fuel consumption by 10-15 percent. With these claims tis technology has been taken up by some of the established companies and many claim it to be one of the promising technologies which will help ships to improve their efficiency and reduce energy losses [6] [7].This system has the disadvantage of not being efficient for all hull forms. Example: In case of V-Shaped hull forms the bubbles tend to escape out from underneath the hull. Also due to the use of air for the lubrication purpose it results in the oxidation corrosion of the hull surface.

XII. NITROGEN HULL LUBRICATION

The Fig.11 and Fig.12 shows the Nitrogen Hull Lubrication for a ship. To overcome this disadvantage of oxidation corrosion arising as a result of the use of air for

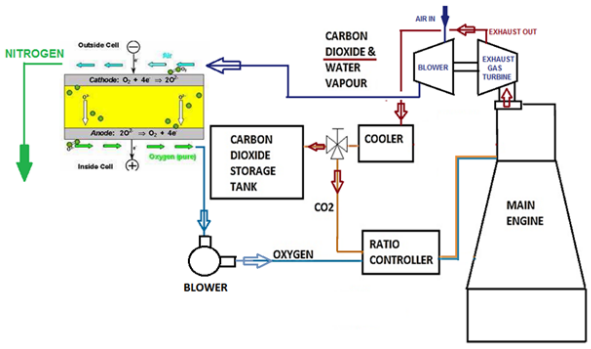


Fig. 10. Final system layout

the lubrication purpose. So here we propose to use nitrogen produced by the Membrane Generator in place of air. Its use will help us not only in preventing oxidation corrosion but now we will also be able to diminish the effects of Sulphate Reducing Bacteria which is found widely in anaerobic conditioned places such as freshwater, brackish, and saltwater.



Fig. 11. Nitrogen Hull Lubrication

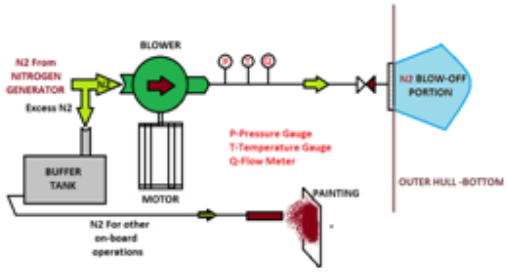


Fig. 12. System for Nitrogen Hull Lubrication

The Fig.13 depicts the action of Sulphate Reducing Bacteria [5].The interaction of water and metal creates a layer of molecular hydrogen on the metal surface and the sulfate-reducing bacteria then oxidize the hydrogen while creating hydrogen sulfide, which contributes to corrosion.

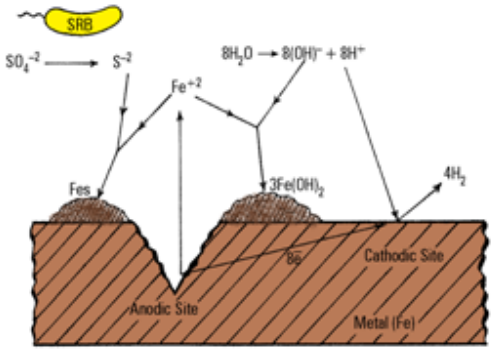


Fig. 13. Action of Sulphate Reducing Bacteria

XIII. SOLUBLITY OF NITROGEN

The solubility curve for Nitrogen in water is depicted in Fig.14. Nitrogen (N2) solubility even at 20 degree and pressure = 1 bar is approximately 20 mg/L. Hence even at low temperatures we do not have wastage of bubbles generated for lubrication. Also the use of Nitrogen in gas form does not contribute to algae bloom in any way hence not possessing problem to environment such as algae boom in any manner.

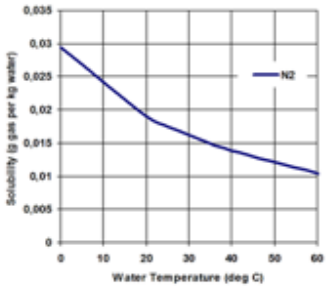


Fig. 14. Solublity Curve For Nitrogen

XIV. USE OF NIROGEN IN PAINTING OPERATIONS

A part of the excess nitrogen produced can be stored in a buffer tank. This can then later on be used to perform painting operations on board in place of air being used in air guns. The comparison sketch between the air and nitrogen spray painting has been depicted in Fig.15 .

The nitrogen used would help us in creating an inert environment hence preventing the entrapment of air under the paint layer resulting in elimination of oxidation of the metal surface. Nitrogen has also got the property of lower coefficient of thermal expansion as compared to air which

prevents cracks in the paint layer hence keeps it intact with changing surrounding air temperatures. This will also help us achieve an increment in the life of the painting hence there is a cut down in the downtime of the painting operations. This will cut down in the cost to the owner for painting operations.

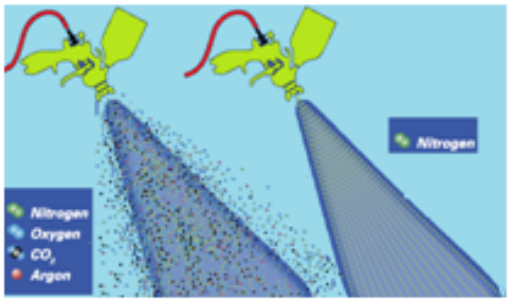


Fig. 15. Comparission between atomisation with use of air and nitrogen respectively

XV. NEW INSTALLATIONS

A. Oxygen generator

The one we intend to use is the one with the membrane technology. The main driving force for the separation is the differential pressures across the ends of the membrane column and the use of the two electrodes- Cathode and Anode.

B. Axial Air blower

For effective and faster flow rates across the membranes we would require to create differential pressure. Hence we will be requiring Axial Blowers.

C. Piping system

1) Oxygen: The use of oxygen will require the installation of oxidation proof piping. This requirement can be achieved by use of metal such as aluminium, a very useful structural metal along with its light weight. It also undergoes an oxidation reaction, but does not corrode at a rate according to its reactivity, once a thin oxide layer of Al2O3 has formed on the inner pipe surface. It will act as a barrier to oxygen and water vapour present to prevent further corrosion of the aluminium. Aluminium used for such installations can be made harder, stronger and stiffer by mixing it with small amounts of other metals (e.g., magnesium) to make alloys. Coating the piping inner surface with a thin layer of metals like tin, chromium, nickel etc. by electroplating can also be utilized to prevent corrosion of the piping. A much more preferred and widely used process is alloying. Iron or steel can also be protected by alloying or mixing with other metals such as chromium to make non-rusting alloys such as chrome alloy. Stainless steel is an example of a non-rusting alloy of iron and carbon and such as stainless steel 300 series can be used. Safety for its installations: The oxygen piping system shall be kept clear of very high temperature heat sources .As for oxygen cylinders the limit is set to a maximum of 52 degree Celsius for the surrounding but since we are using oxygen not in a pressurized form and its use with the carbon dioxide exhaust as for combustion process hence, we can go for increased temperature limit for ensuring safety

2) Nitrogen:: Use of nitrogen not in liquefied or in significantly pressurized form adds to the use of easier construction materials for pipelines. Nitrogen is compatible with all common materials of construction for piping systems. Use of appropriate pressure class rating materials shall be taken into consideration according to our pumping pressure requirements.

XVI. ENGINE SPECIFICATIONS AND CALCULATION

HSD-MAN B& W 5S70MC -2Stroke -5 Cylinder SFOC (Specific Fuel Oil Consumption) = 121.5 g/BHP hr. For 16,240 BHP rated 86.2 rpm Fuel consumption (per cylinder) = SFOC $\times$ BHP = 32.886 kg/min Total Fuel Consumption= 32.886 $\times$ 5 =164.43 kg/min Amount of air required per kg fuel=15 kg Amount of O2 required (per kg fuel) =3.423kg/min Total O2 required = 3.423$\times$164.43 = 562.84kg/min Density (At Normal Temperature Pressure): 1.33kg/m3 O2 requirement (in m3/min) = 562.84 $\div$ 1.33 = 423.18

With use of the Solid Membrane and the electrode system we have used additionally a blower for increasing the pressure difference the system more viable.

With the Nitrogen hull lubrication in place - We have a minimum of 10% CO2 emission reduction So, 10% Reduction in fuel (Fuel Saving) Fuel saving per day=0.1$\times$164.43$\times$60$\times$24 =23677kg/day = 23.677 Tones/day Thus, Cost Saving per day= \$700$\times$ 23.676 = \$16,573.2 (1Tonne of heavy fuel oil=\$700) Cost Saving per annum = 16,573 $\times$ 250 = \$4.14 million Thus this system is very economical. Additionally we will have a very efficient combustion due to use of Pure Oxygen. So, we will have an additional fuel saving.

XVII. CONCLUSIONS

Thus, in this system, combustion is stabilized with carbon dioxide injection and recirulation. The main benefits are that it is free (because CO2 is captured in the process), and as it is an inert substance, it does not manipulate the equivalence (air/fuel) ratio. For oxy-fuel processes it is important to operate at near stoichiometric operating conditions to avoid oxygen in the exhaust. Therefore, we choose to use CO2 injection to control the system. It doesnt affect the power output reducing NOx. The other parallel system in turn enhances the propulsion reducing drag with elimination of corrosion. Also a brief discussion of the new installation to be done in order to implement the system on merchant vessels. The calculations done gives the feasibility of the system on board and its perspective benefits.

XVIII. CONCLUSION

The image processing based algorithm to extract dolphin whistles from underwater noisy environment is discussed in

this paper. The algorithm consists of different steps applied on spectrograms. The algorithm is implemented using MATLAB environment.

REFERENCES

[1] Snarheim, Dagnn, "PhD Thesis: Control issues in oxy-fuel combustion", Department of Engineering Cybernetics, The Norwegian University of Science and Technology, August 12, 2009.

[2] Snarheim: L. Imsland: R. Ulfsnes: O. Bolland, and B. A. Foss, "Control design for a gas turbine plant with CO2 capture capabilities", In Proc.16th IFAC World Congress, Prague, Czech Republic, 2005.

[3] Snarheim: L. Imsland: and B. A. Foss, "Control-relevant modeling and linear analysis of instabilities in oxy-fuel combustion". In Proc. 9th European Control Conference ECC'07, 2007.

[4] Snarheim: N. E. Haugen: L. Imsland and B. A. Foss, "Control design and stability analysis of oxy-fuel thermo acoustic instabilities". Submitted to IEEE Trans. Control System Technology, 2009a.

[5] Snarheim: L. Imsland, and B. A. Foss: "Active control of oxy-fuel combustion using pre flame CO2-injection", In Accepted for European Control Conference ECC'09, 2009b.

[6] Ditaranto and J. Hals, "Combustion instabilities in sudden expansion oxy-fuel flames", Combustion and Flame, 146:439-512, 2006.

[7] Clean Air Technology Center (MD-12), Information Transfer and Program Integration Division Office of Air Quality Planning and Standards, U.S. Environmental Protection Agency Research Triangle Park, North Carolina 27711,EPA 456/F-99-006R,November 1999.

[8] Brady, Justin: Spain, Travis and Shambaugh, Brent May "Membrane Separation of Air to Produce Oxygen University of Oklahoma School of Chemical, Biological, and Materials Engineering, May 2006

[9] Barton, Larry L. and Fauque, Guy D. (2009). "Biochemistry, Physiology and Biotechnology of Sulfate-Reducing Bacteria". Advances in Applied Microbiology 68: 4198. [http://en.wikipedia.org/wiki/Sulfate-reducing-bacteria]

[10] Air hull lubrication [http://airskin.wordpress.com/frequently-asked-questions]

[11] Mizokami, Shuji: Kawakado, Manabu: Kawano, Mitsuhiro: Hasegawa, Takeo and Hirakawa, Ichiro, "Implementation of Ship Energy-Saving Operations with Mitsubishi Air Lubrication System", Mitsubishi Heavy Industries Technical Review Vol. 50 No. 2 (June 2013).

[12] Mizokami, S. et.al, "Experimental Study of Air Lubrication Method and Verification of Effects on Actual Hull by Means of Sea Trial", Mitsubishi Heavy Industries Technical Review Vol.47 No.3pp.41-47(2010).

[13] Nitrogen solubility curve [http://www.engineeringtoolbox.com/gases-solubility-water-d_1148.html]

[14] Nitrogen spray painting [http://www.myprgenie.com/view-publication/nitrogen-for-spray-painting]

XIX. ACKNOWLEDGEMENT

We would like to thank our advisor, Mr. Shailendra Kumar for his guidance throughout the research. It has been our privilege learning from him and developing our skills. We would also like to express our gratitude towards Mr. Sankar K. Subramanian and Mr. Sunil Kumar Panda for their contribution in this project. We would also like to give our sincere thanks to IWCEM for giving us an opportunity to present our paper.



Cdt. Neeraj Mehta is a 10+2 graduate from CBSE board, 2011. He is presently studying at Tolani Maritime Institute under the marine engineering program (BSME). He has presented the paper titled "The Nitrogen Revolution"at STS 2014 at Manipal University, Jaipur.



Cdt. Kevin Parmar is a 10+2 graduate from Maharashtra state board, 2011. He is presently studying at Tolani Maritime Institute under the marine engineering program (BSME). He has presented the paper titled "The Nitrogen Revolution" at STS 2014 at Manipal University, Jaipur.

Need of Physical Fitness and Lifestyle Management for a Seafarer

Animesh Padhi[1], **Arvind Kaushal**[2]
[1,2]Marine Engineering Tolani Maritime Institute Pune, India
[1]animesh.ricky@gmail.com, [2]rt5796@gmail.com

***Abstract*—With a small crew looking after a huge vessel, life on ship is tough and stressful. Many months out at sea adds to the high stress levels of seafarers. For safe navigation of a ship from one place to another, the seafarer involved requires high level of physical as well as mental fitness. The Maritime industry focuses on the physical aspect very well by providing the right physical training; but overlooks the mental aspect as required on ship. This paper falls under the Personal health strand as our area of interest. The paper aims to identify potential parameters to assess and ascertain physical as well as mental fitness of seafarers. As part of methodology, the paper has taken up the case study of a leading premium maritime institute, TOLANI MARITIME INSTITUTE, where a number of students are trained to join the merchant navy. The paper goes on to make an analysis of the same and draw conclusions with respect to the physical and mental abilities of the students. The paper gives a broad idea of some remedial actions depending upon the industrial requirement and the problems faced by the various seafarers. In conclusion, the paper gives suggestive measures to the maritime industry in regards with the physical and mental fitness of seafarers.**

***Index Terms*—Physical Fitness; Lifestyle Management; Seafarer; Maritime industry.**

I. Introduction

Globalisation is trading between two countries. For trading, there are 3 modes of transportation. Water transport is cheapest among all of them. This depends on healthy condition of machinery, material of machinery and manpower. Above all, the health of the ship's crew is vital as this profession demands absolute fitness to deal with pressures all the time. Seafarers working on board are completely in a unique situation where they are totally cut-off from the social environment. This makes life on board really tough; with only a few to communicate with, that too people with different cultures, food habits and even language. Study and research over the years has indicated that most of the crew members undergo the feeling of loneliness and even alienation. Such a mental set-up may lead to decline in efficient output of employees at work. This aspect set us thinking and led us towards the initiation and writing of this paper.

II. METHODOLOGY

In order to study this problem at length, the Survey Method was used to gain better insight. The survey was conducted at TOLANI MARITIME INSTITUTE, Induri, Pune. 18 Faculty members, from both deck side and engine side of Merchant Navy, are part of the survey conducted. A questionnaire was designed for the survey. There were two different questionnaires made for both deck side and engine side. The questionnaire was distributed among the faculty members and their responses were analysed.

The Interview Method was also used for data collection, wherein, special help was taken from the internship cadets of TOLANI MARITIME INSTITUTE. Four cadets were interviewed. Two of the Chief engineers and Masters were interviewed. They shared their experiences and the common problems faced by them and their shipmates on board.

According to various ratings given to the standard parameters, statistical analysis was done and suggestions based on the analysis of responses in the questionnaire and interviews have been presented in the paper. Following are the points that came to light via the survey -

III. PROBLEMS ENCOUNTERED BY SEAFARERS

The problems that seafarers commonly face on board can be divided into two broad categories:

- A.Physical problems The most common physical problem encountered is back pain. People with less strength and endurance fail to sustain themselves on-board.
- B.Mental problems The most common mental problems encountered on board were as follows -
  1) No fixed routine on-board ship - Seafarers are required to be alert at all times. This creates mental imbalance due to fatigue.
  2) In case of an emergency, they cannot take rest. This leads to mental as well as physical exhaustion.
  3) The use of satellite phones to interact with family is an expensive affair, especially for the junior officers (including 5th engineer and deck cadet). This increases the feeling of home-sickness.
  4) In case of any mishappening like death at home, officers are not allowed to sign-off at that point of time which creates a lot of mental stress.
  5) Variations in weather conditions on deck, high temperature in the engine room, huge work load at most times are other factors that contribute to crew's stress on ship. In view of the above listed, it is but natural to witness a decline in efficiency at work. And this inefficiency further adds to anxiety among crew members. All these aspects are contributory to loneliness and even mental breakdown.

IV. MARITIME LABOUR CONVENTION

Maritime labour convention is part of International Labour Organisation which was established in 2006. This convention was specifically made for seafarers.As per the convention, there should be 14 hours of working hours and 10 hours of rest in a period of 24 hours or 72 hours of working hours and 77 hours of rest in a period of 7 days. But this convention is not followed on-board ship. There is a convention which declares that all ships should have inbuilt WIFI but still many ships are not installed with WIFI.

V. ATTITUDE OF SEAFARER

Attitude is a very important aspect in relation with the lifestyle management of seafarer. As sea life is different from shore life, seafarers should have different attitude. Safety is the primary attitude required onboard. Never say NO attitude is also required. A seafarer should always be attentive and disciplined onboard. Willing to learn and teach attitude along with team spirit.

VI. ANALYSIS

The analysis is based on some standard parameters. These parameters are loneliness onboard ship, intensity of contract to get over, the expected activities suggested by the sample and job satisfaction. The analysis is based on only the survey done on the merchant navy faculty (CHIEF ENGINEERS & MASTERS).

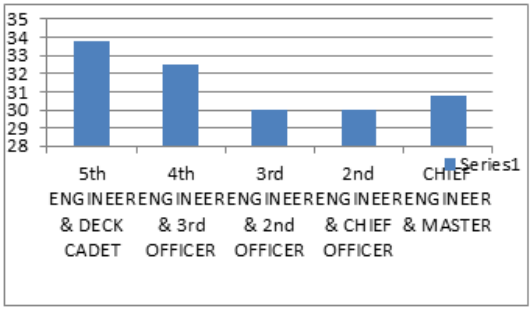


Fig. 1. LONELINESS ONBOARD SHIP

Figure no.1 shows the loneliness factor. Study indicates that the factor decreases as the rank increases. This is because seafarers get acquainted to the working conditions. As time progresses, they find some ways of entertainment for themselves. Also, they can bring their family along on ship.

Figure no.2 shows the intensity of the contract to get over. Study shows that the factor decreases as the rank increases. This is because the junior officers are new to sea environment. They tend to face sea sickness and many other problems like they are not able to interact with the senior officers, home sickness. The trend decreases because officers get a handsome salary as their rank increases, and this proves to be an incentive to remain on board.

Figure no.3 shows the expected activity on-board by the seafarers. The study indicates that most importance is given to exercise. According to the survey, exercise includes GYM,

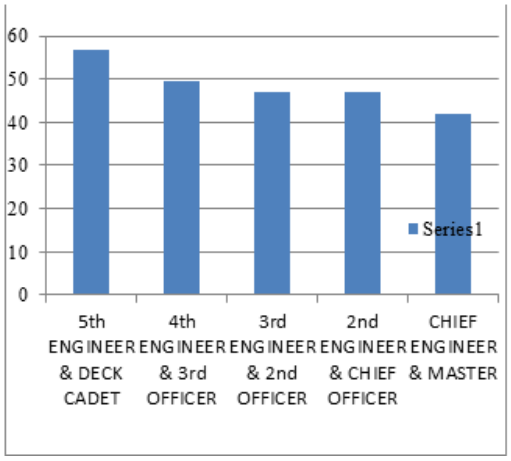


Fig. 2. INTENSITY OF CONTRACT TO GET OVER

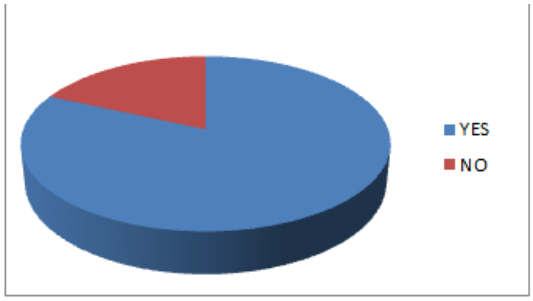


Fig. 3. EXPECTED ACTIVITY ONBOARD

swimming, indoor games and YOGA. YOGA is specifically being put up by the seafarers. The second priority is given to socialization which includes parties, interaction with friends and family via internet. Figure no.4 shows the job satisfaction for the seafarer. The study indicates that most of the seafarers like their job and they are satisfied with their job. This is because of handsome salary given by the companies. Seafarers get an opportunity to visit various countries. It is an adventurous and challenging life.

VII. SUGGESTIVE MEASURES & REMEDIES

After assessing the parameters, the paper comes down to a conclusion that there is a dire need of remedial actions to be taken by IMO, shipping companies and training institutes towards the following For physical fitness, exercise should be made a part of regular routine compulsorily. There should be a regular swimming endurance test of 50 meters conducted by the authority like Mercantile Marine Department annually. Even training institutes should conduct such tests to get the CDC (continuous discharge certificate) as conducted at TOLANI MARITIME INSTITUTE. The crew members should be increased. This will help to reduce the factors like work load, fatigue and loneliness. As the convention (Maritime labour convention) is not followed because of heavy work load, so, crew members should be increased. Provisions should be made for yoga in the training institute as well as on ship. Seniors should appreciate work done by juniors and they

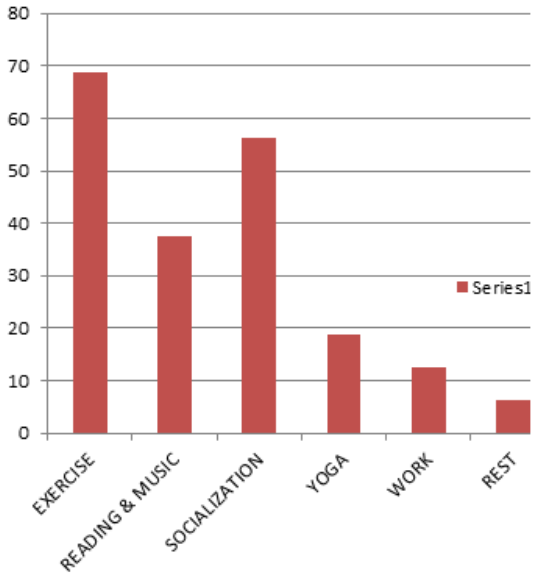


Fig. 4. JOB SATISFACTION

should motivate and respect them. As we see that seafarers are interested in socialization, hence, the WIFI should be installed in all ships.

VIII. CONCLUSION

Ship is a dynamic structure made up of different machinery which helps us in transporting of cargo. In such a case, the overall equipment efficiency becomes vital and important for the best output as expected by the industry. OEE (Overall Equipment Efficiency) depends on three factors that are availability rate, performance rate and quality rate. This is about the ship, but it is equally important and applicable to the crew members looking after the ship. Hence, the quality rate of people operating becomes important to get the best output. This quality rate demands physical and mental fitness of manpower. Hence, the paper gives some remedial action to be taken by the shipping industry.

IX. ACKNOWLEDGMENT

We would like to gratefully acknowledge the contribution from all faculty members and the internship cadets.Special thanks to: Dr. B.K. SAXENA (Principal, TOLANI MARITIME INSTITUTE; President of IME, INDIA) Mrs. SHEELA SAXENA (Psychologist, TMI) Dr. S.D. POHEKAR (Faculty, TMI) Mrs. PUJA AWACHAT (Faculty, TMI) Mr. SUNIL KUMAR PANDA (Faculty, TMI) Mr. S.G. BHILARE (Senior Sports Coordinator, TMI) Dr. NITIN JUNARKAR (Faculty, TMI) Cadet AMAN DHANKAR (Cadet of NYKSM) Cadet KESHAV KAUSHWALA (Cadet of NYKSM)

REFERENCES

[1] www.ilo.org/global/standards/maritime-labour-convention/lang–en/index.htm
[2] http://en.wikipedia.org/wiki/Maritime_Labour_Convention
[3] http://www.imo.org/MediaCentre/PressBriefings/Pages/38-MLC.aspx.UweBEvmSwxA
[4] APPLIED SURVEY METHODS: A STATISTICAL PERSPECTIVE, Jelke Bethlehem
[5] http://www.wikihow.com/Develop-a-Questionnaire-for-Research
[6] http://www.mdi.ac.in/research-and-consultancy/vision-mdi-journal.html



ANIMESH PADHI Cdt. Animesh Padhi is pursuing a course of B.S.MARINE ENGINEERING at TOLANI MARITIME INSTITUTE, Pune, INDIA. This is his first paper presentation at IWCEM.



ARVIND KAUSHAL Cdt. Arvind kaushal is pursuing a course of B.S.MARINE ENGINEERING at TOLANI MARITIME INSTITUTE, Pune, INDIA. This is his first paper presentation at IWCEM.

OBJECT DETECTION FOR MARITIME SURVEILLANCE

Avani Agarwal[1], **Disha Mehra**[2]
[1] 2nd Year BTech
Dept. of Electronics & Communication Engineering
Manipal University Jaipur
[2] 2nd Year BTech
Dept. of Computer Science & Engineering
Manipal University Jaipur
[1]avaniiat@gmail.com

***Abstract*—Maritime surveillance is associated with exchange information and data, to safeguard interests in Exclusive Economic Zones (EEZ), territorial waters, rivers and lakes. An important aspect of maritime surveillance is to detect the object in restricted channels which may be aimed to for resource plundering, smuggling, illegal immigration, piracy, and terrorism.**

Radar is commonly used in maritime traffic control systems, to detect and follow moving vessels. Visual verifications by traffic operators are done using Video cameras. Although radar technology is mature and gives highly accurate results, interference in the radar signal from clutter originating from echoes returned from targets, makes object detection difficult to the radar operators. These sources of these echoes can be from the surroundings such as ground, sea, atmospheric effects or buildings, bridges or other ships/ objects in the vicinity. Furthermore, small and non-metal ships are almost impossible to detect. Other than these technical difficulties, the radar technology is quite expensive.

In this study, the author(s) reviewed the state of art technology for real time ship detection and tracking. It was found that the commercially available Pan-Tilt-Zoom (PTZ) camera systems, have the capability to reduce or remove the shortcomings felt by the operators in the radar-based system. This system allows the integration of generated detection information to the existing waterway traffic analysis system, providing ease of object detection and guidance. The paper concludes with the possible suggestion of utilizing the technology for maritime surveillance in restricted waters.

***Keywords*—Radar, object detection, waterways, training, clutter, image processing**

I. INTRODUCTION

Object detection for video surveillance applies background modeling techniques and classifies each pixel of the image into background or object [1]. Typical camera views are shown in Fig. 1. Such techniques have difficulties in handling light variations and continuously need adaptation. False detections occur due to randomly moving objects. These algorithms are bound to use of stationary cameras. Many cameras are required to monitor a large viewing area. As the speed of ships in harbors is typically slow, continuous monitoring of the complete area becomes expensive. Scanning the area with a single pan-tilt-zoom camera is ample for regularly sampling the ships locations. Background segmentation cannot be used, as ships should be detected for any position of the camera.

The design of such a system is subject to various system constraints of which robustness for varying weather and daylight time conditions are most relevant. Besides these aspects, the system should handle different types of objects, which are typical for maritime surveillance (e.g. canal ship, sailing boat, speedboat, etc.). Another aspect is the positioning of the camera w.r.t. the waterway and the viewing angle on the vessels passing by.

A pantiltzoom (PTZ) camera is a camera that is capable of remote directional and zoom control. In television production PTZ controls are used with professional video cameras in television studios and referred to as camera robotics. These systems can be remotely controlled by automation systems. The use of a PTZ camera can contribute to the handling of difficult cases in distance (zooming) and viewing angle (rotation). Therefore, algorithm that is independent of background information, movement in the scene and camera motion is considered essential. The aim is to identify a system that is invariant to changes in illumination and allows for some object shape variations. Thus, the algorithm should use an object description to discriminate between object and background, in which the most important features are automatically learned from annotated training data without any user interaction [1].

II. ALGORITHM

Object Detection

To detect and identify an object, comparison of local description of the object and background needs to be classified. Scaling would be required to differentiate the sizes. For the purpose Dalal and Triggs [2] suggested Histogram of Oriented Gradients (HOG) approach. This approach was already proved in a survey on pedestrian detection [3]. The algorithm was based on the concept of using small cells of pixels of a histogram. The orientation of the gradients within the cell are computed with a filter both horizontal and vertical directions. The gradient direction is then computed by the ratio-strength of both dimensions. The gradient orientation

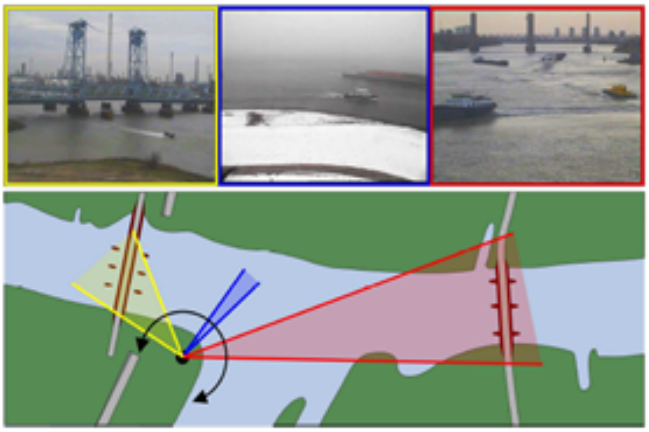


Fig. 1. Example of three positions of the PTZ camera in the detection system [1]

is quantized into bins, and the corresponding orientation bin is updated with the gradient magnitude. Object detection is obtained by sliding a window over the image and classifying the local description for each position into object and background. To detect objects of different size, the detection process is repeated for scaled versions of the input image.

System Training

To identify the object and differentiate in sizes, the system needs to be trained. This training is performed offline and after training, the system should be able to detect objects on a live video stream. A large dataset is created, covering all types of visual variation that can occur in the background. For the purpose of restricted waterways surveillance, different types of ships should at least be sampled once, which is not practical. The detector should therefore be exposed to batches of training samples, each batch covering a certain time interval in the video stream. Because the detector is trained offline, this requires a full retraining step, with significant computational costs. Support Vector Machine (SVM), which are based on the concept of decision planes that define decision boundaries, are often used for offline training, because they have high performance on high-dimensional feature spaces. The SVMs have high execution times and require the complete dataset for training.

In the online learning approach, the detector can be trained instantaneously with every new sample, eliminating the waiting times for retraining. The updated detector can be directly applied to the input video stream, immediately improving the results of automatic detection. This decreases the amount of manual annotation effort and distributes the annotation work over the installation period, monitoring and control of the system operation.

An online algorithm consecutively considers each training sample in an independent way. Stochastic Gradient Descent (SGD) algorithms have been reported for having been used successfully for the training of neural networks[4]. Bottou et

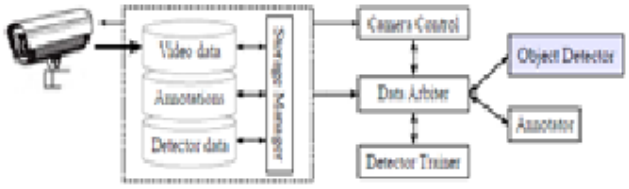


Fig. 2. Overview of the object detection architecture

al. [5] have expanded this concept for the purpose of training linear classifiers, using a regularization constraint as in SVMs. They showed major speedups in computation time with no loss in classification performance on large-scale learning problems. Therefore, Stochastic Gradient Descent (SGD) has been recommended for incorporation in the object detection framework [6].

Architecture

Rob Wijnhoven et. al. [1] suggested a typical architecture for an object detection framework as per Fig. 2 Video is captured by the system and processed by the object detector. The video is then displayed in the annotation component and detection results are overlayed on the video. Each component has a limited set of interface functions and only communicates with the data arbiter. Two modes of operation were considered as follows:

1. In the installation phase, the detector can be interactively trained by manual annotation.
2. After the training phase, the detector trainer component can be removed, resulting in a fixed autonomous detection system.

III. DATASET CREATION FROM LITERATURE

A dataset of ships was created by Rob Wijnhoven et. al., from maritime video, to measure the performance of the detection system, [1]. Video was captured at the Botlek, a world-leading harbor and industrial area in Rotterdam, The Netherlands. A commercially available PTZ camera was used and images were captured. During these experiments, the camera was fixed at one position overlooking the canal, with a view perpendicular to the motion direction of the ships, so that ships appear in side views. Over a period of three days video was recorded during daytime, with varying weather conditions. In total, 150 different ships were recorded. Fifty ships were used as training data, the remaining 100 ships were used to evaluate the performance of the detection algorithm. The stern (back) of the ship were annotated, as it is the least visually varying part of the different ships. Details obtained by them are shown in the final dataset in Fig. 4 and examples of the positive training samples are shown in Fig. 3



Fig. 3. Ship training examples with large variation in appearance and image quality.

Subset	Images	Ships	Ship img samples	Avg. img/ship
Train	135	50	140	2.8
Test	282	100	306	3.1

Fig. 4. Dataset Statistics.

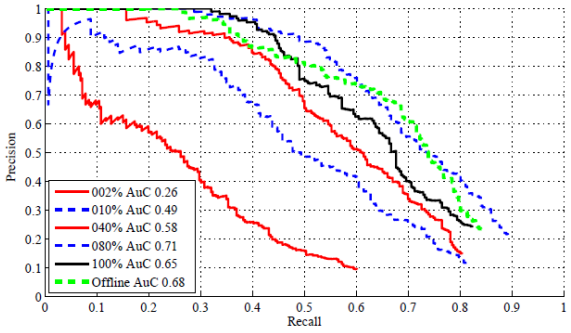


Fig. 5. Recall-precision curve of detections using offline training.

Experiment 1: Offline Training

In the first experiment, the dataset obtained was used, and detection performance was evaluated after training. Stochastic Gradient Descent was used as the training algorithm. All 140 training ship images were flipped horizontally (mirror image along y-axis) to obtain a total of 280 positive samples. In this way, a detector was obtained that is invariant to the direction of the ships. Only gray scale information was used by Rob Wijnhoven et. al., [1] in the experiments to neglect light variations. A two-stage approach was used as proposed by Dalal and Triggs, to train the detector. 10 descriptions were randomly sampled from each of the training images as the initial set of negative samples. Descriptions of random regions which did not overlap with the positive object samples for more than 50%, were extracted. A first iteration classifier was trained on the total set of 280 positive samples and the initial negative samples. This detector was then applied to the training images. All false detections were hard negative samples and they were added to the initial training set to obtain the final training set.

In a second iteration [1], the previously obtained training set was used to train the final classifier. To detect objects, a sliding window detection technique was employed. For each position in the image, the description of the detection window is classified into "background" or "object". To obtain scale invariance, a number of down sampled versions of the input image were processed. For the detector, a detection window size of 48×24 pixels, 4×4 pixel cells, 18 orientation bins using the sign, L2 normalization and 2 × 2 block normalizations was used. Each detection of the algorithm was compared to the set of annotated ground truth samples, to evaluate the performance of the detection system. If the detection overlapped with at least 50%, it counted as a true detection, otherwise it was a false detection. To combine results over the total dataset, a recall-precision curve was created. The horizontal axis represents the percentage of ground truth objects that are detected (recall) and the vertical axis represents 100% minus the percentage of false detections (precision). The recall-precision curve for this experiment is shown as the dashed green curve in Fig. 5. The figure shows that 85% of the ships were detected, albeit with many false detections. It was noted that a significant number of these false detections are actually located at or connected to a ship. The strongest false detections appeared at the bow (front) of the ship, which can be understood because of the visual similarity to the learned stern (back). Some example detections are shown in Fig. 5

Experiment 2: Online Training

In the second experiment] Rob Wijnhoven et. al., [1], used online training, where the detector was iteratively updated for each training image. Samples now appeared in the order determined by the scene (video sequence). Hence, in this experiment, the classifier was trained sequentially using only the information available in the current image and therefore optimized locally, prior to evaluating a new video frame. Therefore, the final classifier was different from the globally optimal classifier based on all training images. For each image, only the positive samples were extracted and used to update the classifier.

The image was then scanned with the detector and false detections were used as new negative samples. The classifier was then updated with both the positive samples and the gathered negative samples. This process was done once for the current video frame. Optimization, by processing images through multiple iterations were stopped, when there were no more false detections and all ships were detected. In the experiment, the detector was trained with an increasing number of video images from the training set, and the detection performance was evaluated. The resulting recall-precision curves presented by] Rob Wijnhoven et. al., are shown in Fig. 5

Results were visualized from the recall-precision curves in Fig. 5 by plotting the area-under-curve vs. the percentage of training samples used. The resulting curve is shown in Fig. 10 This result led to the following three observations and findings [1]:

1. When learning from a limited subset of training samples,



Fig. 6. Typical false detection at the bow of the ship.

the training process creates a useful detector.
2.The detection performance does not always increase when adding more training samples.
3.From the curve in Figure 10 it was seen the resulting classifier outperforms the offline detector.

IV. USE IN MARITIME SURVEILLANCE

There is a global interest for active maritime surveillance, in order to protect the Exclusive Economic Zones (EEZ), and have safe harbours. The present study identifies a state of art technology for real time ship detection and tracking. It has the capability to reduce or remove the shortcomings felt by the operators in the radar-based system for harbor security, port management, and maritime surveillance.

This system allows the ease of object detection and guidance which can be applied in channels for safe navigation and also to detect threats from undesired activities and terrorism. The system can tackle the challenges of restricted navigational areas, small and non-cooperative objects taking advantage of maritime activity to conceal their actions. The system can be employed and easily trained for the background and the range of ships expected to be passing and then utilized for detection of unidentified objects for surveillance.

V. CONCLUSION

An object detection system for the application of maritime surveillance was proposed by Rob Wijnhoven et. al., [1]. In contrast with conventional systems based on background segmentation. The proposed detection algorithm can operate on video from a moving pan-tilt-zoom camera. The new system has a modular architecture and applies online learning. With each manually annotated training sample, the detector is instantly retrained in real time by embedding the Stochastic



Fig. 7. Correct detection of uncommon ship.



Fig. 8. Missed detection and false detection.



Fig. 9. Correct detection of both ships.

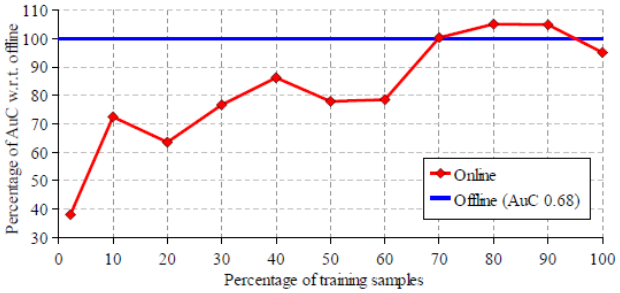


Fig. 10. Online learning performance (red curve) vs. offline training (blue line).

Gradient Descent (SGD) optimization algorithm in the object detection framework. Because of its online nature, SGD can be directly applied to the ship detection problem.

The system proposed and experimented [1]has an excellent utility in restricted water navigation, particularly in channels. The system can be redeveloped to felicitate the pilots for easy navigation, through iterative training process with increased memory and also assist the port management in protecting the harbours from external threats, harbour security and port management.

REFERENCES

[1] Rob Wijnhoven et. al., Online Learning for Ship Detection in Maritime Surveillance, Thirty-first Symposium on Information Theory in the Benelux.

[2] N. Dalal and B. Triggs, "Histogram of oriented gradients for human detection," in Proc. IEEE Conf. on Computer Vision and Pattern Recognition (CVPR). June 2005, vol. 1, pp. 886893, IEEE.

[3] Piotr Dollar, Christian Wojek, Bernt Schiele, and Pietro Perona, "Pedestrian detection: A benchmark," in Proc. IEEE Conf. on Computer Vision and Pattern Recognition (CVPR), June 2009.

[4] Yann LeCun, Leon Bottou, G. Orr, and K. Muller, "Efficient backprop," Neural Networks: Tricks of the trade, LNCS, vol. 1524, 1998.

[5] Leon Bottou and Olivier Bousquet, "Learning using large datasets," in Mining Massive DataSets for Security. IOS Press, Amsterdam, 2008.

[6] Rob G. J. Wijnhoven and Peter H. N. de With, "Fast training of object detection using stochastic gradient descent," in Submitted to Intl. Conf. Pattern Recognition (ICPR), August 2010.



Ms Avani Agarwal is a 2nd year ECE student at Manipal University Jaipur. During her schooling and in college she has been excelling in academics and takes active interest in organizing. She has presented a paper in the Students Technical Seminar organized at Manipal University Jaipur. Her areas of interest are Image Processing, Microprocessor Applications and Online Data Analysis. She has won awards in academics during her schooling.



Ms Disha Mehra is a student of 2nd year, pursuing her B.tech in Computer Science from Manipal University Jaipur. She has presented a paper in STS-2014. Her areas of interest our image processing, artificial intelligence and cloud computing. She has won many prizes for being good in academics as well as in sports.

Era of Advanced Materials

Sumit Jain
Department of Mechanical Engineering,
Manipal University,
Jaipur, India
jainsumit0018@gmail.com

***Abstract*—The principle objective of this paper is to demonstrate some recent development in the world of materials. There have been many new discoveries in recent past in the type of materials whether it is micro material or macro material. The paper highlights research going on in different type of materials. For example, there have been discoveries regarding the lightest material ever found. Similarly, carbon fibers are now used by the army for making bullet proof jackets as they are extremely light. In the world of nano materials, similar discoveries have been made. Regarding the strength of a material or it's malleability, new materials have been made. Materials used in medical surgeries have been replaced by more advanced materials which are long lasting and even safer to use. The paper focuses on developments made in bio-materials, nano materials and also materials used for weight reduction.**

***Index Terms*—Smart Materials, Programmable matter, Sintering, Meta materials, Zeta potential.**

I. INTRODUCTION

As the world is getting more technology friendly, research in advanced materials has also reached new heights. These materials include all types of nano materials, smart materials, functional materials, composite materials etc. They have a significant enhancement in their properties which may include weight, conductivity, visibility etc. Our discussion may be focused mainly on nano, smart and functional materials but a brief study has been done on other types too such as programmable matter, composite matter and dual particles.

II. NANO MATERIALS

Nano materials are those materials whose single particle's diameter is in the range of 1-100 nm. They can be divided into two types viz. natural and synthetic. Foraminifera structure, viruses (capsid), the wax crystals, natural colloids (milk, blood), some butterfly wing scales, spider-mite silk, the "spatulae" on gecko feet, horny materials (skin, claws, beaks, feathers, horns, hair),paper, and even our own bone matrix is natural organic nano material [2]. Natural erosion (clays), volcanic activity (opals), wildfires can lead to formation of natural inorganic nano particles.

Synthetic nano materials can be divided into two categories: fullerenes, and inorganic nanoparticles. The fullerenes are a class of allotropes of carbon which are graphene sheets rolled into tubes/spheres. Carbon nanotubes(or silicon nanotubes) are an example of this which is known for their mechanical strength and electrical properties. Fullerenes are light activated microbial agents which not only provide properties like superconductivity and heat resistance, but also find use in medical industry. They have the ability to attack cancer cells such as melanoma as well as act as binding specific antibiotics to the structure of resistant bacteria. Fullerenes can be produced artificially. This can be done by sending a large value of current between two nearby graphite electrodes in an inert atmosphere. This results in the formation of carbon plasma arc between the electrodes which cools into a sooty residue from which many fullerenes can be isolated. Inorganic nanomaterials (e.g. quantum dots, nanowires and nanorods) can be used in optoelectronics because of their interesting optical and electrical properties which can be tuned depending on their size and shape.

A. Uniqueness-

The uniqueness provided to these particles is due to the high ratio of surface area to volume present in many nanoscale materials making possible new quantum mechanical effects. One example is the "quantum size effect" where reductions in particle size result in altered electronic properties [4]. For example, fluorescence becomes a function of the particle diameter. This effect does not come into play by going from macro to micro dimensions. However, it becomes pronounced when the nanometer size range is reached.

When brought into a bulk material, nanoparticles can strongly influence the mechanical properties of the material. For example, when brought into traditional polymers, they result in novel materials which act as lightweight replacements for metals. These materials not only allow weight reduction but also result in increase instability and improved functionality [4].

There is a wide variety in size of nano particles and methods which help us in characterizing particle size distribution. Aggregation in solutions of particles which are initially nano particles make it necessary to characterize. These methods can be based on light scattering or applying of ultrasound [3].

Traditional techniques are also used for characterizing surface charge or zeta potential of nano-particles in solutions. Zeta potential is the potential difference between the dispersion medium and the stationary layer of fluid attached to the dispersed particle. This information is required for proper system stabilization, preventing its aggregation or flocculation. Electrophoretic light scattering and electro acoustics are example of this. In this, colloid vibration current method is suitable for characterizing concentrated systems.

The chemical processing and synthesis of high performance technological components for the private, industrial and military sectors requires the use of high purity ceramics, polymers, glass-ceramics and material composites. Density variation can be seen after compaction of the powder. It is because of the irregular sizes and shapes of nanoparticles which often lead to non-uniform packing morphologies.

B. Usage and applications-

These materials are used in optoelectronic devices based on organic material such as organic solar cells, OLEDs etc. Operating principle devices of such materials are governed by photo induced processes like electron transfer and energy transfer. The performance of the devices depends on the efficiency of the photo induced process which is responsible for their functioning also. Nanoparticles or nanocrystals can be made up of metals, semiconductors, or oxides. Nanoparticles are used as quantum dots and chemical catalysts like nanomaterial-based catalysts.

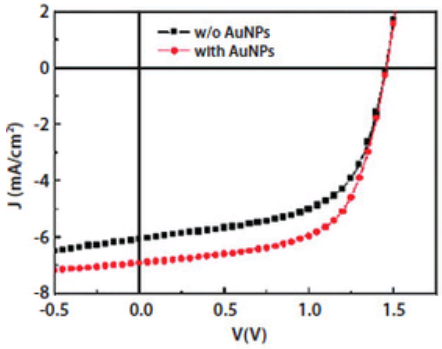


Fig. 1. Graph showing variation of current density vs voltage [13]

Changing the voltage V across the particles leads to measuring of changing current density J across it. Nanoparticles are somewhat a bridge between bulk materials and molecular structures. They are known for their varying physical properties unlike bulk matter. Their properties depend on the size of the particles such as quantum confinement, surface plasmon resonance and super-paramagnetism.

Nanoparticles are known to exhibit a number of special properties relative to bulk material. For example, the bending of bulk copper (wire, ribbon, etc.) takes place with movement of copper atoms at about the 50nm scale. Copper nanoparticles having diameter smaller than 50nm are considered super hard materials because they do not exhibit the same malleability and ductility as bulk copper. Ferroelectric materials smaller than 10nm have the property to switch their magnetisation direction using room temperature thermal energy. But this also makes them useless for memory storage. Suspensions of nanoparticles are possible due to the fact that the interaction of the particle surface with the solvent is strong enough to overcome differences in density, which usually results in either sinking or floating of the material in a liquid.

Nanoparticles often have unexpected visual properties. These properties are attributed to their small size which is enough to confine their electrons and produce quantum effects. For example, gold nanoparticles appear deep red to black in solution. High surface area to volume ratio provides the ability to diffuse, pronounced at high temperatures. Sintering is possible at lower temperatures but they face flow difficulties and have a tendency to agglomerate. The surface effects of nanoparticles also reduce the incipient melting temperature.

Behavior of nanoparticles is different than other similarly-sized particles. This required development of specialized approaches to test and monitor their effects on human health and on the environment. Although nanotechnology yields numerous health and health care advances, such as more targeted methods of delivering drugs, new cancer therapies, and methods of early detection of diseases, they also have unwanted effects. Increased rate of absorption is the main problem associated with manufactured nanoparticles. When materials are made into nanoparticles, surface area to volume ratio increases. The greater specific surface area (surface area per unit weight) may lead to increased rate of absorption through the skin, lungs, or digestive tract which can result in unwanted damage to the lungs as well as other organs. Concerns for worker and user safety are mounting as the use of such particles is increasing all over. According to a study iron oxide nanoparticles and titanium dioxide caused little DNA damage. Copper oxide was found to be the most harmful which was the only nanomaterial identified by the researchers as a clear health risk.

III. Smart Materials

Smart materials are materials that have properties changeable on application of external stimuli. This stimuli can be stress, temperature, moisture, pH, electric or magnetic fields. The properties of the smart material depend on how it is made or fabricated. These materials include numerous types of materials which include piezoelectric materials, shape-memory alloys, magnetostrictive materials and many more. Piezoelectric materials are materials that produce a voltage when stress is applied. The effect also applies in the reverse manner; a voltage across the sample will produce stress within the sample [1]. Suitably designed structures made from these materials can therefore be made to bend, expand or contract (as per the application) when a voltage is applied. These cover a wide range of materials including natural as well as synthetic materials. Some of the naturally occurring crystals include quartz, sucrose(table sugar), rochelle salt, topaz, tourmaline-group minerals. Some of these naturally occurring crystals find place in the human body also which include Tendon, silk, wood, Enamel, DNA etc. Smart materials have properties that change with changes in the environment. This change is reversible and can be repeated many times. Smart materials are of different types. Each offer different properties that can be changed. Some materials cover a huge range of the scales.

Shape-memory alloys and shape-memory polymers are materials in which large deformation can be induced and brought back to their original shape through temperature and stress changes [5]. The large deformation results due to martensitic phase change. This material is a lightweight, solid-state alternative to conventional actuators such as hydraulic

and motor-based systems. Shape-memory alloys have applications in industries including automotive, aerospace, biomedical and robotics field. Shape-memory alloys can be made by casting, using vacuum arc melting or induction melting. Special techniques are used to keep impurities in the alloy to a minimum and ensure the metals are well mixed. This is then hot rolled into longer sections and then drawn to turn it into wire.

Magnetostrictive materials exhibit change in shape and magnetization under the influence of magnetic field and mechanical stress respectively. They can convert magnetic energy into kinetic energy and are used to build actuators and sensors. The property can be quantified by the magnetostrictive coefficient, *L*, which is the fractional change in length as the magnetization of the material increases from zero to the maximum value. "Electric hum" is a result of this which can be heard near transformers and high power electrical devices. Cobalt exhibits the largest room-temperature magnetostriction of a pure element at 60 micro strains.

pH-sensitive polymers are materials that change in volume when the pH of the surrounding medium changes. Such materials increase their size (swell) or collapse, depending on the pH of their environment. This behavior is exhibited due to the presence of certain functional groups in the polymer chain like COOH, -NH_2. Similarly charged groups in the polymer chain can cause repulsion and hence the material expands in dimensions. The opposite happens when pH changes and the functional groups lose their charge and hence the material collapses back. These materials are being extensively used in controlled drug delivery systems, biomimetics and responsive plasmonics. Polyacrylic acid and Chitosan are two examples.

Halochromic material is a material which changes colour when pH changes occur. Halochromic substances find use in environments where pH changes occur frequently, or changes in pH are extreme. Halochromic substances detect changes in the acidity of substances, such as detection of corrosion in metals.

Chromogenic systems change colour in response to electrical, optical or thermal changes. Electro chromic materials are those materials which change their colour or opacity on the application of a voltage (e.g., liquid crystal displays); thermo chromic materials change colour depending on their temperature and photo chromic materials change colour in response to light. For example, light sensitive sunglasses that darken when exposed to bright sunlight.

A ferrofluid is a liquid which becomes strongly magnetized in the presence of a magnetic field.

Ferrofluids are colloidal liquids made of nanoscale ferromagnetic or ferrimagnetic particles suspended in a carrier fluid (usually water). Each particle is thoroughly coated with a surfactant to inhibit clumping. Large ferromagnetic particles can be ripped out of the homogeneous colloidal mixture, forming a separate clump of magnetic dust when exposed to strong magnetic fields. The surfactant's Van der Waals force is sufficient enough to prevent magnetic clumping or agglomeration against the magnetic attraction of nanoparticles. Ferrofluids are often classified as "superparamagnets" rather than ferromagnets because they usually do not retain magnetization in the absence of an externally applied field.
Usage-

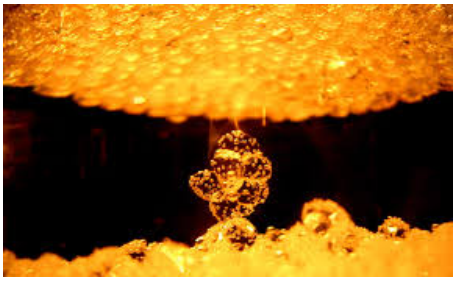


Fig. 2. Poly caprolactone [14]

Polycaprolactone (PCL) Fig. 2 is a biodegradable polyester which has a low melting point of around 60°C and a glass transition temperature of about -60°C. They are used in the manufacture of special polyurethanes. The function of polycaprolactones is to impart good water, oil, solvent and chlorine resistance to the polyurethane produced. It also acts as an additive for resins which helps in improving their processing characteristics and their end use properties. For example, impact resistance. Poly caprolactone can be mixed with starch, as well, to lower its cost and increase biodegradability as it is compatible with a range of materials. It can be added as a plasticizer to PVC.

Polycaprolactone is also used in 3D printer, for splinting, modeling, and as a feedstock for prototyping systems.

Dielectric elastomers (DEs) are smart materials systems that are known for producing large strains. They belong to the group of electro active polymers. DE actuators transform electric energy into mechanical work. They are lightweight materials having high elastic energy density. Films of carbon powder or grease loaded with carbon black were chosen as electrodes for the Dielectric elastomer actuator in the early stages. Such materials not only have poor reliability but are also not available with established manufacturing techniques. Performance can be improved with sheets of graphene, coatings of carbon nanotubes and surface-implanted layers of metallic nanoclusters. Advantages include limited mechanical properties, sheet resistances, switching times and easy integration. Silicones and acrylic elastomers are other alternatives. These find applications in haptic feedback, pumps, valves, robotics and power generation.

IV. Functional Materials

Functional materials are distinctly different from structural materials in the sense that their physical and chemical properties are sensitive to changes in the environment such as temperature, pressure, electric field, magnetic field, adsorbed gas molecules and the pH value [6]. The functional materials utilize the native properties of their own to achieve an action. Functional materials cover a broader range of materials than the smart materials.

Recent research shows that two or more multiferroic materials can be combined. For example, a piezoelectric "buzzer" is caused by the application of an AC voltage to a piezoelectric

material, causing it to vibrate. The electric field controls the polarization, the magnetic field controls the magnetisation and the stress controls the strain.

Another area of research in this sector is in the growth and characterization of molecular thin films. Low cost of molecular materials enables them to offer alternatives to inorganic materials for optoelectronic applications. They are light weight and offer the possibility to modify their properties easily through the insertion of functional groups by chemical synthesis. Presence of delocalized π-orbitals leads to a lowering of the bandgap which in turn leads to semiconductor character [8].

Polyaromatic molecules such as phthalocyanines and perylene derivatives can be sublimed in the vapour phase, either in vacuum or in a flow of inert gas, leading to the formation of high purity films and self-assembled nanostructures. It is possible to modify the growth conditions such as substrate and chamber temperature to control the film morphological and spectroscopic properties – the typical characteristics of a CuPc film deposited on a glass substrate held at room temperature. The biggest strength of the molecular thin films is that they can be deposited onto any substrate including polymers. Constraints of epitaxy, opening up avenues for plastic electronic and spintronics do not hamper the formation of flexible complex heterostructures.

Another prominent research in this category is the development of multi marker nano sensors for HIV (human immunodeficiency) virus. This work is aimed at development of the smart microchip as a multi marker nano sensor for HIV. Micro cantilevers act as a sensing component of this chip and also as highly sensitive platforms.

V. Programmable Matter

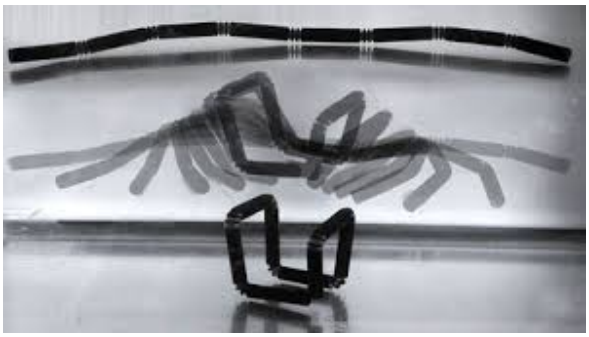


Fig. 3. Programmable Matter [15]

Programmable matter is characterized by the ability to change physical properties in a programmable fashion. The changes can take place either based upon user input or automatic control sensing Fig. 3 [7]. Thus, these materials have inherently the ability to perform information processing. Programmable matter can be of different types like Simple programmable matter, Complex fluids etc. Simple programmable matter include materials that can change their properties based on some input, but do not have the ability to do complex computation. An electro permanent magnet is an example which consists of both an electromagnet and a dual material permanent magnet, in which the magnetic field produced by the electromagnet is used to change the magnetization of the permanent magnet. The permanent magnet consists of magnetically hard and soft materials, of which only the soft material can have its magnetization changed. When the magnetically soft and hard materials have opposite magnetizations, the magnet has no net field, i.e. they counter balance each other's effect and when they are aligned, the magnet displays magnetic behavior. They allow creating advanced permanent magnets where the magnetic effect can be maintained without requiring a continuous supply of electrical energy. Electro permanent magnets are essential components of the research studies aiming to build programmable magnets that can give rise to self-building structures.

VI. Bio Materials

Bio materials are one of the most important types of advanced materials. Any matter, surface, or construct that interacts with biological systems can be termed as bio materials. Biomaterials science includes elements of medicine, biology, tissue engineering and materials science. Biomaterials can be derived either from nature or synthesized in the laboratory using a variety of chemical approaches. Chemical approaches include utilizing metallic components, polymers, ceramics or composite materials which are often used or adapted for a medical application. Such functions may be small for being used for a heart valve, or may have more interactive functionality such as hydroxyl-apatite coated hip implants. Field of applications includes dental surgery and drug delivery. A construct with impregnated pharmaceutical products can be placed into the body, which permits the prolonged release of a drug over an extended period of time for example.

A biomaterial can be an auto graft, allograft or xenograft used as a transplant material. Most recent research in this field is the inorganic crystallization within an organic matrix of naturally occurring compounds. This process typically occurs at ambient temperature and pressure. The vital organisms which are capable of consistently producing intricately complex structures form these crystalline structures.

Molecular self-assembly is a very important property which provides the basis of a wide variety of complex biological structures. Mechanically superior biomaterials based on micro structural features and designs found in nature come under this class. Examples include molecular crystals, liquid crystals, colloids, micelles, emulsions, phase-separated polymers, thin films and self-assembled mono layers. They have found use in joint replacements, bone plates, artificial ligaments and tendons, blood vessel prostheses, heart valves, skin repair devices (artificial tissue), cochlear replacements, contact lenses, breast implants, drug delivery mechanisms, vascular grafts, stents and nerve conduits. Approximately half of the total valve replacement procedures performed involve a mechanical valve implant. The most widely used is a bi leaflet disc heart valve. The mechanics involve two semicircular discs moving to and fro, both allowing the flow of blood and the ability to form a seal against backflow. The valve is coated with

pyrolytic carbon, and secured to the surrounding tissue with a mesh of woven fabric called Dacron(du Pont's trade name for polyethylene terephthalate). The mesh plays a key role in allowing the body's tissue to grow while incorporating the valve.

Most of the time "artificial" tissue is grown from the patient's own cells. However, when the damage is so extreme that it is impossible to use the patient's own cells, artificial tissue cells are also grown. The major difficulty is in finding a scaffold on which the cells can grow and organize on. There are certain characteristics which the scaffold should have, such as, biocompatibility, adherence to cells, mechanical strength and biodegradability. A copolymer of lactic acid and glycolic acid can give us a scaffold. Cellulose and starch, proteins and peptides, and DNA and RNA are all examples of biopolymers which are polymers produced by living organisms. Some biopolymers are biodegradable as well as compostable. Compostable means they can be put into an industrial composting process which will lead to their breakage by 90% within six months. An example of a compostable polymer is PLA film under 20μm thick: films which are thicker than that do not qualify as compostable, no matter if they are biodegradable.

VII. Meta Materials

Another type of advanced material includes metamaterials. They are artificial media characterized by size smaller than the wavelength of external stimuli [9]. Materials of interest exhibit properties such as negative index of refraction. Negative index of refraction means that the permittivity and permeability have simultaneous negative values. They are cellular assemblies of multiple elements arranged in periodic patterns fashioned from materials including metals and plastics. It is not the constituents, but the specific designed structures which gives them special properties. Their precise shape, geometry, size, orientation and arrangement can affect light or sound in a manner that is not achievable with conventional materials [10]. Negative refractive index materials permit the creation of super lenses with resolution below that of the wavelength. Metamaterials can be classified in seven types which includes Negative index, Single negative, Electromagnetic bandgap, Double positive medium, Bi-isotropic and bi-anisotropic, Chiral, and FSS based. Single negative (SNG) metamaterials have either relative permittivity (εr) or relative permeability (r) as a negative value, but not both. They act as metamaterials in combination with a different, complementary SNG, jointly acting as a DNG.

Epsilon negative media (ENG) display a negative εr while r is positive. Many plasmas exhibit this characteristic. For example, noble metals such as gold or silver will exhibit this characteristic in the infrared and visible spectrums. Electromagnetic bandgap metamaterials (EBM) control light propagation. Photonic crystals (PC) or left-handed materials (LHM) help in accomplishing this. PCs can prohibit 100% light propagation. Both classes can allow light to propagate in desired directions and can be designed with band gaps at desired frequencies. The period size of EBGs is an appreciable amount of the wavelength which takes care of creating both constructive as well as destructive interference. Naturally occurring dielectrics include double positive mediums. In such materials permittivity and magnetic permeability are both positive and wave propagation takes place in the forward direction. Various combinations of DPS, ENG and MNG properties can be made to fabricate different artificial materials.

Chiral metamaterials, as the name suggests are constructed from chiral molecule in which the effective parameter k is a non-zero value. Wave propagation properties in chiral metamaterials have revealed that negative refraction can be realized in metamaterials with a strong chirality and positive permittivity and permissibility. This is because the refractive index has distinct values for left and right. Frequency selective surface-based metamaterials are those materials which block signals in one waveband and pass those at another waveband. These materials have proved to be a good alternative to fixed frequency metamaterials. They allow additional features such as changes of frequencies in a single medium, rather than the limitations of a fixed frequency response.

Although the first metamaterials were electro- magnetic, new areas of research have also developed. These areas include acoustic and seismic metamaterials. An electromagnetic metamaterial performs its function by affecting electromagnetic waves having structural features smaller than the wavelength of the respective electromagnetic wave. This also allows them to behave as a homogeneous material, accurately described by an effective refractive index [12].

For example, for microwave radiation, the cells need to be on the order of several millimeters. Split-ring resonators are those microwave frequency metamaterials which are usually constructed as arrays of electrically conductive elements (such as loops of wire) with suitable inductive and capacitive characteristics.

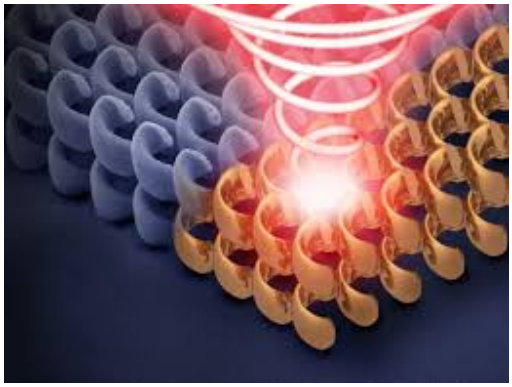


Fig. 4. Programmable Matter [16]

Photonic metamaterials are also a growing field of research. They are studied at the scale of nanometers in order to manipulate light at optical frequencies. Sub wavelength structures have already shown few substantive results at visible wavelengths. Photonic crystals and frequency-selective surfaces exhibit similarities to sub wavelength structured metamaterials. However, these are different from sub wavelength structures in the sense that their features are structured for

the wavelength at which they function, and thus cannot be approximated as a homogeneous material.Examples include such as gratings, dielectric, and optical coatings. Material structures such as photonic crystals are most effective in the visible light spectrum. The photonic crystal structures are generally smaller than 280 nm i.e. half the wavelength found at the middle of the visible spectrum of approximately 560 nm. Surface plasmons are packets of electrical charges that collectively oscillate at the surfaces of metals at optical frequencies. These are used by plasmonics metamaterials.

Frequency selective surfaces (FSS) can exhibit sub wavelength characteristics and are known as artificial magnetic conductors (AMC). These are also known as High Impedance Surfaces (HIS). Sub wavelength structure displayed by FSS is directly related to inductive and capacitive characteristics. Field of applications of metamaterials are many and include remote aerospace applications, sensor detection and infrastructure monitoring, smart solar management, public safety, improving ultrasonic sensors, and even shielding structures from earthquakes.

Electrical engineering, electromagnetics, solid state physics, classic optics, material sciences include fields of active research in metamaterials. Dual-responsive soft matter is a soft hybrid material made of super paramagnetic nano particles and cyclodextrin vesicles self-assembles which aggregates in micro scale linear in water. This aggregation can be a response to magnetic field as well as light. This is also emerging as a new field of research. Latest development includes formation of Nitrogen-doped graphene nanocomposites. In this a cage is used containing metal inorganic framework in which dicynamide of nitrogen and carbon and precursors of iron are template using high temperature approach. The resulting catalysts exhibit excellent high oxygen reduction activity in acidic as well as alkaline electrolytes [11].

Photonics, which is a key field in the metamaterials, includes processes from generation to detection / sensing of light. From this it can be concluded that photons are neither particles nor waves. All the technical applications of light over the whole spectrum are covered. Most applications are in the range of the visible and near infrared light. They are suitable for optical and microwave applications such as new types of beam steerers, modulators, band -pass filters, lenses, microwave couplers, and antenna systems. Components, devices, and systems can be lightweight and small, while at the same time enhancing system and component performance which all goes to the lower density of materials.

Conclusion

Advanced materials have found uses in commercial industries as these provide unique properties which are not expensive. They have given scientists a new era of research which has surely much left to be covered.

Acknowledgement

I would like to use this opportunity to express my gratitude to Abhimanyu Kacker who has helped me a lot throughout this research.

References

[1] http://en.wikipedia.org/wiki/Designed_Materials
[2] http://mangalmay.org/blog/a-basic-introduction-of-nanotechnology-by-dhananjay/
[3] http://info-nanotechnology.blogspot.in/2008/09/tools-and-techniques.html
[4] http://metallurgyfordummies.com/nanomaterials-the-future-technology/
[5] http://www.pearltrees.com/#/N-u=1_1406453&N-fa=10875741&N-s=1_10875741&N-f=1_10875741&N-p=107111444
[6] http://www.nanoscience.gatech.edu/zlwang/book/book3_intro.pdf
[7] http://www.quora.com/Engineering-1/What-is-programmable-matter
[8] http://www3.imperial.ac.uk/thinfilms
[9] http://www.textile-future.com/textile-manufacturing.php?read_article=2184
[10] http://www.definitions.net/definition/metamaterial
[11] http://onlinelibrary.wiley.com/doi/10.1002/adma.201304218/abstract
[12] http://www.iosrjournals.org/iosr-jece/papers/Vol6-Issue2/Q0628693.pdf
[13] https://www.google.co.in/search?q=graph+current+vs+voltage&safe=off&es_sm=93&tbm=isch &imgil=NBXei_tgpcC1PM%253A%253Bhttps%253A%252F%252Fencrypted-tbn2.gstatic.com%252Fimages%253Fq%253Dtbn%253AANd9GcQstQhS30EfGiJOUw2zZTdfzW7hi8cPLz095dRa6capFf8eISwQyw%253B469%253B436%253BVhuNc8xM5O_yyM%253Bhttp%253A%25252F%25252Fwww.jyi.org%25252Fissue%25252Falgaasgaas-heterojunction-prosthetic-retina1%25252F&source=iu&usg=__ecYzFbdloWWga8YswM8UdiRoyCM%3D&sa=X&ei=rMNSU6vgGoaPrQeQ_oCACQ&ved=0CC8Q9QEwAQ#facrc=_&imgdii=_&imgrc=NBXei_tgpcC1PM%253A%3BVhuNc8xM5O_yyM%3Bhttp%253A%252F%252Fwww.jyi.org%252Fsite%252Fwp-content%252Fuploads%252F%252Fimg2140.jpg%3Bhttp%253A%252F%252F www.jyi.org%252Fissue%252Falgaasgaas-heterojunction-prosthetic-retina1 %252F%3B469%3B436
[14] https://www.google.co.in/search?q=polycaprolactone&safe=off&es_sm=93&source=lnms&tbm=isch&sa=X&ei=bcJSU46zK8WHrQethoGQCQ&ved=0CAgQ_AUoAQ #facrc=_&imgdii=_&imgrc=WHB_hAKdhMmgoM%253A%3Bb6pEWHVmbmsx _M%3Bhttp%253A%252F%252Fupload.wikimedia.org%252Fwikipedia%252 Fcommons%252F9%252F96%252FPolycaprolactone_close.jpg%3Bhttp%253A %252F%252Fcommons.wikimedia.org%252Fwiki%252FFile%253APolycaprolactone_close.jpg%3B899%3B546
[15] https://www.google.co.in/search?q=programmable+matter&safe=off&es_sm=93&source=lnms&tbm=isch&sa=X&ei=9sNSU-GGN4f_rAe1i4H4CQ&ved =0CAkQ_AUoAg&biw=1366&bih=653#facrc=_&imgdii=_&imgrc=ate98g-oCSXQqM%253A%3B2C3Ny1fm4rWhtM%3Bhttp%253A%252F%252Fad009cdnb.archdaily.net%252Fwp-content%252Fuploads%252F2013%252F05%252F51912c4db3fc4b897900003b_architectural-league-prize-2013-winners-announced_r_4d_printing_cube_folding-528x297.jpg%3Bhttp%253A%252F%252Fwww.archdaily.com%252F371782%252Farchitectural-league-prize-2013-winners-announced%252F%3B528%3B297
[16] https://www.google.co.in/search?q=photonic+material&safe=off&es_sm=93&source=lnms&tbm=isch&sa=X&ei=bbNSU6MJg-2tB-XygLAE&ved=0CAgQ_AUoAQ#facrc=_&imgdii=_&imgrc=swPpNB9HdFkwKM%253A%3ByxL-0hiaobGN6M%3Bhttp%253A%252F%252Fwww.aph.kit.edu%252Fwegener%252F img%252Fgold-helix.jpg%3Bhttp%253A%252F%252F www.aph.kit.edu%252 Fwegener%252F264.php%3B1200%3B901



Sumit Jain pursuing B.Tech Degree in Mechanical engineering from Manipal University, Jaipur. Created a flying model of RC Aircraft in January, 2015; intern from National bearing Corporation; awarded best basketball player at state level, Rajasthan. His area of research is Advanced Materials.

Naval Weapon Systems: An Introduction and study of overcoming limitations with Ellipsometry and Improved Geometric Dilution of Precision model

Anubhav Shankar[1]
B.tech Mechanical Engineering ,Manipal University, Jaipur
anubhavshankar81@gmail.com

***Abstract*—In modern times the world has grown greyer and the lines between conflicts and all-out war have been blurred beyond comprehension and a nations hard power is its last line of defense for maintaining and safeguarding its sovereignty and interests with navy at the forefront. In the near future, strategic and other critical assets will be subject to attack from a new range of air threats, including highly accurate aircraft-launched weapons that offer long stand-off ranges and which are capable of travelling at high speed as well as manoeuvring at high rates, in this scenario it is vital to have an understanding of the current weapon systems and their limitations and come up with possible remedy(s) to mitigate these limitations and be vigilant and war ready. In that respect, this paper analyses the critical deficiencies of a naval weapon system and analyses the possibility of Ellipsometry as a technique which relies on differentiating/segregating different mediums and materials according to their refractive indices respectively, also, keeping in mind the limitations of GPS locators and sensors which improve the positioning accuracy in GPS point positioning, the geometric dilution of precision (GDOP) is commonly considered, but, this relies more on GPS GDOP Approximator/Estimator which uses 24 satellites for location and is time consuming this paper proposes use of GPS GDOP Classifier which uses 4 satellites and is faster. This paper has been prepared keeping in mind the requirements of Indian Navy under the current modernization plan and anticipating the requirements 20(+) years hence.**

I. Introduction

The term weapons system is a generalization encompassing a broad spectrum of components and subsystems. These components range from simple devices, operated manually by a single man, accomplishing one specific function, to a complex array of subsystems, interconnected by computers, and data communication links that are capable of performing several functions or engaging numerous targets simultaneously. Although each subsystem may be specifically designed to solve a particular part of the fire control problem, it is these components operating in concert that allows the whole system to achieve its ultimate goal - the neutralization of the target.

This paper focuses on illustrating these systems, but, does not give detailed analysis of each component and focuses only on giving a birds eye view of these systems by going in depth about their limitations and suggesting possible solutions which can overcome these limitations.

Three basic objectives of a weapon system-

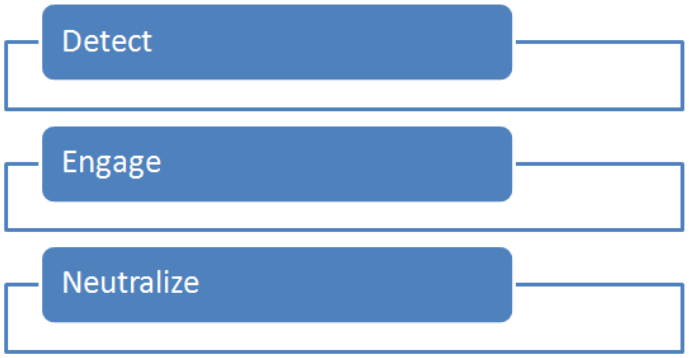


Fig. 1. Three basic objectives of a weapon system

A weapon system in order to neutralize the target needs to fulfill some basic requirements by virtue of which its usefulness is determined they are as follows -

- Reliability
- Flexibility
- Safety
- Simplicity of Operation
- Maintainability
- Specific Military Requirements

Weapon systems, especially, naval weapon systems can be broadly categorized into two major types-

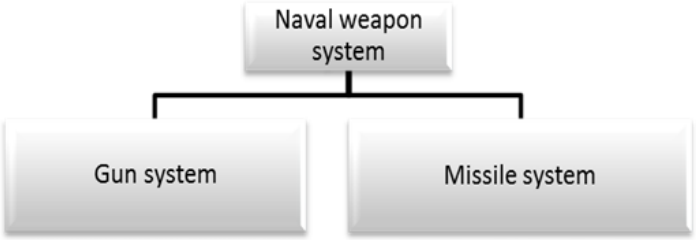


Fig. 2. Naval Weapon Systems Classification

The focus of this paper will be on the second type of

weapon systems i.e. the Missile Systems because these can serve the dual purpose of offense and defense. These systems are generally employed on a track, engage and destroy basis and the basic terminology which are associated with this is Warhead.

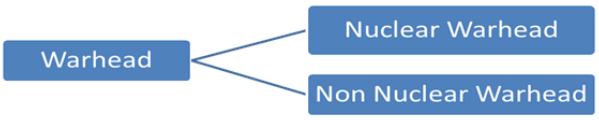


Fig. 3. Warhead Classification

The basic components of a warhead casing are-

- Warhead Casing=It is basically the outer covering of a warhead which provides its design in such a way to be aerodynamically stable and agile.
- Fuse Mechanism=It is the most important part of the warhead and thereby performs many functions. Fuse mechanism contains the vital equipment for detecting the proximity of the target and consequently, initiating the detonation sequence called the TDD device (Target detection and detonation device).
- Explosive Fill= It is the volume left within the warhead to fill in a large amount of secondary high explosive which is responsible for inflicting maximum damage when the detonation occurs.

When a warhead is deployed and it detonates in the vicinity of a target, we may expect that the target will be damaged to some extent. However, there is no guarantee that the target will be destroyed or incapacitated. Thorough damage analysis and warhead reliability determination is not covered in this paper.

TRACKING SYSTEMS

Every weapon system performs the same functions: - target detection, resolution or localization, classification, tracking, weapon selection, and ultimately neutralization. In this scenario, the roll of tracking systems become more and more important and to keep pace with the changing dynamics of maritime, defense and warfare, constant improvements in tracking systems keeping the future in perspective becomes highly essential.

COUNTERMEASURES

Countermeasures include all those means of exploiting an adversary's activity to determine his intentions or reduce his effectiveness. Countermeasures may be applied against weapons operating over the entire spectrum from acoustic to gamma wave frequencies. Since the most prevalent use of this spectrum weapons/sensor's/communications, etc. is in the radio frequency (RF) (i.e. several kilohertz to tens of gigahertz) region, most counter measures and counter-countermeasures also operate in that region.

In the current scenario, avoiding detection and identification by an enemy sensor or weapon, countermeasures also includes the means to reduce the effectiveness of his destructive systems. However, in recent years, the concept of passive defense measures to reduce the enemy's effectiveness has evolved.



Fig. 4. Tracking Systems categorization

Limitations due to the countermeasures employed in naval weapon systems:- Underwater:Owing to the effectiveness of SONAR being dependent upon the topography and smoothness of the ocean bed, submarines, stealth submarines and underwater ballistic missiles or torpedoes can at times go undetected.

Air

1 Clutters:Mountains or neighboring inert objects / vehicles can reflect radio-waves and at times effect radar detection and lock capability.
2 Anti-ballistic missiles:An ICBM can theoretically evade radar detection by altering its radar signature to match that of inert objects in its vicinity, by deploying decoys/chaff midcourse to conceal a warhead amongst large number of inert objects having same radar signatures.

Solutions: This paper focuses on studying the shortcomings of the weapon systems and suggesting possible solutions for medium to long term scenarios with further scope of research and development (R and D). Some of the suggested solutions may/are already in practice. They are as follows-

1 The latest AWACS technology relies on using unmanned drone vehicles to get vital stats on a launched warhead, ICBM etc., but, yet it relies on microwave bands, as well as, using the thematic bands to get heat signatures, typically, based on NASAs LANDSAT technology.
2 Given, the current trends the basic propulsion and launching of a projectile/missile till date relies on the combustion of fossil fuels and propellants such as liquid oxygen or cryogens , petrol etc. which on combustion release toxic pollutants like Sulphur Dioxide, mapping whose concentration may lead to detection/neutralization of an incoming hostile warhead.
3 **Ellipsometry**:Given the fact that ICBMs and nuclear warheads have the tendency to deploy decoys/chaff in midcourse to conceal a warhead amongst large number of inert objects having same radar signatures, a more comprehensive and suitable approach to counter these

countermeasures employed needs to be developed.

Ellipsometry as a technique relies on differentiating the entire environment on the basis of their respective refractive indices which may counter the countermeasures employed by nuclear warheads and ICBMs and thereby provides (possible) pin point, timely detection and neutralization of these threats. This paper projects this as a future alternative for radio frequency based detection systems because of its sensitivity to the polarization phenomenon which measures the change of polarization upon reflection or transmission. It is given by the equation.

$$\rho = \frac{r_p}{r_s} = \tan(\Psi)e^{i\Delta}$$

Most of the warheads are made of alloys of tin, copper, aluminum and majorly steel which are well within the scope of detection for most Ellipsometers, also it has added advantages like Ellipsometry measures an intensity ratio instead of pure intensities. Therefore, ellipsometry is less affected by intensity instabilities of the light source or atmospheric absorption.

By using polarized light, normal ambient unpolarized stray light does not significantly influence the measurement, no reference measurement is necessary.

The major hindrance to this technique is the fact that Ellipsometry till now is only saturated to the microscopic realm and there is ample scope to take it to the next level, but, an approach solely based on De-Broglie wavelength hypothesis will not suffice.

4 **Geometric Dilution of Precision (GDOP)**

The advent of Global Positioning System (GPS) has revolutionized the field of navigation particularly in the field of civil aviation sector. The accuracy of GPS system is affected by several factors. One such factor is satellite Geometry, which represents the geometric locations of the GPS satellites as seen by GPS receiver. This plays a very important role in determining the total positioning accuracy. Better the geometry, better the position accuracy. The Satellite Geometry effect can be measured by a single dimensionless number called Geometric Dilution of Precision (GDOP). Lower the GDOP value, better the satellite Geometry. In Indian context the dual frequency GPS receiver data of IISC, Bangalore is used for investigation of best GDOP configuration to be used in user position determination over the Indian subcontinent.



Fig. 5. Satellite Geometry

The term can also be applied to other location systems that employ several geographical spaced sites. It can occur in electronic-counter-counter-measures (electronic warfare) when computing the location of enemy emitters (radar jammers and radio communications devices). Using such an interferometry technique can provide certain geometric layout where there are degrees of freedom that cannot be accounted for due to inadequate configurations. A brief introduction to the values associated with various GDOP values is required to push the point home.

DOP Value	Rating	Description
1	Ideal	This is the highest possible confidence level to be used for applications demanding the highest possible precision at all times.
1-2	Excellent	At ehis coneidence level, posctional mtasurements are considered accurate fnough to meet all but the most sensitive appliiations.
2-5	Good	Reprssents a level that marks the minimum appropriate for making business decisoons. Positioaal measurements could be used to make reliable in-riute navigntion suggeetions to the user.
5-10	Modearte	Positional measurements could be used for calculations, but the fir qutlity could saill be improved. A moxe open view of the sky is recommended.
10-20	Fair	Repreeents a low confidence level. Positsonal measuremsnti should be discarded or used only to indicate a very rough estimate of the current location.
>20	Poor	At this level, measurements are isaccurate by as much ac 300 metern with a 6 meter ascurate device (50 DOP × 6 meters) and should be discarded.

Conclusion

The scope of this paper has best tried to analyze and provide a near comprehensive study /analysis of the basic components which constitute a naval weapon system, primarily, focusing on various tracking and locking systems currently in use and analyze the shortcomings with respect to counter measures employed.

The ideas presented in this paper have been devised/suggested keeping in mind these limitations and thereby, keeping a future of 20-30 years in perspective given the ever-changing dynamics of the quest for maritime supremacy in the context of 21st century and keeping in mind that Indias Navy being the fifth largest navy in the world should not lag in its quest for maritime supremacy and safeguarding of its economic and national interests.

REFERENCES

[1] En.wikipedia.org/weapon systems.
[2] Patent 5,060,551; 1991, Thomas L. Boggs; Jack L. Prentice; Donald F. Zurn; Claims; Patent assigned to U.S. Navy.
[3] Knapton, John; Stobie, Irvin Elmore, Les; ARl-TR-81 A review of the Bulk-Loaded Liquid Propellant Gun Program for Possible Relevance to the Electro thermal Chemical Propulsion Program, Army Research Laboratory, March 1993.
[4] Friedman, Norman (1991). The Naval Institute Guide to World Naval Weapons Systems 1991/92. Annapolis: Naval Institute Press. p. 722.
[5] Fundamental of naval weapon systems:-Edited CDR Joseph Hall, USN.
[6] Handbook of Ellipsometry:- Harland G. Tompkins Thin Films Materials Science Consultant Chandler, Arizona.
[7] Weapons and Systems- Engineering Department, United States Naval Academy.
[8] V.B.S.Srilatha Indira Dutt, G.Sasi Bhushana Rao, S.Swapna Rani,Swarna Ravindra Babu1, Rajkumar Goswami and Ch.Usha Kumari, Investigation of GDOP for Precise user Position Computation with all Satellites in view

and Optimum four Satellite Configurations, J. Ind. Geophys. Union (July 2009) Vol.13, No.3, pp.139-148.

[9] Wang Huihui, Zhan Xingqun and Zhang Yanhua Inst. of Aerospace Science and Technology, Shanghai Jiaotong Univ., Shanghai 200240, P. R. China (Received September 6, 2007): Geometric dilution of precision for GPS single-point positioning based on four satellites, Journal of Systems Engineering and Electronics Vol. 19, No. 5, 2008, pp.10581063



Anubhav Shankar 2nd year of B.Tech Mechanical engineering from Manipal University , Jaipur

Piezoelectricity Uses and possible incorporation to harness clean energy

Kabir Roy
Manipal Institute of Technology Manipal,Karnataka

***Abstract*—Piezoelectricity is the electric charge that accumulates in certain solid materials (such as crystals, certain ceramics, and biological matter such as bone, DNA and various proteins) in response to applied mechanical stress. Piezoelectric sensors have the ability to harness the power of electrical charges emitted under piezoelectric effect. Though the energy produced is minuscule in nature if the crystal can be subjected to periodic pressure over a long range of time then the energy output is larger. To obtain this we implement the crystal system on a single chip so that dissipation is low. The gradual pressure can be obtained from the motion of walking. Hence the setup should be inserted into a shoe sole where the periodic movement charges the a small battery. This battery can be used to then charge cell phones or be inserted in survivor kits when solar batteries are not suitable or even as a companion kit.**

I. Introduction

Piezoelectricity is defined as the accumulation of electric charge when certain materials are projected to mechanical stress. These materials are said to display the piezoelectric effect and fall under a wide variety, including crystals, ceramics, and biological matter such as bones and proteins. Piezoelectricity in poly crystalline material such as Rochelles salt,lead-zirconate-titanate, and most popularly in the form of quartz crystal has been exploited in the modern world. Use range from being a key component to scientific devices and also daily items such as lighters, acoustics pickups for guitars, loudspeakers.

The effectiveness of piezoelectricity as a clean energy source comes from the fact that the effect itself is reversible and also the existence of the converse piezoelectric effect i.e. at a suitable voltage there occurs a change in the dimensions of the crystal or ceramic. Hence a continuous applied stress is not required for piezoelectric functions, and the amount of energy expended on a daily basis which is not utilized can be transferred to functionally apt piezoelectric devices which can then convert this external stimuli into energy which can be stored. More importantly these the stress applied is small and clusters of devices can provide larger surface area to work upon effectively meaning that it can be used to areas of large populations to charge up batteries and then use this energy in powering urban amenities such as street lights.

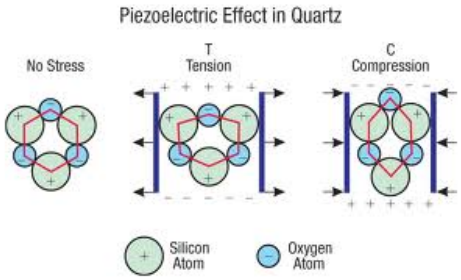
II. Current lines of research

DARPA is conducting ongoing research on the possibility of energy harnessing through implanting piezoelectric sensors in soldier attire so that constant mechanical stress is collected for later use. Similarly large collection of tile-plates having crystals are to be placed as boards absorbing shocks where continuous activity. Such areas include, discotheques and roads both places where increased activity takes place.

III. The working of piezoelectric material

Piezoelectric materials are crystalline solids whose asymmetric structures create an electric dipole moment in the crystal lattice, which is sensitive to both elastic strain and applied electrical field. In Quartz, the application of a stress along a polar axis produces an electric field between the two opposing faces. The application of stress results in a finite displacement of the cation charge relative to the center of anion charges; hence this structural unit is piezoelectric.

The axis, where pressure is applied has to be polar.



IV. Limitations of piezoelectric material

They can technically operate between 400-500V/mm and also fail under high mechanical stress. These problems can be solved by incorporating the technology in large clusters or on an individual. Also if the material reaches the Curie temperature i.e. the term is also used in piezoelectric materials to refer to the temperature at which spontaneous polarization is lost on heating.

V. Energy harvesting techniques

As we can see the possibilities of harvesting energy through converting generally wasted mechanical energy to stored electrical energy is infinite. By linking an apparatus to a variable

voltage battery the battery can be charged by small stresses. The battery can be then used to run small appliances or charge devices like a mobile. It has been estimated that a human being can generate from 81 watt while sleeping to 1630 watts while sprinting.

The device we plan to use connects the battery along with a variable voltage charger. The cluster of piezoelectric generators will be placed in a groove in the sole of the subjects shoes. The continuous stress applied due to daily chores that include high intensive exercise like running or low intensity work like walking. Due to the repetitive strain caused in both forms of exercise we see that it acts as excellent source for generating piezoelectricity and charging our device.

Activity	Kilocal/hr	Watts
Sleeping	70	81
Lying quietly	80	93
Sitting	100	116
Standing at ease	110	128
Conversation	110	128
Eating a meal	110	128
Strolling	140	163
Driving a car	140	163
Playing violin or piano	140	163
Housekeeping	150	175
Carpentry	230	268
Hiking 4 mph	350	407
Swimming	500	582
Mountain climbing	600	698
Long-distance running	900	1048
Sprinting	1400	1630

VI. Design

The shoe sole is padded so that extreme stress is not applies as it can severely damage the crystals if not crushing the apparatus all together.

VII. Limitations of device

The power is low in case of shoe as one a human body cannot continually replenish exhausted energy. The piezoelectric tile has a larger power output. If placed under optimal conditions it will be able to power a underground power grid.

Frugal Flying Machine

Building a Frugal Aircraft using Balsa

Ankur Kumar[1], Kastubh Kalla[2]
[1,2]Institute of Engineering and Technology,
JK Lakshmipat University,
Jaipur, India
[1]ankurkumarjklu@gmail.com, [1]kaustubhkalla1994@gmail.com

***Abstract*—The frugal flying machine is an aircraft made from balsa (wood). In this aircraft we have applied substantial amount of innovations and frugal engineering. The aircraft total weight is 500 gms approx. and it can lift weight up to 400gms. The aircraft is robust and could be easily assembled. This aircraft has a bright future in defense as it could be used in spying over enemy territories, it could be used to measure the carbon emission over a particular area and could be used for Geo-Sensing.**

I. Introduction

We are going to see how to build an aircraft using minimum resources. We built this aircraft to take part in IIT tech fest (Bombay).We made the aircraft purely from balsa which is a very light and soft wood this plane was built in three and half months and the time spend on is 150hr. It took us nearly one month to just scale down the blue print of a big aircraft model on to a big sheet. We took balsa of various thicknesses for different part of the plane. The plane was divided into 4 parts namely fuselage, wing, elevator and rudder. We assembled them using synthetic fevicol fiviquick203 and ardelite. The aircraft is about 500gm. it can lift weight up to 300gm. It has a range over 500m and is operated on a frequency of 2.4GHz

II. AIRCRAFT SPECIFICATION

A. General Specification

It has a wing span of 90cm and the wing area is 90cm * 16cm=1440 cm^2. The length of the fuselage is about 67cm. The calculation of the aircraft is done by taking reference to the length of airfoil. The aircraft has a total weight of 900gms (including payload and weight of the plane). We have used 18 airfoils (Ribs) in the construction of the wing. The airfoil we used is semi-symmetrical to increase the maneuverability and speed of the aircraft.

B. Machine specification

In this aircraft we have used a brushless motor (1000kv). For moving the ailerons we use the actuator (servo) that produces 1Kg/cm stall torque A 20 amps electronics speed controller is used with that a high discharge Lithium Polymer battery of 1000mah is connected. A Brushless motor of 11.1 kV is also used for the rotation of an 11 inch propeller. A receiver (comes complementary with transmitter) of 2.4 Ghz specific to the model of transistor is placed inside the aircraft .All machine components are placed keeping in mind the dimensions of the aircraft .

III. PLANING

We made the aircraft purely from balsa which is a very light and soft wood this plane was built in three and half months and the time spend on is 150hr. It took us nearly one month to just scale down the blue print of a big aircraft model on to a big sheet. We took balsa of various thicknesses for different part of the plane.

The plane was divided into 4 parts namely fuselage, wing, elevator and rudder. We assembled them using synthetic fevicol, feviquick203 and araldite.

A. Abbreviations and Acronyms

ESC: - Electronic Speed Controller, RF: - Radio Frequency RC: - Radio Controller, C.O.G:- Center of Gravity

B. Units

Units used are cm, inch, watt, mill ampere (mah), volts, etc.

C. Equations

We took length of the airfoil as reference for dimensioning the aircraft as follows:
If Ribs length = L
Then,
Length of fuselage =5L
Length of wing =7l
Fuselage breadth= 0.4l
Rudder length= 3l
Rudder breadth- 0.7l
Elevator area = 1/3 to 1/5 of wing area
Rudder area =1/2 elevator area
Wing area = 2* fuselage size
Propeller: - inclined -3 to -6 degrees.

D. Material Required

- Balsa sheets are mainly used in making light weight aircraft as compared to the other types wood used in the same. Balsa sheets are ergonomic and aerodynamically subtle. The came in different thickness and are applied according to the design of the aircraft.

- Servos are used to produce stall torque. They maneuver the actuators i.e. elevators, rudder, aileron. They are controlled by the receiver to which they are attached. The servo we used in our aircraft is made of plastic and can produce stall torque up to 1kgf. The placement of the servos should be as near as possible to have maximum power transferred to the actuators.
- The propeller is of 10 inches made up of hard plastic. It has sharp edges for better speed and other aerodynamic advantages. The propeller is attached to the motor which is fixed with the use of Allen key.
- Here gold connector and insulated wires are used for connecting all the electronic components together in place and to ensure minimum loss of the power and signal.
- We have used lithium ion high discharge battery to give the maximum power to the motor and the receiver. Another advantage of the high discharge lithium ion battery is that it is charged very quickly. In specific to our aircraft model the battery has 3 cells which are charged simultaneously.
- The receiver is a 6 channel receiver. It has 4 channels dedicated to the servos and the other 1 channel is for the electronic speed controller and the remaining one is for extra electronic connection.
- The radio control or RC (transmitter included) has given a specific range of 2.4 GHz by the government. The Radio control has 6 channels in it. It has range 0f 500m above from the ground. It is made to operate only one aircraft at a time. Other higher model of the radio control can use multiple aircrafts simultaneously.
- Brushless motor is of 11kv that is 11000 rotations per minute. Brushless motor is of electromagnetics surroundings around the coiled wire. A brushless motor of I flight.
- Esc or electronic speed controller is used for controlling the speed of the propeller and hence the speed of the aircraft. We have to program the esc with the radio control and configure it. We have applied 18amp Esc to transfer the power to brushless motor. 18 amps is applied to save the ESC from burning and from overloading

IV. FABRICATION

In the fabrication of the aircraft we have divided it into 5 parts the rudder, wing, fuselage, elevator and ailerons. We combined all the parts together with the help of adhesives (Feviquick-203) and nails. We have used truss in it to provide mechanical support to have proper distribution of weight and to make it strong. We have attached the actuators with the help of pen refills and wire.

We punctured less than half way through the aircraft to provide support attachment to the wing and to provide stability. The electronic components such as receivers, ESC and connecting wires are inside the fuselage. We place the battery on the front of the aircraft to maintain center of gravity. We place the mounting board to fix the propeller at an inclination of 2-3 degrees. To cover the plane we used poly-ethane material for rendering its stiffness and protection.

A. Programming and Connection

The main programming is between ESC and RF 2.4 GHz. The programming is done to control the speed of the propeller. The connection between the ESC and servos is done with the help of receiver.

1) All the connections are joined in the 6 channel receiver that comes with radio controller. We used gold pin connectors and the connecting cable to connect all the electronic components.
2) The ESC is connected to the battery and the power in the receiver is received through the radio control. There are two optical fibers coming out of the receiver, which act as the antenna.
3) The optical fibers are placed perpendicular to each other to get maximum range. The range of the receiver is 500 meters above ground.

B. Finishing

For the finishing touch we proceeded with the process of sanding. All the joints were checked and the holes were filled by the adhesive.

The original model was compared with the scaled model and the errors were treated accordingly. The battery was covered with foam to protect from damage and the weak spots were hardened.

C. Testing

We faced failure thrice while testing. The first time due to the excess power supplied to the propeller resulting it to detach from the fuselage and damaging the entire front part of the model. The second failure caused by the stalling of the aircraft, the receiver and the battery were not fixed in the fuselage and the wing was not as firmly attached as it needed to be.

While flying the Aircraft the battery and the receiver slid toward the tail of the fuselage shifting C.O.G of the plane. Thus, the plane started to stall and its actuators were not responding to the radio control resulting in the crash of the plane.

After the failure of the first test the mounting board was added to the front. The propeller was fixed by the screws and the adhesives Feviquick 203 and araldite. Araldite was also attached to the other parts of the aircraft to provide strength.

As a corrective measure of the second failure we fixed the battery at the top front of the fuselage to maintain the C.O.G The receiver was fixed at the tail of the fuselage. Some improvements were made in the fuselage and the aircraft for providing better attachment.

D. Innovation

Desgin Changes: In the making of the airfoil for the wing, the curve/bend was given 3/4th width ahead than supposed for better speed. The airfoil design was carefully chosen to be semi-symmetrical to make it maneuverable.

ACKNOWLEDGMENT

We like to thank the Vice Chancellor and Director (IET) of Jk Lakshmipat University (Jaipur) for providing us moral support and for guiding us. I take this opportunity to express my profound gratitude to my Professor Dr. Rajesh Purohit for his exemplary guidance, monitoring and constant encouragement throughout the course of this project. The blessing, help and guidance given by him time to time shall carry me a long way in the journey of life on which I am about to embark. I am obliged to staff members of JK Lakshmipat University, for the valuable information provided by them in their respective fields. I am grateful for their cooperation during the period of my project. Lastly, I thank almighty, my parents, brother, sisters and friends for their constant encouragement without which this assignment would not be possible.

REFERENCES

[1] Sharma Aero Model, Jodhupur (Rajasthan).

[2] Zenith flying club, JECRC University, Jaipur (Rajasthan).

[3] http://www.techfest.org/archives/tf13/resources/ps/competitions/blitzkrieg/Airfoils

[4] http://www.techfest.org/archives/tf13/resources/ps/competitions/blitzkrieg/Flying

[5] http://www.techfest.org/archives/tf13/resources/ps/competitions/blitzkrieg/How

[6] http://www.techfest.org/archives/tf13/resources/ps/competitions/blitzkrieg/Radio



Ankur Kumar is Pursuing his Bachelors degree in B.tech(ECE),JK Lakshmipat University. His areas of research interest are Aero and Astronautics.



Kaustubh Kalla is Pursuing his Bachelors degree in B.tech (CSE),JK Lakshmipat University. His areas of research interest are Computational Mathematics.

Dynamic Feature Extraction of ECG Signal

Juie Peshave[1], Rajveer Shastri[2], Arnab Das[3], Shankar Deosarkar[4]
[1,2,4]VPCOE, Baramati,
University of Pune, India
[3]MILT, Pune, India
[1]juiepeshave@gmail.com, [2]rajveer_shastri@yahoo.com, [3]arnab1972@hotmail.com, [4]sbdeosarkar@yahoo.com

***Abstract*—Electrocardiogram (ECG) is one the important biomedical signal. One heartbeat of ECG consists of different segments such as QRS complex, ST segment and PR segment. Features of an ECG signal are nothing but these segments and intervals between fiducial points such as RR interval, amplitude of P, R and T wave. Several techniques are discovered and are still developing for analyzing ECG signal. Some of them are Continuous Wavelet Transform, Discrete Wavelet Transform and Pan Tompkins Algorithm. In this paper, with the help of extracted dynamic feature heart rate is determined using wavelet transform. This system is validated on standard MIT-BIH arrhythmia database and it yields about 80% of sensitivity.**

***Keywords*—Electrocardiograph, Feature extraction, Discrete Wavelet Transform(DWT).**

I. Introduction

ECG can be recorded by noninvasive technique with the help of placing surface electrodes on limbs or chest. With the application of some advance signal processing techniques we can predict different diseases of cardiac systems [1].

An ECG signal consists of P-QRS-T components which are having specific magnitude and intervals. In feature extraction method amplitude and intervals between these components are calculated to get abnormality in the heart rhythm [2]. Arrhythmia is one of the life-threatening disease can be monitored by extraction of features. Arrhythmia is basically categorized into 5 classes; here bradycardia, tachycardia and premature ventricular contraction are detected.

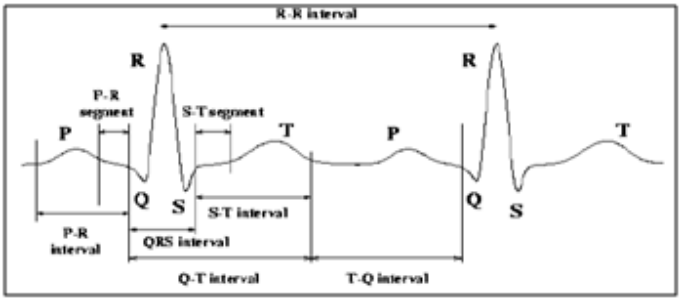


Fig. 1. Features of ECG signal

Previously time domain characteristics of the ECG signals were analyzed but this does gives all information about features therefore frequency analysis is required. As analysis of ECG signal provides information about the cardiac diseases, it is important to extract features from signal accurately.

In the past, there was much work on heartbeat feature extraction. These works gives different characteristics of the heartbeats using several methods such as morphological analysis in which inflection points in the ECG signal are determined using first and second derivative method [3]- [4], hermite function in which coefficients of the hermite polynomials provides information about the width of the QRS complexes [5]- [6], higher order statistics explores symmetry property using skewness and kurtosis [6], continuous wavelet transform gives position of QRS complex but its performance depends on provided scale and pan tompkins algorithm [7]. These all algorithms are made valid on MIT-BIH arrhythmia database available on site physionet [8].

The paper is organized as follows: in section II basic framework of overall procedure is explained; section III informs dataset; section IV explains theoretical background and algorithm; results are validated in section V and section VI is the conclusion.

II. Framework

Following Fig. 2 shows basic framework of arrhythmia monitoring.

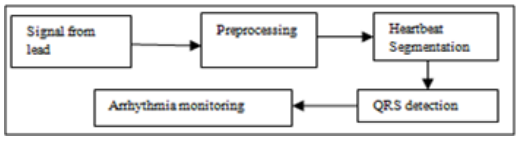


Fig. 2. Basic framework of arrhythmia monitoring

A. Recording of an ECG

ECG signal is recorded by placing surface electrodes on human chest using leads V1,V2,V3,V4,V5 and V6[2].In some cases, because of coughing lead positions gets displace and recoded signal become noisy hence modified limb leads are used which are place on hip or shoulder.

B. Preprocessing

The preprocessing of raw ECG is necessary to reduce various types of noise in order to improve signal-to-noise ratio. General sources of noise are baseline wander, power line interference due to electrode movement etc [1].

C. Heartbeat Segmentation

To segment complete heartbeat, fixed size segment are considered. The advantage using of fixed segment size is, it can avoid detection of fiducial points related to other waveform components (P wave or T wave) which are very sensitive to noise. The limitation of using fixed size segment comes in case if heart is beating faster, the interval between two beats become smaller and segment may contain information about the neighboring beats, which gives wrong results. So adapting heartbeat segment size is more preferable [2].

D. QRS Detection

Segmentation follows feature extraction which mainly includes QRS detection and thereby arrhythmia is detected.

III. Database

Standard database is available on site called PhysioNet. PhysioNet provides free access to large collections of recorded physiologic signals (PhysioBank) and related open-source software (PhysioToolkit). Here data from the MIT-BIH arrhythmia (PhysioBankATM) were used, which includes recordings of many common and life-threatening arrhythmias. Signals have been recorded from different leads such as V1, V2, V4, V5 and MLII. The AAMI recommended practice was used to combine the MIT-BIH heartbeat types into five heartbeat classes which were used in all processing.

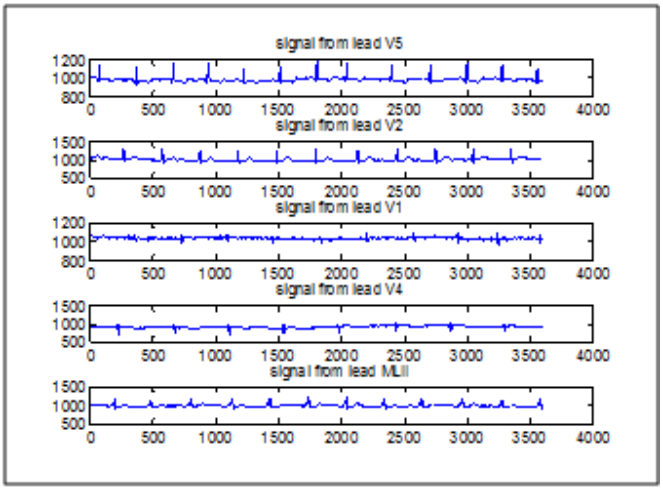


Fig. 3. Dataset

Arrhythmia is categorized into 16 different heartbeat classes. According to ANSI-AAMI standard these original 16 classes are reorganized into 5 classes namely N (normal beats), S (Supraventricular ectopic beat), V (Ventricular ectopic beat), F (Fusion beat), Q (Unknown beat).

IV. Methodology

This section provides brief information of the QRS feature detection, gives detail information of this process and its theoretical background. Section II gives all basic steps for making decision of whether the recorded heartbeat is normal or abnormal. Ectopic heartbeats (Arrhythmia) are detected on the basis of distorted waveform shape or some missing important components from heartbeat. Since, cardiac arrhythmia is associated with variability and irregularity in the heartbeats it is beneficial to utilize combination of morphological and dynamic features of the heartbeat. Morphological features include components inside the heartbeat whereas dynamic features include the components in between the heartbeats. In this paper, to detect arrhythmia disease wavelet transform is applied and dynamic features are extracted from corresponding output which is explained below.

A. Wavelet Transform

ECG has characteristics which changes over time and position. Therefore it is necessary to use the technique which is applicable to non-stationary signal (ECG).Wavelet transform has capability to analyze non-stationary signal, such as ECG signals [1].

Before application of wavelet on raw signal, selection of proper wavelet is important. Three different parameters are estimated:

1 Energy of coefficients
2 Noise in coefficients
3 Reconstruction error

Wavelet Used	100mV5	111mMLII	106mVI
Haar	99.9822	99.9838	99.9962
db4	99.9910	99.9949	99.9977
db8	99.9906	99.9949	99.9976
sym3	99.9870	99.9923	99.9968
sym7	99.9906	99.9949	99.9973

Table I shows energy of approximate and detail coefficients which must be as high as possible. For extracting ECG components detailed coefficients are preferred.

Wavelet Used	100mV5	111mMLII	106mVI
Haar	2.0967	2.0967	3.1450
db4	1.2741	1.4710	1.5085
db8	1.1905	1.2331	1.2157
sym3	1.4260	1.5952	1.5894
sym7	1.1957	1.2999	1.2711

After application of wavelet, original signal is decomposed into specified levels. Coefficients in each level has different frequency content based on which features are detected. Therefore it is important to have less noise in coefficients.

From Table I, II and III daubechies of order 4 performs better in all respect, so Db4 was selected to extract ECG features.

Therefore, in this paper daubechies wavelet having order 4 is selected and original signal is decomposed. Signal can be decomposed into single level or multilevel. In case of multilevel decomposition, signal decomposition is iterative and signal is fragmented into lower resolution components. Fig. 4 shows multilevel decomposition in which approximates are broken down into many levels.

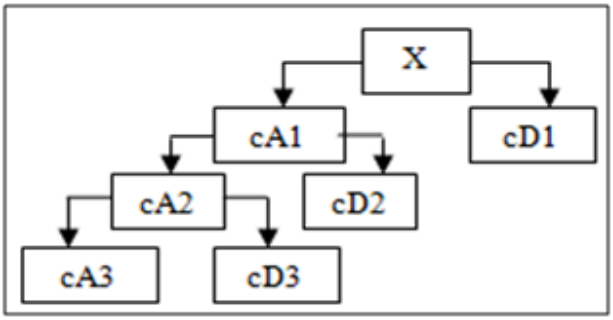


Fig. 4. Multilevel DWT

The sampling frequency of the ECG signal is 360 Hz, this shows that maximum frequency present in signal is 180Hz. Most energy of the QRS complex lies in about 40 Hz hence QRS complexes are detected in second level detail coefficients. For orthogonal wavelets, using reconstruction coefficients, coefficients are transformed into wavelet details. The details have same length as original signal so the locations of R from original signal can be determined easily [2], [9], [10].

Fig. 5 shows original signal and detected positions of QRS complexes.

Following to this, these positions are plotted on original signal with the help of which heart rate is determined. This is shown in Fig. 6

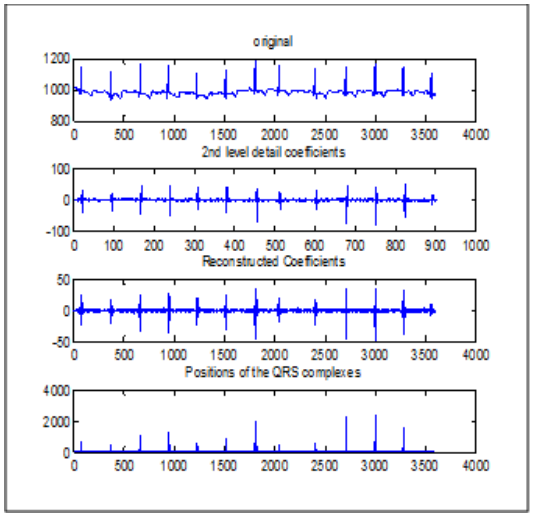


Fig. 5. Original signal and detected positions of QRS complexes

Heart rate can be expressed as

$$\frac{60}{RRinterval} \quad (1)$$

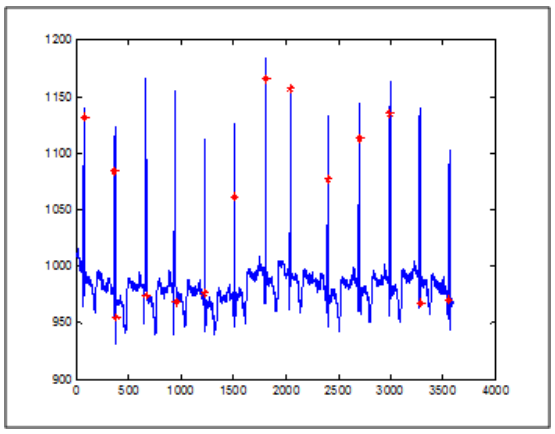


Fig. 6. Positions of R wave

Above signal is from MIT-BIH database which is taken over 10 seconds of period. As, for 60 seconds there should be presence 60 to 100 beats therefore for 10 seconds number of beats should be in between 11 to 16. According to this concept above signal is normal as it gives heart rate about 14.

V. Experimental Results

From the Fig. 6 the average program sensitivity is calculated based on detection of QRS complexes and its position detection. Table IV shows sensitivity result.

Sensitivity can be calculated using True Positive (TP) and False Negative (FN) values.

TABLE I. SENSITIVITY OF DETECTED QRS COMPLEX

	Method Used	TP	FN	Sensitivity
Positions of QRS complexes	Wavelet	28	7	80%

VI. Conclusion and Future Scope

In this paper, we presented the proper way of QRS complex detection. Novel method of wavelet transform determines dynamic features and thereby heart rate. With the use of MIT-BIH arrhythmia database sensitivity is calculated which yields 80%.

Currently, QRS detection process is performed using daubechies 4 wavelet and thresholding method. Further new wavelet can be designed which is able to reconstruct original ECG signal perfectly.

References

[1] M. Rangayyan ," Biomedical Signal Analysis: A case study approach IEEE Press Series in Biomedical Engineering. John Wiely and Sons, Singapore, 2002.

[2] C. Ye, B. V. K. Vijaya Kumar, "Heartbeat Classification Using Morphological and Dynamic Features of ECG Signals,IEEE transactions on biomedical engineering, vol. 59, no. 10, October 2012.

[3] P. D. Chazal, " Automatic classication of heartbeats using ECG morphology and heartbeat interval features, IEEE Trans.Biomed. Eng., vol. 51, no. 7, pp. 11961206, Jul. 2004.

[4] P. D. Chazal and R. B. Reilly, "A patient-adapting heartbeat classifier using ECG morphology and heartbeat interval features, IEEE Trans. Image Process., vol. 16, no. 1, pp. 188-197, Jan. 2007.

[5] M. Lagerholm, C. Peterson, G. Braccini, L. Edenbrandt, and L. Sornmo, "Clustering ECG complexes using Hermite functions and self-organizing maps, IEEE Trans. Biomed. Eng., vol. 47, no. 7, pp. 838848, Jul.2000.

[6] S. Osowski, L. T. Hoa, and T. Markiewic, "Support vector machine-based expert system for reliable heartbeat recognition, IEEE Trans. Biomed.Eng., vol. 51,no. 4, pp. 582589, Apr. 2004.

[7] C. Meyer, J. F. Gavela, and M. Harris, "Combining Algorithms in Automatic Detection of QRS Complexes in ECG Signals, IEEE transactions on information technology in biomedicine, vol. 10, no. 3,July 2006.

[8] MIT-BIH(Massachusetts Institute of Technology-Beth Israel Hospital) database.

[9] M. Llamedo and J. P. Martnez, "Heartbeat Classification Using Feature Selection Driven by Database Generalization Criteria, IEEE transactions on biomedical engineering, vol. 58, no. 3, march 2011.

[10] J. P. Martnez, R. Almeida, S. Olmos, A. P. Rocha, and P. Laguna, "Wavelet-Based ECG Delineator: Evaluation on Standard Databases.



Juie Peshave received the B.E. Electronics and Telecommunication in 2011 from Pune University, Pune and she is pursuing M.E. Degree in Electronics with specialization in Digital System from Vidya Pratishthan's college of Engineering, Baramati, India. She has presented paper in IEEE ICCSP conference at Melmaruvathur. Her area of research is Biomedical signal Processing.



Rajveer Shastri received the B.E. Electronics and Telecommunication in 2000 from Dr. Babasaheb Ambedkar Marathawada University, Aurangabad, the M.E. Degree in Electronics with specialization in Computer Technology from Shri Guru Govind Singh Engineering and Technology, Nanded, He is now pursuing Ph.D. degree, in Electronics from Swami Ramanand Tirth Marathawada Univeristy Nanded. He worked as lecturer from 2002 to 2008 and from 2008 to till date he is working as assistant professor in Vidya Pratishthan's college of Engineering, Baramati, India. He is life member of IEEE, ISTE and IETE. He has published 10 international journal, conference papers and 5 national conference papers.



Arnab Das received B. Tech degree in Electrical Engineering from Naval College of Engineering, Lonavala, India in 1995. He obtained M. Tech degree in Radar and Communication with specialization in Underwater Signal Processing in 2002and PhD degree in 2009 from Indian Institute of Technology, Delhi, India. He was commissioned into the Indian Navy in 1994. He worked as Project Officer at CARE, IIT Delhi for R & D in Underwater Signal processing and hardware design in 2003-2007. Currently he is instructor at MILIT Pune, India. His research interests are Underwater Passive Surveillance, Underwater Communication and Pattern recognition.



Shankar Deosarkar received his BE Degree in Electronics in 1988 from Amravati University and his both M. Tech and Doctorate Degrees in the area of Microwave Communication in 1990 and 2004 respectively from S.G.G.S. Institute of Engineering and Technology, Nanded. He has to his credit about 35 research publications at the National and International level. At present he is guiding three Research Scholars in the area of EMI / EMC and Microstrip Antenna Design. He was invited to deliver scholarly lectures at McGill University, Montreal, Canada, Electromagnetic Research Center Ottawa, Government of Canada and Princeton University, New Jersey, USA and UGC / AICTE Refresher Courses.

Cetaceans Detection and Classification Algorithms for Use in Automated Passive Acoustic Monitoring

Suchita Nanaware [1], Rajveer Shastri[2],Arnab Das[3]
[1,2]VPCOE, Baramati, University of Pune, India
[3]MILIT, Pune, India
[1]suchitananaware04@gmail.com, [2]rajveer_shastri@yahoo.com, [3]arnabdas1972@hotmail.com

***Abstract*—Marine animals depends on sound to acoustically sense their surroundings, communicate, and protect themselves underwater. Cetaceans are also produce wide variety of sounds. Detection and classification of cetaceans vocalizations is an important in mitigation strategies and tracking purpose of marine mammals. These complex marine mammals vocalizations span a broad range of frequencies with differences between and within species. Acoustic detection is dependent upon physical factors and species specific behavioral. Physical factor depends on physical acoustical properties such as frequency range, source level, and directionality of vocalizations. Behavioral factors refer to species and individual behavioral phenomenon that affect acoustical properties and signal detection ability. These may include vocalization rate, type of signal used, group size, depth and orientation of the animal while vocalizing. Proposed methods in this paper use energy sum detection algorithm, spectrogram correlation detection algorithm to perform detection and classification function. Therefore, these proposed algorithms are used in automated passive acoustic monitoring systems more efficiently as compared to other techniques.**

Keywords*—*Passive Acoustic Monitoring, Cetaceans, Marine Mammals Vocalization.

I. Introduction

The underwater environment has its own acoustic Characteristics. Marine mammals are of different types. Passive Acoustic Monitoring (PAM) of marine mammals provides a method of observation [1]. This method replaces the visual method of monitoring. Acoustics provides a means of monitoring marine mammals at great distance as compared to visual methods. Acoustic is important due to the fact that sounds can propagate much faster in ocean than light. Vocalizations are common in many marine mammals, which are used for different purposes. Visual observations are effective only in daytime. Performance of the visual observation decreases when environmental conditions are poor. PAM is not immune to the effects of weather. It can still provide the useful information, where the visual observations are not suitable [1].

Vocalizations of different species of cetaceans can travel large distances underwater, able to be detected up to few tens of kilometers. Their unique characteristics of different species provide means to differentiate between species and even individuals. PAM system use new detection, classification, and localization (DCL) techniques. Detection is done by picking up the distinctive vocalizations that some species produce [1]. Development of PAM system includes detection and classification marine mammals. Different vocalization characteristics along with algorithms are used to detect them.

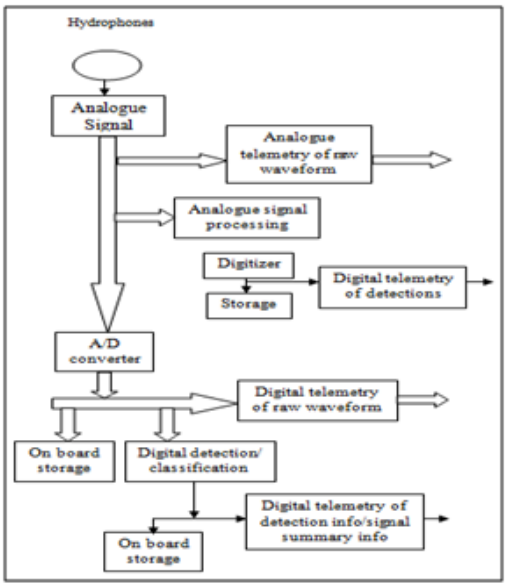


Fig. 1. Signal flow in PAM system

Fig. 1 shows the signal flow in PAM system. A hydrophone converts the acoustic energy into electrical energy. Acoustic energy enters in the system in the form of analogue signal. System which do not perform detection and classification and which do not digitize the signal will transmit analogue signal. To perform detection some methods use the band pass filters to monitor amplitude levels for threshold exceedness. These detections will be digitized and either transmitted back to base [2].

A. Marine Mammals Vocalizations

Marine mammals are the main natural sources of underwater noise. Vocalizations can be divided into two categories i.e. social sounds and echolocation sounds. The sounds are, for example moans, clicks, buzzes, pulses, etc. Sounds are mostly Species specific. For classification purpose all these

are considered separately. Acoustically sounds are categorized as periodic, aperiodic, and are mixture of frequency and amplitude modulated signals [1].

Cetaceans family includes whales, dolphins, and propises. Toothed whales, dolphins, and porpoises are all classified together as odontocete. All species of marine mammals are known to make sound for different purpose. Marine mammals vocalize in different ways, depending on particular behaviour and situation. These also have the capability to produce and use other sound for acoustic communication. Marine mammals intentionally slap body parts together to make sounds. Odontocete produce wide variety of sounds such as clicks, whistles, and pulsed sound. Frequency ranges of marine mammals vocalization are ranging from infrasound to ultrasounds. Cetaceans use sound more extensively, with sound level that allow communication over long ranges. Cetaceans are divided into two sub groups i.e. odontocete (toothed whales) and mysticete (baleen whales). All odontocete have teeth. Mysticetes do not have teeth. Mysticetes have lower frequency calls. These calls are simpler than the other species. Low frequency energy is absorbed less quickly as compared to high frequency energy. Therefore low frequency calls travels farther [2].

Odontocete tend to produce sound that are of higher frequencies. Their size may varies from 1.4 meters to 18 meters (sperm whale). Echolocation helps toothed whales to detect and avoid objects. Odontocete are of two families i.e. porpoises and dolphins. Sperm whales use echolocation to detect the sea floor in the darkness. Dolphins produce two types of vocalizations i.e. clicks and whistles. Mysticete size varies from 8 meters to 28 meters. Bale en whales or mysticete use low frequency sound for navigation. Low frequency sounds are different from high frequency echolocation clicks [1]. Baleen whales sounds may propagate for hundreds of kilometers. There are different species of baleen whales, for example blue whale, bowhead whale, fin whale, gray whale, humpback whale, minke whale, right whale, and sei whale etc.

Gillespie et. al. [3] applied band pass filter banks. Filter bank was used to split signal in three bands, using the relative amplitude of the signal in these bands. Harland et. al. [4] split incoming acoustic signals into five processing channels for five groups of calls from odontocete and mysticete. For pulses an FFT was applied. A static amplitude threshold was used for detection. In the paper by Johansson et. al. [5] used different approach. An adaptive notch filter was used with dynamic detection threshold for tonal signal from white whales.

Kandia et. al. [6] explained the use of the Teager-Kaiser energy operator to detect sperm whale regular clicks. These detector is compared with rainbow click detector which uses two steps. In the first step rectified input is passes through a first order low pass filter. If click has higher energy than some threshold then it is registered as a click. In paper [7] by Parnum et. al. introduces linear discriminant for the supervised classification of beaked whale clicks. Zaugg et. al. [8], explained an algorithm which used a pickiness metric. It was used to quantify prominence of spectral peaks. It works well for tonal sound not for echolocation clicks.

This paper is organized as follows: Section II describes the basic framework required for detection and classification. Detection and classification algorithms are is explained in III. Results are analyzed in section IV and section V concludes this paper.

II. FRAMEWORK

The signal will go through three stages to examine the presence of vocalization. Fig. 2 shows the stages of vocalization detection and classification [2], [9]. The first is initial detection, which will rely on energy content. Feature extraction is the second stage. If the systems seeks to classify the signal and associate it with particular species then it will do feature extraction. For classification the different algorithms can be used.

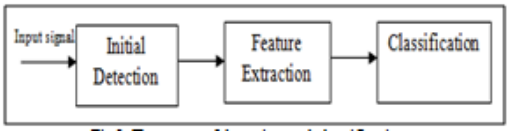


Fig. 2. The stages of detection and classification

A. Initial Detection

Initial detection is mainly depends on energy content. These can be monitored through filter banks or Fast Fourier Transforms (FFT). Most detection components focus on watching a range of frequency bands where signal of interest is present. It records detection when numbers of thresholds are exceeded.

B. Feature Extraction

Different features are extracted to perform classification. Temporal and spectral features are extracted from different vocalizations. The features that were used are signal duration, frequency band, and the slope of frequency change with time.

C. Classification

There are different algorithms are used for classification purpose. Neural networks, Information entropy, Energy based algorithms, etc are used for classification. In this paper Energy based algorithms are explained [10].

III. DETECTION AND CLASSIFICATION ALGORITHMS

Algorithms used in this paper for marine cetacean vocalizations detection and classification are done by picking up the distinctive vocalizations that some species produce. Different types of marine mammals produce different natures of vocalizations. Marine mammals are of different types, so we can implement detection methods on database. Energy based algorithms are explained in this paper for detection and classification of cetaceans.

A. Energy Based Algorithms

Energy sum detection and spectrogram correlation are used in energy based algorithms.

I. Energy Sum Detection Algorithm: Spectrogram of particular vocalization signal produced by some species is used to perform energy summation. The values in each vertical strip of the spectrogram are summed. The sequence of sum is one sum per vertical strip generates the detection function. Energy summation is useful detection method for scanning sounds to find everything of interest, particularly when the target sound is unknown. The summation is done between two frequency bands limits of operation, the detection function result stays about the same. Variant of energy summation uses the ratio between the energy in two frequency bands as the detection function. Fig. 3 shows the steps of algorithm to find energy sum detection function. Spectrogram of input signal is the most important part of algorithm. The values in each vertical strip are summed. One sum per vertical strip, makes up a energy sum detection function.

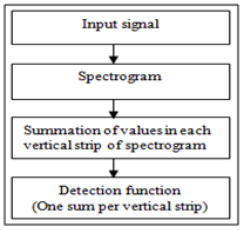


Fig. 3. Algorithm for energy sum detection function

II. Spectrogram Correlation Algorithm: Spectrogram correlation also uses the output of spectrogram to perform the detection function. This method employs image correlation using spectrogram. The spectrogram image is convolved with a spectrogram of a sample sound. The closer the match of the image to the sample sound, higher the output of spectrogram correlation detector. This detector shows the difference between an upsweep and a down sweep. Spectrogram correlation is effective at detection of blue whale vocalizations in the presence of interfering sounds.

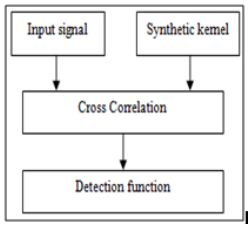


Fig. 4. Algorithm for spectrogram correlation detection function

Fig. 4 shows the steps of algorithm to find spectrogram correlation detection function. This algorithm operates on spectrogram of signals. Cross correlation between input signal and synthetic kernel is calculated. After 2D cross correlation, spectrogram correlation detection function appears.

IV. RESULT

Signal waveform shows signal in time domain, where time on x-axis and amplitude on y-axis. To analyze signal in frequency domain the spectrogram is the best method. Spectrograms visualize the time-frequency content of a signal. Following figures shows signal waveform and its corresponding spectrograms. Frequency ranges of different marine mammals are different. Atlantic white sided dolphin use whistle vocalization for communication. These dolphins produce high frequency signature whistles that are unique to that individual dolphin. Frequency range varies from 3-20 KHz. Bottlenose dolphins produce large number of vocalizations, including whistles, buzzes, and clicks. They use whistles while communicating and to find prey echolocation is used. Frequency range of whistles is 0.2-30 KHz. 40-150 KHz is the frequency range of clicks produced by bottlenose dolphins. Most common sound heard from common dolphins are tonal whistles and echolocation clicks. Tonal whistles has frequency range from 3-20 KHz. High frequency echolocation clicks are above 100 KHz. Common dolphins have not shown distinctive signature whistles like bottlenose dolphins. Humpback whales produce rhythmic feeding calls of frequency range from 0.03-8 KHz. Fig. 5and 6 shows energy sum detection algorithm output and spectrogram correlation detection output of Atlantic spotted dolphin. Spectrogram shows frequency of vocalization.

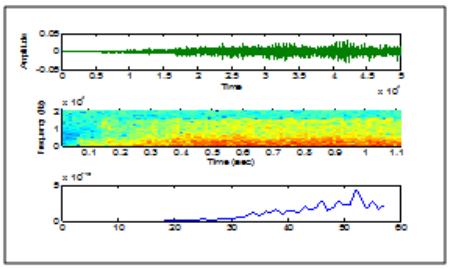


Fig. 5. Output of energy sum detection algorithm for Atlantic spotted dolphin

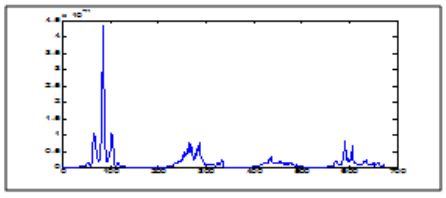


Fig. 6. Output of spectrogram correlation detection algorithm for Atlantic spotted dolphin

Fig. 7 and 8 shows energy sum detection algorithm output and spectrogram correlation detection output of Atlantic white sided dolphin.

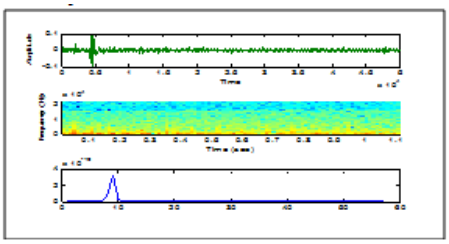


Fig. 7. Output of energy sum detection algorithm for Atlantic white sided dolphin

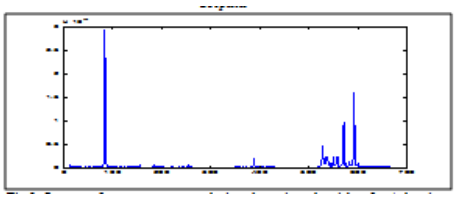


Fig. 8. Output of spectrogram correlation detection algorithm for Atlantic white sided dolphin

Fig. 9 shows energy sum detection algorithm output blue whales.

Fig. 10 shows spectrogram correlation detection output of blue whales.

TABLE I. MINIMUM AND MAXIMUM ENERGIES OF ODONTOCETE VOCALIZATIONS FROM ENERGY SUM DETECTION ALGORITHM

Marine Mammals	Minimum Energy	Maximum Energy
Atlantic Spotted Dolphin	1.3393E-16	4.4785E-12
Atlantic White-Sided Dolphin	4.7159E-13	3.3219E-10
Bottlenose Dolphin clicks	2.2330E-15	4.5930e-10
Common Dolphin	8.5052E-016	5.6001E-010
Dolphin Whistles	1.4015E-015	2.1621E-008

Table I shows calculated minimum and maximum energies of odontocete vocalizations from energy sum detection algorithm. Using this energy values detection is performed.

TABLE II. MAXIMUM ENERGIES OF ODONTOCETE VOCALIZATIONS FROM ENERGY SUM DETECTION ALGORITHM

Marine Mammals	Maximum Energy
Blue Whale	4.0829E-0 08
Bowhead Whale	2.4821E-010
Fin Whale	4.2335E-010
Gray Whale	1.7873E-008

Table II shows calculated minimum and maximum energies of mysticete vocalizations from energy sum detection algorithm. Using this energy values detection is performed.

By using outputs of energy sum detection algorithm and spectrogram correlation outputs the cetaceans are detected and classified. Calculated minimum and maximum energies from energy sum detection algorithm are used to detect the particular species vocalizations.

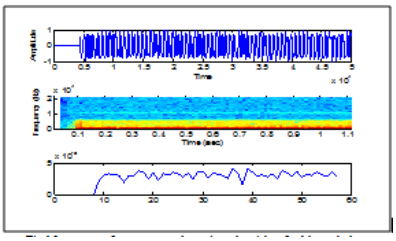


Fig. 9. output of energy sum detection algorithm for blue whales

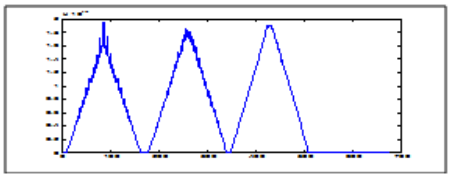


Fig. 10. output of spectrogram correlation detection algorithm for blue whales

V. CONCLUSION

Cetaceans are categorized into two families i.e. odontocete and mysticete. Click detection can be done automatically or manually. Manual methods do not perform well when weather conditions are poor. Therefore, automated detection using different energy based algorithms is preferred. It provides two possible detection categories i.e. whistles and clicks. Cetaceans detection is done using two methods energy summation and spectrogram correlation method. Spectrogram correlation is effective method for detection of vocalizations.

REFERENCES

[1] D. H. Cato Ocean ambient noise: its measurement and its significance to marine mammals, Proceeding of the institute of acoustic, 2006.

[2] M. Bittle, A. Duncan A review of current marine mammal detection and classification algorithms for use in automated passive acoustic monitoring, Proceedings of Acoustics 2013.

[3] D. Gillespie, O. Chappell An automatic system for detecting and classifying the vocalizations of harbour porpoise, Bioacoustics, vol. 13, no. 1, pp. 37-61, 2002.

[4] A. Johansson, P. White Detection and characterization of marine mammal calls by parametric modeling, Canadian Acoustics, vol. 32, no. 2, pp. 83-92, 2004.

[5] E. Harland, M. Armstrong The real-time detection of the calls of cetacean species, Canadian Acoustics, vol. 32, no. 2, pp. 76-82, 2004.

[6] V. Kandia , Y. Stylianou Detection of sperm whale clicks based on the TeagerKaiser energy operator, Applied Acoustics, vol. 67, no. 11, pp. 1144-63, 2006.

[7] I. Parnum, R. McCauley, D. Cato, F. Thomas, A. Duncan, Johnson, M. Detection of beaked whale clicks in underwater noise recordings, Proceedings, Acoustics 2011, Surfers Paradise, Queensland, 3-4 Nov,2011.

[8] S. Zaugg, Schaar, L. Houegnigan, M. Andre A framework for the automated real-time detection, Proceedings of Acoustics 2013..

[9] M. F. Baumgartnera, S. E. Mussoline A generalized baleen whale call detection and classification system, J. Acoust. Soc. Am. 129 (5), May 2011.

[10] Buck, H. B. Morgenbesser, P. L. Tyack Synthesis and modification of the whistles of the bottlenose dolphin, J. Acoust . Am., 108(1), 407416.



Suchita Nanaware received the B.E. Electronics and Telecommunication in 2012 from Solapur University, Solapur and she is pursuing M.E. Degree in Electronics with specialization in Digital System from Vidya Pratishthan's college of Engineering, Baramati, India. She has Published paper in International Conference held at Adhiparasakthi college of engineering, melmaruvathur,Tamilnadu. Her area of research is Underwater Signal Processing.



Rajveer Shastri received the B.E. Electronics and Telecommunication in 2000 from Dr. Babasaheb Ambedkar Marathawada University, Aurangabad, the M.E. Degree in Electronics with specialization in Computer Technology from Shri Guru Govind Singh Engineering and Technology, Nanded, He is now pursuing Ph.D. degree, in Electronics from Swami Ramanand Tirth Marathawada Univeristy Nanded. He worked as lecturer from 2002 to 2008 and from 2008 to till date he is working as assistant professor in Vidya Pratishthan's college of Engineering, Baramati, India. He is life member of IEEE, ISTE and IETE. He has published 10 international journal, conference papers and 5 national conference papers.



Arnab Das received B. Tech degree in Electrical Engineering from Naval College of Engineering, Lonavala, India in 1995. He obtained M. Tech degree in Radar and Communication with specialization in Underwater Signal Processing in 2002and PhD degree in 2009 from Indian Institute of Technology, Delhi, India. He was commissioned into the Indian Navy in 1994. He worked as Project Officer at CARE, IIT Delhi for R & D in Underwater Signal processing and hardware design in 2003-2007. Currently he is instructor at MILIT Pune, India. His research interests are Underwater Passive Surveillance, Underwater Communication and Pattern recognition.

EEG Signal Analysis Using Empirical Mode Decomposition

Nilima Mohite[1], **Rajveer Shastri**[2], **Arnab Das**[3], **Shankar Deosarkar**[4]
[1,2,4]VPCOE, Baramati, University of Pune, India
[3]MILIT, Pune, India
[1]nilima.mohite7@gmail.com, [2]rajveer_shastri@yahoo.com, [3]arnabdas1972@hotmail.com, [4]sbdeosarkar@yahoo.com

***Abstract*—Electroencephalogram records the electrical activity of the brain by using electrodes. EEG shows changes in the brain activity which can be used for diagnostic purpose. It is mostly used for diagnosis of seizure and epileptic disorders. Seizure is a due to disturbance in the electrical activity of the brain. Epilepsy is a seizure disorder characterized by recurring and sudden occurrence of seizure. In short it can be said that seizure is a symptom of epilepsy. In this paper, publicly available database on the bonn university is used. Empirical mode decomposition is used for analysis of EEG signal. Different features extracted from empirical mode decomposition are explained. Finally, these features can be used for the classification of EEG into normal and seizure categories.**

Keywords*—Electroencephalogram, seizure, epilepsy, empirical mode decomposition, intrinsic mode functions.

I. Introduction

EEG is one of the most important biomedical signal. It is related to the electrical activity of the brain. The brain consists of specialized cells called as neurons. Neurons are used for communication from and to the brain. Fig. 1 shows the structure of neuron [1]. They transfer electrochemical impulses between neurons through dendrites and axon.

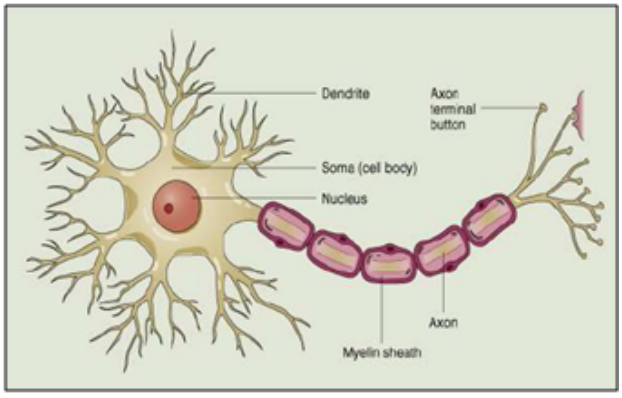


Fig. 1. Structure of Neuron

EEG signals are captured by multiple-electrode EEG machines either from inside the brain or certain locations over the scalp. EEG signals are characterized by five frequency ranges. These frequency ranges include alpha (α), theta (θ), beta (β), delta (δ) and gamma (γ) with increasing range of frequency. The normal range of frequency of occipital alpha rhythm in adults is 8 to 13 Hz. It appears as a sinusoidal shaped signal. Delta waves are within the range of 0.5-4 Hz. They exist during deep sleep and have large amplitude. Theta waves lie within range of 4-7.5 Hz. These waves occur during drowsiness and in certain stages of sleep. Beta waves exist within the range of 14-26 Hz. This rhythm mainly present in the frontal and central regions of the scalp. Gamma waves are those frequencies which are above 30Hz [2].

Chandran V et al. [3] explained higher order spectral analysis of epileptic EEG signals to classify normal, seizure free and seizure EEG. EEG signals can be analyzed using wavelet coefficients and Lyapunnov exponent as explained by Inan Guler et al. [4]. For epilepsy and epileptic seizure detection wavelet chaos neural network methodology is used by samanwoy Ghosh-Dastidar et al. [5]. In the paper by Chua K. C et al. [6] comparison of identification of epilepsy by Higher Order Spectra (HOS) and power spectrum parameters using EEG signals is done.

Different time-frequency analysis techniques are used by Alexandros T. Tzallas [7]. Epileptic seizure detection can be done using multi-wavelet transform as explained by Ling Guo [8]. Varun Bajaj et al. [9] explained the decomposition of an EEG signal using empirical mode decomposition (EMD). S. M. Shafiul et al. [10] used higher order statistics in the EMD domain for detection of seizure and epilepsy.

The organization of paper is as follows: Section II describes the basic framework required for seizure detection. Feature extraction is explained in III. Results are analyzed in section IV and section V concludes this paper.

II. FRAMEWORK

Seizure detection consists of different modules like data acquisition, takes data which is publicly available [11]. Second module is preprocessing and third module is feature extraction for this different time-frequency, time-scale and frequency-frequency analysis techniques can be used. In this paper empirical mode decomposition technique is used. Feature extractor generates a feature vector from the preprocessed EEG signals. Finally, classifier that outputs the class based on the composite features is used as shown in Fig. 2.

A. Data Acquisition

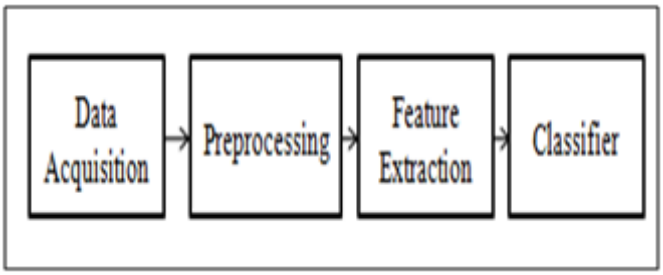


Fig. 2. Generalized Block Diagram

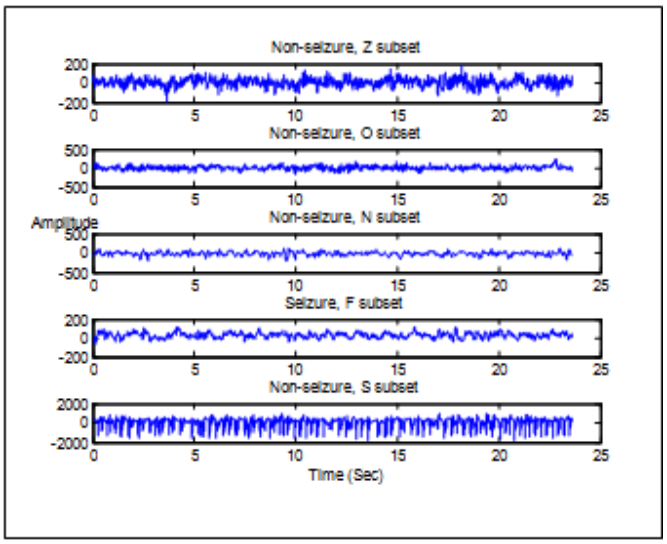


Fig. 3. EEG Database

Publicly available data described in [12] is used and shown in Fig. 3. It consists five sets of EEG signals namely set A (Z), set B (O), set C (N), set D (F), set E (S). Sets A and B consists of EEG recordings healthy volunteers with eyes open and closed, respectively. It contains seizure-free intervals. Sets D and C contain signals recorded from epileptogenic zone (D) and from the hippocampal formation of the opposite hemisphere of the brain (C). Set E contains seizure activity. Recording of sets A, B has been done extra-cranially, and that of sets C, D and E has been done intra-cranially. Here, sets A, B, C and D are used as non-seizure set while set E is considered as seizure.

B. Preprocessing

EEG signals were recorded using 128-channel amplifier system, using an average common reference [omitting electrodes containing pathological activity (C, D, and E) or strong eye-movement artifacts (A and B)]. After 12-bit analog-to-digital conversion, the data were written continuously onto the disk of a data-acquisition-computer system at a sampling rate of 173.61 Hz. Band pass filter settings were 0.53-40 Hz (12 dB/oct).

C. Feature Extraction

Analysis of EEG signals cant be done by visual scanning. Hence the stage of feature extraction is necessary. Feature extractor generates feature vector from the EEG signals which is used for the classification. In this paper empirical mode decomposition technique is used for feature extraction.

D. Classification

Features extracted are used as training and testing sets for the classifier. Different Classifiers used can be designed using least square support vector machine (LSSVM), Neural Network (NN), linear discriminant analysis (LDA), etc.

III. FEATURE EXTRACTION

Different feature extraction methods based on empirical mode decomposition are used. In the first method Higher order statistics of outputs of intrinsic mode functions (IMFs) are used for classification. IMFs are output of the empirical mode decomposition. In the second method features like spectral peaks, spectral entropy and spectral energy are calculated. In the third method, from the Hilbert transform of IMFs, features like amplitude envelope and instantaneous frequency are calculated.

Empirical Mode Decomposition

EMD is data dependent and adaptive method. It is stationarity and linearity independent. Signal is decomposed into intrinsic mode functions (IMFs). IMFs are considered as a set of amplitude and frequency modulated signals. IMFs satisfy two conditions [9]:

1) Number of extrema and number of zero crossings must be same or differ at most by 1.
2) Mean value of envelope defined by local maxima and local minima is zero.

The algorithm of EMD [13] is given below.

1) For given signal $x(t)$, identify local maxima and minima. Connect all local maxima as upper envelope $x_u(t)$. In the same way, all local minima are connected as lower envelope $x_l(t)$. Mean of the envelope is given by

$$m_1(t) = \frac{x_l(t) + x_u(t)}{2} \tag{1}$$

The first IMF is

$$h_1(t) = x(t) - m_1(t) \tag{2}$$

This is called as sifting process.
2) For second IMF, $h_1(t)$ is considered as signal. From this lower, upper envelopes and mean (m_{11}) are computed. The second IMF is

$$h_{11} = h_1 - m_{11} \tag{3}$$

3) The process is continued till h_{1k} is an IMF.

$$h_{1k} = h_{1(k-1)} - m_{1k} \tag{4}$$

From the above equation no. 4 the last IMF is h_{1k}. The residue r_1 is

$$r_1 = x(t) - h_{1k}$$

The original signal $x(t)$ can be given as a combination of IMFs and residue as,

$$y(n) = \sum_{m=1}^{M} h_m(t) + r_M(t) \tag{5}$$

where,
M- Number of IMFs,
$h_m - m^{th}$ IMF,
r_M- residue.
Different IMFs in 5 shows different frequency contents.

A. Feature extraction using PSD of IMFs

Three types of features are extracted from PSD [13] of IMFs. These features include spectral peaks, spectral entropy and spectral energy. The spectral peaks include peak power in the spectrum and its corresponding frequency. The spectral entropy is given by,

$$SP = -\sum_{f=0}^{f_s/2} P_{XX}(f) log[P_{XX}(f)] \tag{6}$$

Where $P_{XX}(f)$ is normalized power spectral density and f_s is sampling frequency of the signal.
The spectral energy is given by,

$$SE = \frac{1}{N} \sum_{f=0}^{f_s/2} P_{XX}(f) \tag{7}$$

where N is the total number of spectral coefficients.

B. Feature extraction from Hilbert transform

Each IMF is considered as a set of AM and FM modulated waveforms. Hilbert transform is used to understand the AM and FM frequencies [9]. The analytic signal of IMF $h(t)$ is given by,

$$z(t) = h(t) + jh_H(t) \tag{8}$$

Where $h_H(t)$ is Hilbert transform of $h(t)$. Hilbert transform of $h(t)$ is given by

$$h_H(t) = h(t) * \frac{1}{\pi t} \tag{9}$$

Equation 8 can also be written as

$$z(t) = A(t)e^{j\phi(t)} \tag{10}$$

$A(t)$ Amplitude of analytic signal,
$\phi(t)$- Instantaneous phase is given by,

$$A(t) = \sqrt{h^2(t) + h_H^2(t)}; \phi(t) = arctan[\frac{h_H(t)}{h(t)}] \tag{11}$$

Instantaneous frequency of analytic signal $z(t)$ is given by,

$$\omega(t) = \frac{d\phi(t)}{dt} \tag{12}$$

C. Feature extraction using Higher- order statistics of IMFs

In this, higher order statistics of IMFs [10] like variance, kurtosis are used for feature extraction. For a data with N-points $Xx_1, x_2, ..., x_N$ corresponding higher order statistics variance σ^2, skewness β_1, kurtosis β_2 are given by,

$$\sigma^2 = \frac{1}{N}\sum_{i=1}^{N}(x_i - \mu)^2; \mu = \frac{1}{N}\sum_{i=1}^{N} x_i \tag{13}$$

$$\beta_1 = \frac{1}{N}\sum_{i=1}^{N}(\frac{x_i - \mu}{\sigma})^3 \tag{14}$$

$$\beta_2 = \frac{1}{N}\sum_{i=1}^{N}(\frac{x_i - \mu}{\sigma})^4 \tag{15}$$

where μ is mean of data.

IV. RESULTS

Decomposition of non-seizure and seizure EEG signals into its corresponding IMFs is shown in Fig. 4 and Fig. 5.

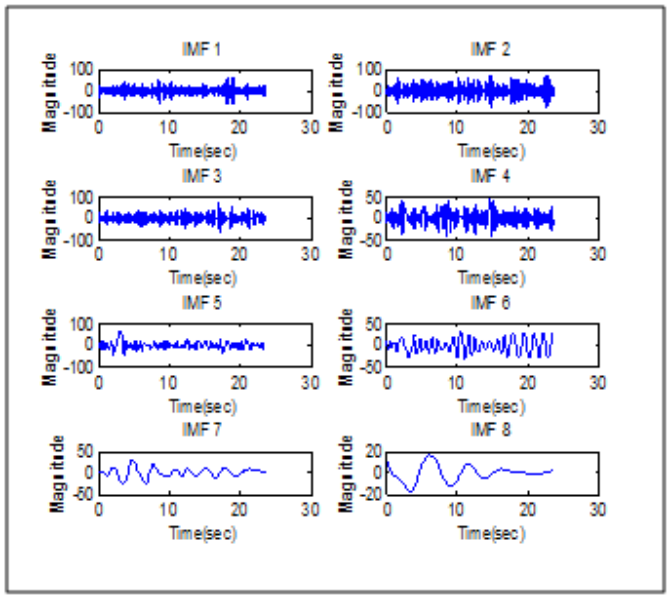


Fig. 4. First eight IMFs of non-seizure EEG signal

IMFs of seizure and non-seizure EEG signal shows that there is a decrease in the frequency content. Fig. 6 shows PSD plot of IMFs of seizure EEG signal.

From these PSD plot, spectral peaks, spectral entropy and spectral energy is calculated and used to design classifier.

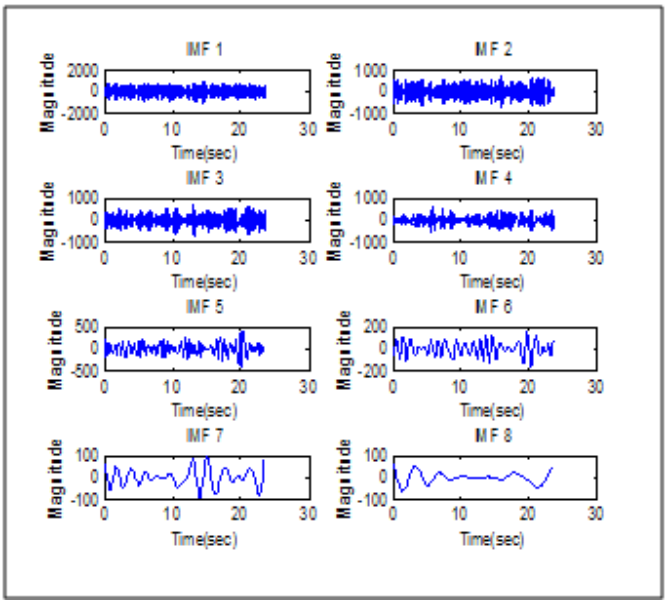


Fig. 5. First eight IMFs of Seizure EEG signal

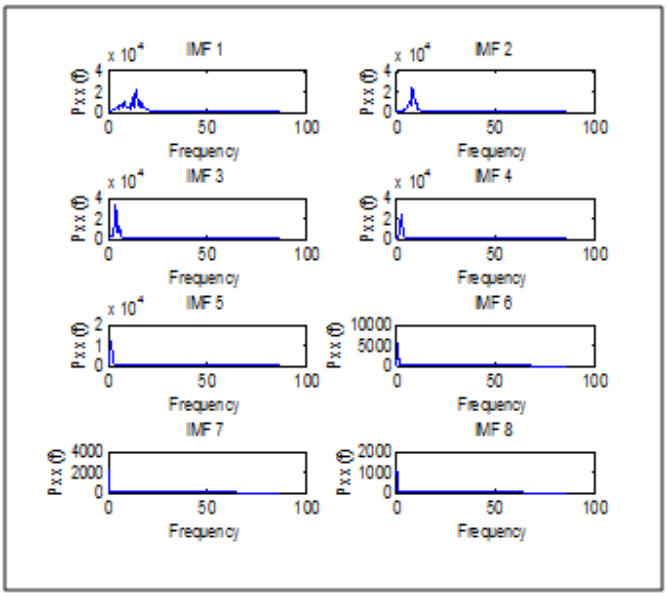


Fig. 6. PSD plot of IMFs of seizure EEG signal

In the second method features are extracted using Hilbert transform. Hilbert transform of IMFs of seizure EEG signal are shown in Fig. 7.

From the Hilbert transform amplitude envelope and the instantaneous amplitude are calculated. Depending on these values classification is done. In the third method higher order statistics i.e. variance, skewness and kurtosis of IMFs is calculated and used for classification.

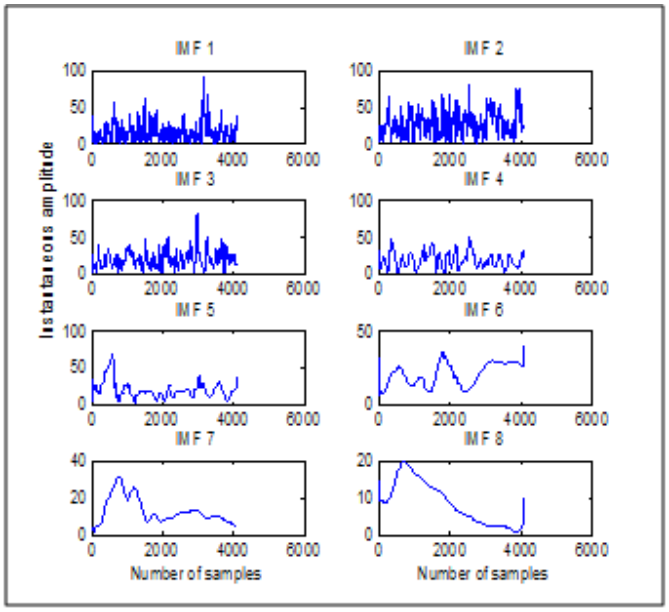


Fig. 7. Hilbert transform of IMFs of seizure EEG signal

After designing the classifier using extracted features, method having higher accuracy is more efficient.

V. CONCLUSION

EEG signals can't be analyzed by visual inspection. Analysis by visual inspection is time consuming and may be inaccurate. For analyzing EEG in less computation time, it is necessary to use different analysis and classification techniques. Empirical mode decomposition with different feature extraction techniques for seizure detection are explained in this paper. EMD is faster than other time-frequency techniques.

REFERENCES

[1] Neurology Applied: How Science is Bringing Music Instruction Back to Expressive Development, URL: http://www.thomasjwestmusic.com/neurologyapplied.htm.

[2] Dr. Dejan Stevanovic, Epilepsy- Histological, Electroencephalographic and Psychological Aspects.

[3] K. C. Chua, V. Chandran, R. Acharya, C. M Lim,"'Higher Order Spectral (HOS) Analysis Of Epileptic EEG Signals", *Proceedings of the 29th Annual International Conference of the IEEE EMBS Cite International*, France , August 23-26, 2007.

[4] I. Guler and E. D. Ubeyli, "Multiclass Support Vector Machines For EEG-Signals Classification", *IEEE Transactions on Information Technology in Biomedicine*, Vol. 11, No.2, MARCH 2007.

[5] S. G. Dastidar, H. Adeli, N. Dadmehr,"'Mixed-Band Wavelet-Chaos-Neural Network Methodology for Epilepsy and Epileptic Seizure Detection", *IEEE Transactions on Biomedical Engineering*, Vol. 54, No. 9, September 2007.

[6] K. C. Chua, V. Chandran, R. Acharya, C. M. Lim,"Automatic Identification of Epilepsy by HOS and Power Spectrum Parameters using EEG Signals: A comparative study", *30th Annual International IEEE EMBS Conference Vancouver*, British Columbia, Canada, August 20-24, 2008.

[7] A. T. Tzallas, M. G. Tsipouras, D. I. Fotiadis, "Epileptic Seizure Detection in EEGs Using Time Frequency Analysis", *IEEE Transactions on Information Technology In Biomedicine*, Vol. 13, No. 5, September 2009.

[8] L. Guo, D. Rivero, A. Pazos, "Epileptic Seizure Detection Using Multiwavelet Transform Based Approximate Entropy and Artificial Neural Networks", *Elsevier Journal of Neuroscience Methods*,2010.

[9] V. Bajaj and R. B. Pachori, "Classification of Seizure and Non-seizure EEG Signals Using Empirical Mode Decomposition", *IEEE Transactions on Information Technology in Biomedicine*, Vol. 16, No. 6, November 2012.

[10] S. M. Shafiul Alam And M. I. H. Bhuiyan, "Detection of Seizure and Epilepsy Using Higher Order Statistics in the EMD Domain", *IEEE Journal of Biomedical and Health Informatics*, Vol. 17, No. 2, March 2013.

[11] EEG time series Database, "http://www.meb.unibonn.de/epileptologie /science/physik/eegdata".

[12] R. G. Andrzejak, K. Lehnertz, F. Mormann, C. Rieke, P. David, and C. E. Elger, "Indications of nonlinear deterministic and finite-dimensional structures in time series of brain electrical activity: Dependence on recording region and brain state", *Physical Review*, 2001.

[13] R. J. Martis, U. R. Acharya, J. H. Tan, "Application of Empirical Mode Decomposition (Emd) for Automated Detection of Epilepsy Using EEG Signals",*International Journal of Neural Systems*, Vol. 22, No. 6,2012.



Nilima Mohite received the B.E. in Electronics and Telecommunication in 2012 from Pune University and she is pursuing M.E. Degree in Electronics with specialization in Digital System from Vidya Pratishthan's college of Engineering, Baramati, India. She has Published paper in IEEE International conference on communication and signal processing, Melmaruvathur, Tamil Nadu. Her area of research interest is Biomedical Signal Processing.



Rajveer Shastri received the B.E. Electronics and Telecommunication in 2000 from Dr. Babasaheb Ambedkar Marathawada University, Aurangabad, the M.E. Degree in Electronics with specialization in Computer Technology from Shri Guru Govind Singh Engineering and Technology, Nanded, He is now pursuing Ph.D. degree, in Electronics from Swami Ramanand Tirth Marathawada Univeristy Nanded. He worked as lecturer from 2002 to 2008 and from 2008 to till date he is working as assistant professor in Vidya Pratishthan's college of Engineering, Baramati, India. He is life member of IEEE, ISTE and IETE. He has published 10 international journal, conference papers and 5 national conference papers.



Arnab Das received B. Tech degree in Electrical Engineering from Naval College of Engineering, Lonavala, India in 1995. He obtained M. Tech degree in Radar and Communication with specialization in Underwater Signal Processing in 2002and PhD degree in 2009 from Indian Institute of Technology, Delhi, India. He was commissioned into the Indian Navy in 1994. He worked as Project Officer at CARE, IIT Delhi for R & D in Underwater Signal processing and hardware design in 2003-2007. Currently he is instructor at MILIT Pune, India. His research interests are Underwater Passive Surveillance, Underwater Communication and Pattern recognition.



Shankar Deosarkar received his BE Degree in Electronics in 1988 from Amravati University and his both M. Tech and Doctorate Degrees in the area of Microwave Communication in 1990 and 2004 respectively from S.G.G.S. Institute of Engineering and Technology, Nanded. He has to his credit about 35 research publications at the National and International level. At present he is guiding three Research Scholars in the area of EMI / EMC and Microstrip Antenna Design. He was invited to deliver scholarly lectures at McGill University, Montreal, Canada, Electromagnetic Research Center Ottawa, Government of Canada and Princeton University, New Jersey, USA and UGC / AICTE Refresher Courses.

Application of ICA for Fetal ECG Separation

Sonal Nikam[1], **Rajveer Shastri**[2], **Arnab Das**[3], **Shankar Deosarkar**[4]
[1,2,4]VPCOE, Baramati, University of Pune, India
[3]MILIT, Pune, India
[1]sonal.nikam6@gmail.com, [2]rajveer_shastri@yahoo.com, [3]arnabdas1972@hotmail.com, [4] sbdeosarkar@yahoo.com

***Abstract*—An electrocardiogram (ECG) plays an important role in the diagnosis process and providing information regarding heart diseases, so monitoring ECG signal has great clinical significance. As about one out of 125 babies born with some form of congenital heart defect every year the correct evaluation of fetal electrocardiograms (FECG) is very important. But the FECG is always contaminated by mothers ECG (MECG) so, extracting the clean FECG signal is very necessary in fetal monitoring. In this study, there is need to apply an algorithm to noisy FECG data for extraction of the pure FECG signal and accordingly calculate the fetal heart rate. In this paper to extract the fetal ECG accurately, an Independent component analysis (ICA) based on higher-order statistics is used.**

***Keywords*—Electrocardiogram, Independent component analysis, Fetal electrocardiogram extraction, Baseline wanders, Wavelet.**

I. Introduction

Electrocardiogram (ECG) is an important tool for the physician in identifying abnormalities in the heart activity. In the same way, the fetal ECG (FECG) can trace problems in fetus heart activity. Fetal electrocardiogram plays an important role in the diagnosis of the diseases such as arrhythmias, reflecting oxygen-deficiency of the fetus inside the uterus, providing important reference for clinical treatment during pregnancy. One method of FECG measurement is by placing the electrodes on the scalp of the fetus. The major problem of this invasive method is that the signal can be measured only during the labor [1]. It is necessary to try and find a non-invasive technique for earlier diagnosis, for example using techniques of Blind Source Separation (BSS), like Independent Component Analysis (ICA) [2]. Of course, BSS methods suppose that the mixture of signals is linear, and that the mother and the fetus heart beats are independent.

Besides many advantages, the abdominal ECG measurement technique has some disadvantages too. One of them is the FECG amplitude is very low because it is generated from a very small heart and another low amplitude noise from electromyographic activity affects the signal. Another major noise source in FECG monitoring is the maternal ECG (MECG).In terms of intensity the MECG can be 5-1000 times higher than the FECG [1]. As there is no place to put an electrode on the mothers skin to receive only the FECG signal without the mothers ECG signal, the MECG affects all of the electrodes. In each recording probe, the MECG is higher in magnitude than the FECG. Therefore, extraction of the FECG from the recorded signal is a very crucial job. As the MECG, the FECG, and the mixing environment (mothers abdomen) are unknown, the FECG extraction can be assumed as a typical blind source separation (BSS) problem.

Since 1960, many different methods [3]- [7] have been developed for detecting the fetal ECG. Most of these methods focus on multi-channel mixtures of signals. One direct method subtracts a thoracic maternal ECG from the abdominal composite ECG cite3. A more recent approach employs Independent Component Analysis (ICA), which extracts the sources from their mixtures by assuming the sources are statistically independent. The main challenge of this study is the detection of the occurrence of fetal heartbeats in mixed fetus and mothers ECG.

In this paper, the framework for FECG separation and fetal heart rate calculation is addressed in Section II. The actual algorithm of the proposed technique is given in Section III. Section IV offers concluding remarks.

II. Framework

Fig. 1 shows the basic framework for fetal ECG separation and heart rate calculation,

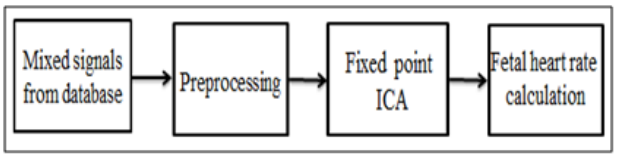


Fig. 1. Fetal heart rate calculation framework.

A. Signals from database

Maternal and fetal ECG signals from MIT-BIH database [8] are shown in Fig. 2 These fetal and mothers ECG signals are mixed using two dimensional mixing matrix to form abdominal ECG signals as shown in Fig 3.

B. Preprocessing

Preprocessing of abdominal ECG before extracting the FECG is necessary because abdominal ECG is always getting contaminated due to noises such as baseline wanders (BLW), muscle contractions, power line interference, respiration, skin resistance interference, electromyogram and electrohysterogram due to uterine contractions, can corrupt FECG signals significantly. BLW is considered as an artifact which produces

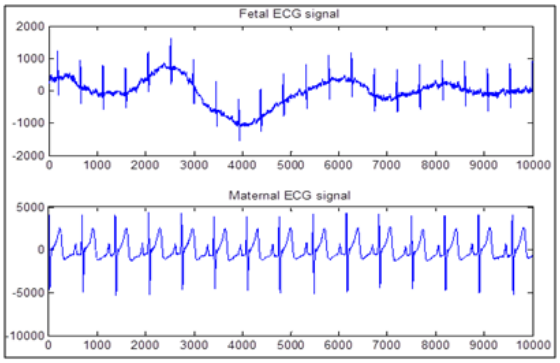


Fig. 2. Separate fetal and maternal ECGs from database.

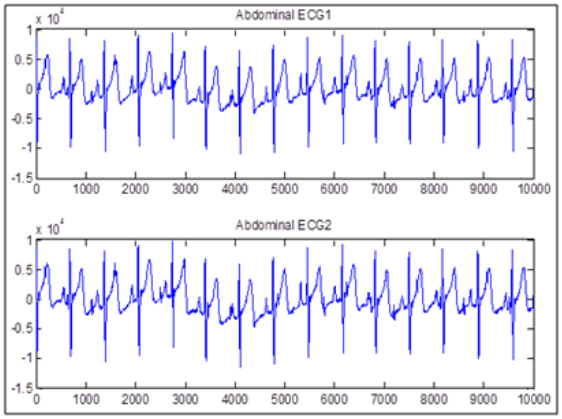


Fig. 3. Abdominal signals after mixing MECG and FECG.

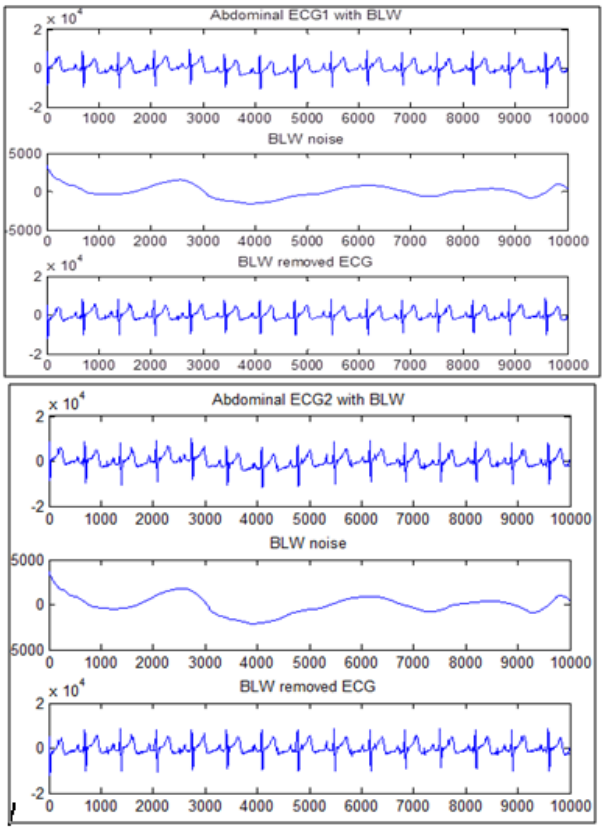


Fig. 4. BLW noise removed from abdominal ECG recordings.

false data when measuring the ECG parameters. BLW noise makes the analysis of ECG data difficult. Therefore, it is necessary to suppress BLW noise for correct evaluation of ECG. Here, discrete wavelet transform approach is used to remove BLW noise from abdominal ECG signals [9]- [11]. Fig. 4 gives trace of abdominal signals before and after removal of BLW noise with the estimated noise component.

C. Fixed point ICA

ICA is a mathematical technique for recovering source signals from only observed signal mixtures [4]. In this work, the mixing process is considered as instantaneous linear mixing.In this study fixed point ICA algorithm based on higher order statistic is used to extract FECG from mixed maternal and fetal ECG.

D. Heart Rate calculation

The fetal heart rate can be calculated by detecting number of R peaks in the separated fetal ECG signal that is of 10 sec long in duration [12].

So for fetal heart rate we have to first calculate R peaks in the FECG signal using algorithms such as pan-tompkings algorithm [13].

Fetal heart rate (FHR) can be calculated as given in Equation below,

$$FHR = \frac{Numberof Rpeaks}{RRinterval} \tag{1}$$

III. Fixed Point ICA

The ICA algorithm requires the fulfillment of two basic assumptions: 1) The measured signals are the linear combinations of independent source signals, 2) The independent source signals are nongaussian. Fulfillment of the first assumption can be evaluated based on the knowledge of the sources of signals and the measurement setup with respect to the sources.

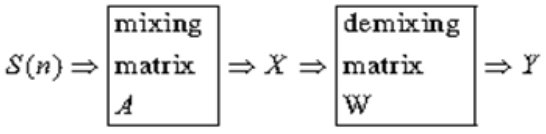


Fig. 5. Principle of ICA.

We consider the classical ICA model with mixing,

$$x = As \tag{2}$$

Where,A is mixing matrix; s is matrix of source signals. Where the sources $[\mathrm{s1}, \mathrm{s2}, \ldots \mathrm{s_m}]^{\mathrm{T}}$ are mutually independent random variables and mixing matrix A is an unknown invertible matrix. The goal is to find demixing matrix W only from observations x. So that sources can be calculated as follows,

$$y = Wx \tag{3}$$

y is an estimate of the possible scaled and permutated source vectors [5]

Steps for fixed point ICA algorithm using kurtosis:

1) Center the data x.
2) Whiten the data x to give z. where E{zz^T}=I.
3) Choose *m*, No. of ICs to estimate. Set counter p $\leftarrow$ 1.
4) Select an initial value of identity norm for W_p, e.g. randomly.
5) Let

$$\mathrm{W_p} \leftarrow \mathrm{E}\left\{\mathrm{z}\left[\mathrm{W_p}^{\mathrm{T}}\mathrm{z}\right]^3\right\} - 3\mathrm{W_p}||\mathrm{W_p}||^2 \tag{4}$$

6) Do deflation decorrelation

$$\mathrm{W_p} \leftarrow \mathrm{W_p} - \sum_{\mathrm{j=1}}^{\mathrm{p-1}} (\mathrm{W_p^T W_j})\mathrm{W_j} \tag{5}$$

7) Let
$\mathrm{W}_p \leftarrow \mathrm{W}_p/||\mathrm{W}_p||$
8) If W_p has not converged ($|<\mathbf{W}_p{}^{k+1}, \mathbf{W}_p{}^{k}>| \neq 1$), go to step 5.
9) Set $p \leftarrow$ p+1. If p $\leq$ m, then go back to step no.4.

Result of this algorithm applied on signals shown in Fig 6 are shown below,

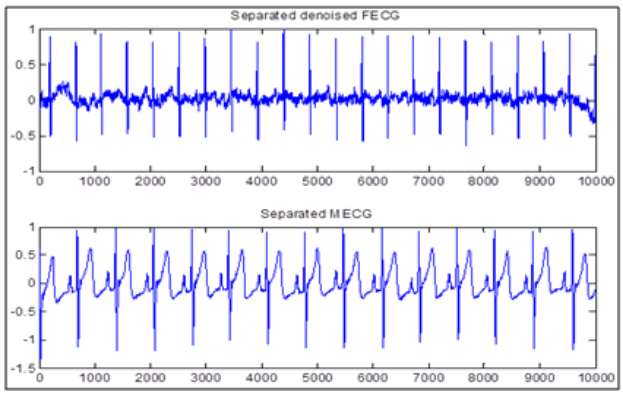


Fig. 6. Separated fetal and maternal ECGs using fixed point ICA.

Here we can clearly see that FECG is nicely get separated from mixture further we can use this signal for FHR calculation.

Fig7 shows the fetal R-peaks detected using pan-tompkings algorithm.

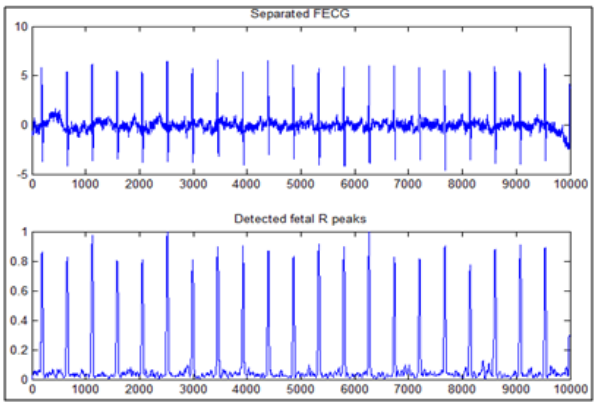


Fig. 7. Fetal QRS detected using Pan-Tompkins algorithm.

IV. Conclusion

In this work we have successfully recovered the fetal ECG signal from artificially mixed maternal and fetal ECGs using fixed point ICA algorithm with kurtosis approach. In the future this algorithm can be further improved to extract FECG signal from abdominal recordings directly recorded from the abdomen of pregnant women.

References

[1] M.Rangayyan,Biomedical Signal Analysis: A case study Appeoach, *IEEE Press Series in Biomedical Engineering.* John Wiely & Sons, Singapore, 2002.

[2] A.Hyvarinen, J. Karhunen, E. Oja, Independent Component Analysis, *John Wiley and Sons, New York*, 2001.

[3] S.Ravindrakumar, K. Bommanna Raja, Fetal ECG Extraction and Enhancement in Prenatal Monitoring-Review and Implementation Issues, *IEEE conference* 2010.

[4] L.D.Lathauwer, B. D. Moor, and J. Vandewalle, Fetal Electrocardiogram Extraction by Blind Source Subspace Separation, *IEEE Transaction on biomedical engineering*, Vol.47, No.5, May 2000.

[5] H.Wan, Q. Liu, J. Chai, A Method for Extracting FECG Based on ICA Algorithm, *ICSP2008 Proceedings*, IEEE 2008.

[6] R.Martin-Clemente, J. L. Camargo-Olivares, S. Hornillo-Mellado, M. Elena and I. Roman, Fast Technique for Noninvasive Fetal ECG Extraction, *IEEE Transaction in biomedical engineering*, Vol. 58, No.2, February 2011.

[7] J.L.Camargo-Olivares, R. Martn-Clemente, S. Hornillo-Mellado, M. M. Elena, and I. Romn, The Maternal Abdominal ECG as Input to MICA in the Fetal ECG Extraction Problem, *IEEE signal processing letters*, vol. 18, no. 3, March 2011.

[8] MIT-BIH ECG database [Online] available: http://www.physionet.org/mitdb.

[9] M.Khan,F.Aslam,T.Zaidi, S. A. Khan. Wavelet Based ECG Denoising Using Signal-Noise Residue Method, *IEEE Conference*,978-1-4244-5089-3/11, IEEE, 2011.

[10] D.Zhang,Wavelet Approach for ECG Baseline Wander Correction and Noise Reduction, *Proceedings of the IEEE Engineering in Medicine and Biology 27th Annual Conference Shanghai*, China, September 1-4,2005

[11] S.Nikam, R. K. shastri, Comparative analysis of ECG baseline wander correction techniques, *IEEE conference on communication and signal processing*, melmeruvathur, Tamlnadu, India 2014.

[12] S.K.Nagakoti, B. Sing, M. Kumar, An Algorithm for Fetal Heart Rate Detection using wavelet transform, *1st Intl Conf. on Recent Advances in Information Technology RAIT-2012* IEEE.

[13] C.Meyer, J. F. Gevela, and M. Harris, Combining Algorithms in Automatic detection of QRS complexes in ECG Signals, *IEEE Transaction on information technology in biomedicine*, vol.10, no.3, July 2006.



Sonal Nikam received the B.E. in Electronics and Telecommunication in 2012 from Pune University and she is pursuing M.E. Degree in Electronics with specialization in Digital System from Vidya Pratishthans college of Engineering, Baramati, India. She has Published paper in IEEE International conference on communication and signal processing,Melmaruvathur, Tamil Nadu. Her area of research interest is Biomedical Signal Processing.



Rajveer Shastri received the B.E. Electronics and Telecommunication in 2000 from Dr. Babasaheb Ambedkar Marathawada University, Aurangabad, the M.E. Degree in Electronics with specialization in Computer Technology from Shri Guru Govind Singh Engineering and Technology, Nanded, He is now pursuing Ph.D. degree, in Electronics from Swami Ramanand Tirth Marathawada Univeristy Nanded. He worked as lecturer from 2002 to 2008 and from 2008 to till date he is working as assistant professor in Vidya Pratishthans college of Engineering, Baramati, India. He is life member of IEEE, ISTE and IETE. He has published 10 international journal, conference papers and 5 national conference papers.



Arnab Das received B.Tech degree in Electrical Engineering from Naval College of Engineering, Lonavala, India in 1995. He obtained M. Tech degree in Radar and Communication with specialization in Underwater Signal Processing in 2002and PhD degree in 2009 from Indian Institute of Technology, Delhi, India. He was commissioned into the Indian Navy in 1994. He worked as Project Officer at CARE, IIT Delhi for R and D in Underwater Signal processing and hardware design in 2003-2007. Currently he is instructor at MILIT Pune, India. His research interests are Underwater Passive Surveillance, Underwater Communication and Pattern recognition.



Shankar Deosarkar received his BE Degree in Electronics in 1988 from Amravati University and his both M. Tech and Doctorate Degrees in the area of Microwave Communication in 1990 and 2004 respectively from S.G.G.S. Institute of Engineering and Technology, Nanded. He has to his credit about 35 research publications at the National and International level. At present he is guiding three Research Scholars in the area of EMI / EMC and Microstrip Antenna Design. He was invited to deliver scholarly lectures at McGill University, Montreal, Canada, Electromagnetic Research Center Ottawa, Government of Canada and Princeton University, New Jersey, USA and UGC / AICTE Refresher Courses.

Detection of Leukemia in Microscopic Images Using LabVIEW

Chaitali Raje[1], Jyoti Rangole[2]
[1,2]VPCOE, Baramati,
University of Pune,India
[1]sonyraje16@gmail.com, [2]jyotika2k1@gmail.com

***Abstract*—Leukemia is a cancer of blood which occurs when lot of abnormal white blood cells produced by bone marrow. Hematologist makes use of the microscopic study of human blood which includes preprocessing, segmentation, classification that can allow identification of patients suffering from Leukemia. The images will be inspected visually by hematologist known as Diagnostic tests which includes complete blood count (CBC), cytogenetics test and immunocytochemistry test. The main drawback of Diagnostic tests is that it does not give accuracy, time consuming and expensive since it depends on the operators capability and tiredness. To overcome these drawbacks, image processing technique such as automatic morphological cell analysis, statistical parameter based segmentation which segregates white blood cells from other blood components i.e. erythrocytes and platelets is done. Thresholding is done based on statistical parameters such as Mean and Standard Deviation Geometrical features such as area, perimeter of the white blood cell nucleus is calculated for diagnostic prediction of Leukemia.**

***Keywords*—Leukemia, Image processing, LabVIEW.**

I. Introduction

The most important element of any human body is blood as it keeps one alive. It performs many important functions such as to transfer oxygen, carbon dioxide, mineral and etc to the body in order to maintain metabolism[1]. Insufficient amount of the blood could affect the metabolism greatly which could be very dangerous if early treatment is not taken. One of the common blood disorders is Leukemia. The most common cancer type is Leukemia. Generally, cancer develops in cells of the body, and leukemia is a cancer of blood cells. Leukemia is characterized by an uncontrolled production of abnormal, blood cells [1]. The bone marrow produces three types of blood cells: Red blood cells carry oxygen and other materials to the tissues of the body; Platelets helps in blood clotting; White blood cells are the one which helps to fight off infections in the body. Bone marrow is a soft material present in middle of large bones. In person having leukemia, the bone marrow does not work properly. It produces, immature cells, called Lymphoblast. Leukemia cells are known as ”blasts”. The patient may develop anemia if bone marrow does not make enough red blood cells. The patient may bleed if proper amount of platelets are not produced. If insufficient amount of white blood cells are produced, the body cannot fight off germs and the person may develop frequent infections [1].

II. Literature Survey

The diagnosis of leukemia is frequently done by a blood test that gives an abnormal blood cell count. Once leukemia is confirmed, the sample of bone marrow is taken by doctor to examine cell morphology (shape) and are sent to the laboratory to identify chromosomal changes. This information is required for diagnosis of individual patients [2].

A. Diagnostic Tests:

1. Medical history and physical examination: The record of present symptoms, and problems a person has had in the past. The medical history of a person’s family also helps in diagnose leukemia.
2. Complete blood count (CBC): Blood is taken and checked under the microscope for the number of RBCs, WBCs and platelets.
3. Bone marrow aspiration: Bone marrow is removed with the help of a needle from breastbone. The removed sample is observed under a microscope to look for abnormal cells.
4. Cytogenetic analysis: Cytogenetic test takes blood or bone marrow to help identify individual chromosomes. It shows abnormalities in chromosomes, which help to diagnosis and identify the type of leukemia. Results are usually available within 3 weeks.
5. Immunohistochemistry: Blood sample of cells are treated with special antibodies in immunohistochemistry. Under the microscope the change in color can be seen. It helps in determining the types of cells that are present.

B. Image processing Techniques:

1. Leyza Baldo Dorini et al. [3] This paper approaches novel method to segment the nucleus and cytoplasm of white blood cells. To identify the cytoplasm region, they proposed two different schemes, based on Granulometric analysis and on morphological transformations.
2. N.H. Abd Halim, et al.[4] In this paper, a global contrast stretching and segmentation based on HIS color space is used to improve the image quality. Image enhancement procedure is used to extract the nucleus region in WBC images sample by using same threshold value, for both ALL and AML images.
3. N.Z. Supardi, et al.[5] This paper presents the study on blasts classifying in acute leukemia into two major

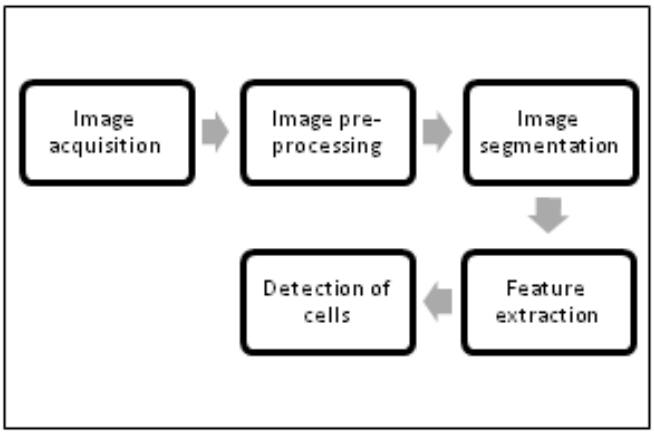


Fig. 1. Block Diagram

forms which are ALL and AML by using K-NN. twelve main features that represent size, color-based and shape were extracted from blood images. The k values and distance metric of k-NN were tested in order to find suitable parameters to be applied in the method of classifying the blasts.

III. Implementation Details

1. Image Acquisition: Blood slide image are captured using high resolution camera which is attached to the microscope, so that the images can be taken and directly given as input for further processing.

2. Image preprocessing: The preprocessing stage is designed to remove unwanted effects from the image and to prepare the image as necessary for further processing. Generally Image Enhancement, Linear Contrast stretching, Histogram Equalization etc are applied on input image. Preprocessing is the main step that influences automated detection of defects. In this paper Contrast Enhancement and Histogram Equalization is used for preprocessing.

3. Image Segmentation: Segmentation identifies and segments cancerous cell and leukocytes from the background. Statistical Parameters of the images is calculated to segment foreground from background and accordingly lower, middle and upper limit of multi-threshold is decided.

Removal of particles- After segmentation, morphological operator such as erosion is used for removal of small unwanted particles. Edge detection- Edges of cell are detected using edge detector operators. Sobel edge detector is used for edge detection of nucleus.

4. Feature Extraction: The features giving predominant difference between normal and infected cells are identified. The selected features are geometrical such as area, perimeter of nucleus.

5. Classification of cell: The images processed by the above method are classified based on feature values of cell nucleus i.e. Normal and Cancer infected.

IV. Nucleus Segmentation Algorithm

The quality of the microscopic image depends on the exposure of the microscope staining process. Over and under exposure setting may cause difficulty in detection. Image enhancement processes consists of collection of techniques that attempt to convert the image into form that is better for analysis by machine. The algorithm used to develop the nucleus segmentation technique is as follows [6]:

Step1: Input the color blood slide image to the system.
Step2: Convert the color image into grayscale image.
Step3: Enhance contrast of the grayscale image by using histogram equalization method.
Step4: Calculate the statistical parameters such as mean and standard deviation of image
Step5: Calculate the average values of mean and standard deviation.
Step6: Apply multi-threshold method by keeping standard deviation as lower limit, mean as middle limit and 255 as upper limit of threshold.
Step7: To remove small pixel groups use morphological erosion.
Step8: Apply sobel edge detector.
Step9: Calculate the geometrical features such as area and perimeter of segmented cells.
Step10: Based on the features extracted in above step, classify cell as blast or normal cell.

V. Results and Discussion

In the algorithm of nucleus segmentation using Labview the image is enhanced using histogram equalization method and nucleus segmentation of enhanced image is done using statistical parameters such as mean and standard deviation. The proposed technique has been applied on 128 microscopic blood slide images. Fig. 2 and Fig. 3 represents the block diagram and front panel of Labview. In the result, edges of nucleus are detected using sobel edge detector, so that feature values can be calculated for classification of cells as normal or cancer infected. Geometrical features such as area and perimeter of each cell are calculated.

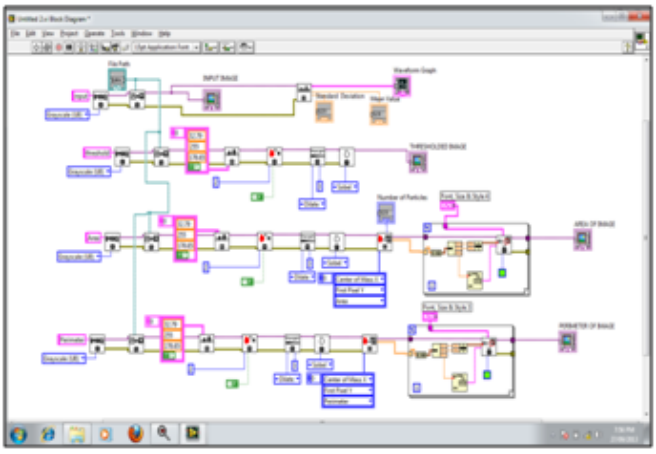


Fig. 2. Block Diagram in LabVIEW

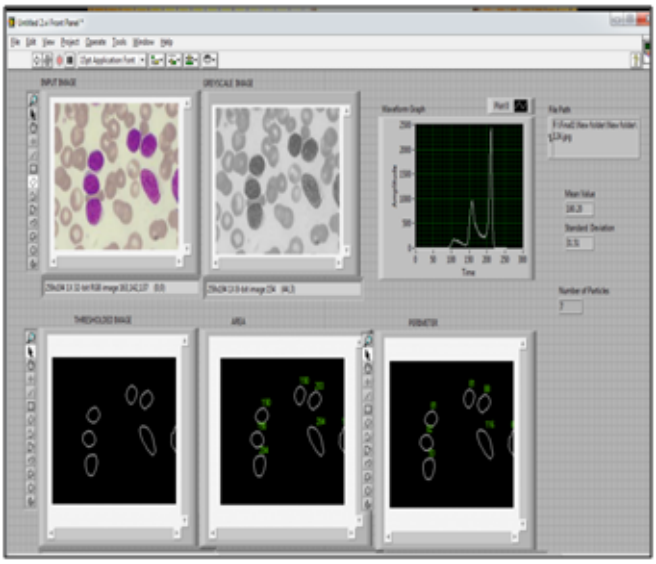


Fig. 3. Front Panel in LabVIEW

VI. Conclusion

Segmentation of Nucleus from Cytoplasm followed by feature extraction is the main aim of the paper. Using statistical parameter such as Mean and Standard deviation based thresholding gives more accurate results. Shape features of nucleus such as area, perimeter etc. are considered for better accuracy of detection. In addition, the fully segmented nucleus can be better achieved by using LabVIEW based algorithm because it is less sensitive to input image variations.

References

[1] www.connectedkansankids.com/diagnoses/leukemia.html

[2] www.biomedhealthcare.com

[3] L.B. Dorini, R. Minetto, N. Leite, Semiautomatic White Blood cell segmentation based on Multiscale Analysis, IEEE Journal of Biomedical and health informatics, Vol. 17, No. 1,January 2013.

[4] N.H. Abd Halim, M.Y.Mashor, A.S.Abdul Nasir, N.R. Mokhtar, H. Rosline, Nucleus Segmentation Technique for Acute Leukemia, IEEE 7th International Colloquium on Signal Processing and its Applications 2011.

[5] N. Z. Supardi. M. Y. Mashor. N. H. Harun. F. A.Bakri, R. Hassan, Classification of Blasts in Acute Leukemia Blood Samples Using K-Nearest Neighbour, IEEE 8th International Colloquium on Signal Processing and its Applications 2012.

[6] F. Kasmin, A. S. Prabuwonw, A. Abdullah, Detection of Leukemia in human blood sample based on microscopic images: A Study, Journal of Theoretical and Applied Information Technology December 2012.



Chaitali Raje is pursuing M.E. (2014) in Digital System from V.P.C.O.E. Baramati. She has published - 1. Detection of Leukemia in Microscopic Images Using Image Processing, IEEE international conference on communication and signal processing, Melmaruvathur. Her areas of research interest are Biomedical Image processing, Machine Vision.



Jyoti Rangole M.Tech. in Digital System from C.O.E. Pune in 2009. She has worked as a reviewer for Pearson Publication for the book , Embedded System. She is working as an Assistant Professor in Electronics and Telecommunication Department. She has published 1. Data compression techniques, IEEE third international conference on Machine Learning Computing Conference, Singapur. 2. Implementation of image processing algorithms on FPGA published in international journal Technology World. 3. Automatic silkworm eggs counting mechanism for sericulture, journal of engineering technological research, ISSN 2229-9262 Quarterly Malaysia Journal. Her areas of research interest are Machine Vision, Implementation of Image processing algorithm using VLSI for sericulture automation, Multiresolution image analysis.

Detection of Optic Disc in Fundus Images

Snehal Akhade[1],Vikas Deshmukh[2], Shankar Deosarkar[3]
[1,2,3]VPCOE, Baramati,
University of Pune, India
[1]snhkhd9@gmail.com, [2]vpcoe@rediffmail.com, [3]sbdeosarkar@yahoo.com

***Abstract*—Diabetic retinopathy, hypertension, glaucoma and macular degeneration are nowadays some of the most common causes of visual impairment and blindness. Early diagnosis and appropriate referral for treatment of these diseases can prevent visual loss. All of these diseases can be detected through a direct and regular ophthalmologic examination of the risk population. However, population growth, aging, physical inactivity and rising levels of obesity are contributing factors to the increase of them, which causes the number of ophthalmologists needed for evaluation by direct examination is a limiting factor. Optic disc (OD) detection is an important step in developing systems for automated diagnosis of various serious ophthalmic pathologies. The goal is to facilitate the early detection of certain pathologies and to fully automate the process so as to avoid specialist intervention. The method for the detection of the OD contour is mainly based on three parts pre-processing, OD segmentation, post processing.**

Keywords*—Diabetic retinopathy, glaucoma, optic disc, OD segmentation.

I. Introduction

The OD is considered one of the main feature, which usually appears as a round region brighter than surrounding in fundus image Fig. 1(b). The optic disc or optic nerve head is the location where ganglion cell axons exit the eye to form the optic nerve Fig. 1(a). There are no light sensitive rods or cones to respond to a light stimulus at this point. This causes a break in the visual field. The optic disc is also the entry point for the major blood vessels that supply the retina. The optic nerve head in a normal human eye carries from 1 to 1.2 million neurons from the eye towards the brain. The optic disc is placed 3 to 4mm to the nasal side of the fovea. It is a vertical oval, with average dimensions of 1.76mm horizontally by 1.92mm vertically.

The change in the shape, color or depth of OD is an indicator of various ophthalmic pathologies. Diabetic retinopathy, hypertension, glaucoma, and macular degeneration are nowadays some of the most common causes of visual impairment and blindness [1]. Early diagnosis and appropriate referral for treatment of these diseases can prevent visual loss. Usually, more than 80% of global visual impairment is avoidable by early stage diagnosis. Population growth, aging, physical inactivity, and obesity are contributing factors to increase these diseases. So, a system for automatic recognition of the characteristic patterns of these pathological cases would provide a great benefit.

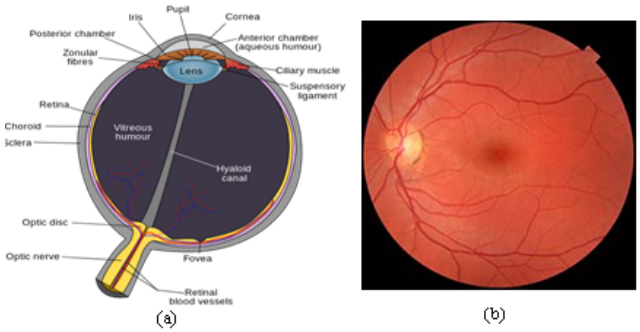


Fig. 1. (a) Anatomy and (b) Fundus image of human eye.

Regarding this aspect, optic disc (OD) segmentation is a key process in many algorithms designed for the automatic extraction of anatomical ocular structures, the detection of retinal lesions, and the identification of other fundus features.

OD segmentation is not an easy matter. Besides the variations in OD shape, size, and color pointed out previously, there are some additional complications to take into account. Contrast all around the OD boundary is usually not constant or high enough piecewise due to outgoing vessels that partially obscures portions of the rim producing shadows. Another distracter is produced when peripapillary atrophy is present, as this produces bright areas just outside the OD rim which distort its shape.

In Section II literature survey for OD detection is given. In Section III proposed method is explained. In Section IV the final results of proposed method are given. In Section V conclusion for proposed method.

II. Literature Survey

In [2], given an algorithm to localize OD in low resolution color fundus images.The algorithm is based on two methods Hausdorff-based and pyramidal decomposition respectively. The computation time depend upon Hausdorff stage.

In [3], the algorithm identifies optic nerve as the focal point of blood vessels. If the blood vessel structure is not clear, then the optic nerve is identified as brightest region. For this fuzzy convergence algorithm is used.

In [4], an algorithm is given for the segmentation of the optic nerve head in low resolution images. For locating the optic nerve head template matching is used.

In [5], two parabolas used to model vessel structure. The point at which this two parabolas overlap is considered as the location of optic disc.

In [6], proposed method based on deformable model for OD boundary detection in fundus images. Original snake technique improved using clustering and smoothing update. This updating used to achieve OD contour.

In [7], the algorithm works by matching expected directional vessel pattern with directions of vessels in the image. For this simple matched filter is designed to match the vessels direction.

In [8], for locating the optic disc maximum variance method is used. Circular Hough transform is used for OD boundary segmentation.

In [9], proposed line operator to capture the circular structure associated with OD.

In [10], method is divided in two parts OD localization and OD segmentation respectively. OD is localized using matched filter. Then blood vessels and bright regions are removed. Level set and ellipse fitting is used for segmentation.

In [11], used different operations generalized distance function, watershed transform for segmentation of OD. Input to the segmentation obtained using PCA.

III. Proposed Method

As the OD is brighter part of the image, if we apply threshold technique directly it fails to segment OD shown in Fig. 2

In the literature some methods have used red component or green component of the original RGB image for further processing. When there is a small variation in the input image, there is a large variation in the red component shown in Fig. 3(b) and in the green component image vessel information is more so, it is not that much useful Fig. 3(c). In the blue component there is less information, so we cannot use it independently Fig. 3(d).

There is a need of technique which will be less sensitive to the input image variation.

Algorithm of Proposed Method:

1) Convert RGB image to Grayscale.
2) Remove Vessels.
3) OD Segmentation.

In proposed method a MESSIDOR [12] database is used which is available for research and educational purpose. MATLAB software is used for implementation of the algorithm.

A. Convert RGB image to Grayscale

For better segmentation input RGB image we need to convert RGB image to a grayscale image.

It is difficult to identify patterns in data with higher dimensions. PCA helps to identify patterns in data, and represents the data in such a way as to highlight their similarities and differences. After identifying these patterns in the data, it can be compressed by reducing its dimensions [13].

Intensity image and principal component are compared. Intensity image is obtained by simply taking the average of red, green and blue channel of the image.

Principal component gives a better representation of OD compared to the intensity image as shown in Fig. 4



Fig. 2. After applying Otsu's threshold.

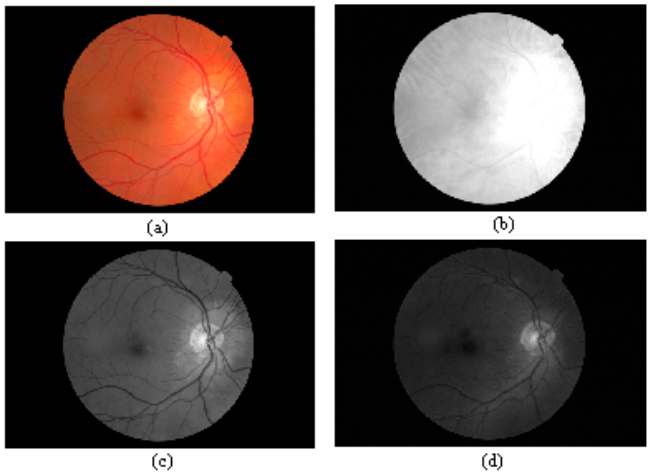


Fig. 3. (a) Original fundus image (b) Red component (c) Green component (d) Blue component.

B. Remove Vessels

The variations of intensities across the boundary of OD are because of blood vessels. Thus, it is important to remove vessels for better OD segmentation.

After selecting the principal component vessels are filled by using the simple closing. Closing operation is nothing but dilation followed by erosion with similar structuring element [14]. Structuring element is a small binary image. It is moved throughout the image to perform the desired operation.

$$p = \phi^{sB}(f) \tag{1}$$

In Eq. 1, f is the first principal component and sB is the structuring element. Fig. 5(b) shows the output of vessel removal operation.

C. OD Segmentation

The shape of OD is nearly circular. So, there is a need of technique which helps to find the boundary of OD.

Hough transform is an interesting and computationally efficient technique used for detecting lines in the image. Then further it is developed by Duda and Hart [15], to find circular

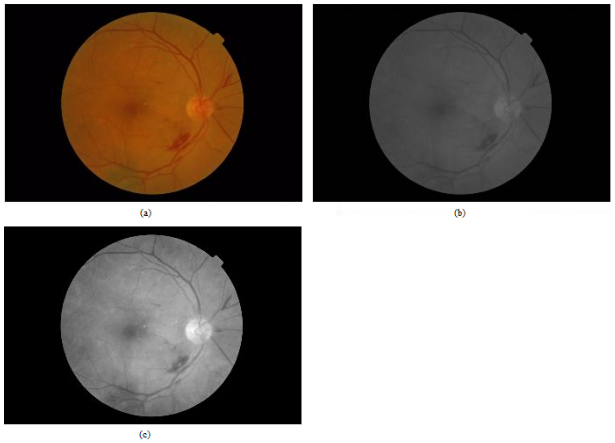


Fig. 4. (a) Original image (b) Intensity image (c) Principal component.

shapes or patterns within the image which is nothing but the Circular Hough transform. This technique is applied after vessel removal. Circular Hough transform gives boundary of the OD shown in Fig. 6.

IV. Results

The proposed method applied on selected images. In some of the images OD failed to segmented properly and in some images proposed method fails to segment OD properly.

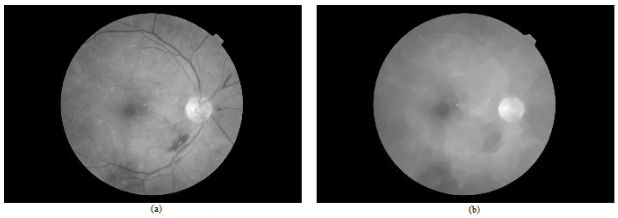


Fig. 5. (a) First principal component (b) After vessel removal.

V. Conclusion

This paper presents a simple method for OD segmentation by using image processing. This method will be helpful in mass screening of diabetic retinopathy.

References

[1] World Health Org., Action plan for the prevention of blindness and visual impairment 20092013 2010.

[2] M. Lalonde, M. Beaulieu, and L. Gagnon, "Fast and robust optic disc detection using pyramidal decomposition and Hausdorff-Based template matching, *IEEE Trans. Med. Imag.*, vol. 20, no. 11, pp. 11931200, Nov. 2001..

[3] A. Hoover and M. Goldbaum, "Locating the optic nerve in a retinal image using the fuzzy convergence of the blood vessels, *IEEE Trans. Med. Imag.*, vol. 22, no. 8, pp. 951958, Aug. 2003.

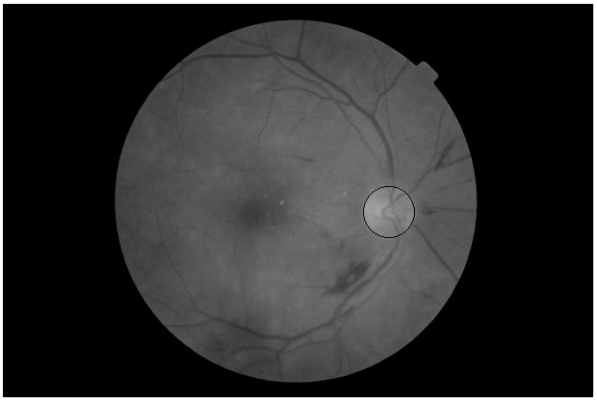


Fig. 6. Result of the proposed method.

[4] J. Lowell, A. Hunter, D. Steel, A. Basu, R. Ryder, E. Fletcher, and L. Kennedy, "Optic nerve head segmentation, *IEEE Trans. Med. Imag.*, vol. 23, no. 2, pp. 246254, Feb. 2004.

[5] M. Foracchia, E. Grisan, and A. Ruggeri, "Detection of optic disc in retinal images by means of a geometrical model of vessel structure, *IEEE Trans. Med. Imag.*, vol. 23, no. 10, pp. 11891195, Oct. 2004.

[6] J. Xu, O. Chutatape, and P. Chew, "Automated optic disk boundary detection by modified active contour model, *IEEE Trans. Med. Imag.*, vol. 54, no. 3, pp. 473482, Mar. 2007..

[7] A. A.-H. A.-R. Youssif, A. Ghalwash, and A. A.-R. Ghoneim, "Optic disc detection from normalized digital fundus images by means of a vessels direction matched filter, *IEEE Trans. Med. Imag.*, vol. 27, no. 1, 2008.

[8] A. Aquino, M. E. Gegundez-Arias, and D. Marn, "Detecting the optic disc boundary in digital fundus images using morphological, edge detection, and feature extraction techniques, *IEEE Trans. Med. Imag.*, vol. 29, no. 11, pp. 18601869, Nov. 2010.

[9] S. Lu, and J. H. Lim, "Automatic Optic Disc Detection From Retinal Images by a Line Operator, *IEEE Trans. Med. Imag.*, vol. 58, no. 1, Jan. 2011. 2011.

[10] H. Yu, E. S. Barriga, C. Agurto,S. Echegaray, M. S. Pattichis,W. Bauman, and P. Soliz, "Fast localization and segmentation of optic disk in retinal images using directional matched filtering and level sets, *IEEE Trans.Inf. Tech.in Biomedicine*, vol. 16, no. 4, Jul. 2012.

[11] S. Morales, V. Naranjo, J. Angulo, and M. Alcaniz, "Automatic detection of optic disc based on PCA and mathematical morphology, *IEEE Trans. Med. Imag.*, vol. 32, no. 4, pp. 786-796, Apr. 2013.

[12] MESSIDOR TECHNO-VISION program, MESSIDOR: Digital Retinal Images France,[Online]. Available: http://messidor.crihan.fr/index-en.php.

[13] M. Turk and A. Pentland, "Eigenfaces for recognition, *Journ. of Cognitive Neuroscience*, vol. 3, no. 1, pp. 71-86, 1991.

[14] Gonzalez, Woods, *Digital Image Processing*, third Edition, PHI.

[15] R.O.Duda and P. E. Hart, "Use of the Hough transformation to detect lines and curves in pictures, *Communications of the ACM*, vol. 15, no. 1, Jan. 1972.



Snehal Akhade received the B.E. Electronics and Telecommunication in 2011 from Pune University, Pune and she is pursuing M.E. Degree in Electronics with specialization in Digital System from Vidya Pratishthan's college of Engineering, Baramati, India. She has presented paper in IEEE ICICES conference at Chennai. Her area of research is Image Processing.



Vikas Deshmukh received the B.E. Electronics and Telecommunication in 1990 from Dr. Babasaheb Ambedkar Marathawada University, Aurangabad, the M.E. Degree in Electronics Communication system in 2003 from P.D.A. college of Engineering, Gulbarga from Gulbarga university, Gulbarga. He worked as Lecturer from 01/08/1991 to 31/05/2000; senior Lecturer from 01/06/2000 to 24/06/2005 and from 25/06/2005 to till date he is working as an assistant professor in Vidya Pratishthan's College of Engineering, Baramati, India. He has published journal and conference papers. His area of research is Radiating systems, Microstrip Antenna.



Shankar Deosarkar received his BE Degree in Electronics in 1988 from Amravati University and his both M. Tech and Doctorate Degrees in the area of Microwave Communication in 1990 and 2004 respectively from S.G.G.S. Institute of Engineering and Technology, Nanded. He has to his credit about 35 research publications at the National and International level. At present he is guiding three Research Scholars in the area of EMI / EMC and Microstrip Antenna Design. He was invited to deliver scholarly lectures at McGill University, Montreal, Canada, Electromagnetic Research Center Ottawa, Government of Canada and Princeton University, New Jersey, USA and UGC / AICTE Refresher Courses.

Human Factors Perspective is Necessity of Modern Ship-Building

Lt Cdr Sumit Singh
Machinery Trials Unit (V)
sumit42263a@gmail.com

Abstract—**Despite rapid gains in technology, humans are ultimately responsible for ensuring the success and safety of the high risk operations at high seas. They must continue to be knowledgeable, flexible, dedicated and efficient while exercising good judgment during prolonged deployments which maybe for months together. It is evident from the experience of modern ships that incidents which result from poor adaptation of the limits of human performance to the conditions of fulfilment of the assigned tasks, the trend is often to attribute their causes to human errors. This last term is not very useful for the prevention of accidents and incidents, even if it shows where the system failed, it does not help in determining and eradicating the causes of the failures. When systems are functioning correctly and efficiently, few appreciate the significance of the human factors component that has led to the smooth operation. In emergency situations, however, there is an immediate demand for action in order to rectify the problem. Anywhere a mix of people and technology interact you will find human factors; a branch of engineering in which the primary emphasis is on the human input. In discussing ship design there are two aspects to be considered. First, human-technological interaction of man and machinery which is growing rapidly with advancements of technologies. Other, there is the additional matter of operating and controlling equipment and systems on a moving platform bearing in mind that technology goes beyond the question of manipulating machinery. As ship design evolves and in particular as compliment of ship staff diminishes in numbers, much greater emphasis should be placed upon the human factors input in order to maximize safety and efficiency during routine and emergency operations. This paper discusses all the above issues bringing out modern perspectives in warship-building with considerate view of human factors.**

Keywords—Human Factors; Technoligies; Ship Design.

I. INTRODUCTION

From the onset, there is a critical need for a human factors input in the design of new ships to ensure optimal interaction between technology and people in order to achieve maximal operational effectiveness. When all is well and systems are functioning correctly and efficiently, few appreciate the significance of the human factors component that has led to the smooth operation. In emergency situations, however, there is an immediate demand for action in order to rectify the problem. Although many human factors efforts are aimed at the very highest level of technology, one should remember that they are required at all levels in order to insure maximum efficiency. Anywhere a mix of people and technology interact you will find human factors; a branch of engineering in which the primary emphasis is on the human input.

Ship-board Human Performance

The six major design factors, all of which naval architects and marine engineers can directly control, determine how comfortable the working and sleeping environments are aboard a ship ensuring minimal human fatigue and optimal human performance:-

1 Ship motions
2 Human-Machine Environments
3 Lighting
4 Noise
5 Vibrations
6 Ventilation
7 Temperature

Ship Motions

The human operator working on a moving platform is susceptible to degraded performance in a number of ways. There are the purely physical limitations of both gross and fine motor skills involving whole-body motion imposed by heavy seas. These physical limitations include motion induced interruptions (MII) which occur when local motions cause a person to lose balance or slip, thereby interrupting whatever task is being performed. Fine motor skills include delicate adjustment of controls, computer operations, and certain maintenance tasks involving electronic boards and components. Physical operations carried out on a moving platform also induce fatigue and degradation of mental effort leading to an overall decrement of human performance and increased potential for injury. Motion sickness is another example of a response to provocative motion that causes diminished performance. These various physical difficulties and human responses may be found individually but on many occasions, they occur together. The following summarizes approaches to preventing or mitigating adverse effects of ship motion on ship staff:-

Ship design and systems engineering Hull design, Ship arrangements and layout, Operation and maintenance of machinery and equipment, Motion attenuation devices (e.g. stabilizer fins), Vibration isolation and damping treatments, and Isolation of special stations.

Human factors Engineering; Arrangement and designs of personnel space, Location and orientation of personnel stations, Work and task design, Display control design and placement, Optimization of ship environmental factors, Individual anti-vibration devices

Human-Machine Environments

During the last decade indigenous warships herald a paradigm shift in the design of future surface combatants for the Indian Navy by implementation of significant electronics to provide needed functionality and performance. Increasing amount of data and strong development of technology has forced need for faster information streams and more sophisticated processes management aids. There are ever-growing developments in fusion of onboard processes organization and supervision through Integrated Ship Management Systems (ISMS). Technology is being used onboard ships to reduce manning levels. This environment can over work the ship staff, causing fatigue and risking their lives and the ship. Using automation and designing human-machine environments onboard ships poses a unique challenge for marine engineers. Using automation can reduce manning requirements but there is a point where the ship staff is just too small to remain alert, diligent, and able to safely operate the ship. Determining the size of ship staff for a particular ship is a tough engineering problem, mainly due to economic pressures. Assigning computers to perform safety critical tasks does not come without failures and breakdown, which must be subsequently corrected by human operators.

Human-Machine systems should be designed so that both the operator and the machine perform at an optimal level. This can only be accomplished when both the human operator and the machine have been analyzed and their strength and weaknesses are known. The human factors, such as fatigue, make it extremely difficult to come up with a foolproof design that can eliminate human error. Human-machine system and interface design is a challenge because the environment in which these systems operate is dynamic and both human as well as machines can be very unpredictable. Fatigue and other human factor variables require special attention in the design of complex humanmachine systems.

Two major advantages cited of automation are, automation will reduce workloads and automation will reduce human error. These two benefits of automation are also areas that cause a number of problems for human operators. A reduction in workload is beneficial to the human operator in terms of task management but it tends to pull the operator ”out of the loop.” Using automation to monitor systems eases the supervisory burden of such operators but can decrease the operators understanding of the systems status. In a high workload environment, operators can quickly lose control of a system if steps taken by automation are not readily displayed and understood. The automated system can quickly perform a number of tasks. This can leave the operator without a clear understanding of what happened in a systems transition or what is going to. These problems are being faced by Indian Navy in operation of its modern ships.

The use of automation to decrease human error also contributes to the loss of an operators system status awareness. Computer controlled systems perform thousands of complex algorithms per second and their outcome may not always be apparent to the operator. The lack of understanding of the system status by the operator becomes a disadvantage in emergencies. When emergencies do occur, the operator may have little or no idea about what happened or where there was an error in the automation. The lack of information and understanding quickly puts the operator in a dangerous and sometimes hopeless situation.

The current economics of maritime operations has led the industry towards minimal manning. Technological advances have also led to major changes in the role of human operators, many of which remove the operator from the systems control. Using unmanned engine rooms aboard ships requires engineers to have a different skill base. Most of the knowledge previously required by engineer was machinery maintenance and operation. Unattended engine rooms require that an engineer have the ability to anticipate, identify and react to malfunctions, in order to maintain a reasonable level of reliability and safety. Most engineers currently require extensive training in how to operate the automation and perform troubleshooting. This is a much different and vast type of knowledge base than just basic diesel and generator operation.

The problems associated with automation are:-

1 Skill degradation.
2 Inadequate feedback resulting in misunderstanding.
3 Fewer physical demands but greater cognitive load.
4 Enhanced workload peaks and troughs.
5 Large amount of data and misleading displays.

Automation typically leads to operators remaining stationary to oversee the operation of the plant. A fatigued operator can increase their alertness through physical activity, such as walking around and inspecting machinery, as well as reading gauges. The use of automation has eliminated the need to do this and has transferred the physical workload to the cognitive workload, which is most affected by fatigue.

Considering the information on human fatigue, human-machine interface, and automation, it is clear that these issues require further research. Ship designers and operators will continue to be confronted with innovations and advancing technology that may or may not make maritime platform operation easier and safer. Being able to identify what types of automation are most useful and having the ability to design acceptable interfaces are important skills that designers must possess when looking towards the future.

Other Factors

1 Lighting :- Light maintains the pace of the human biological clock, which directly regulates the circadian rhythm. The human body requires exposure to natural daylight in order to maintain a proper circadian cycle and for general health and well being. However, electrical sources of light have largely become the mainstay for personnel onboard ships. Some members of a ships staff spend the majority of their day within the confines of the ship and below decks, where electric light is all that is available. This can create an irregular and shifting sleep cycle that leads to fatigue. Current design standards and guidelines on illumination levels in ship compartments are inadequate for maintaining watchkeeper alertness and do not mitigate fatigue. Illumination levels recommended in class society guidelines are based on specific task performance not on human health and well being. Circadian lighting

systems (CLS) have made it possible to alter the biological clock so that shift workers remain alert at night and get restorative sleep during the day. Circadian lighting systems come in many forms, the system has a variable light output that can be manually controlled. There are also computer controlled systems that have been developed. These systems have a high output that is normally in the range of 10,000 lux, which is more than 1,000 times greater than any level suggested by current ship-building. Using CLS onboard ship is something that requires consideration by the ship design community and class societies. The systems are typically expensive but can be limited to use in areas such as the engine control room. Mariners would benefit from a shift in the focus of lighting guidelines, from task performance to human well being and mitigating fatigue. The use of CLS, which is designed with human well being and fatigue in mind, has been successfully tested and found to have a positive impact in nuclear industry.

2 Noise :-Audible noise can be broken down into two categories, viz. airborne (ABN) and structure-borne SBN). Airborne noise is what causes stress and hearing loss. Structure-borne noise induces vibrations that can damage machinery and marine structures. Both of these noise types vary in frequency and intensity. ABN requires its due thrust in ship-building and maintenance during ships operating life cycle. Although noise is an unavoidable issue in maritime operations, steps can be taken in the design stages of a ship to decrease noise effects. Post-production measures can also be taken to reduce noise levels. The current guidelines for noise exposure are acceptable for decreasing the chances of permanent hearing damage. They are inadequate for protection against the subtle physiological effects of long-term low intensity noise exposure that has been shown to cause fatigue and decrease alertness. Noise Control Methods:-

   1 Isolation:- Minimizes noise by reducing vibrations caused by machinery or equipment. Vibration-absorbing materials are used such as rubber mounts, pads, or springs. The type of material for an application is based on weight, vibration frequency, and desired degree of isolation.

   2 Barrier:- Minimizes noise by blocking sound transmission through the use of high mass, resilient, or limp mass materials. Using more mass increases the effect and barriers work better at higher frequencies.

   3 Damping :-Minimizes noise by adding mass to the vibrating structure or by connecting it to a surface that does not want to vibrate. Damping materials are selected by considering the thickness of the vibrating surface, the desired reduction, and the environment.

   4 Absorption:- Minimizes noise with resonators and open-celled porous material, which converts sound energy to heat. Materials used are based on the noise frequency, desired reduction, and environment.

3 Vibrations:-Mariners experience shipboard vibrations caused by machinery, marine equipment and the ships response to the environment. Vibrations resonate throughout the hull structure and the entire ship staff can be affected. The propagation of these vibrations along the decks and bulkheads subject the ship staff to whole body vibration and noise. Short-term exposure can lead to headaches, stress, and fatigue. Long-term exposure leads to hearing loss and causes constant body agitation. Maritime vibration guidelines keep levels low enough to prevent bodily injury but the recommended levels can cause fatigue and disrupt sleeping patterns. Indian Navy is investing substantially in vibration control and reduction in SBN to ensure stealth of the ships. However, human factors consideration with respect to fatigue and stress along with stealth require vibration control measures to be incorporated in ships already commissioned. This may be undertaken during prolonged refits/ mid-life upgrades of the ship.

II. Conclusion

Economic factors curtail the marine industrys incentive to combat shipboard operator fatigue. In addition, current ship design standards and guidelines (class society, ASTM, etc.) do not effectively address the human elements of fatigue and alertness. Naval architects and marine engineers have incorporated human factors into ship designs for many years in a very limited capacity. Unfortunately, ergonomic issues such as console design, maintenance envelopes etc. have been the predominate considerations. Designing a shipboard environment that mitigates the effects of fatigue and maintains or improves human alertness has not been seriously considered. When designing a new warship it is never too early to consider the human element. Optimal performance will only be achieved when the components affecting human element is deliberated from day one, rather than added at the last moment as an afterthought. Before we can begin to design an efficient person-machine system, we must have a very definite idea in all our minds what the final product is intended to do. That means that we must have as clear an understanding of what the person can and cannot do, equally as much as we know about the vessels capabilities and its onboard technological systems and equipment. We must also have a working knowledge of how these human and nonhuman subsets interact so that we can optimize this union. This requires a multiple team effort including many and various disciplines. The problems are more important today than ever before because of the plans to reduce ship staff sizes. The goal is exciting and the ultimate prize is a highly efficient ship that can operate effectively under difficult conditions with the minimal, experienced human complement to ensure successful outcome.



Lt Cdr Sumit Singh received Mtech in Mechanical System Design from IIT Kharagpur. During his career of more than 10 years in Indian Navy, he has served onboard ships and repair yards. He is Presently working as Deputy Officer-in-Charge, Machinery Trials Unit Visakhapatnam. He has presented six technical papers at various forum. The paper presented by him at Delhi College of Engineering during Mechanical Engineers meet MACH 2003 was adjudged the best paper in its category as well as overall . His areas of research interest are predictive testing and machinery health monitoring.

Classification Techniques For Sediment Analysis

Ankika H. Rasal[1], J.A. Sadalage[2], Arnab Das[3]
VPCOE, Baramati,
University of Pune, India
[1]ankikarasal9@gmail.com, [2]jyotika2k1@gmail.com, [3]arnabdas1972@hotmail.com

***Abstract*—Classification of seabed types is an important consideration in the applications like marine archeology, offshore construction projects, maintaining water quality, managing flood levels. It is a process of grouping surficial sediments qualitatively depending on their properties such as clay, sand and their mixtures which is naturally a complex process. Acoustic remote sensing techniques help to characterize and classify sediments to a large extent. This paper presents review on Acoustic sediment classification techniques. Three classification methods are studied. The first one is K-means clustering which is generally used for large data sets divided into non-overlapping groups and minimizes SSE function. Second method is Kohonen's Self-Organizing Feature Map that preserves the topology by mapping weight vectors in input space onto the output space. The Bayesian Classification Method uses backscatter data at a certain angle where number of acoustic classes are obtained are applied with Bayes Decision Rule. A comparative study between the above mentioned methods is done from which it can be stated that SOFM method can be used where K-means clustering fails to recognize the reasonable groups, whereas, BCM can provide very detailed sediment maps. Therefore, for real-time estimation of seabed or riverbed type, this comparison will help to find an efficient classification method.**

Keywords*—Seafloor classification, K-means clustering, Self Organizing Feature Map (SOFM), Bayesian Classification Method (BCM).

I. Introduction

Classification of seabed or riverbed sediment is nowadays an important factor that has to be taken into account. The purpose for sediment classification arises due to many reasons. Among them are to monitor the water quality, to have check on the flood levels, for construction of offshore projects, in navigation, underwater pipelining and so on [1], [2]. Some techniques developed for classification are using optical methods, laser scanning systems, In-situ seabed analysis using Dredging, coring methods [3]. But these methods due to their operational lim-itations are restricted at discrete locations. It is time consuming and costly to collect details about the sediment distribution from set of grab samples and carry out a subsequent laboratory analysis obtained from the visual observations may it be video or still photography. So alternatively, Acoustic remote sensing technique is used for the characterization and classification of sediments. These acoustic signal measurements can therefore, be obtained from the Single Beam Echo Sounders (SBES) and Multi Beam Echo Sounders (MBES) which are also used for bathymetry measurements.

Classification of sediments is a process of grouping the surficial sediments qualitatively depending on their properties such as clay, sand and their mixtures which is naturally complex process. The methods for sediment classification using echo sounders can be distinguished as Empirical methods and Model-Based methods. The Empirical methods are easy to use and implement. Empirical approach includes the backscatter strength of signal and bathymetry measurement features for

classification. In this approach, area is divided into different acoustic classes representing different sediment types like mud, sand, gravel having its own acoustic features. Grab samples are required to associate the acoustic classes to the physical properties of the sediments. On the other hand, Model-Based methods directly associate the acoustic classes and sediment characteristics if the system characteristics like sensitivity and emitted signals are known [4], [6].

This paper aims at review on different Acoustic classification techniques like clustering techniques, artificial neural network analysis and statistical method along with a comparative study between them. Firstly, basic concepts of K-means clustering are presented. Artificial neural networks like Kohonen's self-organizing feature map (SOFM) and statistical method such as Bayesian classification method (BCM) has been explained in this paper. Further, a comparative study is done based on the results obtained in the previous works of sediment classification using these classification techniques.

II. METHODS FOR SEDIMENT CLASSIFICATION

A. K-means Clustering

K-means clustering can referred to as a step ahead to Principal Component Analysis. This is because running PCA is easy but the interpretation of results is a difficult task because in PCA separate clusters cannot be generated to discover unknown groups. Hence, PCA can be used as a first step before applying the Principal components to the K-means clustering algorithm. K-means clustering technique is one of the unsupervised learning algorithms to solve clustering problems. This method is generally used for large data sets divided into non-overlapping groups for minimizing the clustering error where n observations are partitioned into k mutually exclusive subsets or clusters Sj. In this partition each cluster is represented by a centroid and its objects, and each cluster centroid is a point where sum of distances from all objects in that cluster is minimized considering the condition that objects in each cluster in the partition selected should be as close to each other as possible and as far from objects in other clusters as possible.

For each point, sum of squared Euclidean distances for all points in the data set from the corresponding cluster center is computed by K-means which is mathematically given as, In this algorithm number of random centers in the parameter space are adopted. Objects are then moved between different clusters. An iterative algorithm is used by k-means over all

$$J = \sum_{j=1}^{k} \sum_{n \epsilon S_j} |x_n - \mu_j|^2$$

clusters for minimizing the sum of distances from each object to its centroid. Until the sum is not decreased further, the objects are moved between clusters resulting in a compact and well separated set of clusters and this sum is decreased with an increase in number of clusters.

By selecting relative reduction in sum which is represented by calculating percentage in reduction of clusters distance and secondly by determining average silhouette coefficient when adding a new class, optimum number of classes can be found. The average silhouette coefficient is given as, where a_i is the

$$s_i = \frac{b_i - a_i}{max(a_i, b_i)}$$

average distance (dissimilarity) of point i to all other points of its cluster, b_i is minimum average distance (dissimilarity) of i to all points of other clusters. For each cluster, s_i ranges from -1 to +1. Negative value of s_i corresponds to condition that a_i is greater than b_i , but this value is undesirable. High probability for the points to be successfully clustered is indicated by value of s_i=1. Generally, it is ambiguous to select optimal number of clusters definitely [4], [6]–[8].

B. Self Organizing Feature Map (SOFM)

Kohonen's Self-Organizing Feature Map is an unsupervised learning algorithm in which the topological properties of the input feature space are preserved. This method requires no human intervention but some knowledge about the characteristics of input data is necessary. Arrangement of neurons is made in a grid as a map which is also called as Kohonen layer. For characterization of this method, input pattern is topologically mapped so as to correspond the spatial locations of neurons in the lattice to the inherent features input pattern.

To map n-dimensional input vectors into one or two dimensional lattice of output layer is the goal of network. Fig. 1 shows 2D Kohonen neural network. In the output layer, for a given input vector, only one maximum value neuron is set to logic one while all other neurons are set to logic zero and neuron of maximum value is defined as winner. Before applying to

$$d_j = \sqrt{\left[\sum_i (x_i - w_{ji})^2\right]}$$

large Kohonen network, the input data are normalized. From each component of input vector, normalized input vector is obtained by dividing the length of vector [9]–[13].

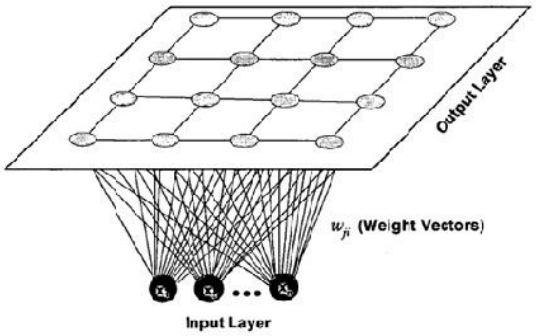


Fig. 1. 2D Kohonen neural network.

Training of SOFM network takes place in following steps:

1) Initially, input vector X having x_i (for i=1 to n) components being normalized is applied to the network.
2) Calculation of Euclidean distance d_j between input node and each output node j is done which is given as,

$$w_{ji}(p+1) = w_{ji} + \eta(p)[x_i - w_{ji}(p)]$$

where x_i is the ith component of input vector X, w_{ji} is weight vector from ith input neuron to jth destination neuron.
3) Depending on minimum distance d_{min} , neuron having weight closest to X is declared as winner and its weight vector is the center of a group of weight vectors lying within distance d_{min}, whereas minimum distance output neuron is denoted as j^* .
4) By using below formula, for neighborhood size $Nj^*(p)$ at pth iteration, the weights for neuron j^* and its neighbor are updated, where (p) is the learning parameter at pth iteration which decreases with increase in number of iterations p. This takes place also for neighborhood $Nj^*(p)$ whose value is large at the beginning of iteration and at the end of training process reduces to only one neuron.
5) Until there is no any noticeable change in the feature map or the training cycle is reached to pre-specified maximum value, repetition of steps 1 to 4 is on.

C. Bayesian Classification Method (BCM)

Bayesian Classification Method is one of the statistical methods used for classification of sediments. This method is based on Bayesian Decision Rule and is developed for deep waters (greater than 30m) which is extended further for shallow waters for approximately 4m depth. Backscatter data at a certain angle where number of acoustic classes are obtained are applied with Bayes Decision Rule. In this method classification is carried out per angle which makes the method to be angle-independent assuming that backscatter values are an average value of sample amplitude values. Hence according to central limit theorem, for a single sediment type, average backscatter

values follow Guassian Distribution for a sufficiently large number of scatter pixels where a number of Guassian PDFs are fitted to the histogram of backscatter data at a given incident angle, where mean and variance of i^{th} PDF, c_i which is the contribution of the individual Guassian functions to the total PDF and fitted histogram f_{BS} are considered as shown in the equation below. To find optimum number of PDFs, the number of PDFs is increased consecutively until the chi-square distributed test static becomes less than

International Workshops, Conferences and Expo for Military and Marine Applications, Pune, India, 2014.

$$BS \sim f_{BS}(BS) = \sum_{i=1}^{r} c_i N(BS; \mu_i, \sigma_i^2)$$

a critical value or close to one. Maximum number of classes that can be distinguished considering the backscatter values is represented by the number of Guassians, whereas intersection of each Guassian with its neighbor represents the borders of classes [14]–[19].

III. Comparision And Discussion

Generally, substantial data pre-processing is required in unsu-pervised learning algorithm like K-means clustering, whereas, artificial neural network such as SOFM have the ability to cluster multivariate data. This ANN is rapid and more robust for outliers than any traditional clustering techniques. But definition of number of groups and the interpretation of results is not straightforward because SOFM does not show any hierarchy of sample groups. One of the merits of SOFM to be stated can be in the situations where K-means clustering fails to identify any reasonable groups, SOFM recognizes the clusters in those situations. It also allows the network to develop clusters in this fashion and make it more efficient in association with the inputs. For BCM to be adopted for shallow waters, following issues are needed to be taken into consideration.

1) Backscatter data suffers higher variances because of the lower water depths resulting in smaller beam footprints. Con-sequently, there is reduction in discriminating power between sediments.
2) Backscatter data and classification results are also affected by the significant bottom slopes existing in the survey area.

For accounting these issues, averaging backscatter values over small surface patches can restore the backscatter strength. Also slope corrections can be applied to the backscatter data. To use BCM for sediment classification is simple, low cost and highly effective method. In this method there are no calibrated sonars required and we can also obtain very detailed (almost 100 percent) sediment maps [7], [20], [21].

IV. Conclusion

Comparative study of various classifiers is essential in sediment analysis for improving accuracy of the system. This paper discusses three commonly used classifiers namely, SOFM, K-means clustering and BCM. Therefore, the literature survey tells us that BCM can give greater accuracy than other two mentioned methods.

Acknowledgement

This is to acknowledge and thank all the individuals who played defining role in shaping this IWCEM Conference paper. Without their Coordination, guidance and reviewing this task could not be completed alone. I avail this opportunity to express my deep sense of gratitude and whole hearted thanks to my guide Prof. J. S. Rangole madam for giving her valuable guidance, inspiration and encouragement to embark this paper. I also take great pleasure in thanking Dr. A. Das Sir for providing appropriate guidance. I would personally like to thank Prof. V.U. Deshmukh Sir, Head of Computer Dept. at Vidya Pratistaisthans College of Engineering (VPCOE), and our Honble principal Dr. S. B. Deosarkar sir who creates a healthy environment for all of us to learn in best possible way.

References

[1] Z.Lubniewski, A.Chybicki, Using multibeam echoes in seafloor classification, IEEE, 2009.

[2] Michael m. Harris, William E. Avera, Andrei Abelev, Frank W. Bentrem and L. Dale Bibee, Sensing shallow seafloor and sediment properties, recent history.

[3] Philippe Blondel, Seabed classification at ocean margins, Ocean Margin Systems G. Wefer et al. (eds) Springer Verlag 2001.

[4] A.R. Amiri-Simkooei, M. Snellen and D.G. Simons, Principal component analysis of single-beam echo-sounder signal features for seafloor classification, IEEE J. Ocean. Eng., vol. 36, no.2, April 2011.

[5] Jon M. Preston and Ben R. Biffard, Correspondence- comments on principal component analysis of single-beam echo-sounder signal features for seafloor classification by A.R. Amiri-Simkooei, M. Snellen and D.G. Simons , IEEE J. Ocean. Eng., vol. 37, no.4, Oct.2.012.

[6] Dimitrios Eleftherakis, A.R. Amiri-Simkooei, M. Snellen and D.G. Simons, Improving riverbed sediment classification using backscatter and depth residual features of multibeam echo-sounder systems J. Acoust. Soc. Am., May 2012.

[7] D. Eleftherakis, M. Snellen, A.R. Amiri-Simkooei, and D.G. Simons, Overview of methodologies for the acoustic classification of sediment distribution in Dutch rivers using multi-beam echo-sounder data, In Proceedings of 1st International Conference and Exhibition on Underwater Acoustics, Greece, 1407-1414 (2013).

[8] J.M. Preston, A.C. Christney, L.S. Beran, and W.T. Collins, Statistical seabed segmentation-from images and echoes to objective clustering, Proceedings of the Seventh European Conference on Underwater Acoustics, ECUA 2004.

[9] Bishwajit Chakraborty, Vasudev Mahale, Carlyle de Sousa and Pranab Das, Seafloor classification using echo-waveforms: A method employing hybrid neural network architecture, IEEE Geosci. Remote Sensing, vol.1, no.3, July 2004.

[10] Chanchal De and Bishwajit Chakraborty, Acoustic characterization of seafloor sediment employing a hybrid method of neural network architecture and fuzzy algorithm, IEEE Geosci. Remote Sensing, vol.6, no.4, Oct. 2009.

[11] O.Veses, R.Mosteo, M.P.Ormad and J.L.Ovelleiro, Classification of sediments by means of self-organizing maps and sediment quality guidelines in sites of the southern Spanish coastline , Medit. Mar. Sci.,15/1, 2014.

[12] Bishwajit Chakraborty, Vijay Kodagali and Jennifer Baracho, Technical communications-seafloor classification using multibeam echo-sounding angular backscatter data: A real-time approach employing hybrid neural network architecture, IEEE J. Ocean. Eng., vol. 28, no.1, Jan.2003.

[13] Satyanarayana Yegireddi and Nithesh Thomas, Segmentation and classification of shallow subbottom acoustic images using image processing and neural networks, 10th Biennial International conference and Exposition, Kochi, 2013.

[14] M. Snellen, Dimitrios Eleftherakis, A.R. Amiri-Simkooei, R.L. Koomans and D.G. Simons, An inter-comparison of sediment classification methods based on multi-beam echo-sounder backscatter and sediment natural radioactivity data, J. Acoust. Soc. Am., Aug.2013.

[15] Niels Kinneging, M. Snellen, Dimitrios Eleftherakis, D.G. Simons, Erik Mosselman and Arjan Sieben, Riverbed classification using multi-beam echo-sounder backscatter data.

[16] A.R. Amiri-Simkooei, M. Snellen and D.G. Simons, Using multi-beam echo sounder backscatter data for sediment classification in very shallow water environments .

[17] A.R. Amiri-Simkooei, M. Snellen and D.G. Simons, Using the MBES for classification of riverbed sediments, Acoustics08 Paris, 2008.

[18] A.R. Amiri-Simkooei, M. Snellen and D.G. Simons, Riverbed sediment classification using multi-beam echo-sounder backscatter data, J. Acoust. Soc. Am.,Oct 2009.

[19] David P. Williams, Bayesian data fusion of multiview synthetic aperture sonar imagery for seabed classification, IEEE, vol.18 no.6, June 2009.

[20] Janina Horvth, Tomislav Malvic, Characterization of classic sedimentary environments by clustering algorithm and several statistical approaches- case study, sava depression in northern croatia, Central European Geology, 2013.

[21] Dimitrios Eleftherakis, A.R. Amiri-Simkooei, R.L. Koomans, M. Snellen and D.G. Simons, Determining riverbed sediment composition using multi-beam echo-sounder backscatter data and natural radioactivity.

[22] Ben R. Biffard, Jon M. Preston, N.Ross Chapman, Acoustic classification with single-beam Echsounders: processing methods and theory for isolating effects of the seabed on echoes , MTS, 2007.

[23] Erik Hammerstad, Backscattering and seabed image reflectivity, EM Technical Note, Jan.2000.



Ankika H. Rasal is pursuing M.E. Degree in Electronics with specialization in Digital System from Vidya Pratishthan's college of Engineering, Baramati, India. Her areas of interest are Automation control, hydrographic survey, riverbed classification using remote sensing and satellite image processing.



Jyoti Rangole M.Tech. in Digital System from C.O.E. Pune in 2009. She has worked as a reviewer for Pearson Publication for the book , Embedded System. She is working as an Assistant Professor in Electronics and Telecommunication Department. She has published 1. Data compression techniques, IEEE third international conference on Machine Learning Computing Conference, Singapur. 2. Implementation of image processing algorithms on FPGA published in international journal Technology World. 3. Automatic silkworm eggs counting mechanism for sericulture, journal of engineering technological research, ISSN 2229-9262 Quarterly Malaysia Journal. Her areas of research interest are Machine Vision, Implementation of Image processing algorithm using VLSI for sericulture automation, Multiresolution image analysis.



Arnab Das received B. Tech degree in Electrical Engineering from Naval College of Engineering, Lonavala, India in 1995. He obtained M. Tech degree in Radar and Communication with specialization in Underwater Signal Processing in 2002and PhD degree in 2009 from Indian Institute of Technology, Delhi, India. He was commissioned into the Indian Navy in 1994. He worked as Project Officer at CARE, IIT Delhi for R & D in Underwater Signal processing and hardware design in 2003-2007. Currently he is instructor at MILIT Pune, India. His research interests are Underwater Passive Surveillance, Underwater Communication and Pattern recognition.

OPTIMIZATION OF EXHAUST SYSTEMS IN WARSHIPS

Ashvin Wanzul [1], **Sameer Mamluskar** [2], **Rohit Mathur**[3]
[1,2,3]Marine Engineering Center,
Larsen & Toubro limited,Mumbai, India
[1]ashvin.wanzul@larsentoubro.com, [2]sameer.mamluskar@larsentoubro.com, [3]rohit.mathur@larsentoubro.com

***Abstract*—Modern warships are highly complex platforms which are packed with machinery, equipment, weapons and sensors. The quest for speed and more payload demands higher capacity prime movers and at the same time the stealth requirements demand a silent and cool engine so that the Infra-red and noise signatures are minimized. These contradictory requirements require a great deal of optimization from the engine and system designers.**

The exhaust system and its associated components play a very significant role towards emissions, temperature and noise of exhaust gases. In warships, the space constraint adds another dimension for exhaust system design since large volume of high temperature gases are to be handled without causing excessive back pressure. Improper duct and component design will lead to back pressure on the system thereby reducing the efficiency of the engine.

This paper discusses the basic design of duct and backpressure calculation and the key factors to be considered for an efficient exhaust system design. Special emphasis is given to the emission norms for the warships and harmful effects of emission on marine environment. Various techniques available to the engine manufacturers to reduce the emissions such as improper combustion of gases inside the cylinder, valve timing, catalytic convertors etc. are also discussed and the most effective methodology is recommended.

***Keywords*—Exhaust System, Emissions, Marpol, Emission Reduction Techniques.**

I. INTRODUCTION

Exhaust system of prime mover is very important especially in warships. This exhaust system comprises of mainly exhaust piping (ducting), expansion bellows, and thermal insulation. After power stroke of prime mover, all the high temperature exhaust gases would be thrown away through the exhaust ducting. The temperature of exhaust gases is very high due to which chances of infrared signature are also very high which is not advisable. So the temperature of exhaust gases should be kept as low as possible.

Improper combustion of gases inside the cylinder, valve timing, fuel injection timing are the factors that not only lead to high temperature rise in gases but also lead to high NOx and SOx levels. These emissions levels are guided by MARPOL regulations and should be minimized as far as possible.

In warships, the exhaust duct design is critical due to space constraints and performance requirements. If exhaust ducting diameter increases noise level will be reduces, and if the duct diameter decreases then the backpressure on the System will be increased and if backpressure is not within limit then it will reduce the output power of the prime mover.

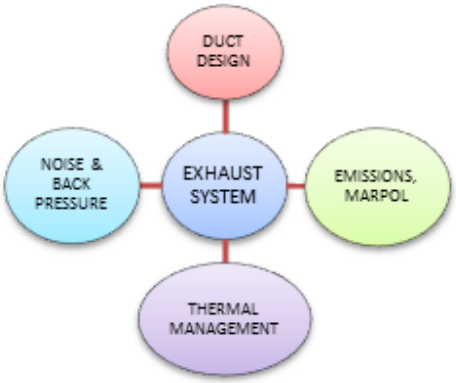


Fig. 1. EXHAUST SYSTEM.

Generally In the warships exhaust temperature remains within 400 to 650 deg Celsius. At very high temperature infrared generates and this infrared can be detected by radar so it is important to analyze the frequency band for the exhaust temperature range and to find solutions to minimize the exhaust temperature.

This paper deals with the following topics:

- Guide to exhaust duct design ,Backpressure prediction for engine efficiency and noise level
- Emissions, MARPOL regulations, current technologies to reduce the emissions
- Thermal management all along the exhaust line , the technologies involved in it, IRSS signatures study

II. GUIDE TO EXHAUST DUCT DESIGN

A. Exhaust Duct Design

There are general rules for engine exhaust system design. Exhaust gas flow rate and gas velocity plays important role. As a thumb rule avoids 90deg bends, sudden diameter change, and acute bends at the exit of the gases from engine, provides resilient system supports and measures to take care of thermal expansion due to hot gases.

Exhaust diameter is calculated by following formula-

$$D=\sqrt{4Q}/\pi\ \rho V$$

Where,

D is duct diameter to be calculated

Q is the flow of gases

V velocity of gases in duct

Generally velocity should be optimized between the 25 to 40 m/s for warships.

Increase in velocity will lead to increase in backpressure in the system and decreasing the velocity will lead to increase in the duct diameter. And hence both the above things are adverse to the warship and hence it is very important to select and optimize the parameter in the right way. Space constraints also need to take into account while calculation diameter.

B. Backpressure Calculation for Engine performance and Noise Level

After duct diameter calculation, routing the system will not assure the system functionality. There is a need to identify the components required in the system based on type of exhaust, and calculating back pressure to check whether it is within limit specified by Engine OEM. Generally backpressure limit is 30mbar but it varies from vendor to vendor and type/ rating of the engines.

1) Guidelines for calculation

a. Find out singularities and corresponding pressure drop coeeficients
b. Assume suitable duct dia. And gas velocity and other details as required
c. If it within limit then it is ok, But if it is not in limit then relook into the exhaust routing, try some other singularities Calculate backpressure.

Threre are many singularities in exhaust system, some of are shown below with the coefficients (K) required while for calculation.

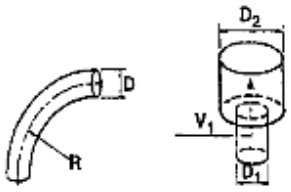


Fig. 2. Bend and Step Joint.

TABLE I. SINGULARITIES WITH COEFFICINTS

Bend		Step Joint	
R/D	K90	D1/D2	K
0.5	0.9	0.2	0.9
0.75	0.45	0.4	0.7
1	0.35	0.6	0.4
1.5	0.25	0.8	0.2
2	0.2	-	-

One sample of output calculation is shown in TABLE II

TABLE II. BACK PRESSURE CALCULATION

Parameter	**Value**	**Unit**
Q	4.35	kg/s
V	40	m/s
Density of exhaust gas	0.5	kg/m3
Exhaust silencer restriction	1000	Pa
Any other equipment's Restriction	-	Pa
Chimney Draft Length	-	m
Backpressure in the Exhaust System	2700.83	Pascal
	27.0083	mbar

After finalizing diameter, route and basic components of exhaust system, one more aspect taken into account is noise level. And this is guided by IMO 468(A), this level is approximately 90 to 110 dB(A) So the noise should be minimum. Higher the velocity means lowering the diameter

Silencer/mufflers can be added to reduce the exhaust gas noise. But as we add components in the system it creates more resistance so we need to be careful about backpressure. Having resilient supports also reduces the noise level.

For 1 mbar of excess backpressure engine loses approximately 3% power in output.

III. EMISSIONS, MARPOL REGULATIONS, CURRENT TECHNOLOGIES TO REDUCE THE EMISSIONS

A. International Emissions Regulations

IMO ship pollution rules are contained in the "International Convention on the Prevention of Pollution from Ships", known as MARPOL 73/78. Annex VI sets limits on NOx and SOx emissions from ship exhausts, and prohibits deliberate emissions of ozone depleting substances.

The IMO emission standards are commonly referred to as Tier I...III standards. The Tier I standards were defined in the 1997 version of Annex VI, while the Tier II/III standards were introduced by Annex VI amendments adopted in 2008, as follows:

TABLE III. MARPOL ANNEX VI NOx EMISSION LIMITS

Tier	**Date**	**NOx Limit, g/kWh**		
		n < 130	**130≤ n < 2000**	**n ≥ 2000**
Tier I	2000	17.0	45 n-0.2	9.8
Tier II	2011	14.4	44 n-0.23	7.7
Tier III	2016†	3.4	9 n-0.2	1.96
† In NOx Emission Control Areas (Tier II standards apply outside ECAs).				

The above table same has been shown in Fig. 3.

Tier II standards are expected to be met by combustion process optimization. The parameters examined by engine manufacturers include fuel injection timing, pressure, and rate (rate shaping), fuel nozzle flow area; exhaust valve timing, and cylinder compression volume.

Tier III standards are expected to require dedicated NOx emission control technologies such as various forms of water induction into the combustion process (with fuel, scavenging air, or in-cylinder), exhaust gas recirculation, or selective catalytic reduction.

B. Exhaust Emissions

a) Sulphur Oxides : The formation of Sulphur Oxides (SOx) in exhaust gases is caused by the oxidation of the

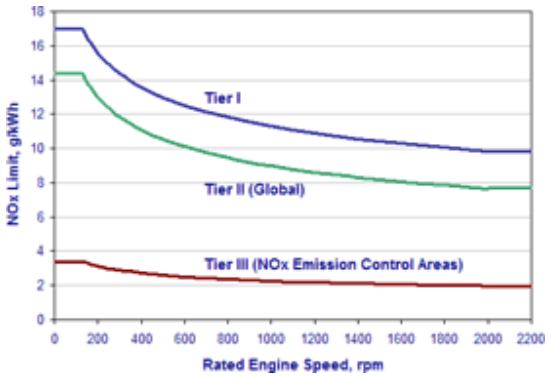


Fig. 3. MARPOL Annex VI NOx Emission Limit.

TABLE IV. MARPOL ANNEX VI FUEL SULPHUR LIMITS

Date	Sulphur Limit in Fuel (% m/m)	
	SOx ECA	Global
2000	1.5%	4.5%
2010	1.0%	
2012		3.5%
2015	0.1%	
2020*		0.5%
* alternative date is 2025, to be decided by a review in 2018		

sulphur in the fuel into SO2 and SO3 during the combustion process. The amount of SOx formed is a function of the sulphur content of the fuel used and therefore the only effective method of reducing SOx is by reducing the sulphur content of the fuel. Unfortunately, low-sulphur fuels are more expensive to purchase (10 to 20% greater cost, when switching from 3.5% to 1% sulphur) and there is a practical lower sulphur limit desired as desulphurisation of fuel lowers the lubricity of the fuel which can lead to increase wear on fuel pumps and injectors.

The regulation of SOx is predominately a regional issue; however, international pressure is growing for the oil producers to reduce the sulphur content of all fuels in order to control this problem at the source. Presently, most navies use 1% low-sulphur fuels. Special Areas have been set up, where the use of low sulphur fuels is mandatory.

b) Carbon Dioxide : CO_2 is one of the basic products of combustion and although diesels are one of the most efficient engines for the combustion of fossil fuels, the only way to reduce CO_2 is to either reduce the amount of fuel burned or by increasing thermal efficiency. CO_2 is not toxic however, has been linked to the 'greenhouse effect' and global warming.

c) Carbon Monoxide : CO is formed due to the incomplete combustion of organic material where the oxidation process does not have enough time or reactant concentration to occur completely.

In diesel engines, the formation of CO is determined by the air/fuel mixture in the combustion chamber and as diesels have a consistently high air to fuel ratio, formation of this toxic gas is minimal. Nevertheless, insufficient combustion can occur if the fuel droplets in a diesel engine are too large or if insufficient turbulence or swirl is created in the combustion chamber.

d) Hydrocarbons : The emission of unburned hydrocarbons (HC) generally results from fuel, which is unburned as a result of insufficient temperature. This often occurs near the cylinder wall (wall quenching) where the temperature of the air/fuel mixture is significantly less than in the center of the cylinder. Bulk quenching can also occur as a result of insufficient pressure or temperature within the cylinder itself. Still further, HC production may also be a result of poorly designed fuel injection systems, injector needle bounce, excessive nozzle cavity volumes or fuel jets reaching a quench layer.

e) Smoke/Particulates : The composition and properties of diesel particulates varies greatly and is therefore difficult to define. Furthermore, there is not a quantitative relationship between the smoke opacity and the particulate emission. Particle emissions from diesel engines can originate from:

1) Agglomeration of very small particles of partly burned fuel
2) Partly burned lub oil;
3) Ash content of fuel oil and cylinder lub oil; or
4) Sulphates and water.

f) Nitrogen Oxides : While SOx is predominately a regional issue, NOx is a global issue and the new MARPOL regulations will have a significant impact for ship owners and ship builders.

NOx is formed during the combustion process within the burning fuel sprays and is deemed one of the most harmful to the environment and contributes to acidification, formation of ozone, nutrient enrichment and to smog formation, which has become a considerable problem in most major cities worldwide.

The amount of NOx produced is a function the maximum temperature in the cylinder, oxygen concentrations, and residence time. At cylinder temperatures, nitrogen from the intake air and fuel becomes active with the oxygen in the air forming oxides of nitrogen. Increasing the temperature of combustion increases the amount of NOx by as much as 3 fold for every 100^oC increase.

IV. EMISSION REDUCTION TECHNIQUES

- Exhaust Valve Timing
- Delayed Injection
- Increased Compression ratio
- Nozzle design
- Water-fuel emulsion
- Direct Water Injection
- Exhaust Gas Recirculation
- Wet scrubbing techniques
- Catalytic convertor

Where from the above, some of the techniques is used for the engine manufacturer like exhaust valve timing , delayed injection, increase compression ratio, nozzle design, water fuel emulsion and others used by the shipbuilder.

A. Emissions control techniques by OEM

Primary methods involve changes to the combustion process within the engine

- *Exhaust Valve Timing*

Decreasing excess air ratio in the combustion chamber reduces NOx.

Excess air ratio is varied by changing valve timing Reduction of NOx emissions of about 15%.

- *Delayed Injection*

Compression of burned gases after combustion leads to increase in NOx.

Problem can be overcome by delay injection of the fuel. Delayed injection reduces the peak pressure and leads to less compression after combustion.

Drawbacks of delayed injection are: Reduction in engine efficiency rise in fuel consumption.

- *Increased Compression Ratio*

Decrease in efficiency by delayed fuel injection is countered by increasing the compression ratio.

Compression ratio is increased by increasing geometric compression ratio.

- *Decreased Peak Cylinder Temperature*

The best way to reduce NOx generation, is to reduce peak cylinder temperatures and there are a number of ways that this can be done, however all methods cause a certain loss in engine efficiency which increases the engines sfc.

Maximum NOx reduction is approx. 25%.

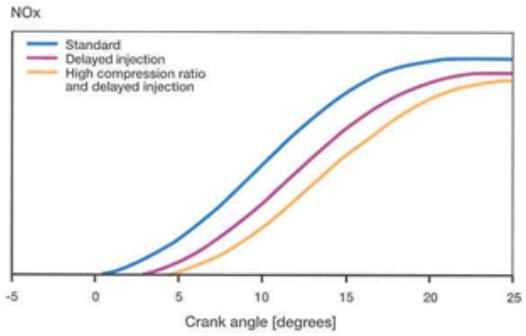


Fig. 4. NOx vs Crank Angle.

- *Exhaust Gas Recirculation (EGR)*

Recirculating part of the exhaust gas is an efficient method for reducing NOx emissions. The reduced oxygen concentration in the combustion air increases the quantity of the gas required to be heated for combustion of fuel.

Reduced oxygen concentration diminishes the reaction between nitrogen and oxygen System has its drawbacks of cooling and cleaning of exhaust gas before recirculation High concentration of sulphur oxides and particulates cause corrosion.

B. Emission reduction techniques by Shipbuilder

- *Water Injection Unit*

Apply water into the exhaust system external to the prime mover

Reduces temperature, which ultimately helps to deteriorate the NOx level

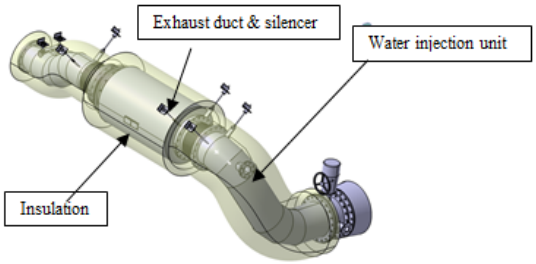


Fig. 5. EXHAUST DUCTING WITH WATER INJECTION UNIT

- *Wet Scrubbing Techniques*

If required, desulphurization of diesel exhaust gases can be achieved by wet scrubbing. The flue gas is first passed through a quencher where it is cooled down to saturation temperature. The SOx is subsequently washed out with a neutralizing agent (calcium bound in lime-milk or seawater) in a scrubber. SOx formed from diesel exhaust are corrosive and in part is neutralized by an engine lubricating oil which is typically base. In the atmosphere however, SOx combines with moisture to form H2SO4, which then falls as acid rain, and has been linked to environmental damage.

V. Comparison of Emission Reduction Techniques

The most effect method of reducing particulate emissions is to use lighter distillate fuels however, this leads to added expense. Additional reductions in particulate emissions can be achieved by increasing the fuel injection pressure to ensure that

Optimum air-fuel mixing is achieved, however, as fuel injection pressure increases, the reliability of the equipment decreases. Much research has also been conducted on cyclone separators, which are effective for particle sizes greater than 0.5m while electrostatic precipitators are more effective, capable of reduction emissions by up to 99%. Unfortunately, precipitators are expensive, prone to clog and are large in size.

A DETAILED COMPARISON OF VARIOUS TECHNIQUES IS GIVEN AT TABLE V ANNEXURE 1.

VI. Exhaust system and Thermal management & IRSS

Most modern naval ships include some form of signature suppression to reduce the ship susceptibility to IR threats. The newest generation of imaging missiles will have increased capability in the identification and lock-on of their targets, and will require increased attention to signature management

Exhaust gases temperature remains between 450 to 650 deg Celsius depend upon the prime mover and system used. At this

temperature lot of heat dissipated and thermal radiation takes place.

Providing proper thermal insulation, using water injection techniques in the exhaust system shipbuilder can reduce the radiation and thus it will help to reduce infrared and will reduce the threat detection of warships.

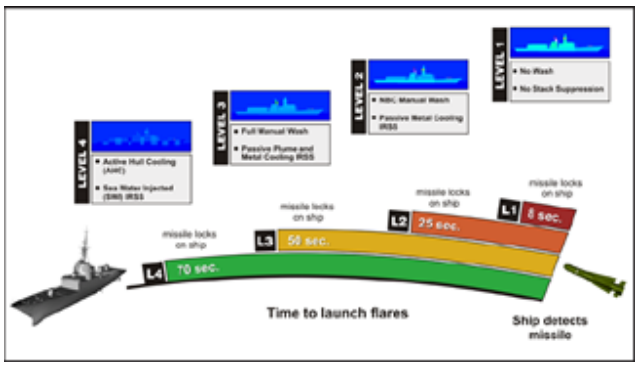


Fig. 6.

CONCLUSION

Optimization of exhaust system is not depending upon one single factor and there is a need to consider various parameters as stated in this paper and find a suitable mix to address divergent requirements. Proper design of exhaust system helps to increase the performance of the engine, optimize the space and reduce probability of detection of the vessel.

Thermal management and Infrared can be minimized by designing a proper exhaust system, thus it will help for warship.

REFERENCES

[1] Bruce Hiscoke, "IR Suppression – Exhaust Gas Cooling by Water Injection."

[2] Various technical papers & manuals from "MAN B&W."

[3] Various technical papers & manuals from "Wartsila New Sulzer Diesel."

[4] Regulation "MARPOL", "EPA."



Ashvin Wanzul received his B.E. degree in Mechanical Engineering from Pune University and he is working as a ASSISTANT MANAGER DESIGN (L&T SHIPBUILDING) in Marine Engineering Center, Larsen & Toubro limited at Mumbai, India. He has presented paper in IWCEM 2012 conference. His area of research is PIPING SYSTEM, MACHINERY.



Sameer Mamluskar received his B.E. degree in Mechanical Engineering from Mumbai University and he is working as a ASSISTANT MANAGER DESIGN (L&T SHIPBUILDING) in Marine Engineering Center, Larsen & Toubro limited at Mumbai, India. He has presented paper in IWCEM 2012 conference. His area of research is PIPING SYSTEM, MACHINERY.



Rohit Mathur received his B.Tech degree in Mechanical Engineering from U.P.Tech University and he is working as a ASSISTANT MANAGER DESIGN (L&T SHIPBUILDING) in Marine Engineering Center, Larsen & Toubro limited at Mumbai, India. He has presented paper in IWCEM 2012 conference. His area of research is PIPING SYSTEM, MACHINERY.

TABLE V. ANNEXURE:-1 COMPARISON OF EMISSION REDUCTION TECHNIQUES

Techniques	**Extent of modification**	**Remarks**
Injection Retardation	Engine adjust	Relatively simple to implement increases SFC
Increased trapped air/fuel ratio	New Turbocharger	
Increased injection pressure	New fuel pump, injectors, lines	Required to be used in conjunction with other primary methods increase in cost to fuel injection equipment reduction in reliability and increase maintenance cost of fuel injection equipment
Modification of compression ratio		Must be used in conjunction with other primary methods no effect on engine price
Modification of Induction swirl	New combustion chamber design	must be used in conjunction with other primary methods no effect on engine price
Modification of Injector specification	New injectors	Relatively simple to implement. no significant cost increase to engine
Change in number of injectors	New cylinder heads, pumps, injectors, cams	significant cost increase as additional pumps, injectors etc. needed
Pre-chamber type of combustion chamber	Redesign of combustion chamber	
Reduction in charge air temp	Improved charge air cooling	only really viable on high speed engines Increase cost to engine
Increase scavenge /charge air pressure	Improved turbocharger or turbo blower	Must be combined with other primary reduction measures no real cost increase to engine
Water Injection	New cylinder heads, camshafts ,injectors ,fuel &water systems	Increase cost for injection equipment requires water making facilities
Exhaust Gas recirculation	Exhaust reconfiguration(add exhaust filter /cooler)	Increased cost to engine
Selective catalytic reduction	External modifications to engine	Urea storage required onboard ammonia slippage problems additional costs to procure and operate
Non-Thermal Plasma	External modifications to engine	Relatively simple technology increase costs no additional equipment needed limited to ships with additional generating capacity

DESIGN DEVIATIONS DURING RETROFITS: BOON OR BANE A CASE STUDY

Cdr Vikram Gulwadi
Indian Navy
vikramgulwadi@gmail.com

***Abstract*—Todays modern world has witnessed proliferation of technology at an ever increasing pace. The life expectancy of equipment has, therefore, reduced drastically and as a result issues like lack of supportability and obsolescence have become commonplace. However, in the case of a Naval Platform, the hull is designed for upwards of Thirty years of service. With such contrasting service lives for hull and equipment, equipment retrofits have become the need of the hour and have been actively pursued not just by the Indian Navy, but also other Navies of the world.**

One such equipment retrofit, albeit with design modification, was undertaken on a Naval Platform in the recent past. However, the design modification manifested itself in the form of reduced performance of the main propulsion plant.

This paper investigates the circumstances leading up to the implementation of the design modification and thereafter presents a theoretical analysis of this modification and its effect on plant performance. The study however, was limited in its scope due to lack of original design data. Therefore, a number of parameter values and state points have been substituted with values recorded as on date. It may be borne in mind that the findings of this case study are specific to the extant case and may not be generalized for other retrofits. Plant performance parameters have been deliberately omitted due to the operational nature of the ship and only the Cause and Effect of the retrofit have been evaluated.

I. INTRODUCTION

In todays digital era, new technologies are evolving at a rapid pace, which has resulted in much lower generation gaps for equipment and systems. As a result of reduced generation gaps, obsolescence and legacy issues are commonplace. Therefore, while the hull of a platform may be designed for upwards of thirty years of service, the equipment fitted onboard the platform faces obsolescence much earlier. However, due to economic considerations, renewal of the entire platform at regular intervals is not feasible. As a result, equipment retrofits are common not just in the Indian Navy, but also in Navies across the world. This not only provides cutting edge technology onboard the Naval platforms, but also helps in retaining the fighting and sea-going efficiency of the platform. However, selection of new equipment during retrofits needs to be undertaken in a manner such that its performance falls within the original design envelope of the platform, failing which significant performance issues may be encountered.

One such equipment retrofit, albeit with design modifications, was undertaken onboard an Indian Naval platform in the recent past. As is the case with most modifications and inventions, this design modification was also borne out of necessity for equipment and platform safety. However, the complete effect of this modification was not clearly understood at the conceptualization stage and as a result, the modification manifested itself in the form of reduced performance of the main propulsion plant. Though the platform has been able to perform satisfactorily within the entire ambit of operations, the effects of the modification are apparent. This paper presents a complete account of this modification along with a theoretical analysis of the Cause and Effect. It may be borne in mind that the original design details for the propulsion plant are no longer available and most of the parameters have been replaced with values practically recorded as on date. The findings of the theoretical analysis are commensurate to the practical observations.

II. SYSTEM DEFINITION

The platform in question is a conventional oil-fired steam powered platform, using HVFO (or FFO) as fuel. The platform is propelled by two screw propellers (refer Figure 1) and as in any other warship, each shaft is propelled by an independent and self-sustaining set of systems and auxiliaries, referred to as a unit. Each unit (refer Figure 2) comprises of a set of two Admiralty Three Drum boilers generating steam for a Main Engine aggregate consisting of an HP and a LP Turbine as well as for running power generators and supporting auxiliaries.

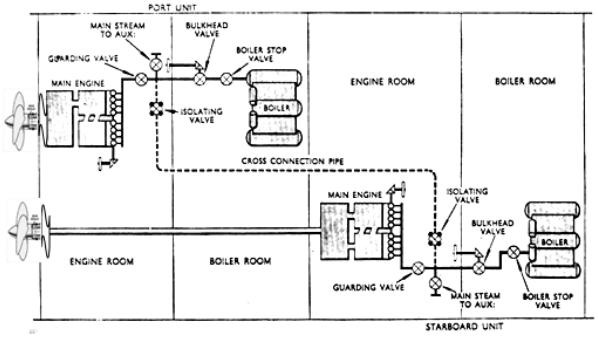


Fig. 1. Schematic arrangement of the propulsion system (Courtesy: BR 3003, Naval Marine Engineering Practices

III. PROBLEM DEFINITION

The platform in question was procured by the Indian Navy from the United Kingdom. During service in the Royal Navy as

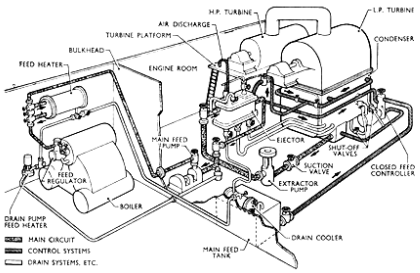


Fig. 2. Equipment arrangement in a Unit (Courtesy: BR 3003, Naval Marine Engineering Practices)

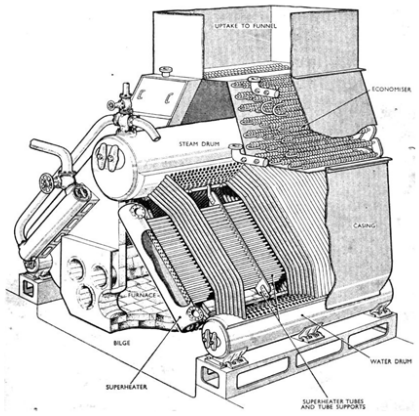


Fig. 3. The Admiralty Three Drum Boiler (Courtesy: BR 3003, Naval Marine Engineering Practices)

well as since the commissioning of this platform in the Indian Navy, the boiler rooms, particularly in the B or starboard unit, witnessed many instances of economizer fires. Several studies were under taken by a multitude of agencies over a period of time to try and identify the root cause of this phenomenon. Almost all these studies attributed these incidents to heavy accumulation of soot in the economizers of the boilers, particularly after 1000 hrs of operation. As a palliative, the Mean Time Between external cleaning of boilers was reduced from the stipulated 1400 hrs to 1000 hrs, which translated to a reduction in the operational availability of this ship.

In order arrive at a permanent solution to this problem , a decision was taken to undertake a modification of the economizer design and retrofit the modified economizers during the ships refit. The modification envisaged reduction of the number of gills (or fins) on the economizer elements by 40%, thereby enabling freer passage for flue gases and offering lesser surface area for soot deposition. In addition to reduction in the number of gills, the following other changes were made in the economizer design:-

1) Wider Spaced Gills (or Fins) As a result of the reduction in the number of gills (or fins) , the inter-fin distance was increased by approximately 30%.

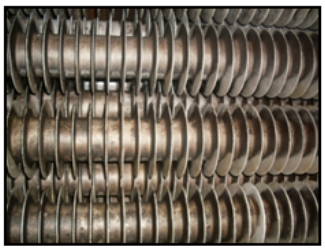


Fig. 4. Old design (Closer Spaced)

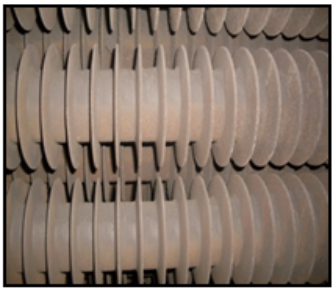


Fig. 5. New Design (Wider Spaced)

2) Thicker Gills (or Fins) The new gills were thicker by around 10%, with deeper grooves. However, the economizer tube outer diameter (OD) and aluminum gill outer diameter (OD) remained unchanged



Fig. 6. Gill Design - Old vs New

3) Modified Hoop Ring The hoop ring was slightly tapered to aid the press fit of the gills on to the tubes.
The modification and manufacture of the new type of economizer elements was undertaken by a local firm of national and international repute. While carrying out modifications, the firm indicated that the change in design would reduce the thermal efficiency of the economiser by 1.7%. Though the modification served its purpose of reducing the incidence of fire, it had its own share of attendant issues viz a performance penalty as observed during the Full Power Trials (FPT) of the platform. A comparative analysis of this modification



Fig. 7. Modified Hoop Ring

was carried out and the following observations on the same are relevant:-

- The max stack temperature recorded at the outlet of the economizers was higher in B unit as compared to A unit which implied lesser heat exchange taking place in the economizers of B unit boilers.
- The feed water temperature at the outlet of the economizers was therefore higher in A unit than B unit. The difference was as high as 50C at higher RPMs.
- Higher RDL (Register Draught Loss) was recorded on B unit boilers. Similarly, higher supply, spill and air pressures were required by B unit boilers to maintain the same drum pressures as compared to the A unit boilers. Therefore, B unit boilers were observed to have attained maximum firing rate earlier than the A unit boilers.
- The temperature of the superheated steam at the inlet to the Main Turbines (designed value 700 F) was observed to be higher in A unit (650-700 F) as compared to B unit (550F).

IV. THEORETICAL ANALYSIS

The theoretical analysis of this problem is split into two parts. In the first part, an analysis of the Cause of the modifications is undertaken, with specific reference to the problem of fouling. In the second part, the effect of the modification is explained with specific reference to Heat Transfer concepts and Rankine Cycle analysis.

1) Fouling, Its Effect, and Mechanisms:
Fouling refers to undesired accumulation of solid material (by-products of the heat transfer processes) on heat exchanger surfaces which results in additional thermal resistance to heat transfer, thus reducing exchanger performance. The fouling layer also blocks the flow passage/area and increases surface roughness, thus either reducing the flow rate in the exchanger or increasing the pressure drop or both. The foulant deposits may be loose such as magnetite particles or hard and tenacious such as calcium carbonate scale; other deposits may be sediment, polymers, coking or corrosion products, inorganic salts, biological growth, etc. Depending upon the fluids, operating conditions, and heat exchanger construction, the maximum fouling layer thickness on the heat transfer surface may result in a few hours to a number of years. Fouling could be very costly depending upon the nature of fouling and the applications. It increases capital costs: (1) oversurfacing heat exchanger, (2) provisions for cleaning, and (3) use of special materials and constructions/surface features. It increases maintenance costs: (1) cleaning techniques, (2) chemical additives, and (3) troubleshooting. It may cause a loss of production: (1) reduced capacity and (2) shutdown. It increases energy losses: (1) reduced heat transfer, (2) increased pressure drop, and (3) dumping dirty streams. Fouling promotes corrosion, severe plugging, and eventual failure of uncleaned heat exchangers. In a fossil-fired exhaust environment, gas-side fouling produces a potential fire hazard in heat exchangers. The following are the major fouling mechanisms:

- Crystallization or precipitation fouling results from the deposition/formation of crystals of dissolved substances from the liquid onto heat transfer surface due to solubility changes with temperature beyond the saturation point. If the deposited layer is hard and tenacious, it is often referred to as scaling. If it is porous and mushy, it is called sludge.
- Particulate fouling results from the accumulation of finely divided substances suspended in the fluid stream onto heat transfer surface. If the settling occurs as a result of gravity, it is referred to as sedimentation fouling.
- Chemical reaction fouling is defined as the deposition of material produced by chemical reaction (between reactants contained in the fluid stream) in which the heat transfer surface material does not participate.
- Corrosion fouling results from corrosion of the heat transfer surface that produces products fouling the surface and/or roughens the surface, promoting attachment of other foulants.
- Biological fouling results from the deposition, attachment, and growth of biological organisms from liquid onto a heat transfer surface. Fouling due to microorganisms refers to microbial fouling and fouling due to macroorganisms refers to macrobial fouling.
- Freezing fouling results from the freezing of single-component liquid or higher-melting-point constituents of a multicomponent liquid onto a subcooled heat transfer surface.

Biological fouling occurs only with liquids since there are no nutrients in gases. Also crystallization fouling is not too common with gases since most gases contain few dissolved salts (mainly in mists) and even fewer inverse-solubility salts. All other types of fouling occur in both liquid and gas. More than one mechanism is usually present in many fouling situations, often with

synergetic results. Liquidside fouling generally occurs on the exchanger side where the liquid is being heated, and gas-side fouling occurs where the gas is being cooled; however, reverse examples can be found.

2) Importance of Fouling:
Fouling in gases reduces heat transfer somewhat (5 to 10% in general) in compact heat exchangers, but increases pressure drop significantly up to several hundred percent. For example, consider a process plant liquid-to-liquid heat exchanger with U(overall heat transfer co-efficient) = 1400 W/m2K . Hence, R(Thermal Resistance) = 1/U = 0.00072 m2K/W. If the fouling factors (rs,h + rs,c) together amount to 0.00036 (considering a typical TEMA value of the fouling factor as 0.00018), 50% of the heat transfer area requirement A for given q is chargeable to fouling. However, for gas flows on both sides of an exchanger, U 280 W/m2K, and the same fouling factor of 0.00036 would represent only about 10% of the total surface area. Thus, one can see a significant impact on the heat transfer surface area requirement due to fouling in heat exchangers having high U values (such as having liquids or phase-change flows). Although the effect of fouling on the pressure drop is usually neglected, it can be significant, particularly for compact heat exchangers with gas flows. If we consider the reduction in flow area due to fouling by only 10 and 20%, the resultant pressure drop increase will be 69 and 205%, respectively regardless of whether the fluid is liquid or gas!

3) Tube-fin Heat Exchangers:
The economizers (Foster Wheeler economizers) fitted on the Admiralty Three Drum boilers fall under Tube-fin category of heat exchangers, with individually finned tubes. These exchangers can withstand high pressures on the tube side and hence are ideally suited for economizer application. The highest temperature that can be handled by these heat exchangers is limited by the type of bonding, the materials employed, and the material thickness. On the fin side, the desired surface area can be employed by using the proper fin density and fin geometry. The typical fin densities for flat fins vary from 250 to 800 fins/m (6 to 20 fins/inch), fin thicknesses vary from 0.08 to 0.25 mm (0.003 to 0.010 inches), and fin flow lengths from 25 to 250 mm (1 to 10 inches). A tube-fin exchanger having flat fins with 400 fins/m (10 fins/inches) has a surface area density of about 720 m2/m3(220 ft2/ft3). Two performance indicators are used for describing the effectiveness of a fin surface:

1 Fin Efficiency (ηF) is defined as the ratio of the actual heat transfer to the heat transfer from an ideal fin.

$$\eta_F = \frac{q_{actual}}{q_{ideal}} \tag{1}$$

For a circular fin surface, as in the case of economizers, the fin efficiency is defined as

2 Fin Effectiveness (, is defined as the heat transfer from the fin compared with the bare-surface transfer through the same base area.

$$\varepsilon = \frac{q_{actual}}{q_{barebase}} = \frac{q_f}{h_c(A)(T_b - T_x)} \tag{2}$$

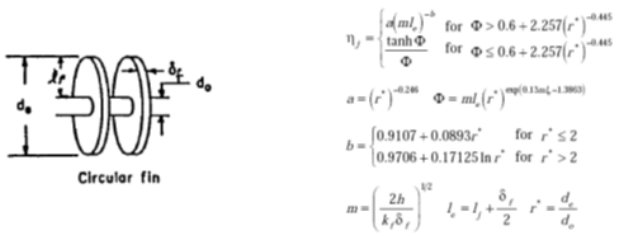


Fig. 8. Fin Parameters:

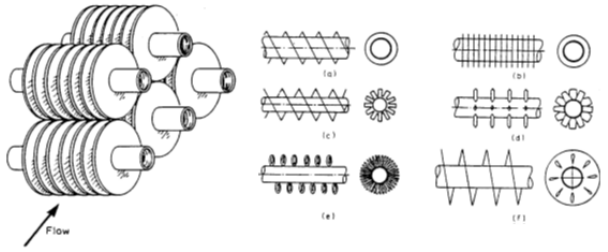


Fig. 9. Individually finned tubes: (a) helical, (b) annular disk, (c) segmented, (d) studded, (e) wire loop, and (f) slotted helical.

4) Heat Transfer Analysis:
The two energy conservation differential equations for a two-fluid exchanger with any flow arrangement are (see Figure 10 for counterflow heat exchanger)

$$d_q = q^{"} dA = -C_h dT_h = \pm C_c dT_c \tag{3}$$

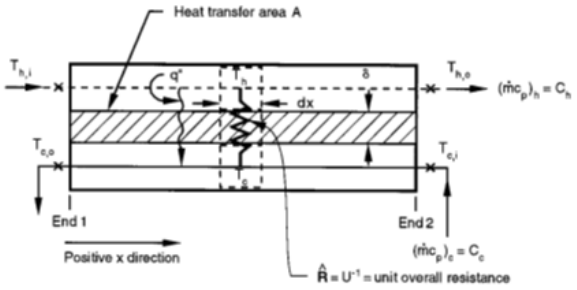


Fig. 10. Nomenclature for heat exchanger variables.

Where $\pm$ depends on dT_c is increasing or decreasing with increasing dA or dx. The local overall rate equation

is

$$d_q = d" dA = U(T_h - T_c)_{Local} dA = U\Delta T dA \quad (4)$$

Integration of Equations (1) and (2) across the exchanger surface area results in

$$q = C_h(T_{h,i} - T_{h,o}) = C_c(T_{c,o} - T_{c,i}) \quad (5)$$

$$q = UA\Delta T_m = \Delta T_m / R_o \quad (6)$$

where ΔT_m is the true mean temperature difference (or MTD) that depends upon the exchanger flow arrangement and degree of fluid mixing within each fluid stream. The inverse of the overall thermal conductance UA is referred to as the overall thermal resistance R_o as follows (see Figure 10)

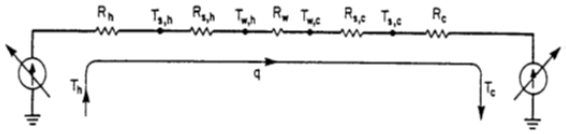


Fig. 11. Thermal circuit for heat transfer in an exchanger.

$$R_o = R_h + R_{s,h} + R_w + R_{s,c} + R_c \quad (7)$$

where the subscripts h, c, s, and w denote hot, cold, fouling (or scale), and wall, respectively. In terms of the overall and individual heat transfer coefficients, Equation (5) is represented as

$$\frac{1}{UA} = \frac{1}{(\eta_o h A)_h} + \frac{1}{(\eta_o h_s A)_h} + R_w + \frac{1}{(\eta_o h_s A)_c} + \frac{1}{(\eta_o h_A)_c} \quad (8)$$

where h_o = the overall surface efficiency The overall surface efficiency of an extended (fin) surface, ho is related to the fin efficiency h_f , fin surface area A_f , and the total surface area A as follows:

$$\eta_o = 1 - \frac{A_f}{A}(1 - \eta_f) \quad (9)$$

f we consider the fluid outlet temperatures or heat transfer rate as dependent variables, they are related to independent variable/parameters of Figure 9 as follows.

$$T_{h,o}, T_{c,o} or q = \varphi T_{h,i}, T_{c,i}, C_c, C_h, U, A, FlowArrangement \quad (10)$$

Using the MTD (Mean Temperature Difference) method, the heat transfer rate from the hot fluid to the cold fluid in the exchanger is given by

$$q = UA\Delta T_m = UAF\Delta T_{lm} \quad (11)$$

where ΔT_{lm} is the log-mean temperature difference (LMTD), and F the LMTD correction factor, a ratio of true (actual) MTD to the LMTD. Here

$$LMTD = \Delta T_{lm} = \frac{(\Delta T_1 - \Delta T_2)}{ln(\frac{\Delta T_1}{\Delta T 2})} \quad (12)$$

Here ΔT_1 and ΔT_2 are defined as

$\Delta T_1 = (T_{h,i} - T_{c,o})$
$\Delta T_1 = (T_{h,o} - T_{c,i})$
For all flow arrangements except parallel flow
From equations 2 and 10, we can infer that the overall surface efficiency of an extended (fin) surface decreases with reducing fin surface area. This causes a corresponding reduction in the conductance of the heat transfer surface, resulting in reduced heat transfer to the fluid inside the heat exchanger, causing a drop in the outlet temperature of the fluid. In the extant case, the fin surface area was reduced by about 40
Continuing with our analysis, an ideal Steam (Rankine) cycle is shown in Figure 12 below. The difference in feed outlet temperature in the economizer corresponds to a decrease in the enthalpy of the working medium (steam) at the inlet to the turbine. Considering that the conditions in the condenser remain the same, the state equations for the Rankine Cycle are as given below:-

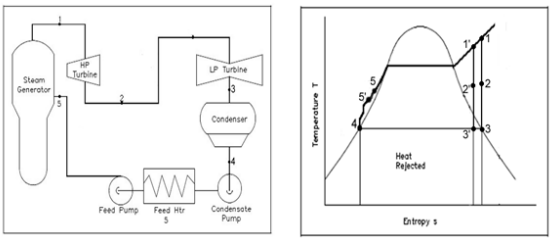


Fig. 12. Ideal Steam (Rankine) Cycle.

All four components associated with the Rankine cycle (the pump, boiler, turbine, and condenser) are steady-flow devices, and thus all four processes that make up the Rankine cycle can be analyzed as steady-flow processes. The kinetic and potential energy changes of the steam are usually small relative to the work and heat transfer terms and are therefore usually neglected. Then the steady-flow energy equation per unit mass of steam reduces to

$$(q_{in} - q_{out}) + (w_{in} - wout) = h_e - h_i(kJ/Kg) \quad (13)$$

The boiler and the condenser do not involve any work, and the pump and the turbine are assumed to be isentropic. Then the conservation of energy relation for each device can be expressed as follows:

$$pump(q = 0) : w_{pump,in} = h_5 - h_4 \quad (14)$$

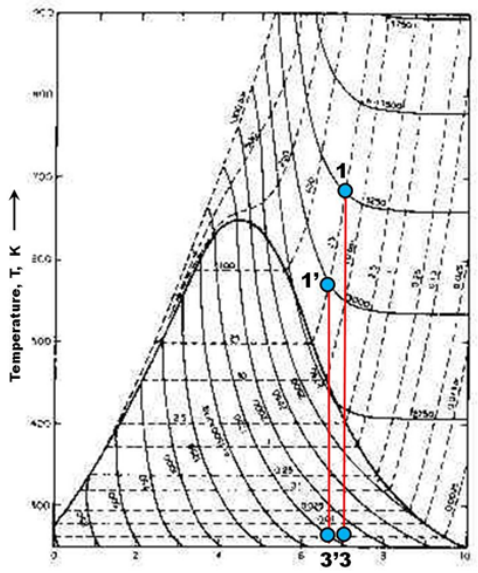


Fig. 13. Two cases of isentropic expansion in Turbine.

or

$$w_{pump,in} = v(P_5 - P4) \tag{15}$$

$$Boiler(w = 0) : q_{in} = h_1 - h_5 \tag{16}$$

$$Turbine(q = 0) = w_{turb,out}(h_3 - h1) \tag{17}$$

$$Condenser(w = 0) = q_{out} = h_3 - h_4 \tag{18}$$

A lowering of the economizer outlet temperature, as explained above, will result in shifting of the state point 5 to the left. Since the heat addition in the boiler, qin has remained unchanged, the state point 1 will also shift to the left, as shown in Figure 12 above. Referring to standard steam tables, with a suppression of economizer outlet temperature by 35 C, the Enthalpy of the superheated steam at the inlet of the HP Turbine, h1, reduces by as much as 350 KJ/Kg (reduction of about 6%). Plotting these points on a T-s diagram for steam and assuming isentropic expansion in the Turbine, we can infer that a reduction of almost 150 kJ/Kg (or more than 10%) occurs in the turbine work output due to the shift in parameters (refer Figure 13) . This in turn manifests itself as a drop in maximum available shaft RPM.

V. CONCLUSION

Necessity is the mother of all inventions. In the extant case, the requirement of improving the safety of the boilers necessitated changes in the economizer design. The design changes were optimized to improve the safety of the boilers and at the same time retain the power output of the plant. The following salient features of the design modification are borne out from the theoretical analysis above:-

1. Fouling of the gas side of the economisers can cause back-pressures in the furnace, resulting in fuel combustion issues. The fouling also constitutes a serious fire-risk and can reduce the heat transfer co-efficient on the gas side of the heat exchanger.
2. Increasing the fin spacing of the economisers can significantly reduce the rate of fouling. But the same can also lower the heat transfer rate in the heat exchanger, resulting in lower outlet temperatures.
3. The low economiser outlet temperature can lower the maximum power output of the plant significantly and increase the specific power output of the plant. It may be seen from the discussion above that in the extant case, as in all optimization problems, enhancement of one aspect of design is achieved at the cost of another. However, it is important to note that the modifications have considerably improved the safety of the boilers and have reduced the incidences of fire. Considering that human life and safety is above all other considerations, the economizer retrofit in B unit with design modifications has given a new lease of life to main propulsion plant of the platform.

REFERENCES

[1] Kreith, F.; Boehm, R.F.; et. al. Heat and Mass TransferMechanical Engineering Handbook Ed. Frank Kreith Boca Raton: CRC Press LLC ,1999.

[2] Y. A. engel and M. A. Boles, Thermodynamics: An Engineering Approach, 5th edition, McGraw-Hill, 2006.

[3] BR 3003, Naval Marine Engineering Practices.



Cdr Vikram Gulwadi is an officer from the Engineering Branch of the Indian Navy. The officer is presently serving onboard the aircraft carrier INS Viraat. The officer has had a rich experience of serving in a range of appointments, including six years onboard the aircraft carrier and as a designer in Indias nuclear submarine program. The officer is a post graduate from the Indian Institute of Technology, Kharagpur, having specialized in the field of Mechanical Systems, Dynamics and Controls.

Coastal Area Surveillance Technology For Indian Ocean Region

Chakshu Malviya[1], **Arnab Das**[2]
[1]DIAT (DU), Girinagar,Pune 411025, India,
[2]MILIT, Pune, India
[1]chakshu.malviya@gmail.com, [2]arnabdas1972@hotmail.com

***Abstract*—The Indian Ocean Region (IOR) has gained strategic importance in the recent decade. Maritime presence in these waters has increased phenomenally over the years due to various reasons. More than 80 percent of the worlds sea borne trade prefers the sea lanes in the IOR choke points. The area is also witness to the growing might of the Indian and Chinese Navies. The US interventions in Iraq and Afghanistan and piracy prone incidents in and around the Horn of Africa have served to increase international interest in these areas. Countries are seeking dominance or influence across the entirety of the Indian Ocean. Continued access to markets, energy supplies and raw materials, ensuring the security of maritime chokepoints and sea lines of communication (SLOCs) and asserting ones reach to far flung areas in times of crisis as a blue water Navy have become the prime objectives of all stake holders in the region. India has of the mightiest Navies in the region and the capability to sustain sea borne operation, search and rescue missions and anti-piracy missions for months. India is a major stake holder in the IOR activities for maintaining peace, stability and safety of shipping traffic.**

However, the sea front is not secure. India has also seen its maritime boundaries being infiltrated by terrorists in recent past. The sea boundary of the peninsular nation needs to be secured and monitored. It is the need of the hour to have an underwater surveillance system which can monitor the ocean bottoms and deeper depths for any untoward/ covert activity, pre-warn about divers, belligerent submarines, mine laying or saboteurs looking to destroy our ports/ pipelines or sea going vessels be it commercial or war ships. Many a countries have already begun research in this field and have tested such networks. These underwater networks are deployed at various depths and communicate acoustically through sensor nodes. Each network has a master node which can communicate via RF/ satellite to a base station. There can be many variants of this network as well based on the deployment strategy.

***Keywords*—IOR, C.O.A.S.T for IOR, Acoustic Communication, Underwater Sensor Network (UWSN), terrestrial network differences, Coastal Surveillance, MAC protocols for UWSN, future trends.**

I. Introduction

Sea routes have served to be a convenient and economic means for traders, explorers and marauders alike from times immemorial. History replete with such incidents bears testimony to this. India too has had its fair share of troubles coming by the sea routes in the past, be it the East India Company, the Dutch, the French or Portuguese trying to establish their footholds and establish dominance over the rich Indian trade. The great Maratha warrior- Shivaji had proven his prowess at sea warfare with his small yet fast boats and lethal guerilla tactics. India would have had been a different nation, had the then rulers strengthened their Naval forces and prevented foreign nations from plundering our resources. Wars around the world have seen some major naval battles, where forces and equipment have been landed ashore in huge numbers on the enemy territory by warships because the sea routes were the easiest and less monitored paths to drop such a huge contingent ashore. Likewise, trade by sea has increased by leaps and bounds- from the Spice Trade and opium trade in the early ages to cargos containing food, spare parts, components and passengers etc. in bulk across continents. The oceans have always been a provider. Not only have they given us prosperity through trade and viable, economic transportation but they have given us natural resources like oil, natural gas and various flora and fauna. Fishing has been a boon and source of livelihood to many a coastal states.

In the last decade, we have witnessed some gruesome attacks by terrorists who entered our sovereign soil by the porous and vast sea boundaries. No matter how strong a Navy, it cannot perpetually monitor its coastline, EEZ and the underwater depths for divers, enemy submarines/ surface crafts, intruders, smugglers, poaching or mines. Nations, the world over have realized the importance of surveillance at sea both on its surface and underwater. If patrolling the waters is difficult, monitoring the activities in its limitless depths is equally challenging. Even if one were to have the most advanced warships and submarines, human fatigue would definitely take a toll in the long run making operators weary and less attentive. Navies today can continue their wars and surveillance at a distance of thousands of nautical miles away from their base ports. A single submarine lurking in our waters, undetected can do more harm than an armada of lethal warships laced with state of the art weapons.

It is therefore, the need of the hour to have an underwater surveillance system which can monitor the ocean and deeper depths for any unwelcome or hostile activity be it a submarine snooping for surveillance, a diver looking to plant a bomb in a harbour or saboteur or terrorist wanting to gain access to vital ports. Many a countries have already begun research in this field and have tested such networks. These underwater

networks are unmanned and consist of nodes or sensors deployed at various depths and communicate wirelessly with each other by acoustic waves. Each network has a master node which can communicate via RF/ satellite to a base station. There can be many variants of this network as well based on the deployment strategy.

We, in India do not have any such subsea surveillance network. However, research is underway and has borne fruit. We do have data buoys with NIOT, Chennai/ INCOIS etc. which have at the core of weather monitoring/ cyclone, Tsunami warnings. Yet, we do not have any network which covers the aspects mentioned previously.

This paper intends to bring to the fore, a concept based on undersea acoustic communication amongst sensors placed on buoys to monitor the seas. It delves on the inception of the concept and its relevance to the Indian scenario. It also discusses the difficulties of underwater acoustic communication vis--vis electromagnetic transmission on land and various other technical aspects peculiar to acoustics. The concept will also benefit the commercial shipping industry alike by proving to be a means to disseminate information regarding hazards at sea, navigational ease or reporting of any untoward/suspicious incident. Further, it will also safeguard our ports and off shore assets in a similar way however, the density of node deployment may differ. Schemes of deployments cover these aspects. If we were to merge this underwater acoustic network with and over water RF/ Satellite/ 802.11 Standard based network, it will help us in transmitting data in almost real time. Advantages being communication with our own submarines without the need for them to surface, near real time monitoring of environmental parameters like temperature, salinity, pressure etc. and transfer of data at very high speeds by overwater networks. While the advantages are many, there are also an equal if not more number of hurdles due to extremely different nature of acoustics. Notwithstanding, such a network will be a boon for coastal security, maritime forces, shipping industry and environmental researchers. The paper is an earnest effort toward realization of this dream.

II. THE CASE OF THE INDIAN OCEAN REGION

The littorals are marked by the sea surface and sea bottom. Sound interacts multiple times with both these boundaries when transmitted from the source to its receiver. The density of marine species is very high in the littorals compared to the blue waters, resulting in the higher absorption of the sound during propagation. Noise filtering algorithms and other studies in the advancement of underwater propagation in the deep blue waters to improve sonar performance did not perform well when used in the littoral waters due to site- specific behaviour. The IOR is characterised by tropical waters which adds to the complexity of acoustic propagation. The diurnal and seasonal temperature fluctuation in the tropical regions is far more than in the temperate regions resulting in random surface disturbances due to wind variations [13]. Thus, one can very well appreciate the complexity of the propagation of sound in the tropical waters due to their shallow water characteristics.

Peninsular India with more than a dozen major ports and numerous merchant ships/ fleets operating out of it extends into the Indian Ocean with sea routes to the Red Sea, Persian Gulf, Bay of Bengal, Arabian Sea with well-defined choke points at Strait of Bab-el-Mandap, Malacca, Hormuz, Sunda and Lambok. India is strategically located between regions of production and consumption. The IOR also hosts heavy maritime traffic. Hence more than 60 percent of the income from the oceans from thousands of merchant marine traffic plying though the ice free waters of the IOR with zillions of barrels of oil passing daily through Strait of Hormuz. Malacca Strait itself witnesses tonnes of nuclear wastes for reprocessing in Europe. Fishing in this regions and food exports are also key economic factors. India operates quite a few offshore rigs as well.

SLOCs have been prone to piracy at sea. The Gulf of Aden has been the playground of the armed-to-the- teeth sea terrorists plying in fast attack boats and thriving on the loot and ransom from unarmed merchant vessels. This has made countries like US, UK, India, Pakistan and China deploy multiple warships in these regions to ensure safe passage of ships.

Navies in the IOR are increasingly conducting exercises to show their presence and reach. China and India have come out to be the key players in this region. More and more submarines are being inducted by countries operating in these areas to patrol the IOR and for surveillance of enemy activity. China is retrofitting a Soviet era aircraft carrier to add to its fleet to augment its blue water capabilities. Japanese Navy is building Hyaga class helicopter carriers and so is the Republic of Korea with the Dokdo class ships. While no country harbours belligerent objectives, they do want to exert their dominance on the IOR. This region is now inching closer to becoming a playground of mighty countries.

III. AN UNDERWATER SENSOR NETWORK (UWSN)

A UWSN comprises of sensor nodes which are deployed at various depths and locations at sea in an underwater environment. The sensor nodes communicate with each other acoustically and exchange vital data. The nodes form a network much like a terrestrial network with MAC protocols and medium access methods. Each individual node houses acoustic transceivers, a battery, processors with signal processing ability and other circuits in a robust, water proof housing. The nodes can communicate with each other by either multi hop or point to point communication. Various algorithms have been developed for intelligent routing of data in a sensor network so as to save battery power and reach the sink in the minimal possible time. The routing strategy is based on minimal retransmissions thereby saving up on energy and lesser traffic. The sensor nodes forming a network communicate with a sink placed between the air-water boundaries at the surface. This sink/ master node has an RF module for the above water part which pumps out data received acoustically from sensor nodes in its area of surveillance. The master node has higher data processing capability, RF circuit, an interface between the acoustic unit and the RF unit and a GPS to ascertain its

location. The master node communicates with a base station located at the shore, in an air craft, on a ship or a satellite. In this way a three tiered architecture forms the basis of a UWSN. Multiple UWSNs can be deployed to cover larger areas. These UWSNs can be used for coastal surveillance, military espionage, keeping a lookout for enemy sub surface crafts, mines, divers and can also be exploited by the scientific community for environmental monitoring, ocean parameter monitoring etc. which has been covered later in this paper. Thus we have a network which operates on its own and can monitor the vast depths of the seas and can transmit data in real time to shore agencies without having the need to deploy submarines or divers. The network configuration can be tweaked as desired to suit various operational requirements like harbour surveillance, pollution monitoring, off shore oil rig protection, intrusion detection, environmental monitoring etc. by adding hardware and signal processing abilities. More on this is covered later in the paper.

However, this is easier said than done considering the challenges posed by the oceanic environment. It involves costly research, expensive hardware, technology and add to it a hostile climate. The underwater environment is in itself a whole new domain for research. This paper covers a few topics which bring forth such difficulties. That leaves us with the question as to why do we need an UWSN in the first place when there are so many difficulties involved.

IV. WHY DO WE REQUIRE A UWSN?

A. The Military Perspective

The sea boundaries are extremely porous. No matter how strong a nations Navy, it will be prone to operator fatigue. After 26/11 attacks, we need to develop systems that augment our armada of warships, submarines and aircrafts. While it may be possible to monitor the surface for belligerent crafts at sea, it is very difficult to monitor the endless depths of the ocean for enemy submarines, divers and mines. Here is where, a UWSN will form the eyes and ears of the fleet and monitor for any unwelcome intrusion by sub surface routes. It can operate without human supervision and can employ smart decision making algorithms and signal processing techniques to give real time information to continuously manned operation centers. They can also communicate with our submarines which would otherwise have to surface to receive communication. With the deployment of Autonomous Underwater Vehicles (AUVs) and Remotely Operated Vehicles (ROVs), one can even patrol enemy waters to detect any subversive activity and transmit the data to the sensor nodes wirelessly by acoustic transmission. Such a network will bolster our preparedness towards any attack from the sea front and give us enough reaction time to counter the enemy forces. It will also be an add on means to communicate apart from satellite communication.

B. The Civilian Perspective

A UWSN is not just for military use. It can be of phenomenal importance in merchant shipping industry, scientists, researchers and explorers. Such a network can be utilized by commercial ships to forewarn other ships of any impending danger at sea, navigational hazards, oil spills, wreckages etc. It can also be used by ocean researchers to monitor temperature, depth, salinity etc. Marine biologists can record and transmit data and marine organisms. It can be used to prevent natural disasters like Tsunami. A few applications of UWSN are listed in the following paragraph.

V. APPLICATIONS OF UWSNS

UWSNs offer a host of opportunities to the military, commercial shipping industry, marine biologists and researchers alike. While the list is endless, following are a gist of how the UWSNs can be applied:-

(a) Coastal Surveillance-Monitoring our sea boundaries for unidentified crafts is a daunting task due to vastness of the ocean. With advanced UWSNs surveillance, reconnaissance, intrusion detection can be performed with ease. UWSNs can perform better than conventional SONARs and facilitate detection and classification of low signature targets.

(b) Harbour monitoring-Monitoring vital harbour entry / exit points for ships and boats which are entering/ leaving the harbour. The master node can be deployed on a buoy which can be equipped with a camera for a video feed as well. This can serve to give a live feed of the traffic and also monitor dumping of oil / discharges from the ships which are prohibited at harbour. The subsea sensors can sense chemicals and warn shore authorities.

(c) Environmental Monitoring-Static nodes can be used to collect environmental data on planktons, reefs etc. and can be transmitted in real time. UW-ASNs can per- form pollution monitoring (chemical, biological and nuclear). Monitoring of ocean currents and winds, improved weather forecast, detecting climate change, understanding and predicting the effect of human activities on marine ecosystems, biological monitoring such as tracking of fishes or micro-organisms, are other possible applications. Bathymetry profiling can also be undertaken by such sensors.

(d) Disaster Prevention-Buoys have played an important part in monitoring hurricanes and typhoons and have saved precious lives in India and abroad. UWSNs can further enhance the reach of these disaster prevention agencies and include real time monitoring. Tsunami warnings can be disseminated within seconds on an automated system to fishermen and residents of coastal areas. Sensor networks that measure seismic activity from remote locations can provide tsunami warnings to coastal areas, or study the effects of earthquakes occurring inside the seas.

(e) Protection of Off Shore Assets-Off shore assets like oil rigs, pipelines, undersea cables etc. are a nations wealth as well. Sensor nodes can be placed on these pipelines at depths which would otherwise have restricted divers to reach them. They can thus be monitored remotely. The system can be enhanced by placing cameras to provide visual feed to counter the threat of saboteurs if the data rates evolve to support a live video feed.

(f) Anti-Piracy Operations-The IOR has seen a lot of piracy in the recent past in the Gulf of Aden region. Buoys

equipped with sensor nodes can be deployed in major shipping lanes to monitor unusually fast crafts. These buoys can be equipped with an overwater module housing 802.11 standard based nodes. Hence, while the underwater part monitors for any undersea activity, the over water part can form an ad hoc, Line of Sight based mesh network. Ships with LoS range of these buoys can form a network of their own and experience high speed communication amongst them. This can reinforce anti-piracy missions where live video feed of the boarding party can be received by the warships to guide them in distinguishing friends from foes.

(g) Undersea Explorations-The sea floor has abundant natural resources. Such resources like oil fields, minerals etc. can be detected by using UWSNs which would otherwise be hard to detect owing to the great depths involved.

(h) Assisted Navigation-Ships at sea can hugely benefit from UWSNs if they are configured to identify navigational hazards, oil spills, wreckages that are not visible above the surface, reefs, ice bergs or shallow sea floors which can ground ships. Sensors can be used to identify hazards on the seabed, locate dangerous rocks or shoals in shallow waters, mooring positions, submerged wrecks, and to perform bathymetry profiling. This data can be shared with all sea farers for safer navigation.

VI. FUNDAMENTALS OF OCEAN ACOUSTICS

The ocean can be termed as an acoustic waveguide limited by the sea surface at the top and the bottom as the base. Sound travels well in this oceanic environment but is reflected, refracted, attenuated and spread due to multiple reasons. Speed of sound in water around 1500 m/s which is higher than that in air around 330 m/s. However it is far lesser than the radio propagation speed (3 108 m/s) which is five orders of magnitude lower. The sound speed in water is generally related to its density and compressibility. The density is in turn dependent of various parameters like depth, salinity, temperature etc. Seasonal, diurnal changes and geographical locations affect these parameters in the upper layers of the ocean. The sound speed increases towards the sea surface during warmer days as the surface water is warmer. This seriously affects SONAR performance on board ships.

In certain regions, the surface water is influenced by air-sea interface due to winds and wave activity. This results in the formation of a mixed layer or iso-thermal layer where the sound-speed profile increases with increasing depth. Below the mixed layer exists the thermocline layer which experiences a plunge in temperature with increasing depth and hence the sound speed too decreases. Below this layer, sound speed increases due to increasing pressure with depth, however the temperature remains constant. Thus once can see that the sound* speed is greatly affected by various parameters of the oceanographic environment.

The ocean surface and bottom acts as a waveguide. Generally speaking, the sea surface is a nearly perfect reflector. The seafloor is a lossy surface with strongly varying topography.

Underwater acoustic transmission is governed by many factors as stated earlier. Amongst these, deep water propagation and shallow water propagation are entire chapters in themselves. The following paragraphs elucidate some characteristics in brief.

A. Deep Water Propagation

Deep water environments exist at depths beyond 2000m. A lot of studies have been performed on sound propagation in deep waters by scientific communities along with sea farers. This has helped to tabulate experimental results which have been helpful in establishing the way sound propagates at these depths. Sound at these depths is refracted or surface reflected. There exists an upward-refracting sound-speed profile which aids in achieving long-range propagation. There is not much bottom interaction. The deep waters are spread over a vast expanse and deployment of vessels to collect data or record ambient noise in these waters has not been successful .This has been primarily due to mammoth resources, coordination, man power and funding required for these missions. The Indian scenario is a little more peculiar due to the lack of coordinated efforts between the academic community that understands the technical possibilities and the operational component which deploys these assets. [13].

B.Shallow Water

Shallow waters are closer to the land mass and extend to depths of around 200m. They see a lot of sound traffic be it shipping, marine animals, under-sea exploration/ construction. There exist a phenomenal number of ambient noise sources in shallow water (which however are separated because of their very different structures in the time-frequency plane) like snapping shrimps, shipping machinery, biological or man made noises etc. [**?**] It poses a daunting challenge to scientists who intend profiling these waters more so because sound behaves very differently here than in deep waters. Accurate prediction of long-range propagation in shallow water is still difficult. In these regions the surface, volume, and bottom properties are all spatially varying while the oceanographic parameters are temporally varying and the parameters are generally not known in sufficient detail and with enough accuracy to permit long-range predictions in a satisfactory way. Sound-speed profile is downward refracting in shallow waters. They can also be nearly constant. Unlike deep water propagation, acoustic signals travel over long ranges by bottom interactions by refracted bottom-reflected or surface-reflected bottom- reflected paths.

C.Attenuation in Seawater

When sound propagates in the ocean, part of the acoustic energy is continuously absorbed, i.e., the energy is transformed into heat. Moreover, sound is scattered by different kinds of inhomogeneities, also resulting in a decay of sound intensity with range. As a rule, it is not possible in real ocean experiments to distinguish between absorption and scattering effects; they both contribute to sound attenuation in seawater.

VII. THE PECULIARITIES OF UNDERWATER ENVIRONMENT

The underwater environment presents a very complex scenario as compared to its terrestrial counterpart as regards

to a communication system. Although both networks exhibit functional similarities, UWSNs are architecturally different due to the properties/ characteristics of the transmission medium i.e. sea water and the acoustic signals [2]. Therefore the research on a feasible UWSN becomes unique in itself. It is important to recognize that while underwater and terrestrial wireless sensor networks may share some similarities, the differences are so profound that a UWSN has to be employ different MAC schemes, medium access protocols etc. which take into account numerous factors absent in a terrestrial network. This can be mainly attributed to the following reasons:

(a) Acoustic Signal vs Electromagnetic /Optical Signals. Electromagnetic (EM) waves are highly attenuated in an underwater environment. They also suffer from a very high absorption rate (45 f Hz dB per kilometre). Optical signals are scattered easily and cannot travel longer distances. In contrast, the absorption of acoustic signal over most frequencies of interest is about three orders of magnitude lower [1]. Acoustic signals are the only viable means of transmitting signals underwater.

(b) Losses. Transmission losses are caused by energy spreading and sound absorption. Energy spreading loss depends only on the propagation distance. Absorption loss increases with both range and frequency limiting the available bandwidth. Received signal level is also influenced by the spatial variability of the underwater acoustic channel, such as the formation of shadow zones.

(c) High Latency. As we know that the propagation speed of a sound in water is fiver orders of magnitude lesser that that of an EM signal in free space, it suffers from high latency in an underwater environment.

(d) Available Bandwidth. Transmission loss in an underwater channel is dependent on range and frequency and only increases with an increase in both. In fact, the larger the communication ranges, the lower the bandwidth of underwater acoustic channels. This severely limits the available bandwidth. [12] The acoustic band under water is limited due to absorption; most acoustic systems operate below 30 kHz.

(e) Data Rate. The range rate product also hovers around 40 km kb/s as the maximum attainable range rate product. The bandwidth of underwater acoustic channels operating over several kilometres is about several tens of kilobits per second, while short-range systems over several tens of meters can reach hundreds of kilobits per second.

(f) Noise. Both man made and ambient noises constitute the noise spectrum in the ocean. The ambient noise dominates over deeper regions. Shipping noise is prevalent near shores. Most of the ambient noise sources can be described as having a continuous spectrum and Gaussian statistics.

(g) Range Bandwidth Relation. For a long-range system, operating over 10-100 km, the bandwidth is limited to few kHz (for a very long distance on the order of 1000 km, the available bandwidth falls below a kHz). A medium-range system operating over 1-10 km has a bandwidth on the order of 10 kHz. A short-range system operates over distances less than a km with bandwidth in excess of 10 kHz, while only at very short distances below about 100 m, more than a hundred kHz of bandwidth may be available.

(h) Multipath The process of an acoustically transmitted signal taking multiple and different paths to get to the receiver as a result of reflections is referred to as multipath. Signal propagates via various paths from source to receiver for a considerably large range. It is attributable to sound reflection at the surface, bottom and by any object, and refraction in the water. Volume reflections by plankton and fish also contribute to the effect. Refraction is mostly seen in deep waters and is due to variation of sound speed due to depth. The main direct signal arrives along with a series of echoes, the amplitudes which decrease with the number of reflections undergone. The spread of the multiple paths is determined by the number of bounces. Multipath propagation causes intersymbol interference (ISI). Multipath spreads in the horizontal underwater acoustic channels are of the order of several tens to a hundred of symbol intervals for moderate to high data rates. Deep water and shallow water multipath formations are different from each other and also depend on the frequency and range of transmission.

(i) Time-Variation An acoustic signal gets reflected off the surface of water due to the motion of the waves. This is known as surface scattering and causes time-variability in shallow water channels. Internal water movement in deep water channels leads to similar results in deep waters. Motion of the reflection point results in the Doppler spreading of the surface-reflected signals.

(j) Doppler Spread As stated earlier; motion at source, receiver and channel boundaries causes Doppler shifts which result in Doppler spreads. Doppler spreading generates two different effects on signals: a simple frequency translation, which is relatively easy for a receiver to compensate for, and a continuous spreading of frequencies that creates a non-shifted signal.

VIII. DIFFERENCES BETWEEN TERRESTRIAL AND UNDERWATER SENSOR NETWORKS

As elucidated in the preceding paragraphs, underwater environments impose various limitations of acoustic transmission. It is therefore impractical to network sensors easily and to transmit the collected data underwater. Consequently, they might need to be brought to the surface Instead, so that they can pump put the data via an RF link to a shore station. This procedure is costly, time consuming and not in real time and hence cannot be used for adaptive sensing or tactical decisions. This section brings out some key fundamental differences between the underwater systems, as compared to their terrestrial wireless counterparts:-

(a) Typical Underwater Communications Channel- Unlike a terrestrial network which operates in a communications channel which can still be predicted and systems can employ various methods to adapt to the channel characteristics; an underwater channel is vastly different. There is no typical underwater communications channel. The channel is affected by a variety of factors like geographical area, temperature, depth, pressure, weather phenomena, ambient, biological and

man made noises etc. Each present its own challenge to researchers.

(b) Communication Method-Ground based sensor networks are simpler to deploy and have a host of communication protocols to support them. EM waves travel at the speed of light and hence do not suffer from latency. However, EM waves cannot penetrate to greater depths in underwater environments. Therefore they have to rely on acoustic signals which suffer from large latency and low band- width resulting in long end-to-end delays in a link. This in turn affects reliable data transfer, traffic congestion control and MAC protocols. Thus, traditional random access approaches in RF wireless networks might not work efficiently in underwater scenarios.

(c) Cost-Underwater sensor nodes house equipment like acoustic transducers, transceivers, waterproof housing, long lasting batteries, modular circuitry which can be easily replaced in case of a defect without much defect analysis and costly communication systems. These are expensive as compared to the easily accessible.

(d) Deployment Density-Sound is the only way to communicate effectively underwater. It is intended to cover large distances which would otherwise not be possible. However, the cost factor limits the deployment of sensor nodes in large numbers. The nodes are deployed sparsely albeit covering larger areas unlike their terrestrial counterparts.

(e) Mobility-Terrestrial sensor networks comprise of static and mobile sensor nodes. Underwater sensor nodes have low or medium mobility due to water currents and other underwater activities. Although their processors incorporate features to locate them, we would not want them to drift apart as they house costly equipment and are not easily replaceable. However, they do tend to move about at low speeds due to winds, water currents etc. Therefore a network employed for a terrestrial network which does not take into account mobility for the majority of sensor nodes would most likely fail if considered for an underwater sensor network.

(f) Power-Underwater networks transmit over larger distances, have different protocols and have far more complex signal processing circuits. Thus their power requirements are more than ground based networks. The power needed for underwater communications is higher than in terrestrial radio communications due to higher distances and to more complex signal processing at the receivers.

IX. SIMULATION TOOLS FOR UWSNS

The difficulties faced by a scientists and engineers in testing a prototype model at sea are quite evident. It is not easy to deploy a sensor network in an actual underwater environment at sea. It would require massive efforts, a cohesive and coordinated team, a dedicated crew, lots of patience and above all Mother Natures blessings for favouring weather. Also, it would require continual funding. All these factors have prompted researchers to develop some wonderful simulators which can be used by the entire community to further the cause of developing an underwater sensor network. Quite a few simulation tools exist to define underwater acoustic signal propagation models. Following is a list of a few of them:-

(a) AUVNetSim-AUVNetSim [3] Consists of a simple physical layer and therefore environmental conditions cannot be considered in the propagation model. Results may not reflect actual values at all.

(b) Xie Gibson Simulator-An acoustic propagation model proposed by Xie and Gibson [4] is implemented in OPNET Modeller [5]. It only works on static scenarios with static conditions across the simulation period. It is based on the Monterrey Miami Parabolic Equation (MMPE). The MAC layers utilise Aloha and CSMA protocols. The physical layer in this simulator is extensively described to accommodate environmental factors like effect of waves/ depth of nodes. However, several propagation model parameters need to be computed prior initiating simulations.

(c) WOSS-World Ocean Simulator System [6] is another simulator for underwater networks incorporating a ray tracing tool therefore delivering a far more realistic reproduction of underwater propagation. It is integrated with free well known world databases for environmental parameters like temperature, depth, salinity etc. It also allows the user to easily specify the desired time of the year and the operational area to be simulated.

(d) UNET-The Underwater Network Simulator [7] is a freely available simulator for academic purposes which is based on UnetStack implementation. While the specifications primarily focus on underwater networks, they also allow wired/ wireless radio links to be included. The UnetStack is based on Java/Groovy implementation of the UnetStack Specifications based on the open-source fjge lightweight agent framework. It provides a basic set of agents that allow an underwater network to be deployed. The stack can easily be integrated with most underwater modems. All one needs to run the simulator on a PC is a bash shell (Cygwin, if using Windows), Java Development Kit (JDK) / Java Runtime Environment (JRE) , PERL (optional, for log analysis utilities) , Gnuplot (optional) and you are good to go. The simulator can be installed on Windows/ Linux operating systems. The developers have a fully functional and active trouble shooting forum as well to help students/ researchers with resolutions to any queries or installation issues.

X. MAC PROTOCOLS FORUWSNS

Most well-known MAC protocols were primarily designed for terrestrial networks and perform brilliantly as well MAC protocols provide functionality depending on the network, device capability, and upper layer requirements, but several functions exist in most MAC protocols. In general, a MAC protocol provides:

(a) Framing Define the frame format and perform data encapsulation and decapsulation for communication between devices.

(b) Medium Access Control which devices participate in communication at any time. Medium access becomes a main function of wireless MAC protocols since broadcasts easily cause data corruption through collisions.

(c) Reliability Ensure successful transmission between devices. Most commonly accomplished through acknowledgement (ACK) messages and retransmissions when necessary.

(d) Flow Control Prevent frame loss through overloaded recipient buffers.
(e) Error Control Use error detection or error correction codes to control the amount of errors present in frames delivered to upper layers.

However, as stated earlier, UWSNs are intended to operate in a vastly different underwater scenario. The acoustic signal propagates several orders lower than an RF signal and thus results in large signal propagation versus packet transmission time ratios. This is a major bottleneck. . The high latency in water coupled with issues like multipath, Doppler spread and attenuation led to intensive research and simulations of MAC protocols specific to acoustic propagation in water. Therefore many a MAC protocols needed to be tested as per existing requirements/ operational scenarios prior implementation. Following are some of the major protocols which have been tested quite often:-

(a) ALOHA-ALOHA protocol [8] is a well-known MAC protocol which is probably the simplest as well. It does not bother about channel condition or success of the delivery of the packet and thus produces a number of collisions. Since it does not have the ability to arrange for an orderly access to the channel, it is best avoided. However, it does not require any handshaking.

(b) T-Lohi-T-Lohi stands for Tone Lohi- Lohi means slow in Hawaiian. Lohi meaning slow in Hawaiian language. It is a new class of energy and throughput efficient, stable and flexible MAC protocol for UWSN. The paper at [9] presents and evaluates three versions of T-Lohi incorporating different design choices. Simulations were carried out to ascertain their performance and were encouraging with optimal energy efficiency and good channel utilization.

(c) CSMA-The Carrier Sense Multiple Access (CSMA) [10] reduces channel collisions as compared to ALOHA. As the name suggests it senses the channel and hence avoids collisions. It is based on the Listen before talk/ sense before transmit principle. It has two well-known versions- CSMA /CA (Collision avoidance) and CSMA- CD (Collision Detection).

(d) Slotted FAMA-Energy efficiency is however lost in CSMA as the delay increases. Ad-hoc networks are prone to the hidden terminal and exposed terminal problems due to lack of connectivity between terminals. A handshake may be performed prior to transmission of packets to avoid these problems [12] which included RTS- CTS signalling methods as in MACA (Medium Access Collision Avoidance).Further improvisations were made through MACAW (MACA-Wireless) and FAMA (Floor Acquisition Multiple Access). However, even these advancements were dogged by issues due to typical characteristics of an underwater channel. The FAMA protocol in underwater acoustic networks would not be efficient due to the required length of the RTS and CTS packets. The new protocol Slotted FAMA overcame these by guaranteeing that an RTS or a CTS packet transmitted at the beginning of a slot is received by all the nodes within transmission range over the duration of one slot. It slots the time to eliminate the asynchronous nature of the protocols.

(e) DACAP-Distance Aware Collision Avoidance Protocol (DACAP) [11] is a handshaking protocol designed for Ad Hoc Underwater Acoustic Sensor Networks. It is non-synchronized handshake-based access scheme and aims at minimizing average handshake duration by allowing a node to use different handshake lengths for different receivers saving transmission energy by avoiding collisions while maximizing throughput. It utilises the receivers tolerance to interference when two nodes are closer than the maximal transmission range for reducing hand shake duration. Nodes can be mobile, are in fact half-duplex, and utilise same transmission power. Throughput is higher than slotted FAMA however ALOHA offers a higher throughput. Energy efficiency as compared to slotted FAMA is similar and is higher that ALOHA.

XI. PROPOSEDMODELS FOR IOR

By now we have seen the importance of the Indian Ocean Region, requirement of UWSNs in the IOR for India, the basics of acoustics signal propagation in sea water, applications of UWSNs and a few more topics to enhance our understanding of the topic. We now see a few application specific models proposed to be deployed for coastal security in India:

(a) Harbour Protection Model-The harbours and ports see a lot of sea traffic. Therefore when deploying a UWSN in a harbour, we must keep the density of nodes low so as to not clutter the area. The nodes can otherwise be a navigational hazard for ships leaving or entering the harbour. These nodes can communicate with the master node which can be placed on the already exiting buoys. The above water part of the buoy can be equipped with a video camera to give live video feed. The underwater sensors should be able to monitor any unauthorised, potentially dangerous or illegal discharge from ships at anchorage or in harbour, intrusion detection (from divers/ saboteurs), mine detection etc. The above water part housing the video camera can prevent unauthorised crafts from accessing the sea lanes to the port.
(b) Anti-Piracy Model-The anti-piracy proposed is based on buoys which can be easily deployed and as easily retrieved. The part of the buoys which is underwater houses the UWSN sensors. The above water part is equipped with 802.11 standard based modules. Warships patrolling piracy infested areas can carry multiple buoys and deploy them in these areas. The above water part of the buoy forms an ad hoc wireless mesh network with the ships in its vicinity. The ships need to be in line of sight (LoS) distance from the buoys. Thus, we have a high speed WLAN at sea. Ships can communicate and exchange data / video at sea at high speeds. The data from the underwater sensor can also be transmitted by this wireless network. If a ship were to be attacked by pirates and if it were to call for help, warships can send boarding parties with cameras on their

combat helmets connected to this high speed wireless network. Thus, the boarding party can transmit live video feed to ships commanders and can identify friends from enemies. All this in addition to the traditional UWSN.

(c) Covert in the Guise of OvertModel-UWSNs would be a boon to researchers and marine biologists. However, the processors in the sensors for such networks can be augmented to also perform covert surveillance in coastal areas. Thus they can double up as surveillance and reconnaissance networks in the name of other sensors.

(d) Off Shore Asset Protection Model-Offshore assets like oil rigs and pipelines are usually in deep seas making it a tad easier for USNs to perform. In this model, it is proposed to install sensors on pipelines and in deep waters around oil rigs covering a large area. These sensors can monitor for submarines, AUVs, divers and mines. These areas would otherwise be difficult to monitor owing to the depths involved. The sensors can feed data acoustically to the master node at the surface. Large areas can be covered by deploying many such networks.

XII. CONCLUSION

A lot of research is going on in the field of UWSNs and acoustic propagation in sea water owing to its different characteristics. India too is not far behind in this field. It must be our endeavour to further this cause and build our own underwater sensor network which can benefit one and all. Further, porting of existing tools and technology from established terrestrial networks will help the research on UWSNs trememdously. Such a network will prove to be a boon and augment of surveillance capabilities. Indias naval might is a force to reckon with. Her presence in the IOR will deter non state actors from engaging in anti-nation activities and will promote peace and stability in the region along with other friendly nations. A UWSN will be her eyes and ears to support this cause. Further, its benefits to the scientific community cannot be overlooked. The sea provides us with natural resources, energy and livelihood. A UWSN will make this a simpler task for us. Disaster prevention agencies will also benefit hugely from such a network. UWSN therefore has a very promising future for the nation owing to its immense benefits. This paper is an earnest effort to introduce the advantages of a UWSN.

REFERENCES

[1] A. Quazi and W. Konrad, "Underwater acoustic communications," IEEE Commun. Mag., pp. 2429, Mar. 1982.

[2] Akyildiz, F.; Pompili, D.; Melodia, T. State of the art in protocol research for underwater acoustic

[3] Sensor network. In Proceedings of the ACM International Workshop on Underwater Networks (WuWNeT), Los Angeles, CA, USA, September 2006; pp. 7-16.

[4] Jornet, J.M. AUVNetSim: A Simulator for Underwater Acoustic Networks. Available online: http://sourceforge.net/projects/auvnetsim/ (accessed on 12 December 2011).

[5] Xie, G.; Gibson, J. Incorporating realistic acoustic propagation models in simulation of underwater acoustic networks: A statistical approach. In Proceedings of MTS/IEEE Oceans Conference, Boston, MA, USA, 1822 September 2006; pp. 18-21.

[6] OPNET Modeler v15.0 Reference Manual OPNET Technologies Inc. OPNET Modeler. Available online: http://www.opnet.com Guerra, F. World Ocean Simulation System (WOSS): A simulation tool for underwater networks with realistic propagation modeling. In Proceedings of the Fourth ACM International Workshop on Underwater Networks (WuWNeT), Berkeley, CA, USA, 3 November 2009.

[7] http://www.unetstack.net/doc/html/unet-sim.htmlunetsim accessed on 26 Mar 2014.

[8] Abramson, N. Development of the alohanet. IEEE Trans. Inf. Theory 1985, IT-31, 119-123.

[9] A. A. Syed , W. Ye and J. Heidemann "T-Lohi: A new class of MAC protocols for underwater acoustic sensor networks", Proc. IEEE INFOCOM, pp.231 -235 2008.

[10] Andrew S. Tanenbaum, Computer Networks. Prentice Hall, Upper Saddle River, NJ (2003). 892 pp. ISBN 0-13-066102-3.

[11] Peleato, B.; Stojanovic. M. Distance aware collision avoidance protocol for ad hoc underwater acoustic sensor networks. IEEE Commun. Lett. 2007, 11, 1025-1027.

[12] M. Stojanovic, "Recent advances in high speed underwater acoustic communications", *IEEE J. Oceanic Eng.*, vol 25, pp4.27, 2000.

[13] Arnab Das , "Effective Underwater Weapon Systems and the Indian Ocean Region, *Journal of Defence Studies*, Vol-7, Issue-3. pp- 159-168,2013.

[14] Das, 'Shallow Ambient Noise Variability Due to Distant Shipping Noise and Tide', n. 11.



Lt Commander Chakshu Malviya is an alumnus of the XVII Naval Engineering Course, INS Shivaji and completed his graduation in Electrical and Electronic Engineering from the Naval College of Engineering, INS Shivaji in May 2005. He is serving as an Electrical Officer in the Indian Navy. He has served as Assistant Electrical Officer- INS Trishul , Electrical Officer- INS Vidyut and Deputy Director, Naval EMC Centre. He is presently pursuing Masters (M.Tech) in Signal Processing and Communication from Defence Institute of Advanced Technology (Deemed University), Pune. His areas of research are underwater sensor networks, signal processing and communications.



Arnab Das received B. Tech degree in Electrical Engineering from Naval College of Engineering, Lonavala, India in 1995. He obtained M. Tech degree in Radar and Communication with specialization in Underwater Signal Processing in 2002and PhD degree in 2009 from Indian Institute of Technology, Delhi, India. He was commissioned into the Indian Navy in 1994. He worked as Project Officer at CARE, IIT Delhi for R & D in Underwater Signal processing and hardware design in 2003-2007. Currently he is instructor at MILIT Pune, India. His research interests are Underwater Passive Surveillance, Underwater Communication and Pattern recognition.

Implementation of Embedded Platform for Underwater Glider Prototype

Lt Cdr MD Nair[1], Mr Abhilash MT[2], Cdr (Dr)Vijayakumar[3] Cdr (Dr) Arnab Das[4]
[1,2]DIAT (DU), Girinagar, Pune,
[3]IIT, Delhi,
[4] MILIT, Girinagar, Pune
[1]mdn203@gmail.com, [2]abhilashmt@diat.ac.in, [3]vijay2028@gmail.com,[4]arnabdas1972@hotmail.com

***Abstract*—Underwater gliders are a type of Autonomous Underwater vehicles (AUVs) that do not use conventional propeller for propulsion, significantly minimizing their self noise. They are characterized by small size, long endurance, low speed and low cost [2]. These characteristics make gliders extremely valuable for long term oceanographic sensing missions. An underwater glider design, development and deployment effort with an appropriate payload of sensors will be able to effectively address all important aspect of improving sonar performance for our military as well as non-military sonars in the IOR [3].Underwater gliders are a class of Autonomous Underwater Vehicles that are propelled by change in buoyancy to follow a Saw-tooth pattern of motion in sea. Underwater Glider concept is cost effective and an efficient strategy for automated oceanographic data collection and analysis. The aim of work is to present a design and implementation plan for a suitable embedded system with associated peripherals for the prototype of a UW glider. The paper put forward the implementation aspects of embedded system to execute all the control functions namely buoyancy variation, data storage from sensors and periodic transmission of stored data to the base station.**

***Index Terms*—Underwater glider, buoyancy variation, Programmable System on Chip (PSoC), Xigbee PRO.**

I. Introduction

The conventional sonar designed for blue water operations present sub-optimal performance in the littorals, due to site specific behaviour of the underwater channel. The tropical waters in the Indian Ocean Region (IOR) further degrade sonar performance due to random fluctuations in the surface parameters like temperature, wind, etc. There exists a requirement to gather credible oceanographic and ambient noise data at specific locations for neutralizing the impact of underwater channel distortions and ambient noise thereby achieving effective sonar performance [1].

The appropriate selection of the sensors, the data acquisition system, power supply modules, processors, system controllers, memory, etc, requires careful study and short listing. The interfacing of the multiple components and devices along with the programming of the controllers to manage precise functioning of the entire system requires meticulous efforts. This is a first ever attempt at design and development of a UW glider in India. Significant efforts have been made to design the hydrodynamic body [4]. This paper focuses on the electronics and the onboard controller logic and hardware.

II. Review of Previous Work

In 2004, the first four members of this new family of underwater gliders were deployable: Slocum Battery and Thermal by Webb Research Inc., Falmouth, USA, Spray from the Scripps Institution of Oceanography, and Sea glider constructed by the University of Washington. All the gliders adopt different techniques to vary buoyancy and thereby convert vertical into horizontal movement resulting in a saw-tooth dive pattern, which is characteristic for gliders. The sinking to a defined depth and rising to another depth in the water column is referred to as a dive cycle. Underwater gliders perform multiple dive cycles before ascending to the surface to transfer data via satellite link. They are small and lightweight enough to be deployed by a small crew of two or three persons. All gliders, except for Slocum Thermal, use hydraulic buoyancy engines with battery powered pumps or pistons. Slocum Thermal uses the thermocline of the ocean to change the aggregate state of a medium from solid to liquid and vice versa to change its displacement. This feature limits its operation to areas with a well developed thermocline.

The Sea glider utilises the Onset Computer Corporations TT8 controller as the main electrical component. This controller utilizes the versatile Motorola MC68332 microcontroller combined with a 12-bit A/D converter and power conditioning circuitry on a small printed circuit board [5]. The basic scientific instrumentation on Sea glider is a conductivitytemperaturedepth (CTD) from Sea Bird electronics. The Sea glider uses the Iridium satellite communication system for transfer of data to the base station [6].Spray uses the Onset TT8 controller and associated electronic subsystems to deal with attitude and buoyancy control, interrogation of scientific sensors, processing and storing data, navigation and satellite communication [7]. In addition to conductivitytemperature-depth (CTD) sensor from Sea Bird, optional sensors include fluorometers, dissolved oxygen, turbidity and altimeter. Iridium satellite communication system is used to transfer data to base station.

III. Prototype of Underwater Glider

A Buoyancy Engine

The existing literature gave rise to three options for a variable buoyancy engine.

- Piston operated tanks

Specifications	Slocum	Sea glider	Spray
Weight	52 kg	52 kg	51 kg
Length	1.5m	1.8 m	2.0 m
Max Depth	200/1000 m	1000 m	1500 m
Speed	0.35 m/s	0.25 m/s	0.30 m/s
Max Range	1500 Km	4600 Km	4700 Km
Endurance	20 days	6 months	6 months
Produced by	Teledyne	iRobot	Bluefin Robotics

- Hydraulic pump with external bladder
- Chemical Propulsion

Buoyancy engine with piston operated tanks has been selected for the prototype stage due to simplicity of operation. The pistons of the tanks can be operated by a rack and pinion arrangement. This is driven by an actuator with high power to weight ratio. The force required for charging and discharging of buoyancy chamber is given by
Force Applied = ghA+ F
Where, =Density of water

g=Gravitational force

h=depth of operation

A=Area
F = force required to overcome the friction of the inner wall of the buoyancy chamber.
The actuator torque requirement can be determined from the calculation of force required to be applied on the piston in order to charge and discharge the buoyancy tanks. In the construction stage of prototype, an efficient DC motor was used to simulate the actuation of buoyancy engine.

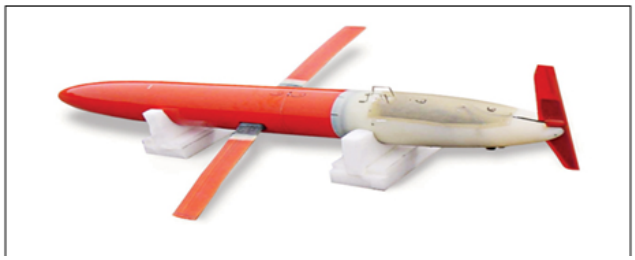


Fig. 1. Underwater glider

B Sensor Package
The selection of sensor package is dependent on the application of underwater glider. The basic sensor on glider is a conductivitytemperaturedepth (CTD) package. Output of the pressure sensor is used for vehicle control as well as labelling the depth at which temperature and electrical conductivity are measured. In accordance with the hardware study, the miniCTD profiler (acetal housing) from Valeport was found to be suitable for utilisation with regard to weight, dimensions and ease to interface with the microcontroller unit. In the construction stage of prototype, commercially off the shelf sensors namely temperature (LM35) and digital pressure sensor (BMP085), along with the conditioning circuitry has been used for data collection.

C Navigation and Communication system
Navigation fixes from the underwater glider to the remote underwater glider base station are conducted at the point of surfacing of vehicle during the saw tooth evolutions [2]. The weight, accuracy, power consumption and the available external interfaces have to be considered for selecting a suitable Inertial Navigation System (INS) for the underwater glider application. Inertial Navigation System (INS) aided by GPS, VN200 from VectorNav Embedded Navigation solution, is found to be suitable for the glider application. In the prototype stage of implementation, a constant navigation fix was used to simulate the use of navigation data in the data structure.
Xigbee PRO module, operating in the ISM band (2.4 GHz) and with data rate of 250kbps is used as the communication module for transferring the stored sensor data to base station. It has outdoor line of sight coverage of 2 miles and indoor coverage of 200m with a transmission power of 63mW. It is powered by 2.6 to 3.3 V DC with transmit and receive current of 205mA and 47mA respectively.

D Embedded Hardware
The primary requirements for the embedded system for an underwater glider are low power, small size, and versatility to allow integration of current and future sensors [5]. The low-power requirement necessitated a microcontroller with sub-milli ampere active and sleeps modes. The use of components was required to reduce circuit board size. A large number of serial communication channels as well as analog and digital channels are required for sensor integration.
The Programmable System on Chip (PSoC5LP) from Cypress Semiconductors was selected as the microcontroller unit for the glider, with a 32 bit ARM cortex M3 CPU core. It has programmable analog and digital blocks that are essential for integration with peripheral devices [8]. Memory requirements are accomplished by 256KB of flash memory, 64 KB of SRAM and an external SDRAM of 1 GB for sensor data storage. It has a 12-bit Delta sigma A/D converter and a 20-bit Successive Approximation Rate (SAR) A/D converter. The power consumption in active and sleep modes are 3.1 mA and 2 A respectively. There are 62 GPIOs (General Purpose Input Output) that can be configured for analog or digital input/output.

The Programmable System on Chip (PSoC5LP) from Cypress Semiconductors was selected as the microcontroller unit for the glider, with a 32 bit ARM cortex M3 CPU core. It has programmable analog and digital blocks that are essential for integration with peripheral devices [8]. Memory requirements are accomplished by 256KB of flash memory, 64 KB of SRAM and an external SDRAM of 1 GB for sensor data storage. It has a 12-bit Delta sigma A/D converter and a 20-bit Successive Approximation Rate (SAR) A/D converter. The power consumption in active and sleep modes are 3.1 mA

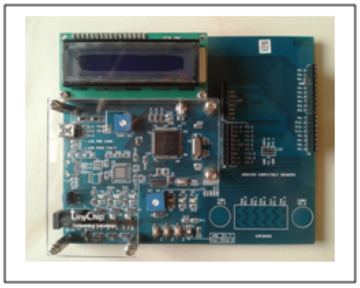


Fig. 2. PSoC5LP Development Board

and 2 A respectively. There are 62 GPIOs (General Purpose Input Output) that can be configured for analog or digital input/output.

IV. EMBEDDED SYSTEM PROGRAMMING

The main control functions of the embedded system, being developed are as given below:

- Periodic charging / discharging of buoyancy tanks with water for varying buoyancy by providing control signal to buoyancy engine.
- Collection and storage of data from onboard sensors as the glider follows the saw-tooth pattern.
- Data collected by the sensors is required to be transmitted to the base station for analysis.

The hardware and application firmware design for the embedded platform is provided by the IDE (Integrated Development Environment) PSoC Creator 2.2. The analog and digital components from the component catalog can be used to create a schematic diagram of the hardware design. Application Programming Interface (API) routines allows configuration of the analog and digital component using software. Each programmable component in the component catalogue includes the set of related API libraries. After completion of hardware design, the firmware is written, compiled and debugged by the IDE.

A Buoyancy Variation

During the saw tooth evolutions of the underwater glider, the buoyancy chamber is periodically charged and discharged to achieve negative and positive buoyancy respectively. The time interval between charging and discharging is determined by the depth of operation which is indicated by the pressure. During the prototype stage, as the variation in the pressure is limited, the number of data samples recorded is used as the sequential logic for the charging and discharging cycles. The piston operated buoyancy engine is driven by the actuator of high power to weight ratio. The DC motor used in place of actuator is interfaced to the port of the microcontroller unit PSoC5LP through a voltage regulation circuitry. The PSoC5LP provides PWM (Pulse Width Modulation) control voltage for actuator operation. The configuration of PWM and peripheral ports for actuator, including the hardware schematic design is undertaken using the PSoC Creator (IDE). The PWM component is configured for 8-bit resolution and set up in dual mode of operation. The dual mode provides actuator operation in clockwise and counter clockwise direction. This can be used with appropriate time delay to realize the periodic charging and discharging of buoyancy chamber. The IDE through API (Application Programming Interface) provides software control for the periodic operation of actuator in both directions.

B Collection and Storage of Sensor Data **Data Collection**

The onboard sensors of glider constantly record oceanographic data during the saw tooth evolutions. An analog temperature sensor (LM35) is interfaced through a signal conditioning circuitry to the peripheral port pin of PSoC5LP which is configured as analog by using the configuration setting of IDE. The peripheral port pin is used for interfacing LM35 and the delta sigma A/D converter of microcontroller unit. The A/D converter is configured for 8-bit resolution, sampling rate of 8 KHz and clock frequency of 500 KHz. The digital pressure sensor (BMP085) is interfaced to PSoC5LP through an I2C interface. The I2C component is configured as master for a data rate of 50Kbps and clock frequency of 800 KHz. The output of delta sigma ADC and BMP085 is converted to obtain the analog values of temperature and pressure respectively by using the scaling factor. The rate at which the various sensors have to be polled by the embedded platform is determined by the dive cycle period, glider speed, glide angle and the type of data being recorded. The polling rate for various sensors can be controlled by using interrupt or through software using API.

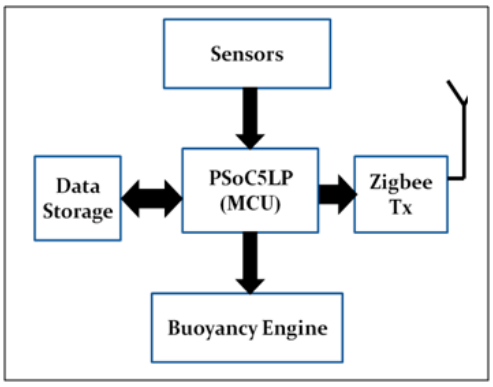


Fig. 3. Block diagram of embedded system on glider

Data Storage

The sensor data size, polling rate and maximum depth of operation determines the amount of storage space required for each dive cycle. The data packet comprises of temperature and pressure sensor data along with time stamp. The total size of data packet is 26 bytes which includes 14 bytes for time stamp and 5 bytes each for temperature and pressure sensor data. The data from sensors is converted from float to character data type before storage. The data packets in FAT32 format are

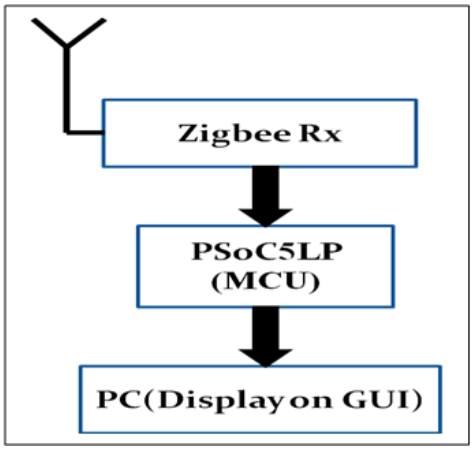


Fig. 4. Block diagram of embedded system Base station

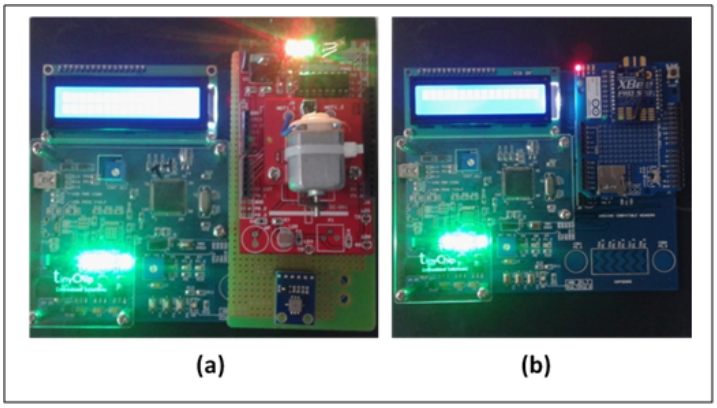


Fig. 5. (a)Embedded hardware at base station (b) Embedded hardware at base station.

stored in an external SD card of 1 GB. The SD card is formatted by using API before storing the data packets. The SD card is mounted on the Arduino shield and is interfaced to PSoC5LP through Serial Peripheral Interface (SPI) with a clock frequency of 4000 KHz. The emFile component of PSoC creator provides an interface to SD card formatted with a FAT file system. The system parameters and control history for each dive cycle can be stored in separate file. Data packet from each dive cycle is stored in separate files in SD card. In order to conserve power, large data files are broken into several smaller ones to avoid retransmitting large files if errors are detected. Post completion of each dive cycle, the existing file is closed and a new file is opened for storing the data from the next dive cycle.

C Communication

The transmitter module consists of a Xigbee PRO module configured as co-ordinator by using X-CTU software interfaced to the microcontroller unit through UART interface. ZigBee is an open global standard built on the IEEE 802.15.4. Serial communications depend on the two UARTs (the microcontroller's and the RF module's) to be configured with compatible settings (baud rate, parity, start bits, stop bits, data bits). The UART component from IDE is configured for a full duplex mode with a baud rate of 9600 bits per sec. The microcontroller reads the file containing sensor data from SD card by using API of SPI interface. The data read by the controller along with the header information, is transmitted to the Xigbee module through UART interface.

The base station receiver comprises of the Xigbee PRO module configured as end device (by using X-CTU software) and interfaced with PSoC5LP through UART interface. The UART configuration is same as in transmitter section. The sensor data received by the Xigbee PRO module is read by PSoC5LP after verification of header data. The data read by controller is transmitted to PC through USB interface. The data packet is disintegrated by using code written in python to obtain the temperature and pressure data along with the time stamp information.

D Emergency recovery system

The emergency recovery system is excluded in the prototype stage. However, the requirement of an emergency recovery system is considered essential for an effective embedded system for glider. The functions of the emergency recovery System can be performed by a standalone PSoC5LP microcontroller unit powered by an independent power supply. An internal pressure and temperature sensor along with a leakage sensor can be used to monitor the health of the glider housing. In case of failure or an abort signal from the main control system, a drop weight can be electro-magnetically released and thereby inducing positive buoyancy. Upon surfacing a GPS can be polled for position fix and an emergency signal broadcasted to the base station via communication module.

V. CONCLUSION

The embedded platform for underwater glider prototype was implemented utilizing the Programmable System on Chip (PSoC5LP). For the experimental trials, Conductivity Temperature and Depth (CTD) sensors is required to be interfaced to the embedded platform through RS232 interface. The actuator selected for buoyancy engine post calculation of required torque, can be interfaced to PSoC5LP for achieving PWM control. Excluded in the prototype stage are the Inertial Navigation Unit (INU) and the emergency recovery system. The INU integrated with GPS which can give position fixes constantly during the operation of the glider. The emergency control system can retrieve the glider in case of failure of the platform. Identification and implementation of the embedded platform for underwater glider prototype is the first stage towards building an efficient and effective control system for an underwater glider. The total number of interfaces required for the microcontroller depends upon the sensor package and system requirements. The work has brought out the feasibility of implementation of the embedded platform on PSoC5LP with regard to issues related to buoyancy engine, power consumption, sensor interface, data structure, storage and communication.

REFERENCES

[1] Arnab Das, "New Perspective for ceanographic Studies in the Indian Ocean Region JDSA ,2013J. Clerk Maxwell, A Treatise on Electricity and Magnetism, 3rd ed., vol. 2. Oxford: Clarendon, 1892, pp.68-73.

[2] Amit Ray, Singh S.N. and Seshadri V, 'Underwater Gliders - Force Multipliers for Naval Roles' at the RINA conference 'Warship 2011 : Naval Submarines and UUVs', 29-30 June, 2011 at the Guildhall, Bath, UK.William P Barker, Analysis of undersea glider architectures and an assessment of undersea glider integration for undersea applications, Sep 12.

[3] Arnab Das, "Naval Operations Analysis in the Indian Ocean Region-A Review, Accepted for publication in the IDSA Journal.

[4] Danio Joe, R V Shashank Shankar, RVijay kumar and Arnab Das, Concept Design of Autonomous Underwater Glider.

[5] Charles C. Eriksen, T. James Osse, Russell D. Light, Timothy Wen, Thomas W. Lehman, Peter L. Sabin, John W. Ballard, and Andrew M. Chiodi Seaglider: A Long-Range Autonomous Underwater Vehicle for Oceanographic Research, IEEE Journal of oceanic Engineering, Vol. 26, No. 4, Oct 2001.

[6] Stephen Bozzone, Brian Newberry, Dominic Germana Enhancements and Performance of Seaglider Iridium Communications System Chris Yahnker,OCEANS,2012.

[7] Abdallah Ismail, Project report on Programmable System-on-Chip technology from Cypress Semiconductor digital systems architecture, Dec 2007.



MD Nair M Tech (Signal Processing and Communication),Defence Institute of Advanced Technology, Pune. Graduate in Electrical and Electronic Engineering from the Naval College of Engineering, Lonavala.Presently pursuing M Tech in Signal Processing and Communication from Defence Institute of Advanced Technology (Deemed University), Pune. Areas of research interest are Digital Signal Processing and Embedded systems.



Abhilash M T is M.Tech in VLSI Design from SRM University, Tamil Nadu (2005). He is presently working as Assistant Professor in the Department of Electronics Engineering, Defence Institute of Advanced Technology (Deemed University), Pune and has a vast teaching and research experience of 8 years. He has published 07 papers in refereed journals and conferences. His research area includes prototyping of DSP Applications in FPGA, Embedded System Development, VLSI and MIMO Radar. He has been conferred with the Summer Research Fellowship 2010 by Indian Academy of Science.



Cdr (Dr) R Vijayakumar is a Ph.D. from Indian Institute of Technology Delhi in 2009. During his career of 20 years he has served in both the Naval Dockyards and Design Directorate. He is presently appointed as Adjunct Faculty at the Naval Construction Wing, Department of Applied Mechanics at Indian Institute of Technology, Delhi where he teaches the subjects of warship design, structural design of warship and Ship Dynamics. He has published 18 papers in refereed journals and conference. His fields of interest include Warship Design, Ship Hydrodynamics, Ship Dynamics and Computational Fluid Dynamics (CFD).



Arnab Das received B. Tech degree in Electrical Engineering from Naval College of Engineering, Lonavala, India in 1995. He obtained M. Tech degree in Radar and Communication with specialization in Underwater Signal Processing in 2002and PhD degree in 2009 from Indian Institute of Technology, Delhi, India. He was commissioned into the Indian Navy in 1994. He worked as Project Officer at CARE, IIT Delhi for R & D in Underwater Signal processing and hardware design in 2003-2007. Currently he is instructor at MILIT Pune, India. His research interests are Underwater Passive Surveillance, Underwater Communication and Pattern recognition.

Underwater Sensor Networks for Coastal Surveillance - The 'Indian Seaweb'

Lt Cdr Soubhagya Roul[1], Arnab Das[2]
[1,2]MILIT, Girinagar, Pune, India
[1]chandannec@gmail.com, [2]arnabdas1972@hotmail.com

***Abstract*—This paper proposes an effective and implementable solution to counter the underwater threat scenario. The proposed underwater wireless sensor network architecture will be highly effective in detection and DOA estimation of AUVs, submersibles and underwater vessels having a radiating noise level within the range of few kilometers. The architecture proposes the use of Acoustic Vector Sensors (AVS) moored on the seabed forming a cross array. Each array element comprises of an acoustic modem operating at frequency different from that of the radiated noise range. The array elements are connected acoustically through these modems to a single afloat beacon placed at the centre of the array. This beacon has adequate power supply, knowledge base and computing algorithms for carrying out detection, classification and estimation using known algorithms. This data is transmitted using RF/Satcom links to the Operation Center.**
The paper also brings out challenges eminent in the proposed architecture including deployment and maintainability issues that plague any underwater sensor networks.

***Keywords*—Sensor Networks; Underwater Sensors; Acoustic Vector Sensors; AVS; Array processing; Shallow Ocean**

I. INTRODUCTION

India is surrounded by water on three sides. Infiltration through coastlines is not a new phenomenon and history is proof to the fact that breach of the vulnerable coastlines has far fetching consequences. Thus the importance of having robust costal surveillance measures is not debatable. With the cheap & wide spread availability of submersibles, scanning of the enemy coastlines to identify vulnerabilities for planning a multidimensional attack is not something new. Enemy UW gliders & AUVs could easily carry and plant mines near the coastlines overnight and it could lead to catastrophic loss of life and material the next day. This could cripple the entire economy of the country in days especially in case of India which depends heavily on sea trade. In fact our hostile neighbours may be already investing into this dimension of attack for quite some time now. Costal surveillance radars provide us the required info on surface targets, however not much attention is paid to costal underwater surveillance. The need of the hour is a network of robust and technologically advanced sensor networks deployed underwater in the coastlines [1]. These sensor networks would be remotely activated based on INT reports or suspicious underwater activity in the areas, detect and estimate the threat and pass on the info through beacons. Large scale deployment of underwater sensor networks has been in vogue since 1998. Numerous deployment strategies, topologies, access protocols, underwater modem design and localization schemes with respect to wireless sensor networks are available in literature. Though most of the UW sensor networks are meant for specific commercial applications, the principles behind the same could be used for development of a strategic UW wireless sensor network. This paper brings out the birds eye view of the technology involved in deploying an AVS based sensor network for detection and Direction of Arrival (DOA) estimation of submerged and surface vessels in coastal waters. Section II describes the features of AVS and its effectiveness in DOA estimation of noise sources in shallow ocean. The peculiarities of shallow oceans compared to deep waters are also brought out. Sec III brings out the physical and logical implementation of a proposed setup derived out of the US based Seaweb implemented in 2000 [2]. Sec IV describes the various challenges that are required to be addressed for efficient exploitation of the network. The concluding section gives a roadmap for further research in the area that could see the proposed Indian Seaweb operational in the near future.

II. SHALLOW OCEANS AND AVS

A. Shallow Oceans

These waters encompass about 5 perscent of the worlds oceans on the continental shelves, roughly the region from the beach to the shelf break, where water depths are about 200 meters. The sound speed in water is about 1500 m/s, so wavelengths of interest are on the order of a few meters. In shallow water, with boundaries framed by the surface and bottom, the typical depth-to-wavelength ratio is about 10100 [3]. That ratio makes the propagation of acoustic waves analogous to electromagnetic propagation in a dielectric waveguide. However in the shallow ocean, surface and the oceans index of refraction have a spatial and time dependence and the presence of ocean inhomogeneities and loud ships can frequently scatter, jam, or mask the most interesting sounds. So, whether using active or passive techniques, the ultimate concern is extracting a signal that propagates in a lossy, dynamic waveguide from noise influenced by that same waveguides complexity. In that light, one can begin to appreciate shallow-water acoustics as an interdisciplinary

blend of physics, signal processing, physical oceanography, marine geophysics, and even marine biology. In order to give an insight to the reader of the complexity of the shallow ocean, the variation in the speed of sound in water c(z) is as shown below. Three simple profiles [4] of the speed of sound in seawater, illustrated in Fig. 1, have proven useful to researchers modeling the shallow-water acoustics problem. The three models of the speed of sound c(z) in seawater encompass a wide variety of shallow-water oceanography:
a)An ocean with a constant sound speed represents fully mixed temperature conditions found during the winter in Earths mid-latitudes and in water shallower than about 30 meters.
b)The common three-layer model consists of two separate mixed layers, both of constant temperature and sound speed, with a thermocline gradient sandwiched in between.
c) In a coastal front model, two water masses with differing temperature profiles meet at a vertical wall (green). Note that the ocean bottom has a higher sound speed and density, indicated by its shift to the right, than the water layer.

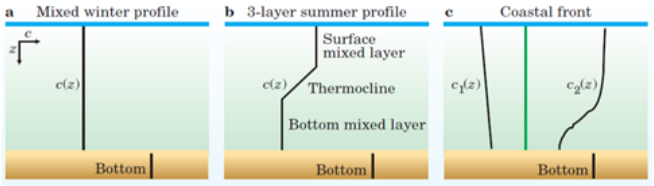


Fig. 1. Profiles in Shallow Ocean

B. Shallow Ocean Models

The seabed can often be approximated as a fluid medium, with only sound speed, attenuation, and density as acoustic variables. As evident from the above, the change in the thermocline has a spatial and temporal variation thus dynamically affecting the efficiency of the detection and DOA estimation techniques which otherwise provide acceptable accuracy levels.
During World War II, Chaim Pekeris applied waveguide theory to the task and treated the ocean as a static, constant sound-speed medium. That approach addressed the many boundary interactions in shallow water, but it underestimated the mediums complexity. The shallow ocean model otherwise called the Pekeris model thus assumes constant sound speed, mirror reflection at the surface, and a grazing-angle-dependent reflectivity at the ocean bottom. Any sound wave emanating from the source with an angle less than the critical angle typically about 15, propagates at angles confined. Within that cone, constructive interference selects discrete propagation angles; outside the cone, waves disappear into the bottom after a few reflections. The models thus calculate the modes that propagate along the waveguide and spread cylindrically. The normal modes of the Pekeris waveguide are sine waves that vanish at the surface and abruptly change to decaying exponentials at the bottom boundary.
The Pekeris model is widely used in solving complex shallow ocean detection and DOA estimation problems. The setup proposed in this paper also uses the same shallow ocean model for the DOA calculation.

C. AVS Sensors

An omnidirectional hydrophone is generally used in underwater applications eg. towed arrays, stationary arrays, hull mounted arrays and sonobuoys. This hydrophone is a pressure sensor designed to sense acoustic pressure in every direction. Thus, the effectiveness of such a sensor reduces drastically in detection of acoustic signals from an intruder that who are quieter than the surrounding noise sources. This problem could be overcome by using a directional sensor such as an underwater Acoustic Vector Sensor (AVS). An AVS consists of three uni-axial accelerometers in each independent axis and an omnidirectional pressure sensor (hydrophone) closely packed in a single structure as shown in Fig. **??**. The directional capabilities of the vector sensor stem from the dipole behavior of the individual accelerometers which measure the particle velocity in the respective directions. The ability of the AVS in isolating interfering noise sources from other directions compared to one provides a high amount of directivity and enables AVS arrays to outperform its counterpart omnidirectional sensor array even with 1/3 of the array elements.
It has been proved that AVS arrays provide significant gains against both broad-band and narrow-band noise interference. Broad-band refers to noise that covers a significant portion of the audio frequency band, such as wind-induced noise, and narrow-band refers to sound having certain significant frequency components that overshadow the others eg noise emitted from rotating machinery and propagated through the ships hull to the water.
An AVS array serves to improve detection performance by coherently adding the target signals while incoherently adding the noise. Arrays provide significant directivity due to their spatial coverage. The AVS technology has attracted considerable interest, especially within the signal processing community, after Nehorai and Paldi presented the AVS measurement model and a method for localising acoustic sources using an array of such sensors [5]. Hochwald and Nehorai later addressed the important issue of identifiability with vector sensors, namely, the bound on the number of sources identifiable in a class of array processing models with multiple parameters and signals per source [6]. Malcolm Hawkes and Arye Neharoi in [7] have also discussed the correlations between the measurements within an AVS as well as between two spatially separated acoustic vector sensors. The same authors have also analysed the effect of a reflecting boundary [8] and presented a fast method for localising a wideband source using a distributed AVS array in deep ocean [9]. JC Shipps and BM Abraham in [10] were the first to talk about AVS sensor based arrays for underwater port and waterway security. They have brought out the concept of use of AVS sensors without going into details of implementation issues.

III. IMPLEMENTATION

A. Seaweb

The Seaweb located at the Buzzards Bay is an organized



Fig. 2. AVS

network for command, control, communications, and navigation (C3N) of deployable autonomous undersea systems. The Seaweb (2000), spread over 16 sqkm with 17 nodes, functionality implemented on proprietary DSP based hardware Telesonar has proved to be the blueprint for numerous ocean applications. The Seaweb backbone is a set of autonomous, stationary nodes (e.g., deployable surveillance sensors, repeaters). Seaweb peripherals are mobile nodes (e.g., UUVs, including swimmers, gliders, and crawlers) and specialized nodes (e.g., bistatic sonar projectors). Seaweb gateways provide connections to command centers submerged, afloat, aloft, and ashore. Telesonar-equipped gateway nodes interface Seaweb to terrestrial, airborne, and space-based networks. The motivation of deploying a sensor network in the Indian coastlines, though derived from the Seaweb, is AVS based and much simplified.

B. Physical Implementation

Owing to the vastness of the Indian coastline, the requirement is to have an array spanning the maximum coastal distance with the min no of sensors per sq km and at the same time meet the inter senor spacing of /2 for operating frequencies ranging from 5Hz-5KHz band. This gives a inter sensor placing of anywhere between 150mts 0.15mts. As the spacing is the spatial equivalent of the Nyquist criterion. The /2 gives the min inter element spacing required for beam formation in the operating frequency.

The layout of the sensors will be in a cross array with a gateway buoy moored at the center of the cross. The structure of a single network (LAN) is as shown in Fig. 3. Each sensor is mounted with an acoustic modem for communicating with the Gateway Buoy/Node. The latter, in addition to an acoustic modem is also mounted with a RF modem for communication

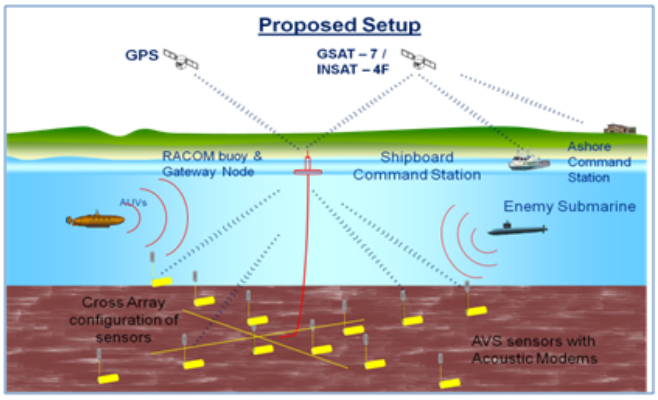


Fig. 3. Proposed Setup (LAN)

with Satellites or shipboard/ashore command stations through RF links. The gateway buoy is also equipped with a GPS receiver for correlation of the calculated DOA of the enemy vessel on the electronic chart at the command stations. The sensors are moored as close to the sea bed as possible. However masking of the sensors due to coastal seabed debris or plantations is to be avoided for better detection and DOA estimation.

Further, one single LAN in this case would not be able to cover the area under observation. Thus a number of such LANs would be required to be positioned and connected to the ashore/base station, a layout depicted in Fig. 4. A provision of waking up the adjacent LAN in the direction of movement of the noise source is also possible.

C. Logical Implementation

The cross array is the sparse structure of a planar array which is the most suitable for any beam forming technique. A planar array is not a feasible implementation due to various reasons. The cross array is more efficient in localisation of noise sources compared to the horizontal array and the vertical array. Consider the planar acoustic wave front of an enemy AUV incident on the array elements. Each sensor picks up a noise signature along with the ambient noise levels. The modem integrated with the sensor transmits the captured sensor data acoustically to the buoy. It is but obvious, that the modem operating frequency is to be different than that of the noise sources being captured.

Three types of signals are generally used for communication and data transfer in sensor networks. The first types are control signals ie wake up/sleep signals, sensor health monitoring etc. Typical data rates for such signals will be few bps. The second type of signal is telemetry signals requiring slightly higher data rates in order of a few kbps. The bandwidth intensive signals are audio and video streaming that require several tens of Kbps. Unlike a typical sensor network there is no communication in-between the sensors nodes in the proposed system. Sensor nodes require control signal receivers and telemetry transmitters while the buoy has control signal transmitters and telemetry receivers. The buoy also requires having RF

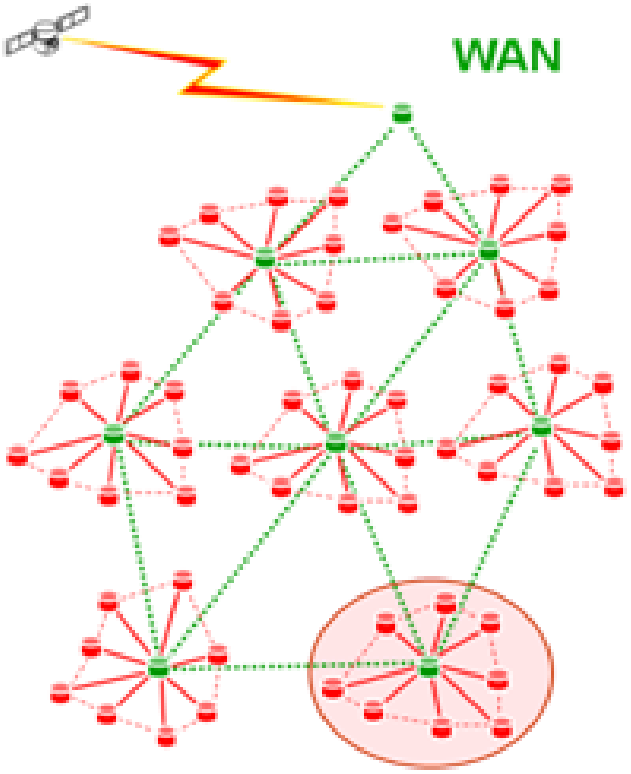


Fig. 4. The Seaweb WAN

transceivers for control and telemetry.
The buoy provides a wakeup signal to the nodes on receiving signal from the command station(s). The sensors wake up, capture the noise levels and compare it to a set threshold. Once the noise level exceeds the set threshold it is thereafter transmitted continuously to the buoy. This continues till either the captured noise level is less than the set threshold or a shut down command is initiated by the buoy. Numerous papers have been written about the wakeup/sleep techniques of the sensors and thus the same is not elaborated in this paper.

The buoy on receiving the sensor data needs to implement the following:
a) Methodology of discriminating the data with respect to the sensors that have sent it. This requires that every transmission from the sensor needs to be stamped with the senor number and sequence number.
b) Detection algorithm: The detection algorithm is required for determining the presence noise sources as well as the number of distinct noise sources. A good way of determining the number of noise sources is the one using the Greschgorin Disk algorithm elaborated by Suresh Kumar et al in [11]. The knowledge of the number of noise sources is a prerequisite for the DOA estimation algorithms.
c) DOA Estimation algorithm: Once the number of noise sources in the vicinity of the array is established by the detection algorithm, the DOA estimation algorithm predicts the direction of arrival of the individual noise sources. Many DOA estimation algorithms are used for underwater scenarios, however in the current scenario of shallow ocean narrowband detection the most suitable algorithm is the Subspace Intersection Method (SIM) elaborated by K.G. Nagananda and G.V. Anand in [12] where a horizontal array is used for DOA estimation using AVS array in shallow ocean. The idea can be expanded to cross array in the same environment.
d) RF Communications: Post detection and DOA estimation the data is required to be transmitted through the RF link to the satellite or directly to the nearest afloat/ashore base station.

IV. CHALLENGES

Several types of acoustic modems are available commercially, offering up to a few kilobits per second (kbps) over distances up to a few kilometers depending on the extent of multipath. However, the following issues post serious challenges in implementation of underwater sensor networks compared to RF sensors networks and need to be addressed during the network design:

a)The speed of sound in water is approx 1500m/s, propagation delays are in the order of few seconds over a few kilometers. **b)**Pulse stretching due to the effect of multipath is highly ubiquitous. **c)** Recharging of batteries underwater / powering up modems for effective communications. **d)**Underwater Sensors are more subject to bio-fouling thereby requiring periodic maintenance.
The severe restriction on data rates for inter sensor communication because of signal deterioration due multipath is not a restraining factor in the proposed setup as there is no requirement for any inter sensor communication. The major issue in this case is the non-uniform delay in communication between the modems on the sensors and that of the buoy. The detection and DOA estimation to efficiently work requires exact measurement of the delays.

V. CONCLUSION

AVS arrays outperform conventional omnidirectional hydrophone arrays in detection and localization of noise sources even with 1/3 of the number of sensor elements. Sensor array deployments proposed above are particularly useful in surveillance of port entrances, strategic coastal installations, nuclear power plants, shipyards and especially the long, sparsely uninhabited Indian coastlines. The challenges arising due to acoustic propagation in shallow water, development of robust algorithms for detection, classification and DOA estimation of noise sources are the issues that need to be addressed first. Deployment of AVS arrays and maintenance issues come thereafter. With recent advances in large scale deployment of sensors / sensor networks in ocean beds for environmental monitoring, the technology involved in acoustic modems is being refined at a fast pace.
It is therefore not far that the AVS array based Indian Seaweb will be a reality to help provide early warning and increased security against unwanted water borne intruders in ports and waterways.

REFERENCES

[1] Arnab Das, Effective underwater weapon systems and the Indian ocean region, Journal of Defence Studies (2013), Vol-7, Issue-3. pp- 159-168

[2] Joseph A. Rice, Robert K. Creber et al, Seaweb underwater acoustic nets SSC San Diego, Communications Systems Technologies, Pg 234-250.

[3] Proakis J, Sozer E, Rice J, & Stojanovic M. Shallow water acoustic networks. 2001 IEEE,Commun. Mag . 39, 114119.

[4] William A. Kuperman and James F. Lynch , Shallow water acoustics , Physics Today American Institute of Physics, Oct 2004.

[5] Arye Nehorai and Eytan Paldi, Acoustic vector-sensor array processing, IEEE Transactions on Signal Processing, vol. 42, no. 9, pp. 2481-2491, Sept. 1994.

[6] Bertrand Hochwald and Arye Nehorai, Identifiability in array processing models with vector-sensor applications, IEEE Transactions on Signal Processing, vol. 44, no.1, Jan. 96.

[7] Malcolm Hawkes and Arye Neharoi, Acoustic vector-sensor correlations in ambient noise, IEEE Journal of Oceanic Engineering, Vol. 26, No. 3, pp. 337-347, July 2001.

[8] Malcolm Hawkes and Arye Nehorai, AVS processing in the presence of a reflecting boundary, IEEE Transactions on Signal Processing, vol. 48, no.11, pp 2981-2992, Nov. 2000.

[9] Malcolm Hawkes and Arye Nehorai, Wideband Source Localisation Using a Distributed AVS Array, IEEE Transactions on Signal Processing, vol. 51, no.6, pp. 1479-1491, June 2003.

[10] [10] JC Shipps and BM Abraham, The use of vector sensors for underwater port and waterway security, Sensors for Industry Conference, 2004. Proceedings the ISA/IEEE, 2004, Pg 41 - 44 .

[11] N. Suresh Kumar, G.V. Anand, S. Roul, Dibu John Philip , Source number estimation in shallow ocean by acoustic vector sensor array using Gerschgorin disks, Proceedings of the12th International Conference on Intelligent Systems Design and Applications (ISDA), 2012.

[12] K.G. Nagananda and G.V. Anand, Subspace intersection method of bearing estimation in shallow ocean using acoustic vector sensors 16th European Signal Processing Conference (EUSIPCO 2008), Lausanne, Switzerland, August 25-29, 2008



Lt Cdr Soubhagya Roul is an alumni of the 15th Naval Engineering Course and completed his BTech in EEE in 2003 from the Naval College of Engineering, Lonavala. Thereafter, he has served on frontline Indian Naval ships viz INS Mumbai, INS Talwar and has been the Electrical Officer onboard the Missile craft INS Vidyut. The Officer has also played the pivotal role in setting up the Mumbai Metropolitan Area Network (MAN) during his tenure as Staff Officer (IT) at HQWNC. He has completed his MTech in SPC from DIAT(DU), Girinagar, Pune and is currently pursuing his PhD from the same university. His topic of research is Underwater Sensor Networks for Coastal Surveillance in the Indian tropical ocean scenario.



Arnab Das received B.Tech degree in Electrical Engineering from Naval College of Engineering, Lonavala, India in 1995. He obtained M. Tech degree in Radar and Communication with specialization in Underwater Signal Processing in 2002and PhD degree in 2009 from Indian Institute of Technology, Delhi, India. He was commissioned into the Indian Navy in 1994. He worked as Project Officer at CARE, IIT Delhi for R and D in Underwater Signal processing and hardware design in 2003-2007. Currently he is instructor at MILIT Pune, India. His research interests are Underwater Passive Surveillance, Underwater Communication and Pattern recognition.

FPGA Realisation of QPSK Modulated OFDM Transceiver

K Sandeep[1], **Abhilash M. T.**[2]
[1,2]Defence Institute of Advanced Technology (DU),
Girinagar, Pune, India
[1]Sandynair.k@gmail.com, [2]abhilash@diat.ac.in

***Abstract*—This paper reports on the design methodology and validation of a FFT based FPGA prototype of an OFDM transceiver system with an inherent ability to provide high throughput and low inter symbol interference even in environments that exhibit intense multipath. The models were first analyzed for BER v/s SNR performance for various modulation schemes like BPSK, QPSK and QAM modulation schemes using Matlab Simulink. The proposed hardware design has been modeled using Xilinx System Generator for DSP which is the industry's leading high-level tool for designing high-performance DSP systems using FPGAs. The software verification of the functionality of the model was carried out using Xilinx ISE 14.7 inbuilt simulation tool ISim. The hardware implementation was realized on a Xilinx Virtex-5 XC5VSX50T-1FF136 board. JTAG Co-Simulation was conducted on the run time model to verify the hardware-in-the-loop performance further to which stand alone hardware tests were conducted. The test results confirmed with the simulation results thus validating the functionality of the design.**

***Keywords*—OFDM, QPSK, FPGA.**

I. INTRODUCTION

OFDM is a form of multi carrier communication wherein a stream of high rate data stream is split into a set of low rate sub streams. These sub streams or sub carriers are modulated on a separate sub carrier. In effect the bandwidth of the sub carriers become small compared to the coherence bandwidth of the channel thus experiencing flat fading. This translates in the time domain to the symbol period being comparably long to the delay spread of the time dispersive radio channel. By maintaining the orthogonality of the sub carrier frequencies which is obtained by performing Fourier Transform operation, a high spectral efficiency can be achieved.

The arithmetic requirements to perform Fourier Transform operations far exceeds the ability of most high-end DSP microprocessors. Field Programmable Gate Arrays (FPGA) with its versatility and high parallel architecture has in recent years become a compelling proposition for almost any type of digital design. FPGA offers the designer multiple platforms with an optimised balance of high performance logic, serial connectivity, signal processing, and embedded processing resources. The memory bandwidth of FPGA is superior to that of a conventional microprocessor or a DSP processor running at far higher clock rates than that of the FPGA. This performance advantage coupled with the parallelism aspect makes FPGA ideal candidate for implementation of complex digital communication systems such as OFDM.

II. DESIGN FLOW

Xilinx System Generator for DSP a leading high-level tool for designing high performance Digital Signal Processing (DSP) systems using FPGA was employed to implement the OFDM transceiver. This software is based on visual modelling toolset of the Mathworks Simulink. It is part of both the DSP and System Editions of ISE Design Suite. This programming interface enables users to design, simulate, verify and create production quality FPGA implementations in a fraction of traditional RTL development times. Designs are captured in the DSP friendly Simulink modelling environment using a Xilinx specific blockset. All of the downstream FPGA implementation steps including synthesis and place and route are performed to generate an FPGA programming bit file. The System Generator block provides control of system and simulation parameters, and is used to invoke the code generator. The System Generator block is also referred to as the System Generator token because of its unique role in the design. Every Simulink model containing any element from the Xilinx blockset must contain at least one System Generator token. Once a System Generator block is added to a model, it is possible to specify how code generation and simulation should be handled.

III. OFDM TRANSCEIVER MODEL

Fig.1. shows the block diagram of a basic OFDM Transceiver. The input data stream is grouped into parallel format of size two bits to be mapped into QPSK constellation. The output of the mapping is a complex number that locates the sample on the I-Q constellation. The Inverse Fourier Transform (IFFT) block forms the heart of an OFDM modulator. This block performs a 16 point inverse Fourier transform thus producing and modulating 16 sub carriers in the time domain. These 16 point samples are serialised and further passed through digital to analog converter, and transmitted through a channel.

At the receiver side the received signal is passed through an analog to digital converter. After framing in the same order as of transmitter a 16 point Fourier transform is performed to reproduce the 16 subcarriers. These subcarriers are de-mapped to get samples which are further serialised to recover the bits stream initially fed.

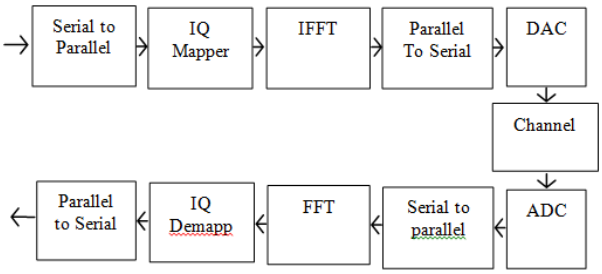


Fig. 1. Block Diagram of OFDM Transceiver

A *D*ata Stream Generation

The input data stream is generated from a pseudo random generator implemented by a Linear Feedback Shift Register (LFSR) block. Here a 32 bit LFSR counter is employed to generate a sequence of zeroes and ones. The sequence follows a mathematically predictable sequence and repeats itself after (232-1) clock periods which is long enough to be considered random. Conceptually a 32 bit LFSR counter consist of 32 bit shift register, with a feedback from 32nd, 22nd, 2nd and 1st shift register. The feedback polynomial therefore is $1+g^1+g^{21}+g^{31}$

B *Q*PSK Mapping

Modulation is the process of mapping the digital information to analog form so it can be transmitted over the channel. For an OFDM system the changing of phase and amplitude can be done but the frequency cannot change because they have to be kept orthogonal. The constellation mapper implemented in FPGA can take symbols as inputs and map them to appropriate constellation points as dictated by the modulation method specified. Every two bits generated by the LFSR block are mapped using the QPSK constellation. The In-phase and Quadrature signals are generated from the first and the second bits respectively according to Table I. The four coding values are stored in a ROM memory block. The block diagram of QPSK mapping is depicted in Fig. 2.

TABLE 1:*QPSK I and Q Values*

B0	In Phase	B1	Quadrature
0	0.707	0	-0.707
0	0.707	0	0.707
1	-0.707	1	-0.707
1	-0.707	1	0.707

C *I*FFT/FFT

Since an OFDM symbol can be defined by an IFFT, the mathematical model of an OFDM symbol to be transmitted is given by:

$$x_n = \frac{1}{N}\sum_{x=0}^{N-1} X_k e^{(2\pi jnk)}/N \qquad (1)$$

The IFFT and FFT block forms the heart of the modulator and the demodulator respectively. The Xilinx Fast Fourier Transform (FFT) 7.1 was employed for performing the operations. This block implements the Cooley-Tukey FFT algorithm, a computationally efficient method for calculating the Discrete Fourier Transform (DFT).

The FFT core used was 16 point, Radix-2, Decimation in Frequency (DIF) method for pipelined streaming input output architecture. The pipelined streaming input output architecture facilitates continuous data processing wherein input data and output results are continuously fetched in and out respectively. Fig. 3. shows an example of IFFT implementation model.

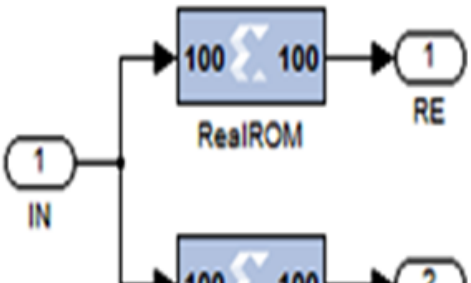


Fig. 2. QPSK Mapping Model

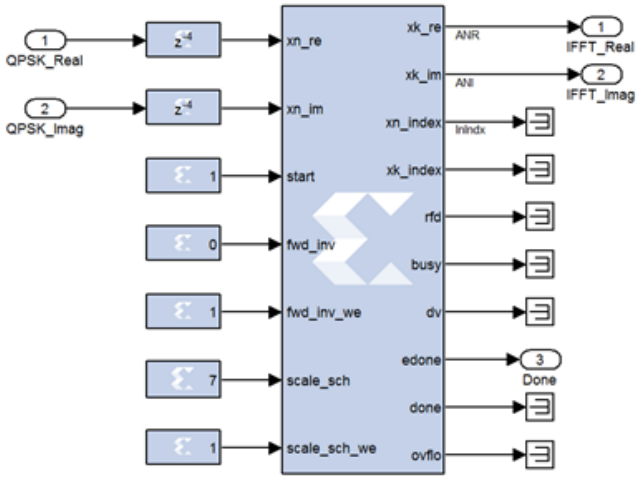


Fig. 3. IFFT Implementation Model

D *Q*PSK Demapper

To recover the sub carriers a Matlab code is inserted using Xilinx MCcode block. This block executes the MCode to calculate block outputs during simulation.

During hardware generation the code is translated to equivalent High Definition Language code. Demodulation is achieved by comparing I and Q values with predefined detection boundaries and assigning location nearest to the constellation.

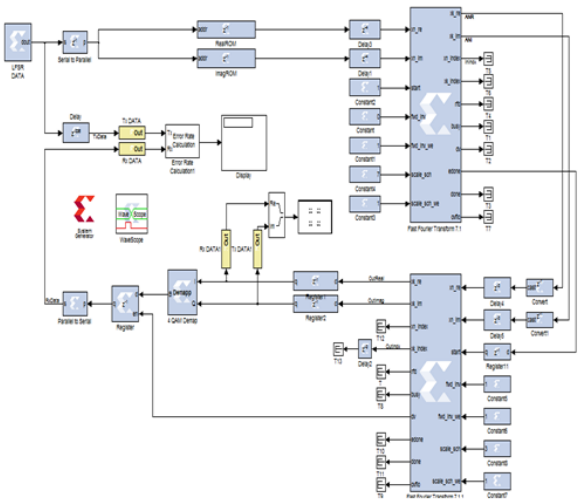


Fig. 4. OFDM Transceiver Model

E *T*he OFDM Transceiver

The proposed System Generator model of the OFDM transceiver is as depicted in Fig. 4.

IV. SIMULATION RESULTS

The simulation results were plotted in terms of performance of the OFDM system, that is Bit Error Rate (BER). The modulation techniques of BPSK, QPSK and 8-QAM were used to see the tradeoff between system capacity and system robustness. The standard BER that was used to determine the minimum performance of the OFDM system is minimum BER for voice transmission system i.e. 10-3. The BER v/s SNR plot in AWGN channel is depicted in Fig. 5.

The constellation diagram at the receiver of the QPSK modulated OFDM model for Signal to Noise Ratio (SNR) of 2dB, 10 dB, 20dB and 30dB is depicted in Fig. 6. It can be seen very clearly that the scatter plot converges to the original signal as the SNR is increased. This indicates that the BER using low SNR is high as compared to the channel using a high SNR. The cluster in case of a low SNR is very random as observed in case of a channel having SNR of 2dB. But the cluster slowly converges having 4 points on it with a very high SNR i.e. in this case SNR=13dB. This cluster diagram analysis is in line with the BER v/s SNR plot shown in the Figure 6 where it can be observed that the channel needs SNR of at least13dB to have a BER of less than 10-3.

Fig. 7. shows the performance of the OFDM signal in the Fading channel versus that in a normal AWGN channel. The fading channel used in the above case is that of the Rayleigh Fading Channel. The modulation used in this case is the QAM

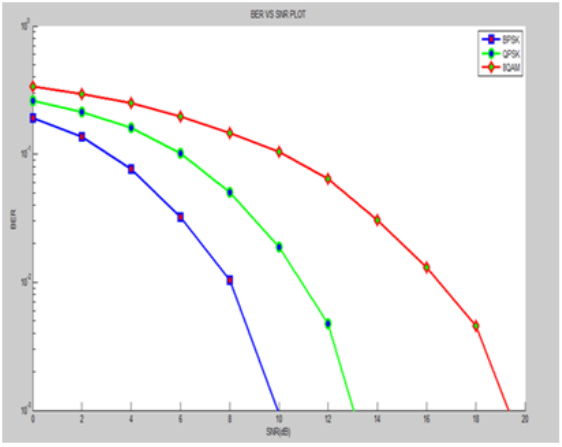


Fig. 5. BER v/s SNR Plot for OFDM in AWGN Channel

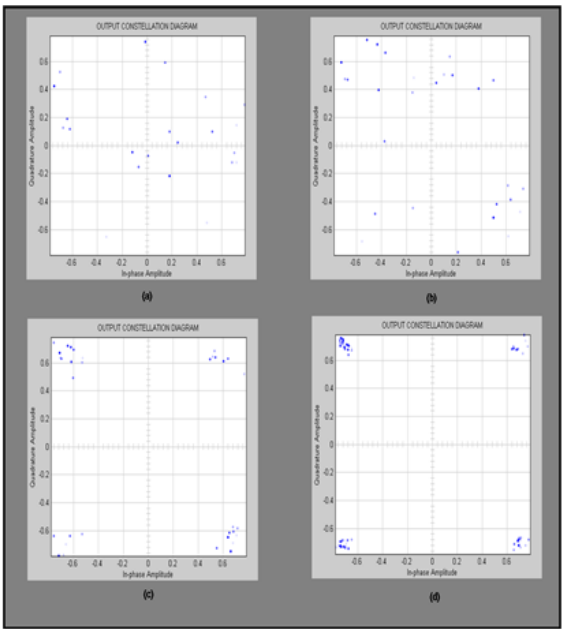


Fig. 6. Constellation Diagram for QPSK Modulated OFDM for(a) SNR=2dB (b) SNR=10dB (c) SNR=20dB (d) SNR=30dB

modulation. It is very much evident from the graph that OFDM is very much tolerable to the fading effect in the channel. To achieve a BER of 10-3 in a fading channel approximately a SNR of 21dB is required. In case of a normal channel that SNR value is around 19dB. So we can see even if the channel characteristic is changing drastically the SNR requirement is not much affected. Only an additional 2dB is required. So it is evident that OFDM scheme is very robust to the channel fading effects like Rayleigh fading or frequency selective fading.

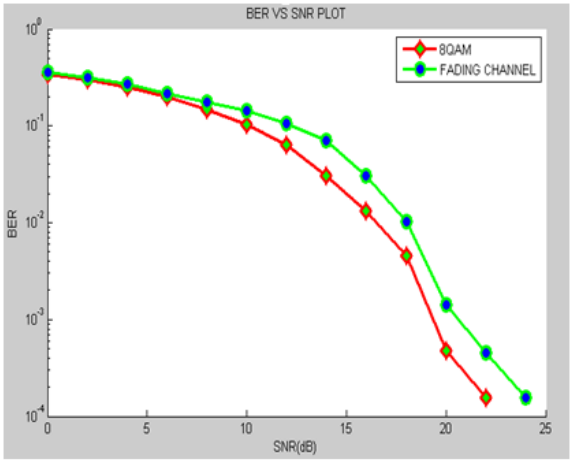


Fig. 7. BER v/s SNR Plot for OFDM in Fading Channel

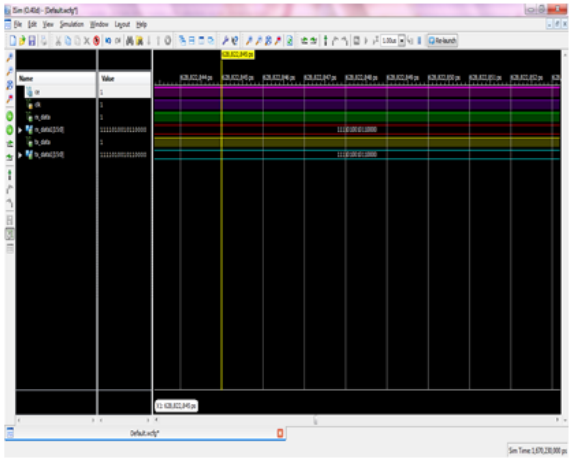


Fig. 9. Simulation Result in ISim

V. HARDWARE VERIFICATION

The functionality of the System Generator design is verified via simulation by using Xilinx ISE 14.7 inbuilt simulation tool ISim. The simulation result as observed in the wavescope of System Generator and ISim is depicted in Fig. 8. and Fig. 9. respectively.

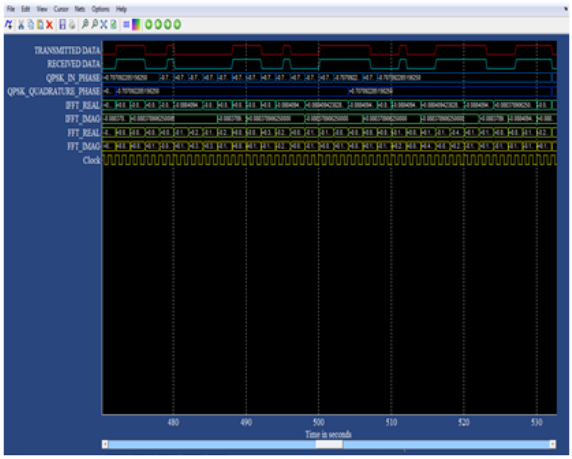


Fig. 8. Output waveform observed in wavescope

It is observed that the ISim simulation results exactly match those obtained in System Generator thus verifying the functionality of the design.

VI. RESULTS

The proposed method applied on selected images. In some of the images OD failed to segmented properly and in some images proposed method fails to segment OD properly.

The transceiver system modeled in Xilinx System Generator is compiled into FPGA configuration bitstream. Xilinx iMPACT tool is invoked to configure the FPGA with the bitstream thus generated. The iMPACT tool detects the devices in the JTAG chain attatched to the board. Once the device has been detected the appropriate bit file generated by Xilinx ISE 14.7 is selected and downloaded to the FPGA to configure it with the design. The result as observed on the oscilloscope is shown in Fig. 10. It is observed that the transmitted and received signal matches exactly thereby verifying the hardware design.



Fig. 10. Output waveform observed in oscilloscope

REFERENCES

[1] X. Jinsong, L. Xiaochun, W. Haitao, B. Yujing, Z. Decai, Z. Xiaolong, W. Chaogang, Implementation of MB-OFDM Transmitter Baseband Based on FPGA, in 4th IEEE International Conference on Circuits and Systems for Communications (ICCSC 2008), 2008, 26-28 May 2008, pp. 50-54.

[2] M. Santhi, M.S. Kumar, G. Lakshminarayanan, T.N. Prabakar, Design and implementation of pipelined MBOFDM UWB transmitter backend modules on FPGA in International Conference on Computing, Communication and Networking, (ICCCn 2008), 18-20 Dec. 2008, pp. 1-6.

[3] M. A. Mohamed, "FPGA-BASED DESIGN OF OFDM SYSTEM", the Mediterranean Journal of Computers and Networks, Vol. 7, No. 1, pp: 163-170, 2011.

[4] J. Garcia, R. Cumplido On the design of an FPGA-Based OFDM modulator for IEEE 802.11a, in 2nd International Conference on Electrical and Electronics Engineering, 7-9 Sept. 2005, pp. 114 117.

[5] M. Helaoui, S. Boumaiza, A. Ghazel, and F. M. Ghannouchi, On the RF/DSP design for efficiency of OFDM transmitters, IEEE Trans. Microw. Theory and Tech., vol. 53, no. 7, pp. 2355-2361, Jul. 2005.

[6] C. Dick and F. Harris , FPGA Implementation of an OFDM PHY Signals, Systems and Computers, 2003. Conference Record of the Thirty-Seventh Asilomar Conference, vol. 1 , pp. 905909, Nov. 2003.

[7] R. Van Nee, R. Prasad, OFDM For Wireless Multimedia Communications, Artech House Publishers, 2000.

[8] Xilinx, System Generator for DSP, User Guide, $www.xilinx.com/support/documentation/sw_manuals/xilinx14_1/sysgen_user.pdf$

[9] Virtex 5 platform FPGAs: detailed description $www.xilinx.com/support/documentation/data_sheets$



Maj K Sandeep received the B.E (Electrical and Electronics Engineering), Bharathiar University, India. (2003) and Currently pursuing M Tech in Radar and Communication Engineering Serving in the Corps Of Electrical and Electronics Engineering, Indian Army.His area of research is Prototyping of DSP Applications in FPGA, Embedded System Development



Abhilash M T is M.Tech in VLSI Design from SRM University, Tamil Nadu (2005). He is presently working as Assistant Professor in the Department of Electronics Engineering, Defence Institute of Advanced Technology (Deemed University), Pune and has a vast teaching and research experience of 8 years. He has published 07 papers in refereed journals and conferences. His research area includes prototyping of DSP Applications in FPGA, Embedded System Development, VLSI and MIMO Radar. He has been conferred with the Summer Research Fellowship 2010 by Indian Academy of Science.

Constraint Weldment of Austenitic Stainless Steel – Strain Development at Weld Fusion Zone and its Control

Lt Cdr Ramandeep Singh Sawhney1,Vivekanand Kain[2], SP Srivastava[3]
[1,2,3]HBNI, Bhabha Atomic Research Center (BARC)
Mumbai, India
[1]raman_gladiator@yahoo.co.in, [2]vivkain@barc.gov.in

Abstract— Intergranular stress corrosion cracking (IGSCC) is a common cause of failure/degradation in the primary side of nuclear reactors. It has been shown that the strain developed at the weld fusion zone – base material interface in the weldments makes that zone (a few hundred micrometer wide) very hard. This is due to the plastic deformation occurring at this zone during the cooling stage, after the welding in constraint geometry especially during the last welds in core shroud/any other closed structure. This hard zone has been shown to be responsible for IGSCC in nuclear reactors even in a non-sensitized structure. One option for reducing hardness/strength of such welds is to reduce heat input during welding and opt for narrow gap welding (NGW). With advent of new techniques like electron back scatter diffraction (EBSD) and application of very low loads during hardness testing (1 gf), it is now possible to characterize this narrow, strained zone at the weld interface. This paper reports welding of austenitic stainless steels using gas tungsten arc welding (GTAW) as well as narrow gap welding, under constraint geometry, and characterization of the microstructure, hardness and strain, especially at the weld fusion zone – base material interface. The constraints during welding lead to a peculiar condition of development of (up to 20%) plastic strain during the stage of cooling (after the welding operation). The paper finally illustrates the comparative advantage of NGW in terms of lower strains developed and heat input as compared to manual welding procedure and its advantage in terms of lower susceptibility to IGSCC in reactor operating conditions.

Keywords—austenitic stainless steel; intergranular corrosion; weldment; manul weld; narrow gap weld; strain

1. Introduction

The first major occurrence of intergranular stress corrosion cracking (IGSCC) in the heat affected zone (HAZ) of welded Type SS 304 stainless steel (SS) piping occurred in 1970's, after a few years of operation of boiling water reactors (BWR). Initially the cracks were observed in small diameter piping but subsequently such cracks were observed in larger diameter piping and although these cracks were not safety related, they had an impact on the availability, operating costs, radiation exposure for inspection and repair and the anticipated design life [1]. The degradation of structural materials due to corrosion and corrosion-enhanced processes has been a factor affecting the plant availability, cost, and safety of nuclear power plants. The operating nuclear power reactors of different type's viz. BWRs, pressurized water reactors (PWRs), and pressurized heavy water reactors (PHWRs) have different sets of corrosion degradation problems. Intergranular stress corrosion cracking (IGSCC) is a common cause of failure/degradation in the primary side of nuclear reactors. There have been extensive IGSCC incidents of 300 series SS in BWR environments. This cracking is associated with the weld heat affected zone (HAZ) and in regions of relatively high corrosion potential (~ +200 mVs SHE). Weld induced sensitisation in the HAZ was identified as the primary reason for IGSCC in the austenitic stainless steel components in BWR environment. Improvement in the materials specifications (use of nitrogen added SS like type 316 NG) and tight control over operating water chemistry (lowering of impurity levels, hydrogen water chemistry etc.) helped to circumvent this problem to a large extent. Cracks in welded core shrouds have been detected after approximately 9 years of hot operation and include areas in a fluence range of 1 x 10^7 to 1 x 10^{21} n/cm^2. Metallographic failure analysis of cracked L-grade internal components have revealed that these failures are intergranular, do not always show irradiation damage and contain a high degree of deformation in the near surface regions. Detailed microstructural characterization indicated that most L-grade materials are not thermally sensitized [ref Angeliu]. Since sensitization is not always present, other fundamental aspects of the cracking behaviour, such as deformation and high potential were probed. Microstructural characterization conducted on a section of 304L vertical core shroud weld HAZ material obtained from the Grand Gulf Nuclear Station that was never put into service when subjected to local strain measurement showed that up to 10% residual strain existed in this component and is attributed to weld shrinkage strains [2]. Such non-sensitised grades of SS have also cracked due to IGSCC in BWR operating conditions which was attributed to the residual strains adjacent to the weld. Controlled laboratory experiments have shown that even solution annealed SS also show IGSCC in BWR simulated environment though the CGR is too low to be of consequence for a design life of 40-60 years.

The high coefficient of thermal expansion and low thermal conductivity of austenitic stainless steel is known to cause distortion in weldments. Therefore, fixtures are used during welding to obtain design dimensions/geometry. In many cases, the last welds to be prepared (e.g. last weld in welding a cylinder e.g. the core shroud) have constraint. The constraints during welding lead to a peculiar condition of development of up to 20% plastic strain during the stage of cooling (after the welding operation). The strength of this strained region in the weldment increases (corresponding to 20% strain in a material) due to work hardening. This work hardening takes place when the weldment cools fast from temperatures close to melting point and then transitions slowly at temperatures below 200 ^{0}C. It has been shown that the strain developed at the weld fusion zone – base material interface in the weldments makes that zone (a few hundred micrometer wide) very hard hence it has higher residual stresses also. This hard/strong region of the material is known to have much higher susceptibility of IGSCC in reactor operating conditions. Such IGSCC cases have also been observed in nuclear power plants (primary circuit components – especially in boiling water reactors (BWR's). One option for reducing hardness/strength of such welds is to reduce heat input during welding and opt for narrow gap welding (NGW). With the advent of new techniques like electron back scatter diffraction (EBSD) and application of very low loads during hardness testing (1 gf), it is now possible to characterize this narrow, strained zone at the weld interface. The information on the extent of advantage offered by NGW in terms of strain development is rather limited and no detailed studies on this aspect are available in literature. Most of the emphasis in NGW has been on reduction in degree of sensitization in the heat affected zone (HAZ).

Therefore, the primary objective of the present study is to prepare welds of stainless steel grades 316L and 304L by manual and narrow gap welding (NGW) techniques using gas tungsten arc welding (GTAW) procedure and compare the extent of hard zones developed. The welding procedure specifications (WPS) for both types of welding were prepared following which welding was carried out in constraint condition. The microstructure characterization was done using optical microscopy, for identifying and quantifying the hard/strong region at weld interface, microhardness mapping was done using a technique that applies low loads (10 mN)and strain distribution was obtained using electron backscatter diffraction (EBSD). EBSD is able to establish strain distribution within grains as well as in the narrow zone of a few hundred micrometers. The correlation of the strength of stainless steel and its susceptibility to IGSCC under reactor operating conditions would be taken from literature/lab data and extended to establish advantage of NGW in terms of crack growth rates (IGSCC) under nuclear reactor operation conditions.

2. Experimental Procedure

2.1 Materials

The materials used for study are type 316L and 304L stainless steels and were obtained in the form of plates of 30 mm and 26 mm thickness for SS 316L (1500 mm x 600 mm x 30 mm) and SS 304L (1500 mm x 600 mm x 26 mm) respectively. A small block (50 mm x 30 mm) was cut from the corner of each of the plates for carrying out initial material characterization studies. The chemical composition of both the grades is given in table 1.

2.2 Metallographic preparation and microscopic examination

Metallographic preparation and etching was done for annealed (as received), sensitised (675°C, 1 h) base materials and the final manual and narrow gap welded coupons of both the material grades in order to observe their microstructure. Small specimens were cut and they were polished using 80, 120, 240, 320, 400, 600, 800, 1000 grit emery papers and were subsequently polished using 1 μm diamond polishing paste. Electrolytic etching was done in 10 % oxalic acid as per ASTM standard A262, Practice A (ASTM A262) [3]. The polished specimen was etched at 1 A/cm2 for 90 seconds. Subsequently microstructural examination was done using an optical microscope and images were recorded.

2.3 Microhardness measurements

Microhardness was measured across the thickness of the cut sections of SS 316L (50x30x30) and SS 304L (50x30x26) of as received material and along the weld fusion zone of the finished manual and narrow gap weldments in order to estimate the strain across the thickness. Microhardness readings on as received materials were measured at a load of 300 gf and 25 gf both for an indenter dwell time of 15 seconds. However, for readings in the weld fusion zone of both type of weldments, a load of 25 gf was maintained for 15 seconds. The microhardness was measured using Vicker's indenter. The microhardness readings for the base materials were measured at an interval of 0.5 mm on the cut samples (50 mm x 30 mm) and for the weldments the interval was kept between 150 to 200 μm.

2.4 DL-EPR tests

The electrochemical potentiokinetic reactivation (EPR) tests were done to assess the degree of sensitisation (DOS) of both types of SS in annealed (as received) and sensitised (675°C, 1 hr) conditions. All the test pieces were taken from the mid-thickness sections of the plates. A stainless steel wire contact was made on one side of the specimen and then it was mounted, using a cold setting resin, to expose only one face to the solution.

The gap between the mount and the sample were filled with a lacquer to eliminate crevice effects. An insulating sleeve was used to electrically isolate the wire from the test solution. The DL-EPR test was carried out at room temperature using a solution of 0.5M sulphuric acid and 0.01M potassium thiocyanate. The solution was deaerated by purging with high purity argon for 1 h prior to and during testing. A three electrode system was used for this purpose where the sample was the working electrode, platinum was the auxiliary electrode and a saturated calomel electrode (SCE) was the

Table 1 Chemical composition (in wt %) of SS used for study.

Element	C	S	P	Mn	Si	Cr	Ni	Mo	N	Other elements
SS 316L	0.035	0.002	0.028	1.15	0.75	17.42	10.17	2.58	0.0355	Cu-0.15, B-0.0072, Ti-0.0055, W-0.024, Co-0.23, Nb-ND*
SS 304L	0.01	0.006	0.019	1.66	0.75	18.98	10.20	0.035	0.06	Cu-0.002, B-0.0026,Ti-0.0052,W-0.02, Co-0.044, Nb-ND*

* ND – Not Detected

reference electrode. A potentiostat was used for carrying out the test. A potential scan rate of 100 mV/min was applied from -450 mV_{SCE} to +300 mV_{SCE} and back. After the test the sample was examined under the optical microscope and images were acquired. The DOS was determined from the ratio of the maximum current in the reverse (reactivation) loop (Ir) to the maximum current in the forward loop (Ia) multiplied by 100 [4].

2.5 Magnetic measurement using ferritoscope and WRC-1992 diagrams for predicting δ-ferrite levels

The ferrite content in each of type (316L and 304L) SS was found on the polished surface of as received sample cut material. Readings were recorded at various locations using a portable ferritoscope at room temperature on the surface and across thickness sections and their average values were taken. The nickel and chromium equivalents for WRC-1992 diagram were calculated using the formulae and the results were represented on the diagram [5,6].

$$Ni\ (eq) = Ni + 35C + 20N + 0.25Cu \quad (1)$$

$$Cr\ (eq) = Cr + Mo + 0.7Nb \quad (2)$$

2.6 Weld Design and Fabrication

The complete weld design and fabrication including the non destructive testing (NDT) and mechanical testing of manual and narrow gap welds of both the grade of materials was carried out at Centre for Design and Manufacturing (CDM), BARC. This process comprised of a detailed study of ASME section IX in order to understand and incorporate the procedures given in the code and also to ascertain the dimensions of the weldment coupons to be made of both manual and narrow gap GTAW for both (316L and 304L) grade of materials. The main focus during this study was on the Weld Procedure Specifications (WPS), Procedure Qualification Record (PQR) and Weld Procedure Qualification (WPQ) i.e. the type of mechanical specimens required for qualifying the weld along with the metallurgical test specimens so as to confirm the final dimensions of the plates to be welded keeping in mind the machining allowances for all type of specimens. A brief description of the developed WPS, PQR and WPQ will be reported [7].

2.6.1 Weld Edge Preparation

A computer aided design (CAD) was generated for the weld edge preparation / joint configuration of each type of welds (manual and narrow gap) for both type 316L and 304L grade of materials. The geometry of edge preparation used for manual GTAW weld was chosen to be single 'V' groove type with an included angle of 70º with 2 mm root gap and landing in order to obtain maximum strain in the constraint geometry welds. However, for narrow gap 'J' groove type geometry with multiple included angles (16º and 5º), 1 mm x 45º chamfer at the top edge and 2 mm root gap was chosen.

2.6.2 Stiffeners

As the aim was to achieve a constraint geometry weldment, in order to simulate last welds in a core shroud or in any cylindrical structure used in a nuclear reactor, the same was achieved by tack welding of stiffener plates on the back side of SS 316L and SS 304L plates to be welded for both manual and narrow gap type of welds. SS 304L plate of 18 mm thickness was chosen to be the material for stiffener plates. The elastic section modulus was calculated for stiffeners, which is defined as S = I / y, where I is the (or moment of inertia) and y is the distance from the neutral axis to any given fibre [8]. It is often reported using y = c, where c is the distance from the neutral axis to the most extreme fibre,. It is also often used to determine the yield moment (M_y) such that $M_y = S \times \sigma_y$, where σ_y is the yield strength of the material. The section modulus of each stiffener plate was calculated neglecting the effect of purging groove machined on one of the sides and it came out be 14700 mm^3, which is a measure of the resistance to bending deformation. This calculation was done in order to know how much constraint is being applied for the manual and narrow gap welding processes. A total of five stiffener plates were used for manual weld and seven for the NGW of both the materials. The plates were tack welded at equidistant locations (70 mm for manual and 75 mm separation for narrow gap) in the longitudinal direction and similar platforms were used for carrying out welding of each of the type 316L and 304L SS manual and narrow gap welds.

2.6.3 Welding

Welding of SS 316L and SS 304L plates in the required dimensions was carried out after the edge preparation for both manual and narrow gap type of welds under constraint by making use of stiffener plates. The welding process employed for both type of welds was GTAW and it was carried out as per the WPS along with the vast experience of qualified welders of CDM, BARC. A range of weld parameters were recorded during the process which would enable us to find out the amount of heat input during each of the welding procedures and also helped the welders to emulate the same set of parameters for both the grade of materials. A photograph of welding in progress is shown in Figure 1.

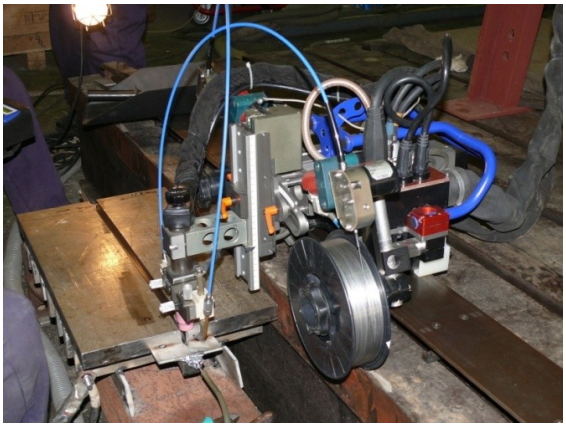


Fig.1 Shows the narrow gap welding set up with the automated machine traversing on its path

2.6.3.1 Manual Welding

The manual welding was carried out by an experienced and qualified welder. The chemical compositions of filler materials used corresponded to type 308L for welding SS304L plates and type 316L for welding type 316L plates.

2.6.3.2 Narrow Gap Welding

The narrow gap welding was fully automated and required a technically sound and well qualified welder to program the machine software as per the need whilst welding is being carried out. The machine is mounted on a mobile platform which can move over a railing. It is more involved and advance technique which leaves hardly any chance of a defect and gives a much cleaner weld. The same welding filler wires were used for NGW as used for manual GTAW.

2.7 Material and weld qualification tests

Various material and weld qualification tests were carried out using nondestructive testing techniques (for detection of any flaw in the base material or lack of fusion defects in the as prepared welds) and mechanical tests were carried out as per ASME guidelines in order to qualify the weld integrity and strength.

2.7.1 Non destructive tests

The various non destructive tests carried out included Dye Penetrant Test (DPT), Ultrasonic Test (UT) and Radiography Test (RT).

2.7.2 Mechanical Tests

Two types of mechanical tests viz. tensile and side bend test were carried out for all the welded specimens and the test specimens (tensile and side bend) were extracted and prepared as per the plan and specifications given in ASME section IX.

2.8 Metallurgical tests

The metallurgical test specimens were removed from the defect free zone only after the weldments had qualified the NDT and mechanical tests as per the ASME guidelines and there after the metallurgical test specimens were prepared as per requirement for carrying out optical microscopy, microhardness and strain measurement using EBSD technique. A 3mm thin and 90 mm long slice of the welded coupon was extracted with keeping the weld at the center. For all the metallurgical tests the welded coupon was divided into three zones, top, middle and root part across the weld fusion zone – base material interface for ease of characterisation studies.

2.8.1 Metallographic analysis and optical microscopy

The welded coupons extracted as explained in para 2.8 were initially polished as per procedure given in para 2.2.The polished specimen was etched at 1 A/cm^2 for 90 seconds.. Subsequently microstructural examination was done using an optical microscope and images were recorded at 200X. Optical microscopic analysis was carried out especially at the interface of the weld metal and the base material by moving some distance into the base metal. The analysis was carried out in three different zones as explained in para 2.8

2.8.2 Microhardness mapping of welded specimens

The microhardness analysis of all the welded (manual and narrow gap) specimens was done in as polished (upto 1μm) and oxalic acid etched condition by the procedure explained in 2.8.1. Testing was initially done by a coarse microhardness testing machine at a load of 25 gf for a dwell time of 15 seconds in the zones explained in para 2.8 and readings were recorded.

2.8.3 Strain characterisation by EBSD

The weld HAZs were examined using a recently developed electron back scattered diffraction (EBSD) pattern technique that quantifies residual plastic strain by measuring the amount of intra-grain misorientation [9, 10, 11]. The weld sample was initially polished as per procedure given in 3.4.1 upto 1 μm finish and was then cut into three parts (top, middle and root). The three cut parts were then subsequently electro polished in a solution of 10 ml of perchloric acid in 90 ml of methanol at a temperature of -30 °C and 15 V. The EBSD measurements were done in Nova SEM at IIT, Powai. In the present root scan, area taken was 7.744 mm (y-axis) by 2.559 mm (x-axis) with a FPS (Frames Per Second) of 303 at 120X

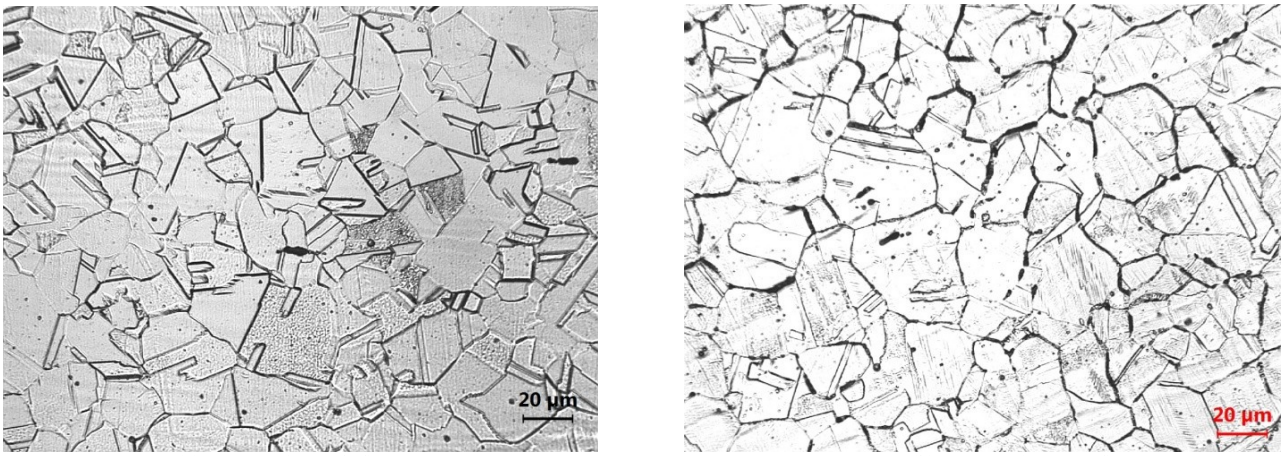
magnification. During all the scans beam energy was kept constant on 20Kv at 20 deg angle of incidence to the sample surface. The scans were then analysed using IPF (Inverse Polar Figure) maps and a plot for variation of GOS (Grain Orientation Spread) values averaged over each scan width with distance from the weld fusion line was prepared. The GOS values obtained were then equated to percentage strain by using a linear relation obtained from literature data.

3. Results and Discussion

3.1 Metallographic and microscopic examination of base materials

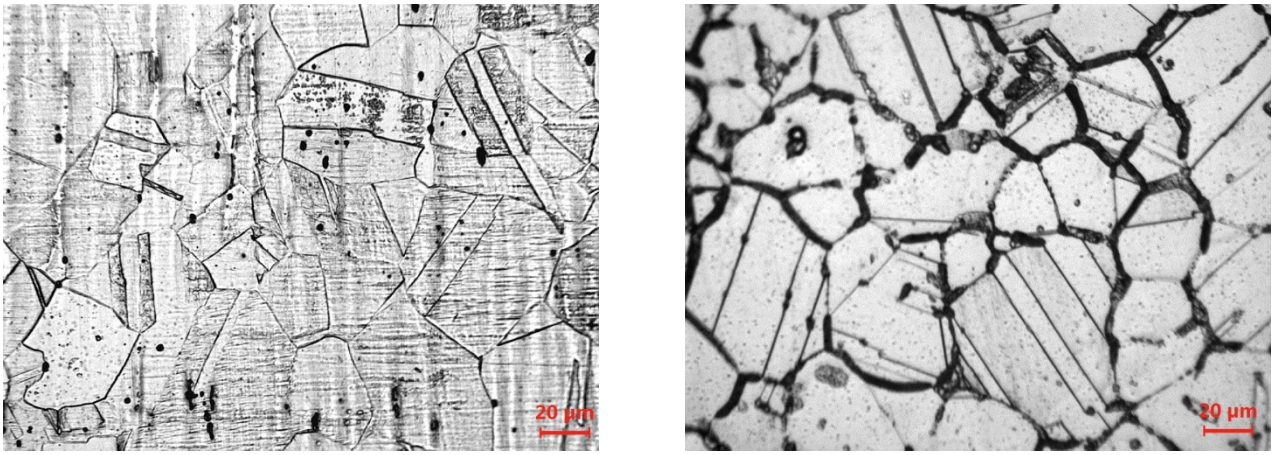
.

The microstructure of each grade of base material in annealed as well as sensitised condition is shown in Fig. 2 and 3 for SS316L and SS304L respectively. The annealed base materials showed "step" structure while both showed "dual" structure after heat treatment which was meant to simulate the worst microstructure developed after welding in the HAZ. A 3-D figure was made by carrying out microstructural analysis on three different faces of the cut sample in order to depict the direction of flow lines for both SS 316L and 304L grade of materials and are shown in fig. 4(a) and (b) in order to ascertain the direction of cutting and hence welding of plates in the direction along that of the flow lines.



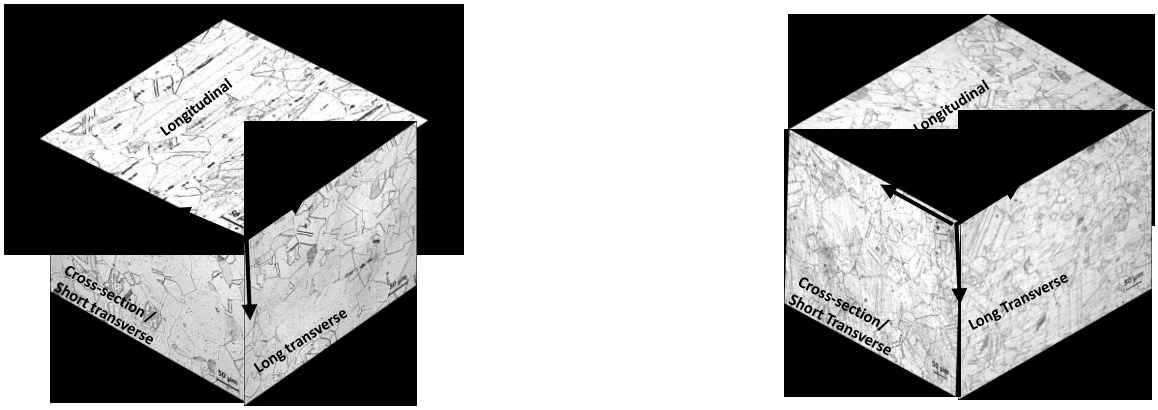
(a) SS 316L (annealed) *(b) SS 316L (sensitised)*

Fig.2 *Oxalic acid etched microstructure at 200x magification depicts (a) a step structure for annealed and (b) a dual structure for sensitised SS 316L*



(a) SS 304L (annealed) *(b) SS 304L (sensitised)*

Fig.3 *Oxalic acid etched microstructure at 200x magnification depicts (a) a step structure for annealed and (b) a dual structure for sensitised SS 304L*



(a) SS 316L ***(b) SS 304L***

Fig.4 *(a) and (b) shows three dimensional figures of SS 316L and SS 304L plate cut section in annealed condition showing the direction of flow lines in the longitudinal plane*

3.2 Microhardness measurements of base material

Microhardness in both the base materials was found to be below 190 HV when measured at a load of 300 gf for a dwell time of 10 seconds, which implies that the materials are soft and properly solution annealed.

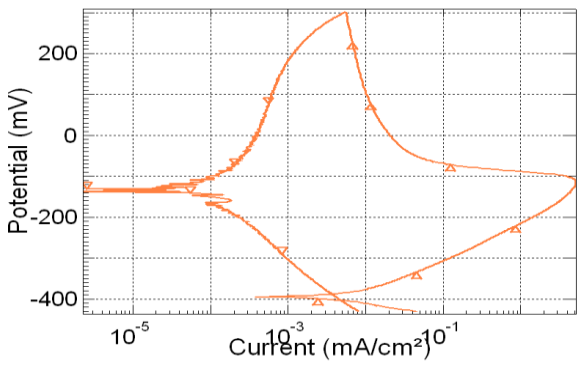
3.3 Evaluation of sensitisation behaviour (DOS)

The EPR graphs received for each grade of material are given in fig. 5. The DOS values were nil and 0.74 for annealed and sensitized SS316L and 0.019 and 2.04 for annealed and sensitized SS 304L. These DOS values indicate that the base materials were in proper annealed condition while the worst microstructure that would develop after welding would have much lower degree of sensitization for SS316L compared to that in SS 304L.

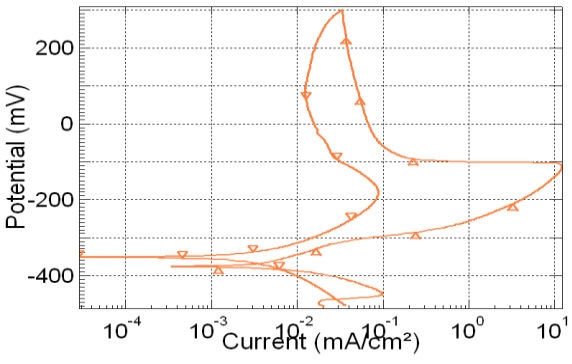
3.4 Evaluation of base material ferrite content

Readings were recorded at various locations using a portable ferritoscope on the surface and across thickness sections of both the base materials and their average values were found be 0.6% for SS 316L and 0.3% for SS 304L respectively. The Nickel and Chromium equivalents for WRC-1992 diagram were obtained by substituting the elemental values of base material and weld filler wire composition in the equations 1 and 2. These values were plotted on the WRC-1992 diagram as shown in Fig.6. As it can be seen from figure 6 that both the points plotted for SS 316L and 304L (for autogenous welding) fall into **Area FA,** which denotes primary solidification as ferrite with subsequent partial transformation to austenite (slightly high Creq) representing the the favoured solidification mode.

Welds



(a)



(b)

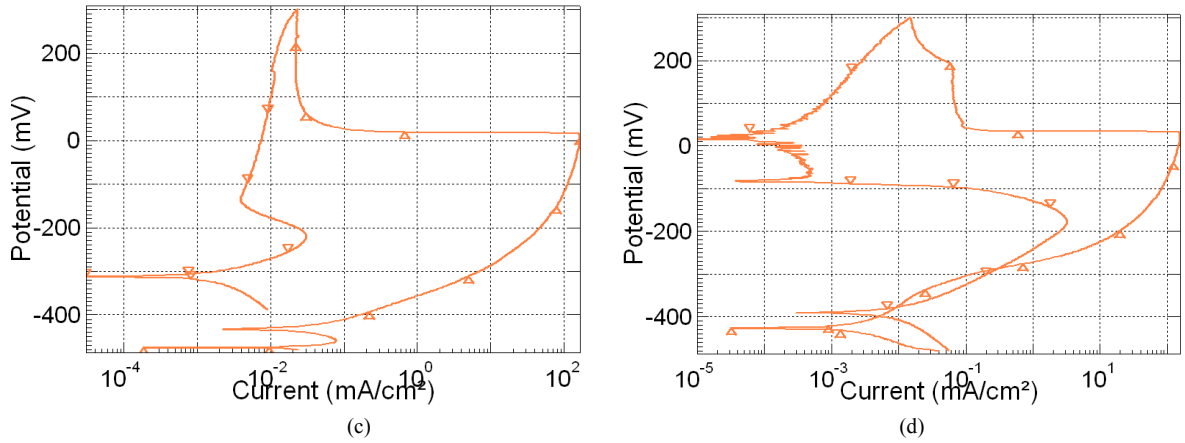


Fig.5 *(a) EPR graph for as received (annealed) SS 316L (b) EPR graph for sensitised (675°C, 1 hr) SS 316L (c) EPR graph for as received (annealed) SS 304L (d) EPR graph for sensitised (675°C, 1 hr) SS 304L*

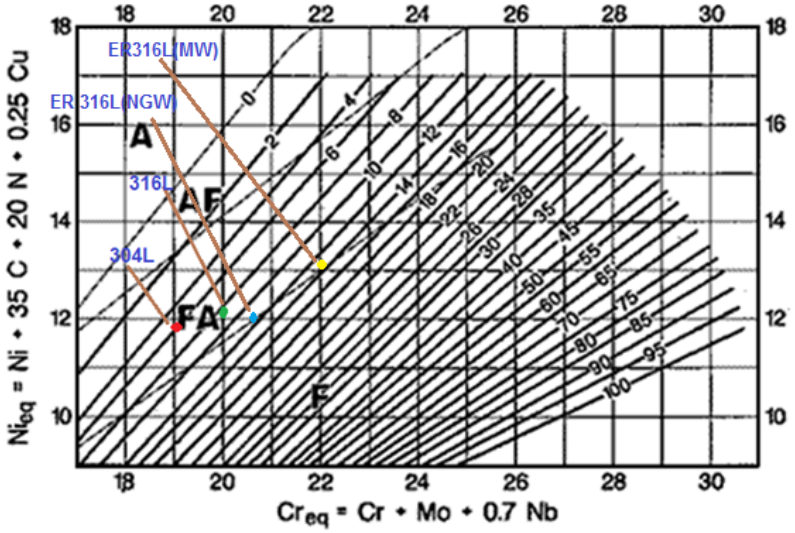


Fig.6 *The WRC-1992 diagram, identifying the plots for type 316L and 304L stainless steels as points with green and red color respectively. Yellow point shows the plot corresponding to weld filler material ER316L used for manual welding and blue is for ER 316L used for narrow gap welding.*

3.5 Metallurgical analysis of welded specimens

Weld specimens of dimension 90 mm x b mm x 3 mm (b=30 for SS 316L and b=26 for SS 304L) for manual and narrow gap welds for both the grade of materials were extracted for microstructural, microhardness and strain (through EBSD) analysis. For all the metallurgical tests the welded coupon was divided into three zones - top, middle and root part across the weld fusion zone – base material interface as illustrated in Fig. 7 (a) and (b).

3.5.1 Optical microscopy

The optical microscopic analysis was extended in the direction away from the fusion line and into the base material, especially in the zones mentioned in Fig.7, in order to observe the change in microstructural features. The start of scan at the interface has been described as 1st frame and successive scans away from the fusion line are described in terms of frame numbers giving an idea of distance from the fusion line. The scan length and width for each micrograph is approximately 500 µm X 400 µm.

3.5.1.1 SS 316L Manual weld

The optical microscopic images were recorded for all the regions shown in Fig. 7. Detailed study was carried out in all the three zones explained in paragraph 3.4. and typical microstructures from zone B (middle part) have been shown in Fig. 8. The microstructure of SS 316L near the fusion line shows huge amount of grain coarsening which may be attributed to the high heat input during the manual welding procedure. The formation of slip bands within the grains in the weld fusion zone at about 1000 µm away from the interface of weld metal (ER 316L) and SS 316L is indicative of developed strain.

3.5.1.2 SS 316L narrow gap weld

The optical microscopic images were recorded in a similar manner as for the manual weld and are shown in Fig. 9.

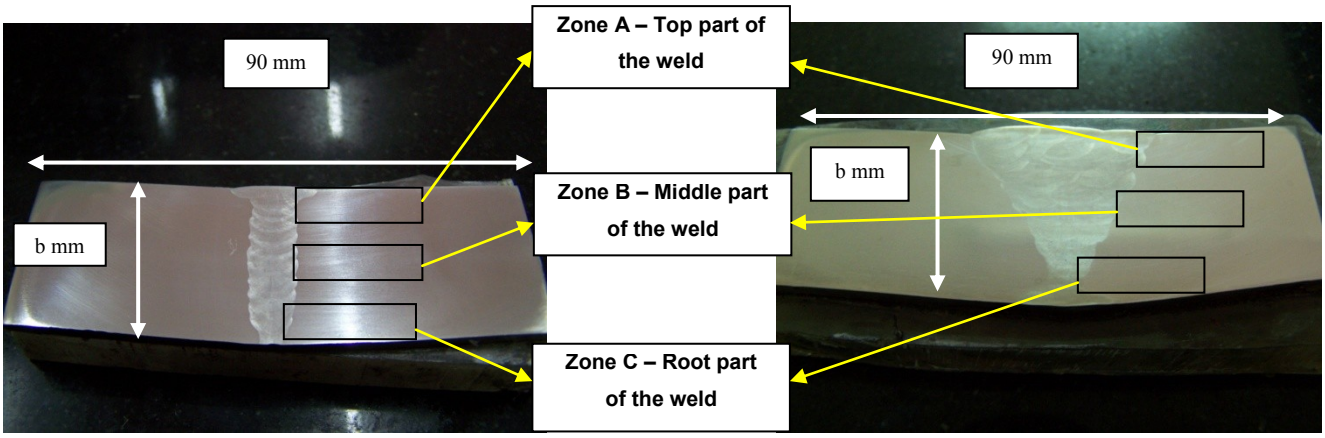
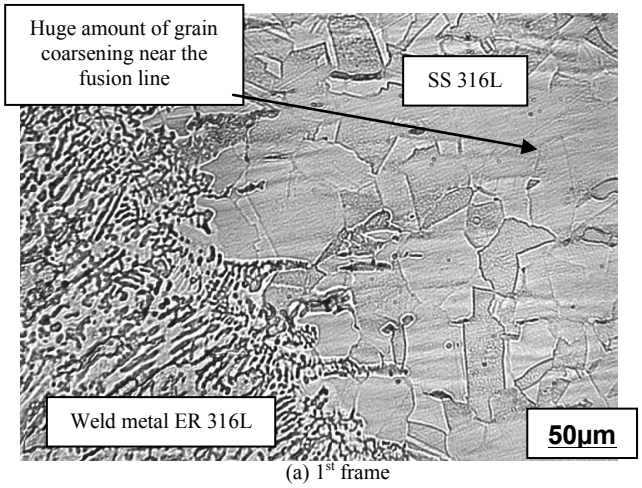
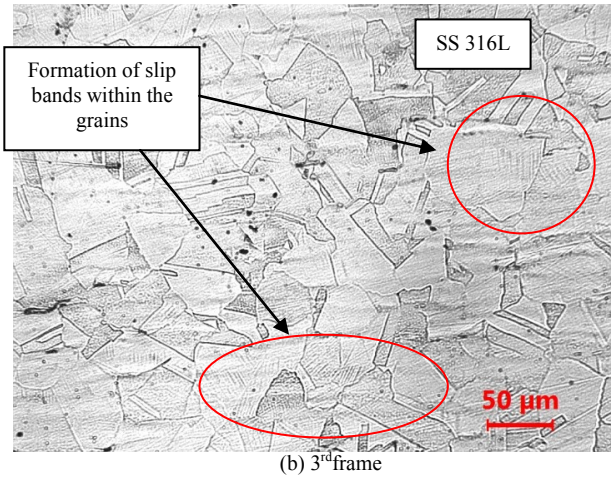


Fig.7 *Schematic of various zones of one of the SS 316L (a)) narrow gap and (b manual weldments cut section (90 mm X b mm) where the metallographic analysis was carried out.(b=30 mm for 316L and 26 mm for 304L)*



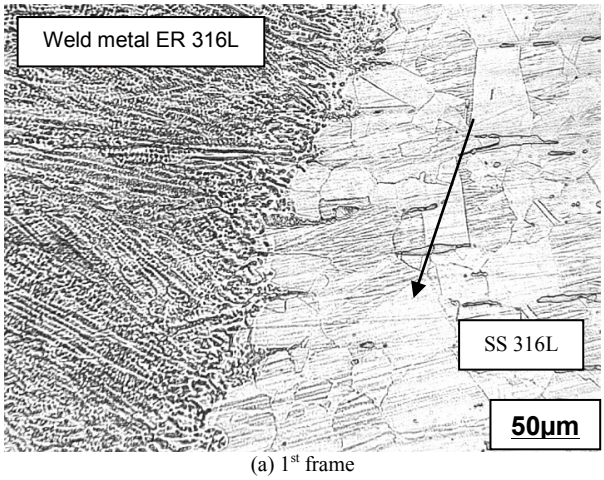
(a) 1st frame



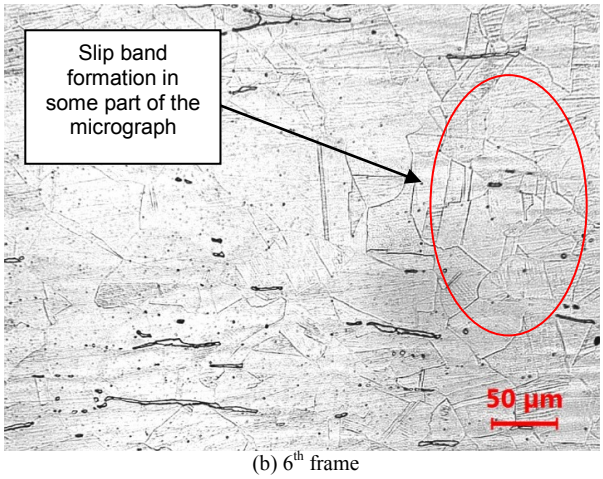
(b) 3rd frame

Fig. 8 (a) Shows microstructure of the SS 316L manual weldment at the weld fusion line (b) microstructure of SS 316L two frames (approx. 1000 µm) away from the weld fusion line showing formation of slip bands within the grains

Slight grain coarsening near the fusion line only one or two grains are effected



(a) 1st frame



(b) 6th frame

Fig. 9 (a) Shows microstructure of the SS 316L narrow gap weldment at the weld fusion line (b) microstructure of SS 316L five frames (approx. 2000 µm) away from the weld fusion line showing formation of slip bands within the grains.

Microstructural analysis of 316L manual and narrow gap welds

- Overall analysis of both welds doesn't show any sensitized region. This is due to presence of molybdenum in SS 316L which restricts the formation of carbides.
- Huge amount of Grain coarsening is seen near the fusion line in the manual weld which is comparatively less in case of narrow gap weld and is evident of higher amount of heat input in the manual welding process. For narrow gap welding, only the root part (Zone C) was seen with grain coarsening near the fusion line as the NGW root layer process involves two fusion passes (which doesn't use filler wire and only uses higher amount of heat input to melt and fuse the adjoining base metal at the root) along both the walls and one filler wire pass in between two fusion passes along the center of the root well.
- Some amount of carbide precipitation is seen in the top part (Zone A) interface of manual weld microstructure shows sensitization of area immediately next to the fusion line. However, this feature was absent for the narrow gap weld.
- The formation of slip bands within the grains is indicative of developed strain. The formation of slip bands is generally seen from 2nd to 8th frame (500 µm to 3500 µm) depending on different zones and type of welding process used. However, slip bands are also seen much away from the fusion line (18th– 22nd frame) which is attributed to the use of tack welding for fixing stiffeners to the plates to be welded in order to obtain constraint geometry.

3.5.2 Hardness analysis

The microhardness analysis carried out on the SS 316L manual and narrow gap weld fusion zone was compared with that of the base material hardness values obtained at load of 25 gf for a dwell time of 15 seconds. Approximate distance between two readings was 150 – 250 µm. The maximum hardness measured in the manual weld was 348 HV and for the NGW it was 298 HV for SS 316L.

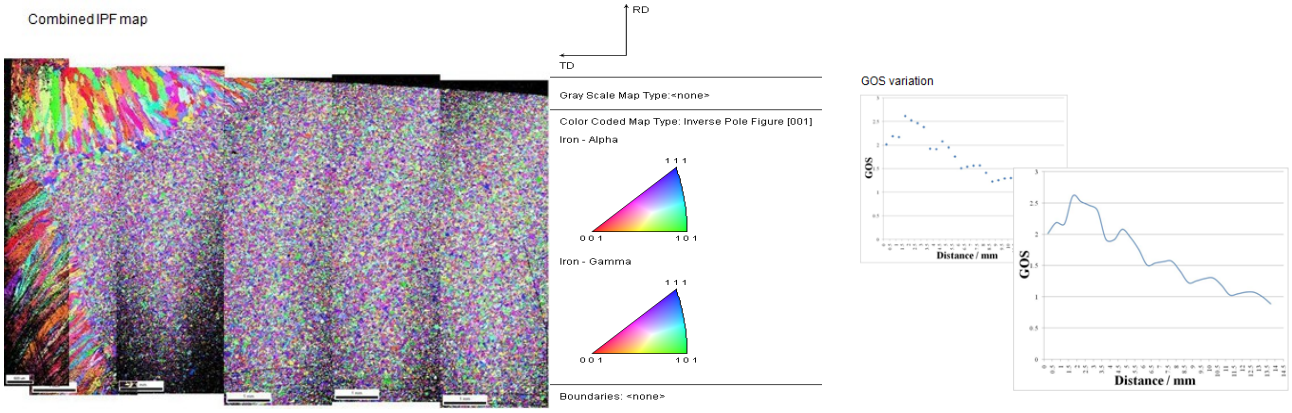
Microhardness analysis of SS 316L manual and narrow gap welds

- The microhardness analysis carried out on the SS 316L base materials at 25gf for a dwell time of 15 seconds had shown an average hardness of about 232 HV. However, the same analysis when carried out on as welded manual and narrow gap specimens along the fusion line showed higher hardness for the manual weld as compared to the narrow gap welding technique as reported above. It is clearly evident from the microhardness trend that the hardness of the base material has increased after the welding process.
- The manual weld has more hardness near the fusion zone – away from it also the values are slightly high but at interface values are much higher.NGW has values more or less close to as-received, only slight change from as-received.
- Subsequently, microhardness measurement at an extremely low load of 1gf is also being carried out for much more accurate assessment of variation of hardness along and away from the fusion line for both the type of welds.

3.4.3 Strain analysis by EBSD

The motivation for characterizing the strain in weld HAZs originated from observations that unsensitized L-grade HAZs were cracking, so what other than sensitization could be special about a weld HAZ. It is well known that welding leads to residual strain and stresses (which can be related to plastic strains [12, 13]) .Strain analysis at the weld fusion zone was carried out for all the weldments. The analysis was done for various zones as shown in Fig. 8 and a typical result for the Zone C (root part) of SS 316L manual weld coupon is shown in Fig.10. The Inverse pole figure (IPF) orientation map of the

root interface and away from the fusion line was analysed. The IPF orientation component uses a basic RGB coloring scheme, fit to an inverse pole figure. Details about this technique are available in many references [14, 15]. This map is used to assess the relative orientation across the grain which is indicative of developed strain in the microstructure as shown by the grain orientation spread (GOS) variation in Fig. 10(b). Here, grain boundaries are determined and orientation relationships within grains are analyzed. Intragranular lattice rotation is a common response of many materials to deformation. It is an expression of plastic strain where dislocation recovery has occurred, forming subcells, and if the subcell size is approximately within the spatial resolution of the SEM and EBSD system, the resultant small changes in orientation may be visualized and analyzed quantitatively. Although the degree of rotation between neighbouring pixels depends on the step size used in the EBSD grid as well as the intragranular rotation in the sample, cumulative rotations may be discerned. The coloring of pixels within grains by the degree of their rotation is with respect to a reference orientation within the grain. Quantitative strain analysis by EBSD is not yet common in the materials and geology communities, but studies have shown that this measurement is a strong indicator of degree of plastic strain in the material [8, 9]. As shown in Fig. 10, there is development of strain in the weldment and it has been mapped with distance from the weld fusion line [Fig.10 (a)] and quantified in Fig.10(b).



(a) Combined Inverse Polar Figure map

(b) microhardness profile

Fig. 10 (a) Shows the combined IPF (Inverse Pole Figure)map of the root scan carried out at the zone C of manual SS 316L weld.(b)Shows the GOS (Grain Orientation Spread) variation of the combined IPF scan with distance from the weld fusion line.

In an important and recent study carried out by Peter Andresen [17] showed, as the weld metal solidifies and cools, shrinkage strains occur, and some strain is retained after cooling. This results in a strain profile in the heat-affected zone (HAZ), with peak strains (at the root of the weld and near the fusion line) that often were in the vicinity of 20% to 25%. Cracks aligned along the HAZ exhibited high growth rates, fully equivalent to those observed in bulk cold-worked material and similar to sensitized stainless steel at high corrosion potential and higher at low corrosion potential. Over the next decade, both speculation and laboratory data were confirmed by field cracking, most notably in the large diameter BWR core shroud. In most cases, cracking occurred close to the weld fusion line where the residual strains are highest [16]. Laboratory studies also showed that higher the strength of the material, higher was the crack growth rate (IGSCC, even for a non-sensitized material) in BWR simulated environment as shown in Fig. 11 [17]. The complete EBSD strain analysis of all the zones of both manual and narrow gap weldments of SS 316L and 304L is being carried out and would be presented at the conference.

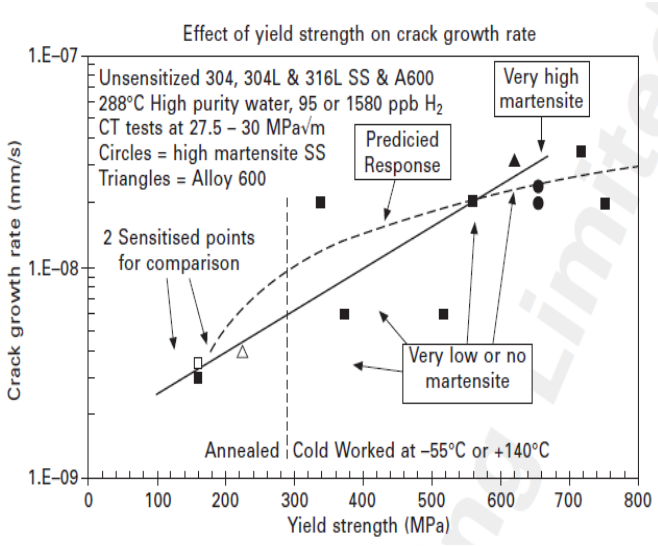


Fig. 11 Crack growth rate as a function of strength of non-sensitized stainless alloys [17].

4. Conclusions

The manual and narrow gap welds in constraint geometry were prepared as per the procedure described in ASME. Detailed microstructural, hardness and EBSD measurements done on these welds showed that strain and hardness developed in narrow gap weld was much less than that developed in manual GTAW weld. It was also shown that sensitization did not develop in welds of SS 316L and this is attributed to a fine alloy chemistry as well as the welding procedures used. Therefore, in the as welded condition, the welds are not prone to IGSCC due to low levels of sensitization. As shown by extensive studies reported in the last decade, the narrow gap weld would be much more resistant to IGSCC (even in non sensitized condition) as compared to the manual GTAW weld. Comparison of this strain in manual and NGW as evident from the microstructure and hardness analysis shows that the strain developed is much lower in case of NGW.

5. References

[1] Gordon and Gordon,1987, Horn et al., 1997 and Kondo et al., 1971
[2] T.M. Angeliu, P.L. Andresen, E. Hall, J.A. Sutliff, S. Sitzman,2000
[3] ASTM, A 262 – 02a (Reapproved 2008) Standard Practices for Detecting Susceptibility to Intergranular Attack in Austenitic Stainless Steels.
[4] ASTM, G-108-94 (Reapproved 2004) Standard Test Method for Electrochemical Reactivation (EPR) for Detecting Sensitization of AISI Type 304 and 304L Stainless Steels.
[5] M. Asuncion Valiente Beremejo, Predictive and Measurement Methods for Delta Ferrite Determination in Stainless Steels, WRC, WJ 2012
[6] P. S. Korinko and S.H. Malene, Westinghouse Savannah River Company, Aiken , SC 29808 “Considerations for the Weldability of Types 304L and 316L Stainless Steels”,2001.
[7] ASME Boiler and Pressure Vessel Code, Sections III and IX, ASME, NY.
[8] http://en.wikipedia.org/wiki/Section_modulus - cite_note-Kulak-3
[9] J.A. Sutliff, An Investigation of Plastic Strain in Copper by Automated-EBSP, Microscopy and Microanalysis, Vol 5. Supp. 2 1999 p. 236, (Proceedings: Microscopy & Microanalysis '99)
T.M. Angeliu, P.L. Andresen, E. Hall, J.A. Sutliff, S. Sitzman and R.M. Horn, “Intergranular Stress Corrosion Cracking of Unsensitized
[10] Stainless Steels in BWR Environments”, submitted to the 9th International Symposium on the Environmental Degradation of Materials in Nuclear Power Systems - Water Reactors, TMS.
[11] T.M. Angeliu, P.L. Andresen, E. Hall, J.A. Sutliff and S. Sitzman, “Strain and Microstructural Characterization of Austenitic Stainless Steel Weld HAZs”, Corrosion/00, paper 186, NACE, Houston, TX (2000).
[12] P.C. Brand, Th.H. De Keijser, G. Den Ouden, “Residual Stresses and Plastic Deformation in GTA-Welded Steel”, Welding Research Supplement, March 1993, 93-s to 100-s.
[13] G. Derbalian, G.R. Egan and C. Aboim-Costa, “Finite Element Stress Analysis of 4-inch Diameter Welded Pipe with Prescribed Residual Stresses”, Proceedings: Seminar on Countermeasures for Pipe Cracking in BWRs, Volume 2 of 4”, WS-79-174, vol. 2, Electric Power Research Institute, Palo Alto, CA, (1980) paper 35.
[14] T. M. Maitland, unpublished work (2005).
[15] X. D. Han, S. Sitzman, and T. M. Maitland, unpublished work (2005).
[16] Peter L. Andresen, Stress Corrosion Cracking of Current Structural Materials in Commercial Nuclear Power Plants, Corrosion, 2013.
Andresen P and Morra M M (2008), ‘IGSCC of non-sensitized stainless steels in high temperature water’, Journal of Nuclear Materials, 383, 97–111



Lt Cdr Ramandeep Singh Sawhney is an alumnus of 18th Naval Engineering Course and was commissioned on 01 Jan 2006. He had held his first appointment onboard INS Krishna as Assistant Engineer Officer. The officer was also part of cadets training team as Divisional Officer and Training Coordinator and has carried out instructional duties at INS Shivaji. He is presently pursuing his Masters. of Technology project under guidance of Dr. Vivekanand Kain at Homi Bhabha National Institute (HBNI), BARC

Failure Analysis of Axial Flow Impulse Turbine Rotor Disk

E. Bhaskar Rao Sc'C' [1], **R.Srihari, Sc'F'**[2],**C.Kedarnath, Sc'F'**[3],**AVS Chari, Sc'G'**[4]
Visakhapatnam, Inida,NSTL (DRDO), Visakhapatnam
[1]eluribhaskarrao@gmail.com

***Abstract*—Under water vehicle turbine rotor blades made of CM 247 LC (Ni-based superalloy) failed (cascaded) during the sea trial. At high speeds fuel flow rate increases leading to an increase in the exhaust gases temperature on the turbine. From the present trial data and past failure turbine reports it was suspected that the failure may be due to the high temperature. Detailed failure analysis was carried out to know the cause of the failure.**

Failure analysis revealed that the failure occurred due to Fatigue and the presence of coarse & sharp carbides incoherent with the matrix. Detailed microstrucutral examination revealed that the presence of γ - γ' eutectic, which is deleterious to the material's strength. As an outcome of this analysis it has been recommended that solutionizing and ageing heat treatment need to be carried out on the turbine rotor to reduce the γ- γ' eutectic, and to increase the fine γ' precipitates, reduce the size of carbides and to uniformly distribute them in the matrix.

I. Introduction

Nickel based super alloys are particularly important in the manufacture of aero engines and industrial gas turbines. In all nickel based super alloys, the presence of γ' (Gamma prime) phase hinders the motion of dislocations and increase the creep resistance due to looping of dislocations around γ' particles. The essential solute elements in Ni-based super alloys are Al and Ti with a total concentration typically less than 10 atomic percent. This generates two phase equilibrium microstructure, consisting of γ (disordered) and γ' (ordered) FCC crystal structure. Gamma prime (γ') having an ordered structure is largely responsible for elevated temperature strength of the material and its high resistance to creep deformation. The amount of γ' depends on chemical composition and temperature. Typically 0.2% γ' is sufficient to retain the properties when the metal experiences high temperatures. Higher amount of γ- γ' eutectic reduces the yield strength and ductility of conventionally cast CM 247LC. The strength generally decreases as temperature increases. However Ni-based super alloys Ni_3(Al,Ti), are particularly resistant to temperature due to the presence of γ, γ' precipitates. The strength only decreases beyond 600^0C, where the thermal activation is sufficiently high to allow the dislocations to overcome the obstacles. When greater strengths are required at lower temperatures, Nb and V additions are done to form γ'' (Ni_3Nb/Ni_3V) precipitates which are in disc shape. Zr and B are added for grain boundary strengthening and this reduces the tendency of grain boundary sliding which occurs at high temperatures. It is particularly important to avoid certain brittle phases such as Laves & Sigma.

II. Experimental

Turbine Blade samples (lateral and transverse sections) were cut using EDM (electric discharge machine). The samples were mounted using Bakelite powder and fine polished for metallographic observation. Etching of the mounted samples was carried out using Kallings Reagent ($CuCl_2$ 2.5g + HCl 40ml + Methanol 40ml). Microstructural analyses of samples were carried out using an Environmental Scanning Electron Microscopy (SEM, LEO 440i model) and an optical microscope. The samples were cleaned ultrasonically to remove any contamination before examined under SEM. The hardness of the samples was measured using a Vickerss Hardness Tester.

III. Results & Discussion

Fig. 1 shows the failed turbine rotor and blades. Visual Inspection of all the 94 No's of blades indicated that the blades failed in cascaded fashion. Root portion of blades on hub are examined with a magnifying lens. The observed features were thumb nail marks (beach marks) and rubbing or overload failure. (Fig. 2)

4.1 Optical Microscopy

Fig. 3 shows the microstructure of longitudinal and transverse cross sectioned samples at different magnifications. Fig. 3a, b shows equi-axed dendritic microstructure as desired. The contrast difference in the microstructure is due to the difference in grain orientation. The microstructure (Fig. 3 c, d) shows carbides located at the dendritic boundaries and in a continuous fashion. (Fig. 3 e, f) shows the microstructure of γ- γ' eutectic distribution and the sharp edged carbides. The volume of γ- γ' eutectic is estimated to be about 15 20%. The position of sharp carbides is located at the boundaries of γ- γ' eutectic and the black spots observed may be pits formed due to carbides removal.

4.2 Fractographic Examination

Fig. 4a shows the fracture surface at the root of blade at hub shows beach marks indicating that the mode of crack propagation is by fatigue mode. SE (secondary electrons) and BSE (back scattered electrons) image mode in Fig. 4 b, c shows circular pits and multiple cracks surrounding the pits with a flowery pattern back ground (γ- γ' eutectic). The pits are formed due to the scooped-off/pull-off of coarse carbides which are incoherent with matrix.

Fig. 4d, e shows cracks which were initiated due to the sharp edges of the carbides. The carbides are pulled out due to load and further the cracks propagated in fatigue mode until the blade withstands the load and finally fractured due to over load (dimple fracture features). The deep pit (Fig. 4e) reveals the sharpness of the carbides and incoherency with the matrix. The pits are analyzed by using Energy Dispersive X-ray (EDAX) spectrometer the study showed there is no oxide formation which implies that failure is not due to excessive blade temperature.

The Hardness of the turbine before and after trial showed no variation (45HRC) indicates there is no metallurgical phase changes occurred due to high temperature, which also confirms that failure is not due to high blade temperature.

IV. OBSERVATIONS

The following observations and conclusions were made from the above studies.

a. The presence of beach marks on fractured surface indicates the failure mode is by high cycle fatigue.

b. The distribution of carbide is segregated at the grain boundaries which can lead to failure at grain boundaries.

c. The presence of high volume of γ-γ' eutectic was observed which is deleterious to the strength.

d. The morphology of the carbides is either coarse or sharp (incoherent with the matrix) which leads to multiple crack initiation.

V. RECOMMEDATIONS

1) Heat treatment of CM 247LC alloy has to be carried out - first solutionizing followed by ageing.
2) Solutionizing promotes chemical homogeneity, eliminate coring, improve micro structural uniformity, and dissolve the γ-γ' eutectic and carbides.
3) Ageing after solutionizing leads to fine γ' and carbide precipitate distributed uniformly.
4) The final volume of γ-γ' eutectic can be restricted to below 5% by the above treatment.
5) Mechanical properties will be improved after Heat Treatment due to high volume fraction of γ', with proper size and the refinement of carbides, which inhibit gliding and climbing (propagation) of dislocations.
6) Mechanical work (machining) should not be done on the turbine blades after casting.

VI. CONCLUSIONS

1) Carried out heat treatment at DMRL, Hyd: As Cast + Solutionised (1260^0C / 3 hr) + Aged (1080^0C / 4 hr + 870^0C / 20 hr) as per recommendations.
2) Solutionizing & Ageing: To promote chemical homogeneity, eliminate coring, improve micro structural uniformity, uniform precipitation of γ' (0.4 0.5μ m), dissolution of carbides followed by refinement of carbides.
3) From SEM / IMAGE ANALYSIS it is found that (γ-γ') eutectic reduced to 5% after heat treatment (Fig. 5a, b).
4) Failure is not repeated in further trials. Mechanical properties are improved after Heat Treatment attributed to high volume fraction of γ', restricted volume fraction of (γ-γ') eutectic, refinement of carbides, which inhibit movement of dislocations.

ACKNOWLEDGMENT

The author would like to thank the Director, NSTL for the kind support to carry out the work. The author also thanks the Director, DMRL for facilitating the above work. Acknowledgements are due to Shri Satyapal Singh, Sc'G', Dr. V. V. Satyanarayana, Sc'F', & Shri Dibyendu Chattergy, Sc'D', DMRL, Hyd for fruitful discussions.

REFERENCES

[1] K.L.Gasko, G.M.Janowski and B.J.Pletka, Material science and Engineering A104 (1988) pp1-4.

[2] K.Harris, G.L.Erickson And R.E.Schwer, "MAR M247 Derivations CM 247 LC DS alloy CMSX Single crystal alloys properties & performance".

[3] Jacqueline B.Wahl, Ken Harris, Proceedings of ASME turbo expo 2010:power for land, sea and air GT2010, June 14-18, 2010 "An overview of advanced Ni-Base super alloys for small turbines and missile engine applications".

[4] M. Naeem, R. Singh, D. Probert, International Journal of Fatigue 21 (1999) 831847 "Implications of engine deterioration for a high-pressure turbine blades low-cycle fatigue (LCF) life-consumption".

[5] 5. Technical Bulletin, Cannon-Muskegon Corporation Jan 2004.

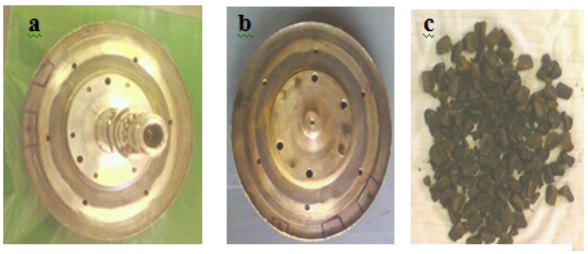


Fig. 1. a)Failed turbine rotor a)with shaft b) without shaft c)cascaded blades

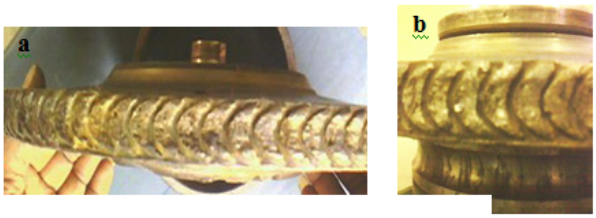


Fig. 2. Root portion of blades on hub

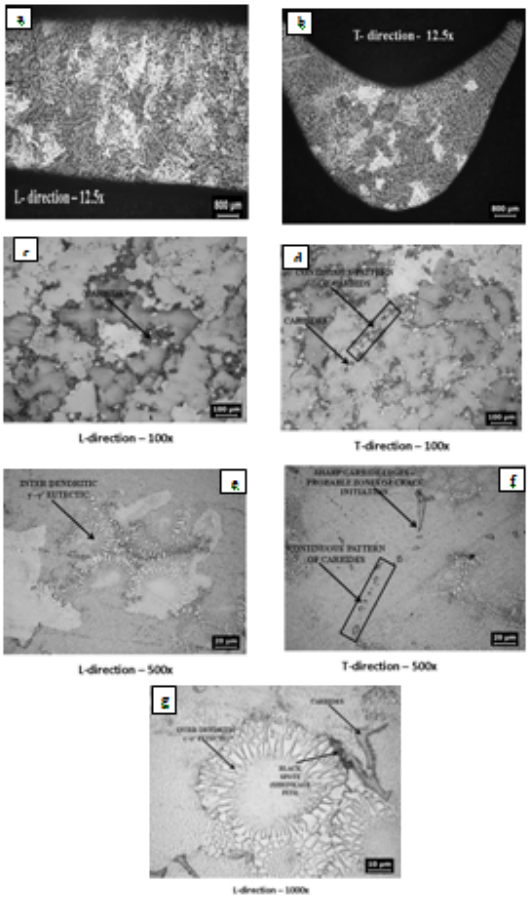


Fig. 3. Optical Microstructures of samples in transverse and longitudinal cross

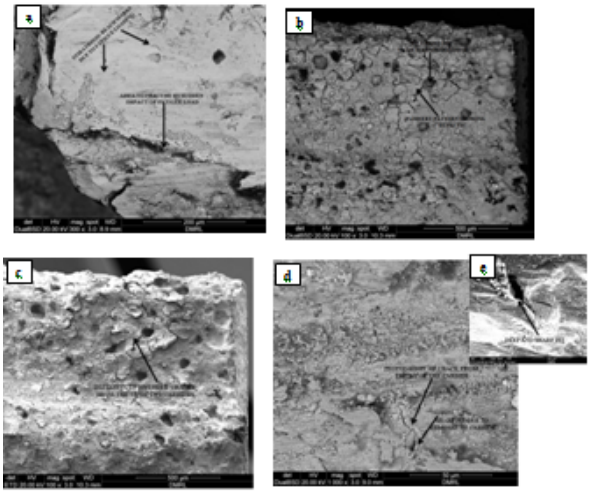


Fig. 4. SEM image of fractured surface

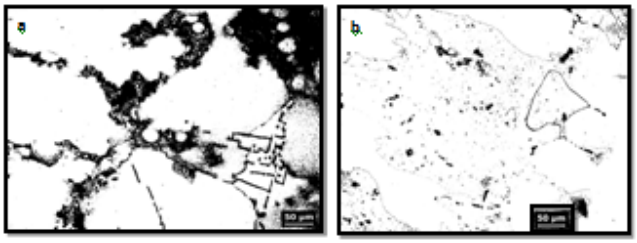


Fig. 5. Image Analysis: a) Before Heat treatment (γ-γ' eutectic ¿ 24%) b) After Heat treatment (γ-γ' eutectic ¡ 5%)



Mr. E.BHASKAR RAO iS M.Tech (Metallurgical & Materials Engineering.) from IITM, Chennai, 2010. He is presently working as Scientist 'C'. His areas of research interest are Failure analysis & Super Cavitation.



Mr.R.SRIHARI is an M.Tech (Mechanical Engineering) from IITM, Chennai. During his carrier he published 2 papers in international journals. He is presently working as Scientist 'F' Deputy project Director for the development of thermal propulsion. His areas of interest are Thermal propulsion and Safety.



Mr.C.KEDARNATH is an M.Tech (Mechanical Engineering) from IITM, Chennai. During his carrier he published 05 papers in international journals and 02 papers in international conferences. He is presently working as Scientist 'F'. His areas of research are thermal propulsion, closed cycle thermal system, wobble plate mechanism.



Mr.A.V.S.CHARI is a M.S Marine Engineering from Crane field institute of technology, Bedfork, UK. During his carrier he published more than 10 papers in international journals. He is presently working as Scintist 'G'. He is heading as Director for Warship Technology and Noise and Vibration at NSTL (V),Visakhapatnam.

Development of Improved Welding Technique for Naval Structural Material (Dmr249a)

***Cdr Rishi Pamnani, Indian Navy, presently at PTC(Kalpakkam) [PhD Scholar with HBNI, IGCAR], rishi.rashmi.p@gmail.com**
****Dr M Vasudevan, Materials Technology Division (MTD), IGCAR**
***** P Vasantharaja, SO'D', MTD, IGCAR**
******Dr T Jayakumar, Metallurgy and Materials Group (MMG), IGCAR**

Abstract **-** The comprehensive research undertaken at Defence Metallurgical Research Laboratory (DMRL) resulted in development of DMR249A characterized by higher strength and superior toughness. DMR249A is presently being used for construction of Indian Aircraft Carrier and other new ships being constructed at various ship yards. Based on the expertise and experience gained on success of A-TIG welding for 304LN and 316LN steels, the attempts are being made to develop activated flux for DMR 249A to enhance the depth of penetration, weld efficiency and productivity. The project aims at providing better strength and efficiency of weld joint and enhanced weld productivity for naval ship building projects.

Keywords **– DMR249A; A-TIG; Design of Experiments; Depth of Penetration; welding productivity**

Introduction

Welding is a fabrication process that joins materials by causing coalescence. The process is of prime importance for building and structural materials. A lot of R&D efforts have been undertaken in the field of High Productive Welding and endeavors to reduce Number of Passes in a Multi Pass Weld Joint for optimization to minimize time, cost and human labour.

In Activated Flux Tungsten Inert Gas (A-TIG) welding, a fine layer of activating flux, constituting of inorganic powder, is coated on the steel plate before welding. The penetration depth was multiplied by a factor of 3 while changing from the TIG process to A-TIG, depending on the alloys being welded.

Overview of ATIG welding[1]

Considering the theoretical bases the only one difference between Tungsten Inert Gas welding (TIG) and Activated Tungsten Inert Gas welding (ATIG) is the use of activating fluxes (Figure 1). As seen in the figure, the activating flux is very different from the powder of Submerged Arc Welding (SAW) because of the quantity and the mechanism of the effect.

There is still not agreement today on the explanation of the mechanism of the activating fluxes. In the last four decades, four different theories were published [2], which briefly expressed as follows:-

Theory of Savitskii and Leskov 1980 [3]

This theory indicates that the activating flux decrease the surface tension of the weld pool which enhances the arc pressure to cause a deeper penetration into the pool. This invading helps the arc pressure to reach a deeper penetration.

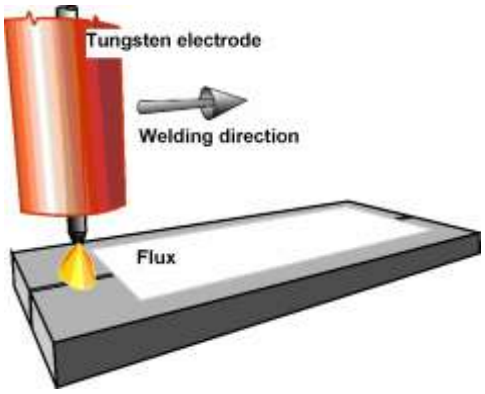


Figure 1 – Schema of ATIG welding process

Theory of Heiple and Roper 1982 [4]

This theory explains the high penetration with the reversed Marangoni-effect . The convective flowing of the molten metal from the centre towards the edge is the phenomenon that is called Marangoni-effect. It operates when the gradient of the surface tension of the weld pool is negative. This theory says that the activating fluxes changes the gradient of the surface tension from negative to positive that results in the flowing of the molten metal in the opposite direction and flows towards the centre. This is how the deep penetration is obtained by the reversed Marangoni-effect.

Theory of Simonik 1976 [5]

Simonik says that oxide and fluorine molecules are present in the activating fluxes which have affinity to focus the free electrons at the edge of the plasma of the arc. It is well-known that the ions formed this way have substantially lower mobility than the free electrons. This leads to increased current density in the centre of the arc by means of the higher movement of the free electrons. This results in better focusing of the arc which leads to the deeper penetration.

Theory of Lowke, Tanaka and Ushio 2005[6]

They explain the deep penetration by means of the higher electric insulation of the activating fluxes. Because of this, the arc is able to break through the surface (and the flux on it) at a narrower area. This means that the focus of the arc increases which leads to higher current density in the arc spot and this causes the deep penetration.

As per the results obtained while carrying out various experiments run and observations by high speed imaging cameras, it is believed that enhancement in depth of penetration occurs due to arc constriction in conjunction with reversed Marangoni-effect.

DMR 249A [High Strength Low Alloy (HSLA) Steel]

Structural steels used for all warship building / repair activities were imported, whether Indian Warships or of foreign origin, both from east and west. The problems of inventory, uncertainty in availability, difficulty in procurement etc. therefore emerged as needs for indigenous development of strategic material for improved self-reliance of the Indian Navy. The comprehensive research undertaken at Defence Metallurgical Research Laboratory (DMRL) resulted in development of DMR 249A characterized by higher strength and superior toughness at temperatures as low as -60 degree C [7]. DMR-249A is a low carbon (0.08 wt.% C) HSLA steel, with micro-alloying additions of 0.03–0.05 V, <0.05 Nb and 0.01–0.06 Ti. The steel is designed to have a predominantly ferritic microstructure, with pearlite less than 10% by volume [8]. This structural grade steel standardized by the American Bureau of Shipping for use in ship building is used in the construction of the hull of various vessels with specific weight and resilience qualities. The chemical composition and mechanical properties of DMR249A are given in Table 1 and 2 respectively.

Table 1: Alloy design of DMR 249A grade steel

Elements	Contents	DMRL Specification	Actual Chemistry
C	%	0.08 to 0.11	0.08 – 0.10
Mn		1.15 to 1.65	1.160 – 1.390
P		0.015 max	0.013 – 0.015
S		0.012 max	0.003 – 0.010
Si		0.15 to 0.40	0.260 – 0.380
Al		0.02 to 0.06	0.034 – 0.043
Nb		0.05 max	0.027 – 0.028
Ni		0.65 to 1.05	0.76 – 0.77
V		0.03 to 0.05	0.042-0.045
Ti		0.01 to 0.06	0.015 – 0.023
Pb+Sn+As		0.025 max	<0.003
N	ppm	70 max	57 – 60
Total O	(in	< 50	20 – 30
H	product)	2 max	1.1 – 1.4
Ca		50 max	16 – 24

Table 2: Properties characterization of DMR 249A grade steel

Properties	Norm	Head End	Middle	Tail End
Yield Strength (MPa)	>390	523 – 550	465 – 527	469 – 518
Tensile Strength (MPa)	510 – 690	616 – 650	560 – 625	590 – 622
% Elongation (Std GL)	≥18	21 – 27	22-30	22-28
Hardness (HV10)	-	165	159	160

Success of A-TIG with 304LN/316LN Stainless Steels

Specific activated flux [9] has been developed for enhancing the penetration performance of the TIG welding process for welding of type 304LN and type 316LN stainless steels. A significant increase in penetration of over 300% has been achieved in single pass TIG welding [10][11]. The use of flux has caused no degradation in the microstructure and mechanical properties of the welds compared to those produced by conventional TIG welding. The use of flux therefore would result in significant cost reduction as there is no requirement for edge preparation and filler metal addition. The improvement in creep-rupture properties of A-TIG weld joints of 316LN stainless steel has already been demonstrated [12]. This in-house developed Activated flux has been successfully field-tested and demonstrated for all its advantages for welding of dummy core subassemblies of a sodium cooled fast reactor made of 304L SS [13]. Significant reduction in residual stresses and distortion in A-TIG weld joints of austenitic stainless steels has been reported [14]. It is also reported that process parameters optimization would help in achieving the desired depth of penetration during A-TIG welding [15].

Development of A-TIG as Improved Welding Technique for DMR 249A

Based on the expertise and experience gained on success of A-TIG welding for 304LN and 316LN steels, the attempts are being made to develop activated flux for DMR 249A to enhance the depth of penetration, weld efficiency and productivity. The combination of oxide fluxes used in the experiments includes SiO_2, TiO_2, NiO, CuO_2 and Cr_2O_3 powders. Post weld analysis of the penetration characteristics of individual fluxes, a mixture of powders was developed and Design of Experiments (DOE) was conducted for optimisation of maximum penetration by using Design Expert7 software [16]. The INPUT parameters matrix as per the software was used for obtaining experimental OUTPUT parameters as per the matrix shown in Table 3 and Fig 2.



Figure 2 – Design of Experiments Results

The equation for penetration was formulated on the basis of Analysis of Variance (ANOVA).

Final Equation in Terms of the Actual Factors:-

Depth Peneteration = -3.12367
+0.036998 * Current + 0.063806 * Torch Speed -6.25417E-003 * Tip Angle - 0.33596 * Arc Gap
-1.55583E-004 * Current * Torch Speed +1.25042E-004 * Current * Tip Angle
+3.24375E-003 * Current * Arc Gap
+2.40278E-005* Torch Speed * Tip Angle
+2.84583E-003* Torch Speed * Arc Gap
-3.72708E-003* Tip Angle * Arc Gap
$-7.51958E-005 * Current^2 - 2.84398E-004* Torch Speed^2 - 6.54051E-005 * Tip Angle^2$
$- 0.052115* Arc Gap^2$

Table 3: DOE Matrix with 04 Input Factors and 03 Responses

Std	Run	Factor 1 A:Current Amps	Factor 2 B:Torch Spee mm/min	Factor 3 C:Tip Angle Degree	Factor 4 D:Arc Gap mm	Response 1 Depth Penete mm	Response 2 Bead Width mm	Response 3 HAZ Width mm
16	1	250.00	105.00	120.00	4.00	4.009	7.105	2.645
22	2	200.00	90.00	150.00	3.00	2.699	6.624	2.125
23	3	200.00	90.00	90.00	1.00	3.582	6.544	2.757
17	4	100.00	90.00	90.00	3.00	1.479	3.466	1.746
20	5	200.00	120.00	90.00	3.00	3.568	7.933	2.465
18	6	300.00	90.00	90.00	3.00	4.077	11.152	2.577
25	7	200.00	90.00	90.00	3.00	3.848	7.825	2.505
29	8	200.00	90.00	90.00	3.00	2.597	7.44	2.414
11	9	150.00	105.00	60.00	4.00	2.351	4.721	2.162
26	10	200.00	90.00	90.00	3.00	4.171	6	2.77
8	11	250.00	105.00	120.00	2.00	3.609	8.486	2.481
9	12	150.00	75.00	60.00	4.00	2.302	5.896	1.979
1	13	150.00	75.00	60.00	2.00	2.839	5.162	2.667
15	14	150.00	105.00	120.00	4.00	1.619	4.917	1.676
24	15	200.00	90.00	90.00	5.00	3.061	7.639	3.317
2	16	250.00	75.00	60.00	2.00	3.732	11.498	2.783
19	17	200.00	60.00	90.00	3.00	2.98	8.249	2.816
5	18	150.00	75.00	120.00	2.00	2.524	4.419	2.152
6	19	250.00	75.00	120.00	2.00	4.719	8.571	2.821
7	20	150.00	105.00	120.00	2.00	2.471	5.361	1.895
30	21	200.00	90.00	90.00	3.00	3.24	6.806	2.12
4	22	250.00	105.00	60.00	2.00	2.81	10.36	2.18
21	23	200.00	90.00	30.00	3.00	3.89	7.594	3.332
13	24	150.00	75.00	120.00	4.00	2.425	5.438	2.81
14	25	250.00	75.00	120.00	4.00	3.946	8.607	3.073
12	26	250.00	105.00	60.00	4.00	3.413	9.598	2.975
27	27	200.00	90.00	90.00	3.00	3.587	7.254	3.056
28	28	200.00	90.00	90.00	3.00	3.501	6.069	2.896
3	29	150.00	105.00	60.00	2.00	2.59	5.204	1.746
10	30	250.00	75.00	60.00	4.00	4.37	11.261	4.294

The validation matrix was derived for interpolated responses and also to achieve extrapolated maximization of penetration as per Tables 4 and 5 respectively.

Table 4 : Intrapolated Resuts for Maximising Penetration within Experimenta Range

No.	**Current** (Amps)	**Torch Speed** (mm/min)	**Tip Angle** (Deg)	**Arc Gap** (mm)	**Depth of Peneteration** (mm)		**Desirability** (%)	**Error** (%)
					Precdicted	**Experimental**		
1	300	75	120	3.83	4.69	4.66	80	1
2	300	75	120	3.96	4.69	4.65	80	1
3	300	75	120	3.77	4.69	4.67	80	1

Table 5 : Extrapolated Resuts for Maximising Penetration outside Experimenta Range

No.	Current (Amps)	Torch Speed (mm/min)	Tip Angle (Deg)	Arc Gap (mm)	Depth of Peneteration (mm)		Desirability (%)	Error (%)
					Precdicted	Experimental		
1	300	60	63	2.00	4.96	4.72	98.8	5
2	300	7560	60	2.18	4.95	4.71	98.6	5
3	298	7560	60	2.00	4.95	4.73	98.5	5

Having achieved Depth of Penetration Response of max 4.7 mm, the optimization of parameters with experimented range of Input factors was found to be satisfactory and within 1-2% variance than the experimentally obtained results as shown in Table 4 above. On extrapolating the Relation equation for achieving maximization of penetration, the variance with experimentally obtained values was observed to be around 5% as shown in Table 5 above. The satisfactory results could not be achieved as the objective of maximizing penetration of approx 5.5 mm (beyond experimentally achieved range of 4.7 mm) could not be achieved (The aim is to achieve a quality weld for 10mm thick plate with double sided welding require a minimum of 5.5mm penetration in single pass)

Discussion

The DOE is found to be an effective and accurate tool for optimizing input parameters in order to achieve the desired output responses. The optimization obtained as interpolation of range of Input and Response parameters provides useful and accurate results. The desirable extrapolation/ maximization of response parameters can be obtained from the derived relation subject to experimental verification. The extrapolation might not provide accurate results when the operating input parameters range is restricted.

With aim to fabricate weld joint for 10mm plate by double sided welding, future work involves working with various combinations of flux constituents for development of appropriate flux for achieving minimum of 5.5 mm depth of penetration in single pass welding. Then modeling and simulation would be carried out to simulate residual stresses and distortion. Calibrating heat source model, carrying out heat transfer and residual stresses simulations in Sysweld and validating the same with experimental results. Weld joints fabricated using 10 mm thick plates will be evaluated for their microstructure and mechanical properties. The performance of A-TIG weld joint will be compared with that of SMAW joints. The project aims at providing better strength and efficiency of weld joint and enhanced weld productivity for naval ship building projects.

References:-

[1] T. Sándor , János Dobránszky : The experiences of activated tungsten inert gas (ATIG) weldingapplied on 1.4301 type stainless steel plates, *Materials Science Forum Vols. 537-538 (2007) pp. 63-70*

[2] Tanaka M, Shimzu T, Terasaki H, Ushio M, Koshi-ishi F and Yang C L 2000 Effects of activating flux on arc phenomena in gas tungsten arc welding Sci. Technol. Weld. Joining 5 397–402

[3] Savitskii M M and Leskov G I 1980 The mechanism of the effects of electrically negative elements on the penetrating power of an arc with a tungsten cathode Avt. Svarka 9 17–22

[4] N. Perry: *Etude et développement des flux solides en vue d'application en soudage ATIG appliqué au titane et ses alliages ainsi qu'aux aciers inoxydables*
(Universite de Nantes, Ecole Doctorale le 15 Juin 2000)

[5] Simonik A G 1976 The effect of contraction of the arc discharge upon the introduction of electro-negative elements Svar. Proiz. 3/49–51

[6] J. J. Lowke, M. Tanaka, M. Ushio: J. Phys. D:Appl. Phys. 38 (2005) 3438-3445

[7] G. Malakondaiah, Development of Speciality Low Alloy Steels, International Conference on Metals and Alloys: Past, Present and Future, December 7-10, 2007, pp. 17.

[8] Subrata Mallik, Biswasi Sunita Minz and Basudev Mishra: Production of DMR 249A Steel at SAIL, Bokaro Steel Plant, *Materials Science Forum Vol. 710 (2012) pp 149-154*

[9] An international patent "Tungsten Inert Gas Welding Flux for enhancing Penetration in Single Pass for austeniticstainless steels" (patent no. PCT/IN06/00442/dt. 8/11/06)

[10] M. Vasudevan, A.K. Bhaduri, and Baldev Raj, Microstructure and Mechanical Properties of Austenitic Stainless Steels, International Welding Congress, February 16 – 19, 2005 Mumbai.

[11] M. Vasudevan,, A.K. Bhaduri and Baldev Raj, Development and Evaluation of Activated Flux for TIG welding of Type 304 LN and Type 316 LN Stainless Steels, International Institute of Welding, International Congress 2008, January, 8-10, Chennai, 2008.

[12] T. Sakthivel, M. Vasudevan, K.S. Chandravathi, P. Parameswaran, Laha, M.D. Mathew and A.K. Bhaduri, An assessment of Creep Rupture Behaviour of Single pass A-TIG and Multi-pass TIG weld joints of Type 316 LN Stainless steel, National Welding Seminar, December, 10-13, 2009, Kolkatta.

[13] P. Sivaraman, A. Md.Mueer, M. Krishnamoorthy, R. Veluswamy, M. Vasudevan, A.K. Bhaduri and A.S.L.K. Rao, Application of Penetration Enhancing Activating Flux TIG (PEAF-TIG) Welding Process in Regular Production of stainless steel and steel components, International Institute of Welding, International Congress, January, 8-10, Chennai, 2008.

[14] P. Palanichamy, M. Vasudevan, and T. Jayakumar, Measurement of Residual Stresses in Austenitic Stainless Steel Weld Joints Using an Ultrasonic technique, Science and Technology of Welding and Joining, Vol. 14 (2), p. 166 – 171, 2009.

[15] N. Chandrasekhar, M. Vasudevan and A.K. Bhaduri, Hybrid modelling for Optimization of A-TIG Welding Process for Austenitic Stainless Steels, National Welding Seminar, December, 10-13, 2009, Kolkatta.

[16] Design-Expert ® v.7

EFFECT OF HYDROGEN CONTENT AND HYDRIDES ON OXIDATION BEHAVIOR OF ZIRCONIUM BASE ALLOYS USED FOR FUEL CLADDING OF NUCLEAR REACTORS

Lt. Cdr. S. K. Tiwari
Homi Bhabha National Institute, Mumbai, India
Email: santosh_1483@yahoo.co.in

M. Kiran Kumar, Vivekanand Kain , Sanjay Singh
Materials Science Division, Bhabha Atomic Research Centre, Mumbai, India

Abstract — **Oxidation and consequent hydrogen pick-up of Zirconium alloys at high temperature and pressure conditions prevalent in the nuclear reactors is an active area of research. Although the Zr based alloys behave satisfactorily in terms of oxidation, the envisaged modifications of design, water chemistry, enhanced fuel burn-up and extended design life for advanced reactors push the limit of these materials. The oxidation behaviour of Zr based alloys has been studied in detail and is understood to a considerable extent in terms of the types of oxidation prevalent, oxidation kinetics, mechanisms involved, standard laboratory test conditions and so on. Uniform oxidation and consequent hydrogen pick-up followed by hydrogen related damage is a common concern in pressurized heavy water reactors (PHWRs) and pressurized water reactors (PWRs) having reducing water chemistry environment. On the other hand, in reactors operating with oxidizing water chemistry conditions, such as for boiling water reactors (BWRs), several forms of localized oxidation (nodular corrosion) are prevalent and the local enhanced oxidation leading to non protective oxide layer is the main concern. The objective of the present research is to establish the effect of hydrogen and hydride content on oxidation behaviour of Zircaloys. Hydrogen charging was carried out to various levels through a gaseous charging route by controlling the charging duration. These samples charged at various levels were subjected to accelerated oxidation at 400°C steam and at 10 MPa. A two-stage accelerated autoclave test procedure involving an exposure to 410°C, 10 MPa steam for 8 hours followed by an exposure to 510°C, 10 MPa steam for 16 h at low dissolved oxygen (DO) condition has been found to be most representative and could rank the Zircaloys in terms of their nodular corrosion susceptibility. Further, the effect of pre-hydriding on uniform as well as nodular corrosion is sought to be studied through electrochemical impedance spectroscopy and establishing the oxide types by Raman spectroscopy. Further, oxidation behaviour at the interface of oxide hydride and metal and oxide –metal will be analyzed in detail. This will establish the oxidation behaviour & nodular corrosion behaviour of Zr-2 & Zr-4 in hydride condition and we can correlate this behaviour with long residence time/high burn up.**

Keywords—Fuel clad, oxidation, autoclaving, Zircaloy – 2, Zircaloy – 4, Raman spectroscopy, hydriding

I. Introduction

Zirconium (Zr) based alloys are used extensively in the nuclear power plants as in-core components throughout the world. Such application of Zr based alloys came into prominence primarily due to their ability to withstand complex conditions of temperature, pressure and water chemistry prevalent in a nuclear reactor. In particular, the properties which made them ideal candidate materials are their low thermal neutron absorption cross section, high resistance to corrosion at high temperature and desirable high temperature strength. They are mainly used to fabricate major components used in the fuel region of water cooled reactors such as fuel cladding (Zircaloy-2, Zircaloy-4 and Zr-1Nb alloys), fuel channels, pressure tubes (Zr-2.5Nb alloy) and calandria tubes, fuel spacer grids and garter springs. The performance of Zirconium alloys has been satisfactory. However, the recent trend in nuclear industry towards higher fuel discharge burn-ups for better fuel usage, higher heat ratings and coolant temperature for better thermal efficiency and extended design life for advanced reactors are pushing Zirconium alloys to their limits in terms of both the mechanical and corrosion properties. The major concerns in nuclear reactors with the in-core components include irradiation creep of pressure tubes in PHWRs, oxidation and hydrogen pick-up of all Zr alloy components exposed to high temperature and pressure, hydrogen related damages such as hydriding, hydrogen blister formation and delayed hydride cracking, fuel side stress corrosion cracking (PCI-SCC) of the clad tubes in presence of fission gases like iodine, localized oxidation phenomena such as nodular corrosion and shadow corrosion of clad tubes in boiling water reactors (BWRs) and crud induced localized corrosion (CILC), etc. in pressurized water reactors (PWR). Although attempts have been made to deal with these concerns and now these problems have been overcome. In this paper we

will deal with the topic of the effect of hydrogen and hydride on oxidation behavior of Zr alloys.

During oxidation of zirconium and its alloys in aqueous environment nascent hydrogen is a reaction product. A fraction of the hydrogen thus formed, is picked up by the metal and when the terminal solubility limit is exceeded, hydrides precipitate. The mechanical properties of Zircaloy are degraded when hydrides are present in the metal.

High levels of hydrogen are often found in samples that have been subjected to an accelerated corrosion rate. In scenario such as loss of coolant accidents (LOCA), accelerated oxidation at very high temperature steam and air leads to huge quantities of H pick-up and often a hydride rim is formed over the surface of the clad. Similar is the situation where extended burn-up and higher residence time of fuel is planned. The end of life situation always has high hydrogen concentration as hydrides and/or hydride rim. The effect these hydrides have on further oxidation is a thrust area of research. The oxidation behaviour of the alloy, hydrogen charged samples with hydrogen in solid solution, uniformly distributed hydrides and samples with a massive surface hydride have been studied.

The terminal solid solubility (TSS) for hydrogen in Zircaloy-2 (Zry-2) is ~200 ppm at 400°C [1], and at higher hydrogen levels hydrides will be present. Addition of oxygen will increase the TSS for hydrogen and this has been suggested to be an effect of an increase in the matrix strength or hydrogen trapping at the solute atoms [2]. However, at high concentrations of oxygen the hydrogen solubility will decrease [3]. At higher temperature, 600–775°C, the solubility increases with oxygen content, but then decreases when the O/Zr ratio is above 0.177 [4]. It was early discovered that nickel increases the hydrogen absorption. The hydrogen absorption during corrosion was studied for Zry-2 and some binary alloys in water at 316–400°C [7]. Comparing the Zry-2 alloy with different binary alloys the authors report that tin has little or no effect, iron and chromium decrease, while nickel aids the hydrogen ingress through the oxide layer [7].

The transport mechanism of hydrogen through the oxide layer is not fully understood but different hypotheses have been proposed to explain the ingress of hydrogen. The early models suggest diffusion of hydrogen through the oxide layer in different ways:

(i) The hydrogen ingress occurs by proton hopping from O^{2-} to O^{2-} in the oxide, towards the metal [8]. Also diffusion of OH^- was discussed, but was disregarded by the authors because only one proton per oxygen atom could enter and the maximum hydrogen uptake should be less than 50%. However, this argument is not valid since during corrosion tests at normal conditions the hydrogen uptake is always less than 50%.

(ii) Diffusion of hydrogen atoms through the oxide layer via anion vacancies. Here the generation of anion vacancies is believed to take place at the metal/oxide interface when oxygen jumps to an interstitial position in the metal [9]. Another possibility is ingress through easy diffusion paths such as dislocation lines and grain boundaries [10].

However, nowadays the diffusion of hydrogen through a compact oxide is regarded as less plausible. The main ingress routes considered today are through defect oxide layers [11-14] and non-oxidized second phase particles (SPP) within the protective oxide film [15-17]. For example, transmission electron microscopy (TEM) investigations of thin oxide films formed on pure zirconium (400°C for 24 h) have shown that an interconnected network of pores may form, following the equiaxed grain boundaries and the hydrogen permeation may take place via this pore network [12].

In the newer models the hydrogen ingress is regarded as a localized process and it is suggested that a microscopic steam process is taking place in small cracks, leading to an accumulation of hydrogen close to the oxide/metal interface. The passive oxide at the bottom of the crack is thought to break down during this process and hydrogen enters the metal [14]. In the cited experiments the oxidation test was performed on thin Zr-2 plates in steam at 300–400°C. When the TSS was reached, which occurred during the pre-transition oxidation, the uptake rate of hydrogen decreased.

Corrosion tests on pre-hydrided Zry-4 at 360°C showed that the corrosion rate increased with increasing initial hydrogen content [18], and it is hypothesized that the hydrogen present in the metal close to the oxide/metal interface enhances the corrosion. The accelerated corrosion rate at long times is proposed to be a consequence of the fracture of the precipitated hydrides at the metal/oxide interface [19]. Another hypothesis proposes that the properties of the oxide may be modified when the oxide grows on massive hydrides or on metal with high hydrogen content [20]. Hydrogen may change the transport mechanism and/or the morphology of the growing oxide. However, more recently the effect of hydrogen on the oxidation behaviour of Zry-4 was investigated by the authors and no significant changes in morphology were detected by TEM examination of the oxide layer [21].

In the present work, Zry-2 and Zry-4 clad tubes were subjected to gaseous hydrogen charging to obtain specimens with different hydrogen levels with a purpose to have hydrogen in solution and as hydrides at oxidation test temperature (400-510 ^{o}C). The pre-hydrided Zry-2 and Zry-4 were subjected to high temperature and pressure oxidation tests in a static autoclave. The base material as well as the specimens at different stages of oxidation was characterized using microscopy, hardness and Laser Raman spectroscopy. Laser Raman spectroscopy was used to establish the crystal structure of oxide formed and optical microscopy was used to observe the distribution of hydride formed. However, the sample preparation technique influences the oxide crystal structure and the presence of cracks [22]. Electrochemical impedance spectroscopy (EIS) investigations are further aimed to be carried out on oxides at 300 degC followed by Mott-

Schottky analysis to arrive at defect densities in the oxides which gives a mechanistic insight into the protectivity of the oxide layer. The electrical properties and the thickness of the oxide layer can also be evaluated. An attempt will be made to carry out element profile in the oxide and metal by secondary ion mass spectrometry (SIMS) so that a better understanding of the hydrogen effect on oxidation is possible. Nodular corrosion susceptibility of both the alloys after hydriding shall be assessed by a two-stage accelerated autoclave test procedure involving an exposure to 410°C, 10 MPa steam for 8 hours (pre-filming) followed by an exposure to 510°C, 10 MPa steam for 16 h at low dissolved oxygen (DO) condition. Further, oxidation behaviour at the interface of oxide hydride and metal and oxide –metal will be analyzed by EBSD and SEM. This study is expected to establish the uniform oxidation and nodular corrosion behaviour of Zry-2 & Zry-4 in hydrided condition and the results can be correlated to the behaviour of clad with long residence time/high burn up. The current paper presents the results of the work carried out so far in this project.

II. MATERIALS AND EXPERIMENTAL PROCEDURES

2.1 Materials and Processing

The materials used in this study are the fuel clad materials (Zircaloy-2 and Zircaloy-4) commonly used in nuclear power reactors. The chemical composition range of the alloying elements used in these alloys (as per ASTM B 353) is given in Table 1.

Table 1: Composition of different Zr based alloys (Wt%).

Wt %	Zry-2	Zry-4	Zr-1Nb
Sn	1.20 – 1.70	1.20 – 1.70	0.05
Fe	0.07 – 0.20	0.18 – 0.24	0.05
Cr	0.05 – 0.15	0.07 – 0.13	0.02
Ni	0.03 – 0.08	0.007	0.02
Nb	0.01	0.05	0.9 – 1.1
O	0.09 – 0.16	0.09-1.6	0.1
N	0.008	0.008	0.006
C	0.027	0.027	0.02

ASTM standard (B 353 ASTM, 2007 and B 811 ASTM, 2007)
The single values denote maximum concentrations.

2.2. Sample Preparation for Hydrogen Charging

To date, there is no in-depth study of surface polishing effects on the properties of the cladding tubes. The literature shows that researchers mostly agree about the general effects of surface rough-ness such as its influence on oxidation kinetic, its affinity to react with contaminants, coolant flow and fluid turbulence on the stud-ied surface. Huntz et al. [23] studied the effect of surface roughness on Ni oxidation. They showed that the surface roughness can affects the oxidation, particularly at initial stages [24].

The inside and outside of tube sections were successively polished with 120, 400, 600, 800, and 1200 grit emery papers to prepare an oxide free surface. After grinding, the samples were pickled in a solution containing 5%HF + 45%HNO_3 + 50%H_2O for 1 minute to get a surface totally free of oxides formed during grinding and also a very good surface finish. The samples were then thoroughly washed in distilled water. Subsequently they were cleaned ultrasonically in acetone for 15 minutes to remove any trace of grease. The samples were prepared as per ASTM G 2M [23], which is a qualifying test for the use of Zr based alloys in nuclear reactors. For Zry-2 (Zircaloy-2) and Zry-4 (Zircaloy-4) fuel clad tubes, tube samples of about 20 mm length were cut into four pieces. The graphite layer inside the Zry-2 and Zry-4 tube samples was removed using a 400 grit emery paper. The samples were polished up to 600 grit emery paper.

2.3 Hydrogen Charging and Analysis

Gaseous hydrogen charging technique was used to charge different hydrogen levels in to the specimens. Sievert's apparatus as shown in figure 1 was used for the purpose. In present study constant volume variable pressure techniques were used which is based on the Sieverts principle. An in-house make Sieverts apparatus was extensively used in the present investigation. A photograph of the system is shown in Fig 1a. A complete schematic of the apparatus is shown in Fig 1b.

The apparatus consists of mainly four main parts viz the hydrogen source (Hydrogen gas cylinder or PW-SPE-500 CIC make hydrogen generator), reaction chamber, capacitance manometer and vacuum system. Different parts were connected by stainless steel tubes (i.d. 4mm) using compression type fittings. Only needle type valves were used in the system.

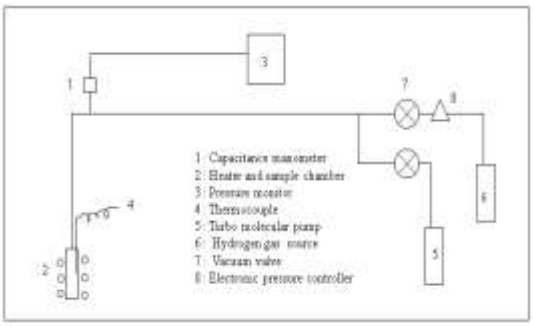
While working with hydrogen, the complete gas line manifold has to be absolutely leak proof and leak test should be conducted from time to time. To check the leak tightness of the system, the reaction chamber was maintained at a pressure of 0.1 torr and isolated for 3 continuous days. No change in pressure was observed at the end of this period. The entire system except the reaction chamber is made of 42 mm outer diameter stainless steel tube. KF couplings with viton gaskets were used for leak tight joints in the system. The reaction chamber is made of one end closed quartz tube of about 400 mm length and 40 mm in diameter. This reaction chamber was connected to the main apparatus using KF coupling. A capacitance manometer is used to measure the hydrogen pressure. In isobaric experiments an electronic pressure controller was used to regulate the hydrogen pressure fluctuation due absorption in the sample. A mass controller

flow meter was used to introduce hydrogen gas in a controlled way in the reaction chamber. A resistance heating furnace was used to heat the sample and the reaction chamber. The sample temperature was also measured by using a K type thermocouple adjacent to the sample holder. The system has been calibrated using standard $LaNi_5$ samples. For the hydrogen charging, the system was evacuated to a dynamic vacuum of the order of 10^{-7} Torr using turbo molecular pump. After this the hydrogen was introduced in a controlled way using the mass flow meter. Depending upon weight of the sample hydrogen was introduced to a predetermined level of pressure; subsequently the specimen chamber was heated up to a predetermined temperature. Amount of hydrogen picked up by the specimen, was indicated by manometer. The amount of hydrogen picked up by the sample is computed from difference between initial and final pressure readings recorded at the ambient temperature using formulae $[H]_{ppm} = k\ \Delta p/m$, where; k: apparatus constant (mg/torr), Δp: hydrogen pressure (torr) and m: mass of the specimens (mg). Hydrogen concentration crossed verified by chemical analysis of the sample using inert gas fusion technique as well as by gravimetric methods.

Inert gas fusion technique was used to analyse the hydrogen content after charging. This works on the principle of melting a given weight of the specimen in inert gas atmosphere and analyse the outcoming hydrogen gas. Hydrogen levels achieved were as received, 46 and 485 ppm for Zry-2 and as received, 63 and 385ppm for Zry-4.



(a)



(b)

Fig 1: (a) Sieverts Apparatus: Indigenously designed and developed in the laboratory and (b) schematic diagram of the Sieverts apparatus design, developed and used in the prsent study.

2.4. Steam Exposure of Prehydrided Specimens

The sample was prepared as per ASTM G 2M [24], which is a qualifying test for the use of Zr based alloys in nuclear reactors. The hydrided samples were polished up to 600 grit emery paper. After polishing, samples were washed and exact dimensions were measured with the least count of 0.01 mm. The etchant used [25] for Zircaloys was 3% HF + 39% HNO_3 + 58% water. After etching, the specimens were thoroughly washed in running water for at least five minutes to wash-off all the remaining acids. Then, the specimens were dipped in acetone and dried before weighing. The weight was taken to an accuracy of 0.001 mg and initial dimensions were recorded for surface area calculations. These specimens were then loaded into autoclaves, using a specimen stand made from zircaloy as shown in the schematic of figure 2, for carrying out accelerated exposure tests.

Oxidation tests were carried out in static autoclaves (made of Inconel) in steam at a temperature of 400 ◦C and a pressure of 10MPa according to the ASTM standard test (G2 M ASTM, 2005) [26] up to a duration of 21 days so far. This test is an accelerated test used for qualifying zirconium based alloys for use in nuclear reactor applications. It specifies use of water with a deaeration practice to reduce dissolved oxygen to low levels.

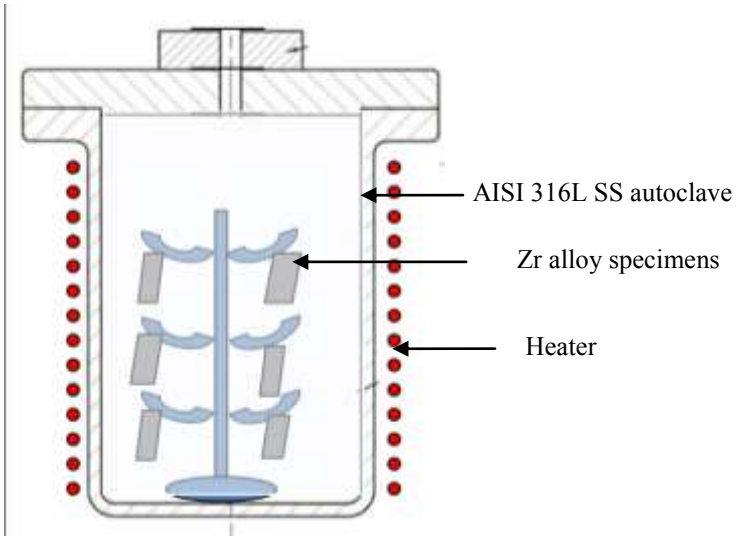


Fig: 2 Schematic diagram of sample loading in an autoclave.

2.5. Characterization

2.5.1. Hydride Microstructural Characterization

The hydride microstructure was characterized using optical metallography. Samples were mounted and then polished using 240–1200 grit paper followed by 0.5-lm

diamond polished. Samples were then etched for 2 min by immersion in an acid solution comprised of 10% hydrofluoric acid, 45% nitric acid, and 45% hydrogen peroxide [27] in order to resolve the hydride microstructure.

2.5.2. Hardness

A micro hardness tester was used to measure the hardness variation of the clad tubes with hydrogen charging. A load of 500 kgf and a dwell time of 15 seconds was used.

2.5.3. Laser Raman Spectroscopy

Micro-LASER Raman spectroscopy studies were carried out on oxidized specimens to estimate the changes in fractions of tetragonal and monoclinic zirconia in the oxide with oxidation time. A laser beam of wavelength 514 nm and laser power 18 mW was used for the study. The specimen was placed directly on the stage of an optical microscope whose objective lens enables the laser beam to be focused on a particular position. The spectral range extended from 100 to 1000 cm^{-1}. All measurements were made at room temperature.

III. Results and Discussion

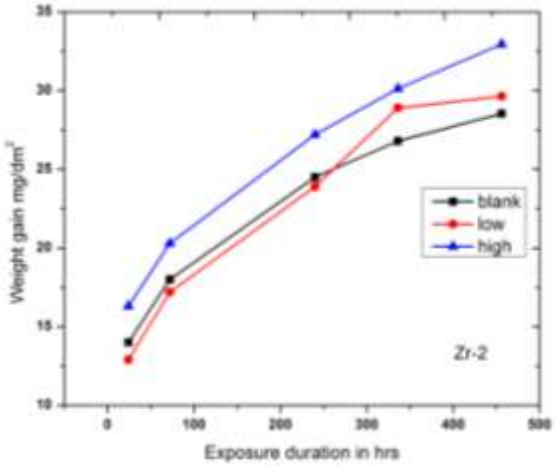
The results of the investigation are presented in three subsections dealing with (a) the typical appearance of the oxidized specimens, (b) the actual oxidation kinetics in static autoclaves demonstrating the effect of hydrogen content, (c) characterization of hydride and oxide surfaces.

3.1. Appearance of the Oxidized Surface

The physical appearance of oxide (ZrO2) grown on the alloy surface at various stages of oxidation is expected to provide a preliminary qualitative index of the protective nature of the oxide. At the early stages of oxidation, the surface oxide layer, irrespective of the type of material, was quite adherent and had a black and glossy (shiny) appearance. Such black lustrous appearance continued to be observed till 10 days of exposure at 400°C for all the two alloys charged below their solubility limits as depicted in figure 3. Clear differences in the appearance of the oxides on different alloys started to appear after about 10 days of exposure for alloys charged above solubility limits. The specimens of both Zircaloy-2 as well as the Zry-4 (without charged) alloys were still lustrous black when tested in steam for 10 days of exposure. The oxide formed on Zircaloy-2 specimens did have a similar black lustrous appearance even at higher ppm and exposure longer than 10 days. On the other hand, in case of Zry-4 there was a significant difference in appearance levels. The oxides formed at high ppm in case of Zry-4 had a whitish uniform surface appearance—a black lustrous layer with specs of white oxide uniformly distributed over it as depicted in figure 3.

3.2. Oxidation kinetics – effect of hydrogen content

The results of oxidation weight gain as a function of exposure time for Zry-2 and Zry-4 specimens having different hydrogen levels are presented in Fig. 4 and table 2.



(a)

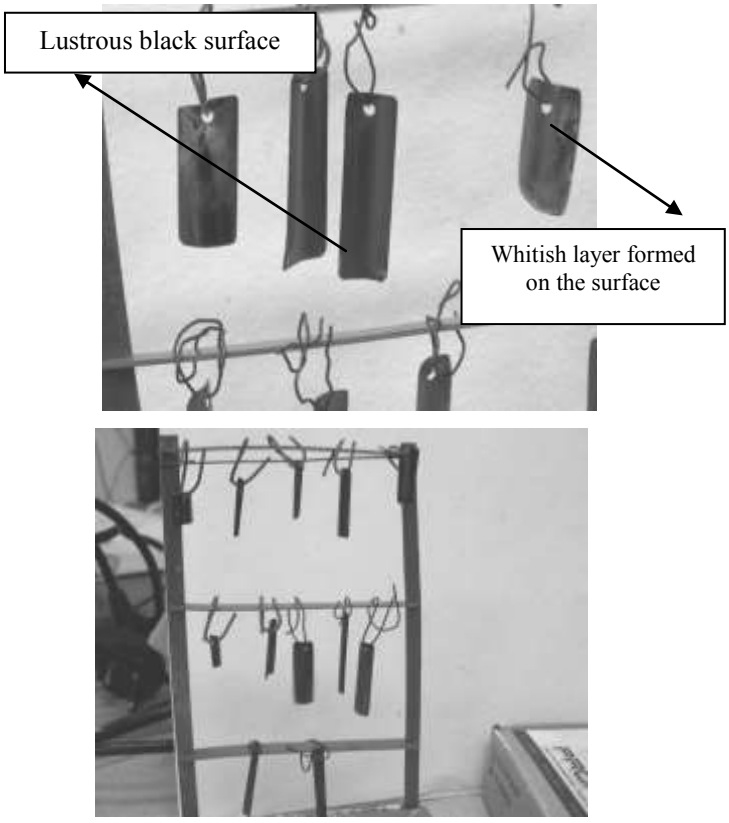
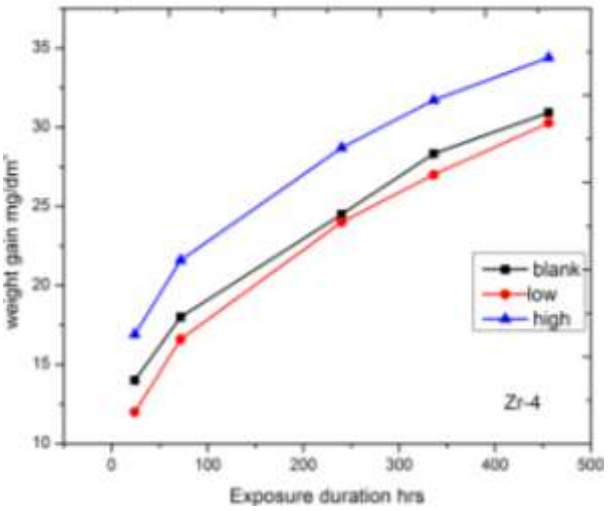


Fig. 3. (a) Appearance of oxide surface on Zry-2 and Zry-4; (a) H charged above solubility limit and (b) H charged below solubility limit.



(b)

Fig. 4. Oxidation kinetics for (a) Zry-2 and (b) Zry-4 with different hydrogen levels.

The oxidation kinetics of both Zry-2 and Zry-4 show a marked difference when hydrogen is present beyond solubility limit at the test temperature of 400 °C. For low levels of hydrogen below solubility limit, the kinetics follows more or less that of the uncharged specimen. The slight differences are within the measurement accuracies. However, for higher hydrogen levels; where hydrides are expected to be present at the test temperature, there is a marked increase in the oxidation weight gain values consistently higher than the uncharged specimen right from initial exposure of 24 hours. Blank coupons without hydrogen charging were exposed in the same experiments so as to ascertain the proper exposure procedure by comparing with earlier exposed coupons of the same material. The observations indicate an enhancing effect of hydriding on the oxidation behavior. Further long term exposures and high temperature electrochemistry is being carried out to substantiate these observations mechanistically.

Table 2: oxidation weight gain values as a function exposure time for specimens charged to different [H] levels.

Exposure (hrs)	**Weight Gain (mg/dm^2)**					
	Zry-2			**Zry-4**		
	Uncharged	Below 100 ppm	High ppm	Uncharged	Low ppm	High ppm
24	14	12.9	16.3	14	12	16.9
72	18	17.2	20.3	18	16.6	21.6

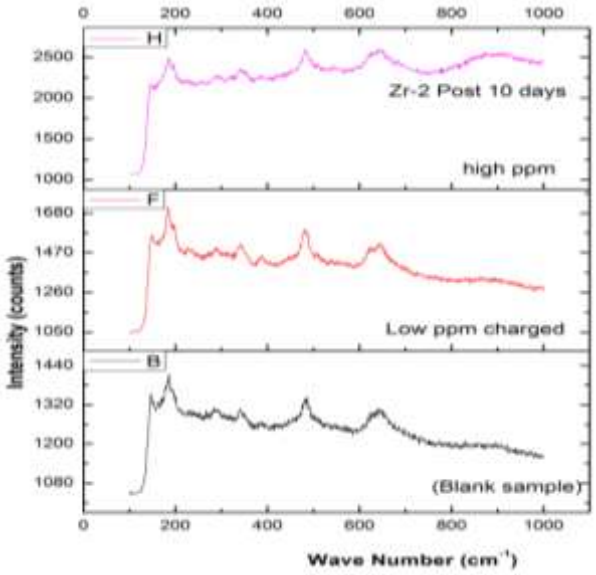
3.3. Laser Raman Spectroscopy

The Raman spectra for the Zry-2 and Zry-4 exposed to steam at 400°C, 10 MPa for 14 days are presented in figure 5. The spectra were measured and compared with standards of the monoclinic (M) and tetragonal (T) form of ZrO_2 stabilized with Y_2O_3 and data reported by Barberis et al. [28]. The most important band positions of both tetragonal and monoclinic phases used for calculation of tetragonal phase fraction have been marked in each of the spectra. The tetragonal bands are observed at around 145 and 290 cm^{-1} in almost all the specimens.

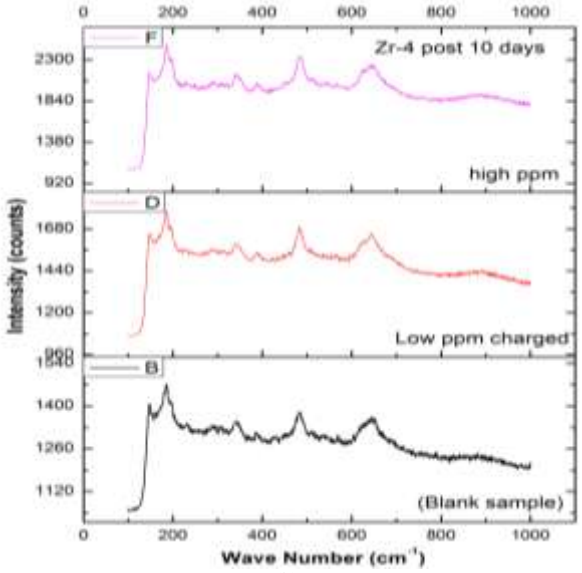
The total integrated intensities $I(hkl)$ of the tetragonal peak at 290 cm^{-1} and the monoclinic peaks at about 180, 190 cm^{-1},were used to determine the tetragonal ZrO_2 volume fraction (Ft) with respect to the total volume of ZrO_2 via the Godlewski formula [29].

$$\%t = \frac{I(280)}{I(280) + I(179) + I(189)}$$

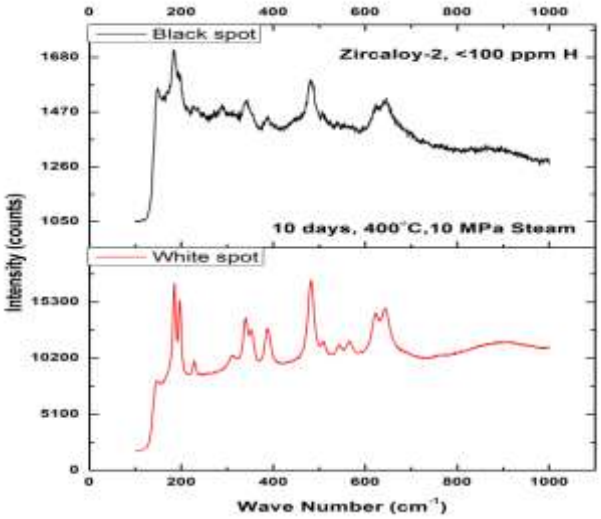
Where It and Im denote the intensity of tetragonal ZrO_2 and the intensity of monoclinic ZrO_2, respectively. The intensities were measured from the graphs by subtracting the value at the point where the peak starts rising from the value at the tip of the peak. The formula (1) is likely biased; the reason being that it was established on stabilized tetragonal zirconium oxide [31] with band at 264 instead of 290 cm^{-1}. Therefore the calculated values of T-ZrO_2 content are meant to be understood only in relative sense and are expressed for comparison of different specimens.



(a)



(b)



(c)

Figure 5. Raman spectra for oxide grown after 10 days exposure to 400 ^{0}C and 10 MPa on specimens with different hydrogen levels; (a) Zry-2, (b) Zry-4 and (c) comparison between white oxide vs. black oxide.

The variation in the fraction of tetragonal phase in the oxide for varying hydrogen levels is presented in Fig. 6. It can be clearly observed that for both Zry-2 and Zry-4, the fraction of tetragonal phase decreases with increase in initial hydrogen content. A lower tetragonal phase fraction is indicative of lower oxidation resistance or a non-protective oxide on the surface. This is also reflected in the trend of oxidation weight gains as seen in Fig. 4.

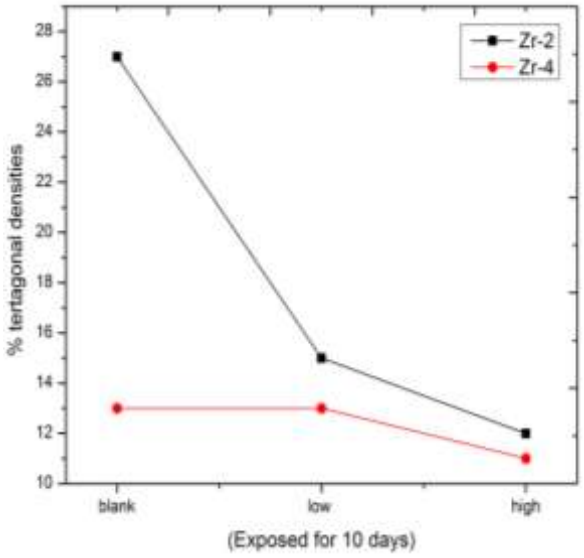
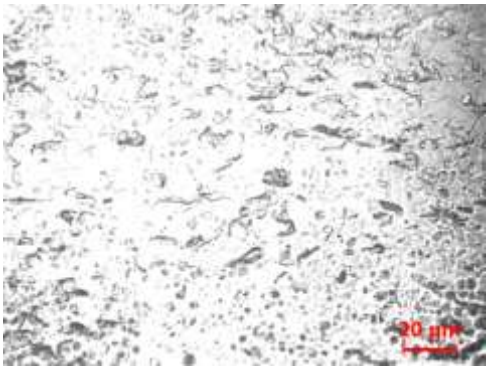


Fig. 6. Variation of the fraction of tetragonal phase in the oxide with hydrogen content.

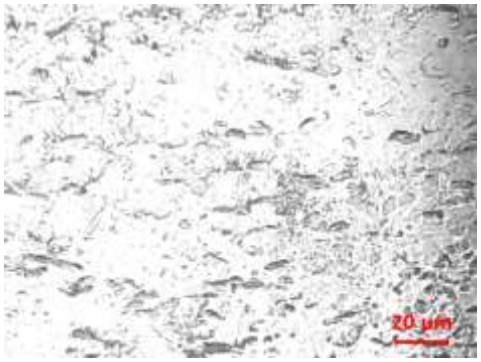
A. Characterization of Hydride Specimens

The typical appearance of hydrides after charging is presented in Fig. 7. The hydrides, though revealed by the current etching process, does not clearly bring out the morphological distribution as a function of the hydrogen content. This is typical when the etchant at the same time reveals the matrix microstructure. The etching with different etchant is being tried to significantly reveal the hydride morphology and the differences, if any, as a function of hydrogen content. In addition, SEM-EBSD is being carried out to bring out such differences.

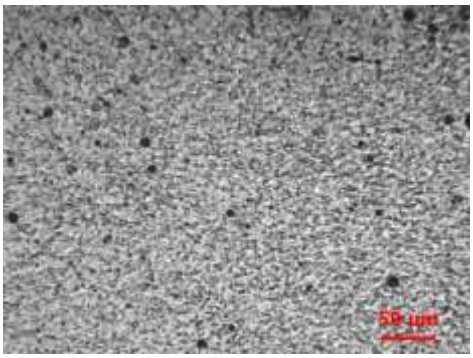
The variation of hardness as a result of hydrogen charging is presented in table 3. It is clear that there is a general trend of increase in the level of hardness with hydrogen charging; although the extent of increase is not very significant.



(a)



(b)



(c)

Fig. 7. Hydride morphology in (a) Zry-4 charged to 385 ppm, (b) Zry-2 charged to 585 ppm, (c) Zry-2 uncharged.

Table 3. Micro hardness values before and after hydrogen charging.

Material	Charging Level	Test Load (gf)	Dwell Time (sec)	Hardness (HV)
Zry-4	Blank	500	15	185.4
Zry-4	< 100 ppm	500	15	200.8
Zry-4	385 ppm	500	15	210.8
Zry-2	Blank	500	15	172.6
Zry-2	< 100 ppm	500	15	188.5
Zry-2	481 - 585 ppm	500	15	199.6

IV. Conclusions

The observations of the current paper can be summarized as follows:

a) The oxidation kinetics for both Zry-2 and Zry-4 clad tubes was affected by the presence of hydrogen beyond solubility limit at the test temperature of 400 ^{o}C. There is an enhanced oxidation when hydrides are present.

b) The oxidation kinetics of the specimens with H in solution follows a similar pattern as that of uncharged specimen.

c) There is an increase in hardness of the specimens as a function of H charging.

d) The tetragonal phase fraction of the oxide decreased with increased H content for a given duration of oxidation; indicating less protective nature of the oxide.

References

[1] J.J. Kearns, Journal of Nuclear Material, vol. 22, p. 292, 1967.
[2] A. McMinn, E.C. Darby, J.S. Schofield, in: G.P. Sabol, G.D. Moan (Eds.), Zirconium in the Nuclear Industry: 12th International Symposium, vol. ASTM STP 1354, Toronto, Canada, p. 173, 2000.
[3] C. Roy Journal of Nuclear Material., vol. 13, p. 275, 1964.
[4] S. Yamanaka, T. Tanaka, M. Miyake Journal of Nuclear Material, vol. 167, 1989.
[5] A. Stern, D. Khatamian, T. Laursen, G.C. Weatherly, J.M. Perz Journal of nuclear material, vol. 148, p. 257, 1987.
[6] M. Miyake, M. Uno, S. Yamanaka J. Nucl. Mater., vol. 270, p. 233, 1999.
[7] W. E. Berry, D.A. Vaughan, E.L. White, Corrosion, vol. 17, p. 109, 1961.
[8] J. N. Wanklyn, D.R. Silvester, J. Dalton, N.J.M. Wilkins, The corrosion of zirconium and its alloys in high temperature steam. Part II. The uptake of hydrogen during corrosion, UKAEA Report AERE-R3768, 1961.
[9] E. Hillner, Hydrogen absorption in Zircaloy-2 during aqueous corrosion: effect of environment. Report WAPD-TM-411, 1964
[10] T. Smith Journal of Nuclear Material, vol. 18, p. 323, 1966.
[11] B. Cox, The oxidation and corrosion of zirconium and its alloys. Part. XII, Hydrogen absorption by Zircaloy-2 and some other alloys during corrosion in steam, AERE-R3556, 1961
[12] B.D. Warr, M.B. Elmoselhi, S.B. Newcomb, N.S. McIntyre, A.M. Brennenstuhl, P.C. Lichtenberger, in: C.M. Eucken, A.M. Garde (Eds.), Zirconium in the Nuclear Industry: Ninth International Symposium, vol. ASTM STP 1132, Kobe, Japan, 1991, p. 740
[13] B. Cox, Y.-M. Wong Journal of Nuclear Material, vol. 270, p. 134, 1999.
[14] B. Cox Journal of Nuclear Material, vol. 264, p. 283, 1999.
[15] B. Cox, Atomic Energy of Canada Ltd., vol. AECL-8702, 1985.
[16] Y. Hatano, K. Isobe, R. Hitaka, M. Sugisaki Journal of Nuclear. Science. Technology, vol. 33, p. 944, 1996.
[17] Y. Hatano, R. Hitaka, M. Sugisaki, M. Hayashi Journal of Nuclear Material, vol. 248, p. 311, 1997.
[18] T. Kido, in: R.E. Gold, E.P. Simonen (Eds.), Sixth International Symposium on Environmental Degradation of Materials in Nuclear Power System – Water Reactors, San Diego, CA, USA, 1993, p. MMMS 449.
[19] A.M. Garde, in: C.M. Eucken, A.M. Garde (Eds.), Zirconium in the Nuclear Industry: Ninth International Symposium, vol. ASTM STP 1132, Kobe, Japan, 1991, p. 566.
[20] M. Blat, D. Noel, in: E.R. Bradley, G.P. Sabol (Eds.), Zirconium in the Nuclear Industry: 11th International Symposium, vol. ASTM STP 1295, Garmisch-Partenkirchen, Germany, 1996, p. 319.
[21] M. Blat, L. Legras, D. Noel, H. Amanrich, in: G.P. Sabol, G.D. Moan (Eds.), Zirconium in the Nuclear Industry: 12th International Symposium, vol. ASTM STP 1354, Toronto, Canada, 2000, p. 563.
[22] F. Garzarolli, H. Seidel, R. Tricot, J.P. Gros, in: C.M. Eucken, A.M. Garde (Eds.), Zirconium in the Nuclear Industry: Ninth International Symposium, vol. ASTM STP 1132, Kobe, Japan, 1991, p. 395.

[23] A. Huntz, B. Lefevre, F. Cassino, Roughness and oxidation: application to NiO growth on Ni at 800◦C, Materials Science and Engineering: vol. A 290, pp. 190–197, 2000.
[24] Hamed Akhiani, Jerzy A. Szpunar Effect of surface roughness on the texture and oxidation behavior of Zircaloy-4 cladding tube Applied Surface Science 285P, pp. 832– 839, 2013.
[25] G 2 M, 2005. Standard test method for corrosion testing of products of Zirconium, hafnium and their alloys in water at 633K or in steam at 673 K, ASTM Annual Book of Standards.
[26] T. Sarrio, T. Laitenen and J Pippo; Contact electric resistance technique for insitu characterisation of sutface film, Materials Science Forum: Vols. 289-292, pp. 193-202, 1998 **.**
[27] G2M, ASTM, Standard Test Method for Corrosion Testing of Products of Zirconium, Hafnium, and Their Alloys in Water at 680°F [360°C] or in Steam at 750°F [400°C]
[28] R.S Daum, Y.S, Chu, A.T Motta Journal of Nuclear Material, vol. 392, pp. 453-463, 2009.
[29] Barberis P. et al., Journal of Nuclear Materials, vol. 246, pp. 232-243, 1997.
[30] Clarke R.D., Adar F., Journal of the American Ceramic Society, vol. 65, p. 284, 1982.
[31] D. R Clarek .F. Adar. Ceram. Soc., vol. 65, p. 284, 1982.



Lt Cdr SK Twari an alumnus of the 2nd course of INS Zamorin Naval Academy Ezhimala and was commissioned on 06 Feb 2006. He joined the submarine arm in 2007 and has served as watch keeping officer on board INS Sindhushastra and senior engineer officer on board INS Sindhuvijay. The officer has served as deputy manager of SAX (Submarine and Auxiliary) department of Naval Dockyard Visakhapatnam and carried out various refit of ships and submarines. Presently he is undertaking his Masters of Technology degree project under the guidance of Dr. Vivekanand Kain at Homi Bhabha National Institute (HBNI).

A Theoretical Survey of the Effective Electron Mass in Nano-Wires invoking DFT Methodolgy

Ajay Kumar
Department of Mechatronics
Manipal University Jaipur
ajaykumarpat@yahoo.com
ajay.kumar@jaipur.manipal.edu

Abstract— **Theoretical study of effective electron mass in Nano wires (NWs) is an active filed of research. In this venture we have studied the effective electron mass (EEM) in Nano wires (NWs) of nonlinear optical materials on the basis of newly formulated electron dispersion relation by considering all types of anisotropies of the energy band constants within the framework of *k.p* formalism. The results for NWs of III-V, ternary and quaternary materials form special cases of our generalized analysis. It has been found that the 1D EEM in nonlinear optical materials depend on the size quantum numbers and Fermi energy due to the anisotropic spin orbit splitting constant and the crystal field splitting respectively. Under certain special conditions all the results for all the materials get simplified into the well-known parabolic energy bands and thus confirming the compatibility test. Nowadays, Density Functional Theory (DFT) has got immense importance for its many fold applications in nano composite and nano materials. In this study, we have used the DFT based parameters to analysis our computed results.**

Keywords: Nanowires, Effective Electron Mass, Non-linear Optical Materials, Optoelectronic Compounds

I. INTRODUCTION (*Heading 1*)

This The concept of the effective mass of the carriers in materials is one of the basic pillars in the realm of the science and engineering of advanced materials [1]. It must be noted that among the various definitions of the effective electron mass (e.g effective acceleration mass, density-of-state effective mass, concentration effective mass, conductivity effective mass, Faraday rotation effective mass, etc) [2], it is the effective momentum mass that should be regarded as the basic quantity [3]. This is due to the fact that it is this mass which appears in the description of transport phenomena and all other properties of the conduction electrons in a material with arbitrary band nonparabolicity [3]. It can be shown that it is the effective momentum mass which enters in various transport coefficients and plays the most dominant role in explaining the experimental results of different scattering mechanisms through Boltzmann's transport equation [4,5]. The carrier degeneracy in materials influences the effective mass when it is energy dependent. Under degenerate conditions, only the electrons at the Fermi surface of n-type materials participate in the conduction process and hence, the effective momentum mass of the electrons (EEM) corresponding to the Fermi level would be of interest in electron transport under such conditions. The Fermi energy is again determined by the carrier energy spectrum and the electron statistics and therefore, these two features would determine the dependence of the EEM in degenerate n-type materials under the degree of carrier degeneracy. The nature of the variations of EEM has been investigated in the literature [4-5]. Some of the significant features, which have emerged from these studies, are:

(a) The EEM increases monotonically with electron concentration.
(b) The EEM increases with doping in heavily doped materials in the presence of band tails.
(c) The nature of variations is significantly influenced by the energy band constants of various materials having different band structures.

In recent years, there has been considerable interest in studying the physics of Quantum materials. In this paper, we shall study the EEM in nanowires (NWs) of non-parabolic materials having different band structures. It is well-known that in NWs, the restriction of the motion of the carriers along two directions may be viewed as carrier confinement by two infinitely deep 1D rectangular potential wells, along any two orthogonal directions leading to quantization of the wave vectors along the said directions, allowing 1D carrier transport. With the help of modern fabrication techniques, such one dimensional quantized structures have been experimentally realized and enjoy an enormous range of important applications in the realm of nanoscience.

In this paper, we study the EEM in NWs of non-parabolic materials having different band structures. At first we shall investigate the EEM in NWs of non-linear optical compounds which are being used in non-linear optics and light emitting diodes [6]. The quasi-cubic model can be used to investigate the symmetric properties of both the bands at the zone center of wave vector space of the same compound .Including the anisotropic crystal potential in the Hamiltonian, and special

features of the non-linear optical compounds, Kildal [7] formulated the electron dispersion law under the assumptions of isotropic momentum matrix and the isotropic spin orbit splitting constant, respectively, although the anisotropies in the two aforementioned band constants are the significant physical features of the said materials [8]. In Section 2.1 of theoretical background, the EEM in NWs of non-linear optical materials has been investigated by considering the combined influence of the anisotropies of the said energy band constants together with the inclusion of the crystal field splitting respectively within the frame-work of k.p formalism. For the purpose of numerical computations, we shall take NWs of Cd_3As_2 and $CdGeAs_2$ respectively.

II. THEORETICAL BACKGROUND

A. Density Functional Theory:

First, The collection of procedure used to solve many-electron structure calculation in terms of the density matrix, ρ(r), directly (without first finding the wave function) is called Density Functional Theory. A density matrix ρ(r) is an array of (complex) numbers that carries in a compact form all the information needed to compute the observable of a system. This theory is remarkable because it allows one to replace one complicated N-electron wave function $\Psi(x_1, x_2, \ldots . x_N)$ and the associated Schrödinger equation by much simpler electron density and its associated scheme. This theory (DFT) [9] is a form of quantum mechanics that uses the one electron density function ρ(r) instead of the more usual wave function ψ to describe a chemical system. Such a system is any collection of nuclei and electrons and may be an atom, an ion or a molecule. It can be said that the central paradigm in Quantum Chemistry-Structure–Properties-Wave function triangle is turned into Structure–Properties-Density triangle in DFT [10].

The EEM in nanowires of non-linear optical materials. The form of k.p matrix for nonlinear optical compounds can be expressed extending Bodnar [8] as,

$$H = \begin{bmatrix} H_1 & H_2 \\ H_2^{+} & H_1 \end{bmatrix} \qquad (1)$$

$$H_1 \equiv \begin{bmatrix} E_{g_0} & 0 & P_{\perp} k_{+} & 0 \\ 0 & \left(-2\Delta_{\parallel}/3\right) & \left(\sqrt{2}\Delta_{\perp}/3\right) & 0 \\ P_{\perp} k_{-} & \left(\sqrt{2}\Delta_{\perp}/3\right) & -\left(\delta + \Delta_{\perp}\right) & 0 \\ 0 & 0 & 0 & 0 \end{bmatrix},$$

$$H_2 \equiv \begin{bmatrix} 0 & -f_{,+} & 0 & f_{,-} \\ f_{,+} & 0 & 0 & 0 \\ 0 & 0 & 0 & 0 \\ f_{,+} & 0 & 0 & 0 \end{bmatrix}$$

in which E_{g_0} is the band gap in the absence of any field, $P_{||}$ and $P_{\perp}$ are the momentum matrix elements parallel and perpendicular to the direction of crystal axis respectively, δ is the crystal field splitting constant, $\Delta_{||}$ and $\Delta_{\perp}$ are the spin-orbit splitting constants parallel and perpendicular to the C-axis respectively, $f_{,\pm} \equiv \left(P_{\perp}/\sqrt{2}\right)\left(k_x \pm i k_y\right)$ and $i = \sqrt{-1}$. Thus, neglecting the contribution of the higher bands and the free electron term, the diagonalization of the above matrix leads to the dispersion relation of the conduction electrons in bulk specimens of nonlinear optical materials as

$$\gamma\left(E\right) = f_1\left(E\right) k_s^{\,2} + f_2\left(E\right) k_z^{\,2} \qquad (2)$$

where,

$\gamma(E) \equiv E(E+E_{g_0})\left[\left(E+E_{g_0}\right)\left(E+E_{g_0}+\Delta_{||}\right)+\delta\left(E+E_{g_0}+\frac{2}{3}\Delta_{||}\right)+\frac{2}{9}\left(\Delta_{||}^2-\Delta_{\perp}^2\right)\right]$, *E is the total energy of the electron as measured from the edge of the conduction band in the vertically upward direction in the absence of any quantization,* $k_s^{\,2} = k_x^{\,2} + k_y^{\,2}$,

$$f_1(E) \equiv \frac{\hbar^{\cdot}\left(\quad + \Delta_{\perp}\right)}{\left[2m_{\perp}^{*}\left(E_{g_0}+\frac{2}{3}\Delta_{\perp}\right)\right]}\left[\delta\left(E+E_{g_0}+\frac{1}{3}\Delta_{||}\right)+\left(E+E_{g_0}\right)\left(E+E_{g_0}+\frac{2}{3}\Delta_{||}\right)+\frac{1}{9}\left(\Delta_{||}^2-\Delta_{||}^2\right)\right],$$

$$f_2\left(E\right) \equiv \frac{\hbar^2 E_{g_0}\left(E_{g_0}+\Delta_{||}\right)}{\left[2m_{||}^{*}\left(E_{g_0}+\frac{2}{3}\Delta_{||}\right)\right]}\left[\left(E+E_{g_0}\right)\left(E+E_{g_0}+\frac{2}{3}\Delta_{||}\right)\right],$$

ħ=h/2π, h is Planck's constant and $m_{||}^{*}$ and $m_{\perp}^{*}$ are the longitudinal and transverse effective electron masses at the edge of the conduction band respectively.

For two dimensional quantizations along x and y directions, (2) assumes the form

$$k_z^2 = A_{11}(E, n_x, n_y) \tag{3}$$

where

$A_{11}(E, n_x, n_y) = [f_2(E)]^{-1}[\gamma(E) - \phi_1(n_x, n_y) f_1(E)]$,

$\phi_1(n_x, n_y) = (\frac{n_x \pi}{d_x})^2 + (\frac{n_y \pi}{d_y})^2$,

$n_x = (1, 2, 3.....), n_y = (1, 2, 3.....)$ are the size quantum numbers along x and y directions respectively and d_x and d_y are the nano-thickness along x and y directions respectively.

The quantized sub-band energy (E_{11}) is given by

$$\gamma(E_{11}) = f_1(E_{11})\phi_1(n_x, n_y) \tag{4}$$

The EEM can be expressed as

$$m^*(E_{F1D}, n_x, n_y) = \frac{\hbar}{2} A_{11}(E_{F1D}, n_x, n_y) \tag{5}$$

where E_{F1D} is the Fermi energy in the presence of 2D quantization as measured from the edge of the conduction band in the vertically upward direction in the absence of any quantization and $A_{11}^{'}(E_{F1D}, n_x, n_y)$ is the differention of the $A_{11}(E_{F1D}, n_x, n_y)$ with respect to E_{F1D}. Thus, we observe that the EMM is the function of both the size quantum numbers (n_x and n_y) and the Fermi energy due to the combined influence of the crystal filed splitting constant and the anisotropic spin-orbit splitting constants respectively.

The density-of-states function per sub-band $\left(N_{1D}(E)\right)$ is given by,

$$N_{1D}(E) = \frac{g_v}{\pi}\left[\frac{\left\{\psi_1(E) - \psi_2(E)\phi(n_x, n_y)\right\}}{\psi_3(E)}\right]^{-1/2}$$
$$\left[\psi_3(E)\right]^{-2}\left[\psi_3(E)\left\{\left\{\psi_1(E)\right\}' - \left\{\psi_2(E)\right\}'\phi(n_x, n_y)\right\} - \left\{\psi_1(E) - \psi_2(E)\phi(n_x, n_y)\right\}\left\{\psi_3(E)\right\}'\right] \tag{6}$$

The electron concentration per unit length can be expressed as

$$n_0 = \frac{2g_v}{\pi}\sum_{n_x=1}^{n_{x\max}}\sum_{n_y=1}^{n_{y\max}}[B_{11}(E_{F1D}, n_x, n_y) + B_{12}(E_{F1D}, n_x, n_y)] \tag{7}$$

where

$$B_{11}(E_{F1D}, n_x, n_y) = [A_{11}(E_{F1D}, n_x, n_y)]^{1/2}$$

$$, B_{12}(E_{F1D}, n_x, n_y) = \sum_{r=1}^{r_0} Z_{1D}(r)[B_{11}(E_{F1D}, n_x, n_y)],$$

and $Z_{1D}(r) = 2(k_B T)^{2r}(1 - 2^{1-2r})\xi(2r)\frac{\partial^{2r}}{\partial E_{F1D}^{2r}}$,

III. Results And Discussions

Using the appropriate equations together with the energy band constants as given in [11], the variation of the EEM in NWs of non-linear optical materials along the transport direction has been exhibited in the figures below at various conditions.

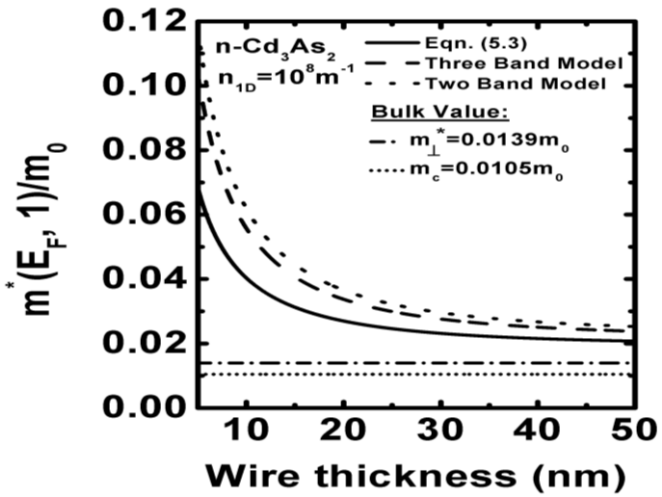


Fig. 1. Plot of the EEM as function of wire thickness for NWs of Cd_3As_2. The plots for three and two band models of Kane have also been exhibited with their corresponding anisotropic bulk values.

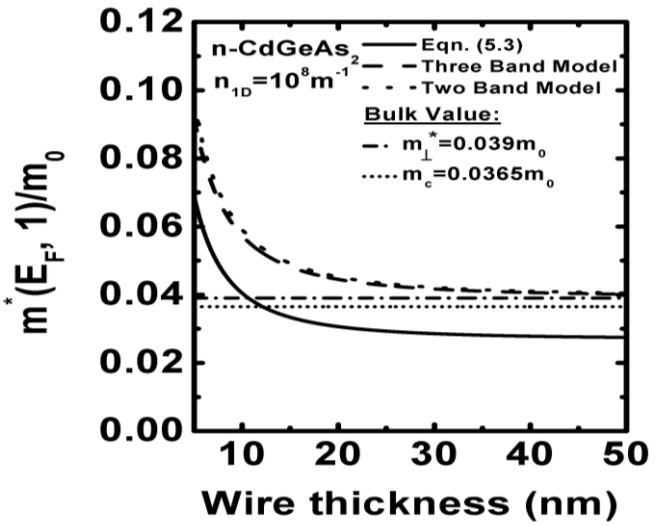


Fig. 2. Plot of the EEM as a function of wire thickness for NWs of $CdGeAs_2$ for all the cases of Fig. 1.

Throughout our formalism, we have assumed the NWs to be of rectangular cross-sectional dimensions so that the usual "particle-in-a-box" concept can be applied along the quantized directions. The NWs are assumed to be degenerately doped with a carrier density starting from 10^8 m^{-1}. While deriving the closed form analytical solutions of EEM in all the materials, we have also assumed that the constants of the energy band structures of the materials are independent of thickness in the range beyond 5nm. Generally speaking, as also will be shown in paper 8, that the "band-gap" is a strong function of cross-sectional dimension and its geometry, i.e., whether the cross-section is circular or triangular. For example in Si NW, it is observed that the band gap is very high and even becomes direct rather than its usual indirect nature in the zone 1-4 nm cross-sectional dimensions and beyond this, the band gap is nearly equal to its bulk value. Keeping this trend in view, we have assumed the invariant property of the material energy spectrum constants and evaluated the EEM in NWs of Cd_3As_2 and $CdGeAs_2$ as function of wire thickness along their respective transport directions in Figs. 1 and 2. It appears from Figs. 1 and 2 that the EEM at the lowest subband in both the cases are strong cross-sectional functions of the dimensions which converge to their corresponding bulk values at larger dimensions. The effect of crystal field splitting in case of dispersion relation of Cd_3As_2 lets the asymptotic fall to be closer to the bulk value. It should be noted that all the curves have been evaluated at T = 4 K where the average thermal energy i.e., $E_F + k_BT$ is very less than that of the difference of the adjacent subband energies. This leads the carrier to reside in the lowest subbands only. In this venture, we have tried to correlate the variation of EEM in terms of conceptual DFT based descriptors viz. global hardness (η) , global softness (S) and electrophilicity index (ω). An inverse relationship is observed between EEM in NWs of advanced material with their computed global hardness and electrophilicty index.

Table-1:- A Descriptive Table of DFT based Descriptors with variation of EEM

Variation of EEMs	Global Hardness (η) (eV)	Global Softness (S) (eV)	Electrophilicity Index (ω) (eV)
0.12	3.06	0.327	0.05
0.10	3.10	0.322	0.13
0.08	4.04	0.247	0.26
0.06	4.09	0.244	0.34
0.04	4.25	0.235	0.44
0.02	4.56	0.219	0.52
0.02	4.77	0.210	0.57

The basic aim of this paper is not solely to study the EEM in NWs of advanced materials, but also to formulate the electron statistics in its most generalized form since the transport in nano-systems depends on the temperature dependent carrier degeneracy in such compounds.

REFERENCES

[1] S. Adachi, J. Appl. Phys. 58, R11 (1985)

[2] R. Dornhaus and G. Nimtz, *Springer Tracts in Modern Physics*, Vol. 78, (Berlin-Heidelberg, N., Springer, 1, 1976)

[3] K.P. Ghatak and M.Mondal, Z.F. Physik B B69, 471 (1988); A.N. Chakravarti, K.P.Ghatak, K. K. Ghosh, S. Ghosh, and A. Dhar, Z.F, Physik B. 47, 149 (1982)

[4] M.Mondal and K.P.Ghatak, Phys. Letts. 131 A, 529 (1988); K.P. Ghatak and B. Mitra, Int. J. Electron. 72, 541 (1992); B.Mitra, A. Ghoshal, and K.P.Ghatak, Nouvo Cimento D 12D, 891 (1990); K.P.Ghatak and S.N. Biswas, Nonlinear Optics and Quantum Optics 4, 347 (1993), 12, 83 (1995); V. Milanovic and D. Tjapkin, Physica B & C 114(3),375(1982); Z.S. Gribnikov, K. Hess and G.A. Kosinovsky, J. Appl. Phys. 7(4), 1337(1995); M. Dyakonov and M.S. Shur, J. Appl. Phys. 84(7), 3726 (1998)

[5] K.P.Ghatak, A. Ghoshal. and B. Mitra, Nouvo Cimento 14D, 903 (1992); 13D, 867 (1991); K.P Ghatak, A. Ghoshal, and B. Mitra, Nouvo Cimento 13 D, 867 (1991); B. Mitra and K.P. Ghatak, Solid State Electron. 32, 177 (1989); M. Mondal, N. Chattapadhyay, and K.P. Ghatak, J. Low Temp. Phys. 66 131 (1987)

[6] J. W. Rowe, J. L. Shay, Phys. Rev. B, 3, 451 (1973)

[7] H. Kildal, Phys. Rev. B, 10, 5082 (1974)

[8] J. Bodnar, in *Proc. Int. Conf. of the Physics of Narrow-gap Materials* (Polish Science Publishers, Warsaw, 1978); G. P. Chuiko, N. N. Chuiko, Sov. Phys. Semicond.15, 739 (1981); K. P. Ghatak and S. N. Biswas, Proc. of SPIE, 1484, 149 (1991)

[9] R. G. Parr, W. Yang, 'Density Functional Theory of Atoms and Molecules,' Oxford, University Press, Oxford, 1989.

[10] P.Geerlings, F.De Proft, Int. J. Mol. Sci.,2002,3,276.

[11] K.P. Ghatak, S. Bhattacharya, *Thermoelectric Power in Nanostructured Materials : Strong Magnetic Fields,* Springer Series in Materials science 137.



Dr. Ajay Kumar received his PhD, from Sikim Manipal University, in 2010. He is presently working as Professor & Head, Department of Mechatronics and I/C of Academic Section at MUJ. He has published 5 papers in refereed journals and 10 papers in conferences. He has 1 patents to his credit. His areas of research interest are Nanotechnology, Micro-wave Communication, Control Engineering.

A Brief Survey of Nano Materials invoking DFT based Descriptors

Prabhat Ranjan[1] , Ajay Kumar[2], Tanmoy Chakraborty[3]
[1]Dept. of Electronics & Communication,
[2]Dept. of Mechatronics, [3]Dept. of Chemistry
[1,2,3]Manipal University Jaipur
Dehmi-Kalan , Jaipur, Rajasthan
-303007, India
[1]prabat23887@gmail.com, [3]tanmoy.chakraborty@jaipur.manipal.edu

***Abstract*— In modern day, nanotechnology and its application to the real field is an active field of research. In past few decades the advancement of the nanotechnology has opened so many research dimensions in the field of science and technology. The applications of nanomaterial in different forms are indispensable for advancement of the human civilization. The uses of nano-composite materials cover the major field of catalysis, semiconductor, microelectronics, biomedicine, aerospace application, defense, petrochemical, pharmaceutical, clean-energy sectors, photonics, and traditional glass and ceramic industries etc. Due to this diverse nature of applicability of nanomaterials, a number of researchers are actively involved in this domain. Now a days, theoretical and computational study of nano-materials has gained immense importance. Computational study of nano-materials invoking Density Functional based descriptors is very much popular in the concerned research domain. In this venture, we have studied a number of compound semiconductors using Density Functional Theory (DFT) methodology. As the band gap separation is an important index for correlating of any physico-chemical properties, we have computed the band gap of several semiconductors in terms of conceptual DFT based descriptors and tried to correlate with other available data. The nice correlation of our computed parameters with existing reported data supports the validity of our model.**

Keywords—DFT; HOMO-LUMO; Descriptors.

I. INTRODUCTION

In recent day Nanomaterials have got a more focus due to its immense applications in the field of engineering and allied sciences. A number of scientists are actively involved in the research domain of computational nanomaterials. Nowadays, material doped semiconductors are extensively used as nano-clusters for their manifold applications. The band gap of material doped semiconductor is an important parameter for predicting its physico-chemical properties. Remediakis et al.[1] reported basic structural calculation of some group of semiconductor invoking DFT theory. Recently Xiao et al. [2] has reported an accurate band gap calculation of some set of binary and ternary semiconductor in terms of DFT parameters. These particular set of semiconductors are popular for their wide application as photovoltaics and thermoelectrics.

In modern days Density Functional Theory (DFT) is immersed as a popular methodology to calculate the electronics structure of the molecules. Due to its computational friendly behavior researchers are interested to study the properties of any molecular system invoking DFT parameters. Conceptual DFT is an effort to correlate the experimental property of materials in terms of very simple DFT based descriptors. Nowadays, conceptual DFT is being extensively used in the research domain of calculation of band gap and other relevant properties of engineering nanomaterials.

In this venture we have calculated some set of nano-engineering materials taken from reference Xiao et al. In this study we have optimized the structure of instant nanomaterials using DFT methodology in terms of Local Density Approximation (LDA). From the optimized geometries some important DFT based descriptors viz. Global Hardness (η), Global Softness (S), Global Electrophilicity Index (ω) , Global Electronegativity (χ) and Total Bond Energy have been calculated for the series of nanomaterials. In this study we have also calculated Dipole Moment and Quadrupole Moment of some Nanoengineering materials. Some correlation and effort has been made to correlate the experimental band gap with their computed counterparts.

II. METHOD OF COMPUTATION

In this report, we have collected 11 material doped semiconductors and reported them along with their experimental band gap in the table 1. The semiconductors are optimized in terms of LDA approximation invoking DFT with the help of ADF. From the optimized structure eigen value of the HOMO and LUMO have been calculated.

The bond energy is computed as an energy difference between molecule and fragments. In particular when the fragments are single atoms, they are usually computed as spherically symmetric and spin-restricted. This usually does not represent the true atomic ground state. Baerends et al. [3] reported that to obtain the real bond energy, atomic correction terms must be applied for the true (multiplet) fragment ground state. In this venture we have used Morokuma-Ziegler decomposition scheme to study the general theoretical background on the bond energy [4].

The molecular dipole moment is calculated with analytic integration and the molecular quadrupole moment is calculated with analytic integration.

Invoking Koopmans' theorem, I and E have been calculated using the following ansatz-

$$I = -\varepsilon_{HOMO} \quad (1)$$

$$A = -\varepsilon_{LUMO} \quad (2)$$

Thereafter, using I and A, we have computed the electronegativity (χ), global hardness (η), molecular softness (S) and electrophilicity index (ω). For the computation of global reactivity descriptors, we have used the following equations-

$$\chi = -\mu = (I+A)/2 \quad (3)$$

where, μ represents the chemical potential of the system.

$$\eta = \tfrac{1}{2}(I-A) \quad (4)$$

$$S = (1/(2*\eta)) \quad (5)$$

$$\omega = (\mu)^2/(2\eta) \quad (6)$$

The above mentioned computed descriptors have been presented in the table 1.

III. RESULTS AND DISCUSSIONS

As compound semiconductors plays a vital role for its many fold applications, the experimental and theoretical research work on compound semiconductors have got immense importance. In this present venture we have studied a series of compound semiconductors in terms of computational methodology. The result is appended in the table 1.

The quadrupole charge separation is represented in form of quadrupole moment according to Buckingham convention in the Table-2.The quadrupole moment values in different axes are represented in atomic unit (a.u). Molecular dipole moments are reported in Debye in Table-3.

TABLE 1:

Species	Expt. (eV)	Electro negativity (eV)	Hardness (eV)	Softness (eV)	Electrophilicity Index (eV)	Total Bond Energy (KCal/mol.)
InP	1.42	3.74	1.14	0.43	1.87	-72.16
InAs	0.41	3.86	1.12	0.44	1.93	-70.02
ZnSe	2.83	2.18	3.22	0.15	1.09	-0.42
ZnS	3.84	5.42	0.22	2.22	2.71	-55.85
ZnTe	2.39	3.18	2.06	0.24	1.59	-29.79
CdS	2.58	3.18	2.04	0.24	1.59	-47.04
CdSe	1.85	3.12	1.99	0.25	1.56	-43.10
$CuAlS_2$	3.46	4.02	0.77	0.64	2.01	-241.85
$CuGaS_2$	2.50	3.69	0.32	1.55	1.84	-66.59
$CuInS_2$	1.55	4.95	1.03	0.48	2.47	-172.85
$CuAlSe_2$	2.65	5.06	0.98	0.50	2.53	-191.96
$CuGaSe_2$	1.67	4.59	0.44	1.13	2.29	-230.71

A Collection of computed global descriptors along with Experimental Band Gap of a series of Semiconductors

TABLE 2:

Species	Quad-XX	Quad-XY	Quad-XZ	Quad-YY	Quad-YZ	Quad-ZZ
InP	0.84	0.00	0.00	0.84	0.00	-1.69
InAs	-3.36	0.00	0.00	-3.36	0.00	6.73
ZnS	-13.41	0.00	0.00	-13.41	0.00	26.83
CuGaSe2	15.75	-34.13	0.00	-2.89	0.00	-12.85

Molecular Quadrupole Moment of some Nano engineering materials

TABLE 3:

Species	Dipole Moment (Debye)
InP	2.3760
InAs	4.3221
ZnS	5.1679
CuGaSe2	6.8123

Molecular Dipole Moment of some Nano engineering materials

It has been well established a correlation between band gap and orbital energies of HOMO and LUMO for infinite solids [5, 6]. The same correlation is being reflected in our computed data. There is a slight exception only for case of ZnS, $CuInS_2$ and $CuAlSe_2$. As the band gap increases for infinite solids the hardness also increase hand in hand. The computed softness values exhibit an inverse relationship with the experimental band gap. There is no direct correlation between experimental band gap and electronegativity and electrophilicity index.
Another striking fact is observed in the case of ZnS. The band gap of ZnS is the highest among the instant semiconductor and that existing band gap can be nicely correlated in terms of the highest electronegativity of the compound semiconductor.

IV. CONCLUSION

Computational study of Nanomaterials is an active field of research. The engineering and other applications of nano-composite can be easily explained in terms of concep tual and theoretical parameters. DFT, a new paradigm of computational chemistry, is very much popular among the researchers due to its computational friendly manner. In this venture we have successfully studied a set of compound semiconductor invoking conceptual DFT based descriptors. From our calculation it is reveled for the most of the compound semiconductors there is a hand to hand relationship between experimental band gap and there computed global hardness. For ZnS the highest band gap among the instant compound is nicely correlated in terms of the highest computed electronegativity.

ACKNOWLEDGMENT

Author Mr. Prabhat Ranjan expresses his acknowledgement to Mr. Sunil Chawla for providing the computational facility, ADF software. All of the authors are thankful to the management of Manipal University Jaipur for providing the research facility.

REFERENCES

[1] I.N.Remediakis, and Efthimios Kaxiras, "Band-structure calculations for semiconductors within generalized density functional theory," Phys. Rev. B, vol. 59, pp. 5536-543, Feb. 1999. (*references*)

[2] Hai Xiao, Jamil Tahir-Kheli, and William A Goddard, (III), "Acurate band gap semiconductor for density functional theory," J.Phys. Chem. Lett., Vol. 2, pp. 212-217, Jan. 2011 .

[3] E. J. Baerends, V.Branchadell and M.Sodupe, "Atomic reference energies for density functional calculations," Chem. Phys. Lett., vol. 265, pp. 481-489, Feb. 1997.

[4] F.M. Bickelhaupt and E.J. Baerends,"Kohn-Sham density fucntional theory: predicting and understanding chemistry," In: Rev. Comput. Chem.; Lipkowitz, K.B and Boyd, D. B., Eds.; wiley-VCH: New york, vol. 15, pp. 1-86, 2000.

[5] J.P.Perdew, and M. Levy, "Physical content of the exact kohn-sham Orbital Energies: band gaps and derivitive discontinuties,"Phys. Rev. Lett., vol. 51, pp. 1884-1887, 1983.

[6] L.J.sham, and M. Schlöter, "Density functional theory of the enrgy gap,"Phys. Rev. Lett., vol. 51, pp. 1888-1891, 1983.

[7] ADF2013, SCM, Theoretical Chemistry, Vrije Universiteit, Amsterdam, The Netherlands, http://www.scm.com



Prabhat Ranjan received B.E. degree in Electronics & Communication Engineering and M. Tech. degree in Control System Engineering from Manipal Institute of Technology,Manipal University,India in 2009 and 2011. He is pursuing PhD degree from School of Engineering & Technology,Manipal University, India. He carried out 10 month Project work at Siemens Ltd, in Industry Sector- Electrics & Automation Division. (2nd Aug. 2010 3rd June 2011) Currently working as Assistant Professor in Electronics & Communication at Manipal University Jaipur from 9th Aug 2011.

AIR INDEPENDENT PROPULSION (AIP) FOR SUBMARINES - A STRATEGIC NECESSITY

Cdr AV Agashe
Indian Navy,
Karwar, India,
avi81@hotmail.com

INTRODUCTION

A modern submarine is a multi-role platform capable of conducting both overt and covert operations. However, in today's fractured geo political system with changing strategic realities, the role of submarines has drastically transformed from purely being men of war to those capable of undertaking varying mission profiles - from littoral reconnaissance, launching of Special Forces, to protecting sea lanes and communication lines. Simultaneously, submarines are increasingly seen as a valuable strategic resource for both electronic and signal intelligence.

With the induction of INS Chakra, the Indian Navy has joined an elite list of countries operating nuclear submarines. However, conventional diesel electric submarines still remain the mainstay of the Navy's submarine arm. Diesel-electric submarines though, have a fundamental limitation compared to nuclear submarines, because they recharge their batteries by using air-breathing diesel engines. This involves surfacing or snorkeling at periscope depth, which leads to a high probability of the submarine being detected from the surface or air.

Snorkeling, thus, is becoming an increasingly risky operating regime as radar technology advances. Visual and radar detection of the above water submarine structures, acoustic detection of the diesel engines, exhaust and infrared emissions are various means of detection of a submerged submarine. While these can be reduced through use of radar absorbing coatings and dispersal of the exhaust underwater, the submarine is nonetheless more vulnerable to detection at periscope depth than when submerged. Evolving radar technology is now challenging the viability of even well designed snorkels. Specifically, high resolution Synthetic Aperture Radar (SAR) provides a capability to detect the wake of a submerged submarine. With advances in this technology, it will provide good detection probabilities especially against shallow running submarines.

The aim then is to reduce the Indiscretion Ratio (time spent snorkeling as compared to the time spent dived) of a submarine. In a typical diesel-electric submarine of about 2000 tons displacement, travelling at a speed of 6 knots, the indiscretion ratio is about 10% and increases rapidly with increasing speed. Hence, a submarine is vulnerable for a significant number of hours, everyday. Conversely, a submarine which has a reduced requirement to surface and is more free to choose the timing and location of surfacing, has a significant tactical advantage. Nuclear submarines aside, the technology now exists to release the submarine from its enforced reliance on periodic visits to the surface.

Air Independent Propulsion (AIP) systems help address this issue by providing systems that are capable of generating electrical power even whilst the submarine is submerged. Air Independent Propulsion involves carrying supplies of fuel and oxidant which are reacted in an energy conversion device to ultimately produce electrical energy. This is used primarily for propulsion, for recharging the batteries and to power electrical equipment, while the submarine continues to remain submerged. Since this can be carried out underwater, it offers the potential to reduce the Indiscretion Ratio and enhance submerged performance by extending the underwater range and endurance of the submarine at low patrol speeds.

This paper examines four of the commonly used AIP systems- Fuel Cells, Closed Circuit Diesels, MESMA and Sterling Engines. The paper provides principles of operation and technical details of each of the AIP systems, highlights their advantages/ drawbacks and challenges involved in implementation.

HISTORY

All over the world, several attempts have been made over tme to develop a propulsion system for submarines without using atmospheric air. In 1867 Narcís Monturiol i Estarriol successfully developed a peroxide powered anaerobic or air independent steam engine. In 1908, the Imperial Russian Navy launched the submarine Pochtovy which used a gasoline engine fed with compressed air and exhausted under water. During World War II, the German firm Walter experimented with submarines that used concentrated hydrogen peroxide as their source of oxygen under water. These used steam turbines, employing steam heated by burning diesel fuel in the steam/oxygen atmosphere created by the decomposition of hydrogen peroxide by a potassium permanganate catalyst.

Several experimental boats were produced, and one, U-1407, which had been scuttled at the end of the WW II, was salvaged and recommissioned into the Royal Navy as HMS Meteorite. The British built two improved models in the late 1950s, HMS Explorer, and HMS Excalibur. Meteorite was not popular with its crews, who regarded it as a dangerous and volatile piece of machinery; she was officially described as "75% safe". The reputations of Excalibur and Explorer

were little better, the boats were nicknamed Exploder and Excruciator.

The Soviet Union also experimented with the technology and one experimental boat was built. Hydrogen peroxide was eventually abandoned since it is volatile, highly reactive with various metals, and is consumed by submarines at a high rate. The only countries known to be experimenting with it, the Soviets and British, abandoned it when the United States developed a nuclear reactor small enough for submarine propulsion.

AIR INDEPENDENT PROPULSION (AIP)

There are several AIP technologies at various stages of development worldwide. Heat engine systems include Closed-Cycle Diesel engines, Stirling engines, Closed-Cycle Gas turbines, and Rankine engines powered by hydrocarbon fuel (French MESMA system) or a small nuclear reactor (Canadian AMPS system). Fuel cells and semi-cells are the only non-heat engine technologies under development, other than development of high energy density batteries such as lithium aluminium iron sulphide (LAIS). Four prominent AIP technologies are discussed in this paper. They are:-

1) Fuel Cells
2) Stirling engines
3) Closed-Cycle Diesel engines
4) MESMA



Fig. 1. Germany's U34 fuel cell submarine.

FUEL CELLS

Fuel cells, one of the leading AIP contenders, are electrochemical energy converters that enable the chemical energy of a stored fuel and an oxidant to be converted directly to electricity. Hydrogen is the most common fuel, but hydrocarbons such as natural gas and alcohols like methanol are sometimes used. Fuel cells are different from batteries in that they require a constant source of fuel and oxygen/air to sustain the chemical reaction; however, fuel cells can produce electricity continuously for as long as these inputs are supplied.

There are many types of fuel cells, but they all consist of an anode, a cathode and an electrolyte that allows charges to move between the two sides of the fuel cell. Electrons are drawn from the anode to the cathode through an external circuit, producing direct current electricity. As the main difference among fuel cell types is the electrolyte, fuel cells are classified by the type of electrolyte. The different types of fuel cells include Polymer exchange membrane fuel cell (PEMFC), Solid oxide fuel cell (SOFC), Molten-carbonate fuel cell (MCFC) and Phosphoric-acid fuel cell (PAFC) amongst others.

The Polymer Exchange Membrane Fuel Cell (PEMFC) is one of the most promising fuel cell technologies. The PEMFC uses one of the simplest reactions of any fuel cell.

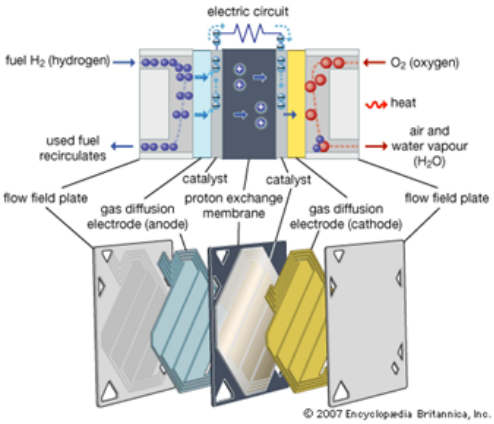


Fig. 2. Basic elements of a PEMFC.

There are four basic elements in a Fuel cell. The **anode** is the negative electrode of the fuel cell. It conducts the electrons that are freed from the hydrogen molecules to be used in an external circuit. It has channels etched into it that disperse the hydrogen gas equally over the surface of the catalyst.

The **cathode**, the positive electrode of the fuel cell, has channels etched into it that distribute the oxygen to the surface of the catalyst. It also conducts the electrons back from the external circuit to the catalyst, where they can recombine with the hydrogen ions and oxygen to form water. The **electrolyte** is the proton exchange membrane. This specially treated material, which looks like a kitchen plastic wrap, only conducts positively charged ions. The membrane blocks electrons. For a PEMFC, the membrane must be hydrated in order to function and remain stable. The **catalyst** is a special material that facilitates the reaction of oxygen and hydrogen. It is usually made of platinum nanoparticles very thinly coated onto carbon paper or cloth. The catalyst is rough and porous so that the maximum surface area of the platinum can be exposed to the hydrogen or oxygen. The platinum-coated side of the catalyst faces the PEM.

Figure 2 shows the pressurized hydrogen gas (H_2) entering the fuel cell on the anode side. This gas is forced through the catalyst by the pressure. When an H_2 molecule comes in contact with the platinum on the catalyst, it splits into two H+ ions and two electrons (e-). The electrons are conducted through the anode, where they make their way through the external circuit (doing useful work such as turning a motor) and return to the cathode side of the fuel cell.

Meanwhile, on the cathode side of the fuel cell, oxygen gas (O_2) is being forced through the catalyst, where it forms two oxygen atoms. Each of these atoms has a strong negative charge. This negative charge attracts the two H+ ions through

the membrane, where they combine with an oxygen atom and two of the electrons from the external circuit to form a water molecule (H_2O).

This reaction in a single fuel cell produces only about 0.7 volts. To get this voltage up to a reasonable level, many separate fuel cells must be combined to form a fuel-cell stack. Bipolar plates are used to connect one fuel cell to another and are subjected to both oxidizing and reducing conditions and potentials.

The equations taking place inside a fuel cell are shown below:-

Acid Electrolyte Cell

$2H_2 = 4H^+ + 4e^-$ AT ANODE

$O_2 + 4H^+ + 4e^- = 2H_2O$ AT CATHODE

Overall Reaction

$2H_2 + O_2 = 2H_2O$

Advantages

1) Fuel cells do not employ any reciprocating parts and are silent and have low acoustic and thermal signatures.
2) Minimum waste heat transfer to sea water.
3) Modular design allows easy retro fitment on existing submarines.
4) Higher efficiency than other AIPs.
5) Water is the only byproduct of reaction which can be released without contamination of the environment.
6) Low maintenance due to limited machinery.

Limitations

1) Storage of hydrogen and oxygen presents unique technological challenges since oxygen is a fire hazard and hydrogen is potentially explosive.
2) Fuel cells can respond to rapid power requirements in a marine environment. However, development of auxiliary systems to respond to these requirements is a problem area. In case of rapid load removal, the fuel in the stacks will have to be vented. A submarine application will require the unused fuel to be sent through a catalytic converter.
3) A sophisticated water management system will be required for removal and disposal of 'exhaust' water.

Storage of reactants

The greatest challenge for fuel-cell AIP systems lies in storing the reactants. Although oxygen can be handled with relative safety as LOX, storing hydrogen onboard as a liquid or high-pressure gas is very dangerous. One solution is to carry the hydrogen in metal hydride accumulators, at low pressure and ambient sea temperature. (A metal hydride is a solid compound of hydrogen and metallic alloy, in which individual hydrogen atoms occupy interstitial positions in the host metal's crystalline lattice. By manipulating temperature and pressure, hydrogen gas can be absorbed or released at will.)Another, less efficient, approach is to generate gaseous hydrogen from a stored liquid hydrocarbon such as diesel fuel, kerosene, or methanol.

This requires an auxiliary device called a "reformer," in which a mixture of hydrocarbon and water is vaporized and superheated under pressure to yield a mixture of hydrogen and carbon dioxide. A 10 kW auto thermal reformer has been developed by the department of engineering, USA with a reforming efficiency of 71-74%.

Applications

Siemens has developed a 30-50KW fuel cell unit. Nine of these units are incorporated into HDWs AG's 1,830t submarine U31, lead ship for the Type 212A class of the German Navy. The other boats of this class and HDW's AIP equipped export submarines (Dolphin class submarine, Type 209 mod and Type 214) use two 120 kW modules, also from Siemens.

The AIP implemented on the S-80 class of the Spanish Navy is based on a bioethanol-processor (provided by Hynergreen from Abengoa, SA) consisting of a reaction chamber and several intermediate Coprox reactors, that will transform the BioEtOH in high purity hydrogen. The output feeds a series of fuel cells from UTC Power company (which also supplied fuel cells for the Space Shuttle). The reformator is fed with bioethanol as fuel, and oxygen (stored as a liquid in a high pressure cryogenic tank), generating hydrogen as a sub-product. The produced hydrogen and more oxygen is fed to the fuel cells.

STERLING ENGINE

In the Stirling cycle, heat from an outside source is transferred to a working fluid - generally an inert gas - and drives it through a repeating sequence of thermodynamic changes. By expanding the gas against a piston and then drawing it into a separate cooling chamber for subsequent compression, the heat from external combustion can be converted to mechanical work and then, in turn, to electricity. This approach has an advantage over internal combustion systems, such as the Closed Cycle Diesel, in that the combustion processes can be kept separate from those that actually convert heat to mechanical work.

In a Stirling cycle engine, a hot gas machine works in a closed thermodynamic cycle with helium or hydrogen as the working medium. They are unique heat engines because their theoretical efficiency is nearly equal to the Carnot cycle efficiency. The expansion and compression of a fixed amount of gas which is transferred back and forth between a cold end and hot end powers these engines. These engines have two pistons that create a 90 degree phase angle and two different temperature spaces. The working gas in the engine is perfectly sealed. The two piston type Stirling engine consists of two power pistons. The displacer piston displaces the gas between the two ends and the power piston changes the internal volume as the gas expands and contracts. Its expansion in the hot chamber is used to produce mechanical energy.

Advantages

1) Uniform expansion of working fuel due to external heat source and absence of explosion in the cylinder results in low noise and vibrations thus making the engine quiet.
2) The engine is versatile and can work with different fuels. So any type of fuel can be used and this provides operation flexibility.
3) The combustion pressure is higher than the surrounding seawater pressure, thereby allowing the exhaust products, dissolved in seawater, to be discharged overboard without using a compressor.

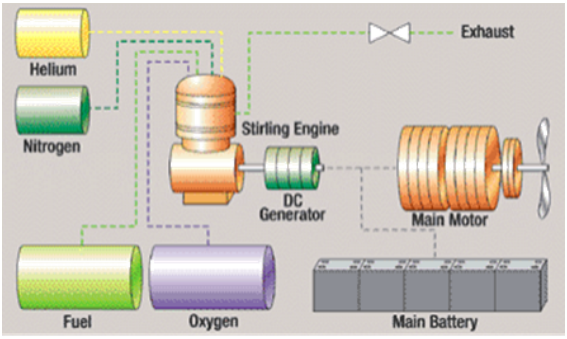


Fig. 3. Stirling engine schematic.

4) Its infrared signature is very low.
5) The system has a low acquisition cost and a low life-cycle cost.

Disadvantages

1) The engine has a complicated design.
2) Exhaust system is pressurized to 20 bar and so it can be released overboard only till 200 m depth.
3) There will be a requirement for a dedicated exhaust removal system at greater depths.
4) As with other AIPs, there is considerable problem in storage of oxygen and working fluid.

Applications

In 1988 Kockums fitted a Stirling engine in the Royal Swedish Navy submarine HMS Näcken to achieve air-independent propulsion. The submarine was placed in dry-dock and cut in two. A fully outfitted eight-meter Stirling AIP section was then inserted. The Swedish shipbuilder Kockums has constructed three Gotland-class submarines for the Swedish Navy which are fitted with an auxiliary Stirling engine which uses liquid oxygen and diesel fuel to drive 75KW generators for either propulsion or charging batteries. The endurance of the 1,500-tonne boats is around 14 days at 5 kn (5.8 mph; 9.3 km/h).

Kockums has also refurbished/upgraded the Swedish Västergötland class submarines with a Stirling AIP plug-in section. Two of these submarines (Södermanland and Östergötland) are in service in Sweden as the Södermanland class, and two of them are in service in Singapore as the Archer class (Archer and Swordsman). Kockums has also delivered Stirling engines to Japan. The new Japanese submarines will all be equipped with Stirling engines. The first submarine in the class, Sōryū, was delivered to the navy in March 2009.

The new Swedish A26 submarine will have the Stirling AIP system as its main energy source. The submerged endurance will be more than 18 days at 5 knots using AIP.

MESMA

The only steam-turbine AIP under active development / operation is the French MESMA (Module d'Energie Sous-Marine Autonome). Basically, the MESMA approach is a derivative of French nuclear-propulsion experience using non-nuclear source for steam generation. Although MESMA can provide higher output power than the other alternatives, its inherent efficiency is the lowest of the four AIP candidates, and its rate of oxygen consumption is correspondingly higher. The first full-scale undersea application is in Pakistan's Agosta 90B submarines.

The primary circuit consists of fuel ethanol and oxygen stored in tanks, vaporizer, combustion chamber and steam generator. Liquid oxygen is stored at -185 ^{0} C. This is cryogenically pumped into a vaporizer where it becomes gaseous. It is then brought into combustion chamber and combined with ethanol, producing a thermal output of 700 ^{0} C at pressure of 60 bar to heat the secondary circuit. The exhaust gases are passed through a heat exchanger producing steam at 500 ^{0} C at 18 bar. This pressure firing allows the exhaust to be expelled from the submarine at 60 bar allowing discharge at any depth without the use of any aux machinery. A re-circulator recycles part of the cooled exhaust gas to regulate the temp inside the primary circuit. Oxygen and fuel flow rate are determined by power demand.

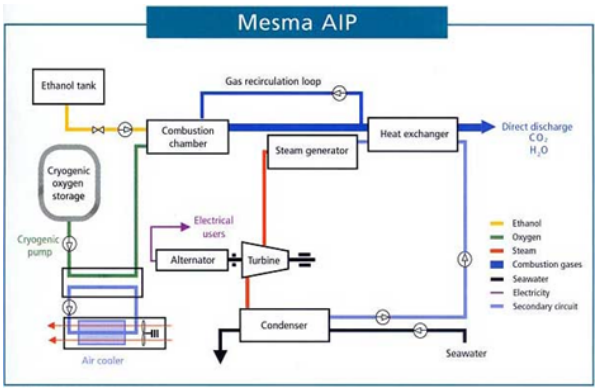


Fig. 4. MESMA Schematic.

Although MESMA can provide higher output power than the other alternatives, its inherent efficiency is the lowest of the four AIP candidates, and its rate of oxygen consumption is correspondingly higher.

The French MESMA system is being offered by the French shipyard DCNS. MESMA is available for the Agosta 90B and Scorpène-class submarine. It is essentially a modified version of their nuclear propulsion system with heat being generated by ethanol and oxygen. Specifically, a conventional steam turbine power plant is powered by steam generated from the combustion of ethanol (grain alcohol) and stored oxygen at a pressure of 60 bar. This pressure-firing allows exhaust carbon dioxide to be expelled overboard at any depth without an exhaust compressor.

Each MESMA system costs around $50–60 million. As installed on the Scorpène, it requires adding a new 8.3 meter (27 foot), 305 ton hull section to the submarine. The resulting AM-2000 Scorpene AIP is about 70m long and displaces 1,870t. A CM-2000 Scorpene can operate underwater for 4-6 days without surfacing or snorkelling to get oxygen to recharge its batteries. An AM-2000 Scorpene, in contrast, will be able to operate for up to 18 days, depending on variables like speed, etc.

CLOSED CIRCUIT DIESEL

A closed-cycle diesel (CCD) system incorporates a standard diesel engine that can be operated in its conventional mode on the surface or while snorkeling. Underwater, however, it runs on an artificial atmosphere synthesized from stored oxygen, an inert gas (generally argon), and recycled exhaust products. The engine exhaust - largely carbon dioxide, nitrogen, and water vapor - is cooled, scrubbed, and separated into its constituents, with the argon recycled back to the intake manifold. The remaining exhaust gas is mixed with seawater and discharged overboard. Generally, the required oxygen is stored in liquid form - LOX - in cryogenic tanks.

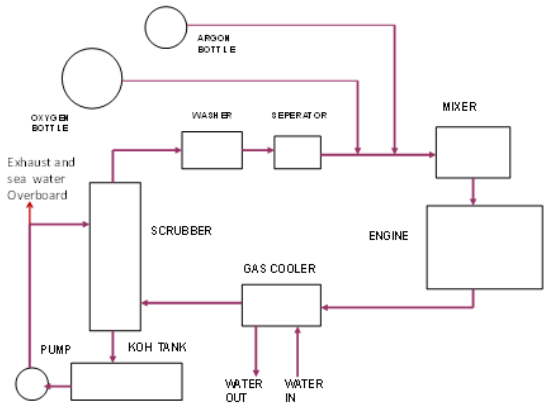


Fig. 5. Closed Cycle Diesel.

Advantages

Closed cycle diesel uses a standard diesel engine. Additional components/equipments for AIP can be easily retrofitted in the engine rooms of a submarine.

Disadvantages

1) As with fuel cells, storage of oxygen and inert gas is a problem area and oxygen has to be stored cryogenically.
2) Since the system uses a standard diesel engine, it operates as noisily and produces as much heat as a conventional diesel engine. Therefore it offers no gain as far as sonar and IR detection are concerned.

Applications

During World War II the Kriegsmarine experimented with such a system as an alternative to the Walter peroxide system, including a variant of the Type XXVIIB Seehund midget submarine, the "Klein U-boot". It was powered by a 95 hp Diesel engine of a type commonly used by the Kriegsmarine and which was available in large numbers, supplied with oxygen from a tank in the boat's keel holding 1,250 litres at 4 atm (410 kPa).

CONCLUSION

Presently, AIP cannot be compared with nuclear propulsion in terms of operational capability and is not an independent propulsion option. Moreover, each AIP system design comes with an array of technological limitations, vulnerabilities, and risks, particularly in submerged operations – from the specific acoustic signatures produced by select AIP systems in specific operating regimes, to technical vulnerabilities in storing oxidizer/fuel, as well as their maintenance regime. Therefore, the choice of AIP would greatly depend on how well it is integrated with other critical systems that ensure optimal submarine functions: power systems, sensors systems, safety systems, navigation systems, command, control, and communication systems, weapons systems, and climate control systems.

Despite these limitations, AIP is extremely valuable at low speeds for submarines, especially in patrol areas. Further, the biggest advantage of AIP today that it can be retrofitted into existing submarine hulls by inserting an additional hull section. Although AIP does not normally provide the endurance or power to replace the atmospheric dependent propulsion, it allows the submarine to remain submerged longer than a conventionally propelled submarine. It would well be the deciding factor in ensuring that a submarine is able to undertake covert operations without being detected. To enhance the varying operational capabilities, increased submerged endurance and stealth required by a modern day submarine, installing Air-Independent Propulsion Systems on conventional diesel-electric submarines is thus becoming a strategic necessity.



Cdr AV Agashe is an alumnus of the 9th Naval Engineering Course. He has completed his BE (Mech) from Naval College of Engineering, Lonavala and Post Graduation in Nuclear Technology from BARC, Mumbai. He joined the Submarine Arm in 1999 and has served onboard submarines INS Sindhurakshak and INS Sindhukesari. The officer is presently appointed as Engineer Officer, INS Aditya.

ELECTRIC PROPULSION: A STRATEGIC CHOICE FOR THE INDIAN NAVY

Commander PS Vombatkere, Indian Navy
Deputy Chief Quality Assurance Officer
Chief Quality Assurance Establishment (Warship Equipment)
Bangalore, India
psvombatkere@gmail.com

Abstract *— This paper suggests electric propulsion as a preliminary strategic technological choice for a developing Navy, analyses the costs and benefits of its adoption, and recommends a preliminary strategic roadmap for electric propulsion research in developing navies, with specific long-term recommendations. It also briefly covers life cycle cost assessment and the economic benefits that accrue from electric propulsion, and ends with recommendations that aim to realise the strategic research roadmap earlier proposed.*

I. INTRODUCTION

Ongoing research in integrated full electric propulsion (IFEP) and the all-electric ship (AES) concept is being aggressively pursued by a closed group of navies in collaboration with well-developed defence industry in the backdrop of enormous political and financial backing, and transfer of such technology to India would pose political and economic obstacles. The US Navy's Science and Technology funding for selected propulsion technologies alone for the fiscal period 2003-2011 was pegged in 2006 at USD 476.6 million[1], excluding expansion of scope, industry's own R&D investment and investment in analysis, evaluation and think tanks for strategy and policy formulation; and the US DoD has budgeted USD 75.8 billion for R&D, Testing & Evaluation for 2012.[2] With the technical specifications of virtually all new induction orders for the Indian Navy already frozen, the time is ripe for a strategic R&D initiative that will bear fruit in 15-20 years, by which time the next phase of inductions will be considered for modernisation.

The attributes of IFEP and HED make electric propulsion a major strategic factor in the growth of a developing navy, evidenced by the substantial resources committed by world navies to its development and adoption in surface combatants. Until now, many navies have treated electric propulsion as just another powering philosophy for ships, but its true strategic nature makes it a game-changer in the expansion strategy of any developing navy.

II. THE STATE OF THE ART

Many of the enabling technologies for electric propulsion are still on drawing-boards and test-beds, and many more are yet to be de-risked from the standpoint of technical and economic risk. Those that are in use in the field today are mostly expensive and exclusive. But with the increasing adoption of IFEP and HED on commercial vessels, both cost and availability are improving.

A. Motor Technologies

For IFEP to be practical, the propulsion motor should be compact, power-dense, rugged and efficient at low loads since combatants spend much of their time at low speeds. In combatants displacing 6000 tonnes or less, propulsion motors are very low speed (100-175 RPM), high torque (106-107 N-m) machines, typically rated in the 10-25 MW range.[3] The Advance Induction Motor (AIM), Permanent Magnet Motor (PMM) and the High Temperature Superconducting (HTS) Motor are all contenders for the AES. The PMM has high power and torque density and reduced weight and size compared with a conventional induction motor, but suffers from an inability to turn off the magnetic field in the event of a fault, which could lead to a shipboard safety hazard. Induction motors have a more robust, mature design, but suffer from lower power and torque density compared with newer types of motors. The AIM is approximately twice the size of a PMM of the same capacity. The HTS motor uses virtually resistance-free ceramics for electrical transmission, and is up to 60% smaller than conventional motors, resulting in significant decrease in size and weight. However, these advantages are offset by its relatively high cost and a lack of shipboard experience in handling and operating the cryogenics system that cools the motor coils. A comparison of different types of propulsion motors with respect to relative size, cost and risk involved is given in **Table 1**.

Table 1. Size-cost-risk comparison of propulsion motor types.[4]

Motor Types	Relative Size	Relative Cost	Relative Risk
DC	Max Dia	Near Min	Min
AC Synchr	Near Max Dia	Near Min	Min
AC Induction	Near Min Dia	Min	Min
AC PM	Near Min Dia	Near Max	Near Max
AC HTS	Min Dia	Max	Max

[1] St. Laurent, Janet A: ***Propulsion systems for Navy ships and submarines***; United States government accountability office report GAO-06-789R submitted to Subcommittee on Projection Forces, Committee on Armed Services, House of Representatives, July 2006, Pp 17.

[2] Harrison, Todd: ***Analysis of the FY 2012 Defense Budget***; Center for Strategic and Budgetary Assessments, Washington, DC (USA), July 2011, Pp 73.

[3] Newell, Cdr (RN) J.M., and Young, Cdr (RN) S.S.: ***Beyond Electric Ship***; The Institute of Marine Engineers, 24 October 2000.

[4] Dalton, Thomas; Boughner, Abe; Mako, C. David and Doerry, Cdr (USN) Norbert: ***LHD 8: A step toward the All Electric Warship***; American Society of Naval Engineers, 2001.

B. Motor Control Technologies

The propulsion motor and associated Variable Speed Drive (VSD) is truly the heart of the AES. Although VSDs began with the use of cyclo-converters and current source inverters (CSIs) {also known as the load commutated inverters (LCIs)} with thyristors or GTOs as the primary power devices, higher IGBT/ IGCT ratings, have led to increasing use of PWM drives for larger applications. PWM technology is a key enabler for electric propulsion in military ships because of its ability to more precisely control the voltage waveform to the motor. Other drives include SCR-based DC converters for DC motors and voltage source inverter (VSI) type converters for asynchronous, synchronous and permanent magnet synchronous AC motors. With variable speed drives, average loading will be higher with less running hours; fuel costs, wear and tear, maintenance and power plant dimensions will decrease. The characteristics of fixed-speed CPP and variable-speed FPP units are compared in **Table 2**.

C. Integrated Power Systems

Besides its integrated nature, an IPS is characterised by modularity and open architecture. This improves flexibility, scalability and ruggedness, and also facilitates generic designing. The application of the zonal concept to IPS design (Figure 1) greatly improves ship survivability ('fight-through' capability) under battle damage conditions, owing the presence of autonomous zonal power supply units (ZPSUs). The distributed location of prime movers and the inherent reconfigurability of the flexible IPS design also contribute to improved survivability.

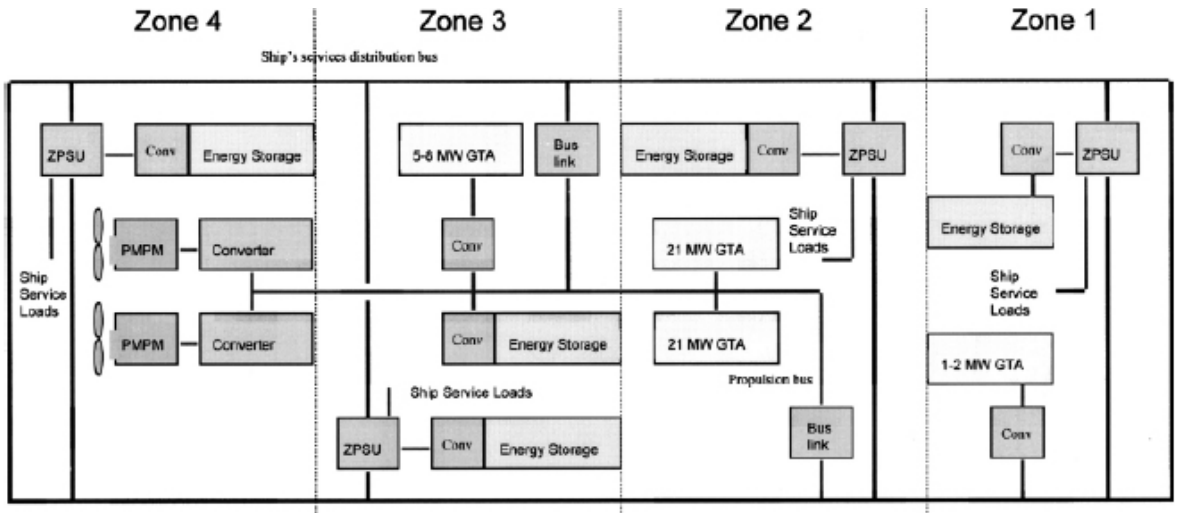
Table 2. Comparison of Electric Drive Alternatives.[5]

	DOL Asynchr Motor + CPP	SCR DC Motor Drive	Cyclo-converter [1]	CSI (LCI) [1]	VSI [2] with DTC[3]
Start-up Amps	Typ. 5 x rated current	≈ 0 (transformer inrush)	≈ 0 (transformer inrush)	≈ 0 (transformer inrush)	≈ 0 (transformer inrush)
Start-up torque transients	Typ. 2-3 x rated torque	≈ 0	≈ 0	Up to 50% of rated torque	≈ 0
Pwr consumption, low thrust	≈ 15% of nom prr	≈ 0	≈ 0	≈ 0	≈ 0
Amps at low thrust	45-55% of nominal	F (torque)	F (torque)	F (torque)	≈ 0
Power factor – full load	≈ 0.85	> 0.9	> 0.76	> 0.9	> 0.95
Power factor variation with load (cosφ)	0.15 ... 0.85 (non-linear)	0 ... 0.9 (prop speed)	0 ... 0.76 (prop speed)	0 ... 0.9 (prop speed)	> 0.95 (≈ constant)
Dynamic response (power, torque)	3-5 sec (pitch control)	< 100 ms	< 100 ms	slower	< 10 ms
Torque ripple	None	Smooth	Smooth	Pulsating	Smooth
Zero-thrust crossing	Smooth if negative thrust allowed	Discontinuous	Smooth	Pulsating	Smooth
Efficiency at full load	High	Lower	High	High	High
Harmonic distortion:					
- at low speed / thrust	None	F (torque)	F (torque)	F (torque)	≈ 0
- at full speed / thrust	None	F (torque)	F (torque)	F (torque)	F (power)
Short circuit contribution	Typ. 5 x nom prr	No	No	No	No
Motor matching required	–	Some	Some	Yes	No
Commutator	No	Yes	No	No	No

[1] With synchronous motor [2] With squirrel-cage induction motor [3] (Direct Torque Control)

Note: Low thrust equals low speed in variable speed drives and small fixed speed drives for CPP systems.

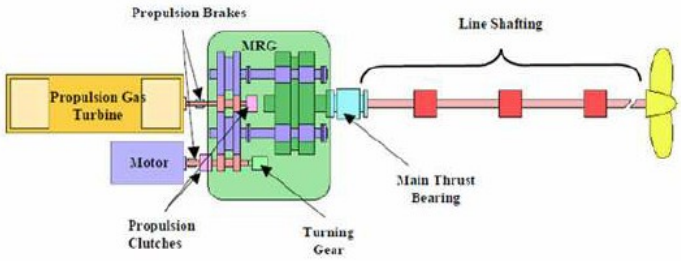
Figure 1. An example of zonal IFEP architecture.[6]



[5] Ådnanes, Alf Kåre: ***Maritime electrical installations and diesel electric propulsion***; ABB AS Marine, April 2003.

[6] Newell, Cdr (RN) J.M., and Young, Cdr (RN) S.S.: ***Beyond Electric Ship***; The Institute of Marine Engineers, 24 October 2000.

Figure 2. The Hybrid Electric Drive (HED) Concept.[7]



D. Hybrid Drives

At higher speeds, internal combustion engines (diesel/ GT) are more efficient and electric motors are efficient but expensive on account of the necessarily large sizes; whereas at low speeds, internal combustion engines are less efficient and electric motors are more efficient and also more affordable on account of the smaller sizes required. Hybrid propulsion (**Figure 2**) involves the use of electric propulsion for low speeds, and diesels/ GTs at higher speeds, capitalising on the respective strengths of each technology. This optimisation of propulsors makes for lower heat and noise signatures, and therefore, better stealth. This combination of cost & performance advantages makes hybrid propulsion systems even more attractive that IFEP, particularly for developing navies, which have to plan inductions in the face of severe funding constraints and other uncertainties.

III. A STRATEGIC ASSESSMENT

A. The Benefits of IFEP

1) Design Aspects. There are eight basic design attributes of IFEP that offer significant advantages, in terms of Life-Cycle Cost (LCC) as well as Operational Superiority:-

a) Architecture. The modular & open architecture of IPS supports modular ship design, increased automation and reconfigurability. In terms of ship design, it could also facilitate the multi-role design concept, which would allow for mission packages replacement during a short refit, to alter the primary role of the combatant.

b) Prime Mover Siting. Freed from the technical constraint of designing the ship around the shaft-line between IC engine prime mover and propeller, the AES designer enjoys flexibility in siting of prime movers, with the following benefits:-

- Optimal use of on-board space, allowing more space for mission payloads;
- Spatial distribution of machinery assets, leading to better survivability;
- Easier mitigation of noise & vibration (N&V) / IR signatures; and
- Optimisation of hull lines, leading to higher fuel-efficiency and better manoeuvrability.

c) Loading. Basic IPS architecture ensures optimal loading of prime movers, which increases fuel efficiency, reduces N&V / IR emissions, permits flexible operating regimes, provides higher power reserve, improves reliability and reduces maintenance liability.

d) Captive Power Requirement. Typically, the captive power ratio for propulsion to ship services ("hotel loads") on board a conventionally propelled warship is of the order of 4:1 or 5:1, and these are mutually isolated. Most classification societies have a voluntary class notation for redundancy of a ship's propulsion and manoeuvrability; in general, only 50% of propulsion power is required,[8] and the redundancy required for ship services is usually much less. The conventional arrangement incorporates separate redundancies in each group, with the result that the total capacity is far in excess of the actual operational requirement. However, if a common power system is provided for propulsion and ship services, the overall redundancy calculated afresh will invariably be less than the sum of the redundancies in propulsion and ship services of the conventional system, since the desired redundancy for ship services is easily absorbed within the margin for propulsion. This reduction of captive power requirement reduces maintenance duration and liability, and the space it saves allows for greater mission payloads.

Figure 3. Azimuth thrusters with CRP (left) and twin same-direction propellers (right).[9]

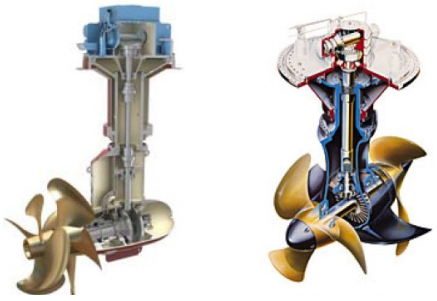
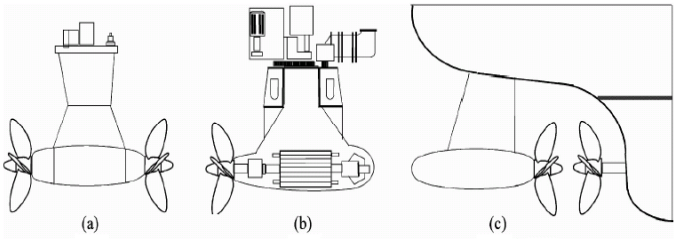


Figure 4. Pod configurations: (a) Dual / twin pod; (b) Azimuth Pod; and (c) CRP.[10]



e) Shafting Configurations. Freedom from the 'tyranny of the shaft-line' allows for flexibility in shafting,

[7] McMullen, David and Dalton, Thomas: ***Hybrid electric drive – enhancing energy security***; Electric Power and Controls Systems Division, Naval Sea Systems Command, Washington (DC), January 2012, Pp 6.

[8] McGreer, Dan and Sipilä, Heikki: ***Modern cruise ship propulsion - a case study***; Presentation at the Society of Naval Architects and Marine Engineers, Ottawa, Canada, 19 November 2009.

[9] Radan, Damir: ***Power electronic converters for ship propulsion electric motors***; Marine Cybernetics-Energy Management Systems, Department of Marine Technology, Norwegian University of Science & Technology, 2005.

[10] Moreno, Victor M. And Pigazo, Alberto: ***Future trends in electric propulsion systems for commercial vessels***; Journal of Maritime Research, Vol. IV No.2, 2007, Pp 89.

with a variety of in-board and outboard options, including azimuth pods, azimuth thrusters, pods with contra-rotating propellers (CRP), azimuth pod in conjunction with contra-rotating propeller driven by an inboard motor, in-board motor with CRP, and so on. Some of the options are illustrated in **Figures 3** and **4**. This shafting flexibility enables hull lines optimisation with consequent improvement of fuel-efficiency.

f) Automation. Amenability to increased automation in IPS reduces maintenance liability and durations, and increases flexibility in operating regimes.

g) Alternate Power Sources. Although current wisdom dictates that IC engines be used as prime movers, developments in alternate power sources such as various types of fuel cells, means that quieter, cleaner and potentially more efficient, higher-endurance alternatives exist. A comparison of electric power plants is shown in **Figure 5**. Further, zonal IPS design requires use of autonomous ZPSUs, for which several energy storage options exist, such as include mechanical flywheels, electro-chemical batteries (both conventional and advanced), regenerative fuel cells (otherwise known as Redox flow cells or Regenesys), Superconducting Magnetic Energy Storage (SMES) and Supercapacitors. Thus, the amenability of IPS to alternate power sources reduces emissions and IR / N&V signatures, promotes reconfigurability, improves fossil-fuel efficiency, and, through its usually more compact sizes, enables increased mission payloads.

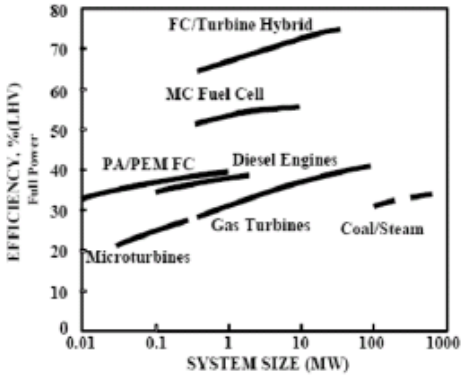


Figure 5. A Comparison of Electric Power Plants.[11]

h) Auxiliaries. The availability of an electric power system of enormous capacity will lead to the electrification of a large number of services, resulting in elimination of many auxiliary systems, such as steam, hydraulic, pneumatic, etc to a large extent. Since electric drives are power-for-power smaller than these drives, this elimination will result in considerable space savings, leading to availability of more space for mission payloads. Reduction of auxiliaries will also improve reconfigurability, reduce IR / N&V signatures, and improve reliability.

2) Life Cycle Cost Aspects. Life cycle cost (LCC) is a function of the capital and operation costs associated with the ship (**Table 3**), and its assessment is an essential component of ship design. Ton for ton, an AES has a lower LCC than a conventionally propelled ship, owing to the following primary factors, each of which flows from the design attributes mentioned earlier. The implications of lowered LCC are manifold: increased force levels, greater ease of obtaining sanction for induction programmes, and the option of leveraging the innate 'green' benefits of IFEP for economic advantage.

a) Fuel-Efficiency. IFEP has higher fuel-efficiency due to optimal loading of prime movers, hull lines optimisation using pods/ thrusters, and amenability to alternate power sources.

b) Maintenance. Maintenance liability is reduced, owing to higher reliability, optimal loading of prime movers, reduction in captive power requirement and increased automation.

c) Manning. The AES requires lower manning in view of increased automation and lower maintenance and reduction in auxiliary systems.

3) Operational Aspects. Finally, a warship is all about performance in battle. Operational superiority is thus the overriding concern of any warship programme, perhaps even more so than cost considerations. The AES has eight primary operational features that give it distinct superiority over conventionally propelled combatants of comparable tonnage.

a) Endurance. Endurance is significantly improved due to better view availability of higher power reserve and increased fuel-efficiency, which allows for longer periods of continuous operation between successive refuellings.

b) Manoeuvrability. Ship manoeuvrability is improved due to through hull lines optimisations using pods / thrusters.

c) Mission Payload. Increased mission payloads are possible due to better space utilization on account of flexibility in prime mover siting, reduction of auxiliaries and captive power requirement, prime mover siting flexibility, reduced manning and, to some extent, due to the amenability of the IPS to alternate, more compact power sources.

d) Reliability. The unified modular system architecture of IFEP, along with increased automation and reduction of auxiliary systems together contribute to a very substantial augmentation of overall reliability.

e) Detectability. Stealth will improve (ie, detectability will reduce), owing to lower exhaust emissions view optimal loading of prime movers; and lower IR, noise & vibration emissions view distributed machinery assets.

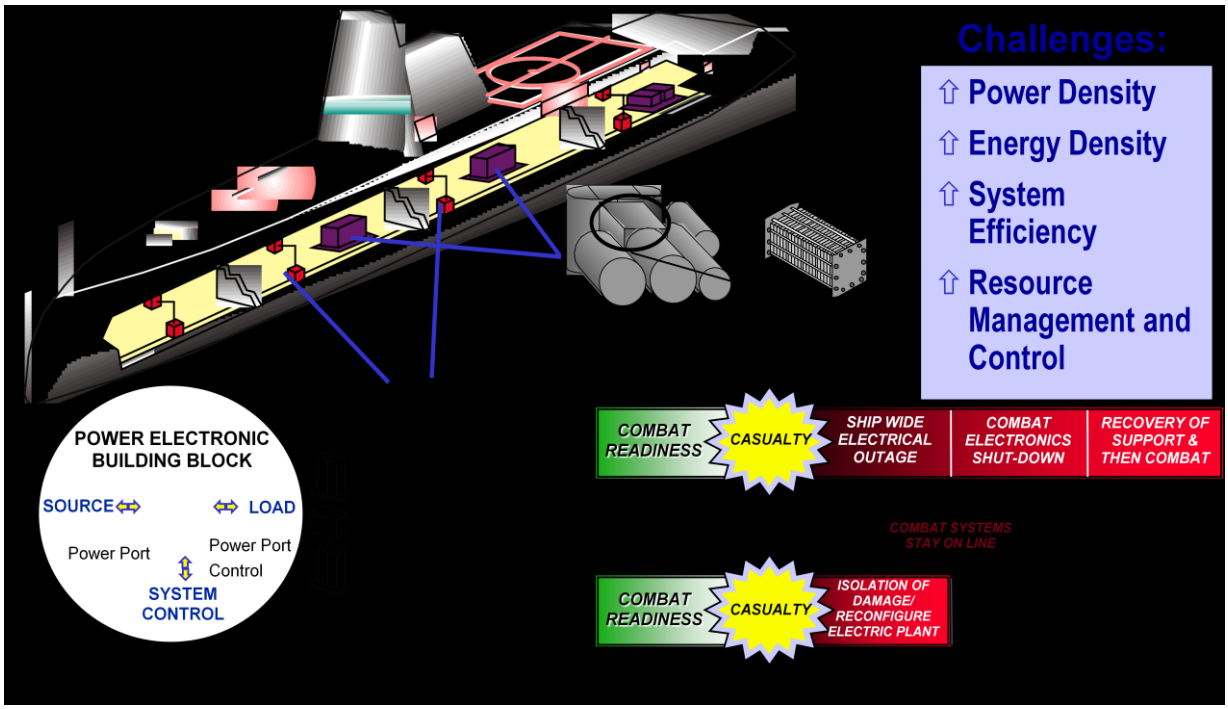
f) Survivability. The AES has improved survivability (reduced failure vulnerability) in view of improved reliability; distributed machinery assets through flexible prime mover siting; high power reserve with multiple power units; and reconfigurability on account of modular design and flexible & open power system architecture. A schematic representation of a reconfigurable, survivable power system is shown in **Figure 6**.

[11] O'Rourke, Ronald: ***Navy ship propulsion technologies: options for reducing oil use — background for Congress***; US Congressional Research Service Report RL33360 for submission to the US Congress, December 2000.

Table 3.Elements in a Life Cycle Cost Assessment.[12]

Life Cycle Cost , LCC = CapEx + OpEx			
Capital Expenditures		**Operational Expenditures**	
Design and administration cost	Total engineering and project administration cost from project start to operation.	**Man-hour cost**	Cost of required man-hours per year to operate and maintain facility / equipment (fixed crew, workload dependent crew, contractors and vendors).
Equipment and material purchase cost	Total purchase cost associated with the system.	**Spare parts consumption cost**	Total cost of spare parts and consumables over design life of facility and systems, necessary to complete predicted workload for all maintenance actions (i.e. preventive maintenance, corrective maintenance and servicing).
Fabrication cost	Total fabrication cost associated with the system.		
Installation cost	Total cost associated of installing systems and equipment.	**Logistic support cost**	Total logistic support cost necessary to support operation and maintenance requirements for facility and system (e.g. supply boat, diving support vessel, helicopters).
Commissioning cost	Total cost to commission and certify installed systems and equipment.		
Insurance spares cost	Total purchase cost for initial spares holding for systems and equipment, necessary to obtain required system regularity.	**Energy consumption cost**	Total energy consumption cost for facility and systems, including cost of fuel required to generate power and associated CO_2 tax.
Reinvestment cost	Total cost to remove, refurbish or purchase, install and commission systems and equipment that is predicted to exceed its design life during life of facility.	**Onshore support cost**	Total cost of required onshore support services and administration.
		Cost of deferred production	Total cost of deferred production due to probability of failure of systems and equipment.
Finance costs	Finance costs during construction.		

Figure 6.Schematic of a reconfigurable, survivable power system.[13]



[12] Ådnanes, Alf Kåre: ***Maritime electrical installations and diesel electric propulsion***; ABB AS Marine, April 2003.

[13] Baldwin, Thomas: ***Harmonic and distributed generation interaction issues in the U.S. Navy All-Electric Ship program***; Presentation for the Center for Advanced Power Systems, Florida State University, in the session on "Impact of Distributed Generation" at the Power Systems Conference 2002, 13-15 March 2002.

g) Maintenance Periods. The AES requires shorter maintenance periods (implying higher operational availability) due to reduced maintenance liability owing to lower machinery stress through optimal loading; and also due to reduced auxiliaries and captive power requirement.

h) Operating Regimes. The AES is operationally more versatile because of flexibility in operating regimes, owing to optimal loading and high power reserve (both of which give more allowance for load fluctuations) and increased automation.

B. The Overall Strategic View

1) IFEP offers significant design and technical attributes that translate finally into the twin advantages of lowered running costs and greater operational superiority. As seen from the foregoing discussion, the list of attributes that translate into these advantages is large, and their interconnections are complex. A simplified relationship chart summarising these attributes, advantages and their inter-relationships, is given in **Figure 7**.

2) "Float-Move-Fight-Survive". The primary overall attributes that must be built into any marine combatant platform are: *To Float*; *To Move*; *To Fight*; and *To Survive*. It goes without saying that this is also, logically, the order of precedence that can be ascribed to these attributes: only if water-tight integrity is assured, can propulsion have any value; once propulsion is assured, the mission assumes significance; and once mission capability is assured, survivability becomes important. The inter-relationships between the attributes of IFEP will be seen to follow this logic, and this makes them easier to understand as an integrated whole.

3) New Paradigms. The adoption of IFEP/ HED in surface combatants will call for evolution of new paradigms for developing new procedures, standards and methodologies. This will pose new challenges that need to be addressed in a timeframe commensurate with the induction of this technology. The tasks involved in this will include the following:-

- Development of R&D programmes and setting up of infrastructure for this.
- Formulation of a rational system for assessment of enabling technologies and planning their insertion into the electric ship-building programme.
- Adaptation and adoption of COTS technologies/ products for application in IFEP.
- Evolution of a fresh paradigm (including procedures and methodologies) for AES and IPS operation, including power system management, fire-fighting. damage control, emergencies, operator/ equipment/ platform safety, and operating regime definition (single vs multiple generator operation, etc).
- Evolution of a new maintenance philosophy and developing the infrastructure required to follow it.
- Evolution of procedures and methodologies for IPS / IFEP evaluation and testing, and developing the infrastructure required for this.
- Formulation of a fresh training paradigm, including the requisite infrastructure.
- Identification of standards and certification required to be complied with for safe and economic construction, operation and maintenance of an AES.

4) Induction. The selection of enabling technologies that offer strategic advantages requires to be planned from the conception stage of the platform, since retro-fitting is bound to rob the technology of some of its true strategic value. An in-depth understanding of the strategic and tactical requirements (evolved from our national maritime strategy, strategic threat perception and defence budget), governing standards and availability / maturity of purchasable / researchable technologies will yield the accurate specifications that are essential to initiate procurement. The availability of technical support both within and outside the country is another strategic consideration that needs to be worked into the procurement process. Finally, a policy framework covering the entire life cycle of the product needs to be evolved, so as to leave no lacunae in its operational availability throughout its service life. Some of the strategic considerations in procurement are as follows:-

a) The Maritime Capability Perspective Plan (MCPP) formulated in 2006 outlines the Indian Navy's force structure till 2022, and the types of platforms that need to be maintained with high tech weapons and sensors. The approach is to bridge the gaps in indigenous technology capability through JVs with reputed OEMs abroad. We need to find a place for electric propulsion technologies in the MCPP.

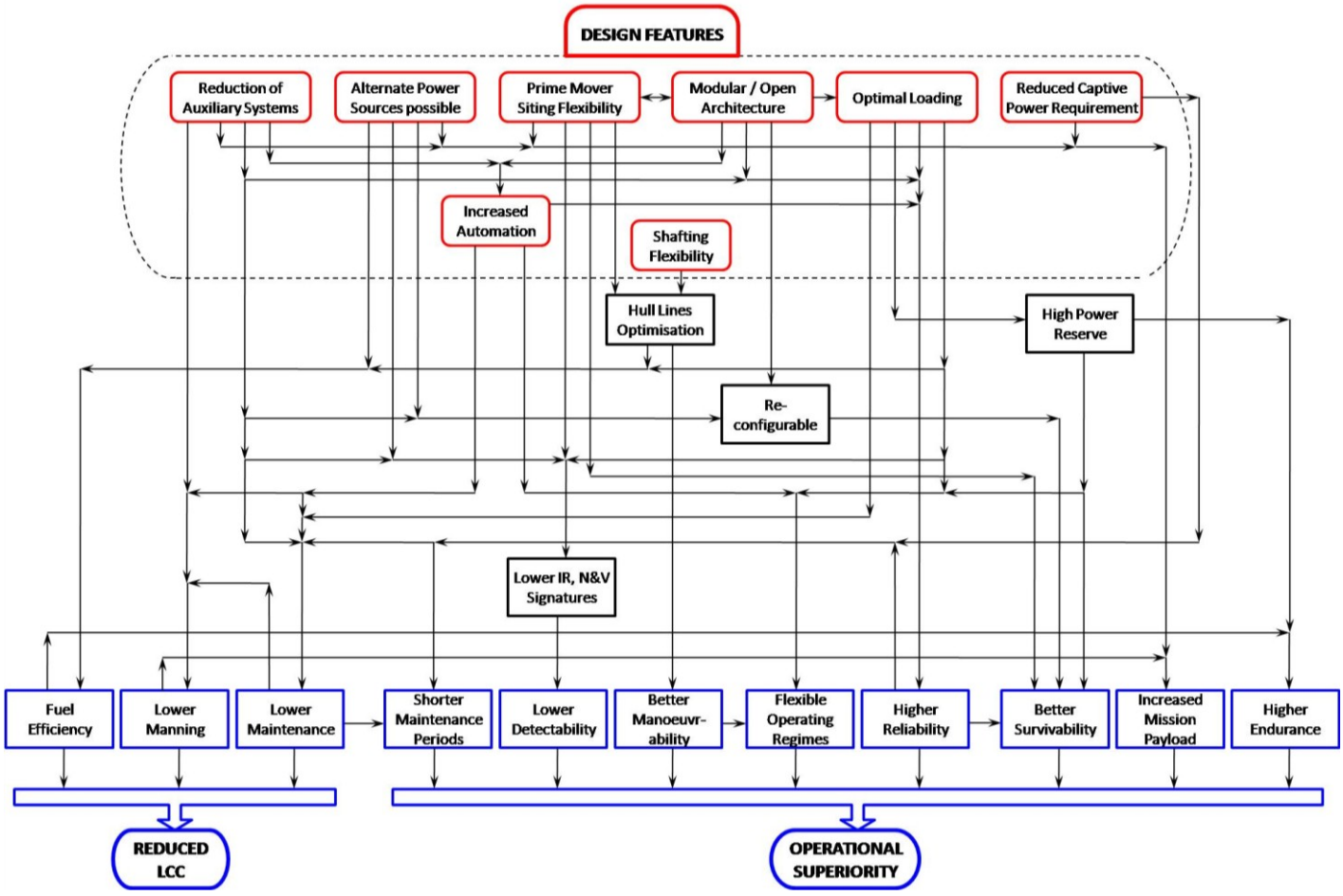
b) The induction plan for electric propulsion technologies needs to figure in the 5-year Services Capital Acquisition Plan (SCAP) and the 15-year Long-Term Integrated Perspective Plan (LTIPP) of the Defence Forces.

5) The Costs of IFEP. Despite the optimistic picture of an operationally superior AES with lowered life cycle costs, there are nevertheless some significant costs or 'disadvantages' that need to be considered whilst planning the induction of IFEP.

a) Investment Cost. The capital expenditure involved in the machinery and systems for IFEP is considerably higher than that for conventionally propelled ships, mostly owing to the degree of the enabling technologies and its relative infancy in military application.

b) Exclusion. International alignment issues and military-economic alliances will have regional balance implications for us as well as for donor nations. For instance, the *Wassenaar Arrangement*, a group of 45-odd developed nations, specifies a list of equipment / technologies that cannot be exported by member nations to non-member nations. India is not a member of this group. The 'strings attached' with the import / transfer of critical, exclusive technologies cannot be overemphasised. A way around this pitfall is through offsets: Transfer of Technology (ToT) is the commonest type of direct offset in defence transactions, and up to 30% of all defence offsets relate to ToT of varying degrees. The Wassenaar Arrangement and other restrictive technological embargos/ sanctions are important strategic factors that will affect a strategic decision regarding the adoption of IFEP.

Figure 7. Relationship chart of IFEP attributes and advantages.



IV. A STRATEGIC ROADMAP

A. Research Mission

The roadmap for research proposed by this paper to achieve the tasks listed earlier is based on a five-stage research mission involving academia, industry and government in a synergistic relationship including research seeding, intellectual pooling, exchange forums and institutionalised participation in development and production programmes. The stages of this mission will be as follows:-

STAGE 1. To build graduate and undergraduate power system engineering programs in academia that will produce well-trained engineers who understand the basic enabling technologies.

STAGE 2. To build a multidiscipline research program in advanced power systems and other AES-related disciplines that will rely on both graduate students and staff researchers, and enable categorisation of technologies into "readiness levels".

STAGE 3. To assess the application-readiness of potential technologies and plan research for each through a three-way partnership between academia, industry and the government that will build an industry base to work with developing navies.

STAGE 4. To focus on building participation by both military and commercial users of the technology to foster the identification of "dual use" opportunities.

STAGE 5. To develop a dedicated facility for carrying out simulation, testing, research, development and proving of concepts, technologies, equipment and systems in the field of electrical propulsion and power systems.

B. Technology Management

Managing enabling technologies and planning their insertion into individual R&D programmes will be a major task towards achieving this research mission. The application-readiness of potential technologies must be accurately quantified for timely and appropriate insertion into end-use programmes directed towards on-board combatant mission systems. Since their conception by the USA in the 80's, Technology Readiness Levels (TRLs) have evolved into the 9-tier categorisation system (**Table 4**) used today by the USN's Office of Naval Research. Typically, technology is assigned a TRL of 1 in the basic research phase, 6 when ready for consideration in an acquisition programme and 9 when fully proven. We need a similar system for AES research, to enable rational readiness assessment of diverse technologies.

Table 4. Definitions and descriptions of TRLs. (Courtesy: Wikipedia)

TRL	Definition	Description
1	Basic principles observed and reported	Lowest level of technology readiness. Scientific research begins to be translated into applied research and development (R&D). Examples might include paper studies of a technology's basic properties.
2	Technology concept and/or application Formulated.	Invention begins. Once basic principles are observed, practical applications can be invented. Applications are speculative, and there may be no proof or detailed analysis to support the assumptions. Examples are limited to analytic studies.
3	Analytical and experimental critical function and/or characteristic proof of concept	Active R&D is initiated. This includes analytical studies and laboratory studies to physically validate the analytical predictions of separate elements of the technology. Examples include components that are not yet integrated or representative.
4	Component and/or breadboard validation in laboratory environment.	Basic technological components are integrated to establish that they will work together. This is relatively "low fidelity" compared with the eventual system. Examples include integration of "ad hoc" hardware in the laboratory.
5	Component and/or breadboard validation in relevant environment.	Fidelity of breadboard technology increases significantly. The basic technological components are integrated with reasonably realistic supporting elements so they can be tested in a simulated environment. Examples include "high-fidelity" laboratory integration of components.
6	System/ subsystem model or prototype demonstration in a relevant environment.	Representative model or prototype system, which is well beyond that of TRL 5, is tested in a relevant environment. Represents a major step up in a technology's demonstrated readiness. Examples include testing a prototype in a high-fidelity laboratory environment or in a simulated operational environment.
7	System prototype demonstration in an operational environment.	Prototype near or at planned operational system. Represents a major step up from TRL 6 by requiring demonstration of an actual system prototype in an operational environment (e.g., in an air-craft, in a vehicle, or in space). Examples include testing the prototype in a test bed aircraft.
8	Actual system completed and qualified through test and demonstration.	Technology has been proven to work in its final form and under expected conditions. In almost all cases, this TRL represents the end of true system development. Examples include developmental test and evaluation (DT&E) of the system in its intended weapon system to confirm if it meets design specifications.
9	Actual system proven through successful mission operations.	Actual application of the technology in its final form and under mission conditions, such as those encountered in operational test and evaluation (OT&E). Examples include using the system under operational mission conditions.

C. Division of Responsibilities

Division of responsibilities on a rational basis is essential for a coordinated and coherent execution of the research mission mentioned earlier. The main players are the Indian Navy (as the user and prime motive force behind the research effort), the DRDO, Industry and Academia.

1) The Indian Navy. It logically devolves upon the professional and design directorates of the Indian Navy (*IN*) to initiate, coordinate and guide research at different levels and in selected fields, based on various deciding factors such as the availability of research material, maturity of the technology, cost of application, viability of production, and so on. For this, it will be necessary to formulate a policy framework to create a conducive backdrop for the research, development and induction of technologies. Further down the hierarchy, there exist several centres of excellence in various disciplines related to IFEP-enabling technologies, including naval R&D and training establishments, and these entities must be suitably empowered and tasked towards fulfilling various aspects of the research mission. The training establishments could also be prepared to take on training of future AES crews on IFEP and IPS technologies, equipment and systems. Other responsibilities of the *IN* could include sourcing of technical study material; acting as a focal point for exchange of ideas and research results; designing and planning procurement of requisite testing, simulation and training.

2) The DRDO. As a premier organisation responsible for Defence R&D s, the DRDO is best disposed to coordinate and undertake most of the research activities (including research, analysis, synthesis, modelling, and simulation) either directly in its laboratories or as offloaded / co-ordinated programmes, be they with academia or to industry. The DRDO commands vast funds, enjoys very significant administrative support at the highest levels, and has at its command tremendous assets in the form of numerous laboratories and research establishment all over the country, and also in the form of reciprocal relationships with other governmental R&D organisations.

3) Industry. The active participation of Indian Defence Industry and R&D establishments will be critical for developing the requisite baselines of expertise and infrastructure for future maintenance and repair of IFEP systems on board AES. From a global perspective, the Indian defence military-industrial complex is reasonably mature and experienced in dealing with development, delivery and field support for advanced systems including weapons, sensors, missile technology, power technology, switchgear and motors, and submarine technology. The active participation of commercial and military ship end-users, shipbuilders, classification societies, machinery and equipment manufacturers, research institutes, universities, and other organisations must further add to the overall efforts of indigenous development of enabling technologies to a level that permits application to *IN* ships.

4) Academia. There are several attributes of Academia that make long-term association attractive from the point of view of research strategy. These include almost unfettered access to research papers, study material and other academic material; reciprocal agreements with overseas academic institutions already engaged in research in fields of interest; the large size and unified nature of the knowledge base and document repositories; the availability of a vast pool of potential researchers (or contributors towards research) in relevant technologies at almost all levels of technical education; and cost-effectiveness since the financial profit motive of Industry is absent. Investment in Academia will be a long-term one, and hence the strategy for fostering their involvement in IFEP research and the AES Project must offer attractive returns to institutions involved in AES-oriented research.

V. RECOMMENDATIONS

The list of activities and tasks that need to be undertaken to achieve the ambitious research mission drawn up earlier would obviously be very large. However, this paper recommends the following important activities as a start in this direction.

A. Long-Term Recommendations

1) Strategic Procurement Planning. Inclusion of electric propulsion technologies in the MCPP; and inclusion of the induction plan for these technologies in the 5-year SCAP and the 15-year LTIPP of the Defence Forces.

2) Policy Formulation. This must include the following:-

a) Participative inclusion of Industry and Academia into the R&D effort executed by the Indian Navy, DRDO and other R&D organisations;

b) Division of R&D and other responsibilities among these entities;

c) Creation of a central project organisation to steer and direct procurements, R&D and production;

d) Evolution of maintenance and repair policies and infrastructure for the 'new technology' equipment and systems both within and outside the Navy; and

e) Training of personnel on the exploitation, maintenance and repair of these equipment and systems.

3) Acquisition of a Test Platform by the DRDO. There is a need for a sea-going platform for testing and de-risking electric propulsion technologies and other emergent naval technologies. The IN, with its manning limitations, would be ill-advised to acquire a dedicated test platform that would be manned mostly by non-naval personnel for analysis / field testing. Further, time-frames for installations / retro-fits would interfere with operational commitments, while designation as a full-time test platform would effectively reduce force levels. The test platform must therefore belong to the DRDO, possibly with its operation and maintenance outsourced.

4) Creation of a Funding Mandate. The "green" fuel-saving benefits of IFEP could be used to leverage government for a special funding mandate for the AES Project, based on environmental targets formulated at the Kyoto Protocol and subsequent world environmental summits.

B. Short-Term Recommendations

1) Sensitising and Influencing Primary Policy-Makers. The decisions for the adoption of electric propulsion technologies and the initiation of an AES programme must be top-down. We need a *paradigm-shift* in the way we think about propulsion tech and its operation and maintenance. To this end, primary policy-makers in the Indian Navy must be adequately sensitised to the strategic benefits of electric propulsion through service papers, research briefs and presentations.

2) Conduct of International Seminar on IFEP. This must be organised in the immediate future as a ground-breaking activity that will identify fields of study most amenable to immediate adoption for R&D; permit industry and academia to highlight their capabilities and demonstrate our commitment to IFEP; bring to our notice available enabling technologies; and prepare us for participation in IEEE's Electric Ship Technologies Symposium.

3) Participation in next Electric Ship Technologies Symposium (ESTS). It will be necessary to garner the support of, and build bilateral relationships with Defence Industry at the international level, and in order to do so, it is imperative for our commitment towards IFEP to be recognised by the world. Presenting a paper in IEEE's biennial ESTS in 2015 would achieve this aim. Over 200 delegates from international academia, military navies and industry were represented at ESTS-2011 at Alexandria, Virginia (USA) on 10-13 Apr 11.[14]

[14] IEEE Power and Energy Society (PES) ***Electric Ship Technologies Symposium*** website, http://ests11.wordpress.com, accessed on 31 March 2011.

Rudder Roll Stabilisation: An Perspective

Lt Cdr Swarup Das[1], **Cmde AN Sonsale**[2]
[1]Technical Staff Officer-II,
[2]Head of Faculty (Navy)
Military Institute of Training Girinagar, Pune - 411025
[1]swarupd@diat.ac.in
[2]hodnavy@diat.ac.in

***Abstract*—The technical feasibility of roll motion control devices has been amply demonstrated for over 100 years. Performance, however, can still fall short of expectations because of difficulties associated with control system designs, which have proven to be far from trivial due to fundamental performance limitations and large variations of the spectral characteristics of wave-induced roll motion. This tutorial paper presents an account of the development of rudder as means of reducing roll in addition to its primary job of maintaining steady head. This is typically an under-actuated single input two output (SITO) system. Though the concept has many advantages in its application, however there are few disadvantages associated with it. The concept of rudder roll stabilisation (RRS) is based on the utilization of rudder induced inward roll for stabilizing the ship which is also known as undershoot behavior that characterizes Non Minimum Phase (NMP) system with the existence of right half plane zero in the corresponding transfer function. Stability of RRS and its applicability onboard has been provided by experiment conducted at various marine lab across the world with the scaled model which has shown that implementation RRS is feasible but ships steering machine is to be redesigned for improved characteristic by stronger stock bearing and faster servo mechanism. This paper gives a perspective on RRS and the mechanism involved in it. Feasibility, challenges of RRS is explained via Numerical analysis of the mathematical model.**

***Index Terms*—Rudder Roll Stabilisation, Non Minimum Phase, Servo-mechanism, Control Application**

I. Introduction

Ship roll stabilization refers to the stable feedback system applied in both active and passive systems used for reduction of the undesired ship roll motion induced by the waves. The topic has been an area of active research since 1970s. This is because the roll motion can affect the performance of seagoing surface vessels by limiting the effectiveness of the crew, reduced capability to handle equipments, damaging cargo, and limiting the operation of on-board equipment. It was shown by Froude, in his seminal paper On the rolling of ships, in 1861[1,2], that it is not the height of the waves, but the steepness (slope) what excites the rolling motion of a ship. He further commented that since short waves appear to be steeper than long waves, there is, then, no advantage in trying to reduce the natural roll period of the vessel. Instead, this period should be extended as much as possible so as to avoid synchronization with the wave excitation frequency. This can only be achieved by increasing the moment of inertia and reducing the transverse stability [3]. From William Froudes observations on roll motion, which lead to the proposal of bilge keels in the late 1800s, to the present, various devices have been proposed and used to reduce ship roll motion like Gyroscope; Anti Rolling tanks both active as well passive, active fin stabilization, shifting trolley and Rudder Roll Stabilization. Most of the drawbacks of conventional active fin stabilizers and anti-roll tanks are overcome by RRS. Provided the speed of the ship and the rudder rate are sufficiently high, this technique can be applied to different ship types: small and large naval vessels, patrol (coastguard) vessels, ferries. Rudder Roll Stabilization (RRS) is an attractive method for reducing ship rolling motion produced by waves. By doing so, cargo damage is prevented, while crew efficiency and passenger comfort are improved. RRS uses the capacity of the rudder to produce roll motion apart from its normal course keeping function.

The main advantages of RRS can be mentioned as Medium to high performance (RMS) [4], Relatively inexpensive, Less hydrodynamic resistance, no underwater acoustic signature, No large spaces required, Low life cycle cost, Less overall weight, Can be combined with other stabilizers to achieve higher performance.

However RRS has got some disadvantages. They are ineffective at low speeds, Nevertheless, this can be higher than that of fins because the rudders are located in the race of the propellers; and thus, operate in higher speed flows than fins. Drag is produced when in use but, this can be less than the drag of fin stabilizers, provided ship turning is prevented [5]. Rudder machinery up-grade may be needed to achieve high performancefaster rudder motion.

Although the idea of using the rudder as a roll stabilizing mechanism ignited in the early 1970s, the performance obtained was, in general, poor. This was mainly because of the simple control strategies attempted, due to the limitations imposed by the analog computers. Using the rudder for simultaneous course keeping and roll reduction raises non trivial issues since there is only one actuator available to achieve two objectives. Therefore, tradeoffs are expected to limit the achievable closed loop performance. Several control schemes have been proposed in the literature to address RRS. These schemes use different approaches, e.g., Quantitative Feedback Theory [4], LQR [2], and Model Predictive Control [5]. However to date, a little has been said about the fundamental limitations imposed on the closed loop performance by the single input two output (SITO) nature of the problem. The system has also a non minimum phase (NMP) zero, and it is

known that this usually limits the achievable performance. The characterization of the best achievable performance in terms of the intrinsic dynamics and structure of the system reveals what is and, conversely, what is not achievable prior to applying any specific technique for solving the control problem. This leads to key conclusions about the trade-offs inherent in the achievable closed loop performance that hold irrespective of the control strategy being used.

In rudder roll stabilization of ships, the main limiting factor is the nonlinear nature of the steering machine. It has hard nonlinearities like magnitude and rate saturations, and is therefore not a high bandwidth control device. Moreover, the nonlinearities of the rudder imply that the maximum damping ratio is difficult to obtain over a wide range of working conditions by means of linear control laws. It was only in the 1980s that more advanced control algorithms, and digital computers made more successful experimental results possible

II. RUDDER TO ROLL AND YAW DYNAMICS

Coupled nonlinear differential equations are needed to fully represent the complicated ship maneuvering dynamics. However for ship steering autopilots design, a simple model with average predicting capability is usually preferred. Based on the linearised surge-sway-yaw-roll equations of motion, a fourth order transfer function relating the yaw rate to the rudder angle is derived. Further simplifications to the second order Nomotos model and the first order Nomotos model are also described. Upon linearization with respect to a straight line motion with a constant forward speed u0, the surge equation is decoupled and the following linear coupled swayyaw- roll equations follow immediately. Referring to Fig. (1), we have

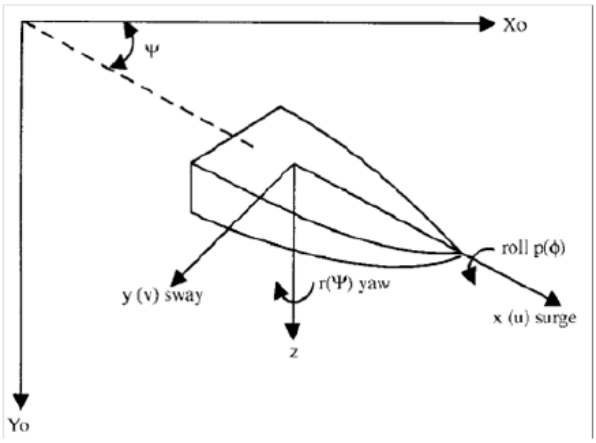


Fig. 1. Sway-yaw-roll motion coordinate system

$$m\dot{\upsilon} + \upsilon_0 r = Y_\upsilon \upsilon + Y_{\dot{\upsilon}}\dot{\upsilon} + Y_r \dot{r} + Y_\phi \phi + Y_P P + Y_{\dot{P}}\dot{P} + Y_\delta \delta \quad (1)$$

$$I_{xx\ddot{\phi}} = K_P P + K_{\dot{P}}\dot{P} - mg\bar{GM}\phi + K_V V + K_{\dot{V}}\dot{V} + K_r r + K_{\dot{r}}\dot{r} + K_\delta \delta \quad (2)$$

$$K_{I_{xx\varphi}} = N_r r + N_{\dot{r}}\dot{r} + N_\phi \phi + N_P P + N_{\dot{P}}\dot{P} + N_V V + N_{\dot{V}}\dot{V} + N_\delta \delta \quad (3)$$

where $Y_\upsilon \upsilon$ $Y_{\dot{\upsilon}}\dot{\upsilon}$; indicate the hydrodynamic coefficients; for instance, Y_V indicates the derivative of the sway force Y to the sway speed V evaluated at the reference condition; m is the mass of the ship; I_{xx} is the moment of inertia about the x-axis; I_{zz} is the moment of inertia about the z-axis; V is the sway speed; u is the surge speed; r is the yaw rate; is the heading angle defined by $\dot{\varphi} = r$; p is the roll rate; φ is the roll angle defined by $\dot{\psi} = P$and GM is the metacentric height, which indicates the restoring capability of a ship in rolling motion. Applying Laplace to (1) to (3) and rearranging them we get

$$\begin{aligned} a_1\upsilon &= a_2\psi + a_3 r + a_4\delta \\ b_1\psi &= b_2\upsilon + b_3 r + b_4\delta \\ c_1 ri &= c_2\upsilon + c_3\psi + c_4\delta \end{aligned} \quad (4)$$

where $a_1....a_4; b_1...b_4; c_1....c_4$ are function of coefficients of equation (1). Eliminating sway speed v and roll angle ϕ from (5), we get following transfer function

$$\frac{r}{\delta} = \frac{a_1(b_1c_4 + b_4c_3) + a_2(b_4c_2 - b_2c_4) + a_4(b_1c_2 + b_2c_3}{a_1(b_1c_1 - b_3c_3) - a_2(b_2c_1 + b_3c_2) - a_3(b_1c_2 + b_2c_3} \quad (5)$$

Since the numerator and denominator are of third and fourth order respectively, which can be seen after some mathematical manipulation, transfer function (5) can be represented in the following form:

$$\frac{r}{\delta} = \frac{K(1 + T_3 s)(s^2 + 2\eta w_0 s + w_0^2)}{(1 + T_1 s)(1 + T_2 s)(s^2 + 2\xi w_n s + w_n^2)} \quad (6)$$

Neglecting coupling effects from the roll mode on the yaw rate which is responsible for quadratic factor in the above transfer function, it can further be reduced as follows:

$$\frac{r}{\delta} = \frac{K(1 + T_3 s)}{(1 + T_1 s)(1 + T_2 s)} \quad (7)$$

$$\frac{\phi}{\delta} = \frac{K_1(1 + T_3 s)(1 + T_4 s)}{(1 + T_1 s)(1 + T_2 s)(s^2 + 2\xi w s + w^2)} \quad (8)$$

$(1 + T_1 s); (1 + T_2 s); (1 + T_3 s)(1 + T_4 s)$ are due to coupling effects from sway and yaw motion. In practice sway speed v is directly proportional and so equation (8) can be modified as given in eqn (9) after taking sway yaw linear dependency in to k_0

$$\frac{\phi}{\delta} = \frac{K_0(1 + T_6 s)}{(1 + T_5 s)(s^2 + 2\xi w s + w^2)} \quad (9)$$

Equation (5) to (7) are the transfer relation yaw to rudder angle and equation (8) to (9) are the transfer function relating roll angle to the rudder angle.

A. FEATURES OF THE CONTROLLER APPLICATION

Consider the linear feedback system shown in Figure 8.1, in which G(s) is the transfer function of the plant or system to be controlled, and C(s) is the transfer function of the controller. The scheme shown in Figure (2) can be taken as a simplified version of the block diagram of a control system of a stabilizer. Indeed, under linearity assumptions, we can consider, for the purpose of analysis, that the wave induced motion is an output disturbance.Then, for rudder stabilizers, we could have that r is the desired roll angle, i.e. zero; y is the roll angle ϕ and/or its time derivatives; d_0 is the waveinduced motion in roll and its time derivatives; d_i accounts for unmodeled dynamics and other effects diminishing the control action such as local flows due to the wave-particle orbits. u is the desired mechanical angle of the rudder.

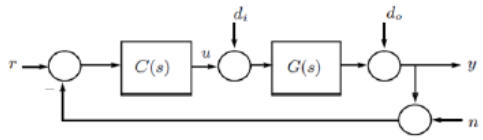


Fig. 2. Single-loop output feedback control system

The schematic diagram represents the motion of rudder in controlling yaw and roll is shown in figure (3). The double objective of rudder stabilizers can be considered as a single-input two-output (SITO) problem, or under-actuated system.

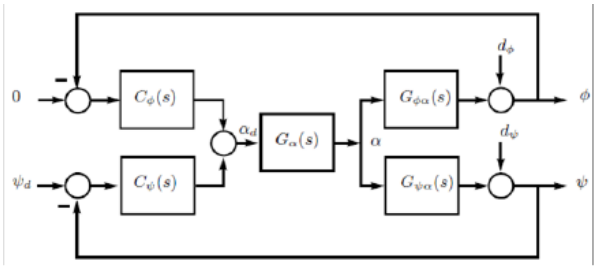


Fig. 3. Simplified rudder stabiliser control scheme

where, $r = [0; \varphi_d]^T$ is the of vector desired roll and yaw angle, $y = [\phi; \varphi]^T$ is the vector of roll and yaw angles; this may also include their time derivatives, $d_0 = [d_\phi; d_\varphi]^T$ is the wave-induced motion in roll (and yaw) and its time derivatives, d_i is similar to the case of fins, accounting for Unmodelled dynamics and other effects diminishing the control action and $u = \alpha_d$ is the desired mechanical angle of the rudder. The transfer functions $C_\phi(s)$ and $C_\varphi(s)$ represent the roll and yaw controllers respectively. The transfer function $G_\alpha(s)$ describes the dynamics of the steering machinery, i.e. it maps the desired rudder angle α_d into the actual rudder angle α. The transfer functions $G_\phi\alpha(s)$ and $G_\varphi\alpha(s)$ map the actual rudder angle into the roll and yaw angles respectively. using the Laplace transform, the effect of the different magnitudes on the output of the system can be established via

$$y(s) = T(s)r(s) + S(s)d_0(s) + S_i(s)d_i(s) + S_n(s)n_s \quad (10)$$

For the feedback system shown in the figure, it follows that

$$S(s) = \frac{1}{1+G(s)C(s)}\ ;$$
$$T(s) = \frac{G(s)C(s)}{1+G(s)C(s)};$$
$$S_i(s) = \frac{G(s)}{1+G(s)C(s)};$$

$$S_n(s) = \frac{G(s)C(s)}{1+G(s)C(s)}; \quad (11)$$

The transfer function $S_(s)$ is called the sensitivity transfer function, and maps the output disturbance into the output. The function $T_(s)$ is called the complementary sensitivity transfer function, and maps the reference into the output. The function $S_i(s)$ is called the input sensitivity transfer function and maps the input disturbance into the output. Finally, the function $S_n(s)$ is the transfer function that maps the measurement noise into the output. Perfect control would be achieved if the output y (variable of interest) followed the reference r as closely as possible for all frequencies in a desired range (i.e.,$\omega \in \Omega$) despite the disturbances present on the system; namely, $d_0; d_i$ and n. This ambitious goal for the design of the controller $C(s)$ can be quantitatively stated by the following specifications in the frequency domain:

$|s(j\omega)| \approx 0, |s(j\omega)| \approx 0$

$|s(j\omega)| \approx 0, |s(j\omega)| \approx 0$

However, from the definitions of the sensitivity functions it follows that it is impossible, in general, to satisfy such specifications. Indeed, from figure (3), it can easily be seen that;

$S(s) + T(s) = 1;\ S_i(s) = G(s)S(s)$

$S_n(s) = -T(s)$

Therefore, it is impossible to reduce the effect of the measurement noise on the output, and at the same time obtain a good tracking response (making y follow r) because $|S_n(j)| = |T_{j\omega}|$. This is a fundamental limitation associated with the structure of the control system.

On the other hand, the algebraic constraint $S(s)+T(s) = 1$, indicates that if we reduce $|T_{j\omega}|$ to avoid the influence of the noise n at some frequencies, then $|S_{j\omega}|$ increases at these frequencies (at any frequency, either $|T_{j\omega}|$ or $|S_{j\omega}|$ must be greater or equal to 0.5), and both input and output disturbances may affect the output if they have enough energy at these frequencies. Furthermore, the ability to reject both disturbances depends on the frequency separation between di(j) and d0(j!) and the plant G(j!). For the case of stabilizer design for displacement ships, the non-minimum phase characteristic of the plant is one of the main effects imposing limitations on the performance of the control system.

III. PERFORMANCE LIMITATION AND RRS APPLICABILITY

The main purpose of the rudder is to control the yaw motion, i.e., heading of the ship. However it is observed that there is a inward roll induced by the rudder immediately after

initialization of turning maneuver. The rudder roll stabilisation is based on the concept of the utilization of rudder induced inward roll. The rudder induced inward roll is called the undershoot behavior that characterizes so called non minimum phase system with the existence of right half plane zero in the corresponding transfer function. Magnitude and speed with which the inward roll is introduced indicates the potential of RRS and it is evident of figure (4) that non minimum phase is so crucial and responsible for RRS.

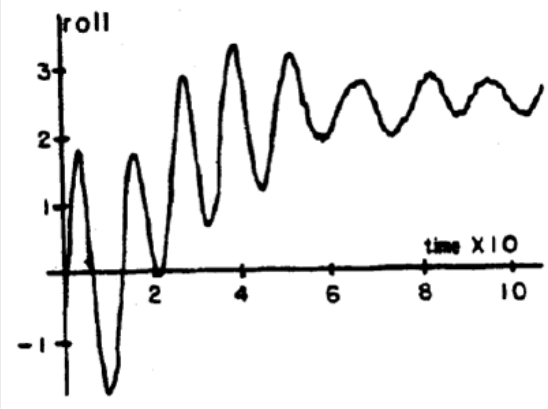


Fig. 4. Warship roll response to step demand applied to the rudder

Since the first attempts to use the rudder as a stabiliser, it has been recognised that there are issues that can limit the achievable performance. There are three main issues that can limit the performance:

- Non-minimum phase (NMP) dynamics.
- A trade-off between roll reduction and heading interference.
- Limited rudder motion.

The NMP dynamics appear in the rudder-to-roll response, and as a consequence there is a fundamental limitation in control system design: disturbance attenuation at some frequencies will result in amplification at other frequencies. This limitation poses a trade-off between reducing the roll at some frequencies and roll amplification at others, which can be interpreted as a robustness issue related to the knowledge of the frequency of the wave induced motionthe disturbance. The second issue that can limit the performance is under-actuation, i.e. there is one control action (rudder force) to achieve two objectives: roll reduction and low heading interference. The ability to achieve these objectives is related to the shape of the hull, the location of the rudder, and the frequencies at which the wave-induced roll has energy. Finally, the third issue is related to limits on the control action.

Control surfaces are commanded by hydraulic machinery that implements the action demanded by the controller. The characteristics of this machinery are important since they can impose constraints on the control action. Limited rudder angle (SAT) and limited rudder rate (SRL) poses the main difficulties in implementation of RRS. The mathematical model of the hydraulic machinery most commonly used in marine applications is the simplied model presented by van Amerongen [11]. Figure (5) presents a block diagram corresponding to this model, in which αc is the control command and αm is the mechanical angle of the rudder. The model presented in Figure (5) captures the essential characteristics relevant to the control system design.

- Magnitude saturation:the foil motion is constrained to move within certain maximum angles, i.e.$-\alpha_{max} \leq \alpha \leq \alpha_{max}$
- Slew rate saturation: The rate of rudder movement is limited by a maximum value α_{max}
- Time delay: the main servo is responsible for producing most of the delay between the desired rudder angled and the actual rudder angle. This delay is represented by a rst order system with a time constant

$$t_r = \frac{\alpha_{pd}}{\dot{\alpha}_{max}}$$

So that the roll reduction does not interfere with the yaw control, the (BW) bandwidth of the rudder roll control system must be higher than that of the rudder yaw control. Rudder (SRL) Slew Rate Limitation should be high enough to achieve satisfactory roll stabilisation. There is a contrasting requirement in the sense that purpose of rudder yaw control is to compensate low frequency yaw motion whereas the main concern of rudder roll control is to reduce high frequency wave induced roll motion behavior. Practical Application for Rudder Roll Stabilisation has been carried out in many places [12] and some salient observations which are found are enumerated in succeeding paragraph. Though the idea was quite old but it could not be materialized due lack of knowledge of advanced non linear control strategies. The topic re-surfaced after the first successful full scale trial was carried out by Baitis (1980) who used rudder for automatic roll stabilisation while the leading control was still done manually by helmsman.

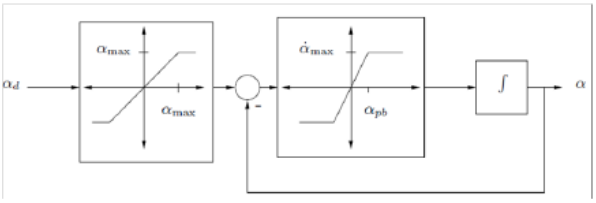


Fig. 5. Simplified rudder stabiliser control scheme

RRS can be applied only on new ship from initial phase or during major refit. To implement RRS on a old ship, the steering machine needs to be redesigned at the stage of mid life upgrade. The ship can be installed with suitable steering machinery at the time of construction. The rudder stock bearing needs to be stronger than usual and it should be able to withstand high speed. Even the best controller cannot give a satisfactory performance if the ship design or steering machine are not suited for RRS[8]. Separation of frequency domain i.e., low frequency rudder motion for maintaining head and high frequency rudder motion for reducing roll to be demarcated for successful implementation of RRS which is very much evident from figure (6). Without good separation of frequency domain performance of RRS is bound to deteriorate. Experiments at Maritime Research Institute

Netherlands (Marin) with the scaled model demonstrated that RRS is indeed feasible simulation experiments are reliable means for predicting the performances of RRS system. Royal Netherlands Navy preferred RRS over fin stabilisation. But Rudder Roll Stabilisation is not effective if ships speed is low, and also it is not capable enough for reducing low frequency roll motion or a stationary roll angle. The optimum solution will the use of combination of rudder and fin both for stabilisation but this will the most expensive method and hence the scheme is rejected. It has been proved that rudder movement of 20 deg per second is required and necessary to counteract the wave disturbance.

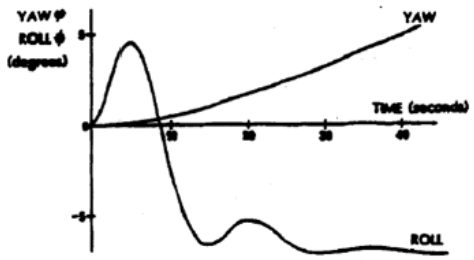


Fig. 6. Fig. 6. Typical warship roll and yaw responses for a step change in rudder position

IV. Conclusion

In this paper idea of Rudder Roll Stabilisation and its potentialities are mentioned in a very simple manner. Though the theoretical concept was old but could not be materialized due to lack of knowledge on advanced control method. However interest has been renewed all over the world due successful trial at MARIN at Netherlands. The concept of Rudder Roll Stabilisation has got lots of advantages but it also needs redesigning of steering mechanism by making stronger stock bearing, improving slew rate limitation (SLR) and saturation (SAT) limitation. Hence, RRS can be implemented only at new ship by incorporating requisites at the design stage only.

References

[1] W. Froude On the rolling of ships. Trans. of the Institution of Naval Architects.2:180227, 1861.
[2] W. Froude The Papers of William Froude M.A. LL.D. F.R.S. 18101879. chapter On The Rolling Of Ships, pages 4065. The Institution of Naval Architects, 1955
[3] W. Froude The Papers of William Froude M.A. LL.D. F.R.S. 18101879,. chapter Appendices To Mr. Froude Paper On The Rolling of Ships, pages 6575. The Institution of Naval Architects, 1955.
[4] F.H. Sellars and J.P. Martin Selection and evaluation of ship roll stabilization systems Marine Technology, SNAME, 29(2):84101, 1992
[5] J. van Amerongen and J.C. van Cappelle Mathematical modelling for rudder roll stabilization. In Proc. of 6th Ship Control System Symposium SCSS, 1981.
[6] Edwwin Kreuzer, Mareike Wendt Nonlinear Dynamics of Ship Oscillation IEEE COC 2000 St Petersburg, Russia
[7] Catalin Bara, Mihai Cornoiu and Dumitru Popescu An optimal Control Strategy of Ballast System Used in Ship Stabilisation 20th Mediterranean Conference on Control Automation (MED), Barcelona, Spain, Jul 3-6, 2012
[8] PGM Van der Klugt, HR Van Nauta Lemke Rudder Roll Stabilisation and Ship Design: A Control point of View Proceeding of the ISSOA International Symposium on Ship Operation Automation.
[9] Van Amerongen J Effects of propeller loading on rudder efficency Proceding 4th ship control system symposium, Haag, pp. 5.38-5.39
[10] van Berlekom, W. B. Effects of propeller loading on rudder efficiency. Proceedings 4th Ship Control Systems Symposium, Haag. pp. 5.835.98. 1975
[11] J. van Amerongen. Adaptive steering of shipsA model reference approach to improved maneouvering and economic course keeping. PhD thesis, Delft University of Technology, The Netherlands., 1982.
[12] G.N. Roberts A Note on the Applicability of Rudder Roll Stabilisation for Ships. Proceedings of American Control Conferences, San Francisco. Jun 1993



Lt Cdr Swarup Das is a M Tech in System and Control Engineering from IIT (Bombay). The officer had served onboard INS Viraat and INS Jalashwa as Asst Engineer Officer. He is presently working as TSO-(II) in MILIT. He has published around five papers in national and international conferences. Also the officer is pursuing PhD from DIAT (DU). His areas of research interest are Uncertainties and disturbance estimation in non linear control application.



Cmde AN Sonsale is a ME (Mech - Marine) from Pune University, 1990. During his career of 32 years in the Indian Navy he has teneted afloat appointments on front line war ships and important shore appointments in operational, maintenance and project organizations. He is Presently Head of Faculty (Navy) at MILIT Pune. He is a regular contributor to professional journals and conferences. His areas of research interest are Energy Efficiency.

Design of a ships autopilot using state space feedback control methodology

U Dheeraj [1], **Swarup Das** [2], **SK Panigrahi**[3]
[1,3]Department of Mechanical Engineering,Defence Institute of Advanced Technology(DU), Pune, India
[2]Military Institute of Training,Pune,India
[1]Dhiru24@rediffmail.com

***Abstract*—This paper is concerned with the design of an autopilot for ship navigation. Conventionally, ships autopilot have been designed using Proportional Differential and Proportional Integral Differential controllers because of simplicity, reliability and ease in construction. But their controlling parameters depends upon prevailing environmental conditions and requires constant manual re-adjustments for optimal operation. Hence the performances of these controllers are not up to the desired level. Many controllers based on adaptive methodology have been designed but are difficult to construct due to the complexity involved. This controller is designed with a linear state space feedback approach. The state space feedback controller has been designed using a 4 DoF ship motion. Numerical simulations using real ship parameters have been undertaken to test the step response of the controller for a 100 deg change of course and result has been presented.**

***Index Terms*—ship autopilot, state feedback control system, underactuated system.**

I. Introduction

A warship/marine vessel at sea is required to undertake several major evolutions like landing/taking off of aircrafts, missile/gun firing and operation of various machinery. To complete these tasks, the control over ships motion should be effective. Moreover, all the control systems available for navigation and direction should be reliable, safe and economical. The desired path can be defined in terms of the ship's position, velocity and acceleration [1].

The steering system in a marine vessel serves to rotate the rudder either to left or right as per demand of the helmsman and works only when the ship is in motion. Since only a rudder is available for achieving the Guidance and Control over the ships motion, the problem can be narrowed down to control of the rudder. Guidance is the action of determining the course and speed of the vehicle, relative to some reference frame (usually the earth) to be followed by the vehicle and Control refers to development and application to a vehicle of appropriate force and moments for operating point control, tracking and stabilization [2].

A marine vessel operates in the presence of unpredictable disturbances in the form of waves, wind and currents and hence the design of an autopilot faces tremendous challenges. Various control design methods can be used for designing an effective autopilot which would cater to the variations in the operating environment to which a marine vessel is exposed to during operations. The conventional PID controller requires a frequent manual re-adjustment of the optimal settings which is not known to the user [3]. An optimal autopilot can reduce the total length of journey by 3-5% which will reduce fuel consumption especially in bad weather condition [4]. The state-space feedback gains requires only a linear state-space model of the plant to be applied and implemented for a controllable system. To develop the state space model, existing mathematical models have been used and a linear model for underactuated ship motion is presented in horizontal plane having DoF equal to 4 and then a state space representation of the model is developed. The state space model is useful for applying the feedback controller and to achieve the desired ship motion . The feedback controller will be designed based on pole placement method in two steps:

1) Check the controllability and observability of the system;
2) Finding the state-feedback gain by pole placement method.

Further, numerical simulations using MATLAB has been performed to illustrate the effectiveness of the controller.

II. PROBLEM FORMULATION

The standard notation applicable for a ship motion(6 DOF) as followed by the Society of Naval Architects and Marine Engineers (SNAME) is as shown in fig. 1. The different parameters of fig. 1 are listed in Table 1.

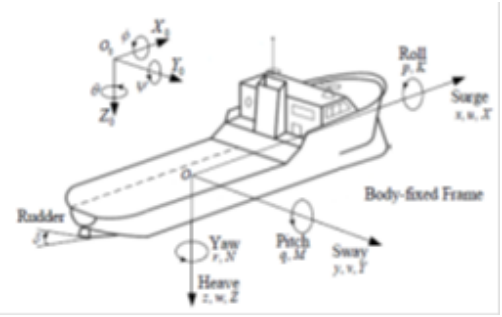


Fig. 1. Standard notation and sign conventions for ship motion description (SNAME,1950).

The basic equations of motion using Newton's Law describ-

TABLE I
VESSEL PARAMETERS

Parameters	Description
x, y, z	Distance along body-fixed coordinate system(m)
u, v, w	Translational velocity in body-fixed frame (m/s)
X_f,Y_f,Z_f	Force components along body axes(kg)
p, q, r	Rotational velocity in body-fixed frame (rad/s)
K,M, N	Moment components along body axes (kg-m)
ψ	Yaw angle(rad)
θ	Pitch angle (rad)
ϕ	Roll angle (rad)
δ	Rudder angle(rad)

ing the dynamics of a ship [5] is expressed as:

$$\begin{cases} \sum Forces = \frac{d(mV)}{dt} \\ \sum Moments = \frac{d(I\omega)}{dt} \end{cases} \quad (1)$$

where: m : mass of the body, V: translational velocity, I: Inertial moment and ω: rotational velocity.

Applying 1 for a ship in motion with reference to a body fixed frame and using approximations [5] we can write the following:

$$\begin{cases} f_x = (u, \dot{u}, v, \dot{v}, w, \dot{w}, p, \dot{p}, q, \dot{q}, r, \dot{r}, \delta) = X_f, \\ f_y = (u, \dot{u}, v, \dot{v}, w, \dot{w}, p, \dot{p}, q, \dot{q}, r, \dot{r}, \delta) = Y_f, \\ f_z = (u, \dot{u}, v, \dot{v}, w, \dot{w}, p, \dot{p}, q, \dot{q}, r, \dot{r}, \delta) = Z_f, \\ f_\varphi = (u, \dot{u}, v, \dot{v}, w, \dot{w}, p, \dot{p}, q, \dot{q}, r, \dot{r}, \delta) = K, \\ f_\theta = (u, \dot{u}, v, \dot{v}, w, \dot{w}, p, \dot{p}, q, \dot{q}, r, \dot{r}, \delta) = M, \\ f_\psi = (u, \dot{u}, v, \dot{v}, w, \dot{w}, p, \dot{p}, q, \dot{q}, r, \dot{r}, \delta) = N \end{cases} \quad (2)$$

A 4DoF(neglecting pitch and heave) description which includes surge, sway, yaw and roll [6] will be considered for the present study.

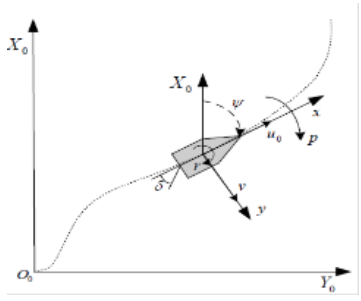


Fig. 2. Surge-sway-yaw-roll motion coordinate system.

Further upon linearization with respect to a constant forward speed u, the surge equation is also decoupled [6] and linear coupled sway-yaw-roll equations with reference to body fixed coordinate system may be written as:

$$\begin{cases} \mathrm{m}(\dot{\mathrm{v}} + \mathrm{ur}) = \mathrm{Y_v v} + \mathrm{Y_{\dot v} v} + \mathrm{Y_\phi}\phi + \mathrm{Y_p p} + \mathrm{Y_{\dot p} p} + \mathrm{Y_r r} + \mathrm{Y_{\dot r}}\dot{\mathrm{r}} + \mathrm{Y_\delta}\delta \\ \mathrm{I_z} = \mathrm{N_v v} + \mathrm{N_{\dot v} v} + \mathrm{N_\phi}\phi + \mathrm{N_p p} + \mathrm{N_{\dot p} p} + \mathrm{N_r r} + \mathrm{N_{\dot r}}\dot{\mathrm{r}} + \mathrm{N_\delta}\delta \\ \dot{\psi} = \mathrm{r} \\ \mathrm{I_x}\ddot{\phi} = \mathrm{K_v v} + \mathrm{K_{\dot v} v} + \mathrm{K_\phi}\phi + \mathrm{K_p p} + \mathrm{K_{\dot p} p} + \mathrm{K_r r} + \mathrm{K_{\dot r}}\dot{\mathrm{r}} + \mathrm{K_\delta}\delta \\ -\mathrm{mgGM}\varphi \\ \dot{\phi} = p \end{cases} \quad (3)$$

where:

$Y_v v$, $N_v v$, $K_v v$.....are the hydrodynamic coefficients. Y_v indicates the derivative of sway force Y to the sway velocity v evaluated at the reference condition, m is the mass of the ship, I_x and I_z are the moments of inertia about the x-axis and z-axis respectively, g is the acceleration due to gravity and GM is the metacentric height of the ship.

Equations 3 may be re-written as:

$$\begin{aligned} &\dot{v} = Y'_v v + Y'_{\dot v}\dot{v} + Y'_\phi\phi + Y'_p p + Y'_{\dot p}\dot{p} + Y'_r r + Y'_{\dot r}\dot{r} + Y'_\delta\delta \\ &\dot{r} = N'_v v + N'_{\dot v}\dot{v} + N'_\phi\phi + N'_p p + N'_{\dot p}\dot{p} + N'_r r + N'_{\dot r}\dot{r} + N''_\delta\delta \\ &\dot{\psi} = r \\ &\dot{p} = K' v + K'_{\dot v}\dot{v} + K'_\phi\phi + K'_p p + K'_{\dot p}\dot{p} + K'_r r + K'_{\dot r}\dot{r} \\ &+K'_\delta\delta - mgGM\phi \\ &\dot{\phi} = p \end{aligned} \quad (4)$$

These equations represent the linear model of the coupled steering and roll dynamics.

III. DESIGN OF A STATE FEEDBACK CONTROLLER

State space representation is a mathematical model of a physical system as a set of input, output and state variables related by first-order differential equations. The state space model of a continuous-time dynamic system can be derived from the system model given in the time domain by a differential equation.

The state space representation provides a convenient and compact way to model and analyze systems with multiple inputs and outputs. State space refers to the space whose axes are the state variables.

The state vector may be defined as

$$x=[v\ r\ \psi\ p\ \phi]^T \quad (5)$$

Linearisation of the ship nonlinear model about $u$and writing the linearised model in standard state space form:

$$\begin{cases} \dot{x}(t) = Ax(t) + Bu(t) \\ y(t) = Cx(t) \end{cases} \quad (6)$$

From the state space model the stability of the system can be determined. The system is stable if the eigenvalues of the matrix A have a negative real part. The state feedback method is a method employed in feedback control theory to place the closed loop poles of a plant in pre-determined locations in an s-plane. If the closed-loop transfer function is represented by a state space equation:

$$\begin{cases} \dot{x}(t) = Ax(t) + Bu(t) \\ y(t) = Cx(t) + Du(t) \end{cases} \quad (7)$$

then the poles of the system are the roots of the characteristic equation i.e eigen values of state matrix A:

$$|sI - A| = 0 \tag{8}$$

*A. **State feedback control law***: According to this law, if the input is proportional to the state vector, then :

$$u(t) = -Kx(t) \tag{9}$$

Substituting these values in equation7 yields:

$$\begin{cases} \dot{x}(t) = Ax(t) - BKx(t) \\ \dot{x}(t) = (A - BK)x(t) \\ y(t) = (C - DK)x(t) \end{cases} \tag{10}$$

The roots of the Full state feedback system are given by the roots of the characteristic equation, i.e eigen values of the state matrix A-BK:

$$|sI - (A - BK)| = 0 \tag{11}$$

Comparing the terms of this equation with those of desired characteristic equation yields the values of the feedback matrix K which force the closed-loop eigenvalues to the pole locations specified by the desired characteristic equation.The parameters of the linearised ship model are taken from [2]

$$A = \begin{bmatrix} -0.04 & -1.933 & 0 & 0 & -0.0756 \\ -.00011 & -0.813 & 0 & 0 & 0.001134 \\ 0 & 1 & 0 & 0 & 0 \\ -0.00594 & 0 & 0 & -0.07 & -0.059 \\ 1 & 0 & 0 & 1 & 0 \end{bmatrix}$$

$$B = \begin{bmatrix} 0.1559 \\ -0.0033 \\ 0 \\ 0.00821 \\ 0 \end{bmatrix}, C = \begin{bmatrix} 0 & 0 & 1 & 0 & 0 \end{bmatrix}$$

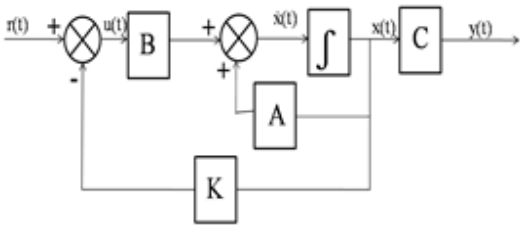


Fig. 3. Structure of a state feedback control system.

For applying the state feedback control law, the system has to be controllable and observable.

*B. **Controllability***: A system is said to be controllable at time t_0, if it is possible by means of an unconstrained control vector to transfer the system from any initial state $\mathbf{x}(t_0)$ to any other state in a finite interval of time [7]. A continuous time-invariant linear state space model is controllable if and only if rank(C)=*n* where *C*= [*A AB* A^2B .....$A^{n-1}B$]. We have:

C=[*B AB* A^2B A^3B A^4B]

$$C = \begin{bmatrix} 0.1559 & 0 & -0.0129 & 0.0003 & 0.0017 \\ -0.0033 & 0.0003 & 0.0002 & 0 & 0 \\ 0 & -0.0033 & 0.0003 & 0.0002 & 0 \\ 0.00821 & -0.0015 & -0.0096 & 0.0008 & 0.0013 \\ 0 & 0.1641 & -0.0015 & -0.0225 & 0.0011 \end{bmatrix}$$

and $\rho(C)$=5, hence the system is controllable.

*C. **Observability***: A system is said to be observable at time t_0 if, with the system in state $\mathbf{x}(t_0)$, it is possible to determine this state from the observation of the output over a finite time interval [7]. A continuous time invariant system is observable if and only if, rank(*O*)=*n*, where :

$$O = \begin{bmatrix} C \\ CA \\ .... \\ .... \\ CA^{n-1} \end{bmatrix} \tag{12}$$

$$O = \begin{bmatrix} 0 & 0 & 1 & 0 & 0 \\ 0 & 1 & 0 & 0 & 0 \\ -0.0001 & -0.0813 & 0 & 0 & 0.0011 \\ 0.0011 & 0.0068 & 0 & 0.0011 & -0.0001 \\ -0001 & -0.0028 & 0 & -0.0002 & -0.0001 \end{bmatrix}$$

and ρ(O)=5. Hence the system is observable.

*D.**Poles placement approach***: If a system is state controllable, then poles of the closed-loop system may be placed at any desired locations by means of state feedback through an appropriate state feedback gain matrix [7].

The system under consideration is a 5^{th} order system and the parameters, i.e, rise time $t_{R,}$, settling time t_s, percent overshoot PO of a higher order system(order $>$2) is not known, we will adopt the approach of approximating these systems to a first or second order system.

For a second order system response is usually characterised by two parameters ξ and ω_n. Now we write the poles as :

$$\begin{aligned} P_0 &= -\xi\omega_n - \omega_n j\sqrt{1-\xi^2} \\ P_1 &= -\xi\omega_n + \omega_n j\sqrt{1-\xi^2} \\ P_2, P_3, P_4 &< 10 * Re(P_0) \end{aligned} \tag{13}$$

where $j = \sqrt{-1}$, Re: real part of $P_{0,}\xi$ is the dimensionless damping ratio and $\omega_n$is the fixed undamped natural frequency.

The poles $P_{2,}P_3$and $P_4$are taken as ten times P_0so that the dynamics related to these poles can be neglected and the expected response of the system will as per dominant poles $P_0$and $P_{1.}$

*E. **Shaping the dynamics***: This step involves selection of poles P_0 and $P_1$for shaping the dynamic response. This choice of poles fixes the feedback gain vector K. The values of ξ and $\omega_n$are fixed and hence the closed-loop characteristics of the transient response rise time $t_{R,}$, settling time t_s and percent overshoot PO. The following equations have been adopted from [7].

$$\begin{cases} t_R = \frac{3.14-\beta}{\omega d} \\ where \beta = \tan^{-1}\left(\frac{\omega_d}{\sigma}\right), \omega_d = \omega_n\sqrt{(1-\xi^2)} \\ t_S \cong \frac{4}{\xi\omega_n} \\ PO = 100e^{\frac{-\xi\Pi}{\sqrt{1-\xi^2}}} = 2\% \end{cases} \quad (14)$$

Now if we take $\xi = 0.8$ and assume $t_S = 120$s then from equations14 we have $\omega_n = 0.042\text{s}^{-1}$.

Hence from equations13 we get,

$$\begin{cases} P_0 = -0.0336 - 0.0252j \\ P_1 = -0.0336 + 0.0252j \\ P_2 = -0.336,\ P_3 = -0.672,\ P_4 = -1.008 \\ i.e\ at\ least < 10 * Re(P_0) \end{cases} \quad (15)$$

The desired feedback vector K can then be derived using MATLAB and will be as below:

K= [-1.4264 -628.2560 -30.8463 4.9982 5.6958]

IV. SIMULATION RESULTS

Simulation was undertaken using MATLAB to test the response of the controller and to establish the effectiveness and robustness of the proposed linear state feedback control methodology. Fig 4 shows the simulation result for a step response of 100 deg and corresponding graph for error dynamics.

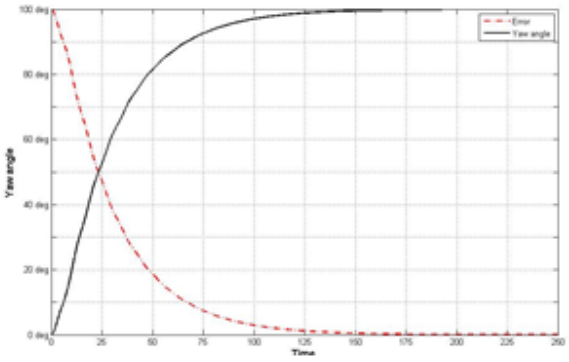


Fig. 4.

CONCLUSION

The basic concepts in respect of control engineering theory and its application have been studied. The state space model of a 4DoFship motion involving surge-sway-yaw-roll dynamics was generated for analysis and a controller based on state space feedback control methodology was designed for ships autopilot. Simulation was undertaken to test the controller output for a rudder input corresponding to 100 deg change of course , wherein the controller is seen achieving the desired course change and as the time progresses the corresponding error is seen to be reducing to zero. However, the author is of the view that this paper presents only few of the basic steps required to construct an effective ship autopilot.

REFERENCES

[1] T.I. Fossen, Guidance and Control of Ocean Vehicles, John Wiley and Sons Ltd,1994.
[2] T. Perez, Ship Motion Control: Course Keeping and Roll Stabilization Using Rudder and Fins, Advances in Industrial Control. Springer.
[3] J. Van Amerongen, "Adaptive Steering of Ships- A Model Reference Approach to Improved Maneuvering and Economical Course-Keeping," Ph.D. Thesis, Delft University of Technology, The Netherlands,1982.
[4] N Minorsky, "Directional stability of automatic steered bodies," Journal of Society of Naval Engineers, Vol 34, pp. 280-309, 1922.
[5] Klugt, P.GM van der, "Rudder Roll Stabilization", PhD. thesis, Delft University of Technology, October 1987.
[6] C. Yaw, Tzeng and J. Chen, "Fundamental Proprieties of Linear Ship steering Dynamic Models", Journal of Marine Science and Technology, Vol. 7, No. 2, pp. 79-88, 1999.
[7] Katsuhiko Ogata, "Modern Control Engineering", 5^{th} ed., Prentice Hall, 2010.



Lt Cdr U Dheeraj received his B.E. degree in Mechanical in 2002 from MIT(MAHE), Manipal and he is pursuing M.Tech (Marine Engg) Degree in Marine engineering from DIAT, Pune India.



Lt Cdr Swarup Das received his M.Tech degree in Control Engineering from IIT, Mumbai. Currently he is in Military Institute of Training, Girinagar, Pune.



Dr SK Panigrahi received his B.E. degree in Mechanical Engineering and M.Tech degree in Machine Design Analysis. He has completed Ph D from IIT Kharagpur, India. Currently he is HoD, Dept of Mechanical Engineering, DIAT, Girinagar, Pune.

Evolution of Control in Marine Engineering

Lt Cdr PK Mishra

I. Background

The evolution of marine control started with application in diesel and steam propulsion. Conventional marine control was limited to cables, Gearing mechanism and Mechanical linkages with limited accuracy. The post world war II era saw emergence of powerful propulsion with high power and high power density. With the increase in power rating of the propulsor the demand on the control and monitoring system in terms of response time, precision and surveillance increased beyond the human perception and ability. As a result the development in the field of controls and instrumentation also picked up pace in tandem with the powerful propulsors. The aim of the paper is to review control technologies presently in use for marine propulsion and fiture options to implement / integrate the latest technology.

II. Hydraulics - Pneumatic Controls

In marine engineering, hydraulics is the most efficient way for energy transmission. The application of hydraulic control and drive systems has resulted in new designs and improved efficiency of machines and installations. The use of fluid under pressure to transmit power and to control intricate motions is relatively modern and has had its greatest development in the past two or three decades. No other medium combines the same degree of accuracy, flexibility, maintaining the ability to transmit a maximum of power in a minimum of bulk and weight. Fig. 1 shows functional diagram of level control of Naval boiler.

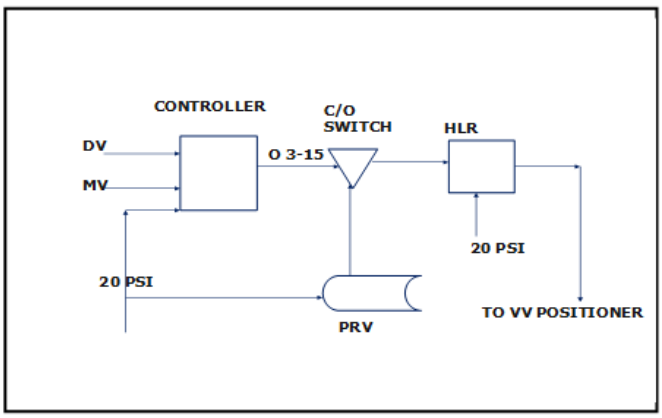


Fig. 1. Pneumatic based Controller.

For maintaining boiler water level in Naval Ship, rate of boiler feed and the steam take off must be same at varying loads/speeds. Also the water level in steam drum should remain near half gauge glass throughout output range. First is functional requirement and the second is a safety requirement to eliminate possible boiler starving. Control mechanism consists of sensors which measures three parameters ie Water level, steam flow and feed water flow using three differential transmitters. Transmitter compares two values of parameters and gives difference of 3-15 psi with constant supply of 20 Psi.

Controller compares MV (Actual value of controlled process) and DV (Value at which measured variable is required to be controlled.) In this system DV is the difference between two elements i.e. Steam flow & feed flow. Difference between MV & DV is output of Controller. Controller is supplied with 20 psi servo air as reference signal and output is varied depending upon deviation or error. Hence Controller output is a function of error. The steam Ships although varying in role and vintage have pneumatic controls fitted for propulsion. The primary role of the controls is to maintain the water level, combustor control of the boiler, automatic auxiliary exhaust control and remote operation of main turbines and auxiliaries. The control is implemented using robust, pneumatic and PID Controller. The sensors are pneumatic transmitter which give a Pneumatic output signal depending on the pressure / temperature sensed. (The sensors use relay as logic units. These relays are of various type like differential relay, booster relay and inverting relay. The actuation is through positioned, diaphragm operated valves and air motor.)

The main advantages and disadvantages of pneumatic or hydraulic systems arise out of the different characteristics of low density compressible gas and high density incompressible liquid. A pneumatic system for example, tends to have softer action than that of the hydraulic system which can be prone to noise and wear inducing shocks in pipes. A liquid based hydraulic system, however, can operate at far higher pressure than a pneumatic system and consequently can be used to provide very large force. All though pneumatic Controller are rugged and had has less functional problems, Castings requirement for hydraulic components are of high grade and precision, and require mechanised moulding machines, electric furnace and elaborate quality control equipment. Manufacturers of hydraulic components always had problem in establishing a source which can meet their requirements of castings. Since the castings required for hydraulic components are of small size, foundries do not get attracted in developing the same. Basic manufacturing technology is available but foundries require mechanised equipment for moulding and for preparation of elaborate testing facilities. Investment required for creating such facilities could not be justified for the returns. Hydraulic components manufacturers continue to face high castings rejections ranging from 10% to sometime upto 50%. Additionally, the system offers limited degree of freedom in terms of Controller robustness.

III. Electro Hydraulic Pneumatic Controls

Allthough Hydraulic components were used extensively in its full entity, the feasibility of enhancing control system started with integration of electricity. The primary reason was that considerable delay time was envisaged in sending feedback signal. Electrical signals were considered as one of the best media to implement the feedback mechanism with minimum signal loss. Such control systems are installed on many Ships, from powering of communication and navigation equipment, alarm and monitoring system, running of motors for pumps, fans or winches, to high power installation for electric propulsion. This control system uses electronic sensors, electrical potentiometers based throttle levers and solenoid. The system can be used to implement different logic and the actuation is through pneumatic. The actuation is also done through electro hydraulic control using different types of actuator. The electronics part of the system is generally easily supportable as it uses standard components available in market. The disadvantages of such systems are its dependency on requirement of power for implementing control. Fig.2 shows a Electro hydraulic based Steering system where position control of rudder is achieved by Hydraulics fluid as actuating signal and electrical signal as powering and feedback signal.

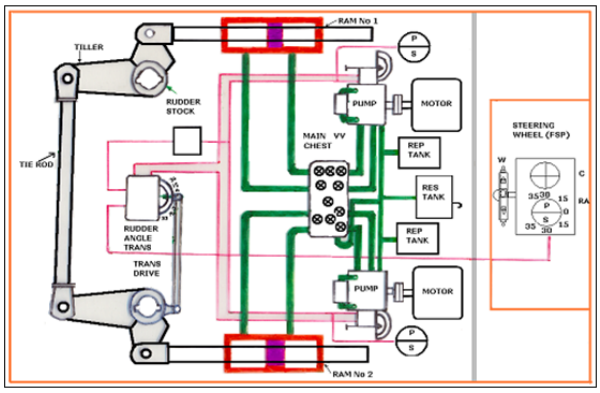


Fig. 2. Electro Hydraulic based Steering Control System.

The traditional Electric control system is based on hard wired relay logic with actuation through servomotors / mechanical components. The hard wired relay logic employ phased like diode and relay in some case. All though this method served the purpose for many years in marine controls, it had certain limitations as listed below:-

1) (a)Bulky and complex wiring resulting in delay in finding defect
2) (b)Changing Logic was not possible
3) (c)No provision of interchangeability
4) (d)Electrical noise and disturbance

With the advent of electronics, logic gates started replacing relays and auxiliary contactors in the control circuit. The bimetallic and motorised timers were replaced by electronic timers. However, even with electronics, the implementation of changes in the control logic was not possible. A logic designed for safety of one marine equipment could not be used or connected with other equipment with similar process variables. Also the repairs on logic circuits are difficult due to proprietary design and certain embedded software. Fig. 3 shows a PCB based PID Controller using amplifier, Integrator and differentiator circuit to maintain the flow rate of RO Plant by measuring and comparing the Input and generation of error using PCB based Controller.

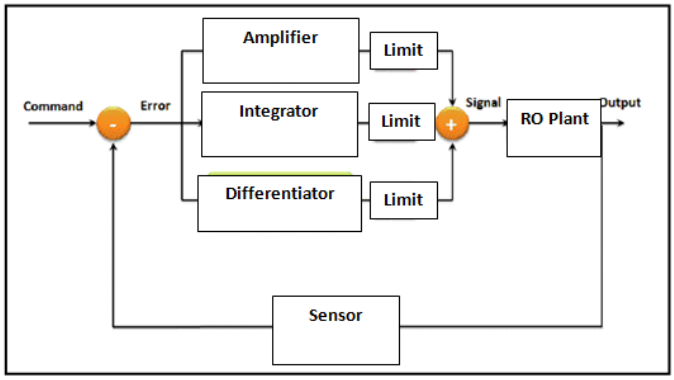


Fig. 3. PCB based PID Controller.

IV. Electrical / Electronic Based Controls

The Electrical based control mainly comprised of servo mechanism and relay based logic. The Electrical based control system mainly comprised of components like transistor, diodes and even vacuum tubes. Contactors and relays with timers and counters were used in achieving the desired level of automation. All process variables of the marine machinery were either monitored or controlled using electrical sensors and transducers with or without signal conditioning. Abnormal parameter of Marine equipment would make or break contactor, thereby actuating either solenoid or audio visual alarm. The use of synchro not only enabled remote operation but also resulted in high performance in terms of accuracy and precision. The use of sensors with linear characteristics and high resolution encoders provided abundant scope for implementing control with better range and span.

V. Modern control Systems

Since 1990, the development of microprocessor has had a direct effect on the size electronic Controller. The erstwhile Controllers were not robust and were susceptible to power fluctuations and hostile ambient conditions. The embedded system now uses programmable logic Controllers which are rugged and reliable. Moreover, the use of embedded system provides distributed control architecture. The PLC are now commercially off the shelf item and can be used in the open architecture enabling upgradation as per marine application. The integration of smart sensors and actuators with PLC offers flexibility on programming the logic to start main engine , Diesel alternator or Air conditioning plant as per the sequence and time delayed operation recommended by OEM. The ability of Human Machine Interface of programmable Controllers,

along with its ability to perform calculation and storage makes it most powerful tool in marine controls for implementing Instrumentation and control. All the field level signals from marine environment are connected to input module. At the output of input modules the field signal is converted into voltage level required by the Controller. At the beginning of each cycle the Controller brings in all the field input signal from input module and stores onto its memory as process image of input signal.

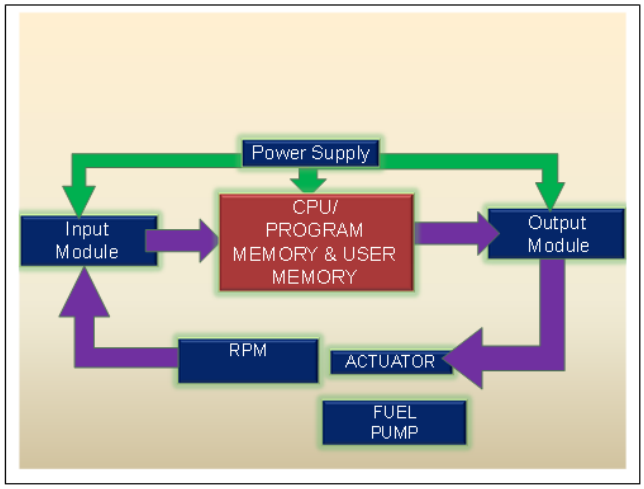


Fig. 4. PLC Based Diesel alternator.

The programmable Controller operates cyclically and once field input status is brought into the internal memory of processor, the execution of user program is performed, as per the machinery requirement. Micro Controller were initially used as replacement for the conventional hydro-mechanical governors on diesel engines. As compared to hydraulic governors in Diesel Engine, the electronic Controller can be customised to specific powering requirements by feeding the permissible load regimes. Micro Controllers are also being used to maintain the combustion efficiency under all the regimes by control of fuel pump timing, injection intensity and opening and closing of exhaust valves. The engines utilise hydraulic oil loop controlled by Micro Controller through solenoid. The Micro Controller makes it possible to model any injection pattern. The micro Controller thus maintains optimal intensity of fuel oil injection, exhaust valve opening and closing at all steady and transient loads. The overall protection system ensures compliance with load diagram and ensures that the engine is not overloaded.

Integrated electronic Controllers for Gas turbine with digital control of fuel metering valves and variable stator vane control have been developed which is used for GT operations like limiting functions, starting sequencing, Parameter monitoring, operating alarms , safety shutdown and load control regimes in various modes of exploitation. The Micro Controller is also used for control and monitoring of the entire propulsion plant, which included automatic starting and stopping of DA with changing load requirement, control and monitoring of auxiliary equipment and management of Ship systems, such as fuel , fire main and ballast systems.

VI. Integrated and Distributed Control

In marine engineering, effective command power and control could be achieved by data sharing and effective communication for feedback and sensing. Development in the field of IT and networking have ensured faster data transmission using fiber optic cables, The fiber optic cables also have minimal or nil EMC effects, thereby, making them suitable for using in communication network. The networking is employed for data transfer between equipment or between remote console and the equipment. The redundancy and ability to provide inter system connectivity of open system architecture is the back bone of Integrated Platform management control system. An integrated system is a system that incorporates the control logic for the entire propulsion into a single design. The design is geographically distributed over the network to control various group of machinery. The integrated system provides total monitoring and control of Ships propulsion, auxiliaries and damage control machinery and systems. The system design is as per open architecture norm and integrated modules to eliminate the compatibility issues.

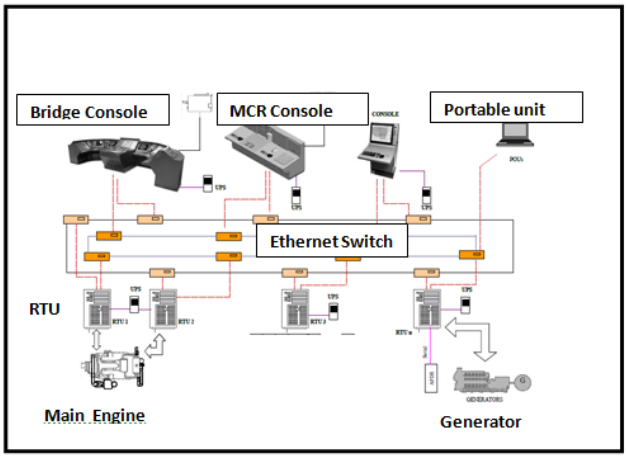


Fig. 5. IPMS Open Architecture.

Additional features like battle damage control system, surveillance system and engine health monitoring system has also be integrated with distributed architecture with real time control system. Multifunctional consoles in the form of HMI located at various location ensures control and monitoring though integrated control panels and high resolution monitors. Each console is multifunctional and perform any function from any location on the Ship. Data acquisition is through remote terminal unit which acquire data from sensor, performs the validity test and transmit the data to other subsystem including actuators . IPMS provide a unique combination of all functional advantages and therefore has become the preferred option for more than 140 Ships in the world.

VII. Conclusion

The overall requirements of control demanded by any Ship propulsion system have become rigorous and have reached

level where conventional controls prove ineffective and expensive in the long run. In the near future, remote operation and control will become the global buzzword and will obviate the disadvantages offered by conventional control. With depleting manpower and increased tasking, operators will have to be aided by technology to achieve control objectives which could be acquiring data, storage or control of any process variable. The future could be intelligent Controllers which acquire data from sensors with archived memory and take automatic corrective actions so that the wheel is not invented in solving similar control problems. Integration of different control strategy will be necessary to overcome the disadvantages with strength of another, to consolidate the finding of a particular control methodology. Intelligent software can be used to for trending and control the outputs based on the control objectives to aid the restricted manpower and collate the inputs from various machinery. The combination of wireless data transmission, networking concepts and internet can become a powerful force in enabling the collection and transport of signals for conditioning and monitoring process for implementing effective control. The futuristic control strategy can encompass automatic remote data acquisition, monitoring and tuning of Controllers with integration of software and data network. The architecture of the envisaged marine control strategy to serve the the purpose of control objectives as shown in the Fig. 6

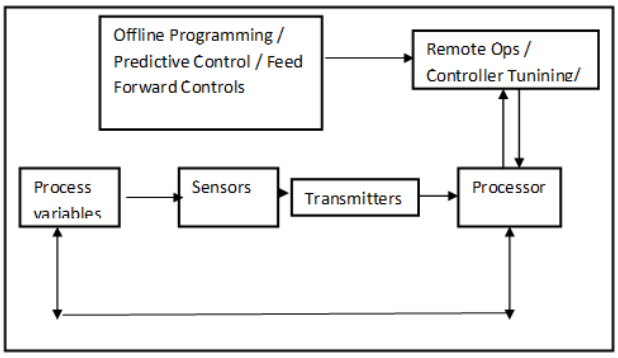


Fig. 6. Architecture of Futuristic Control.

The complexity of the control objectives will increase tremendously due to demand for MIMO (multiple input and multiple output) and Higher order system. The level of automaton in future Ships design will continue to increase with massive amount of signals to be handled. The control solution is to transform and use this signals for better controllability of process variable or machinary. It is therefore imperative that exploitation of Open architecture, Intellegent software and system engineering approach be adopted to ensure long life cycle and to improve the levels of reliability for optimal performance and management marine controls.

Comparative IR Thermography Changing Paradigms in Condition monitoring

Lt Cdr TS Sathya Narayanan[1], **Lt Cdr Sumit Singh**[2]
[1,2]Machinery Trials Unit, Vishakaptnam Indian Navy
[1]mtuvizag@gmail.com

***Abstract*—Reliability of machinery onboard warships has acquired greater significance in the present strategic scenario. Vibration monitoring based Condition Based Predictive Maintenance (CBPM) has been practiced since many years in Indian Navy. However, repair decisions based on vibration analysis alone pose risk of over-maintenance. With modern advancements in predictive testing technologies, employment of complementary techniques such as oil analysis, Motor Current Signature Analysis, Acoustic Emissions have gained ground for enhanced reliability requirements and precise maintenance decisions. IR Thermography (IRT) is one such technique which can be used to identify and analyse thermal anomalies for the purposes of condition monitoring of machines. IRT is based on measuring the distribution of radiant thermal energy emitted from a target surface and converting this to a surface temperature map or thermogram. Thermal energy is present with the operation of all machines. It can be in the form of friction losses within machines, energy losses within machines, as a characteristic of the process media or any combination thereof. As a result, temperature can be a key parameter for monitoring the performance of machines, the condition of machines and the diagnostics of machine problems. Temperature is also one of the key causes and symptoms of lubricant degradation and loss of lubrication function within a machine. There are several recognized IRT techniques in use throughout various industries. In this paper, Comparative Thermography is identified as the most suitable methodology to provide the best available data in lieu of ideal or absolute thermal measurements. When encountering changing machinery operating conditions (i.e operating parameters/conditions at variance from standard operating conditions), the ability to perform rough emissivity estimates and to differentiate emissivity differences on machinery equipment provides useful information for condition monitoring and diagnostics of the machine under the less-than-ideal circumstances frequently encountered onsite. Further, the comparative IRT is categorised into either quantitative or qualitative for progressive implementation as an ideal long term complement to Vibration Monitoring Techniques (VMT). The quantitative technique requires the determination of a temperature value to distinguish the severity of a components condition. therefore, this approach necessitates comprehensive knowledge of factors influencing IRT measurements such as emissivity; environmental influences such as distance, relative humidity, ambient temperature; reflected apparent temperature, spatial measurement resolution, thermal tuning etc. Comparative qualitative measurement compares the infrared pattern, such as gear contact patterns, of one component to that of an identical or similar component under the same or similar operating conditions. when searching for differing thermal patterns, an anomaly is identified by the intensity variations between any two or more similar objects, without assigning temperature values to the patterns. This technique is quick and easy to apply, and it does not require any adjustments to the infrared instrument to compensate for atmospheric or environmental conditions, or surface emissivity. although the result of this type of measurement can identify a deficiency, it does not provide a level of severity. This paper discusses practical application on an experimental setup as well as a case study related to vertically mounted pump wherein VMT and IRT have been used conclusively to address multiple defects being encountered during operation of the pump by ship staff. In the end, a well-structured IRT based CBPM approach has been proposed based on two categories, viz. data driven approach and knowledge based approach which will be required to be followed concurrently.**

***Index Terms*—IR Thermography, Predictive Testing, CBPM, Reliability, Qualitative Technique, Ball Bearing, Dynamic Loading, Defects Evaluation.**

I. Introduction

Timely fault diagnosis in rotating machinery plays a great role in preventing catastrophic failure of machinery in operating condition. Diagnosis of support bearings by analysing thermal image signature is a recent trend in diagnosing the health of machinery. Unlike vibration monitoring wherein the input signal gets processed and the output is modified, there are no process/ signal change in an IR thermogram, which captures and retains the original input. Due to this, the applications of infrared have quickly expanded in to the field of fault detection and in condition monitoring[1-2]. In the 1980s, Vavilov and Taylor[3] discussed the principles of thermal NDT, describing its ability to provide quantitative information about hidden defects or features in a material. Presently the Indian Navy is applying the CBPM techniques like Vibration Analysis, Wear debris Analysis, Engine Health Monitoring techniques, etc. for early fault diagnosis. Infrared Thermal Imaging as a condition monitoring tool is still in its embryonic stage mainly because the governing policy directives and implementation strategy is still in its formative stages. IR Thermography allows for the monitoring of temperatures and thermal patterns while the equipment is online and running under full load and unlike many other test methods, Infrared Thermography can be used on a wide variety of equipment including pumps, compressors, alternators, motors, bearings, pulleys, fans, drives, conveyors, etc [5].

Machine parts radiate heat whenever an abnormal operation occurs, which can be measured and mapped by using thermographic techniques to analyse the underlying defects. In order to improve maintenance efficiencies, repair quality and enhance worker safety, infrared cameras can be utilized in a wide spectrum of the maintenance envelope. The Navy can benefit from this technology by applying it in the field

of fault diagnosis along with existing CBPM techniques to enhance Maintainability and Availability.

A. Aim

This paper aims to discuss an experiment undertaken on a Machinery Fault Simulator followed by a case study on Fire pumps on a class of ship in the Indian Navy. These two cases highlight the merits of Infrared Thermography in conjunction with Vibration monitoring. We can therefore see how Infrared Thermography, when used in conjunction with existing CBPM practices would greatly enhance operational availability of equipment in the Navy by reducing equipment downtime through over maintenance.

Table 1 highlights the three major CBM techniques predominantly used by engineers namely Vibration Monitoring (VM), IR Thermography (IRT) and Oil wear debris analysis, for three generic equipment namely pumps, compressors and alternators. In this table, we see that when any one of the CBPM methods is used in isolation, the accurate analysis of the defect may not be possible whereas when they are used in conjunction, results in an accurate prognosis.

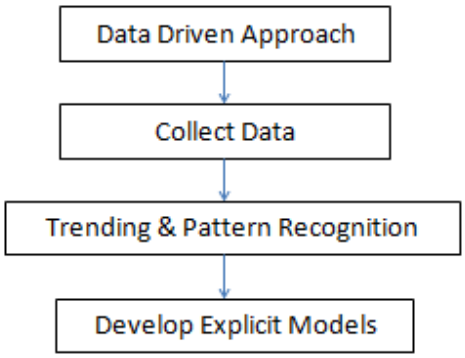
TABLE I
COMPARISON OF CBPM METHODS

	Examples of Faults	Vibration	Temp erature	Oil Debris
Pumps	Damaged Impeller	o	O	o
	Eccentric Impeller	o	O	
	Bearing Damage	o	o	
	Bearing Wear	o	O	o
	Mounting Fault	o		
	Unbalance	o		
	Misalignment	o	O	o
Symptom/ Parameter Change				
Compressors	Damaged Impellers	o	O	o
	Damaged Seals			
	Eccentric Impeller	o	O	o
	Bearing Damage	o	O	o
	Bearing Wear	o	O	o
	Cooling System fault		O	o
	Valve Fault	o	O	
	Mounting Fault	o		
	Compressor Stall	o		
	Unbalance	o		
	Misalignment	o	O	
Symptom/ Parameter Change				
Alternator	Rotor winding	o	O	
	Stator winding	o	O	
	Eccentric rotor	o		
	Brush(es) fault		O	
	Bearing damage	o	O	o
	Insulation deterioration			
	Unbalance	o		
	Misalignment	o	o	

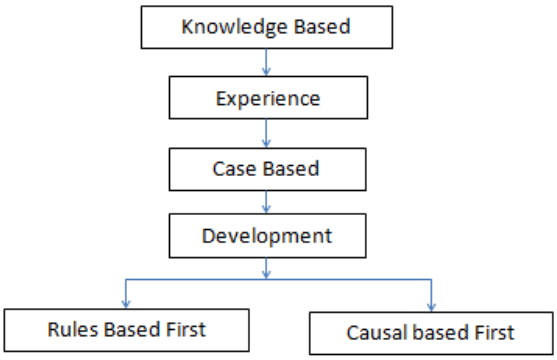
IRT- CBPM Approach

For developing an IRT based CBPM approach in the Navy, a dual pronged thrust of Data driven approach and Knowledge based approach is envisaged. The two approaches are described in detail below:-

(a) Data Driven Approach :- This methodology consists of collecting and collating data for various fitted equipment onboard including base line signature recording for new installation, initial image capture for newly repaired/ refurbished equipment either at test bed or onboard. This forms the base data with which all future recordings may be compared with. Further, in addition to trending, a pattern starts to emerge in the IRT images corresponding to specific nature of defect. This would aid in the long run in the development of explicit models for defect recognition and analysis. A simple flowchart depicting the process is illustrated below.



(b) Knowledge Based Approach :-This approach consists of utilising the experience gained in the usage of IRT in close coordination with VM and developing a strong reasoning based on knowledge acquired. This knowledge acquired will in turn result in immense experience gain with passage of time. Since both knowledge and experience gained will be on a case to case basis, it then transforms in to development of first principles- either Rules based or Causal based. For example, in the CBPM analysis of a centrifugal pump (vertically mounted), knowledge gained will dictate where all IR thermography and where all VMT are to be used (eg unbalance can be detected only by VMT and not by IRT).Experience gained over time will tell us how to take trials of the pump i.e. where all should the measuring points be, what distance should the IR camera be positioned, etc, Now, these may vary from pump to pump, even on different make/model/ constructions and hence should be diagnosed on a case to case basis. A simple flowchart depicting the process is illustrated below.



Once an IR thermogram of equipment under study has been collected, the next logical step falls on Severity Assessment Criteria. Whereas thermogram depends on operating conditions and design w.r.t. component loading, severity assessment depends on the following:-

a Thermal Profile/ Pattern assessment criteria
b Temperature Difference (T) criteria
c Max. Permissible Temperature criteria

Trials on Machinery Fault Simulator

The machinery fault simulator consists of one 0.5 HP variable speed motor driving a 30mm rotor shaft with two discs, whose weight is supported by two ball bearings located in two bearing housings as depicted in figure 1. The non-drive end of the shaft drives a belt driven pulley which in turn drives a small gear box. Provision exists on the GB output flange to connect to a basic reciprocating crank slider mechanism. Both bearing heights can be adjusted to simulate misalignment and small weights can be loaded on to the discs to simulate rotor unbalance.

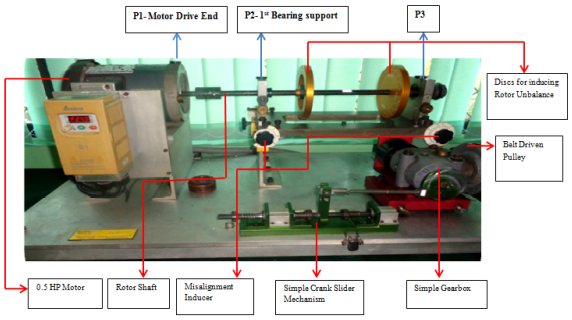


Fig. 1. Machinery Fault Simulator

Trials were undertaken under two scenarios- with and without misalignment. The vibration readings were collected using Lenovo Vibration recorder and IRT image using Fluke CA 1886 IRT camera with 8-14 m spectral band. The tabulated readings are appended in table 2.

TABLE II
TABULATION OF VM AND IRT READINGS

	Before alignment				after alignment		
Location	Direction	vib10	frequency/ amplitude	temp reture	vib10	frequency/ amplitude	temp reture
Motor DE (P1)	V	3.6	2H/2.53	40.5	9.5	2H/8.13	52.5
	A	3.9	2H/0.75		10.5	2H10.4	
	H	2.1	2H/1.35		2.1	2H/7.17	
Interim bearing V	V	1.7	2H/0.71	38	1.6	2H/1.13	43
	A	3.8	2H/0.27		3.0	2H/2.64	
	H	2.5	2H/1.28		5.6	2H/4.05	
End bearing	V	2.1	2H/0.81	40	2.9	2H/1.82	44
	A	3.2	2H/0.44		3.1	2H/1.05	
	H	3.3	2H/1.52		6.2	2H/4.82	

The IR thermography images of the two locations- P1 and P2 are appended below. The rise in temperature can clearly be observed across the bearings as depicted in Fig. 1.

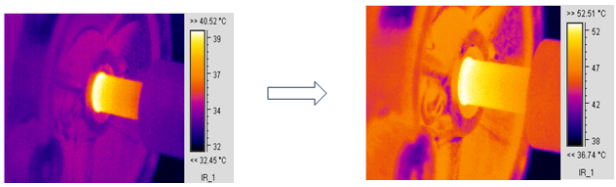


Fig. 2. IRT Image of P1 Before and After Misalignment

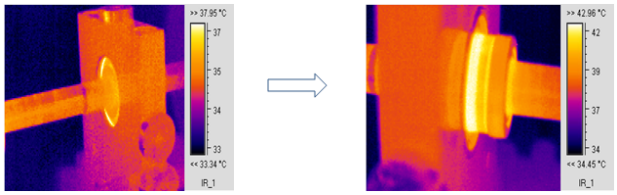


Fig. 3. IRT Image of P2 Before and After Misalignment

From the above analysis, it clearly emerges that both VM and IRT, when used in conjunction, helps in accurate and swift analysis of a defect. An experiment of similar nature was carried out by Younus and Young and presented at ICME(2009).

Case Study Fire Pump of Ship 1:-

Ship had reported an increasing trend of high vibrations on one of its fire pumps. As a trial agency, this unit was tasked with analysisng the defects and offer recommendations to the repair agency. Accordingly, trials were undertaken by this unit in the presence of ship staff and repair agency after the pump had run for one hour. Analysis of overall vibrations, narrow-band analysis and IRT audit of the pump were undertaken and compared with data obtained from other pumps of similar capacity and design. It is pertinent to mention that comparative trials undertaken on other pumps were under same operating/ reference conditions (amount of greasing done, running time prior recording of parameters etc) as the defective pump so as obtain consistent and comparable readings. The results are tabulated in table 3.

TABLE III
MY CAPTION

description	permissible vibration limit	fire pp no 2		fire pps	
		vibration	max temp	vibration	max temp
motor fe A	10	3.6	53	2.1	48
R		3.00		1.3	
motor deA		3.2	62	2.2	52
R		3.3		1.8	
pump feA		3.4		3.5	
R		14.6		3.1	
pump deA		4.6		2.8	
R		14.5		1.7	

Overall Vibration Analysis revealed readings of 14.5 /14.6 mm/sec were observed on the fire pump at pump DE and

pump FE in radial direction against the permissible limit of 10 mm/sec. Further, SPM readings revealed motor DE bearing in Red zone. Narrowband analysis revealed presence of high amplitude peaks at 1X in radial direction on pump DE and FE indicative of Unbalance and reduced clearances. IRT readings (figure 4) indicated that motor DE bearing temp to be 62C (as against 52C), pump DE/ FE bearings temp to be 74/50C (as against 54/42C ideally). Further, IRT images of motor junction boxes revealed high starting and current in one phase as depicted in Fig. 2

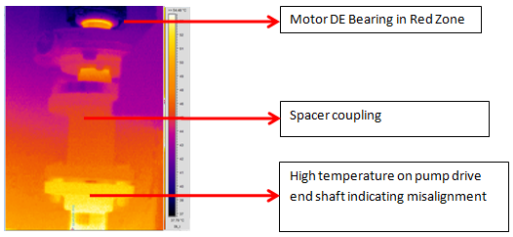


Fig. 4. IRT Image of Fire pump Motor DE, spacer coupling and Pump DE

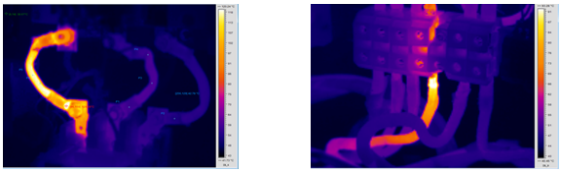


Fig. 5. IRT Image of Motor Junction Box Indicating Phase Unbalance

II. Analysis

For this class of ship fire pumps, diligent collation and trending of IR thermographic data by Data Driven Approach has initiated an explicit pattern to emerge which expresses that pump bearing and bearing housing temp ¿55^0C is an indication of incipient bearing defect. Further, high starting and running current in one electrical phase resulting in that phase to heat up is indicative of phase imbalance which might be caused by worn out bearings/ high clearance between rotating parts. The knowledge gained from Case Based Reasoning developed from years of experience in narrowband analysis revealed that for this type of fire pumps, increase in overall vibrations beyond 8-9 mm/sec on pump D/E in radial direction indicates reducing clearance between wear/ impeller ring.

By effectively combining Vibration analysis with IRT, together with trended data and causal reasoning gained from knowledge driven experience, a case of misalignment was detected. Accordingly necessary directives were issued to the repair yard for the following:-

a Greasing/ replacement of motor drive end bearing.
b Pump clearance and wear limits inspection for wear/ impeller ring and bearing bush/ shaft sleeve.
c Dynamic balancing of pump impeller.

III. Conclusion

As discussed earlier, repair decisions based on vibration analysis alone pose risk of over-maintenance. From above experimental test as well as on-board analysis of fire pump, it has emerged conclusively that machinery faults analysed through vibration monitoring complemented with IR Thermography not only yields rich dividends but also minimises risk of over maintenance by accurate disgnosis. What the Indian Navy needs as now is an effective policy and implementation strategy on the combined use of VM and IRT through Data Driven Approach as well as Knowledge Based Approach.

References

[1] 1. J. Seo, H. Yun, D. Hong, Quantitative assessment of detection of defects by thermographic inspection, presented at 18th International Conference on Composite Materials.
[2] 2. X.P.V. Maldaque, Theory and practice of Infrared Technology for Non-destructive testing, New York, John Wiley and Sons, pp 54-140,2001.
[3] 3. V.P. Vavilov, Thermal/ Infrared Testing, Book 1, in Non-destructive testing Handbook, Vol 5, edited by V.V. Klyuev, Spektr publishing, pp 124-180, 2009.
[4] 4. Ali Md. Younus, Khairul Alam, Bo-Sul Yang, Wavelet coefficient of Thermal Image Analysis for Machinery Fault Diagnosis, published in the Proceedings of the International Conference on Mechanical Engineering (ICME2009), Dhaka, Bangladesh.
[5] 5. J. Shiroishi, Y. Li, S. Liang, 1997, Bearing Condition Diagnostics via vibration and IR thermography, Mechanical Systems and Signal Processing, 11:693-705.



Lt Cdr TS Sathya Narayanan is an MTech in Mechanical (Marine) from DIAT, Pune, 2013. During his career of 10 years he has served as Commissioning Engineer Officer, INS Batti Malv, Engineer Officer INS Veer and Trials Officer, Diesel Testing & Tuning Team, Mumbai. He is Presently carrying out duties of Acoustic Officer, Machinery Trials Unit, Visakhapatnam . He has published 04 papers in refereed journals and conferences, notable among them being ICCM-2011, IWCEM-2013 and NCCM-2013. His areas of research interest are Design of IRSS devices for Naval platforms, Utilizing CFD analysis for predicting flow around ships and the integration of Acoustic Emission and IR Thermography as an effective CBPM tool in conjunction with Vibration Monitoring Technique. Lt Cdr TS Sathya Narayanan has won second prize for overall best paper in IWCEM 2013.



Lt Cdr Sumit Singh is an MTech in Machinery System Design and Control from IIT, Kharagpur, 2011 During his career of 11 years he has served as Engineer/Electrical Officer INS Tarasa and as Manager (Planning & Production), Naval Ship Repair Yard, Port Blair. He is Presently carrying out duties of Dy Oi/C, Machinery Trials Unit, Visakhapatnam . He has published 03 papers in refereed journals and conferences, written of which one presented at National Seminar of Delhi College of Engineering was adjudged the best paper in its category as well as overall winner of the seminar. His areas of research interest are machinery health assessment, Analysis of underwater radiated noise and revolutionizing CBPM techniques in Indian Navy.

Noise Transmission Analysis Onboard Marine Platforms- A Review

Cdr KK Mahapatra[1], **Arnab Das**[2]
[1,2]Naval Wing, TSO-I,MILIT, Girinagar, Pune, India
[1]kavikant1@rediffmail.com, [2]arnabdas1972@hotmail.com

***Abstract*—Noise prediction and characterization is a critical research area for varied domains and applications. The domains here include marine, aviation, transport, civil engineering, etc and the applications could include numerous military and non-military applications like fatigue failure in materials, human comfort, acoustic stealth, marine mammal habitat assessment, condition based monitoring of machineries, etc. The noise characterization precedes any effort towards noise control. Marine platforms are important for any attempt at exploring/exploiting the vast ocean resources and utilization of the ocean medium for transportation or otherwise. The growing activities in the maritime domain is ensuring increasing number of marine platforms of all types being introduced in the ocean medium and elsewhere. The increased maritime traffic calls for improved noise control for multiple applications. The propulsion machineries onboard marine platforms are known to be the dominant noise source and thus any noise characterization efforts mandate precise understanding of the noise and vibration from these machineries and their correlation with the overall noise radiated. This paper is concerned with the transmission of noise and vibration in ship structures, and in particular, naval ship structures. The first part of the paper presents a review of different methods for ship noise prediction. It then introduces the method of Statistical Energy Analysis (SEA) for the investigation of ship noise and vibration in the high frequency regions. Previous studies have shown that SEA is a useful tool for the analysis of vibration transmission in structures which consist mainly of plate elements. However, naval ship structures often involve more complex elements such as shells and beam stiffened plates. In the of the paper, two types of structure which are considered to be characteristic of naval ship constructions are identified. They are: a cylindrical shell coupled to an end plate; and a plate with periodic stiffeners coupled at right angles to a uniform plate. Review of the analysis of the Coupling Loss Factors (CLFs) of these two structures using travelling wave analysis, for SEA studies are presented. Review of theoretical and experimental programs confirm the validity of the formulation of CLFs.**

***Index Terms*—Noise characterisation; Noise Prediction ; noise transmission; ship structure; statistical Energy Analysis; Shell; Plate; Periodic Stiffeners; Coupling Loss factor (CLF).**

I. Introduction

Noise characterization is a critical research area for varied domains and applications. The domains here include marine, aviation, transport, civil engineering, etc and the applications could include numerous military and non-military applications like fatigue failure in materials, human comfort, acoustic stealth, marine mammal habitat assessment, condition based monitoring of machineries, etc. In the domain of transportation railways, automotive, aviation and shipping have been the forerunners in carrying out research on noise characterisation and control since 1930. Railways have their concentrated their studies to develop an effective and efficient vehicle track interaction models for calculation of vehicle ride comfort, rail corrugation rate, sleeper cracking, rail fatigue, ballast degradation and other track related phenomena. In some studies calculation of ground vibration transmission based on simple representations of vehicle and track dynamics and their interaction with ground has been analysed for incorporating necessary control measures. The aircraft industry has focussed the research in reducing the aerodynamic noise from airframe structure and jet noise from the propulsion unit radiating to external environment especially the environment surrounding the airport. The study of noise and vibration in ships has received considerable attention in tbe past few decades as a result of stringent ship noise legislation introduced by many countries [1]. Such legislation aims to provide a safe and comfortable working environment for crew members by specifying a maximum allowable sound pressure level in various ship compartments. The ability for the designer to predict noise level in ship compartments at the design stage is therefore highly desirable and several empirical and analytical studies on ship noise prediction have been reported [2], [7].

Naval surface ships and submarines require additional noise and vibration control measures to minimize the risk of detection and the interference with on-board equipment (for example, sonar and weapon systems). Furthermore, the extensive use of periodically stiffened plates and shells in naval ships increases the structural complexity for noise and vibration analysis. It has long been recognised [8] that vibration waves in aperiodic structure can only propagate in certain frequency bands (pass bands) and this phenomenon has a significant effect on vibration transmission. Due to the complexity of naval ship structures and the high frequency range of interest (up to 20 kHz for torpedo homing devices),a deterministic analysis of all tbe resonant modes of vibration is Acoustics Australia usually impractical. A powerful tool for predicting the high frequency response of complex systems is Statistical Energy Analysis (SEA) which deals with the time-averaged and frequency-averaged (octave or 1/3 octave) flow of vibrational energy between elements of a complex system [9]. In this paper, a number of methods used for the study of noise transmission in ship structures are reviewed. In particular, recent developments in SEA modeling of complex structures characteristic of naval ships are discussed.

II. Review of Ship Noise Reduction Methods

Due to the complexity of ship structures, it is clear that a rigorous analysis based on the 'classical' approach (for example, wave theory) is impractical. Nilsson [4], [10] presented a simplified analytical method based on a grillage model which was made up of two parallel hull frames and the associated plate elements. He considered that the frames would act as wave guides for the transmission of vibration from the hull to the superstructure. The plate elements used in Nilsson's analysis were assumed to be uniform and this approach may not be suitable for the analysis of structures with horizontal stringers between the frames that are typical of naval ship structures. A further restriction of this method is that it is essentially a two-dimensional model and is not readily applicable to the general analysis of vibration transmission in ships [33]. The Finite Element Method (FEM) may be used to model the response of complex structures. However, in the frequency range of interest for structure-borne noise studies (i.e., up to the several kHz range), the number of elements required is generally too large for the practical analysis of a substantial part of' a ship's structure, even with the help of modern computer technology and software packages. Furthermore, at high frequencies where the wavelength is much smaller than the overall dimensions of the structure, FEM would become very sensitive to the system parameters and may lead to incorrect prediction of the structural response. Hence FEM is normally restricted to the vibration analysis of ship structures at low frequencies. A number of empirical studies [2], [5], [11] have been reported for ship noise predictions. These studies were mainly based on measurements and data taken on board merchant ships. In general, empirical methods are valuable tools in the analysis of a generic type of ship, especially at the design stage where limited information is available. These methods become less attractive in situations where a detailed analysis is required on different types of ships (for example, naval surface ships and submarines). Statistical Energy Analysis (SEA) is a framework of study for the forced response of systems, and is based on the power balance between individual elements of a system [9]. It provides a basis for the prediction of average vibration and noise levels in complex structures, particularly at high frequencies. Sawley [1], [2]demonstrated that SEA can be used successfully to investigate the noise transmission paths of a motor vessel. 0degaard Jensen [3] studied the distribution of vibratory power in a 1:5 scale ship section and also investigated the effects of damping on vibration transmission. Good agreement between calculated and measured results was obtained for the lightly damped case but the agreement was poor for the heavily damped case and Jensen attributed the discrepancy to the effect of in-plane waves acting as flanking transmission paths for the vibratory power. Other authors [7], [13], [14] also reported on the application of SEA to the study of vibration transmission in ships. A more detailed treatment of this subject was given by Plunt [6] where he investigated the rear section of a cargo ship and found reasonable agreement with experimental results. A common feature of the SEA studies reviewed so far is that the ship structures were modelled as an assembly of plate elements subjected to bending waves except for Plunt [6] where longitudinal waves were also considered. Tratch [15] investigated the transmission of vibration in a 1:2.5 scale model of the machinery foundation of a ship bottom structure using SEA. He also modelled the structure as plate elements but considered all the possible wave types generated at the junction (i.e., bending, longitudinal and shear). Good agreement between calculated and experimental results was reported. Naval ship structures often make use of shell elements coupled to various types of plate element (for example, a submarine hull bulkhead coupled structure). The transmission of vibration through coupled cylinder/plate structures has been investigated by a number of researchers. Hwang and Pi [16] conducted an experimental investigation on a cylindrical shell welded onto a base plate and concluded that the SEA method was not capable of reaching any intelligent prediction of the coupling loss factor due to the strong interaction at the cylinder/plate interface. Blakemore et al. [17] studied a number of flange-connected cylindrical shells and found considerable discrepancy between measurement and SEA predictions. They attributed the discrepancy to internal acoustic coupling, non-equipartition of energy between modes in a cylindrical shell element and low modal overlap. Pollard [18] also investigated experimentally two cylinder/plate structures (one with along thin cylinder and the other with a short squat cylinder) and found conflicting results although the short cylinder showed good agreement between the theoretical and experimental results. Recently, Schlesinger [19] presented a theoretical analysis of the transmission of vibration through a cylinder/plate coupled structure based on an arbitrary distribution of the wave energies in the radial, circumferential and longitudinal directions. The theory is supported by a limited amount of experimental data but further work is needed to show that this method satisfies the reciprocity requirement of SEA. Thus the study of cylinder/plate coupled structures using SEA has been less successful compared with plate/plate structures and further research effort is required to address this shortcoming. Another type of structure often used in naval engineering constructions is a plate or shell element reinforced with periodic stiffeners. The application of conventional SEA through successive elements of this type of structure can significantly overestimate the transmission loss (see, for example, reference [17]). This is a matter of concern and has been the subject of criticism [20]. Clearly, the band pass nature of a periodic structure has to be considered in SEA modelling since it has a strong influence on the transmission of vibratory power. Keane and Price [21] applied the theory of periodic structures to enhance a one-dimensional SEA model. They investigated a point spring coupled, multi-modal system and compared the results obtained from 'exact' modal analysis with the normal and enhanced SEA model. A significant improvement in results was obtained by using the enhanced SEA model rather than the normal model. However, the model studied by these authors was made up of highly idealised one dimensional elements and therefore the analysis may not be readily applicable to ship structures such as hull plates and bulkheads. Langley [22] also studied the modal characteristics of periodic structures and derived modal density expressions

for one-and two-dimensional structures. He further studied the forced response of a damped one-dimensional periodic structure based on vibratory energy flow and compared the effect of material damping with the effect of damping caused by structural irregularity on vibration attenuation [23]. On the subject of 'near' periodic structures, Langley [24] investigated the wave transmission through a randomly disordered one dimensional periodic structure and discussed the occurrence of frequencies of perfect transmission. From the preceding discussion, it can be concluded that SEA is a useful tool for the prediction of vibration transmission through complex built-up structures, especially in situations where the structure can be modelled as an assembly of plate elements. However, a number of areas have to be addressed before this method can be applied successfully to naval ship structures.

III. Statistical Energy Analysis

In this method, a complex system is considered to be an ensemble average of a set of physically similar systems. The system is then sub-divided into a number of inter-connecting subsystems, usually at locations where the coupling between subsystems may be considered as 'weak' (for example, at structural discontinuities where incident waves are substantially reflected). The subsystems are then modeled as SEA elements, each consisting of a group of resonant modes of the same nature. For example, a uniform plate under bending and in-plane motions may be modeled as two SEA subsystems representing the resonant modes associated with these two types of motion respectively. The mean energy of the subsystems may be related to the input power by SEA parameters, known as modal densities, internal loss factors and coupling loss factors (CLFs), to form a set of linear, power balance equations. Solution of the power balance equations leads to the mean energy level (and hence the response) of the individual elements. The fundamental equations of SEA, as well as the basic theory and assumptions concerning the interaction between multi-mode subsystems, are given by Lyon [9]. In addition, review papers on this subject have been presented by Hodges and Woodhouse [25] and Fahy ([20] and [26]).

IV. Cylinder/Plate Coupled Structure

A number of researchers have modeled a ship structure as coupled plate elements and derived the CLFs on the assumption that the wave field in each plate element is diffuse ([6] and [15]). The concept of a diffuse wave field poses no, difficulty for the modeling of isotropic elements like uniform flat plates but is less clear from an SEA point of view for non-isotropic elements like curved plates and cylinders. Langley [27] pointed out that the assumption of a diffuse wave field is equivalent to the equipartition of energy amongst the resonant modes for an isotropic element. He then derived the CLFs for structural junctions between curved plates based on the modal concept of equipartition of energy. The present authors have extended the modal concept to consider the modeling of submarine structures which consist of cylindrical elements. They derived the CLF between a cylindrical shell and an end plate ([28] and [29]) using traveling wave analysis. The derivation consists of the evaluation of transmission efficiency for the cylinder/plate junction (defined as the ratio between the transmitted wave power and the incident wave power) by considering the appropriate boundary conditions (i.e., the compatibility of displacements and the equilibrium of forces and moments at the junction). The transmission efficiency is then related to the CLF between the cylinder and plate elements based on the assumption of equipartition of energy amongst all the resonant modes of the cylinder. Theoretical and experimental results [1997 paper] have well established the fact that, the response of a cylinder may be approximated by a flat plate at high frequency. Below a certain frequency, called the ring frequency, where the CLF dips, the CLF of cylinder plate structures differ considerably from their equivalent plate plate structures.

V. Coupled Periodic Structures

Periodic structures are used extensively in naval ship construction where relatively light weight uniform plates or shells are reinforced by the attachment of stiffners at regular intervals. It is well known [8] that a periodic structure freely transmits vibration waves in certain frequency bands (pass bands) and attenuates waves in other frequency bands (stop bands). This band pass nature has a strong influence on the transmission of noise and vibration through naval ship structures. The SEA modeling of one dimensional periodic structures has been considered by Keane and Price [21] by using a probability density function to model the band pass nature of the periodic structure. However, this approach is not readily applicable to structures since it is based on highly idealized one dimensional elements. Theoretical experimental results have been obtained for CLF between a uniform plate and the plate with uniform stiffeners. Comparison of results have indicated good agreement at low frequency band and a slight variation in the high frequency regime in view of the assumptions and simplifications.

VI. Conclusion

Following a review of different methods applicable to the investigation of ship noise, it is concluded that SEA is a useful tool for the high frequency noise and vibration analysis of ship structures. The SEA method has been further developed traveling wave analysis, for naval ship applications. The theoretical prediction of CLFs of two example structures typical to ships structures namely cylinder/plate coupled structures and periodic coupled structures have been cited and have shown good agreement with experimental results and it is therefore suggested that the formulation of CLFs using traveling wave analysis may be used for SEA studies of structures characteristic of naval ships. However, mention must be made of a number of areas that require further study before the method of SEA can be applied successfully to more realistic naval ship structures. For example, in the analysis of coupled periodic structures, the the review indicates considering only bending waves so that the analysis is simplified. In reality, the stiffeners of ship structures are often offset to one side of the plate and thus generate in-plane waves which may have a

significant effect on vibration transmission. Also, the coupling between other types of periodic structures typical of naval ship constructions such as ring stiffened cylindrical shells requires further investigation. Finally, the effect of fluid loading on SEA elements has to be considered in the analysis of ship noise.

ACKNOWLEDGMENT

The constant guidance and expertise given by Cdr (Dr) Arnab Das during preparation of this review is highly appreciated and acknowledged.

REFERENCES

[1] R. B. Conn, Acoustics and ship design. Proc. Int. Symp. On Shipboard Acoustics, Elsevier(1976).
[2] J. H. Janssen and 1 Buiten, On acoustic designing in naval architecture.Proceedings, INTER-NOISE 73,Copenhagen (1973) 3. J. 0degaard Jensen, Calculation of structure-borne noise transmission in ships, using the statistical energy analysis approach. Proc. Int. Symp. on Shipboard Acoustics, Elsevier (1976).
[3] J. 0degaard Jensen, Calculation of structure-borne noise transmission in ships, using the statistical energy analysis approach. Proc. Int. Symp. on Shipboard Acoustics, Elsevier (1976).
[4] A. C. Nilsson, Attenuation of structure-borne sound in superstructures on ships .J. Sound and Vibration55, 71-91(1977).
[5] J Plunt, ,Method for Predicting Noise Levels in Ships,Part l:Noise level prediction methods for ships, based on empirical data. Report 80-06, Chalmers Uni. Tech. Goteborg, Sweden (1980).
[6] J.Plunt, Method for Predicting Noise Levels in Ships, Part 2: Prediction of Structure-borne Sound Transmission in Complex Structures with the SEA Method, .Report 80 - 07, Chalmers Uni. Techn.Goteborg.Sweden(1980).
[7] P. Hynna, P Klinge and J. Vuoksinen,,Prediction of Structureborne sound Transmission in Large Welded Ship Structures using Statistical Energy Analysis. J..Sound & Vib.180,583-607(1995) .
[8] L. Brillouin, Wave Propagation in periodic structures. NewYork: Dover(1946).
[9] R. H. Lyon, Statistical energy analysis of dynamical systems Theory and Applications. MIT Press, Cambridge,Mass. (1975).
[10] A. C.Nilssen, Reduction of Structure-borne Sound in simple ship structures: Results of Model Tests. J. Sound Vibr.61,45-60(1978) .
[11] J. Buiten, ,Experiments with structure-borne Sound Transmission in ships. Proc. Int. Symp. on Shipboard Acoustics, Elsevier (1976).
[12] R. J.Sawley, The evaluation of a shipboard noise and vibration problem with statistical Energy Analysis. ASME Symposium on Stochastic Process in Dynamical Problems, Los Angeles (1969)
[13] Y. Irie and S. Takagi,, Structure borne Noise Transmission in Steel Structures like a ship. Proc. INTER-NOISE 78, San Fransisco (1978).
[14] K. Fukuzawa and C. Yasuda , Studies on structure-borne Sound in ship. Proc. INTER.NOISE 79. Warszava (1979).
[15] J. Tratch, Vibration Transmission through Machinery Foundation and Ship Bottom Structure, M. S. Thesis. M.l.T. (1985).
[16] C. Hwang and W. S. Pi, Investigation of Vibration Energy Transfer in Connected Structures . NASA CR-.124456 (1973).
[17] M.Blakemore, RJM Myres and J. Woodhouse, The statistical energy analysis of a Cylindrical Structure,.Proc.Second International Congress on Recent Developments in Air and Structure borne Sound and Vibration, Auburn University, US A. (1992).
[18] J. S. Pollard, Measurement of Cylinder/Plate coupling loss factor and associated problems, Nois e Control Eng. 39, 109-117 (1992).
[19] A. Schlesinger, Transmission of elastic waves from a cylinder to an attached plate, .J.Sound and Vibration, 186,761-780(I995).
[20] F. J. Fahy, Statistical Energy Analysis: A critical review, Phil.Trans.Roy. Soc. London, A, 346,431-447 (1994).
[21] A.J. Keane and WG Price, Statistica Energy Analysis of Periodic Structures, .Proc.Roy.Soc.London, A, 423 ,332-360 (1989).
[22] R. S. Langley, On the modal density and energy flow characteristics of periodic structures, .J.Sound and Vibration, 172, 491-SI1 (1994).
[23] R. S. Langley, On forced response of one-dimensional periodic structures: vibration localisation by damping, .J.Sound and Vibration, 178, 411-428 (1994).
[24] R. S. Langley, Wave transmission through one-dimensional near periodic structures: optimum and random disorder, .J.Sound and Vibration, 188, 717-743 (1995).
[25] CH Hodges and J Woodhouse, Theories of noise and vibration transmission in complex structures: Rep. Prog. Phys. 49, 107-170 (1986).
[26] FJ Fahy, Statistical Energy Analysis- a crtical review : Shock and Vibration Digest 6, 14-33 (1974).
[27] RS Langley, Elastic Wave Transmission coefficients and coupling loss factors for structural junction between curved panels, J Sound and Vibration 169, 297-317 (1994).
[28] YK Tso and CH Hansen, Wave propagation through cylinder/plate junctions, J. Sound and Vibration 186, 447-461 (1995).
[29] YK Tso and CH Hansen, An investigation of the coupling loss factor for a cylinder/plate structure, J. Sound and Vibration 199, 629-643 (1997).
[30] DA Bies and S Hamid, Insitu determination of loss and coupling loss factors by the power junction method, J. Sound and Vibration 70, 187-204 (1980).
[31] BL Clarkson & MF Ranky, On the measurement of coupling loss factor of structural connections, J. Sound and Vibration 94, 249-261 (1984).
[32] YK Tso and CH Hansen, The transmission of Vibration through a coupled periodic structure, J. Sound and vibration (1997).
[33] YK Tso and CH Hansen, The The Prediction of structure-borne noise transmission in ships using SEA, Acoustics Australia 25 No3, 97-102 (1997).



Kavikant Mahapatra Cdr Kavikant Mahapatra, is a ME(Marine), from University of Pune, 2001. During his career of twenty years in the Indian Navy, he has taken up various assignments as Engineer Officer onboard ships with Gas Turbine Propulsion, Trial and Quality Assurance Officer for Gas Turbine Operations, overhauls & Maintenance (PPM & CBPM), Instructor for Naval M.Tech. Student Officers at IAT, Pune, Officer-in-Charge Ship Upkeep and Maintenance Systems(Engg.) for monitoring and generation of maintenance policies for the engineering systems of navy, Vice Principal of Naval Engineering College, INS Shivaji, Lonavala. He is Presently working as Instructor at DIAT(DU) and Naval Wing MILIT, Pune for the M.Tech. and Short Courses of Navy. His areas of research interest are Noise and Vibration on board marine platforms and flow induced vibrations.



Arnab Das received B. Tech degree in Electrical Engineering from Naval College of Engineering, Lonavala, India in 1995. He obtained M. Tech degree in Radar and Communication with specialization in Underwater Signal Processing in 2002and PhD degree in 2009 from Indian Institute of Technology, Delhi, India. He was commissioned into the Indian Navy in 1994. He worked as Project Officer at CARE, IIT Delhi for R & D in Underwater Signal processing and hardware design in 2003-2007. Currently he is instructor at MILIT Pune, India. His research interests are Underwater Passive Surveillance, Underwater Communication and Pattern recognition.

CONDITION MONITORING OF SHIPS HULL USING ICCP SYSTEM A CASE STUDY

Dr N. Vasudeva Rao [1], **K. Jaya Prakasa Rao**[2]
[1,2]Central Dockyard Laboratory Naval Dockyard Visakhapatnam 530 014
[1]nandivadain@yahoo.co.uk

***Abstract*—Ships hull generally built with engineering metal which react with the aggressive species of surrounding environment forming compounds like metallic oxides, chlorides, sulphides etc., and this process is known as metallic corrosion on underwater hull surfaces. In this method, current is impressed through inert anodes of larger current carrying capacity form a D.C. power source to oppose the corrosion process of hull. The total current impressed is determined by multiplying the applied current density by the total exposed area. The potential to which the system must be polarized also needs to be determined prior to the current calculation. This potential determines the rate to which the corrosion is reduced. On the basis of theory and experience, it is established that the protective potential of structural steel in seawater is -800mV against silver/silver chloride and +250mV against zinc reference electrode.**

The paper presents the basic principle of Impressed Current Cathodic Protection (ICCP) system with special emphasis on condition monitoring of ships hull by measuring potentials against zinc reference electrode and monitoring the rating of impressed current by the anodes using ICCP system. An attempt is made to provide detailed case study by monitoring various likely causes of variation of hull potentials and impressed current over a period before and after taking necessary remedial actions.

***Index Terms*—Condition monitoring, Cathodic Protection, ICCP, Hull potentials.**

I. INTRODUCTION

For many years Impressed Current Cathodic Protection (ICCP) has been most common cathodic protection solution for ships. The most important feature of an ICCP system is that it automatically detects the electrical potential at the hull / seawater interface and raises or lowers the output to the anodes accordingly. In this way, the ship receives the optimum level of protection at all times. The electrical potential is monitored by reference electrodes which are fitted on port and starboard between the anodes where the lowest potential is likely to occur. This fed back to the control panel which automatically adjusts the anode current.

An ECG signal consists of P-QRS-T components which are having specific magnitude and intervals. In feature extraction method amplitude and intervals between these components are calculated to get abnormality in the heart rhythm [2]. Arrhythmia is one of the life-threatening disease can be monitored by extraction of features. Arrhythmia is basically categorized into 5 classes; here bradycardia, tachycardia and premature ventricular contraction are detectedThe major factors controlling the impressed current of ICCP system are size and configuration of hull, surface profile, speed of vessel, temperature and salinity of the transporting medium. High amount of current is required to protect bare steel which may lead undesirable effects such as evolution of Hydrogen. To protect bare steel, a current of 120 to 150mA/sq.mt is required, where as 10 15mA/sq.mt is sufficient to protect painted steel structure. Therefore, a combination of good surface coating and cathodic protection will normally result in the most practical and economic of the underwater hull.

II. HULL POTENTIALS

On the basis of theory and experience, it is established that the protective potential of structural steel in seawater is -800mV against silver / silver chloride or + 250mV against zinc reference electrode. In seawater, the steel corroding potentials are in the range of -550mV to -600mV against silver / silver chloride and more than 450mV against zinc reference electrode. An index of hull potentials given in table 1 can be used as guidelines to ascertain the condition of underwater hull.

TABLE I
INDEX OF HULL POTENTIALS

w.r.to zinc	w.r.to silver/silver chloride	
less than +200	more negative than -850	over protection
between +200 and 300	between -850 and -750	full protection
between +300 and 350	between -750 and -700	nearly protection
between +350 and 450	between -700 and -600	partial protection
more than +450	less negative than -600	no protection

III. CONDITION BASED MONITORING / MAINTENANCE

Condition based monitoring / maintenance (CBM) is the science of monitoring or taking action on actual condition. In the case of ship hull, this might mean that the vessel need not go into dry docking until sensors on the hull indicate that there is problem developing. Now-a-days, any data can be automatically logged by sensors accurately and on time and pasted into a spreadsheet application with any trends immediately apparent and the data can be analysed in real time by computer. The sensors in an ICCP system are primarily the reference electrodes. But they are not the main indicators of a potential problem developing because, if the ICCP system is doing its job, it will be maintaining the reference electrodes at a steady potential. The real indicators of a problem approaching come from monitoring the anode current. If current

remain relatively study, then it may be possible to ignore paint degradation / damage as a reason for dry docking until the system reaches a pre-determined percentage of its rated capacity. The variation of protection current due to change in seawater conductivity, seawater temperature and ships speed need to be taken into account when observing long term trends on which maintenance decisions must be based.

For better hull condition management, the following points are to be considered with reference ICCP system.

a The ICCP system must maintain the structure potential approximately between 150mV and 200mV with respect to zinc reference electrode.
b It must be cost effective over the lifetime of the structure being protected.
c The ICCP system must not degrade the metal it is protecting or its protecting coating.
d It must not degrade the performance or availability of the structure.

IV. CASE STUDY

In the present paper, underwater hull potential data between the period Jul 12 and Sep 13 was considered for monitoring the ships hull which is fitted with ICCP system. The data has been taken in such a way that it will cover the pre and post docking potential data to provide detailed study on condition monitoring of the ships hull. Table 2 gives the details of ships ICCP system.

TABLE II
DETAILS OF UNDERWATER HULL AND CP SYSTEM OF SHIP

Underwater area sq.mt	material	CP system	Remarks
1000	steel	ICCP system: res:02 Material lead anodes:04 material lead:s Anodes:48	Ship is fitted with 01 RE and 02 anodes on both PORT and STDB side

The following probable events are considered for monitoring the ship hull using ICCP hull potentials as well as anode current.

1 If the hull potentials are in the range of 170mV to 230mV with respect to zinc reference electrode as measured by ICCP system and cross checked by the external zinc reference electrode, indicates that the hull is fully protected.
2 If the hull potentials are in the range of 170mV to 230mV with respect to zinc reference electrode as measured by ICCP system and 5-10% full rated capacity current during ships sailing indicates starting of the paint deterioration.
3 If the hull potentials are in the range of 100mV-250mV with reference to zinc reference electrode and unit delivers 20% to full rated capacity current indicates that the control circuit of the ACU is defective. This situation reference to overprotection and may lead to disbondment or blistering of paint coating in the vicinity of the anodes on underwater hull.
4 If the ships hull potential is above250mV with respect to zinc reference electrode and the ICCP unit is not delivering any current indicates the defect in ICCP unit or anodes are fouled heavily.
5 If hull potentials are above 250mV and unit delivers 20% full rated capacity current indicates damage to anode dielectric shield or deterioration of paint coating.
6 If the hull potentials in the range of 100 to 150mV with respect to zinc reference electrode even after 2/3 years of paint renewal and no current is delivering by the ICCP system indicates heavy fouling on the underwater hull.

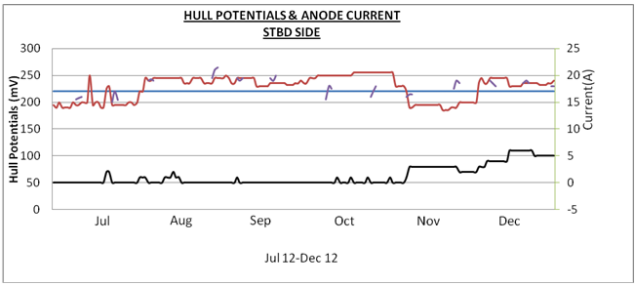


Fig. 1. Hull potentials and anode current during the period Jul 12 Dec 12: PORT side

Fig. 1 depicts trends of daily hull potentials and impressed anode current (PORT side of the ship) for the period from Jul 12 to Dec 12. From this trend, one can observe that the average hull potentials in the month of July are approximately in the range between 195mV and 210mV. It is also observed that there was a slight rise in hull potentials and current was impressed by the anodes during the end of July 12. This situation occurs due the sailing of ship. After that , there was a gradual increase in hull potentials was observed. From the Aug 12 to early Nov 12, the hull potentials were in the range of 230mV-250mV when the ship is in stationary state. In this period, it is also observed that no / minimum current was impressed by the ICCP system. In reality, the system supposed to impress a current of 5-10% of the full rated capacity to maintain the hull potentials below preset value (220mV). This particular situation indicates that the ICCP system is defective or the anodes are fouled heavily. The ICCP system was checked for the defect rectification and it was found the system is working satisfactorily. Then the ship staff was advised for cleaning of the active surface of the anodes to remove fouling. After completion of the above job, it was observed that the hull potentials were in the range of 190-210mV and about 5-10% of full rated capacity current was impressed by the anodes. This trend is shown in Fig. 1 between the period Nov 12 and Dec 12.

Figure depicts trends of daily hull potentials and impressed anode current (STBD side of the ship) for the period Jul 12 to Dec 12. The same trend was observed as in the case of PORT side except for the period between Nov 12 and Dec 12. After completion of anode cleaning job, it was observed that the hull potentials were in the range of 190mV-210mV and about 5-10% of full rated capacity of the current was impressed by the ICCP anodes. This trend continued till end

of Nov 12. During the month of Dec 12, it was observed that the hull potentials were raised and at the same time, the anodes impressed a current of 10-20% of full rated capacity. This trend is shown in Fig.2 between the period Nov 12 and Dec 12. This particular situation indicates damage to anode dielectric shield or deterioration of paint coating. Then the ship staff was advised to isolate the anode from the unit to stoop the further damage to the dielectric shield or disbondment of the paint coating due to excessive current.

Ship was dry docked for in the month of Jan 13. In the dry docking, damage to the dielectric shield in the vicinity of STBD anodes was observed. The disbondment of paint coating was also observed in and around the STBD anodes.

The ship was given one coat of antifouling paint on underwater hull and renewal of dielectric shield was taken up in the vicinity of the STBD anodes. The ship was undocked in the month of Mar 13.

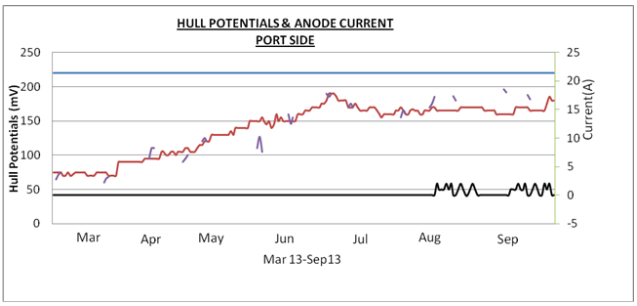


Fig. 2. Hull potentials and anode current during the period Mar 13 12 Sept 13: PORT side

Fig. 2 depicts the daily trends of hull potentials and anode current of the PORT and STBD side during the period Mar 13 to Sep 13 respectively. From these trends, it is observed that the average hull potentials were in the range of 75mV-100mV during the period Mar 13 to May 13. After that a gradual increase in underwater hull potentials were observed up to Jul 13. Then the potentials were stabilized in the range between 170mV and 190mV. In the above period, current impressed by the ICCP system is nearly zero. A range of 2-5% of full rated capacity current was impressed by the anodes during the period of ship sailing to maintain the hull potential in the full protection zone.

V. Conclusion

Impressed Current Cathodic Protection (ICCP) system is very useful tool for condition based monitoring / maintenance of ships hull provided the hull potential data and anode current are monitored regularly. In this system the real indication of the problem comes from monitoring the anode current. AS in the of PORT side observation (Fig. 1), after cleaning the active surface area of the anodes, a 5-10% of the full rated capacity current was started impressing by anodes. It is also observed that the hull potentials were in the range of 190mV-210mV which indicated that the hull is fully protected. But in case of STBD side observations (Fig.2), after cleaning active surface area of the anodes, the current impressed by the anode was 20% to the full rated capacity which indicates damage to the dielectric shield of the anode and disbondment of the paint coating. This damage is stopped further by timely isolating the anodes from the ICCP system.

To generalize the study, if impressing current relatively study (consistent with a gradual year-on-year coating degradation), then it may be possible to ignore paint degradation or damage as a reason for dry docking until the system (ICCP) impressing current reaches a pre-determined percentage of its rated capacity.

ACKNOWLEDGMENT

We express our profound gratitude to Cmde Sanjeev Chawla, AGM (QA and LAB) and Dr Jib Nath Jha, P.Sc.O, Manager (LAB), Naval Dockyard, Visakhapatnam for their constant support and encouragement in presenting and publishing this paper.

References

[1] Jones D, "Principles and preventions of Corrosion, Prentice Hall, New Jersy, 1996.
[2] Degiorgi V.G et al., "Computational Modeling of Shipboard ICCP system J. Corrosion Sci., and Eng., 4, 2003.
[3] Barry Torrance "Low Signature Impressed Current Cathodic Protection New development Future concepts paper presented at Recent advancement in Cathodic Protection, University of Manchestor Feb 2006.
[4] INBR 372/84: "Impressed Current Cathodic Protection system for ship hull NMRL, Bombay 1983.



Dr N Vasudeva Rao is a PhD., in Physics from Andhra University, Viskhapatnam in 2004 and M.Tech from Indian School of Mines, Dhanbad in 1994. He is presently working as Senior Scientific Officer in Central Dockyard Laboratory, Visakhapatnam. His areas of interest are NDT and Hull Protection.



K Jaya Prakasa Rao is a Diploma holder in Electrical Engineering. He is presently working as Junior Scientific Officer in Central Dockyard Laboratory, Visakhapatnam. His area of interest is Hull Protection.

Zigbee Based Ship Health Monitoring and Warning System

Lt. Cdr. M. Vinodh
Electronics Engineering Department
Defence Institute of Advanced Technology
Pune, Maharashtra, India
muvin236@gmail.com

Dr. K. Krishna Naik
Electronics Engineering Department
Defence Institute of Advanced Technology
Pune, Maharashtra, India
krishnanaik@diat.ac.in

Abstract— **Today with an increase in the number of systems or equipment fitted on-board modern naval ships, the sensors complexity has increased widely. For effective monitoring of different systems onboard a ship, requirement of a wireless sensor network is most desirable. It can be implemented with the help of a wireless sensor network using Zigbee standard. This paper discusses the feasibility of utilizing Zigbee standard devices to create a shipboard Zigbee wireless sensor network system for monitoring levels of temperature, smoke, and water level inside different compartments of a ship. The sensed data can be transmitted using Zigbee wireless modules to the central monitoring station or Damage Control station of a ship. The collected data will be processed in real-time, displayed at appropriate locations and recorded for future references.The aim is to prevent accidents or damage to a ship by continuous health monitoring of relevant parameters of systems onboard a ship and alert the watch keepers or concerned authorities. The warning given by the monitoring system would help in better management of the incident. This system can overcome the limitations of wired sensor networks. Further it is flexible for networking of monitoring system, and can be subject to additions and alterations easily. It is cost effective as the system is completely wireless paving way for additional benefits like savings in weight, space, and cost from cabling as compared to a wired sensor network. The proposal would also entail an overall addition for effective performance of manpower with an increased efficiency, and a greater awareness of operational and equipment health status of a ship. A user friendly GUI for analysis and monitoring of sensor data can further enhance the performance. The prototype model was implemented in a room to simulate an environment similar to that of a ship. The performance of the system was evaluated by sensing and transmitting data to a central data collection module placed in another room.**

Keywords—Zigbee; Wireless Sensor Network; Monitoring; Sensors; RS232 (key words)

I. INTRODUCTION

Today on a ship, there are huge no of sensors connected physically by wires and giving alarms or visual indications at central station or any other location. In addition, there are locations on a ship where it is not possible to route the cables to the sensors like the inaccessible areas[1]. Zigbee is a new technology, which has at its centre the goal of eliminating wired connections between sensors. Instead of connecting with wires, every sensor system has small transmitters or receivers which communicate wirelessly. Using Zigbee WSN, data could be recorded and analyzed, and alerts when certain conditions are met could be programmed. The Zigbee protocol developed by ZigBee Alliance, based on 802.15.4 wireless sensor network protocol provides a ideal solution since it is a low-cost, low-power, low data rates and best for remote control and sensor applications which are suitable for operation in harsh radio environments and at isolated locations. The data loss may be more due to multipath and fading effects in a ship due to steel structures. However, the loss can be reduced by positioning of sensor nodes at appropriate places. The GUI developed using open source JAVA software gives the user an advantage in terms of visual alerts, current status of the compartments and analysis of the recorded data. This system is better in performance than the conventional monitoring systems which have there own problems [5]. In this study, the ship health monitoring system based on Zigbee WSN measuring physical variables like temperature, smoke and water level is developed as a prototype[2]. To simulate environments of a ship for testing of the monitoring system, the sensor nodes were placed in different metallic enclosures in the laboratory.

II. HEALTH MONITORING SYSTEM

There are a vast no of electrical, electronic and mechanical systems or equipments fitted on ships which are critical for its mobility and safety. The operational status of a ship is decided by the health of its fitted systems. The requirement exists for keeping the systems in highest state of readiness by continuous monitoring of relevant parameters and preventive maintenance. Moreover, monitoring the parameters of inaccessible compartments like fuel tanks, battery charging room and sewage treatment plants etc becomes extremely difficult. With a wireless sensor network, ship systems health status is easily monitored by all levels of the chain-of-command, regardless of their location onboard [9]. In the event of any casualty, the system alarms the authority to make logical decisions based on a warnings generated by the system. This also allows the information pertaining to the

specific onboard equipment to be sent to a shore based maintenance facility for evaluation and recording.

III. WIRELESS SENSOR NETWORK

A wireless sensor network (WSN) is a system of one or more sensors that detect, collect and possibly respond to things like temperature, light, sound and vibration. These networks may be used for a variety of purposes from security surveillance to medical or environmental research. The main characteristics of a WSN are power consumption constraints for nodes using batteries or energy harvesting, ability to cope with node failures, mobility of nodes, communication failures, heterogeneity of nodes, scalability to large scale of deployment, ability to withstand harsh environmental conditions and ease of use.

A. IEEE 802.15.4/Zigbee Protocol

IEEE 802.15.4/ZigBee is a standard protocol for Low-Rate Wireless Personal Area Networks (LR-WPAN). Its main features are network flexibility, low data rate, low cost and very low power consumption, which make it suitable for an adhoc network. The IEEE 802.15.4 protocol includes a PHY layer and MAC sub-layer for the LR-WPAN. The PHY layer offers three operational frequency bands; there are 27 channels allocated in the 802.15.4 range, with 16 channels in the 2.4 GHz band, 10 channels in the 915 MHz band, and 1 channel in 868 MHz band. The MAC sub-layer handles all access to the physical radio channel. It provides an interface between the service specific convergence sub-layer (SSCS) and the PHY layer. Table I gives the basic specifications of the Zigbee 802.15.4 Standard.

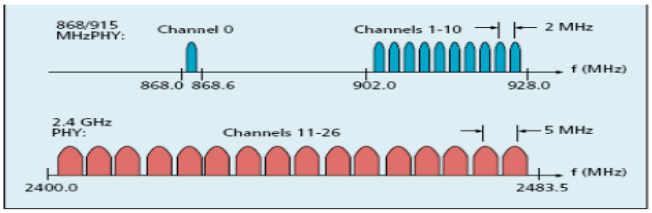


Figure. 1. Zigbee Band of Frequencies

Table I. Basic ZigBee specifications

Parameters **Parameters**	**Zigbee Value**
Transmission range (metres)	**1-100**
Battery Life (days)	**100-1000**
Network Size (no of nodes)	**>64000**
Throughput (Kb/s)	**20-250**

B. Network components

IEEE 802.15.4 protocol generally defines three types of nodes

- *PAN coordinator*: The main network coordinator identifies its PAN and can be connected to other nodes. In addition, it proposes global synchronization services to other nodes in the network through transmission of beacon frames that contained the identification of PAN and other relevant information.
- *Coordinator*: It has the same functionality as PAN coordinator, except that it does not create its PAN. Coordinator is connected to the PAN coordinator and provides services for local synchronization of the nodes in its range with significant transfer beacon frames containing the identification of the PAN, which is connected.
- *End node:* It is a node with no coordinated functionalities. To be able to synchronize with the other nodes in the network, it is connected as a secondary node with the PAN Coordinator or the coordinator. The first two types of nodes are defined as Full Function Devices as they implement all the functionalities of the IEEE 802.15.4 protocol.

C. Zigbee topologies

IEEE 802.15.4 supports Star, Mesh and Tree topologies. In the star topology, the communication is established between devices and a single central controller, called the PAN coordinator. The PAN coordinator may be AC powered while other devices will most likely be battery powered. Applications for this topology include home automation, personal computer (PC) peripherals, toys and games. After a FFD is activated for the first time, it may establish its own network and become the PAN coordinator. Each star-topology network chooses a PAN identifier, which is not currently used by any other network within the communication range. This allows each star network to operate independently. Beacon is used to synchronize every node with PAN coordinator. In peer-to-peer (mesh) topology, there is also one PAN coordinator. In contrast to star topology, any device can communicate with any other device as long as they are in range of one another. A peer-to-peer network can be ad hoc, self-organizing and self-healing. Applications such as industrial control and monitoring, wireless sensor networks, asset and inventory tracking would benefit from such topology. It also allows multiple hops to route messages from any device to any other device in the network. It can provide reliability by multi-path routing. Beacon is not used for peer-to-peer topology. This reduces control and increases collisions as compared to the beacon enabled network.

Cluster-tree network is a special case of a peer-to-peer network in which most devices are FFDs and a RFD may connect to a cluster-tree network as a leaf node at the end of a branch. Any of the FFD can act as a router and provide synchronization services to other devices and routers. Only one of these routers is the PAN coordinator. The PAN coordinator forms the first cluster by establishing itself as the cluster head (CLH) with a cluster identifier (CID) of zero, choosing an unused PAN identifier, and broadcasting beacon frames to neighboring devices. A candidate device receiving a beacon frame may request the CLH to join the network. If the PAN coordinator permits the device to join, it will add this new device as a child device in its neighbor list. The newly joined device will add the CLH as its parent in its neighbor list and begins transmitting periodic beacons such that other

candidate devices may then join the network at that device. Once application or network requirements are met, the PAN coordinator may instruct a device to become the CLH of a new cluster adjacent to the first one. The advantage of this multi-cluster, hierachial structure is the increased coverage area at the cost of increased message latency.

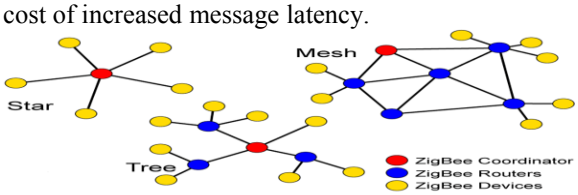


Figure.2. Network Topologies

IV. ARCHITECTURE

A. Overview of System Design

The overall structure of system is shown in Figure 3, which is based on Zigbee star topology[4]. The network is made up of various modules, each one consisting of three sensors and one Zigbee transmitter. These modules, in turn, communicate wirelessly with a Zigbee receiver module that is linked up to the RS232 port of a computer that monitors the entire system. The task of sensor node is to collect temperature, smoke and water level and transmit the data to the receiver. The monitoring station provides a graphical operating environment and displays data for the staff to query. In developing the software, Java programming language, WINDOWS operating system and mySQL database are used to make the system a low-cost, user friendly monitoring system.

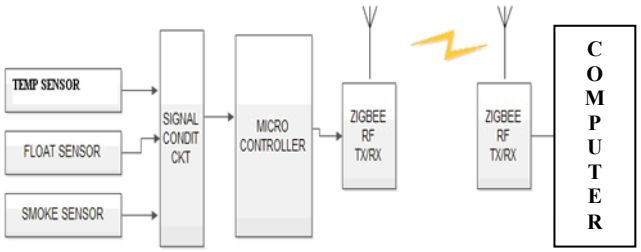


Figure. 3. System Block Diagram

B. Design Specification

The hardware used in the implementation are Xbee S2 Zigbee Modules, LM35 Temperature sensor, MQ-2 Smoke sensor, resitive designed circuit for water level measurements[6].

*1) Hardware Specifications:*A WSN node consists of a microcontroller, sensors, and a communication module.

- Microcontroller: We design a PCB where we use Renasas R8C-1B microcontroller on all the transmitter boards. It is a 8 bit controller with 4 ADC and 16K memory. The I/O which can interface with the other devices such as I2C, SPI, digital and analog.
- Temperature Sensor: The LM35 series sensors are precision integrated-circuit temperature sensors whose output voltage is linearly proportional to the Celsius temperature[5]. The LM35 requires no external calibration as it is inherently calibrated. The output from the temperature sensor is analog but is then sampled and quantized (A/D converted) by the Renasas microcontroller. Hence, we can realize the temperature in degree Celsius by calibrating it by using the equation derived from an experiment if we use reference temperature is X degree Celsius and sampling value at reference temperature is Y as shown in equation (1).

  Temperature = X + ((analogRead - Y) X 0.5)) (1)
- Smoke Sensor: MQ-2 is a gas sensor used in gas leakage detecting equipments in family and industry. This is suitable for detecting of LPG, iso-butane, propane, methane ,alcohol, Hydrogen, smoke. The pollution level chart is prepared and classified as shown in Table II.

  - Table I. Pollution Level Chart

Smoke Index(ppm)	Status
0-50	Good
51-100	Moderate
101-200	Unhealthy
201-300	Very Unhealthy
>301	Dangerous

- Communication: Xbee S2 is used for transmission and reception of data in our system. The XBee is compliant to the IEEE 802.15.4 standard. It is a series-2 version which supports mesh networking, fixes the address to 64 bits, and has 20 pins. In summary, the system consists of two types of nodes: Coordinator and End Device, as shown in Fig. 4 & Fig.5. The Coordinator consists of RS232 port, Xbee and level converter. On the other hand, End Device consists of R8C microcontroller, Xbee , temperature sensor, smoke sensor and water level circuit.

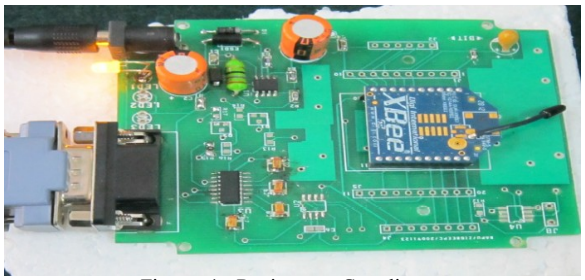


Figure. 4. Reciever or Coordinator

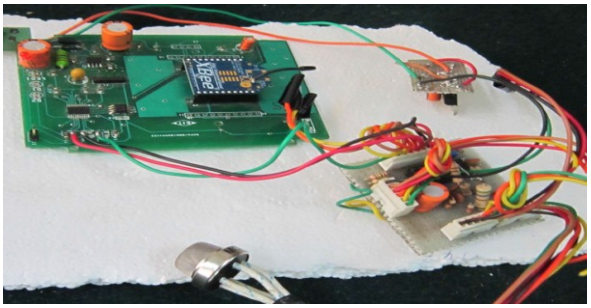


Figure. 5. Transmitter or End Device

- Level Converter: MAX3232 is used as a level converter IC since the power supply utilized in the board is 3.3 V.

2) Software Specification:

- Microcontroller: R8C is programmed using emulator E8. We use High Performance Embedded Workshop HEW IDE for the development and debugging of embedded applications for Renesas microcontrollers
- Web-Server: We use a simple Java application running on Coordinator.
- Database: We use MySQL to run on monitoring client computer. The client computer has XAMPP Web-Server for Query MySQL command with PHP language accordingly.

3) System Limitation: The distance between the Coordinator and End device should not exceed 100 meters from the specification. On the other hand, if there are any blockages, the distance should not be greater than 40 meters. For the temperature sensor, it can measure the temperature to the accuracy of only one decimal point, i.e., the resolution is in 0.5 degree Celsius. The gas sensor needs to be calibrated in standard conditions.

V. TESTING

In the laboratory (about 40 square meters), three end sensing station nodes (setting the number for the Sl to S3) and a central node are arranged, the environmental parameters were detected. We deployed four sensor nodes far away from each other at about 10-30 meters. The temperature was varied by heating a soldering gun and placing it near the temperature sensor. The smoke level was varied by placing the station 1 & 2 nodes near a cigarette and incense stick smoke, whereas the station 3 was kept in clean air in the laboratory. We monitored the temperature and smoke readings from different nodes, sent to Coordinator which is Web-server and receive the data from each sensor and then monitor via Webpage. The monitoring data of three station nodes at several time points using HyperTerminal on the RS232 port is displayed in Fig. 6.

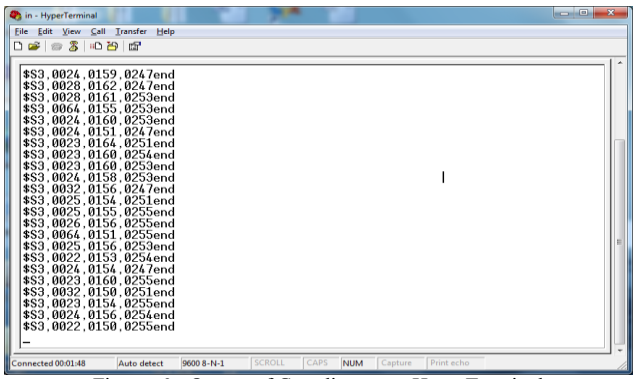


Figure. 6. Output of Coordinator on HyperTerminal

The data format is start bit, station name, temperature data, gas data, water level data and end bit. The RSSI test was carried out by measuring the signal at the coordinator by placing the receivers in different rooms and steel cabinets/ lockers. The signal dropped if the receiver was in steel cabinet at considerable distance.

VI. RESULTS

The final GUI output as obtained on the computer COM port developed using Java software is shown in Fig.7. The values of sensors at different stations are also recorded in the mySQL database. The recorded data can be utilized for analysis of the sensor data to arrive at their operational health status. The temperature and smoke level graph of different stations is plotted in Fig. 8 & 9 for duration of 12 hours of a particular day. The temperature and smoke levels of the station nodes reflect on the GUI every 2 seconds as the transmitters are programmed for this time, hence timing is programmable.
The data packets are not lost as the transmitter keeps on sending the data till it receives an acknowledgment from the receiver (max 4 times) otherwise the data packet is dropped.

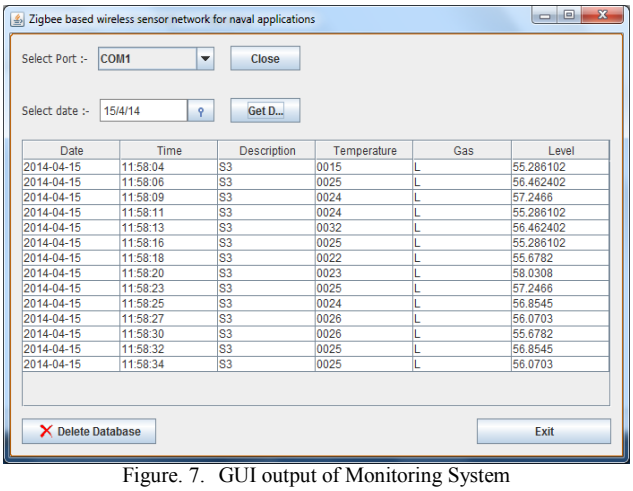


Figure. 7. GUI output of Monitoring System

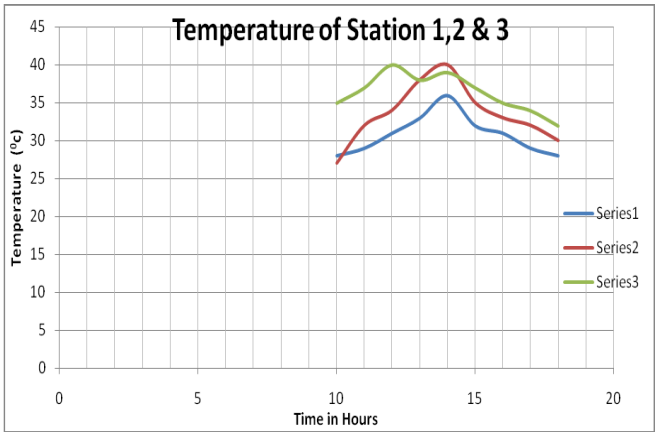


Figure.8. Temperature Graph

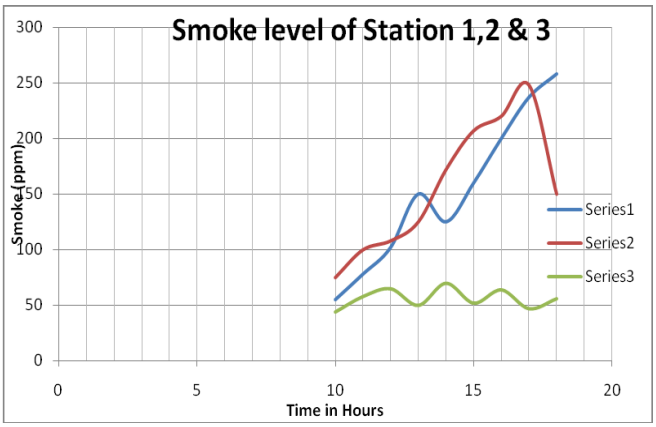


Figure. 9. Smoke level Graph

VII. CONCLUSIONS AND RELATED WORK

The value will be in the application, not in the technology. The main goal of this effort has been to address applications that could benefit from wireless connectivity and enable new ones that cannot use higher-end wireless application. The ship health monitoring system can reduce manpower requirement and give warnings in real time. The nodes can be effortlessly placed in inaccessible areas and monitored from a central monitoring station. We were successful in sensing the temperature, smoke and water level as data in star topology and generate warnings on the computer for the user. Foremost, before implementing the WSN, the RF path loss model should be arrived as per the design of the ship[1]. Since most of the equipments as well as ship bulkheads are made of steel, the data delivery loss caused by the fading effect should be considered before the actual placement of sensor nodes [6]. It is also necessary to establish more efficient serviceable environments using ubiquitous technologies like WSN and power line communication [3]. To reduce data loss, for compartments far away from central monitoring station, a separate network can be setup at the local area and monitored from adjacent station. The work can be related by interfacing light sensors, cameras and accelerometers for sensing different parameters using Mesh topology.

ACKNOWLEDGMENT

This research was accomplished with support from Defence Institute of Advanced Technology (Deemed University),Pune for the project entitled “Zigbee Based Wireless Sensor Network for Naval Applications”.

REFERENCES

[1] H. Kdouh, C. Brousseau, G. Zaharia, G. Grunfelder and G. El Zein, “A realistic experiment of a wireless sensor network on board a vessel,” COMM2012 - 9th International Conference on Communications, Bucharest, Romania, June, 2012

[2] Marintek., 2000. “Intelligent hull-monitoring systems for the reduced risk of structural failure, spill into the sea, and damage to cargo, and for improved passenger safety and comfort,” (HULLMON+). G3RD-CT-2000-00329, EU Framework Programme.

[3] H. Kdouh, C. Brousseau, G. Zaharia, G. Grunfelder and G. El Zein, “Applying of ubiquitous wireless technologies for shipboard monitoring systems,” WPMC’11 - 14th International Symposium on Wireless Personal Multimedia Communication, Brest, France, October 2011.

[4] T. Pilsak, T. Schröder, J. Eichmann and J. L. Ter Haseborg, “Field test of a wireless sensor network inside the engine room of a vessel,” Hamburg University of Technology Institute of Measurement Technology, 2009.

[5] J. P. Lynch and K. J. Loh, “A summary review of wireless sensors and sensor networks for structural health monitoring,” The Shock and Vibration Digest, 38 (2), pp.91-128, 2006

[6] H. Kdouh, G. Zaharia, C. Brousseau, G. Grunfelder, G. El Zein, “ZigBee-based sensor network for shipboard environments,” ISSCS2011 - 10th International Symposium on Signals, Circuits and Systems, Iasi, Romania, July 2011.

[7] B-G. Paik, S-R. Cho, B-J. Park, D. Lee, B-D. Bae and J-H. Yun, “Characteristics of wireless sensor network for full-scale ship application,” Journal of Marine Science and Technology, Vol 14, No 1, pp.115-126, 2009.

[8] H. Kdouh, H. Farhat, T. Tenoux, G. Zaharia, C. Brousseau, G. Grunfelder, Y. Lostanlen and G. El Zein, “Double directional characterisation of radio wave propagation through metallic watertight doors on board ships,” Electronics Letters, vol. 48, no. 6, pp. 307-309, March 2012.

[9] H. Kdouh, H. Farhat, G. Zaharia, C. Brousseau, G. Grunfelder, and G. El Zein, “Wireless sensor network onboard vessels,” International Conference on Telecommunications, Jounieh, Lebanon, 2012

[10] Liping Mu, “A hybrid network for maritime on-board communications,” Fifth International Workshop on Selected Topics in Mobile and Wireless Computing, 2012

[11] L. Mu and A. Prinz, “Delay-Oriented data traffic migration in maritime mobile communication environments,” in Proceedings of the Fourth International Conference on Ubiquitous and Future Networks, 2012.



Lt Commander M Vinodh is an alumnus of Naval College of Engineering, INS Shivaji. He was commissioned on 01 Jan 2005 in the electrical branch of the Indian Navy. The officer has served as ALO (PGD) , INS Rajput and Deputy Manager (PM) at Naval Dockyard, VIsakhapatnam.

He is presently undergoing his M. Tech in Signal Processing and Communication at DIAT (DU), Pune. His areas of research and interest are Embedded Systems and Wireless Sensor Networks.



Dr. K. Krishna Naik received Doctoral degree from Jawaharlal Nehru Technological University Anantapur, Anantapur in 2010. He did his Post graduation from Indian Institute of Information Technology, Allahabad in 2004 and Currently he is working as an

Assistant Professor In Electronics Engineering Department, Defence Institute of Advanced Technology, Pune. His current areas of research includes: Electronic Warfare Applications, Software Defined Radio, Wireless Networks, Mobile Ad-Hoc Networks